Universidade de Lisboa
Faculdade de Ciências
Departamento de Biologia Vegetal

Revealing Host Factors Important for Hepatocyte Infection by *Plasmodium*

Cristina Dias Rodrigues

Universidade de Lisboa

Faculdade de Ciências

Departamento de Biologia Vegetal

Revealing Host Factors Important for Hepatocyte Infection by *Plasmodium.*

Cristina Dias Rodrigues

Dissertation submitted to obtain a PhD Degree in Biology, speciality of Cellular Biology by the Universidade de Lisboa.

Supervisor
Maria Manuel Mota, MsD, PhD.
Principal Investigator of Instituto de Medicina Molecular
and Auxiliary Professor at Faculdade de Medicina,
Universidade de Lisboa.

Co-Supervisor
Maria da Graça Alves Vieira, PhD.
Auxiliary Professor of Faculdade de Ciências,
Universidade de Lisboa.

**Research is to see what everybody else has seen, and
to think what nobody else has thought.**
Albert Szent-Györgi

**All truths are easy to understand once they are discovered;
the point is to discover them.**
Galileo Galilei

Preface

The present thesis embraces the data obtained during my Ph.D. research project developed from November 2003 to June 2007.

The experimental work was supervised by Prof. Doutora Maria Manuel Mota and was carried out at Instituto de Medicina Molecular, in Lisboa and Instituto Gulbenkian de Ciência, in Oeiras, Portugal. The RNAi screens were performed at Cenix BioScience, Dresden, Germany.

This Ph.D. was supervised by Prof. Maria da Graça Alves Vieira from Departamento de Biologia Vegetal, Faculdade de Ciências, Universidade de Lisboa, Portugal.

The financial support was provided by the portuguese Fundação para a Ciência e Tecnologia, through the Ph.D. fellowship grant SFRH/BD/14232/2003.

This thesis is structured in 5 chapters, which are preceded by a summary, both in Portuguese and in English.

Chapter 1 comprises a general introduction to malaria and its current world situation, followed by an overview on the *Plasmodium* life cycle, the state of the art on the liver stage biology and the objectives of this thesis.

Chapters 2 to 4 consist of the results obtained throughout the research project, which are presented in a publication format. Each results chapter includes an abstract, an introduction, the results and discussion, as well as the methods, acknowledgments and references.

Chapter 5 encloses a general discussion and the future perspectives of the work develop.

In Appendix are supplied my *Curriculum Vitae* and the publications in which I have participated until the date of printing this thesis.

Agradecimentos
Acknowledgements

Ao longo do meu doutoramento "cresci" em termos científicos mas acima de tudo como pessoa. Estes quatro anos foram muito intensos em sentimentos totalmente diferentes: entusiasmo *vs.* desânimo, alegria *vs.* tristeza, partilha *vs.* inibição, convicção *vs.* dúvida, sorrisos *vs.* lâgrimas, companheirismo *vs.* momentos de solidão. Durante esta jornada foram várias as pessoas que me acompanharam e às quais faço questão de agradecer.

À Maria.

Um bem-haja à minha orientadora científica e amiga.

É díficil conseguir expressar em palavras tudo pelo qual gostaria de te agradecer. Obrigada pela oportunidade de poder trabalhar contigo e pela tua constante presença e apoio. Obrigada pela orientação científica e por me ensinares a fazer Ciência, pelo teu entusiasmo contagiante, pelas discussões científicas, por compreenderes os meus erros, por toda a preocupação, carinho e amizade e por respeitares as minhas ideias e o meu ritmo de trabalho e de escrita.

À Professora Graça.

Obrigada por ter aceite ser a minha orientadora interna ao nível da Faculdade de Ciências da Universidade de Lisboa. Foi um prazer partilhar e discutir o meu trabalho consigo... Muito obrigada por todo o apoio, ajuda e carinho.

Ao Miguel.

Quando começámos a trabalhar juntos foi um pouco difícil para mim. De repente ter de partilhar ideias, opiniões, horários, material, preocupações, definir prioridades e até partilhar uma vida/casa num país frio foi um desafio. Aprendi imenso contigo durante o meu doutoramento e sem ti os 6 meses em Dresden teriam sido ainda mais difíceis. Crescemos como colegas e amigos! Miguelito, muito obrigada por todo o apoio científico e pessoal.

À Sónia.

Muito obrigada pela constante boa disposição, companheirismo, ânimo, amizade no lab e principalmente durante as nossas mil viagens épicas. Estás nas minhas memórias de NY, Dresden, Berlim, Praga, Budapeste e Londres. E espero que em breve de Barcelona, mas desta vez espera-se que sem quedas!!

To Michi.

When I think about the first time that I went to Cenix BioScience, it comes to my mind the picture of you and Christian. Two friendly guys!! At that time I had never thought that we would still be working together after 4 years, which is spectacular. We were involved since the beginning and together we have been able to build an amazing story. Thank you for your

support to the development of malaria research at Cenix. Many thanks for all the help, your work and input, your enthusiasm and all the scientific discussions.

To Cécilie.

I have learned a lot working with you, especially in what regards a good laboratory methodology. Thank you for your excellent work, your availability to answer my questions, your support and friendship and for the evenings and dinners while we were in Dresden. I hope to see you and Régis soon here in Lisbon.

To Chris.

Thank you for embracing the malaria research. To be able to work directly with you is a great honor and I have been learning constantly. Thanks for all your amazing input to our work and I will never forget your support and advices at the Keystone Meeting.

À Sílvia.

Agradeço-te pela tua constante disponibilidade em ajudares e especialmente por o fazeres com um sorriso. Sei que posso contar sempre contigo. Muito obrigada pelo apoio, energia e positivismo em termos profissionais e pessoais. O teu bom humor e espírito de amiga têm-me contagiado! Si, mil "thanks".

À Sabrina.

Muito obrigada pela ajuda no trabalho, pelo apoio na recente cruzada de se fazer hepatócitos primários, pela tua amizade repleta de energia e sabedoria de vida. Desejos de muitas felicidades e havemos de nos cruzar algures no mundo! Não desanime nunca!

À Lígia.

Muito obrigada pelos teus maravilhosos hepatócitos primários de ratinhos, por me ensinares o protocolo que tão arduamente optimizaste e por estares sempre disponível a ajudar. Obrigada por todo o apoio e carinho. Mantém esse sorriso lindo!

A todos os meus colegas que constituem a *Unidade de Malária*.

Vocês estiveram presentes durante o meu doutoramento em fases diferentes... Se não me falha a memória, aqui vai por ordem de chegada ao grupo.

Patrícia, muito obrigada por toda a ajuda, constante disponibilidade, amizade e contagiante gosto de se fazer Ciência sem deixar de se viver e explorar o Mundo e os sentidos. Admiro a tua capacidade de conciliar tantas actividades. Bjinho gde Linda!

Daniel, muito obrigada pela paciência e muitos ensinamentos aquando da minha chegada ao grupo. Foste espectacular!

Casanova, pelo apoio inicial e por me ensinares princípios laboratoriais básicos. Força para o teu doutoramento. Pensamento positivo!

Bruno, muito obrigada por todo o apoio e força de que tudo vai correr bem. Desejos de muitas felicidades e se falhei na Holanda espero não falhar em Itália. Tudo de bom.

Margarida, marcaste-me desde o primeiro dia em que fui ao IGC. Ainda me lembro da tua disponibilidade e simpatia a falares comigo. Foi muito bom trabalhar contigo, muito obrigada por todos os teus concelhos. Fica bem!

Ana, o teu percurso constitui para mim um exemplo de como é possível mudar. Admiro a tua coragem, perseverança e luta. Obrigada por todo o apoio, ombro amigo e concelhos. Coragem, energia e sorriso estampado!

Marta, a tua forte personalidade em prosseguires as tuas convicções é marcante. Muito obrigada pelas constantes perguntas e pelo apoio e compreensão em momentos difíceis. Desejos de muitas felicidades na tua nova etapa de vida em Londres and "see u"!

Nuno, aprendi muito ao trabalhar contigo e obrigada por toda a ajuda. Espero que alcances todos os teus objectivos profissinais e pessoais. Nunca desistas!

Cristina, muito obrigada pela tua visão do que é fazer Ciência, pelo exemplo de organização e capacidade de trabalho, pelo apoio e amizade. Ao te observar parece tão fácil!

Ataíde, obrigada pelo trabalho indispensável com os nossos amigos mosquitos, pela constante boa disposição, companheirismo e gargalhadas. Boa sorte na Austrália e vê-se estás por lá em Fevereiro para fazeres as honras. Arrasa!

Iana, thanks for your example of courage for going after of what you really wanted. I wish you all the best.

Carina, és um exemplo de perseverança e insistência. Não percas estas qualidades e apesar de o tempo passar a correr lembra-te que durante um doutoramento também se deve aproveitar. Força!

Kirsten, thanks for all the scientific questions, conversations about different subjects and help with the english. A smile!

Catarina, obrigada pelo teu empenho no trabalho de produção de mosquitos. Bjinho!

Luís, muito obrigada por toda a tua ajuda preciosa nesta fase final e por respeitares a minha agitação. Boa sorte por NY e aproveita ao máximo esta nova fase da tua vida.

Inês e Ana, parte essencial do grupo sem vocês tudo seria muito mais difícil. *Ana*, um especial obrigado por todo o teu apoio.

A special thanks to ***all at Cenix BioScience***.
Thank you for the exceptionable working environment, all the help and company outside the lab that has allowed me to enjoy Dresden.

Thank you to ***Geert-Jan Gemert*** and ***Robert Sauerwein*** for providing precious *P. berghei* infected mosquitoes.

Thank you to ***Jean-François Franetich*** and ***Dominique Mazier*** for the primary human hepatocytes and *P. falciparum* sporozoites.

Thank you to **Hans-Peter Vornlocher** from **Alnylam** for providing us the siRNAs and experimental protocol used in the RNAi *in vivo* experiments.

Muito obrigada a todos que constituem o **IMM** e o **IGC** e que tornam estes dois institutos locais excepcionais para se fazer investigação.
Um especial obrigada à **Unidade Patogénese Viral** no IMM com quem partilhámos o espaço, material e o dia-a-dia a fazer experiências e a todos os membros dos **grupos de Malária** no IGC por toda a ajuda.
Muito obrigada à **Alina** e **Dolores**, responsáveis pelo biotério do IMM e IGC. O vosso trabalho é essencial à realização e sucesso das nossas experiências *in vivo*. Obrigada pela vossa compreensão e ajuda em momentos em que os resultados são para ontem!

Muito obrigada à **Margarida Vigário** e **Moises Mallo**, membros do meu comité de tese no IGC, pelo apoio e discussão científica.

Obrigada à **Fundação para a Ciência e Tecnologia** pelo financiamento da minha bolsa doutoramento e por ter patrocinado a minha participação em encontros científicos internacionais.

À **Isa** e **Maf** muito obrigada pela vossa amizade e pelos bons momentos de lazer que foram indispensáveis para descomprimir. É sempre garantida muita diversão e muitas gargalhadas.

À **Vera**, apesar de estarmos em países diferentes, a tua presença nos bons e maus momentos foi uma constante durante estes anos de doutoramento. Através de um mail, um telefonema, uma viagem senti sempre o teu apoio e amizade. Á minha grande amiga ;)

À **Graça** e **Jorge Henriques** por me terem acolhido como parte integrante da vossa família. Todo o vosso apoio e carinho tem sido imprescendíveis. Muito obrigada!

Ao meu **mano David**, por estar sempre presente, pela sua contagiante boa-disposição, pelos seus sorrisos e carinho, pelo seu imenso apoio à nossa família, por toda a força e apoio e pelo teu exemplo de ambição e constante luta. Ao meu **pai Henrique** por me ter dado o possível e impossível, por todos os "patrocínios", pela sua visão sonhadora, a sua força de que basta querermos para sermos capazes, por me ensinar a nunca desistir e por todo o seu carinho. À minha **mãe Branca** por ter me ter transmitido os valores por que me guio, pela educação que me proporcionou e sempre acompanhou de perto, por valorizar o que sou e faço, por me apoiar em tudo e por todos os pequenos gestos que transmitem o seu amor por mim. Dou graças todos os dias por vos ter... Amo-vos muito!

E a ti, **Ricardo**... por viveres comigo todos os momentos que marcaram este projecto. Pela tua paciência, disponibilidade, compreensão, ajuda e força. Pela tua constante presença e disponibilidade para ouvir e me "guiar" durante os momentos complicados. Pelas tuas tentativas de me alegrares e por apoiares as minhas decisões. Por todo o teu amor... Que seria de mim sem ti... Amo-te! Te!!

Abstract

Malaria remains the most important parasitic infection in humans and one of the most prevalent infectious diseases worldwide. It is estimated that 350–500 million people become infected and one million of children under the age of five years die every year. This disease is caused by a protozoan parasite of the genus *Plasmodium* and is transmitted by mosquitoes of the genus *Anopheles*. During a malaria infection, the parasite undergoes intracellular development within two different host cells, hepatocytes and erythrocytes. The first stage of a malaria infection, the liver stage, is asymptomatic while the second phase, the blood stage, is responsible for all the disease-associated symptoms. Although clinically silent, the liver stage is an obligatory and extremely important step in *Plasmodium* life cycle. Therefore, understanding the parasite's requirements during this period is crucial for the development of any form of early intervention. Despite this awareness, the strategies developed by *Plasmodium* to allow its survival and development inside host liver cells remain poorly understood. We have sought to disclose some of these strategies through the identification of host factors which are important for hepatocyte infection by *Plasmodium*. For this purpose, RNA interference (RNAi) was extensively applied to an *in vitro* model of *Plasmodium* infection. The infection outcome of the rodent *P. berghei* parasite was addressed in the context of individual gene loss of function of a total of 830 different genes.

In chapter 2 of this thesis, it was studied the functional relevance of a selection of 50 genes differentially expressed by hepatocytes throughout *Plasmodium* infection, revealed by a microarray approach. Two host transcription factors, the Activating Transcription Factor 3 (Atf3) and the Myelocytomatosis oncogene (c-Myc), were recognized as important for sporozoite infection. It was observed that their individual silencing led, respectively, to an increase and to a decrease in *P. berghei* hepatocyte infection levels. In addition, Atf3's functional relevance was confirmed *in vivo*.

In chapter 3, the role of host kinases and kinase-interacting proteins was explored. From the 727 genes investigated at least six host kinases, namely the Met proto-oncogene (MET), Protein Kinase C iota (PKCι), Protein Kinase C zeta (PKCζ), WNK lysine deficient protein kinase 1 (PRKWNK1), Serum/Glucocorticoid Regulated Kinase 2 (SGK2) and Serine/Threonine Kinase 35 (STK35) were identified as playing important roles during *Plasmodium* sporozoite infection. Moreover, the importance of one of these kinases, PKCζ, was further demonstrated for *in vivo P. berghei* infection,

and also for human primary hepatocytes infection by *P. falciparum,* the deadliest of the human malaria parasites.

Finally, in chapter 4, the function of 53 host lipoprotein pathway genes was investigated and the Scavenger Receptor Class B member 1 (SR-BI) was identified as being crucially required for hepatocyte infection by *P. berghei*. In addition, SR-BI's importance in *Plasmodium* infection was also observed *in vivo* for *P. berghei* and *ex vivo* for *P. falciparum*. Further detailed analyses revealed that SR-BI is required for both sporozoite invasion and development within the hepatocyte.

Altogether, the work presented in this thesis reveals different host factors that play important roles during hepatocyte infection by *Plasmodium* sporozoites and, therefore, offers new insights into the processes underlying *Plasmodium* liver infection.

Resumo

A malária é uma das doenças infecciosas em humanos com maior prevalência em todo o mundo, sendo a mais importante de todas as doenças parasitárias. Esta doença afecta cerca de 40% da população mundial e estima-se que, todos os anos, entre 250 a 500 milhões de pessoas ficam infectadas e que morrem aproximadamente um milhão de crianças com menos de cinco anos. O parasita responsável por esta doença é um protozoário que pertence ao género *Plasmodium* e é transmitido por mosquitos do género *Anopheles*. O parasita humano *P. falciparum* provoca as formas mais severas da doença e é responsável pela maior parte das mortes por malária.

O parasita *Plasmodium,* no estadio de esporozoíto, após ter sido transmitido ao hospedeiro mamífero através da picada de um mosquito infectado, migra até ao fígado onde infecta hepatócitos. No interior dos hepatócitos, cada parasita replica-se e diferencia-se no estadio seguinte, em merozoítos. Estes são libertados na corrente sanguínea e infectam eritrócitos. Assim sendo, uma infecção de malária caracteriza-se pelo desenvolvimento intracelular do parasita em dois tipos de células hospedeiras, hepatócitos e eritrócitos. A primeira fase de uma infecção de malária, a fase hepática, é assintomática, enquanto que a segunda, a fase sanguínea, é responsável pelos sintomas associados à doença. Apesar do desenvolvimento de esporozoítos de *Plasmodium* em hepatócitos decorrer sem qualquer sintoma associado, a fase hepática é um passo importante devido à sua obrigatoriedade para o estabelecimento da infecção. Como tal, a compreensão das necessidades do parasita durante este período é fundamental para o desenvolvimento de qualquer tipo de intervenção precoce.

Apesar disso, as estratégias que o parasita *Plasmodium* desenvolveu para conseguir sobreviver e desenvolver-se no interior dos hepatócitos são ainda desconhecidas. O presente trabalho teve como objectivo revelar algumas destas estratégias através da identificação de factores do hospedeiro importantes para a infecção de hepatócitos pelo parasita *Plasmodium*. Para tal, recorreu-se a utilização da técnica conhecida por RNA de interferência (RNAi). Esta técnica baseia-se no mecanismo celular em que moléculas de RNA na forma de dupla cadeia silenciam o gene alvo através da degradação específica do seu RNA mensageiro. Deste modo, através da inserção em células de duplas cadeias de RNA é possível induzir especificamente o silenciamento do gene desejado e analisar o seu papel funcional ao nível de um determinado fenótipo. No presente trabalho aplicou-se a técnica RNAi a um modelo *in vitro* de infecção com *Plasmodium* e avaliou-se qual o efeito do silenciamento de genes

específicos em termos de infecção do parasita de ratinhos, *P. berghei.* Ao todo foram analisados 830 genes, de diferentes categorias, nomeadamente genes expressos ao longo de uma infecção por *Plasmodium*, genes que codificam cinases e proteínas associadas e ainda genes associados ao metabolismo de lipoproteínas. Estes estudos são apresentados como parte integrante da presente tese em três capítulos distintos de resultados.

No capítulo 2, foi estudada a relevância funcional de 50 genes que são expressos diferencialmente por hepatócitos ao longo de uma infecção por *Plasmodium*, genes que foram seleccionados a partir de um estudo anterior em que se utilizaram *microarrays*. Através da utilização de RNAi procedeu-se ao silenciamento individual de cada um dos 50 genes seleccionados e, após diferentes passos experimentais de confirmação, os factores de transcrição, *Activating Transcription Factor 3* (Atf3) e *Myelocytomatosis oncogene* (c-Myc), foram reconhecidos como sendo importantes para a infecção hepática por esporozoítos, dado que quando silenciados, a infecção com *P. berghei* aumenta e diminui, respectivamente. Adicionalmente, foi confirmada *in vivo* a relevância funcional para o factor de transcrição Atf3. Em ratinhos da estirpe BALB/c observou-se cinco horas depois da infecção com esporozoítos de *P. berghei* um aumento na quantidade de RNA mensageiro do gene *Atf3* ao nível do fígado. E ratinhos *Atf3 knock-out* quando infectados com esporozoítos de *P. berghei* apresentam um nível de infecção mais elevado que ratinhos controlo, sem qualquer deficiência ao nível da expressão do gene *Atf3*.

No capítulo 3, foi explorado o papel de um total de 727 cinases do hospedeiro ou proteínas que interagem com cinases. A relevância de cada gene foi estudada através do seu silenciamento individual com três *small interfering RNAs* (siRNAs), tendo sido realizadas três experiências de rastreio em que os genes candidatos foram seleccionados progressivamente de acordo com os resultados obtidos. Na última experiência, confirmou-se ainda o nível de silenciamento atingido, através da quantificação do nível de RNA mensageiro específico para uma das cinases identificadas como sendo potencialmente importante(s) para a infecção da linha celular de hepatócitos humanos (Huh7) por esporozoítos de *P. berghei*. No final, foram seis os genes de cinases para os quais se observou uma correlação entre o nível de silenciamento e um fenótipo em termos da infecção, mais especificamente *Met proto-oncogene* (MET), *Protein Kinase C iota* (PKCι), *Protein Kinase C zeta* (PKCζ), *WNK lysine deficient protein kinase 1* (PRKWNK1), *Serum/Glucocorticoid Regulated Kinase 2* (SGK2) e *Serine/Threonine Kinase 35* (STK35). Para as cinases MET, PKCζ, SGK2, PRKWNK1 e STK35 observou-se que o seu silenciamento está associado a uma redução ao nível de

células infectadas com *P. berghei*, enquanto que para a cinase PKCι observou-se que o seu silenciamento leva a um aumento do nível de células infectadas com *P. berghei*.

A importância de uma destas cinases, PKCζ, foi ainda explorada através da realização de experiências adicionais. O tratamento de células Huh7 *in vitro* com um inibidor para a cinase PKCζ, que funciona como um pseudo-substracto, teve como resultado uma redução no nível de infecção. Este resultado foi também observado *ex vivo* em hepatócitos primários de ratinhos da estirpe C57BL/6 e em hepatócitos primários humanos sujeitos ao tratamento com o inibidor da PKCζ, e que foram posteriormente infectados com esporozoítos do parasita *P. berghei* ou *P. falciparum*, respectivamente.

Através da realização de RNAi *in vivo* para a cinase PKCζ, em que se induziu uma redução da expressão desta cinase ao nível do fígado, foi demonstrado que esta cinase também desempenha um papel na infecção de malária *in vivo*, já que se observou uma significativa diminuição no nível de parasita no fígado. Todos estes resultados adicionais para a cinase PKCζ apoiam de certo modo a validade dos genes candidatos identificados através da utilização de RNAi, e demonstram também que esta cinase específica é importante para a infecção de *Plasmodium*.

Finalmente, no capítulo 4, foi investigada a função de 53 genes associados a vias metabólicas que envolvem lipoproteínas, e o receptor *Scavenger Receptor Class B member 1* (SR-BI) foi identificado como sendo fundamental para a infecção de hepatócitos por *P. berghei*. A relevância deste receptor para a infecção *in vitro* de *P. berghei* foi demonstrada através da realização de diferentes experiências em que se recorreu ao tratamento da linha celular Huh7 com diversos reagentes que permitiram silenciar o gene *SR-BI* ou bloquear a actividade do receptor SR-BI. O silenciamento do gene *SR-BI* foi realizado através da utilização de três siRNAs diferentes, e o nível de silenciamento obtido foi comprovado ao nível de RNA mensageiro e também ao nível da quantidade de proteína. Para bloquear a actividade de SR-BI recorreu-se a um anticorpo contra este receptor e a compostos que bloqueiam a actividade de transporte de lípidos (BLTs de *blocker lipid transport*) pelo receptor SR-BI. Em todas as experiências realizadas observou-se que o silenciamento ou bloqueio de SR-BI conduz a uma redução ao nível da infecção por *P. berghei*. O papel deste receptor na infecção de *P. berghei* foi confirmado em hepatócitos primários de ratinhos C57BL/6 sujeitos ao silenciamento de SR-BI ou ao bloqueio da sua actividade através do tratamento com o composto BLT-1 e ainda em experiências *in vivo,* em que ratinhos C57Bl/6 foram tratados por RNAi para induzir o silenciamento do gene SR-BI. Em todas estas experiências observou-se uma redução na infecção de *P. berghei*. A importância de SR-BI foi também observada em experiências *ex vivo* para o parasita *P. falciparum*. Uma análise extensiva revelou que o receptor SR-BI é necessário não só para a invasão dos

esporozoítos, mas também para o seu desenvolvimento no interior dos hepatócitos. O papel exacto que cada um dos factores do hospedeiro identificados desempenha na infecção de hepatócitos por *Plasmodium* tem ainda de ser determinado.

O trabalho apresentado nesta tese identifica já diferentes factores do hospedeiro que desempenham papéis importantes durante a infecção de hepatócitos por esporozoítos de *Plasmodium,* oferecendo assim uma nova perspectiva acerca dos processos que decorrem durante a fase hepática de uma infecção de malária.

Palavras Chave:

Malária, *Plasmodium,* fase hepática, factores do hospedeiro, RNA de interferência.

Abbreviations

A13009K04RIK	RIKEN cDNA A13009K04 gene
acLDL	acetylated low density lipoprotein
AMA-1	apical membrane antigen 1 protein
aPKCs	atypical protein kinase C
ApoA1	apolipoprotein A-I
ApoA1BP	apolipoprotein A-I binding protein
ApoE	apolipoprotein E
Atf2	activating transcription factor 2
Atf3	activating transcription factor 3
BLTs	blockers of lipid transport
Bst1	bone marrow stromal cell antigen 1
cAMP	cyclic adenosyl monophosphate
CD36	CD36 molecule
cDNA	complementary deoxyribonucleic acid
Cebpb	CCAAT/enhancer binding protein (C/EBP), beta
CelTOS	cell traversal protein for ookinete and sporozoite
c-Jun	Jun oncogene
c-Myc	myelocytomatosis oncogene
CO_2	carbon dioxide
CREB	cAMP-response-element-binding protein
cRNA	complementary ribonucleic acid
CSP	circumsporozoite protein
CTL	cytotoxic T-cell
DAPI	4'6-diamidino-2-phenylindole
DCs	dendritic cells
DDT	Dichloro-Diphenyl-Trichloroethane
DEPC	diethylpyrocarbonate
DMEM	Dulbecco's MEM medium
DMSO	dimethyl sulfoxide
dsRNA	double stranded RNA molecules
e.g.	*exempli gratia* (for example)
EBA 175	erythrocyte-binding antigen 175
EDTA	ethylenediamine tetraacetic acid
EEF	exoerythrocytic form
EGF	epidermal growth factor
EURYI	European Science Foundation Young Investigator Award
FACS	fluorescence activated cell sorting
FC	fold change
FCS	fetal calf serum

FCT	Fundação para a Ciência e Tecnologia
Fos	FBJ osteosarcome oncogene
gadd153/CHOP10	DNA-damage inducible transcript 3
GAS	genetically attenuated sporozoites
GFP	green fluorescent protein
GFP+	GFP-positive population
HCV	Hepatitis C virus
HDL	high density lipoprotein
HGF	hepatocyte growth factor
HPRT	hypoxanthine guanine phosphoribosyltransferase
Hsp70	heat shock protein 70
HSPGs	heparan sulphate proteoglycans
i.v.	intra-venous
IC_{50}	half maximal inhibitory concentration
ICAM-1	intercellular adhesion molecule 1
ICAM-2	intercellular adhesion molecule 2
IPA	ingenuity pathway software
ITNs	insecticide-treated bednets
JunB	Jun-B oncogene
Kif5c	kinesin family member 5C
KO	knock-out
LDL	low density lipoprotein
LDLR	low density lipoprotein receptor
L-FABP	liver-fatty acid binding protein
LPDS	lipoprotein-deficient serum
LRP	low density lipoprotein receptor-related protein
MET	met proto-oncogene
modLDL	modified forms of low density lipoprotein
mRNA	messenger RNA
MSR1	macrophage scavenger receptor 1
NCBI	national center for biotechnology information
NF-κB	nuclear factor kappa-B
op	osteopetrosis
oxLDL	oxidized low density lipoprotein
P.	*Plasmodium*
p.i.	post infection
PBS	phosphate buffered saline solution
pen/strep	penicillin/streptomycin
PFA	paraformaldehyde
PfEMP3	*Plasmodium falciparum* erythrocyte membrane protein 3
PK	protein kinase
PKC	protein kinase C
PKCζ	protein kinase C zeta

PKCι	protein kinase C iota
PKCζInh	PKCζ pseudo-substrate inhibitor
PL	phospholipase
PPLP1	*Plasmodium* perforin-like protein 1
PRKWNK1	WNK lysine deficient protein kinase 1
PV	parasitophorous vacuole
qRT-PCR	quantitative real-time polimerase chain reaction
RAS	radiation attenuated sporozoites
RNA	ribonucleic acid
RNAi	RNA interference
rRNA	ribosomal RNA
RT	room temperature
s.d.	standard deviation
SGK2	serum/glucocorticoid regulated kinase 2
siRNA	small interfering RNA
Slc7a11	solute carrier family 7, member 11
SPATR	secreted protein with altered thrombospondin repeat
SPECT	sporozoite microneme protein essential for cell traversal
spp.	species
SR-AI	scavenger receptor class A member 1
SR-AII	scavenger receptor class A member 2
SR-BI	scavenger receptor class B member 1
SR-BII	scavenger receptor class B member 2
Src	Rous sarcoma oncogene
STARP	sporozoite-threonine-asparagine-rich protein
STK35	serine/threonine kinase 35
Syn	syndecan
TNF	tumor necrosis factor
TRAP	thrombospondin related anonymous protein
TRSP	thrombospondin related sporozoite protein
TSR	thrombospondin motif
UIS	upregulated in infective sporozoites
UV	ultraviolet light
Zbtb20	zinc finger and BTB domain containing 20

Table of Contents

Chapter 1 | General Introduction

Chapter 1

1.1. Malaria: from ancient times to modern scientific discoveries

Malaria is one of the most important infectious diseases in the world, and its history dates back to ancient times. The characteristic periodic fevers of malaria are recorded from every civilized society from China in 2700 BC through the writings of Greek, Roman, Assyrian, Indian, Arabic, and European physicians up to the 19th century (Cox, 2002). The earliest detailed accounts are those of Hippocrates in his Book of Epidemics in the 5th century BC, and thereafter there are increasing numbers of references to the disease in Greece and Italy and throughout the Roman Empire (Sherman, 1998). Over this period, it became clear that malaria was associated with marshes, and there were many ingenious explanations to enlighten the disease in terms of the miasmas rising from the swamps (Cox, 2002). In fact the disease was initially called ague or marsh fever due to its association with swamps and only later, in 1740, was the term malaria coined from the italian *"mala aria"* meaning "bad air" (Bruce-Chuvatt, 1981).

Malaria scientific studies made their advance in the 19th century. The German Heinrich Meckel, in 1847, noted the presence of a brown pigment in the organs of people who died of fever and proposed that the pigment was the malaria cause (Bruce-Chuvatt, 1981). However, in 1880, it was the French Charles Louis Alphonse Laveran who associated malaria to a living organism when he observed the malaria parasite in a fresh blood specimen from patients with fever episodes. Laveran named these parasites *Oscillaria malariae* (Bruce-Chuvatt, 1981; Sherman, 1998). In 1907 Laveran was awarded the Nobel Prize for Physiology or Medicine for these discoveries [see http://nobelprize.org/nobel_prizes/medicine/laureates/ and (Nobel, 1967)]. In 1884, the Italians Ettore Marchiafava and Angelo Celli, with the help of microscopes with oil immersion lenses, were also able to observe the parasite development within the red blood cell, confirming Laveran's theory of a parasite. However, since the parasite they observed had no resemblance to the one described by Laveran, they named it as *Plasmodium malariae* (Sherman, 1998). The genus name *Plasmodium* of Marchiafava and Celli became the one chosen for the malaria parasite. The Italian Camillo Golgi, in 1886, established that there were at least two forms of the disease, one with tertian periodicity (fever every other day) and one with quartan periodicity (fever every third day). Golgi also noticed that the fever coincided with the rupture and release of new parasites into the blood stream (Sherman, 1998).

The malaria transmission mystery was solved independently by the British Ronald Ross and the Italians Giovanni Battista Grassi, Amico Bignami, and Giuseppe Bastianelli. In 1897, when studying malaria in birds, Ronald Ross described oocysts of

the malarial parasite in the walls of the stomach of an unclassified mosquito. Giovanni Battista Grassi and colleagues confirmed experimentally that the human malaria parasites go through the same stages as the bird parasites and are transmitted by mosquito bite. However, by the time the Italians began working in human malaria transmission, Ross's proof was complete and parts had already been published (Sherman, 1998; Capanna, 2006). Ross received the 1902 Nobel Prize in Medicine for his achievements [see http://nobelprize.org/nobel_prizes/medicine/laureates/ and (Nobel, 1967)]. For nearly 50 years, the life cycle in humans remained poorly understood as it was not known where the parasites, which could not be seen in the blood in the first days after infection, developed during this period. Finally, in 1947, Henry Shortt and Cyril Garnham showed that a phase of division in the liver preceded the development of parasites in the blood (Shortt and Garnham, 1948).

1.2. The malaria burden reality

The malaria burden is not evenly distributed since the global pattern of malarial transmission suggests a disease centered in the tropics, but with a reach into subtropical regions in five continents. As of 2004, 107 countries and territories were reported as exposed to malaria transmission (Figure 1.1) with 40% of the world total population at risk (WHO and UNICEF, 2005). Current estimates are that around 350–500 million clinical disease episodes occur annually, with about 90% of these occurring in sub-Saharan Africa. This inequality is due to the fact that the majority of infections in Africa are caused by *Plasmodium falciparum*, the most deadly of the human malaria parasites, and also because the *Anopheles gambiae* mosquito, the most effective malaria vector and difficult to control, is largely widespread in this continent. Malaria is thought to kill between 1.1 and 2.7 million people worldwide each year, about 1 million of which are children under the age of 5 years (WHO and UNICEF, 2000). These estimates render malaria the most pre-eminent tropical parasitic disease and one of the top three killers among communicable diseases. Moreover, malaria has also a major economic and social burden in endemic areas. Malaria endemic countries are not only poorer than non-malarious countries, but they also have lower rates of economic growth (Sachs and Malaney, 2002). The malaria burden falls disproportionately on poor and vulnerable individuals (Barat *et al.*, 2004).
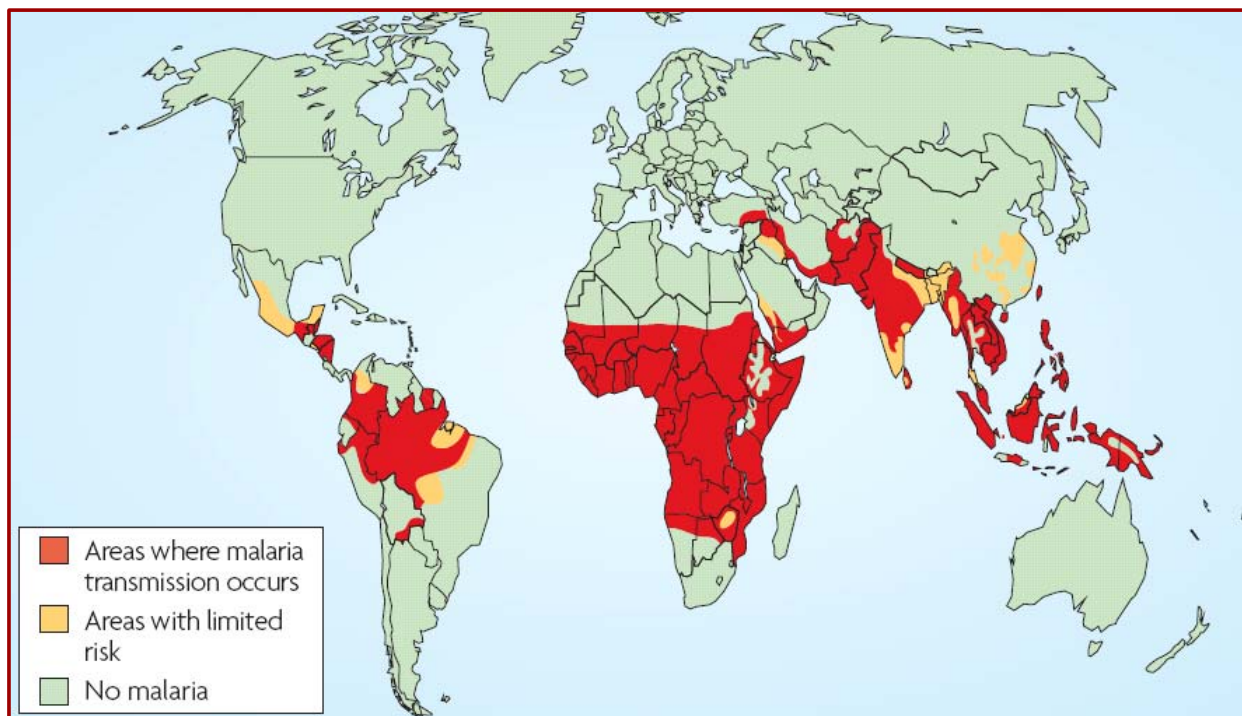
Figure 1.1 | Global distribution of malaria incidence in 2003.

Malaria is found in tropical regions throughout sub-Saharan Africa, Southeast Asia, the Pacific Islands, India, and Central and South America [adapted from (Todryk and Hill, 2007), with original data taken from World Malaria Report, WHO and UNICEF, 2005].

During the 20th century, the Global Malaria Eradication Programme attempted to reduce the malaria spread through vector control combined with improved access to treatment. The Programme's effort was able to reduce or eliminate malaria transmission but only in areas where transmission occurred at low intensity, such as the Americas, Asia, Europe and Transcaucasia. Recent evidence shows that the burden of malaria increased in several areas in terms of proportions of population at risk, of the severity of infections and of the number of deaths. Factors contributing to malaria increase consist of parasite resistance to the common used antimalarial drugs, breakdown of control programmes, complex emergencies, collapse of local primary health services and resistance of mosquito vectors to insecticides (WHO and UNICEF, 2005).

As consequence of the present malaria reality, a wide-ranging coalition of interests has been gathering to fight this disease, namely: the World Health Organization's "Roll Back Malaria" campaign, which aims at halving the burden of disease by 2010 in the participating countries through interventions that are adapted to local needs and by reinforcement of the health sector; pharmaceutical industry support; research coordination, with the main funding agencies coming together in the Multilateral Initiative on Malaria; and philanthropy, most notably the Malaria Vaccine Initiative

supported by the Bill and Melinda Gates Foundation (Nabarro and Tayler, 1998; WHO and UNICEF, 2000; Remme *et al.*, 2001; Carucci, 2004).

1.3. Overview of the *Plasmodium* life cycle

Plasmodium, the causative agent of malaria belongs to the *Apicomplexa* phylum. The *Apicomplexa* are named after their distinctive organelle, the apical complex, which plays a central role in cell invasion. Several other intracellular animal parasites belong to this phylum, for example *Cryptosporidium*, *Eimeria*, *Leishmania*, *Theileria*, and *Toxoplasma*.

The *Plasmodium* genus includes more than 100 species that infect a wide range of vertebrate hosts such as reptiles, birds, rodents, non-human primates and humans. Under natural conditions only four *Plasmodium* (*P.*) species can infect humans: *P. falciparum*, *P. vivax*, *P. ovale* and *P. malariae*. The first two species are responsible for most infections worldwide.

P. falciparum, most prevalent in Africa south of the Sahara and in certain areas of South-East Asia and the Western Pacific, is the agent of severe, potentially fatal malaria, causing around 1.1 - 2.7 million deaths annually, most of them in young children in Africa. The second most common species, *P. vivax*, found in Asia, Latin America and in some parts of Africa, can cause symptoms that are incapacitating and only exceptionally leads to death (often due to rupture of an enlarged spleen). *P. vivax* contributes substantially to malaria social and economic burden. *P. ovale* is found in West Africa and the islands of the western Pacific. *P. vivax* and *P. ovale* form resting stages in the liver, called "hypnozoites", which can reactivate leading to a clinical relapse several months or years after the infecting mosquito bite. *P. malariae*, found worldwide, produces long-lasting infections and if untreated can persist asymptomatically in the human host for lifetime [reviewed in (Despommier *et al.*, 2000)].

The *Plasmodium* life cycle comprises two different hosts, a mammalian and a female anopheline mosquito. The life cycle is rather complex and begins when a *Plasmodium* infected mosquito probes for a blood source under the skin of the mammalian host. During this process sporozoites, the parasite's designation at this stage, are deposited in the skin together with anticoagulant saliva that ensures an even flowing meal (Ponnudurai *et al.*, 1991; Matsuoka *et al.*, 2002). These sporozoites reach the circulatory system and are transported to the liver (Sidjanski and Vanderberg, 1997; Vanderberg and Frevert, 2004; Amino *et al.*, 2006). Once in the liver, sporozoites migrate through several hepatocytes by breaching their plasma membranes until they infect a final one

with the formation of a parasitophorous vacuole (PV) (Mota *et al.*, 2001a; Frevert *et al.*, 2005). After several days of development inside a hepatocyte, between 2 and 16 days depending on the *Plasmodium* species (spp.), 10000 to 30000 merozoites per invading sporozoite are released via budding of parasite-filled vesicles (merosomes) into the blood stream [reviewed in (Prudêncio *et al.*, 2006)]. Each released merozoite invades an erythrocyte, again with the formation of a PV, and undergoes a replication cycle that ends with the release of new 16 to 32 merozoites from the mature infected erythrocyte (schizont), which go on to infect other erythrocytes [reviewed in (Sturm and Heussler, 2007)]. This cyclic blood stage infection occurs with a periodicity of 48 to 72 hours, depending on the *Plasmodium* spp.. Malaria associated symptoms only occur during the blood stage of infection. Furthermore, some merozoites develop into sexual parasite stages, the male and female gametocytes (micro- and macro-gametocytes, respectively), which can be taken up when another female mosquito feeds off an infected mammalian host. The *Plasmodium* life cycle continues in the mosquito midgut, where the exflagellation of microgametocytes occurs and the macrogametocytes are fertilized. The resulting ookinete migrates through the mosquito midgut into the hemocele and develops into an oocyst, where sporozoites are formed. When the oocyst is fully matured it bursts and the released sporozoites migrate into the mosquito's salivary glands, where they become more infective and, therefore, ready for the next transmission step [reviewed in (Barillas-Mury and Kumar, 2005; Matuschewski, 2006; Vlachou *et al.*, 2006)] (Figure 1.2).
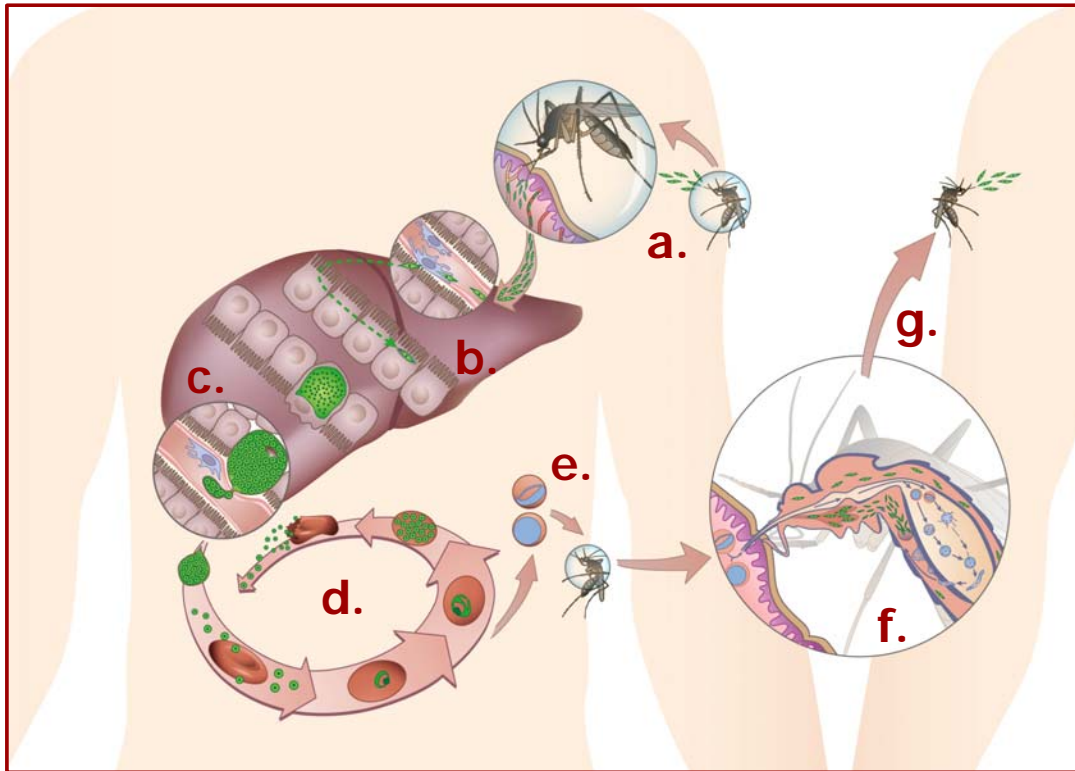
Figure 1.2 | *Plasmodium* **life cycle in the human and mosquito hosts.**
(a.) The parasite's life cycle in the human host begins when sporozoites are inoculated into the host's skin through the bite of an infected female *Anopheles* mosquito. The sporozoites are rapidly transported to the liver as soon as they reach the blood stream. **(b.)** In the liver sporozoites migrate through several hepatocytes before infection of a final host cell with the formation of a parasitophorous vacuole. **(c.)** The liver schizonts, named exoerythrocytic forms (EEFs), proliferate and differentiate into thousands of merozoites that will ultimately be released through merosomes into the blood stream. **(d.)** Each merozoite will recognize, bind to, and invade an erythrocyte, initiating a replication cycle that ends with the release of new merozoites. **(e.)** Some merozoites develop sexual parasite morphologies (male and female gametocytes), which can be ingested by a mosquito during a blood meal. **(f.)** Once in the mosquito midgut, the parasite undergoes a series of transformations, culminating in the development of new sporozoites that invade the salivary glands and **(g.)** consequently can be inoculated into another host .

1.4. A glimpse at the malaria clinical features and pathogenesis

Malaria infection manifestations include a wide variety of symptoms, ranging from absent or very mild symptoms to severe disease and even death. Symptoms and signs of uncomplicated malaria comprise sensation of cold, shivering, fever, headaches, vomiting, sweats and tiredness. Severe malaria manifestations include metabolic acidosis which leads to respiratory distress, severe anemia, thrombocytopenia (blood platelets decrease), organ failure, cerebral malaria (impairment of consciousness, seizures, coma, or other neurological abnormalities) and placental malaria in pregnant

women. Overall patterns of disease depend markedly on the age and the previous immunological experience of the host [reviewed in (Greenwood *et al.*, 2005; Schofield and Grau, 2005)]. The multiplicity of severe malaria syndromes has confounded the identification of unifying mechanisms of the disease. Research studies support the idea that these several syndromes arise from the intersection of a few basic processes: rapid expansion of infected erythrocytic mass; destruction of both infected and uninfected erythrocytes; adhesion and sequestration of infected erythrocytes in the vasculature; release of bioactive parasite products in host tissues molecules; local and systemic production of cytokines and chemokines by the innate and adaptive immune systems in response; and activation, recruitment and infiltration of inflammatory cells (Table 1.1) [reviewed in (Malaguarnera and Musumeci, 2002; Clark and Cowden, 2003; Rasti *et al.*, 2004; Hisaeda *et al.*, 2005; Schofield and Grau, 2005; Boutlis *et al.*, 2006)]. Over the last few years, significant progress has been made towards the identification of both parasite and host molecules that actively participate in these processes. This is particularly important because understanding the biology associated with the malaria disease is an essential key for the development of successful tools for intervention.

Syndrome	Clinical features	Possible sequence or mechanism of disease
Cerebral malaria	Sustained impaired consciousness, coma, long-term neurological sequelae	Cerebral parasite sequestration; bioactive GPI; pro-inflammatory cytokine cascade; endothelial-cell activation; natural killer T-cell activation; T_H1/T_H2-cell balance; chemokine production; monocyte, macrophage and neutrophil recruitment; platelet and fibrinogen deposition; $CD4^+$, $CD8^+$ and $\gamma\delta$ T-cell involvement; IFN-γ production; neurological metabolic derangements; possibly hypoxia
Placental malaria	Placental insufficiency, low birth weight, premature delivery, loss of fetus	*Plasmodium falciparum* EMP1-mediated binding to placental endothelium and syncytiotrophoblast through chondroitin sulphate A and hyaluronic acid; cytokine production; chemokine-mediated recruitment and infiltration of monocytes; intravascular macrophage differentiation
Severe malarial anaemia	Pallor, lethargy, haemoglobin level of 4–6 g per 10 ml	Erythropoietic suppression by toxins and cytokines; increased RBC destruction, owing to parasitization, RBC alterations, complement and immune complex or antigen deposition, erythrophagocytosis, splenic hyperphagism, $CD4^+$ T cells, T_H1/T_H2 cytokine balance (TNF and IFN-γ versus IL-10)
Metabolic acidosis	Respiratory distress, deep breathing (Kussmaul breathing), hypovolaemia	Molecular mechanisms unknown. Possibly widespread parasite sequestration; bioactive toxins; increased vascular permeability; reduced tissue perfusion; anaemia; pulmonary airway obstruction; hypoxia; increased host glycolysis; repressed gluconeogenesis. Some overlap with shock-like syndrome
Shock-like syndrome (systemic inflammatory-response-like syndrome)	Shock, haemodynamic changes, impaired organ perfusion, disseminated intravascular coagulation	Bioactive toxins; T_H1 cytokines; acute-phase reactants

EMP1, erythrocyte membrane protein 1; GPI, glycosylphosphatidylinositol; IFN-γ, interferon-γ; IL-10, interleukin-10; RBC, red blood cell; T_H, T helper; TNF, tumour-necrosis factor.

Table 1.1 | Severe malaria clinical features and underlying mechanisms.
Severe malaria comprises a variety of diverse syndromes that present singular and distinguishing clinical features. The comprehension of the mechanisms that lead to the development of each syndrome constitutes a leading area of malaria research. A remarkable knowledge has been achieved, however there is still a great deal to be understood [adapted from (Schofield and Grau, 2005)].

1.5. The fight against malaria: available tools

1.5.1. Anti-malarial tools: the present

Currently, the fight against malaria is focused on mosquito eradication, reduction of human–vector contact and disease prevention and treatment using antimalarial drugs. A viable vaccine is not yet available, despite the significant efforts that have been made to develop one.

Mosquito eradication is mainly achieved through indoor residual spraying and environmental management to eliminate breeding sites. Global control efforts from the 1950s to the 1970s, mainly through the use of the insecticide Dichloro-Diphenyl-Trichloroethane (DDT), virtually eliminated malaria transmission in the subtropics (Greenwood *et al.*, 2005). However, the programme was abandoned due to the negative impact of the use of high concentrations of DDT, namely resistence developed by mosquitoes and toxic effects to humans (Turusov *et al.*, 2002). A deeper reason for abandoning the campaign might have been geopolitical (Sachs, 2002). Despite attempts to ban DDT completely, the use of small amounts of DDT (allowed under the Stockholm Convention on persistent organic pollutants) still plays a major role in malaria control (Schapira, 2004; Greenwood *et al.*, 2005). A new and alternative approach, the deployment of mosquito-killing fungi, has been recently shown as possible (Blanford *et al.*, 2005; Scholte *et al.*, 2005) and has been extensively discussed [see (Michalakis and Renaud, 2005; Kanzok and Jacobs-Lorena, 2006; Thomas and Read, 2007)]. Although vector control strategy is very effective in reducing malaria in some regions of Africa, it is also expensive, logistically demanding and has been undermined by problems of insecticide resistance, environmental contamination and risks to human health.

Reduction of human–vector contact is achieved through insecticide-treated bed nets (ITNs) and is more appropriate for malaria control in Africa (Klausner and Alonso, 2004). Randomized trials of the ITNs in diverse settings have established their effectiveness at cutting malaria-related morbidity and mortality (Lengeler, 2000). Nonetheless, though ITNs are inexpensive and effective, fewer than 2% of Africans sleep under them, which means that considerable campaigns to increase their use are urgently required (Monasch *et al.*, 2004). Furthermore, the regular ITN re-treatment with insecticide has proved difficult to sustain on a large scale. However, this might be overcome by the development of long lasting insecticidal ITNs and in fact different prototypes are being produced and two have already been approved by the WHO and are undergoing large-scale production (WHO and UNICEF, 2004).

Antimalarial drugs have been quite essential in the combat against malaria, but parasite resistance problems are arising. The used antimalarials are quinolines (amodiaquine, piperaquine, primaquine, quinine, mefloquine and chloroquine), antifolate drugs (pyrimethamine, chloroguanide, sulfadoxine, sulfalene and dapsone), artemisinins and derivatives (artemether, arteether, artesunate and dihydroartemisinin), atoquavone, and antibiotics (such as, tetracycline, doxycycline, and clindamycin) [reviewed in (Cunha-Rodrigues *et al.*, 2006b; Schlitzer, 2007; Vangapandu *et al.*, 2007)]. The choice of the drug to use is usually driven by what drugs the parasites in the area are resistant to, as well as their side-effects. To counteract the rapid development of resistance some drugs are used in fixed combinations [reviewed in (Fidock *et al.*, 2004)].

The increasingly serious problem of malaria parasite resistance to the currently used antimalarials discloses the urgent need to develop new and effective antimalarial molecules. This goal can be achieved in two ways: either by focusing on validated targets in order to generate new drug candidates or by identifying new potential targets for malaria chemotherapy [see (Jana and Paliwal, 2007)].

1.5.2. Anti-malarial tools: the future

Sadly, the available tools against malaria mentioned above provide no strategy to sustainably reduce or eliminate the burden of malarial disease. A vaccine against malaria could lead the way given that this has been the most cost-effective health intervention for a range of other infectious diseases. However, despite the extensive research that is developed in this area, there is still no vaccine available. Malaria vaccine research has focused on different approaches: an anti-infection vaccine aimed at protecting malaria-naive travelers or residents of low endemic areas from becoming infected; an anti-disease/anti-mortality vaccine aimed at children, pregnant women and migrants living in endemic areas; and an anti-mosquito-stage vaccine aimed at preventing the transmission of malaria from one person to another. Different pre-erythrocytic, blood stage, and transmission-blocking vaccines are the focus of ongoing research [reviewed in (Richie and Saul, 2002; Moorthy *et al.*, 2004; Todryk and Hill, 2007)]. The currently most advanced malaria vaccine candidate in development is the pre-erythrocytic RTS,S/AS02A [state of the art addressed in (Alonso, 2006; Hill, 2006)]. RTS,S/AS02A comprises a hybrid molecule in which the circumsporozoite protein of *P. falciparum* is expressed with hepatitis B surface antigen in yeast (Stoute *et al.*, 1997). This is the only vaccine candidate shown in field trials to prevent malaria and, in one instance, to limit disease severity. RTS,S/AS02A has provided substantial, short-lived protection in volunteers, exposed experimentally to bites by infected

11

mosquitoes (Kester *et al.*, 2001), and substantial (71%) but only short-term protection in naturally exposed, semi-immune adults from The Gambia (Bojang *et al.*, 2001). In a subsequent trial in Mozambican children, RTS,S/AS02A gave 30% protection against the first clinical episode of malaria and 58% protection against severe malaria (Alonso *et al.*, 2004).

Another approach for malaria control focuses on the development of transgenic or genetically modified genetic mosquitoes in order to convert them into inefficient parasite vectors (Moreira *et al.*, 2002; Marrelli *et al.*, 2006; Marrelli *et al.*, 2007).

In addition, the availability of genome sequences, such as the ones from the three most relevant organisms to malaria, *Homo sapiens* (Nature, 2001; Science, 2001), *Anopheles gambiae* (Holt *et al.*, 2002) and *Plasmodium falciparum* (Gardner *et al.*, 2002), together with bioinformatics tools and high-throughput technologies (microarrays, RNA interference, proteomics) will ultimately provide an integrated picture of the parasite biology and malaria pathogenesis and hopefully facilitate the development of the existing and new approaches [see (Hoffman *et al.*, 2002; Ghosh *et al.*, 2003; Carucci, 2004; Johnson *et al.*, 2004)].

1.6. A close look at the pre-erythrocytic stage

Although the clinical symptoms only appear during the erythrocytic stage of *Plasmodium*'s life cycle it should not be disregarded that the asymptomatically pre-erythrocytic stage (also referred to as liver stage) is essential for the malaria infection outcome. During this stage *Plasmodium* develops inside hepatocytes and there is an amazing parasite multiplication. Still, relatively little knowledge exists on *Plasmodium*-hepatocytes interactions, which is due to the fact that the blood stage, being the pathogenic stage of the parasite's life cycle, has soon attracted much more attention than the asymptomatic liver stage. Also, large and detailed studies of liver stage development are difficult because of the prerequisite of freshly extracted infectious sporozoites (breeding of infectious mosquitoes is a necessity) and to the low infection rates obtained *in vitro* (Prudêncio et al., 2007) and *in vivo* (Heussler *et al.*, 2006). Despite these restrictions, malaria researchers have been working towards an understanding of the biology behind the malaria liver stage and, during this journey, huge steps have been made to disclose the processes involved in this stage.

1.6.1. *Plasmodium* models for liver stage research

Liver stage research of human malaria is not feasible *in vivo*, therefore, several studies have successfully accessed the complete development of hepatic stages of human

Plasmodium sps. in human primary hepatocytes (Mazier *et al.*, 1984; Smith *et al.*, 1984; Mazier *et al.*, 1985; Mazier *et al.*, 1987). Still, these are technically challenging because they do not grow continuously in culture and, consequently, their availability is dependent on often scarce and unpredictable material. Thus, several studies have focused on the development of model systems using human hepatocyte cell lines (Uni *et al.*, 1985; Calvo-Calle *et al.*, 1994; Karnasuta *et al.*, 1995; Sattabongkot *et al.*, 2006). Initially, *P. vivax* and *P. falciparum* development *in vitro* was shown to be possible, although in different cell lines. Complete liver stage development for *P. vivax* was shown in HepG2-A16 cells (Uni *et al.*, 1985) while *P. falciparum* liver stage growth was achieved in Huh1 cells (Calvo-Calle *et al.*, 1994) as well as HHS-102 cells (Karnasuta *et al.*, 1995). Only recently has a human hepatocyte cell line, HC-04, been shown to support the complete liver stage development of both *P. vivax* and *P. falciparum* (Sattabongkot *et al.*, 2006). The main advantage of this cell line over the ones previously mentioned is the fact that it allows the development of the two most prevalent human malaria parasites with greatly improved infection rates. In addition, mouse models with humanized livers have been shown to represent a promising new tool for *P. falciparum in vivo* studies (Morosan *et al.*, 2006; Sacci *et al.*, 2006). These recent developments are extremely important because they might finally bring new avenues to human malaria liver stage research. Nevertheless, it should not be disregarded that human malaria research also requires the production and handling of human malaria parasite infectious mosquitoes, which involves very controlled conditions.

As a result of the difficulties mentioned above, liver stage malaria research progress has been achieved through the use of rodent *Plasmodium* spp., in particular *P. berghei* and *P. yoelii*. These parasites are established as well-suited models for *Plasmodium* pre-erythrocytic stage biology, immunology and vaccine development (Hafalla *et al.*, 2006; Prudêncio *et al.*, 2006). *P. berghei* and *P. yoelii* share more than 90% genome identity (Kooij *et al.*, 2005). Although the *P. yoelii* model is generally thought to reflect human malaria better than the *P. berghei* model (Calvo-Calle *et al.*, 1994; Doolan and Hoffman, 2000; Mota *et al.*, 2001b), the latter is the most widely used because the technologies to enable its transfection were developed earlier (van Dijk *et al.*, 1996) than for *P. yoelii* (Mota *et al.*, 2001b; Jongco *et al.*, 2006). Moreover, green or red fluorescent protein-tagged parasites have been developed first for *P. berghei* (Natarajan *et al.*, 2001; Franke-Fayard *et al.*, 2004; Frevert *et al.*, 2005) and these have already allowed extensive *in vivo* studies focused in sporozoite transmission by mosquito bite (Frischknecht *et al.*, 2004), its subsequent journey from the skin to the liver (Vanderberg and Frevert, 2004; Frevert *et al.*, 2005; Amino *et al.*, 2006) and liver stage

development (Sturm *et al.*, 2006). Only recently were GFP-tagged *P. yoelii* parasites developed (Tarun *et al.*, 2006; Ono *et al.*, 2007) and used for *in vivo* liver stage studies (Tarun *et al.*, 2006).

Both *P. berghei* and *P. yoelii* are able to infect primary mouse hepatocytes (Meis *et al.*, 1984; Millet *et al.*, 1985; Davies *et al.*, 1989; Long *et al.*, 1989) and these cells have often been used in liver stage research. However, since primary cells have to be freshly prepared and can only be maintained in culture for a short period of time, established cell lines have been more widely used. Cell lines, easily maintained in culture through several passages, constitute an extremely important tool that provides useful information to be subsequently tested *ex vivo* and/or *in vivo*.

The hepatoma cell lines that present a relatively high level of infectivity for *P. berghei* and *P. yoelii* and, therefore, are widely used in *in vitro* studies are the human hepatoma cell lines, HepG2 and Huh7 (Aikawa *et al.*, 1984; Calvo-Calle *et al.*, 1994) and the murine hepatoma cell line, Hepa1-6 (Mota and Rodriguez, 2000). *P. berghei* is known to be more promiscuous than *P. yoelii*, since the former is able to efficiently infect both the human and the murine hepatoma cell lines (Aikawa *et al.*, 1984; Calvo-Calle *et al.*, 1994; Mota and Rodriguez, 2000) whereas the latter only infects the murine Hepa1-6 cells efficiently (Mota and Rodriguez, 2000). *P. berghei* sporozoite invasion and exoerythrocytic forms (EEFs) development has also been observed in some non-hepatic cell lines, namely the human lung cell line WI38 (Hollingdale *et al.*, 1981; Hollingdale *et al.*, 1983) and the human epithelial cells HeLa (Calvo-Calle *et al.*, 1994). Additionally, it has been shown that *P. berghei* and *P. yoelii* sporozoites incubated, without any host cells, at 37º C in the presence of serum develop into early EEFs (Kaiser *et al.*, 2003; Wang *et al.*, 2004). Although at the morphological level axenically cultured EEFs are indistinguishable from those that develop within hepatocytes, intracellular residence is essential for parasite's further growth.

P. berghei and *P. yoelii* display different infection efficiencies *in vitro* and *in vivo*. There is an inverse relationship between the two species in their *in vitro* and *in vivo* infection rates. *P. yoelii* infection rate is high *in vivo* but low *in vitro*, whereas *P. berghei* stands in the opposite situation with the highest infection rate of malaria models *in vitro*, both in primary hepatocytes and hepatoma cell lines, and comparatively low *in vivo* success in mice (Khan and Vanderberg, 1991; Briones *et al.*, 1996; Druilhe *et al.*, 1998). Moreover, *P. berghei* and *P. yoelii* infectivity differences *in vivo* not only depend on the parasite but also on the clone and the genetic background of the rodent host (Jaffe *et al.*, 1990; Scheller *et al.*, 1994; Belmonte *et al.*, 2003). All these aspects should be considered while extrapolating results obtained with the different experimental models.

1.6.2. Introducing the *Plasmodium* sporozoite

The invasive *Plasmodium* stage that is transmitted by mosquitoes and is responsible for initiating the infection in the vertebrate host is called sporozoite and it is distinguished by specific features. Sporozoites are small unicellular organisms, about 10 µm long and 1 µm wide. At the anterior cell pole, they possess the apical polar ring, which serves as a microtubule-organizing center, and a unique set of secretory organelles, termed micronemes and rhoptries, that belong to the apical complex. Micronemes are small vesicles of varying electron density while rhoptries are large, usually paired, pear-shaped organelles. Both these organelles discharge at the anterior pole and their contents are involved in the three basic types of tissue interaction in the mammalian host cell environment: gliding motility (a substrate-dependent form of locomotion), migration through cells by membrane rupture wounding and invasion of the host cell with the formation of a PV. The micronemes, rhoptries and also dense granules (microspheres of approximately 200 nm in diameter) are characteristic organelles of other invasive forms of apicomplexa parasites. Interestingly, dense granules have not yet been observed for the sporozoite invasive form. Another unique organelle of the sporozoite is the inner membrane complex, a flattened vesicle underneath the cell membrane that is associated with a set of subpellicular microtubules. An actin-myosin motor essential for sporozoite motility and invasion is located in the narrow space between the plasma membrane and the outer membrane of the inner membrane complex [reviewed in (Kappe *et al.*, 2004)] (Figure 1.3). The *Plasmodium* sporozoite's features outlined above are essential for sporozoite expedition to the liver's host cell.
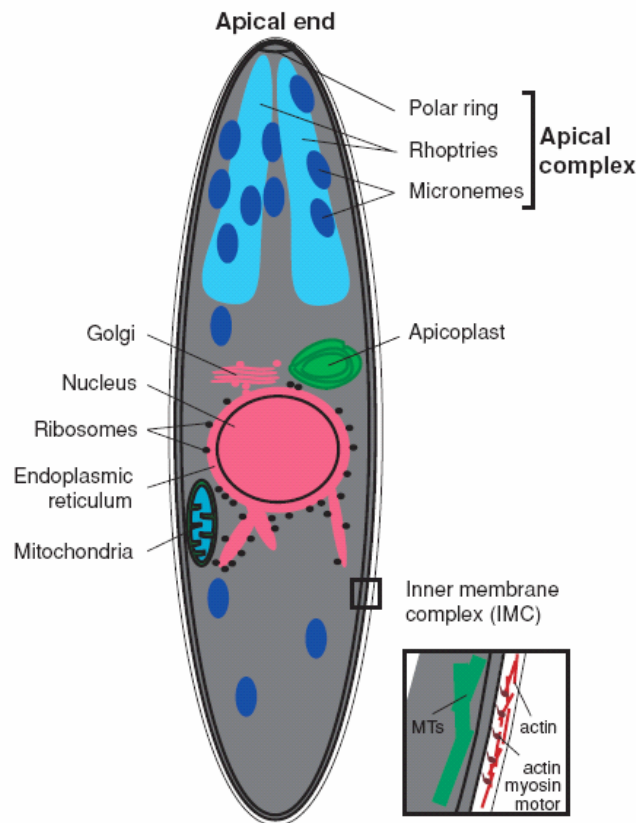
Figure 1.3 | The *Plasmodium* sporozoite.

Schematic representation of a *Plasmodium* sporozoite, showing some of its organelles and subcellular structures. At the anterior cell pole is positioned the apical complex which is formed by the apical polar ring and the secretory organelles, micronemes and rhoptries. Underneath the sporozoite's cell membrane is the inner membrane complex with an actin-myosin motor and associated to subpellicular microtubules [adapted from (Kappe *et al.*, 2004)].

1.6.3. The sporozoite journey from the skin to the liver

Malaria transmission takes place when an infected mosquito bites a mammalian host while probing for a blood source under the skin (Matsuoka *et al.*, 2002). During the mosquito bite saliva containing sporozoites, vasodilators and anticoagulants is released (Griffiths and Gordon, 1952). Although mosquitoes can harbor thousands of sporozoites in their salivary glands, the number of sporozoites delivered in each bite rarely exceeds 200 and most estimates from experimental infections record numbers around 20 (Vanderberg, 1977; Rosenberg *et al.*, 1990; Ponnudurai *et al.*, 1991; Rosenberg, 1992). Recently, 2 different studies (Frischknecht *et al.*, 2004; Medica and Sinnis, 2005) report higher numbers (sporozoite means 114 and 123, respectively). Nevertheless, considering the total number of sporozoites present in the salivary glands the number of sporozoites injected is quite low.

Sporozoites are deposited into the skin (Sidjanski and Vanderberg, 1997; Amino *et al.*, 2006), where they migrate for at least 30 min (Vanderberg and Frevert, 2004; Amino *et al.*, 2006). Recently, a study using quantitative Real-Time Polimerase Chain Reaction (qRT-PCR) has determined the kinetics with which *P. yoelii* sporozoites leave the injection site and arrive in the liver and has shown that the majority of infective sporozoites can remain in the skin for hours (Yamauchi *et al.*, 2007). A sporozoite surface phospholipase (PL) was shown to be required for host cell membrane breaching during migration in the skin (Bhanot *et al.*, 2005). Sporozoites migrate extensively through the avascular dermis until they reach a vessel and enter the circulatory system, which transports them into the liver. It has been proposed that sporozoites may also travel using the lymphatic system (Vaughan *et al.*, 1999; Krettli and Dantas, 2000). Intravital microscopy observations have showed that within 1 hour after *P. berghei* injection a proportion of sporozoites invades blood vessels and gets carried away by the blood flow, whereas others actively enter lymph vessels or remain in the skin after exhaustion of their motility (Amino *et al.*, 2006) (Figure 1.4).
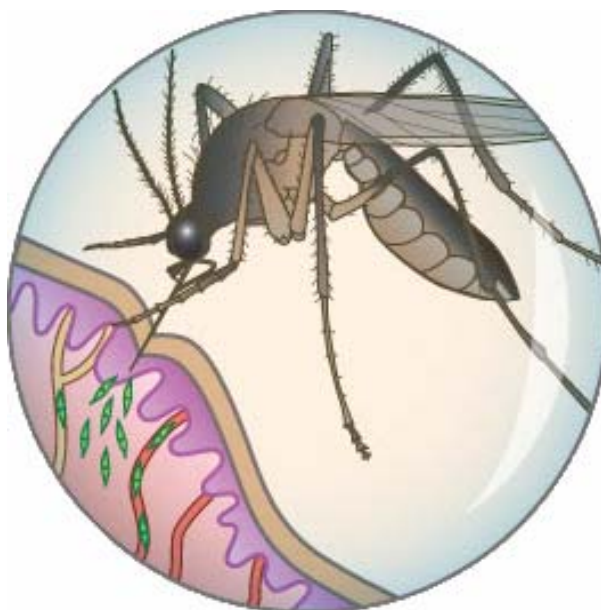
Figure 1.4 | *Plasmodium* sporozoites are deposited in the skin and enter the circulatory and lymphatic systems.

Sporozoites (in green) are placed under the skin of the mammalian host while an infected female *Anopheles* mosquito probes for a blood meal. Sporozoites migrate in the skin until they come into contact with a blood vessel (in red) and enter the circulatory system, being then transported into the liver. A small proportion of sporozoites can enter the lymphatic system (in yellow). Adapted from the *Plasmodium*'s life cycle presented on Figure 1.2.

Most of the sporozoites that enter the lymphatic vessels do not reach the circulatory system; instead, they are trapped in the lymph nodes. Some of these sporozoites

partially develop into small-sized EEFs before eventually being degraded (Amino *et al.*, 2006). The relevance of presence of parasites in such an important organ of the immune system has been under investigation by Chakravaraty and Zavala. It has been observed a sporozoite-specific cytotoxic T-cell (CTL) response in the draining lymph node just 2 days after intradermal immunization with irradiated sporozoites. When the draining lymph node was surgically ablated to prevent early local priming, the number of sporozoite-specific CTLs in the liver was significantly reduced, highlighting the importance of skin-draining lymph nodes in the initiation of the immune response to sporozoites during natural infection [Chakravaraty and Zavala, unpublished data referenced in (Sinnis and Coppi, 2007)].

1.6.4. Sporozoite arrest in the liver

Once in the circulatory system, sporozoites are rapidly arrested in the liver. Sporozoites are found in hepatocytes within 2 minutes after intravenous injection into rats (Shin *et al.*, 1982). The speed and selectivity of this process suggests specific interactions between parasite surface protein(s) and host molecule(s).

The major surface protein of *Plasmodium* sporozoites, the circumsporozoite protein (CSP), appears to have an essential role by interacting with the heparan sulphate proteoglycans (HSPGs) of liver cells. It has been reported that recombinant CSP binds specifically to HSPGs from the basolateral cell surface of hepatocytes in the Disse space (region that separates the sinusoidal endothelium from hepatocytes) and that this interaction occurs between the CSP's conserved I and II-plus regions and heparin-like oligosaccharides and/or heparan sulfate (Cerami *et al.*, 1992; Pancake *et al.*, 1992; Frevert *et al.*, 1993; Cerami *et al.*, 1994; Sinnis *et al.*, 1994; Rathore *et al.*, 2002; Ancsin and Kisilevsky, 2004). Although HSPGs are present in most tissues, liver HSPGs are known to be more highly sulphated than those in other tissues (Lyon *et al.*, 1994). This feature has been proposed to be responsible for the selective recognition of recombinant CSP and *Plasmodium* sporozoites in the liver (Ying *et al.*, 1997; Pinzon-Ortiz *et al.*, 2001).

Between the blood and hepatocytes there is a layer of liver endothelial cells that have open fenestrations which allow direct contact between the circulation and the space of Disse (Wisse *et al.*, 1985). Lipoproteins, because of their small size (90 nm of diameter), are able to freely diffuse through the endothelial fenestrations and access directly the space of Disse while sporozoites cannot due to their larger size (1µm). It has been proposed that hepatocyte HSPGs may extend through endothelial fenestrations to the lumen of blood vessels where they would sequester sporozoites (Sinnis *et al.*, 1996). More recently, it has been shown that CSP and another parasite protein,

thrombospondin-related anonymous protein (TRAP), recognize HSPGs, not only on hepatocytes, but also on Kupffer cells (resident macrophages of the liver) and stellate cells (highly branched fat-storing cells that embrace the sinusoids from within the Disse space) (Pradel *et al.*, 2002). Stellate cells synthesize eight times more sulphated HSPGs than hepatocytes and incorporate twice the amount of sulphate into heparan sulphate (Gressner and Schafer, 1989). Therefore, it has been suggested that *Plasmodium* sporozoites initial arrest in the liver sinusoids (blood vessels in the periphery of the liver lobules) is mediated by matrix HSPGs that are produced by stellate cells and protrude through the endothelial fenestrations (Pradel *et al.*, 2002, , 2004) (Figure 1.5).
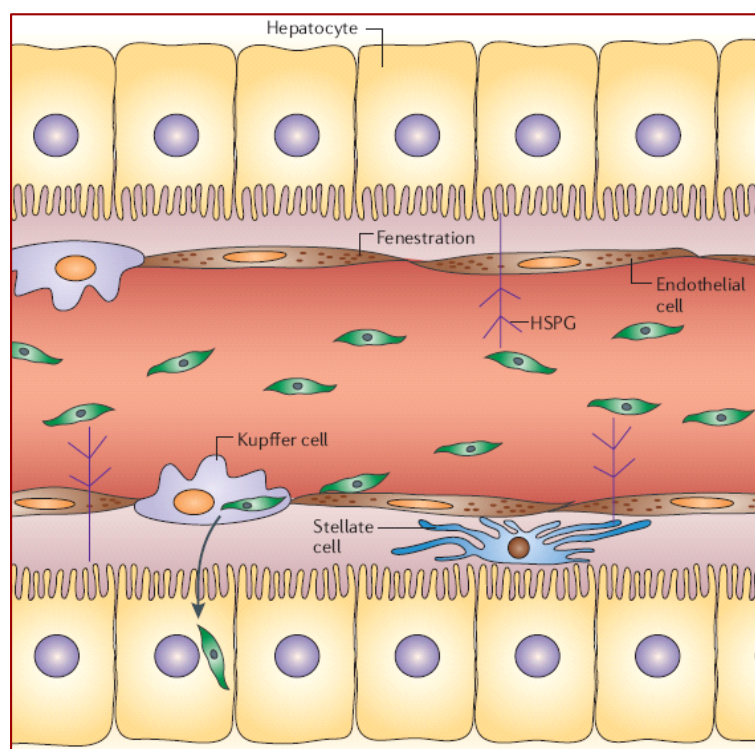
Figure 1.5 | *Plasmodium* sporozoite arrest in the liver.
Sporozoites (in green) reach the liver sinusoids, where they are arrested due to interactions with heparan sulphate proteoglycans (HSPGs) from hepatocyte and stellate cells [adapted from (Prudêncio *et al.*, 2006)].

In addition, it has also been proposed that the highly selective sporozoite arrest in the liver involves at least two different cell surface receptors, a highly sulfated HSPG that associates with CSP region I-plus together with another receptor that would bound to CSP region II-plus (Ancsin and Kisilevsky, 2004). A similar co-receptor strategy is employed by the fibroblast growth factor (HSPG + tyrosine kinase receptor) (Rapraeger *et al.*, 1991; Yayon *et al.*, 1991) and Apolipoprotein E (ApoE) containing lipoproteins [HSPG + low density lipoprotein receptor (LDLR) or low density

lipoprotein receptor-related protein (LRP)] (Willnow *et al.*, 1994; Rohlmann *et al.*, 1998). In fact, malarial sporozoites may be using an existing host lipoprotein clearance pathway since lipoproteins (such as chylomicrons, very low lipoprotein and low density lipoprotein) are removed from circulation by binding to liver-specific HSPG in the space of Disse (Herz *et al.*, 1995; Ji *et al.*, 1995) and recombinant *P. falciparum* CSP can compete with lipoproteins for binding and clearance (Sinnis *et al.*, 1996). High affinity binding between CSP and LRP has been reported and shown to be inhibited using a LRP specific blocker (Shakibaei and Frevert, 1996). However, when another study demonstrated that LRP-deficient hepatocytes *in vivo* and LRP-null cells *in vitro* showed an infection efficiency equal to controls (Marshall *et al.*, 2000) it was considered that LRP and HSPGs may not function in a coordinated fashion during sporozoite entry, as in remnant lipoprotein metabolism, but instead may be used as alternate binding sites during sporozoite passage to the liver.

The identity of the liver HSPG receptor remains elusive. Possible candidates are members of the syndecan family, a major class of vertebrate membrane-bound proteoglycans (Couchman, 2003). The multi-functional cell surface co-receptors Syndecans-1, -2, -3 and -4 (Syn-1, -2, -3 and -4) are type 1 transmembrane proteins expressed in a wide variety of tissues. Syn-1 and -2 are considered as possible candidates for the HSPG receptor for *Plasmodium* sporozoites since they are expressed in the liver (Bernfield *et al.*, 1999). Syn-1 seems not an important sporozoite receptor because *P. yoelii* infection in Syn-1 deficient mice showed that these mice are as susceptible to sporozoite infection as the wild-type controls (Bhanot and Nussenzweig, 2002). It is possible that Syn-1 function as a hepatic HSPG receptor for *Plasmodium* is redundant, and that in its absence its role is fulfilled by another molecule. Syn-2 is probably the CSP receptor since it is an unusual member of the family of HSPGs, with a large proportion of heparin like, highly sulfated structures at the distal end of the glycosaminoglycans chains (Lyon and Gallagher, 1991; Pierce *et al.*, 1992). Notably, among glycosaminoglycans, heparin is the most efficient inhibitor of CSP binding to HepG2 cells. A well-defined decasaccharide isolated from heparin, which has a structure commonly found in liver Syn-2, blocks the interaction between CSP and HepG2 cells (Rathore *et al.*, 2001). The same decasaccharide binds specifically to apolipoprotein E (Dong *et al.*, 2001), providing additional support for the view that sporozoites and chylomicron remnants compete for the same liver sites. Syn-2's role in this process can be clarified when Syn-2 deficient mice become available.

1.6.5. Hepatocyte infection

1.6.5.1. Reaching hepatocytes

After sporozoites are arrested in the liver sinusoid, they must reach and invade the hepatocytes. The liver sinusoid is composed of a single cell layer of fenestrated endothelial cells along with interspersed Kupffer cells, the liver resident macrophages. Although liver endothelial cells have fenestrations, these are too small (about one tenth of the diameter of a sporozoite) to allow sporozoite passage. Research in this matter has provided strong evidence that sporozoites cross the sinusoidal layer primarily through Kupffer cells [reviewed in (Frevert *et al.*, 2006)] (Figure 1.6).
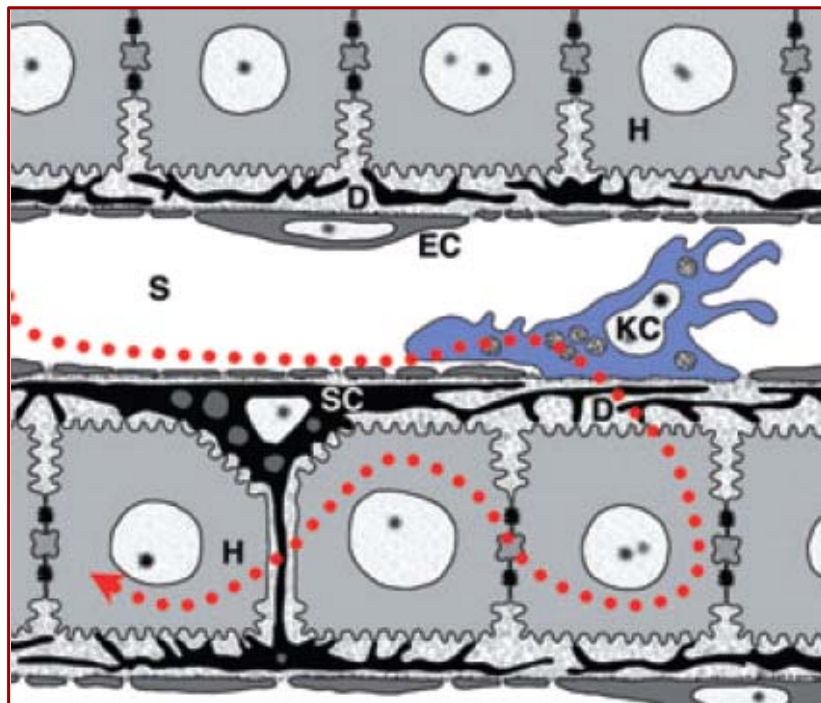
Figure 1.6 | *Plasmodium* **sporozoite's arrival at hepatocytes through Kupffer cells.**
Liver sinusoids (S) are lined by fenestrated endothelia (EC) and interspersed Kupffer cells (KC). Stellate cells (SC) are located inside the narrow Disse space (D), which is formed by sinusoidal cell layer and hepatocytes (H). Sporozoites (represented by the red dotted line) are transported through liver sinusoids, until they encounter a Kupffer cell. Then, sporozoites reach hepatocytes by traversing the Kupffer cell [adapted from (Baer *et al.*, 2007)].

In vitro observations of the interaction between sporozoites and sinusoidal cells found that sporozoites preferentially invaded Kupffer cells (Pradel and Frevert, 2001). More recently, Baer *et al.* (2007) provided strong evidence that Kupffer cells represent the sporozoite's doorway to hepatocytes. *In vivo*, *Plasmodium* infection of homozygous op/op mice, known to have fewer Kupffer cells than their wild-type counterparts

[because they lack macrophage colony stimulating factor 1 due to a mutation in the osteopetrosis (op) gene], led to the observation that infection in homozygous mice was decreased by 84% when compared with their heterozygous siblings, which have normal Kupffer cell numbers (Baer *et al.*, 2007).

The Kupffer cell invasion process was observed to occur with the formation of a PV, which allows sporozoites to go through Kupffer cells avoiding lysosomal fusion (Pradel and Frevert, 2001). Intravital microscopy provided evidence that sporozoites arrested in the liver sinusoids were found to move towards the hepatocytes through Kupffer cells at a lower speed than the normal speed measured when sporozoites traverse cells using plasma membrane disruption (Frevert *et al.*, 2005). Furthermore, it was shown that *Plasmodium* sporozoites are able to survive the Kupffer cell passage unharmed through the suppression of the respiratory burst in these cells (Usynin *et al.*, 2007). Sporozoites exploit the overall macrophage deactivating and anti-inflammatory properties of cyclic adenosyl monophosphate (cAMP) to suppress reactive oxygen species production in Kupffer cells. cAMP concentration in Kupffer cells was previously shown to be increased by the high-affinity interaction between CSP and the scavenger receptor LRP (Shakibaei and Frevert, 1996), which suggests that HSPGs might also contribute to the induction of the signaling cascade by facilitating CSP binding to LRP (Usynin *et al.*, 2007).

Nevertheless, it has been also been suggested that crossing of the sinusoidal layer might occur by the disruption of cell plasma membranes since *P. berghei* parasites deficient in the SPECT1 (sporozoite microneme protein essential for cell traversal) and SPECT2 (also called *Plasmodium* perforin-like protein 1, PPLP1) proteins, known to confer a defect in the ability to traverse cells, have low infectivity *in vivo* (Ishino *et al.*, 2004; Ishino *et al.*, 2005a). More studies are needed to reconcile these results with the previously described ones.

1.6.5.2. Migration through hepatocytes

Sporozoites migrate through several hepatocytes before finally engaging the mechanism to enter hepatocytes with formation of a PV. It has been shown both *in vitro* and *in vivo* that during migration through cells, *Plasmodium* sporozoites breach the plasma membranes of several hepatocytes and these can rapidly be repaired (Mota *et al.*, 2001a; Frevert *et al.*, 2005) (Figure 1.7).
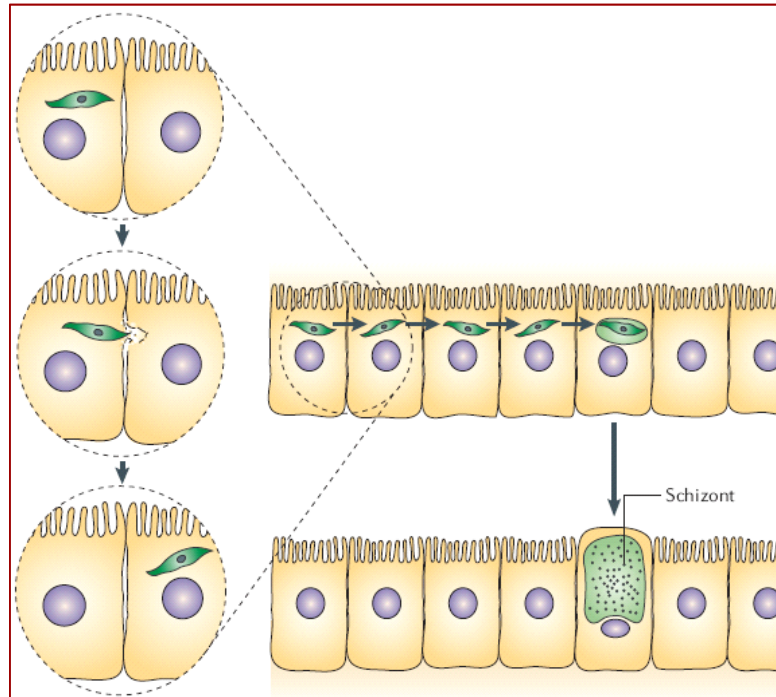
Figure 1.7 | *Plasmodium* **sporozoite migration through hepatocytes.**
Sporozoites (in green) migrate through several hepatocytes until infection of a final one. The migration process involves hepatocyte plasma membrane breaching while hepatocyte infection occurs with the formation of a parasitophorous vacuole [adapted from (Prudêncio *et al.*, 2006)].

Migration through host cells induces exocytosis from sporozoite apical organelles and parasite molecules, such as TRAP, are released (Mota *et al.*, 2002). Sporozoites usually present a faint TRAP surface staining pattern but, after incubation with host cells, high concentrations of TRAP are observed forming an apical "cap" on the sporozoite surface (Gantt *et al.*, 2000). Elevated cytosolic concentrations of Ca^{2+} in sporozoites induce exocytosis (Gantt *et al.*, 2000; Mota *et al.*, 2002), which suggests that signaling cascades might be activated in the parasite during migration through cells. In addition, the host cell wounding by sporozoite migration was also shown to induce the secretion of a host factor, hepatocyte growth factor (HGF), which renders surrounding hepatocytes more susceptible to infection (Carrolo *et al.*, 2003). By activating its receptor, MET, HGF induces important rearrangements in host cell cytoskeleton (Carrolo *et al.*, 2003) and protects the host cell(s) from apoptosis (Leirião *et al.*, 2005a).

Although a full understanding of the molecular mechanisms associated with cell migration is still far, four *P. berghei* proteins involved in this process have been identified. These are SPECT1, SPECT2, PL and CelTOS (cell traversal protein for ookinete and sporozoite) (Ishino *et al.*, 2004; Bhanot *et al.*, 2005; Ishino *et al.*, 2005a; Kariu *et al.*, 2006). Sporozoites in which either one of the SPECT proteins or CelTOS

were deleted show similar phenotypes: *in vitro* they lack the ability to traverse cells but when placed directly on hepatocytes they invade and develop normally. *In vivo* it was observed that these mutants lack infectivity for the mammalian host when injected intravenously and this phenotype was inverted in mice whose liver Kupffer cells were depleted because sporozoites access hepatocytes directly through gaps in the sinusoidal barrier (Ishino *et al.*, 2004; Ishino *et al.*, 2005a; Kariu *et al.*, 2006). These proteins may also be required for sporozoite exit from the dermis and in fact this has been demonstrated by intravital microscopy for the SPECT1 mutant [Amino and Menard, unpublished data referenced in (Sinnis and Coppi, 2007)]. Altogether, the SPECT and CelTOS mutant data suggest that, although migration through cells is necessary to reach the hepatic parenchyma, migration through hepatocytes may not be necessary for infection. This is in disagreement with the notion that migration is a prerequisite to enable sporozoites to invade the appropriate host cell and therefore, these different perceptions need further attention to be reconciled.

Mutant sporozoites in which PL is deleted or its catalytic site altered also show a reduced cell traversal activity. Although, these mutants are impaired in reaching the liver when injected intradermally, they present a normal infectivity when injected intravenously (Bhanot *et al.*, 2005). Therefore, PL appears to be required only for crossing cell barriers in the skin suggesting that the migration mechanism in the skin might differ from the one in the liver.

1.6.5.3. Hepatocyte invasion

Following migration through cells, *Plasmodium* sporozoites engage in a final invasion, with the formation of a parasitophorous vacuole, which is essential for further differentiation of the parasite. The parasite and host molecules involved in hepatocyte invasion process have been under investigation. Several parasite proteins were shown to be involved in this process and these are described below.

CSP has been extensively shown to be essential for sporozoite localization to the liver but the role of CSP–hepatocyte interactions during the invasion process itself is still under investigation. Recently, it was found that CSP is proteolytically cleaved by a parasite cysteine protease upon contact with hepatocytes and this cleavage process seems to be specifically associated with productive sporozoite invasion (Coppi *et al.*, 2005). In addition, CSP intracytoplasmic deposition was shown to take place during sporozoite attachment to the host cell, reaching its peak 4 to 6 hours after invasion. CSP interacts initially with cytosolic as well as endoplasmic reticulum-associated ribosomes and throughout parasite development CSP binding becomes restricted to ribosomes lining in the outer membrane of the host cell nuclear envelope (Hugel *et al.*,

1996). Moreover, it was shown that CSP leads to the inhibition of protein synthesis in host cells (Frevert *et al.*, 1998).

TRAP, normally present in small amounts on the sporozoite surface, is released in large amounts onto the sporozoite surface upon parasite contact with hepatocytes or during the migration process (Gantt *et al.*, 2000; Mota *et al.*, 2002). TRAP is a transmembrane protein whose extracellular portion has two cell-adhesive sequences, an A-domain (or I-domain of integrins) and a type I thrombospondin motif (TSR) [reviewed in (Menard, 2000)]. TRAP's role in hepatocyte invasion has been elucidated thanks to the generation TRAP mutants in these domains (Wengelnik *et al.*, 1999; Matuschewski *et al.*, 2002). Mutations in only one of the adhesive domains were shown to significantly decrease infectivity for hepatocytes while mutations in both domains completely abolished infection.

The apical membrane antigen 1 protein (AMA-1), known to be involved in *Plasmodium* merozoite invasion of erythrocytes, was also shown to be expressed in sporozoites (Florens *et al.*, 2002; Silvie *et al.*, 2004) and to have a role in hepatocyte invasion by *P. falciparum* parasites *in vitro* (Silvie *et al.*, 2004). This protein is initially found intracellularly and is secreted onto the sporozoite surface in the presence of hepatocytes.

P. berghei P36p and Pb36 proteins, members of a small family of *Plasmodium* proteins that have 6 conserved cysteine residues, were also shown to be important for sporozoites to recognize hepatocytes and commit to infection (Ishino *et al.*, 2005b).

The Py235 rhoptry protein, first described in *P. yoelii* but with clear homologues in other rodent and human malaria species (Gruner *et al.*, 2004), was also involved in sporozoite invasion of hepatocytes (Preiser *et al.*, 2002).

A role in hepatocyte invasion has been suggested for other proteins, namely the secreted protein with altered thrombospondin repeat (SPATR) (Chattopadhyay *et al.*, 2003), the erythrocyte-binding antigen 175 (EBA 175) (Gruner *et al.*, 2001b), the sporozoite-threonine-asparagine-rich protein (STARP) (Pasquetto *et al.*, 1997) and the *Plasmodium falciparum* erythrocyte membrane protein 3 (PfEMP3) (Gruner *et al.*, 2001a), due either to their localization in the sporozoite or to the fact that antibodies directed against them can decrease sporozoite infectivity.

More recently, a new parasite protein called thrombospondin related sporozoite protein (TRSP) initially described in *P. yoelii* (Kaiser *et al.*, 2004) was shown to facilitate host cell entry (Labaied *et al.*, 2007a).

Regarding the host cell molecules that the parasite exploits, so far only a few have been described and these are presented below.

The HSPGs already mentioned to be involved in sporozoite arrest in the liver may also be involved in invasion [see (Sinnis and Coppi, 2007)]. More recently, an interaction between fetuin-A glycoprotein on hepatocyte membranes and the extracellular region of TRAP has been shown to enhance the parasite's aptitude to invade hepatocytes (Jethwaney *et al.*, 2005).

Another host molecule identified as essential for sporozoites invasion is the tetraspanin CD81 (Silvie *et al.*, 2003). This membrane protein is expressed on the surface of hepatocytes and has been previously shown to be a putative receptor for hepatitis C virus (Pileri *et al.*, 1998). CD81 appears to have an important role in the invasion of mouse hepatocytes by *P. yoelii* and human hepatocytes by *P. falciparum* (Silvie *et al.*, 2003), which has been proposed to be linked with CD81 being localized in tetraspanin-enriched microdomains (Silvie *et al.*, 2006a). On the other hand, *P. berghei* was shown to use both CD81-dependent and -independent pathways to enter the hepatocyte (Silvie *et al.*, 2006b; Silvie *et al.*, 2007).

To date, the precise role of CD81 remains elusive, as attempts to identify a sporozoite ligand for CD81 have not yet allowed the identification of a binding partner (Silvie *et al.*, 2003). Therefore CD81 may not function as a receptor but, instead, might regulate the activity of another host molecule that has an essential role in sporozoite invasion. This hypothesis is in agreement with the reported ability of tetraspanins to associate with, and regulate the function of, molecular partners. Another possibility is that CD81 functions during the early stages of PV formation, which is suggested by the finding that the small proportion of *P. yoelii* sporozoites that invade CD81-negative cells are found developing in the nucleus without a PV (Silvie *et al.*, 2006b).

Research focused on the identification of host receptors essential for sporozoite infection has also revealed host molecules that seem not to play a role in this process. *Plasmodium in vivo* infection was accessed in mice deficient in molecules such as ICAM-1 and ICAM-2 (intercellular adhesion molecule 1 and 2, respectively, expressed in endothelial and epithelial cells) (Sultan *et al.*, 1997), CD36 (scavenger receptor found on many cells including Kupffer and endothelial cells) (Sinnis and Febbraio, 2002), Syn-1 (HSPG expressed by many cell types, including hepatocytes) (Bhanot and Nussenzweig, 2002), SR-AI and SR-AII (scavenger receptors class A, member 1 and 2 expressed by Kupffer and liver endothelial cells) (Cunha-Rodrigues *et al.*, 2006a). In these studies it was observed that mice deficient in these proteins showed levels of *Plasmodium* infection similar to those of wild-type mice. However, it is possible that *Plasmodium* can invade host cells using multiple, alternative pathways, with significant redundancy. Therefore, it remains to be elucidated whether any of the receptors mentioned above plays (a) specific role(s) in malaria infection.

As mentioned above, sporozoite hepatocyte invasion is characterized by the formation of a PV. The processe(s) involved in PV formation is (are) unknown. Three different models have been proposed to explain PV formation in apicomplexan parasites: (i) *de novo* PV formation through the discharge of proteins and membranous material from the parasite rhoptries; (ii) PV formation by direct invagination of the host cell membrane and (iii) PV formation through the discharge of material from the rhoptries along with cell membrane invagination [reviewed in (Mota and Rodriguez, 2002)]. If any of these model(s) applies to the PV formation at the time of hepatocyte infection still has to be determined.

1.6.5.4. Development within the hepatocyte

After invasion, the sporozoite resides inside the PV and differentiates into an EEF, which grows (trophozoite stage), multiplies (schizont stage) and, within a few days (only 2 days for the murine *Plasmodium* models), generates thousands of erythrocyte-infectious merozoites. The initial phase of sporozoite differentiation into an EEF probably occurs without nutrient acquisition from the host cell but, afterwards, in order to develop and multiply, the parasite must establish an extensive system to remodel and exploit the host hepatocyte [reviewed in (Mikolajczak and Kappe, 2006)]. During EEF development within the hepatocyte the parasite notably outgrows the normal host cell limits (Figure 1.8). During this phase there is certainly a huge membrane and nucleic acid synthesis and an important question that remains unanswered is how the parasite acquires the nutrients required for this process. The hepatocytes' unique properties of metabolic "superachievers" (e.g. for major lipids and purines) and "storehouses" (e.g. for glycogen) could be one reason why mammalian species have acquired the ability to infect hepatocytes, whereas the evolutionarily older avian and reptilian species develop in the sinusoidal cells (Frevert, 2004; Bano *et al.*, 2007). A recent study shows that, during its development, the EEF is found in the juxtanuclear cell region where optimal replication occurs and their PV is associated with the host endoplasmic reticulum. The PV membrane was shown to be cholesterol-enriched and the lipids are likely to be derived from the host plasma membrane. Moreover, *Plasmodium* transforms its vacuole into a highly permeable compartment by creating channels within the PV membrane, which allow the trafficking of a wide range of small metabolites from the host cytosol to the PV (Bano *et al.*, 2007).
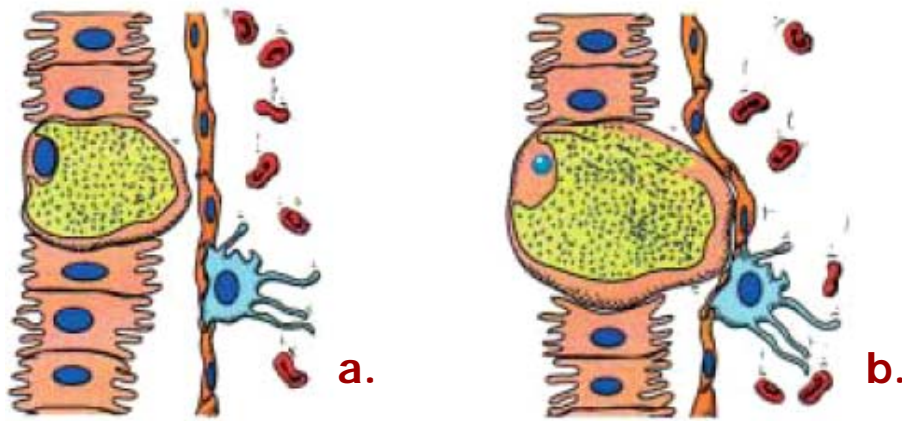
Figure 1.8 | *Plasmodium* **development within the hepatocyte.**

(a.) *Plasmodium* EEF development within the hepatocyte occurs indoors the parasitophorous vacuole. **(b.)** Infected hepatocytes are enormously increased in cell volume when compared to a non-infected cell [adapted from (Sturm *et al.*, 2006)].

The molecular mechanisms that occur in the parasite or the hepatocyte to establish the intrahepatocytic niche are still poorly understood.

To date only a few sporozoite proteins, namely UIS3, UIS4 and Pb36p (Mueller *et al.*, 2005a; Mueller *et al.*, 2005b; van Dijk *et al.*, 2005; Tarun *et al.*, 2007), have been shown to be essential for parasite development within the hepatocytes.

UIS3 and UIS4 (UIS for upregulated in infective sporozoites) knock-out (KO) *P. berghei* and *P. yoelii* sporozoites were shown to successfully invade hepatocytes with the formation of a PV and transform into EEFs but, subsequently, to present a severe growth defect (Mueller *et al.*, 2005a; Mueller *et al.*, 2005b; Tarun *et al.*, 2007).

For *P. berghei* P36p KO sporozoites, while one study shows that these invade hepatocytes but are not able to maintain the PV and consequently their early development is arrested (van Dijk *et al.*, 2005), a different study shows that P36p KO sporozoites are able to infect cells with the formation of the PV, although with reduced efficiency (Ishino *et al.*, 2005b). In the latter study a significant increase in cell traversal activity of KO parasites was also observed and it was proposed that these fail to switch to the "infection mode" and keep on traversing host cells. A recent study, shows that a *P. yoelii* P36p and P36 double mutant can enter and traverse host cells normally (no increase in traversal activity was observed) but cannot establish a PV early in hepatocyte infection (Labaied *et al.*, 2007b). Thus, although P36p-deficient sporozoites might be impaired in both invasion and intracellular development within the host cells, it is likely that P36p plays a critical role in the pathway that leads to the formation of the PV membrane.

Even if the exact role of all of these proteins in EEF development remains to be elucidated, a remarkable application of these genetically attenuated sporozoites (GAS) is their use as live attenuated vaccines, similarly to radiation attenuated sporozoites (RAS), which also present a deficient growth within hepatocytes (Sigler *et al.*, 1984). Immunization with RAS was shown to induce protection against challenge with infectious sporozoites (Nussenzweig *et al.*, 1967) and this model has allowed an understanding of the basic immune mechanisms that mediate sterile protection against infection (Doolan and Hoffman, 2000; Doolan and Martinez-Alier, 2006; Hafalla *et al.*, 2006). Immunization with GAS was also shown to confer full protection against a subsequent challenge with fully infective sporozoites (Mueller *et al.*, 2005a; Mueller *et al.*, 2005b; van Dijk *et al.*, 2005; Douradinha *et al.*, 2007; Labaied *et al.*, 2007b; Tarun *et al.*, 2007), which has already been shown to occur through the induction of protective immune responses for the UIS-deficient parasites (Jobe *et al.*, 2007; Mueller *et al.*, 2007; Tarun *et al.*, 2007).

Barely any host factors important for EEF development in the host cell are known. As mentioned before, HGF is secreted by hepatocytes damaged during sporozoite migration (Carrolo *et al.*, 2003). Through HGF/MET signaling, this host factor induces rearrangements of the host cell actin cytoskeleton that might play a role during the early development of the parasites within the hepatocyte (Carrolo *et al.*, 2003). Moreover, it was also shown that HGF/MET activity on infection is also due to apoptosis prevention in infected host cells, a crucial requirement for the full parasite development (Leirião *et al.*, 2005a).

Studies focused on the role of the UIS4 and UIS3 parasite proteins, essential for EEF development, have revealed that they seem to interact with the host proteins ApoA1 (apolipoprotein A-I) and L-FABP (liver-fatty acid binding protein), respectively.

ApoA1 and UIS4 were observed to co-localize in the PV 24 hours after sporozoite infection and ApoA1 relevance in *Plasmodium* infection was confirmed *in vitro* and *in vivo* [Mueller and Matuschewski, unpublished data referenced in (Prudêncio *et al.*, 2006)]. ApoA1 is a major protein component of high density lipoprotein (HDL) and therefore it is speculated that its role in *Plasmodium* intrahepatocytic development might be related with the synthesis of large amounts of additional membrane essential for the considerable PV expansion that must occur to allow intra-vacuolar replication of malaria sporozoites [reviewed in (Prudêncio *et al.*, 2006)].

UIS3 was shown to interact directly with L-FABP, using a two-hybrid system (Mikolajczak *et al.*, 2007). L-FABP expression down-regulation in hepatocytes severely impairs parasite growth and L-FABP overexpression promotes growth. As the main cytoplasmic carrier of fatty acids in hepatocytes, L-FABP acts as a shuttle of fatty acids

for import, storage, export and delivery to intracellular destinations. Even though whether a direct interaction of UIS3 and L-FABP takes place in infected hepatocytes remains to be demonstrated, the authors suggest a major pathway for fatty acid acquisition by *Plasmodium* from the host hepatocyte via docking of L-FABP to UIS3 (Mikolajczak *et al.*, 2007). Further studies are needed to prove the speculated roles for ApoA1 and L-FABP.

During schizogony the parasite grows considerably in size and infected hepatocytes become several times larger than non-infected ones. Although this enormous growth is certainly an important stress factor for the host cell, and stress normally induces apoptosis, infected cells surprisingly do not exhibit signs of cell death [reviewed in (Sturm and Heussler, 2007)]. In fact there is accumulating evidence for parasite-dependent survival of the host cell during liver stage development. A recent study suggests that irradiated dying parasites induce apoptosis of the host cell confirming that viable parasites are required to constantly stimulate host cell survival pathways (Leirião *et al.*, 2005b). Moreover, it was shown that dendritic cells (DCs) phagocytose apoptotic cells containing the remains of intracellular parasites (Leirião *et al.*, 2005b). It is possible to extrapolate that apoptotic infected cells may play a role in the protective immune response since it has previously been demonstrated that DCs mediate the protective immune response induced by irradiated sporozoites (Hafalla *et al.*, 2003). Another piece of evidence that parasite death results in host cell apoptosis arises from the observation that host cell apoptosis occurs upon parasite death (van de Sand *et al.*, 2005). Moreover, *P. berghei* infected hepatocyte analysis revealed that the presence of the parasite protects the host cell from apoptosis induced *in vitro* by peroxide treatment or serum deprivation and *in vivo* by TNF-α. This parasite-dependent inhibition of apoptosis although more pronounced at 48 h post infection (p.i.) is already detectable at 24 h p.i.

1.6.6. The parasite breaks away from the hepatocyte

Ultimately *Plasmodium* intrahepatocytic development comes to an end and the thousands of newly formed merozoites must be released into the blood stream, where they will invade erythrocytes, initiating the blood stage of malaria infection. These merozoites must leave the PV membrane and the host cell membrane, cross the space of Disse and penetrate endothelial cells to enter blood vessels and finally infect erythrocytes. For many years it has been assumed that merozoites would be liberated by rupture of the host cell membrane, but this does not explain how they can cross the extracellular matrix-filled space and the endothelium of the blood vessels, being also able to escape the host immune system. Recently, it was proposed that *P. berghei* liver

stage parasite manipulates their host cells to guarantee the safe delivery of merozoites into the blood stream (Sturm *et al.*, 2006). Parasites induce the death and the detachment of their host hepatocytes, followed by the budding of parasite-filled vesicles, named merosomes (Figure 1.9).
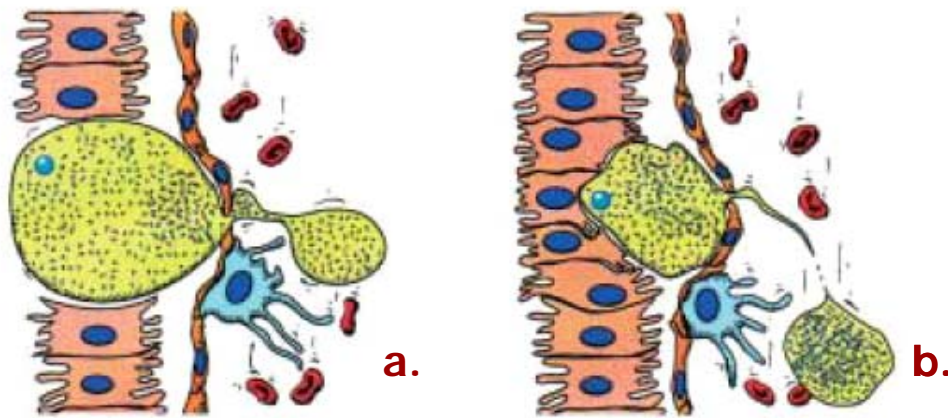
Figure 1.9 | *Plasmodium* **exit from the liver into the blood stream.**
(a. and **b.)** *Plasmodium m*erozoites are released from the liver via merosomes, merozoite-filled vesicles, that bud off from infected hepatocytes into the sinusoidal lumen [adapted from (Sturm *et al.*, 2006)].

Merosomes, which can contain from just a few to several thousand merozoites, bulge into liver sinusoids and appear to act as shuttles that ensure the release of living merozoites directly into the circulation. Interestingly, although merosomes present apoptotic features they are able to act as protective shields against phagocytosis due to the lack of the phosphatidylserine signature of a dying cell. This mechanism of cell death and cell movement of the host cell seems to be controlled by cysteine proteases as well as factors that mediate Ca^{2+} accumulation (Sturm *et al.*, 2006). Merosome-like structures have also been reported for *P. yoelii* (Tarun *et al.*, 2006).

1.7. Objectives

The biological events that take place throughout the liver stage of *Plasmodium* infection are obligatory during the establishment of a natural malaria infection and therefore constitute an ideal target for potential anti-malarial vaccines and prophylactic drugs. Although there have been recent significant advances in our understanding of the mechanisms by which *Plasmodium* sporozoites establish infection in the mammalian host, there is still insufficient information on the host and parasite molecules involved in *Plasmodium* invasion and development within hepatocytes.

The overall goal of the research proposal that led to the work presented in this thesis was to identify host factors playing a role on *Plasmodium* liver stage infection. To this end, we sought to apply an RNA interference (RNAi) approach, which allows selective down-regulation of gene expression. RNAi is an evolutionarily conserved mechanism by which double stranded RNA molecules (dsRNA) silence a target gene through the specific destruction of its messenger RNA (mRNA) [reviewed in (Meister and Tuschl, 2004)]. In mammalian cells small interfering RNA (siRNA) molecules (with 21 to 23 nucleotides) are capable of specifically silence gene expression without induction of the interferon response pathway [see (Echeverri and Perrimon, 2006)]. RNAi's ability to induce the destruction of individual targeted mRNAs with high efficacy and specificity enables the generation of direct relationships between a gene's expression level and its functional role in any biological process being studied (Sachse *et al.*, 2005). Basically, we used an *in vitro* assay in which *Plasmodium* infection was accessed in host cells treated with siRNAs to specifically silence the genes under investigation.

Initially, we tested the feasibility of a high throughput RNAi procedure in our *in vitro P. berghei* infection system by performing a small screen in which a total of 96 genes expressed in liver cells and involved in different processes (such as cytoskeleton, signaling, apoptosis and others) were targeted. This initial screen allowed the optimization and the standardization of all experimental conditions. More, regarding the RNAi screen system itself, it allow us to realize the crucial importance of: (i) use of at least three different siRNAs to target each gene to avoid false-negative results; (ii) confirmation rounds in order to achieve reproducible results for a specific gene with at least two different siRNAs; and (iii) a final confirmation step in which the observed phenotypic effect in infection is correlated with gene knock-down. Concerning the *in vitro Plasmodium* infection system it was understood that the widely used human HepG2 hepatoma cell line was not appropriate for the high-throughput type of

reading used. HepG2 cells in culture show a high aggregation level, which makes the automated acquisition of images at different focusing levels rather difficult. All these conclusions allowed us to better plan the different steps of the RNAi screen(s). Subsequently, three different sets of genes were screened:

(i)   host hepatocyte genes differentially expressed throughout *Plasmodium* infection, which were identified using microarray technology;

(ii)   host genes encoding kinases and kinase-interacting proteins and

(iii)   host lipoprotein pathway genes.

Why were these genes chosen? The explanation for the first screen involves previous work performed in our laboratory, namely the identification of host genes that are differentially expressed as a result of *Plasmodium* infection. Briefly, a microarray approach was used to compare gene expression of infected cells to the one of non-infected cells. Although this study has disclosed valuable information regarding the host genes specifically modulated throughout *Plasmodium* infection, by itself it did not supply evidence on their functional relevance. In order to achieve this some candidate genes were selected from the microarray analysis and their function was further studied by gene silencing using RNAi.

The second RNAi screen sought to determine host kinases and kinases-interacting proteins role in *Plasmodium* infection. It is known that these proteins are important intracellular signaling players and tightly control numerous cellular processes (Manning *et al.*, 2002). Therefore, it seemed likely that kinases and kinases-interacting proteins modulate the cell's behaviour during the infection process by an intracellular pathogen.

Finally, in a follow-up work from previous reports, in which a link between host lipoprotein clearance pathways and *Plasmodium* sporozoite infection of the liver was suggested (Shakibaei and Frevert, 1996; Sinnis *et al.*, 1996), we observed a lipoprotein-mediated inhibition of *Plasmodium* hepatocyte invasion. To better understand this observation the role of lipoprotein pathway genes in the liver stage of *Plasmodium* infection was accessed by RNAi.

Data from these three studies has revealed several host factors that seem important for the establishment and development of *Plasmodium* infection. Other approaches have been employed to further validate their role. The choice of the different approaches used was made according with the question to address and the tools available such as antibodies, inhibitory compounds and transgenic mice among others. The data obtained for the host factors studied provides strong evidence of their role in liver stage *Plasmodium* infection.

Plasmodium liver stage infection represents the most appealing stage for prophylaxis and vaccine strategies and effective intervention will only become realistically attainable by understanding the crucial host-parasite interactions. Therefore, the knowledge of important host factors for liver stage *Plasmodium* infection might provide new targets for drug and vaccine development.

1.8. References

Aikawa, M., Schwartz, A., Uni, S., Nussenzweig, R., and Hollingdale, M. (1984). Ultrastructure of in vitro cultured exoerythrocytic stage of Plasmodium berghei in a hepatoma cell line. Am J Trop Med Hyg *33*, 792-799.

Alonso, P.L. (2006). Malaria: deploying a candidate vaccine (RTS,S/AS02A) for an old scourge of humankind. Int Microbiol *9*, 83-93.

Alonso, P.L., Sacarlal, J., Aponte, J.J., Leach, A., Macete, E., Milman, J., Mandomando, I., Spiessens, B., Guinovart, C., Espasa, M., Bassat, Q., Aide, P., Ofori-Anyinam, O., Navia, M.M., Corachan, S., Ceuppens, M., Dubois, M.C., Demoitie, M.A., Dubovsky, F., Menendez, C., Tornieporth, N., Ballou, W.R., Thompson, R., and Cohen, J. (2004). Efficacy of the RTS,S/AS02A vaccine against Plasmodium falciparum infection and disease in young African children: randomised controlled trial. Lancet *364*, 1411-1420.

Amino, R., Thiberge, S., Martin, B., Celli, S., Shorte, S., Frischknecht, F., and Menard, R. (2006). Quantitative imaging of Plasmodium transmission from mosquito to mammal. Nat Med *12*, 220-224.

Ancsin, J.B., and Kisilevsky, R. (2004). A binding site for highly sulfated heparan sulfate is identified in the N terminus of the circumsporozoite protein: significance for malarial sporozoite attachment to hepatocytes. J Biol Chem *279*, 21824-21832.

Baer, K., Roosevelt, M., Clarkson, A.B., Jr., van Rooijen, N., Schnieder, T., and Frevert, U. (2007). Kupffer cells are obligatory for Plasmodium yoelii sporozoite infection of the liver. Cell Microbiol *9*, 397-412.

Bano, N., Romano, J.D., Jayabalasingham, B., and Coppens, I. (2007). Cellular interactions of Plasmodium liver stage with its host mammalian cell. Int J Parasitol.

Barat, L.M., Palmer, N., Basu, S., Worrall, E., Hanson, K., and Mills, A. (2004). Do malaria control interventions reach the poor? A view through the equity lens. Am J Trop Med Hyg *71*, 174-178.

Barillas-Mury, C., and Kumar, S. (2005). Plasmodium-mosquito interactions: a tale of dangerous liaisons. Cell Microbiol *7*, 1539-1545.

Belmonte, M., Jones, T.R., Lu, M., Arcilla, R., Smalls, T., Belmonte, A., Rosenbloom, J., Carucci, D.J., and Sedegah, M. (2003). The infectivity of Plasmodium yoelii in different strains of mice. J Parasitol *89*, 602-603.

Bernfield, M., Gotte, M., Park, P.W., Reizes, O., Fitzgerald, M.L., Lincecum, J., and Zako, M. (1999). Functions of cell surface heparan sulfate proteoglycans. Annu Rev Biochem *68*, 729-777.

Bhanot, P., and Nussenzweig, V. (2002). Plasmodium yoelii sporozoites infect Syndecan-1 deficient mice. Mol Biochem Parasitol *123*, 143-144.

Bhanot, P., Schauer, K., Coppens, I., and Nussenzweig, V. (2005). A surface phospholipase is involved in the migration of plasmodium sporozoites through cells. J Biol Chem *280*, 6752-6760.

Blanford, S., Chan, B.H., Jenkins, N., Sim, D., Turner, R.J., Read, A.F., and Thomas, M.B. (2005). Fungal pathogen reduces potential for malaria transmission. Science *308*, 1638-1641.

Bojang, K.A., Milligan, P.J., Pinder, M., Vigneron, L., Alloueche, A., Kester, K.E., Ballou, W.R., Conway, D.J., Reece, W.H., Gothard, P., Yamuah, L., Delchambre, M., Voss, G.,

Greenwood, B.M., Hill, A., McAdam, K.P., Tornieporth, N., Cohen, J.D., and Doherty, T. (2001). Efficacy of RTS,S/AS02 malaria vaccine against Plasmodium falciparum infection in semi-immune adult men in The Gambia: a randomised trial. Lancet *358*, 1927-1934.

Boutlis, C.S., Yeo, T.W., and Anstey, N.M. (2006). Malaria tolerance--for whom the cell tolls? Trends Parasitol *22*, 371-377.

Briones, M.R., Tsuji, M., and Nussenzweig, V. (1996). The large difference in infectivity for mice of Plasmodium berghei and Plasmodium yoelii sporozoites cannot be correlated with their ability to enter into hepatocytes. Mol Biochem Parasitol *77*, 7-17.

Bruce-Chuvatt, L.J. (1981). Alphonse Laveran's discovery 100 years ago and today's global fight against malaria. J R Soc Med *74*, 531-536.

Calvo-Calle, J.M., Moreno, A., Eling, W.M., and Nardin, E.H. (1994). In vitro development of infectious liver stages of P. yoelii and P. berghei malaria in human cell lines. Exp Parasitol *79*, 362-373.

Capanna, E. (2006). Grassi versus Ross: who solved the riddle of malaria? Int Microbiol *9*, 69-74.

Carrolo, M., Giordano, S., Cabrita-Santos, L., Corso, S., Vigario, A.M., Silva, S., Leiriao, P., Carapau, D., Armas-Portela, R., Comoglio, P.M., Rodriguez, A., and Mota, M.M. (2003). Hepatocyte growth factor and its receptor are required for malaria infection. Nat Med *9*, 1363-1369.

Carucci, D. (2004). Know thine enemy. Nature *430*, 944-945.

Cerami, C., Frevert, U., Sinnis, P., Takacs, B., Clavijo, P., Santos, M.J., and Nussenzweig, V. (1992). The basolateral domain of the hepatocyte plasma membrane bears receptors for the circumsporozoite protein of Plasmodium falciparum sporozoites. Cell *70*, 1021-1033.

Cerami, C., Frevert, U., Sinnis, P., Takacs, B., and Nussenzweig, V. (1994). Rapid clearance of malaria circumsporozoite protein (CS) by hepatocytes. J Exp Med *179*, 695-701.

Chattopadhyay, R., Rathore, D., Fujioka, H., Kumar, S., de la Vega, P., Haynes, D., Moch, K., Fryauff, D., Wang, R., Carucci, D.J., and Hoffman, S.L. (2003). PfSPATR, a Plasmodium falciparum protein containing an altered thrombospondin type I repeat domain is expressed at several stages of the parasite life cycle and is the target of inhibitory antibodies. J Biol Chem *278*, 25977-25981.

Clark, I.A., and Cowden, W.B. (2003). The pathophysiology of falciparum malaria. Pharmacol Ther *99*, 221-260.

Coppi, A., Pinzon-Ortiz, C., Hutter, C., and Sinnis, P. (2005). The Plasmodium circumsporozoite protein is proteolytically processed during cell invasion. J Exp Med *201*, 27-33.

Couchman, J.R. (2003). Syndecans: proteoglycan regulators of cell-surface microdomains? Nat Rev Mol Cell Biol *4*, 926-937.

Cox, F.E. (2002). History of human parasitology. Clin Microbiol Rev *15*, 595-612.

Cunha-Rodrigues, M., Portugal, S., Febbraio, M., and Mota, M.M. (2006a). Infection by and protective immune responses against Plasmodium berghei ANKA are not affected in macrophage scavenger receptors A deficient mice. BMC Microbiol *6*, 73.

Cunha-Rodrigues, M., Prudêncio, M., Mota, M.M., and Haas, W. (2006b). Antimalarial drugs - host targets (re)visited. Biotechnol J *1*, 321-332.

Davies, C.S., Suhrbier, A.S., Winger, L.A., and Sinden, R.E. (1989). Improved techniques for the culture of the liver stages of Plasmodium berghei and their relevance to the study of causal prophylactic drugs. Acta Leiden *58*, 97-113.

Despommier, D., Gwadz, R.W., Hotez, P.J., and Knirsch, C.A. (2000). Parasitic Diseases. Apple Trees Productions, New York.

Dong, J., Peters-Libeu, C.A., Weisgraber, K.H., Segelke, B.W., Rupp, B., Capila, I., Hernaiz, M.J., LeBrun, L.A., and Linhardt, R.J. (2001). Interaction of the N-terminal domain of apolipoprotein E4 with heparin. Biochemistry *40*, 2826-2834.

Doolan, D.L., and Hoffman, S.L. (2000). The complexity of protective immunity against liver-stage malaria. J Immunol *165*, 1453-1462.

Doolan, D.L., and Martinez-Alier, N. (2006). Immune response to pre-erythrocytic stages of malaria parasites. Curr Mol Med *6*, 169-185.

Douradinha, B., van Dijk, M.R., Ataide, R., van Gemert, G.J., Thompson, J., Franetich, J.F., Mazier, D., Luty, A.J., Sauerwein, R., Janse, C.J., Waters, A.P., and Mota, M.M. (2007). Genetically attenuated P36p-deficient Plasmodium berghei sporozoites confer long-lasting and partial cross-species protection. Int J Parasitol.

Druilhe, P.L., Renia, L., and Fidock, D.A. (1998). Immunity to liver stages. In: Sherman IW, editor. Malaria: Parasite Biology, Pathogenesis, and Protection. ASM Press, Washington DC, 513–543.

Echeverri, C.J., and Perrimon, N. (2006). High-throughput RNAi screening in cultured cells: a user's guide. Nat Rev Genet *7*, 373-384.

Fidock, D.A., Rosenthal, P.J., Croft, S.L., Brun, R., and Nwaka, S. (2004). Antimalarial drug discovery: efficacy models for compound screening. Nat Rev Drug Discov *3*, 509-520.

Florens, L., Washburn, M.P., Raine, J.D., Anthony, R.M., Grainger, M., Haynes, J.D., Moch, J.K., Muster, N., Sacci, J.B., Tabb, D.L., Witney, A.A., Wolters, D., Wu, Y., Gardner, M.J., Holder, A.A., Sinden, R.E., Yates, J.R., and Carucci, D.J. (2002). A proteomic view of the Plasmodium falciparum life cycle. Nature *419*, 520-526.

Franke-Fayard, B., Trueman, H., Ramesar, J., Mendoza, J., van der Keur, M., van der Linden, R., Sinden, R.E., Waters, A.P., and Janse, C.J. (2004). A Plasmodium berghei reference line that constitutively expresses GFP at a high level throughout the complete life cycle. Mol Biochem Parasitol *137*, 23-33.

Frevert, U. (2004). Sneaking in through the back entrance: the biology of malaria liver stages. Trends Parasitol *20*, 417-424.

Frevert, U., Engelmann, S., Zougbede, S., Stange, J., Ng, B., Matuschewski, K., Liebes, L., and Yee, H. (2005). Intravital observation of Plasmodium berghei sporozoite infection of the liver. PLoS Biol *3*, e192.

Frevert, U., Galinski, M.R., Hugel, F.U., Allon, N., Schreier, H., Smulevitch, S., Shakibaei, M., and Clavijo, P. (1998). Malaria circumsporozoite protein inhibits protein synthesis in mammalian cells. Embo J *17*, 3816-3826.

Frevert, U., Sinnis, P., Cerami, C., Shreffler, W., Takacs, B., and Nussenzweig, V. (1993). Malaria circumsporozoite protein binds to heparan sulfate proteoglycans associated with the surface membrane of hepatocytes. J Exp Med *177*, 1287-1298.

Frevert, U., Usynin, I., Baer, K., and Klotz, C. (2006). Nomadic or sessile: can Kupffer cells function as portals for malaria sporozoites to the liver? Cell Microbiol *8*, 1537-1546.

Frischknecht, F., Baldacci, P., Martin, B., Zimmer, C., Thiberge, S., Olivo-Marin, J.C., Shorte, S.L., and Menard, R. (2004). Imaging movement of malaria parasites during transmission by Anopheles mosquitoes. Cell Microbiol *6*, 687-694.

Gantt, S., Persson, C., Rose, K., Birkett, A.J., Abagyan, R., and Nussenzweig, V. (2000). Antibodies against thrombospondin-related anonymous protein do not inhibit Plasmodium sporozoite infectivity in vivo. Infect Immun *68*, 3667-3673.

Gardner, M.J., Hall, N., Fung, E., White, O., Berriman, M., Hyman, R.W., Carlton, J.M., Pain, A., Nelson, K.E., Bowman, S., Paulsen, I.T., James, K., Eisen, J.A., Rutherford, K., Salzberg, S.L., Craig, A., Kyes, S., Chan, M.S., Nene, V., Shallom, S.J., Suh, B., Peterson, J., Angiuoli, S., Pertea, M., Allen, J., Selengut, J., Haft, D., Mather, M.W., Vaidya, A.B., Martin, D.M., Fairlamb, A.H., Fraunholz, M.J., Roos, D.S., Ralph, S.A., McFadden, G.I., Cummings, L.M., Subramanian, G.M., Mungall, C., Venter, J.C., Carucci, D.J., Hoffman, S.L., Newbold, C., Davis, R.W., Fraser, C.M., and Barrell, B. (2002). Genome sequence of the human malaria parasite Plasmodium falciparum. Nature *419*, 498-511.

Ghosh, A., Srinivasan, P., Abraham, E.G., Fujioka, H., and Jacobs-Lorena, M. (2003). Molecular strategies to study Plasmodium-mosquito interactions. Trends Parasitol *19*, 94-101.

Greenwood, B.M., Bojang, K., Whitty, C.J., and Targett, G.A. (2005). Malaria. Lancet *365*, 1487-1498.

Gressner, A.M., and Schafer, S. (1989). Comparison of sulphated glycosaminoglycan and hyaluronate synthesis and secretion in cultured hepatocytes, fat storing cells, and Kupffer cells. J Clin Chem Clin Biochem *27*, 141-149.

Griffiths, R.B., and Gordon, R.M. (1952). An apparatus which enables the process of feeding by mosquitoes to be observed in the tissues of a live rodent; together with an account of the ejection of saliva and its significance in Malaria. Ann Trop Med Parasitol *46*, 311-319.

Gruner, A.C., Brahimi, K., Eling, W., Konings, R., Meis, J., Aikawa, M., Daubersies, P., Guerin-Marchand, C., Mellouk, S., Snounou, G., and Druilhe, P. (2001a). The Plasmodium falciparum knob-associated PfEMP3 antigen is also expressed at pre-erythrocytic stages and induces antibodies which inhibit sporozoite invasion. Mol Biochem Parasitol *112*, 253-261.

Gruner, A.C., Brahimi, K., Letourneur, F., Renia, L., Eling, W., Snounou, G., and Druilhe, P. (2001b). Expression of the erythrocyte-binding antigen 175 in sporozoites and in liver stages of Plasmodium falciparum. J Infect Dis *184*, 892-897.

Gruner, A.C., Snounou, G., Fuller, K., Jarra, W., Renia, L., and Preiser, P.R. (2004). The Py235 proteins: glimpses into the versatility of a malaria multigene family. Microbes Infect *6*, 864-873.

Hafalla, J.C., Cockburn, I.A., and Zavala, F. (2006). Protective and pathogenic roles of CD8+ T cells during malaria infection. Parasite Immunol *28*, 15-24.

Hafalla, J.C., Morrot, A., Sano, G., Milon, G., Lafaille, J.J., and Zavala, F. (2003). Early self-regulatory mechanisms control the magnitude of CD8+ T cell responses against liver stages of murine malaria. J Immunol *171*, 964-970.

Herz, J., Qiu, S.Q., Oesterle, A., DeSilva, H.V., Shafi, S., and Havel, R.J. (1995). Initial hepatic removal of chylomicron remnants is unaffected but endocytosis is delayed in mice lacking the low density lipoprotein receptor. Proc Natl Acad Sci U S A *92*, 4611-4615.

Heussler, V., Sturm, A., and Langsley, G. (2006). Regulation of host cell survival by intracellular Plasmodium and Theileria parasites. Parasitology *132 Suppl*, S49-60.

Hill, A.V. (2006). Pre-erythrocytic malaria vaccines: towards greater efficacy. Nat Rev Immunol *6*, 21-32.

Hisaeda, H., Yasutomo, K., and Himeno, K. (2005). Malaria: immune evasion by parasites. Int J Biochem Cell Biol *37*, 700-706.

Hoffman, S.L., Subramanian, G.M., Collins, F.H., and Venter, J.C. (2002). Plasmodium, human and Anopheles genomics and malaria. Nature *415*, 702-709.

Hollingdale, M.R., Leef, J.L., McCullough, M., and Beaudoin, R.L. (1981). In vitro cultivation of the exoerythrocytic stage of Plasmodium berghei from sporozoites. Science *213*, 1021-1022.

Hollingdale, M.R., Leland, P., Leef, J.L., and Schwartz, A.L. (1983). Entry of Plasmodium berghei sporozoites into cultured cells, and their transformation into trophozoites. Am J Trop Med Hyg *32*, 685-690.

Holt, R.A., Subramanian, G.M., Halpern, A., Sutton, G.G., Charlab, R., Nusskern, D.R., Wincker, P., Clark, A.G., Ribeiro, J.M., Wides, R., Salzberg, S.L., Loftus, B., Yandell, M., Majoros, W.H., Rusch, D.B., Lai, Z., Kraft, C.L., Abril, J.F., Anthouard, V., Arensburger, P., Atkinson, P.W., Baden, H., de Berardinis, V., Baldwin, D., Benes, V., Biedler, J., Blass, C., Bolanos, R., Boscus, D., Barnstead, M., Cai, S., Center, A., Chaturverdi, K., Christophides, G.K., Chrystal, M.A., Clamp, M., Cravchik, A., Curwen, V., Dana, A., Delcher, A., Dew, I., Evans, C.A., Flanigan, M., Grundschober-Freimoser, A., Friedli, L., Gu, Z., Guan, P., Guigo, R., Hillenmeyer, M.E., Hladun, S.L., Hogan, J.R., Hong, Y.S., Hoover, J., Jaillon, O., Ke, Z., Kodira, C., Kokoza, E., Koutsos, A., Letunic, I., Levitsky, A., Liang, Y., Lin, J.J., Lobo, N.F., Lopez, J.R., Malek, J.A., McIntosh, T.C., Meister, S., Miller, J., Mobarry, C., Mongin, E., Murphy, S.D., O'Brochta, D.A., Pfannkoch, C., Qi, R., Regier, M.A., Remington, K., Shao, H., Sharakhova, M.V., Sitter, C.D., Shetty, J., Smith, T.J., Strong, R., Sun, J., Thomasova, D., Ton, L.Q., Topalis, P., Tu, Z., Unger, M.F., Walenz, B., Wang, A., Wang, J., Wang, M., Wang, X., Woodford, K.J., Wortman, J.R., Wu, M., Yao, A., Zdobnov, E.M., Zhang, H., Zhao, Q., Zhao, S., Zhu, S.C., Zhimulev, I., Coluzzi, M., della Torre, A., Roth, C.W., Louis, C., Kalush, F., Mural, R.J., Myers, E.W., Adams, M.D., Smith, H.O., Broder, S., Gardner, M.J., Fraser, C.M., Birney, E., Bork, P., Brey, P.T., Venter, J.C., Weissenbach, J., Kafatos, F.C., Collins, F.H., and Hoffman, S.L. (2002). The genome sequence of the malaria mosquito Anopheles gambiae. Science *298*, 129-149.

Hugel, F.U., Pradel, G., and Frevert, U. (1996). Release of malaria circumsporozoite protein into the host cell cytoplasm and interaction with ribosomes. Mol Biochem Parasitol *81*, 151-170.

Ishino, T., Chinzei, Y., and Yuda, M. (2005a). A Plasmodium sporozoite protein with a membrane attack complex domain is required for breaching the liver sinusoidal cell layer prior to hepatocyte infection. Cell Microbiol *7*, 199-208.

Ishino, T., Chinzei, Y., and Yuda, M. (2005b). Two proteins with 6-cys motifs are required for malarial parasites to commit to infection of the hepatocyte. Mol Microbiol *58*, 1264-1275.

Ishino, T., Yano, K., Chinzei, Y., and Yuda, M. (2004). Cell-passage activity is required for the malarial parasite to cross the liver sinusoidal cell layer. PLoS Biol *2*, E4.

Jaffe, R.I., Lowell, G.H., and Gordon, D.M. (1990). Differences in susceptibility among mouse strains to infection with Plasmodium berghei (ANKA clone) sporozoites and its

relationship to protection by gamma-irradiated sporozoites. Am J Trop Med Hyg *42*, 309-313.

Jana, S., and Paliwal, J. (2007). Novel molecular targets for antimalarial chemotherapy. Int J Antimicrob Agents *30*, 4-10.

Jethwaney, D., Lepore, T., Hassan, S., Mello, K., Rangarajan, R., Jahnen-Dechent, W., Wirth, D., and Sultan, A.A. (2005). Fetuin-A, a hepatocyte-specific protein that binds Plasmodium berghei thrombospondin-related adhesive protein: a potential role in infectivity. Infect Immun *73*, 5883-5891.

Ji, Z.S., Sanan, D.A., and Mahley, R.W. (1995). Intravenous heparinase inhibits remnant lipoprotein clearance from the plasma and uptake by the liver: in vivo role of heparan sulfate proteoglycans. J Lipid Res *36*, 583-592.

Jobe, O., Lumsden, J., Mueller, A.K., Williams, J., Silva-Rivera, H., Kappe, S.H., Schwenk, R.J., Matuschewski, K., and Krzych, U. (2007). Genetically Attenuated Plasmodium berghei Liver Stages Induce Sterile Protracted Protection that Is Mediated by Major Histocompatibility Complex Class I-Dependent Interferon- gamma -Producing CD8+ T Cells. J Infect Dis *196*, 599-607.

Johnson, J.R., Florens, L., Carucci, D.J., and Yates, J.R., 3rd. (2004). Proteomics in malaria. J Proteome Res *3*, 296-306.

Jongco, A.M., Ting, L.M., Thathy, V., Mota, M.M., and Kim, K. (2006). Improved transfection and new selectable markers for the rodent malaria parasite Plasmodium yoelii. Mol Biochem Parasitol *146*, 242-250.

Kaiser, K., Camargo, N., and Kappe, S.H. (2003). Transformation of sporozoites into early exoerythrocytic malaria parasites does not require host cells. J Exp Med *197*, 1045-1050.

Kaiser, K., Matuschewski, K., Camargo, N., Ross, J., and Kappe, S.H. (2004). Differential transcriptome profiling identifies Plasmodium genes encoding pre-erythrocytic stage-specific proteins. Mol Microbiol *51*, 1221-1232.

Kanzok, S.M., and Jacobs-Lorena, M. (2006). Entomopathogenic fungi as biological insecticides to control malaria. Trends Parasitol *22*, 49-51.

Kappe, S.H., Buscaglia, C.A., and Nussenzweig, V. (2004). Plasmodium sporozoite molecular cell biology. Annu Rev Cell Dev Biol *20*, 29-59.

Kariu, T., Ishino, T., Yano, K., Chinzei, Y., and Yuda, M. (2006). CelTOS, a novel malarial protein that mediates transmission to mosquito and vertebrate hosts. Mol Microbiol *59*, 1369-1379.

Karnasuta, C., Pavanand, K., Chantakulkij, S., Luttiwongsakorn, N., Rassamesoraj, M., Laohathai, K., Webster, H.K., and Watt, G. (1995). Complete development of the liver stage of Plasmodium falciparum in a human hepatoma cell line. Am J Trop Med Hyg *53*, 607-611.

Kester, K.E., McKinney, D.A., Tornieporth, N., Ockenhouse, C.F., Heppner, D.G., Hall, T., Krzych, U., Delchambre, M., Voss, G., Dowler, M.G., Palensky, J., Wittes, J., Cohen, J., and Ballou, W.R. (2001). Efficacy of recombinant circumsporozoite protein vaccine regimens against experimental Plasmodium falciparum malaria. J Infect Dis *183*, 640-647.

Khan, Z.M., and Vanderberg, J.P. (1991). Role of host cellular response in differential susceptibility of nonimmunized BALB/c mice to Plasmodium berghei and Plasmodium yoelii sporozoites. Infect Immun *59*, 2529-2534.

Klausner, R., and Alonso, P. (2004). An attack on all fronts. Nature *430*, 930-931.

Kooij, T.W., Carlton, J.M., Bidwell, S.L., Hall, N., Ramesar, J., Janse, C.J., and Waters, A.P. (2005). A Plasmodium whole-genome synteny map: indels and synteny breakpoints as foci for species-specific genes. PLoS Pathog *1*, e44.

Krettli, A.U., and Dantas, L.A. (2000). Which routes do Plasmodium sporozoites use for successful infections of vertebrates? Infect Immun *68*, 3064-3065.

Labaied, M., Camargo, N., and Kappe, S.H. (2007a). Depletion of the Plasmodium berghei thrombospondin-related sporozoite protein reveals a role in host cell entry by sporozoites. Mol Biochem Parasitol *153*, 158-166.

Labaied, M., Harupa, A., Dumpit, R.F., Coppens, I., Mikolajczak, S.A., and Kappe, S.H. (2007b). Plasmodium yoelii sporozoites with simultaneous deletion of P52 and P36 are completely attenuated and confer sterile immunity against infection. Infect Immun.

Leirião, P., Albuquerque, S.S., Corso, S., van Gemert, G.J., Sauerwein, R.W., Rodriguez, A., Giordano, S., and Mota, M.M. (2005a). HGF/MET signalling protects Plasmodium-infected host cells from apoptosis. Cell Microbiol *7*, 603-609.

Leirião, P., Mota, M.M., and Rodriguez, A. (2005b). Apoptotic Plasmodium-infected hepatocytes provide antigens to liver dendritic cells. J Infect Dis *191*, 1576-1581.

Lengeler, C. (2000). Insecticide-treated bednets and curtains for preventing malaria. Cochrane Database Syst Rev, CD000363.

Long, G.W., Leath, S., Schuman, R., Hollingdale, M.R., Ballou, W.R., Sim, B.K., and Hoffman, S.L. (1989). Cultivation of the exoerythrocytic stage of Plasmodium berghei in primary cultures of mouse hepatocytes and continuous mouse cell lines. In Vitro Cell Dev Biol *25*, 857-862.

Lyon, M., Deakin, J.A., and Gallagher, J.T. (1994). Liver heparan sulfate structure. A novel molecular design. J Biol Chem *269*, 11208-11215.

Lyon, M., and Gallagher, J.T. (1991). Purification and partial characterization of the major cell-associated heparan sulphate proteoglycan of rat liver. Biochem J *273(Pt 2)*, 415-422.

Malaguarnera, L., and Musumeci, S. (2002). The immune response to Plasmodium falciparum malaria. Lancet Infect Dis *2*, 472-478.

Manning, G., Whyte, D.B., Martinez, R., Hunter, T., and Sudarsanam, S. (2002). The protein kinase complement of the human genome. Science *298*, 1912-1934.

Marrelli, M.T., Li, C., Rasgon, J.L., and Jacobs-Lorena, M. (2007). Transgenic malaria-resistant mosquitoes have a fitness advantage when feeding on Plasmodium-infected blood. Proc Natl Acad Sci U S A *104*, 5580-5583.

Marrelli, M.T., Moreira, C.K., Kelly, D., Alphey, L., and Jacobs-Lorena, M. (2006). Mosquito transgenesis: what is the fitness cost? Trends Parasitol *22*, 197-202.

Marshall, P., Rohlmann, A., Nussenzweig, V., Herz, J., and Sinnis, P. (2000). Plasmodium sporozoites invade cells with targeted deletions in the LDL receptor related protein. Mol Biochem Parasitol *106*, 293-298.

Matsuoka, H., Yoshida, S., Hirai, M., and Ishii, A. (2002). A rodent malaria, Plasmodium berghei, is experimentally transmitted to mice by merely probing of infective mosquito, Anopheles stephensi. Parasitol Int *51*, 17-23.

Matuschewski, K. (2006). Getting infectious: formation and maturation of Plasmodium sporozoites in the Anopheles vector. Cell Microbiol *8*, 1547-1556.

Matuschewski, K., Nunes, A.C., Nussenzweig, V., and Menard, R. (2002). Plasmodium sporozoite invasion into insect and mammalian cells is directed by the same dual binding system. Embo J *21*, 1597-1606.

Mazier, D., Beaudoin, R.L., Mellouk, S., Druilhe, P., Texier, B., Trosper, J., Miltgen, F., Landau, I., Paul, C., Brandicourt, O., and et al. (1985). Complete development of hepatic stages of Plasmodium falciparum in vitro. Science *227*, 440-442.

Mazier, D., Collins, W.E., Mellouk, S., Procell, P.M., Berbiguier, N., Campbell, G.H., Miltgen, F., Bertolotti, R., Langlois, P., and Gentilini, M. (1987). Plasmodium ovale: in vitro development of hepatic stages. Exp Parasitol *64*, 393-400.

Mazier, D., Landau, I., Druilhe, P., Miltgen, F., Guguen-Guillouzo, C., Baccam, D., Baxter, J., Chigot, J.P., and Gentilini, M. (1984). Cultivation of the liver forms of Plasmodium vivax in human hepatocytes. Nature *307*, 367-369.

Medica, D.L., and Sinnis, P. (2005). Quantitative dynamics of Plasmodium yoelii sporozoite transmission by infected anopheline mosquitoes. Infect Immun *73*, 4363-4369.

Meis, J.F., Verhave, J.P., Meuwissen, J.H., Jap, P.H., Princen, H.M., and Yap, S.H. (1984). Fine structure of Plasmodium berghei exoerythrocytic forms in cultured primary rat hepatocytes. Cell Biol Int Rep *8*, 755-765.

Meister, G., and Tuschl, T. (2004). Mechanisms of gene silencing by double-stranded RNA. Nature *431*, 343-349.

Menard, R. (2000). The journey of the malaria sporozoite through its hosts: two parasite proteins lead the way. Microbes Infect *2*, 633-642.

Michalakis, Y., and Renaud, F. (2005). Malaria: fungal allies enlisted. Nature *435*, 891-893.

Mikolajczak, S.A., Jacobs-Lorena, V., MacKellar, D.C., Camargo, N., and Kappe, S.H. (2007). L-FABP is a critical host factor for successful malaria liver stage development. Int J Parasitol *37*, 483-489.

Mikolajczak, S.A., and Kappe, S.H. (2006). A clash to conquer: the malaria parasite liver infection. Mol Microbiol *62*, 1499-1506.

Millet, P., Landau, I., Baccam, D., Miltgen, F., and Peters, W. (1985). [Cultivation of exo-erythrocytic schizonts of rodent Plasmodium in hepatocytes: a new experimental model for chemotherapy of malaria]. C R Acad Sci III *301*, 403-406.

Monasch, R., Reinisch, A., Steketee, R.W., Korenromp, E.L., Alnwick, D., and Bergevin, Y. (2004). Child coverage with mosquito nets and malaria treatment from population-based surveys in african countries: a baseline for monitoring progress in roll back malaria. Am J Trop Med Hyg *71*, 232-238.

Moorthy, V.S., Good, M.F., and Hill, A.V. (2004). Malaria vaccine developments. Lancet *363*, 150-156.

Moreira, L.A., Ghosh, A.K., Abraham, E.G., and Jacobs-Lorena, M. (2002). Genetic transformation of mosquitoes: a quest for malaria control. Int J Parasitol *32*, 1599-1605.

Morosan, S., Hez-Deroubaix, S., Lunel, F., Renia, L., Giannini, C., Van Rooijen, N., Battaglia, S., Blanc, C., Eling, W., Sauerwein, R., Hannoun, L., Belghiti, J., Brechot, C., Kremsdorf, D., and Druilhe, P. (2006). Liver-stage development of Plasmodium falciparum, in a humanized mouse model. J Infect Dis *193*, 996-1004.

Mota, M.M., Hafalla, J.C., and Rodriguez, A. (2002). Migration through host cells activates Plasmodium sporozoites for infection. Nat Med *8*, 1318-1322.

Mota, M.M., Pradel, G., Vanderberg, J.P., Hafalla, J.C., Frevert, U., Nussenzweig, R.S., Nussenzweig, V., and Rodriguez, A. (2001a). Migration of Plasmodium sporozoites through cells before infection. Science *291*, 141-144.

Mota, M.M., and Rodriguez, A. (2000). Plasmodium yoelii: efficient in vitro invasion and complete development of sporozoites in mouse hepatic cell lines. Exp Parasitol *96*, 257-259.

Mota, M.M., and Rodriguez, A. (2002). Invasion of mammalian host cells by Plasmodium sporozoites. Bioessays *24*, 149-156.

Mota, M.M., Thathy, V., Nussenzweig, R.S., and Nussenzweig, V. (2001b). Gene targeting in the rodent malaria parasite Plasmodium yoelii. Mol Biochem Parasitol *113*, 271-278.

Mueller, A.K., Camargo, N., Kaiser, K., Andorfer, C., Frevert, U., Matuschewski, K., and Kappe, S.H. (2005a). Plasmodium liver stage developmental arrest by depletion of a protein at the parasite-host interface. Proc Natl Acad Sci U S A *102*, 3022-3027.

Mueller, A.K., Deckert, M., Heiss, K., Goetz, K., Matuschewski, K., and Schluter, D. (2007). Genetically Attenuated Plasmodium berghei Liver Stages Persist and Elicit Sterile Protection Primarily via CD8 T Cells. Am J Pathol.

Mueller, A.K., Labaied, M., Kappe, S.H., and Matuschewski, K. (2005b). Genetically modified Plasmodium parasites as a protective experimental malaria vaccine. Nature *433*, 164-167.

Nabarro, D.N., and Tayler, E.M. (1998). The "roll back malaria" campaign. Science *280*, 2067-2068.

Natarajan, R., Thathy, V., Mota, M.M., Hafalla, J.C., Menard, R., and Vernick, K.D. (2001). Fluorescent Plasmodium berghei sporozoites and pre-erythrocytic stages: a new tool to study mosquito and mammalian host interactions with malaria parasites. Cell Microbiol *3*, 371-379.

Nature. (2001). The Human Genome, Nature *409*, 745-964.

Nobel. (1967). Nobel Lectures, Physiology or Medicine 1901-1921. Elsevier Publishing Company, Amsterdam.

Nussenzweig, R.S., Vanderberg, J., Most, H., and Orton, C. (1967). Protective immunity produced by the injection of x-irradiated sporozoites of plasmodium berghei. Nature *216*, 160-162.

Ono, T., Tadakuma, T., and Rodriguez, A. (2007). Plasmodium yoelii yoelii 17XNL constitutively expressing GFP throughout the life cycle. Exp Parasitol *115*, 310-313.

Pancake, S.J., Holt, G.D., Mellouk, S., and Hoffman, S.L. (1992). Malaria sporozoites and circumsporozoite proteins bind specifically to sulfated glycoconjugates. J Cell Biol *117*, 1351-1357.

Pasquetto, V., Fidock, D.A., Gras, H., Badell, E., Eling, W., Ballou, W.R., Belghiti, J., Tartar, A., and Druilhe, P. (1997). Plasmodium falciparum sporozoite invasion is inhibited by naturally acquired or experimentally induced polyclonal antibodies to the STARP antigen. Eur J Immunol *27*, 2502-2513.

Pierce, A., Lyon, M., Hampson, I.N., Cowling, G.J., and Gallagher, J.T. (1992). Molecular cloning of the major cell surface heparan sulfate proteoglycan from rat liver. J Biol Chem *267*, 3894-3900.

Pileri, P., Uematsu, Y., Campagnoli, S., Galli, G., Falugi, F., Petracca, R., Weiner, A.J., Houghton, M., Rosa, D., Grandi, G., and Abrignani, S. (1998). Binding of hepatitis C virus to CD81. Science *282*, 938-941.

Pinzon-Ortiz, C., Friedman, J., Esko, J., and Sinnis, P. (2001). The binding of the circumsporozoite protein to cell surface heparan sulfate proteoglycans is required for plasmodium sporozoite attachment to target cells. J Biol Chem *276*, 26784-26791.

Ponnudurai, T., Lensen, A.H., van Gemert, G.J., Bolmer, M.G., and Meuwissen, J.H. (1991). Feeding behaviour and sporozoite ejection by infected Anopheles stephensi. Trans R Soc Trop Med Hyg *85*, 175-180.

Pradel, G., and Frevert, U. (2001). Malaria sporozoites actively enter and pass through rat Kupffer cells prior to hepatocyte invasion. Hepatology *33*, 1154-1165.

Pradel, G., Garapaty, S., and Frevert, U. (2002). Proteoglycans mediate malaria sporozoite targeting to the liver. Mol Microbiol *45*, 637-651.

Pradel, G., Garapaty, S., and Frevert, U. (2004). Kupffer and stellate cell proteoglycans mediate malaria sporozoite targeting to the liver. Comp Hepatol *3 Suppl 1*, S47.

Preiser, P.R., Khan, S., Costa, F.T., Jarra, W., Belnoue, E., Ogun, S., Holder, A.A., Voza, T., Landau, I., Snounou, G., and Renia, L. (2002). Stage-specific transcription of distinct repertoires of a multigene family during Plasmodium life cycle. Science *295*, 342-345.

Prudêncio, M., Rodrigues, C.D., Ataide, R., and Mota, M.M. (2007). Dissecting in vitro host cell infection by Plasmodium sporozoites using flow cytometry. Cell Microbiol.

Prudêncio, M., Rodriguez, A., and Mota, M.M. (2006). The silent path to thousands of merozoites: the Plasmodium liver stage. Nat Rev Microbiol *4*, 849-856.

Rapraeger, A.C., Krufka, A., and Olwin, B.B. (1991). Requirement of heparan sulfate for bFGF-mediated fibroblast growth and myoblast differentiation. Science *252*, 1705-1708.

Rasti, N., Wahlgren, M., and Chen, Q. (2004). Molecular aspects of malaria pathogenesis. FEMS Immunol Med Microbiol *41*, 9-26.

Rathore, D., McCutchan, T.F., Garboczi, D.N., Toida, T., Hernaiz, M.J., LeBrun, L.A., Lang, S.C., and Linhardt, R.J. (2001). Direct measurement of the interactions of glycosaminoglycans and a heparin decasaccharide with the malaria circumsporozoite protein. Biochemistry *40*, 11518-11524.

Rathore, D., Sacci, J.B., de la Vega, P., and McCutchan, T.F. (2002). Binding and invasion of liver cells by Plasmodium falciparum sporozoites. Essential involvement of the amino terminus of circumsporozoite protein. J Biol Chem *277*, 7092-7098.

Remme, J.H., Binka, F., and Nabarro, D. (2001). Toward a framework and indicators for monitoring Roll Back Malaria. Am J Trop Med Hyg *64*, 76-84.

Richie, T.L., and Saul, A. (2002). Progress and challenges for malaria vaccines. Nature *415*, 694-701.

Rohlmann, A., Gotthardt, M., Hammer, R.E., and Herz, J. (1998). Inducible inactivation of hepatic LRP gene by cre-mediated recombination confirms role of LRP in clearance of chylomicron remnants. J Clin Invest *101*, 689-695.

Rosenberg, R. (1992). Ejection of malaria sporozoites by feeding mosquitoes. Trans R Soc Trop Med Hyg *86*, 109.

Rosenberg, R., Wirtz, R.A., Schneider, I., and Burge, R. (1990). An estimation of the number of malaria sporozoites ejected by a feeding mosquito. Trans R Soc Trop Med Hyg *84*, 209-212.

Sacci, J.B., Jr., Alam, U., Douglas, D., Lewis, J., Tyrrell, D.L., Azad, A.F., and Kneteman, N.M. (2006). Plasmodium falciparum infection and exoerythrocytic development in mice with chimeric human livers. Int J Parasitol *36*, 353-360.

Sachs, J., and Malaney, P. (2002). The economic and social burden of malaria. Nature *415*, 680-685.

Sachs, J.D. (2002). A new global effort to control malaria. Science *298*, 122-124.

Sachse, C., Krausz, E., Kronke, A., Hannus, M., Walsh, A., Grabner, A., Ovcharenko, D., Dorris, D., Trudel, C., Sonnichsen, B., and Echeverri, C.J. (2005). High-throughput RNA interference strategies for target discovery and validation by using synthetic short interfering RNAs: functional genomics investigations of biological pathways. Methods Enzymol *392*, 242-277.

Sattabongkot, J., Yimamnuaychoke, N., Leelaudomlipi, S., Rasameesoraj, M., Jenwithisuk, R., Coleman, R.E., Udomsangpetch, R., Cui, L., and Brewer, T.G. (2006). Establishment of a human hepatocyte line that supports in vitro development of the exo-erythrocytic stages of the malaria parasites Plasmodium falciparum and P. vivax. Am J Trop Med Hyg *74*, 708-715.

Schapira, A. (2004). DDT still has a role in the fight against malaria. Nature *432*, 439.

Scheller, L.F., Wirtz, R.A., and Azad, A.F. (1994). Susceptibility of different strains of mice to hepatic infection with Plasmodium berghei. Infect Immun *62*, 4844-4847.

Schlitzer, M. (2007). Malaria Chemotherapeutics Part I: History of Antimalarial Drug Development, Currently Used Therapeutics, and Drugs in Clinical Development. ChemMedChem.

Schofield, L., and Grau, G.E. (2005). Immunological processes in malaria pathogenesis. Nat Rev Immunol *5*, 722-735.

Scholte, E.J., Ng'habi, K., Kihonda, J., Takken, W., Paaijmans, K., Abdulla, S., Killeen, G.F., and Knols, B.G. (2005). An entomopathogenic fungus for control of adult African malaria mosquitoes. Science *308*, 1641-1642.

Science. (2001). The Human Genome, Science *91*, 1145-1434.

Shakibaei, M., and Frevert, U. (1996). Dual interaction of the malaria circumsporozoite protein with the low density lipoprotein receptor-related protein (LRP) and heparan sulfate proteoglycans. J Exp Med *184*, 1699-1711.

Sherman, I.W. (1998). A brief history of malaria and discovery of the parasite's life cycle. In: Sherman IW, editor. Malaria: Parasite Biology, Pathogenesis, and Protection. ASM Press, Washington DC, 3-10.

Shin, S.C., Vanderberg, J.P., and Terzakis, J.A. (1982). Direct infection of hepatocytes by sporozoites of Plasmodium berghei. J Protozool *29*, 448-454.

Shortt, H.E., and Garnham, P.C.C. (1948). Pre-erythrocytic stages in mammalian malaria parasites. . Nature *161*, 126.

Sidjanski, S., and Vanderberg, J.P. (1997). Delayed migration of Plasmodium sporozoites from the mosquito bite site to the blood. Am J Trop Med Hyg *57*, 426-429.

Sigler, C.I., Leland, P., and Hollingdale, M.R. (1984). In vitro infectivity of irradiated Plasmodium berghei sporozoites to cultured hepatoma cells. Am J Trop Med Hyg *33*, 544-547.

Silvie, O., Charrin, S., Billard, M., Franetich, J.F., Clark, K.L., van Gemert, G.J., Sauerwein, R.W., Dautry, F., Boucheix, C., Mazier, D., and Rubinstein, E. (2006a). Cholesterol contributes to the organization of tetraspanin-enriched microdomains and to CD81-dependent infection by malaria sporozoites. J Cell Sci *119*, 1992-2002.

Silvie, O., Franetich, J.F., Boucheix, C., Rubinstein, E., and Mazier, D. (2007). Alternative invasion pathways for Plasmodium berghei sporozoites. Int J Parasitol *37*, 173-182.

Silvie, O., Franetich, J.F., Charrin, S., Mueller, M.S., Siau, A., Bodescot, M., Rubinstein, E., Hannoun, L., Charoenvit, Y., Kocken, C.H., Thomas, A.W., Van Gemert, G.J., Sauerwein, R.W., Blackman, M.J., Anders, R.F., Pluschke, G., and Mazier, D. (2004). A role for apical membrane antigen 1 during invasion of hepatocytes by Plasmodium falciparum sporozoites. J Biol Chem *279*, 9490-9496.

Silvie, O., Greco, C., Franetich, J.F., Dubart-Kupperschmitt, A., Hannoun, L., van Gemert, G.J., Sauerwein, R.W., Levy, S., Boucheix, C., Rubinstein, E., and Mazier, D. (2006b). Expression of human CD81 differently affects host cell susceptibility to malaria sporozoites depending on the Plasmodium species. Cell Microbiol *8*, 1134-1146.

Silvie, O., Rubinstein, E., Franetich, J.F., Prenant, M., Belnoue, E., Renia, L., Hannoun, L., Eling, W., Levy, S., Boucheix, C., and Mazier, D. (2003). Hepatocyte CD81 is required for Plasmodium falciparum and Plasmodium yoelii sporozoite infectivity. Nat Med *9*, 93-96.

Sinnis, P., Clavijo, P., Fenyo, D., Chait, B.T., Cerami, C., and Nussenzweig, V. (1994). Structural and functional properties of region II-plus of the malaria circumsporozoite protein. J Exp Med *180*, 297-306.

Sinnis, P., and Coppi, A. (2007). A long and winding road: The Plasmodium sporozoite's journey in the mammalian host. Parasitol Int *56*, 171-178.

Sinnis, P., and Febbraio, M. (2002). Plasmodium yoelii sporozoites infect CD36-deficient mice. Exp Parasitol *100*, 12-16.

Sinnis, P., Willnow, T.E., Briones, M.R., Herz, J., and Nussenzweig, V. (1996). Remnant lipoproteins inhibit malaria sporozoite invasion of hepatocytes. J Exp Med *184*, 945-954.

Smith, J.E., Meis, J.F., Ponnudurai, T., Verhave, J.P., and Moshage, H.J. (1984). In-vitro culture of exoerythrocytic form of Plasmodium falciparum in adult human hepatocytes. Lancet *2*, 757-758.

Stoute, J.A., Slaoui, M., Heppner, D.G., Momin, P., Kester, K.E., Desmons, P., Wellde, B.T., Garcon, N., Krzych, U., and Marchand, M. (1997). A preliminary evaluation of a recombinant circumsporozoite protein vaccine against Plasmodium falciparum malaria. RTS,S Malaria Vaccine Evaluation Group. N Engl J Med *336*, 86-91.

Sturm, A., Amino, R., van de Sand, C., Regen, T., Retzlaff, S., Rennenberg, A., Krueger, A., Pollok, J.M., Menard, R., and Heussler, V.T. (2006). Manipulation of host hepatocytes by the malaria parasite for delivery into liver sinusoids. Science *313*, 1287-1290.

Sturm, A., and Heussler, V. (2007). Live and let die: manipulation of host hepatocytes by exoerythrocytic Plasmodium parasites. Med Microbiol Immunol *196*, 127-133.

Sultan, A.A., Briones, M.R., Gerwin, N., Carroll, M.C., and Nussenzweig, V. (1997). Sporozoites of Plasmodium yoelii infect mice with targeted deletions in ICAM-1 and ICAM-2 or complement components C3 and C4. Mol Biochem Parasitol *88, 263-266*.

Tarun, A.S., Baer, K., Dumpit, R.F., Gray, S., Lejarcegui, N., Frevert, U., and Kappe, S.H. (2006). Quantitative isolation and in vivo imaging of malaria parasite liver stages. Int J Parasitol *36*, 1283-1293.

Tarun, A.S., Dumpit, R.F., Camargo, N., Labaied, M., Liu, P., Takagi, A., Wang, R., and Kappe, S.H. (2007). Protracted Sterile Protection with Plasmodium yoelii Pre-erythrocytic Genetically Attenuated Parasite Malaria Vaccines Is Independent of Significant Liver-Stage Persistence and Is Mediated by CD8+ T Cells. J Infect Dis *196*, 608-616.

Thomas, M.B., and Read, A.F. (2007). Can fungal biopesticides control malaria? Nat Rev Microbiol *5*, 377-383.

Todryk, S.M., and Hill, A.V. (2007). Malaria vaccines: the stage we are at. Nat Rev Microbiol *5*, 487-489.

Turusov, V., Rakitsky, V., and Tomatis, L. (2002). Dichlorodiphenyltrichloroethane (DDT): ubiquity, persistence, and risks. Environ Health Perspect *110*, 125-128.

Uni, S., Aikawa, M., Collins, W.E., Campbell, C.C., and Hollingdale, M.R. (1985). Electron microscopy of Plasmodium vivax exoerythrocytic schizonts grown in vitro in a hepatoma cell line. Am J Trop Med Hyg *34*, 1017-1021.

Usynin, I., Klotz, C., and Frevert, U. (2007). Malaria circumsporozoite protein inhibits the respiratory burst in Kupffer cells. Cell Microbiol.

van de Sand, C., Horstmann, S., Schmidt, A., Sturm, A., Bolte, S., Krueger, A., Lutgehetmann, M., Pollok, J.M., Libert, C., and Heussler, V.T. (2005). The liver stage of Plasmodium berghei inhibits host cell apoptosis. Mol Microbiol *58*, 731-742.

van Dijk, M.R., Douradinha, B., Franke-Fayard, B., Heussler, V., van Dooren, M.W., van Schaijk, B., van Gemert, G.J., Sauerwein, R.W., Mota, M.M., Waters, A.P., and Janse, C.J. (2005). Genetically attenuated, P36p-deficient malarial sporozoites induce protective immunity and apoptosis of infected liver cells. Proc Natl Acad Sci U S A *102*, 12194-12199.

van Dijk, M.R., Janse, C.J., and Waters, A.P. (1996). Expression of a Plasmodium gene introduced into subtelomeric regions of Plasmodium berghei chromosomes. Science *271*, 662-665.

Vanderberg, J.P. (1977). Plasmodium berghei: quantitation of sporozoites injected by mosquitoes feeding on a rodent host. Exp Parasitol *42*, 169-181.

Vanderberg, J.P., and Frevert, U. (2004). Intravital microscopy demonstrating antibody-mediated immobilisation of Plasmodium berghei sporozoites injected into skin by mosquitoes. Int J Parasitol *34*, 991-996.

Vangapandu, S., Jain, M., Kaur, K., Patil, P., Patel, S.R., and Jain, R. (2007). Recent advances in antimalarial drug development. Med Res Rev *27*, 65-107.

Vaughan, J.A., Scheller, L.F., Wirtz, R.A., and Azad, A.F. (1999). Infectivity of Plasmodium berghei sporozoites delivered by intravenous inoculation versus mosquito bite: implications for sporozoite vaccine trials. Infect Immun *67*, 4285-4289.

Vlachou, D., Schlegelmilch, T., Runn, E., Mendes, A., and Kafatos, F.C. (2006). The developmental migration of Plasmodium in mosquitoes. Curr Opin Genet Dev *16*, 384-391.

Wang, Q., Brown, S., Roos, D.S., Nussenzweig, V., and Bhanot, P. (2004). Transcriptome of axenic liver stages of Plasmodium yoelii. Mol Biochem Parasitol *137*, 161-168.

Wengelnik, K., Spaccapelo, R., Naitza, S., Robson, K.J., Janse, C.J., Bistoni, F., Waters, A.P., and Crisanti, A. (1999). The A-domain and the thrombospondin-related motif of Plasmodium falciparum TRAP are implicated in the invasion process of mosquito salivary glands. Embo J *18*, 5195-5204.

WHO, and UNICEF. (2000). WHO Expert Committee on Malaria. Twentieth report. (WHO technical report series; 892) World Health Organization and

UNICEF (2000) *(available at www.rbm.who.int/docs/ecr20.pdf)*.

WHO, and UNICEF. (2004). Report of the fourth meeting of the global collaboration for development of pesticides for public health (WHO/CDS/WHOPES/GCDPP/2004.8). World Health Organization and UNICEF *(available at http://whqlibdoc.who.int/hq/2004/WHO_CDS_WHOPES_GCDPP_2004.8.pdf)*.

WHO, and UNICEF. (2005). World Malaria Report 2005. World Health Organization and UNICEF *(available at http://rbm.who.int/wmr2005)*.

Willnow, T.E., Sheng, Z., Ishibashi, S., and Herz, J. (1994). Inhibition of hepatic chylomicron remnant uptake by gene transfer of a receptor antagonist. Science *264*, 1471-1474.

Wisse, E., De Zanger, R.B., Charels, K., Van Der Smissen, P., and McCuskey, R.S. (1985). The liver sieve: considerations concerning the structure and function of endothelial fenestrae, the sinusoidal wall and the space of Disse. Hepatology *5*, 683-692.

Yamauchi, L.M., Coppi, A., Snounou, G., and Sinnis, P. (2007). Plasmodium sporozoites trickle out of the injection site. Cell Microbiol *9*, 1215-1222.

Yayon, A., Klagsbrun, M., Esko, J.D., Leder, P., and Ornitz, D.M. (1991). Cell surface, heparin-like molecules are required for binding of basic fibroblast growth factor to its high affinity receptor. Cell *64*, 841-848.

Ying, P., Shakibaei, M., Patankar, M.S., Clavijo, P., Beavis, R.C., Clark, G.F., and Frevert, U. (1997). The malaria circumsporozoite protein: interaction of the conserved regions I and II-plus with heparin-like oligosaccharides in heparan sulfate. Exp Parasitol *85*, 168-182.

Chapter 2 | Results

Identification of host molecules involved in the liver stage of malaria infection using transcriptional profiling followed by RNAi analysis

Sónia S. Albuquerque[1,2]*, Cristina D. Rodrigues[1,2]*, Miguel Prudêncio[1,2]*, Michael Hannus[3], Cécilie Martin[3], Sabrina Epiphanio[1,2], Geert-Jan van Gemert[4], Adrian J.F. Luty[4], Robert Sauerwein[4], Christophe J. Echeverri[3] and Maria M. Mota[1,2]#

[1]Unidade de Malária, Instituto de Medicina Molecular, Universidade de Lisboa, 1649-028 Lisboa, Portugal. [2]Instituto Gulbenkian de Ciência, 2780-156 Oeiras, Portugal. [3]Cenix BioScience GmbH, Tatzberg 47, Dresden 01307, Germany. [4]Department of Medical Microbiology, University Medical Centre, P.O. Box 9101, 6500 HB Nijmegen, The Netherlands.

*These authors contributed equally to this work.

#Correspondence should be addressed to M.M.M. (mmota@fm.ul.pt).

After entering their mammalian host via the bite of an *Anopheles* mosquito, *Plasmodium* sporozoites are arrested in the liver. There, they traverse several hepatocytes before invading the one in which they develop and multiply into thousands of merozoites (Mota *et al.*, 2001). *Plasmodium* strategies that enable its survival and development inside host liver cells remain a poorly understood, yet essential step in malaria infection (Prudêncio *et al.*, 2006). A molecular analysis of this process was initiated using a post-genomics approach that comprises host cell transcriptional profiling of *P. berghei*-infected hepatoma cells followed by functional testing of identified genes using RNA interference (RNAi). The data revealed differential expression patterns for 611 host genes, with the largest proportion correlating specifically with the early stages of the infection process. Of these genes, RNAi-induced loss of functions implicated two transcription factors, Atf3 and c-Myc, whose silencing leads, respectively, to a significant increase and decrease in *Plasmodium* hepatocyte infection levels. The *in vitro* result was confirmed *in vivo* by our finding that Atf3-deficient mice have significantly higher liver parasite loads than wild-type mice.

The pre-eminent tropical malaria disease is one of the top three communicable diseases in the world today. Forty percent of the world's population is at risk of infection, with 500 million clinical cases every year and up to three million deaths, mostly of children, being attributable to this disease (Sachs and Malaney, 2002). Malaria infection is initiated when *Plasmodium* sporozoites are injected into a mammalian host during the bite of an infected female *Anopheles* mosquito while probing for a blood meal. These sporozoites rapidly reach the liver, where inside hepatocytes they develop into thousands of merozoites within 2 to 16 days, depending on the *Plasmodium* species [reviewed in (Prudêncio *et al.*, 2006)]. When released into the blood stream each merozoite rapidly invades an erythrocyte, thus initiating the erythrocytic stage of infection, responsible for all the malaria symptoms and associated pathology. Although clinically silent, the pre-erythrocytic stage is critical for malaria infection establishment and constitutes an ideal target for potential anti-malarial vaccines or prophylactic treatments [reviewed in (Cunha-Rodrigues *et al.*, 2006)]. However, the host factors that constitute an adequate environment for sporozoite development within hepatocytes remain largely unknown and consequently their identification along with the underlying molecular mechanisms in which they participate are extremely important. With the aim of identifying such factors, we have used an established *in vitro* malaria model, infection of mouse hepatoma Hepa1-6 cells with *P. berghei* sporozoites (Mota and Rodriguez, 2000), to identify host factors involved in *Plasmodium*-host cell interactions. Initially, a genome-wide microarray technology was employed to define the temporal host cell transcriptional response to *Plasmodium* sporozoite infection. The transcriptome of infected cells was compared with that of non-infected cells using Affymetrix oligonucleotide chips.

Plasmodium sporozoite infection *in vitro* is characterized by a very low efficiency, with an average of only 2.7 ± 0.7 % infected cells (n=8) in our chosen model. Therefore, *P. berghei* sporozoites expressing Green Fluorescent Protein (GFP) (Franke-Fayard *et al.*, 2004) during all stages of parasite development (including the stages within hepatocytes) were used in cell infection and the GFP-positive (GFP+) population, i.e. *Plasmodium* infected cells, were isolated from the total cell population by Fluorescence Activated Cell Sorting (FACS). In order to obtain an overview of the host cell response to parasite development until it reaches a fully replicating schizont, infected samples were collected at four different time points post-infection (p.i.), namely 6 h (early infection), 12 h (intermediate development), 18 h (early parasite replication) and 24 h (late parasite replication and differentiation). *In vitro* Hepa1-6 infection with GFP-expressing *P. berghei* always yielded infection levels lower than 4% and the proportion

of infected cells decreased throughout the infection period (Figure 1a, b), which can be explained by the fact that infected cells might not cope with parasite development and/or by cell proliferation through time and, therefore, dilution of the infected cell population. After selection by FACS, the infected cell population adhered successfully, did not show any morphological defect and was able to support parasite development (Figure 1c). In parallel, control non-infected samples were prepared by incubating cells with salivary glands material obtained from uninfected mosquitoes.

For each selected time point, two replicate samples were analyzed in two independent experiments. RNA obtained from an average of $7x10^4$ cells per sample was processed to obtain labeled cRNA, which was then hybridized to the oligonucleotide GeneChip® Mouse Genome 430 2.0 Array (Affymetrix), which represents the whole mouse transcriptome. Comparison between non-infected and infected samples was carried out using a Fold Change (FC) ratio threshold of 1.4 (putative up-regulation or down-regulation). To exclude false positives due to cross-hybridization of parasite RNA with the mouse probes, *P. berghei* sporozoites were cultured axenically (without intracellular residence in host hepatocytes) (Kaiser *et al.*, 2003) and samples were collected at the same time points as those used when the parasites were incubated with cells. cRNA from axenic cultures of *P. berghei* sporozoites was pooled and hybridized with the same GeneChip type used for the cell samples. No match was found between the genes differentially expressed in the array incubated with *P. berghei* infected cells and the genes expressed in the array incubated with parasite cRNA, indicating that the parasite RNA did not interfere with the mouse expression profiles obtained in the infected samples.

The comparison of the transcriptome of infected cells with that of non-infected cells at the four time points post-infection assessed in this study, reveals a total of 611 genes differentially expressed during infection of Hepa1-6 cells by GFP-expressing *P. berghei* sporozoites (Figure 2a and Supplementary Table 1a,b). A hierarchical clustering analysis shows a clear segregation between non-infected (n=8) and infected cell samples (n=8) (Figure 2a). These results suggest that *Plasmodium* parasites induce host cell responses during their development within the host cell. Interestingly, we find that the number of differentially expressed host genes decreases, from 330 at 6h to 115 at 24 hours post-infection (Figure 2b). This suggests that the initial invasion of hepatocytes by *Plasmodium* leads to more profound changes in the host cell gene expression than the subsequent intracellular parasite development occurring within the study's timeframe. Indeed, these early effects may reflect host cell responses to the known traversal of sporozoites through several hepatocytes, which precedes the final

productive infection event (Mota *et al.*, 2001; Frevert *et al.*, 2005) and leads to changes at the microenvironment level (Carrolo *et al.*, 2003).

In order to determine which of these host cell changes modulate the infection process, we sought to manipulate the expression levels of a selection of these genes prior to and during infection. To this end, we used RNA interference (RNAi) to silence the expression of 50 genes deemed of highest priority based on our transcriptional profiling results. Of these, 46 genes were among those differentially expressed during infection (a FC ratio threshold of 1.2 was applied) (Figure 2c and Supplementary Table 2). Moreover, 4 additional genes were chosen based on gene network analysis with the Ingenuity Pathway Software (Ingenuity Systems, USA; www.ingenuity.com). This software was used to perform a dynamic computational analyses of the microarray results in terms of gene networks formed by the genes differentially expressed throughout infection and also other associated genes, for which molecular interaction information was obtained from the Ingenuity Pathway Knowledge Base. The biological networks included information such as the gene molecular interactions, functions and pathways and revealed recurrent genes that, although not differentially expressed during infection, are tightly associated to the later (Supplementary Figure 1a-d and Supplementary Table 3). These genes, referred to as "central genes", are mostly kinases or transcription factors, which are regulated at the phosphorilation level and therefore did not appear as modulated at the transcriptional level.

Each of the 50 selected genes was targeted with three different small interfering RNAs (siRNAs) individually and in triplicate samples, following the experimental workflow summarized in Figure 3a. Briefly, each siRNA was transfected into Hepa1-6 cells which were seeded 24 hours earlier in 96-well plates. Forty-eight hours later cells were infected with *P. berghei* sporozoites freshly extracted from the salivary glands of *Anopheles stephensi* mosquitoes. Infected samples were fixed 24 hours after sporozoite addition, immuno-stained for nuclear DNA, host cell actin and *Plasmodium* EEF-specific antigen. Infection rates were then quantified with fluorescence microscopy and automated image analysis. Basically, the number of stained EEFs that developed inside Hepa1-6 cells was determined and normalized to the cell confluency, quantified through the host cell actin staining, to account for potential differences in the total cell surface available for infection in each well. As controls, untransfected samples and cells transfected with a negative control siRNA not targeting any annotated genes in the mouse genome were used. In order to compare the data between the different experimental plates the infection rate in each experimental well was calculated as a percentage of the negative control infection rate, which was considered as 100%. To account for cell proliferation or toxicity effects, the infection

data obtained through the described analysis was plotted against the number of cell nuclei in the same experimental well, calculated as a percentage of the average number of nuclei within each experimental plate.

The first screening pass includes data from two independent runs for all the tested siRNAs. The genes for which treatment with at least one siRNA yielded a statistically significant infection rate increase or decrease greater or smaller than one standard deviation (s.d.) of the average of all the experimental sample data were selected to undergo a second confirmation pass (Figure 3b). A total of 11 out of the 50 initial genes, corresponding to 22% of the screened genes, were chosen for the second screening pass (Figure 3b and Supplementary Table 4 and 7). From these 11 genes there are: (i) two genes, Fos and c-Myc, for which two distinct siRNAs lead to an increase and decrease in infection, respectively; (ii) six genes, Atf3, Bst1, Cebpb, Kif5c, Slc7a11 and Zbtb20, for which one siRNAs leads to an increase and (iii) three genes, A130090K04RIK, Ldlr and Src, for which one siRNA leads to a decrease in infection rate (see Supplementary Table 4 and 7). In this confirmation round each gene was re-assayed with a set of three independent siRNAs, i.e., the siRNAs from the first screening pass were re-assayed and one or two additional siRNAs, depending on the gene, were designed and included in the experiment (Figure 3c). The experimental procedure and data analysis performed in the second screening pass was the same as the one used in the first screening pass, already described above. To ensure that the observed infection phenotype is due to the siRNA specific-gene silencing and not to siRNA sequence-dependent off-target effects [see (Echeverri and Perrimon, 2006)] in this second pass only the genes for which at least two distinct siRNAs reproducibly yield the same *Plasmodium* infection outcome were considered as candidate genes. Two genes, Atf3 and c-Myc yielded a statistically significant (P < 0.05) infection phenotype with two distinct siRNAs (Figure 3c and Supplementary Table 5 and 7). These genes underwent a final confirmation pass in which the levels of specific-gene silencing were determined in parallel with the infection phenotype. Briefly, as described previously, siRNAs were transfected individually into Hepa1-6 cells and, 48h later, cells were either infected with *P. berghei* sporozoites or lysed for quantitative RT-PCR (qRT-PCR) analysis of the target mRNA remaining level at the time of sporozoite addition. Analysis of the infection phenotype plotted against cell nuclei revealed an effect on the infection outcome greater or smaller than 1 s.d. of the untreated and negative control samples for both genes with at least two distinct siRNAs (Figure 4a). Actually, Atf3 silencing with all the six siRNAs tested led to a statistically significant (P < 0,05) increase in infection which correlated well with Atf3 mRNA remaining levels (Figure 4b and Supplementary Table 6 and 7). On the other

hand, c-Myc silencing effect at the time of infection was only statistically significant with two out of the four independent siRNAs tested (Figure 4b and Supplementary Table 6 and 7).

The combination of the microarray and RNAi approaches allowed the identification of two host genes Atf3 and c-Myc, which likely play a role during infection of host hepatocytes by *Plasmodium*. Nevertheless, it should not be disregarded that from all the genes differentially expressed throughout infection only about of 8% were selected to undergo a functional confirmation by RNAi and, moreover, the present RNAi screen data does not completely rule out the possible involvement of other genes among those tested since negative results in RNAi screens are generally inconclusive [see (Echeverri *et al.*, 2006)]. Therefore, future follow-up studies will be extremely valuable to elucidate the potential participation of other host genes and also to characterize the function(s) of the two genes already implicated in *Plasmodium* infection in the present study.

The c-Myc protein, encoded by the myelocytomatosis oncogene, is a basic region helix–loop–helix leucine zipper transcription factor and is involved in the regulation of cellular proliferation, apoptosis and cell growth [reviewed in (Dang, 1999; Levens, 2002)]. In particular, c-Myc was shown to regulate the size and ploidy of hepatocytes, being involved in liver regeneration (Baena *et al.*, 2005). c-Myc expression promotes the transition from G0/G1 to S phase of the cell cycle in multiple cell types, including hepatocytes, by regulating cyclin/cyclin-dependent kinase complexes (Obaya *et al.*, 1999) while the absence of sufficient c-Myc turns hepatocytes susceptible to TNF-induced apoptosis and necrosis (Liu *et al.*, 2000).

In the present work we observed that, although not differentially expressed throughout *Plasmodium* infection, this gene appeared as a central gene in the microarray analysis and, moreover, when silenced by RNAi a decrease in infection was observed. Therefore, c-Myc seems to play a role in *Plasmodium* infection which might be associated with c-Myc regulation of apoptosis since it has been showed that an active inhibition of apoptosis in host cell during infection by *Plasmodium* is required for a successful infection (Leirião *et al.*, 2005; van de Sand *et al.*, 2005). In addition, since c-Myc is a transcription factor, it is possible that this modulates other(s) target and/or modulator gene(s) that mediate(s) the host cell response to *Plasmodium* infection. In fact, recently several studies have revealed that candidate c-Myc target genes fall into a broad spectrum of diverse functional categories, ranging from metabolic enzymes, biosynthesis of macromolecules such as RNA, protein and DNA, transcription, and cell signaling (Menssen and Hermeking, 2002; O'Connell *et al.*, 2003; Remondini *et al.*, 2005). Therefore, it is possible that c-Myc role in *Plasmodium*

infection is related with the latter pathways, a possibility that remains to be elucidated.

The activating transcription factor 3 gene (*Atf3*) encodes a member of the ATF/CREB (cAMP-response-element-binding protein) family of basic region leucine zipper transcription factors. Atf3 can act as a transcriptional repressor or activator depending on whether it forms homodimers with Atf3 or heterodimers with other proteins, such as c-Jun, Atf2, JunB, and gadd153/CHOP10 [reviewed in (Hai and Hartman, 2001)]. Atf3 is a stress-inducible transcription factor, expressed at low levels in quiescent cells and rapidly and highly induced in different cell types by multiple and diverse extracellular signals, such as mitogens (serum, epidermal growth factor and hepatocyte growth factor) (Weir *et al.*, 1994; Allan *et al.*, 2001), cytokines (interferon-γ and interleukin-4) (Drysdale *et al.*, 1996) and genotoxic agents (ionizing radiation and UV light) [reviewed in (Hai *et al.*, 1999)].

The early stress response, important for the maintenance of cell homoeostasis under adverse conditions, activates cascades of phosphorylation events. These, in many cases, increase the expression of the immediate early genes that encode transcription factors, which regulate downstream genes and initiate a network of transcriptional regulation. Atf3 has already been involved in diverse cellular functions, i.e., stress response, regulation of the cell cycle and apoptosis (Hartman *et al.*, 2004; Yan *et al.*, 2005; Lu *et al.*, 2006; Lu *et al.*, 2007). Moreover, Atf3 has been shown to be regulated upon diverse microbe infections [reviewed in (Jenner and Young, 2005)]. In fact an Atf3 increase was observed in response to bacteria and viral infections, such as spiral *Helicobacter pylori* (Liu *et al.*, 2006), hepatitis B virus (Tarn *et al.*, 1999) and adenovirus (Zhao *et al.*, 2003; Granberg *et al.*, 2006).

The microarray data presented here (see Figure 2c and Supplementary Table 2) also shows an increase in Atf3 in response to hepatocyte infection by *Plasmodium*. Moreover, although Atf3 increase is observed throughout all the infection time points accessed, the highest expression level occurs in the earliest infection time point assessed, namely at 6h post-infection. This is in agreement with the kinetics of Atf3 induction being immediate and transient [reviewed in (Hai and Hartman, 2001)]. The early and transient nature of Atf3 induction suggests the existence of a mechanism that turns off *Atf3* gene expression after its induction, and in fact, Atf3 itself can repress the activity of its own promoter (Wolfgang *et al.*, 2000).

The functional genomics data from the RNAi screen reveals *atf3* as a promising gene candidate to have a role in *Plasmodium* infection since a statistically significant increase on infection was observed with treatment with 6 distinct siRNAs in the third confirmation pass. In order to determine the physiological relevance of the *in vitro*

results for Atf3, BALB/c mice were infected with different amounts of *Plasmodium* sporozoites (2×10^4 or 10×10^4) and the Atf3 mRNA levels, quantified by qRT-PCR at different time points post-infection, were compared to the levels present in non-infected mice (Figure 4c and Supplementary Figure 2). Atf3 mRNA level was found to be upregulated 5 h after sporozoite infection, which is in agreement with the microarray data since it was in the 6 h time point post-infection that Atf3 was found to be more up-regulated (see Supplementary Table 2).

Furthermore, *Plasmodium in vivo* infection was accessed in Atf3 deficient mice. Basically, Atf3 deficient mice were infected with 2×10^4 *P. berghei* sporozoites and the liver infection load was compared with that of wild-type littermate mice (Figure 4d). Forty-hours post-infection, i.e., immediately prior to parasite passage into the blood stream, livers were dissected and the infection load was determined by qRT-PCR. The results show that infection is higher in Atf3 deficient mice and are in agreement with those of the RNAi functional screen whilst lending further support to the notion that the absence of Atf3 leads to a significant increase of liver infection by *P. berghei*. All the data taken together suggest that hepatocytes may respond to *P. berghei* infection by increasing expression of Atf3, which, in turn, plays a role in countering infection. Therefore, the results yielded by the *in vitro* approach employed in this study are of significance to *Plasmodium berghei in vivo* infection.

In conclusion, the genomics approach employed to identify host molecules that may play relevant roles during the liver stage of malaria unequivocally showed that at least 2 host cell factors, c-Myc and Atf3, play a relevant role during *Plasmodium* infection of hepatocytes, which can readily be rendered rate-limiting even with partial RNAi-induced gene expression silencing. The fact that the two host cell factors identified in the present study are transcription factors is consistent with the notion that the primary response to the stress induced by the intracellular parasite must include the activation of transcription factors which will subsequently control the second wave of the host cell response. Moreover, several microarray studies demonstrate that the genes regulated by diverse microbe infections converge towards a common set of alert genes, from which *Atf3* identified here as important for *Plasmodium* liver stage infection belongs to [reviewed in (Jenner and Young, 2005)]. The study of the mechanism(s) by which these host molecules, c-Myc and Atf3, modulate *Plasmodium* infection of hepatocytes will be of considerable interest since this knowledge might shed light into the host cell response not only to *Plasmodium* but also other microorganisms infections.

Previous genomic studies on malaria pre-erythrocytic stage have focused exclusively on the parasite (Kappe *et al.*, 2001; Le Roch *et al.*, 2003; Kaiser *et al.*, 2004; Le Roch *et al.*,

2004; Wang *et al.*, 2004; Sacci *et al.*, 2005). The present study constitutes, to our knowledge, the first genomic study aimed at identifying the host liver molecules that influence infection by *Plasmodium* through the use of microarray and/or RNAi technologies. Moreover, the success of this initial targeted application of RNAi technology suggests that larger scale and more systematic approaches hold an enormous potential for further advances in the malaria liver stage field.

Methods

Cells and parasites

Hepa1-6 (murine hepatoma cell line) cells were cultured in Dulbecco's MEM medium (DMEM) supplemented with 10% fetal calf serum (FCS, Gibco/Invitrogen), 1% penicillin/streptomycin (pen/strep, Gibco/Invitrogen) and 1 mM glutamine (Gibco/Invitrogen) and maintained at 37 °C with 5% CO_2. Cells were routinely screened and found to be negative for mycoplasma.

Green fluorescent protein (GFP) expressing *Plasmodium berghei* (parasite line 259cl2) sporozoites (Franke-Fayard *et al.*, 2004) were obtained from dissection of infected female *Anopheles stephensi* mosquito salivary glands.

Sample preparation and collection for microarrays

Hepa1-6 cells were seeded ($2x10^5$ cells per well) in 24-well plates twenty-four hours before infection. At the infection time the cell confluency was approximately of 80% and $2x10^5$ GFP-expressing *P. berghei* sporozoites were added per well (referred to as infected samples). Salivary glands from non-infected mosquitoes were extracted and the same volume of the extraction solution was added to control samples (referred to as non-infected samples). All plates were then spun down at 1800xg for 7 min and incubated at 37°C with 5% CO_2.

Infected samples were collected at 6, 12, 18 and 24 hours after sporozoite addition and fluorescence activated cell-sorting (FACS) was used to select and collect infected cells among the total cell population within each well. Briefly, cells were collected using Trypsin (Gibco), washed with 10% FCS in PBS and resuspended in 2% FCS in PBS. Infected hepatocytes were separated from non-infected cells using the high speed cell sorter Dako-Cytomation (Mo-Flo MLS, 1999). Only infected samples with approximately 90% purity (confirmed in the FACSCalibur 4 Color Analyser; Becton Dickinson, FACSCalibur, 1998) were selected. Two replicates from independent experiments were prepared and for further processing, only replicates with similar infection and parasite development rates were used. In parallel non-infected samples were collected at the same time points and passed through the cell sorter.

Sorted cells were collected in cell lysis buffer (RLT, Qiagen) and total RNA was extracted with the Rneasy Micro Kit (Qiagen), according to the manufacturer's instructions. RNA concentration and quality of all replicates was evaluated with the NanoDrop ND-1000 UV-Vis Spectrophotometer (NanoDrop Technologies) and Bioanalyser 2100 (Agilent). The extracted RNA was used as template to synthesize double-stranded cDNA and processed for usage on Affymetrix GeneChip® Mouse

Genome 430 2.0 Array, according to the manufacturer's small sample labeling protocol version II. Data were filtered to include only those spots for which the ratio of Fold Change (FC) was ≥ 1.4 (putative up-regulation or down-regulation) in at least one time point post-infection but in both replicates for each time point. For *P. berghei* cross-hybridization RNA control experiments, *P. berghei* sporozoites were cultivated as previously described (Kaiser *et al.*, 2003), and collected 6, 12, 18 and 24 hours post-incubation. Total parasite RNA was pooled and further sample processing was performed as described above.

Microarray replicates infection quantification

Replicate infection and parasite development data were obtained at the same time points by processing parallel infected samples for immunofluorescence. Briefly, cells were washed with PBS, fixed with 4% paraformaldehyde (PFA) and permeabilized with 0.1% saponin in blocking solution (3% bovine serum albumin, 100mM glycine and 10% FCS). Exoerythrocytic forms (EEFs) were detected using the mouse monoclonal antibody 2E6 against the parasite heat shock protein 70 (Hsp70) (Tsuji *et al.*, 1994) and an AlexaFluor555 labeled goat anti-mouse secondary antibody (Molecular Probes/Invitrogen). Cell nuclei were stained with 4'6-diamidino-2-phenylindole (DAPI, Sigma) and host cell actin with AlexaFluor488 Phalloidin (Molecular Probes/Invitrogen). Infection was assessed by manual quantification of the number of EEFs per sample.

Microarrays accession codes

The array data files are available online on http://www.ebi.ac.uk/arrayexpress/ under the accession number E-MEXP-667.

siRNA design, siRNA library and screening controls

All siRNAs were purchased from Ambion's *Silencer* genome wide library (Ambion/Applied Biosystems, Austin USA). The siRNA library screened included a total of 50 genes selected from the microarray study analysis. Each gene was initially targeted with 3 distinct siRNAs used individually in all cases and in the following confirmation steps more siRNAs per gene were tested. Each siRNA was transfected in triplicate. Negative control samples included untransfected cells and cells transfected with a negative control siRNA not targeting any annotated genes in the human genome. A full list of gene names and siRNA ID numbers are shown in Supplementary Table 7.

High-throughput siRNA screening of *Plasmodium* infection

Hepa1-6 cells ($4{,}5 \times 10^3$ per well) were seeded in 100 µl of complete DMEM medium in optical 96-well plates (Costar) and incubated at 37°C and 5% CO_2. Twenty-four hours later, growth medium in each well was replaced by 80 µl of serum-free medium and cells were transfected with 1 µl of 10 µM siRNA diluted in 16 µl of Opti-Mem (Invitrogen) complexed with 0.4 µl Oligofectamine (Invitrogen) diluted in 2.6 µl OptiMem. Transfection was performed following the recommended manufacturer instructions. Four hours after cell transfection, 50 µl of fresh DMEM medium supplemented with 30% FCS, 3% pen/strep and 3% glutamine were added to the cells. Two days later, cells were infected with 20×10^5 *P. berghei* sporozoites per well. Twenty-four hours after infection, cells were fixed with 4% PFA in PBS and permeabilized with 0.2% saponin in PBS. Cell nuclei and actin were stained with Hoeschst-33342 (Molecular Probes/Invitrogen) and Phalloidin AlexaFluor 488 (Molecular Probes/Invitrogen), respectively. EEFs were detected with the mouse monoclonal 2E6 antibody (Tsuji *et al.*, 1994) and an AlexaFluor555 goat anti-mouse secondary antibody (Molecular Probes/Invitrogen).

Automated image acquisition and analysis

Images were acquired with a Discovery1 automated fluorescence microscope (Molecular Devices Corporation, CA, USA) using a 10x lens. In each well, cell nuclei, actin and EEFs were imaged in 9 fields covering a total area of 2.7 x 2.0 mm. Image data was analyzed using a custom MetaMorph (Molecular Devices Corporation, CA, USA) based algorithm extracting the following values for each imaged field: cell proliferation as measured by the number of nuclei per imaged field (Hoechst staining), cell confluency as measured by the percentage of the imaged field covered by actin staining and number of EEFs as number of compact, high contrast objects in a size range from 16 to 150 pixels. Within each field, the number of EEFs was normalized to the cell confluency. Normalized EEF numbers and number of nuclei were averaged between the 9 imaged fields within each well. Mean and standard deviations were calculated for each experimental triplicate. Final readouts included number of EEFs shown as a percentage of the negative control and number of nuclei as a percentage of the plate mean.

Gene-specific expression and infection quantification by qRT-PCR

For gene-specific expression *in vitro*, total RNA was isolated from Hepa1-6 cells 48 h after cell transfection (Invitek Invisorb 96-well plate kit) and converted into cDNA

(ABI's HighCapacity cDNA reagents) with random hexamers, following the manufacturer recommendations. qRT-PCR used the SybrGreen method with Quantace qPCR mastermix at 11 μl total reaction volume, containing 500 nM of the target-specific primers, and primers that were designed to specifically target the selected genes. Real-time PCR reactions were performed on an ABI Prism 7900HT system. Relative amounts of remaining mRNA levels of RNAi targets were calculated against the level of the housekeeping gene *18S* rRNA. Remaining mRNA levels of RNAi-treated samples were compared with those of samples transfected with Negative siRNA, which were considered as 100% expression of the specific gene under study. *18S* rRNA-specific primer sequences were: 5′- CGG CTT AAT TTG ACT CAA CAC G -3′ and 5′- TTA GCA TGC CAG AGT CTC GTT C -3′.

The determination of liver parasite load *in vivo*, was performed according to the method developed for *P. yoelii* infections (Bruna-Romero *et al.*, 2001). Livers were collected and homogenized in denaturing solution (4 M guanidine thiocyanate; 25 mM sodium citrate pH 7, 0.5 % sarcosyl and 0.7 % β-Mercaptoethanol in DEPC-treated water), at different time points after sporozoite injection depending on the experiment. Total RNA was extracted using Qiagen's RNeasy Mini kit, following the manufacturer's instructions. RNA for infection measurements was converted into cDNA using Roche's Transcriptor First Strand cDNA Synthesis kit, according to the manufacturer's protocol. The qRT-PCR reactions used Applied Biosystems' Power SYBR Green PCR Master Mix and were performed according to the maunufacturer's instructions on an ABI Prism 7000 system (Applied Biosystems). Amplification reactions were carried out in a total reaction volume of 25 μl, containing 0,8 pmoles/μl or 0,16 pmoles/μl of the *Atf3*-, Pb*A*- or housekeeping gene-specific primers, respectively. Relative amounts of *Atf3* and Pb*A* mRNA were calculated against the Hypoxanthine Guanine Phosphoribosyltransferase (*HPRT*) housekeeping gene. *Atf3*-specific primer sequences were 5′- CCA GGT CTC TGC CTC AGA AG -3′ and 5′- TCC AGG GGT CTG TTG TTG AC -3′. For Pb*A 18S* the primers used were 5′- AAG CAT TAA ATA AAG CGA ATA CAT CCT TAC -3′ and 5′- GGA GAT TGG TTT TGA CGT TTA TGT G -3′. For *HPRT* the specific primer sequences were 5′- TGC TCG AGA TGT GAT GAA GG -3′ and 5′- TCC CCT GTT GAC TGG TCA TT -3′, respectively.

Plasmodium berghei in vivo infection

BALB/c mice were bred and housed in the pathogen-free facilities of the Instituto Gulbenkian de Ciência and Instituto de Medicina Molecular, respectively. All protocols were approved by the Animal Care Committee of both Institutes.

BALB/c mice (male, 6-8 weeks) were infected with 2 or 10×10^4 *P. berghei* sporozoites by intra-venous (i.v.) injection. At different time points post-infection, namely 5, 10, 20 and 40 h after sporozoite injection, the Atf3 mRNA level (determined by qRT-PCR) was compared to the level in non-infected mice (considered as 100%).

Atf3 knock-out mice and wild-type littermates (male, 6-8 weeks) were infected i.v. with 2×10^4 *P. berghei* sporozoites and PbA infection level, determined 40 h after sporozoite injection by qRT-PCR, was compared between the two experimental groups.

Statistical analysis

Statistical analysis was performed using unpaired Student *t* or ANOVA parametric tests. *P* < 0.05 was considered significant.

Acknowledgments

References

Allan, A.L., Albanese, C., Pestell, R.G., and LaMarre, J. (2001). Activating transcription factor 3 induces DNA synthesis and expression of cyclin D1 in hepatocytes. J Biol Chem *276*, 27272-27280.

Baena, E., Gandarillas, A., Vallespinos, M., Zanet, J., Bachs, O., Redondo, C., Fabregat, I., Martinez, A.C., and de Alboran, I.M. (2005). c-Myc regulates cell size and ploidy but is not essential for postnatal proliferation in liver. Proc Natl Acad Sci U S A *102*, 7286-7291.

Bruna-Romero, O., Hafalla, J.C., Gonzalez-Aseguinolaza, G., Sano, G., Tsuji, M., and Zavala, F. (2001). Detection of malaria liver-stages in mice infected through the bite of a single Anopheles mosquito using a highly sensitive real-time PCR. Int J Parasitol *31*, 1499-1502.

Carrolo, M., Giordano, S., Cabrita-Santos, L., Corso, S., Vigario, A.M., Silva, S., Leiriao, P., Carapau, D., Armas-Portela, R., Comoglio, P.M., Rodriguez, A., and Mota, M.M. (2003). Hepatocyte growth factor and its receptor are required for malaria infection. Nat Med *9*, 1363-1369.

Cunha-Rodrigues, M., Prudêncio, M., Mota, M.M., and Haas, W. (2006). Antimalarial drugs - host targets (re)visited. Biotechnol J *1*, 321-332.

Dang, C.V. (1999). c-Myc target genes involved in cell growth, apoptosis, and metabolism. Mol Cell Biol *19*, 1-11.

Drysdale, B.E., Howard, D.L., and Johnson, R.J. (1996). Identification of a lipopolysaccharide inducible transcription factor in murine macrophages. Mol Immunol *33*, 989-998.

Echeverri, C.J., Beachy, P.A., Baum, B., Boutros, M., Buchholz, F., Chanda, S.K., Downward, J., Ellenberg, J., Fraser, A.G., Hacohen, N., Hahn, W.C., Jackson, A.L., Kiger, A., Linsley, P.S., Lum, L., Ma, Y., Mathey-Prevot, B., Root, D.E., Sabatini, D.M., Taipale, J., Perrimon, N., and Bernards, R. (2006). Minimizing the risk of reporting false positives in large-scale RNAi screens. Nat Methods *3*, 777-779.

Echeverri, C.J., and Perrimon, N. (2006). High-throughput RNAi screening in cultured cells: a user's guide. Nat Rev Genet *7*, 373-384.

Franke-Fayard, B., Trueman, H., Ramesar, J., Mendoza, J., van der Keur, M., van der Linden, R., Sinden, R.E., Waters, A.P., and Janse, C.J. (2004). A Plasmodium berghei reference line that constitutively expresses GFP at a high level throughout the complete life cycle. Mol Biochem Parasitol *137*, 23-33.

Frevert, U., Engelmann, S., Zougbede, S., Stange, J., Ng, B., Matuschewski, K., Liebes, L., and Yee, H. (2005). Intravital observation of Plasmodium berghei sporozoite infection of the liver. PLoS Biol *3*, e192.

Granberg, F., Svensson, C., Pettersson, U., and Zhao, H. (2006). Adenovirus-induced alterations in host cell gene expression prior to the onset of viral gene expression. Virology *353*, 1-5.

Hai, T., and Hartman, M.G. (2001). The molecular biology and nomenclature of the activating transcription factor/cAMP responsive element binding family of transcription factors: activating transcription factor proteins and homeostasis. Gene *273*, 1-11.

Hai, T., Wolfgang, C.D., Marsee, D.K., Allen, A.E., and Sivaprasad, U. (1999). ATF3 and stress responses. Gene Expr *7*, 321-335.

Hartman, M.G., Lu, D., Kim, M.L., Kociba, G.J., Shukri, T., Buteau, J., Wang, X., Frankel, W.L., Guttridge, D., Prentki, M., Grey, S.T., Ron, D., and Hai, T. (2004). Role for activating transcription factor 3 in stress-induced beta-cell apoptosis. Mol Cell Biol *24*, 5721-5732.

Jenner, R.G., and Young, R.A. (2005). Insights into host responses against pathogens from transcriptional profiling. Nat Rev Microbiol *3*, 281-294.

Kaiser, K., Camargo, N., and Kappe, S.H. (2003). Transformation of sporozoites into early exoerythrocytic malaria parasites does not require host cells. J Exp Med *197*, 1045-1050.

Kaiser, K., Matuschewski, K., Camargo, N., Ross, J., and Kappe, S.H. (2004). Differential transcriptome profiling identifies Plasmodium genes encoding pre-erythrocytic stage-specific proteins. Mol Microbiol *51*, 1221-1232.

Kappe, S.H., Gardner, M.J., Brown, S.M., Ross, J., Matuschewski, K., Ribeiro, J.M., Adams, J.H., Quackenbush, J., Cho, J., Carucci, D.J., Hoffman, S.L., and Nussenzweig, V. (2001). Exploring the transcriptome of the malaria sporozoite stage. Proc Natl Acad Sci U S A *98*, 9895-9900.

Le Roch, K.G., Johnson, J.R., Florens, L., Zhou, Y., Santrosyan, A., Grainger, M., Yan, S.F., Williamson, K.C., Holder, A.A., Carucci, D.J., Yates, J.R., 3rd, and Winzeler, E.A. (2004). Global analysis of transcript and protein levels across the Plasmodium falciparum life cycle. Genome Res *14*, 2308-2318.

Le Roch, K.G., Zhou, Y., Blair, P.L., Grainger, M., Moch, J.K., Haynes, J.D., De La Vega, P., Holder, A.A., Batalov, S., Carucci, D.J., and Winzeler, E.A. (2003). Discovery of gene function by expression profiling of the malaria parasite life cycle. Science *301*, 1503-1508.

Leirião, P., Albuquerque, S.S., Corso, S., van Gemert, G.J., Sauerwein, R.W., Rodriguez, A., Giordano, S., and Mota, M.M. (2005). HGF/MET signalling protects Plasmodium-infected host cells from apoptosis. Cell Microbiol *7*, 603-609.

Levens, D. (2002). Disentangling the MYC web. Proc Natl Acad Sci U S A *99*, 5757-5759.

Liu, H., Lo, C.R., Jones, B.E., Pradhan, Z., Srinivasan, A., Valentino, K.L., Stockert, R.J., and Czaja, M.J. (2000). Inhibition of c-Myc expression sensitizes hepatocytes to tumor necrosis factor-induced apoptosis and necrosis. J Biol Chem *275*, 40155-40162.

Liu, Z.F., Chen, C.Y., Tang, W., Zhang, J.Y., Gong, Y.Q., and Jia, J.H. (2006). Gene-expression profiles in gastric epithelial cells stimulated with spiral and coccoid Helicobacter pylori. J Med Microbiol *55*, 1009-1015.

Lu, D., Chen, J., and Hai, T. (2007). The regulation of ATF3 gene expression by mitogen-activated protein kinases. Biochem J *401*, 559-567.

Lu, D., Wolfgang, C.D., and Hai, T. (2006). Activating transcription factor 3, a stress-inducible gene, suppresses Ras-stimulated tumorigenesis. J Biol Chem *281*, 10473-10481.

Menssen, A., and Hermeking, H. (2002). Characterization of the c-MYC-regulated transcriptome by SAGE: identification and analysis of c-MYC target genes. Proc Natl Acad Sci U S A *99*, 6274-6279.

Mota, M.M., Pradel, G., Vanderberg, J.P., Hafalla, J.C., Frevert, U., Nussenzweig, R.S., Nussenzweig, V., and Rodriguez, A. (2001). Migration of Plasmodium sporozoites through cells before infection. Science *291*, 141-144.

Mota, M.M., and Rodriguez, A. (2000). Plasmodium yoelii: efficient in vitro invasion and complete development of sporozoites in mouse hepatic cell lines. Exp Parasitol *96*, 257-259.

O'Connell, B.C., Cheung, A.F., Simkevich, C.P., Tam, W., Ren, X., Mateyak, M.K., and Sedivy, J.M. (2003). A large scale genetic analysis of c-Myc-regulated gene expression patterns. J Biol Chem *278*, 12563-12573.

Obaya, A.J., Mateyak, M.K., and Sedivy, J.M. (1999). Mysterious liaisons: the relationship between c-Myc and the cell cycle. Oncogene *18*, 2934-2941.

Prudêncio, M., Rodriguez, A., and Mota, M.M. (2006). The silent path to thousands of merozoites: the Plasmodium liver stage. Nat Rev Microbiol *4*, 849-856.

Remondini, D., O'Connell, B., Intrator, N., Sedivy, J.M., Neretti, N., Castellani, G.C., and Cooper, L.N. (2005). Targeting c-Myc-activated genes with a correlation method: detection of global changes in large gene expression network dynamics. Proc Natl Acad Sci U S A *102*, 6902-6906.

Sacci, J.B., Jr., Ribeiro, J.M., Huang, F., Alam, U., Russell, J.A., Blair, P.L., Witney, A., Carucci, D.J., Azad, A.F., and Aguiar, J.C. (2005). Transcriptional analysis of in vivo Plasmodium yoelii liver stage gene expression. Mol Biochem Parasitol *142*, 177-183.

Sachs, J., and Malaney, P. (2002). The economic and social burden of malaria. Nature *415*, 680-685.

Tarn, C., Bilodeau, M.L., Hullinger, R.L., and Andrisani, O.M. (1999). Differential immediate early gene expression in conditional hepatitis B virus pX-transforming versus nontransforming hepatocyte cell lines. J Biol Chem *274*, 2327-2336.

Tsuji, M., Mattei, D., Nussenzweig, R.S., Eichinger, D., and Zavala, F. (1994). Demonstration of heat-shock protein 70 in the sporozoite stage of malaria parasites. Parasitol Res *80*, 16-21.

van de Sand, C., Horstmann, S., Schmidt, A., Sturm, A., Bolte, S., Krueger, A., Lutgehetmann, M., Pollok, J.M., Libert, C., and Heussler, V.T. (2005). The liver stage of Plasmodium berghei inhibits host cell apoptosis. Mol Microbiol *58*, 731-742.

Wang, Q., Brown, S., Roos, D.S., Nussenzweig, V., and Bhanot, P. (2004). Transcriptome of axenic liver stages of Plasmodium yoelii. Mol Biochem Parasitol *137*, 161-168.

Weir, E., Chen, Q., DeFrances, M.C., Bell, A., Taub, R., and Zarnegar, R. (1994). Rapid induction of mRNAs for liver regeneration factor and insulin-like growth factor binding protein-1 in primary cultures of rat hepatocytes by hepatocyte growth factor and epidermal growth factor. Hepatology *20*, 955-960.

Wolfgang, C.D., Liang, G., Okamoto, Y., Allen, A.E., and Hai, T. (2000). Transcriptional autorepression of the stress-inducible gene ATF3. J Biol Chem *275*, 16865-16870.

Yan, C., Lu, D., Hai, T., and Boyd, D.D. (2005). Activating transcription factor 3, a stress sensor, activates p53 by blocking its ubiquitination. Embo J *24*, 2425-2435.

Zhao, H., Granberg, F., Elfineh, L., Pettersson, U., and Svensson, C. (2003). Strategic attack on host cell gene expression during adenovirus infection. J Virol *77*, 11006-11015.
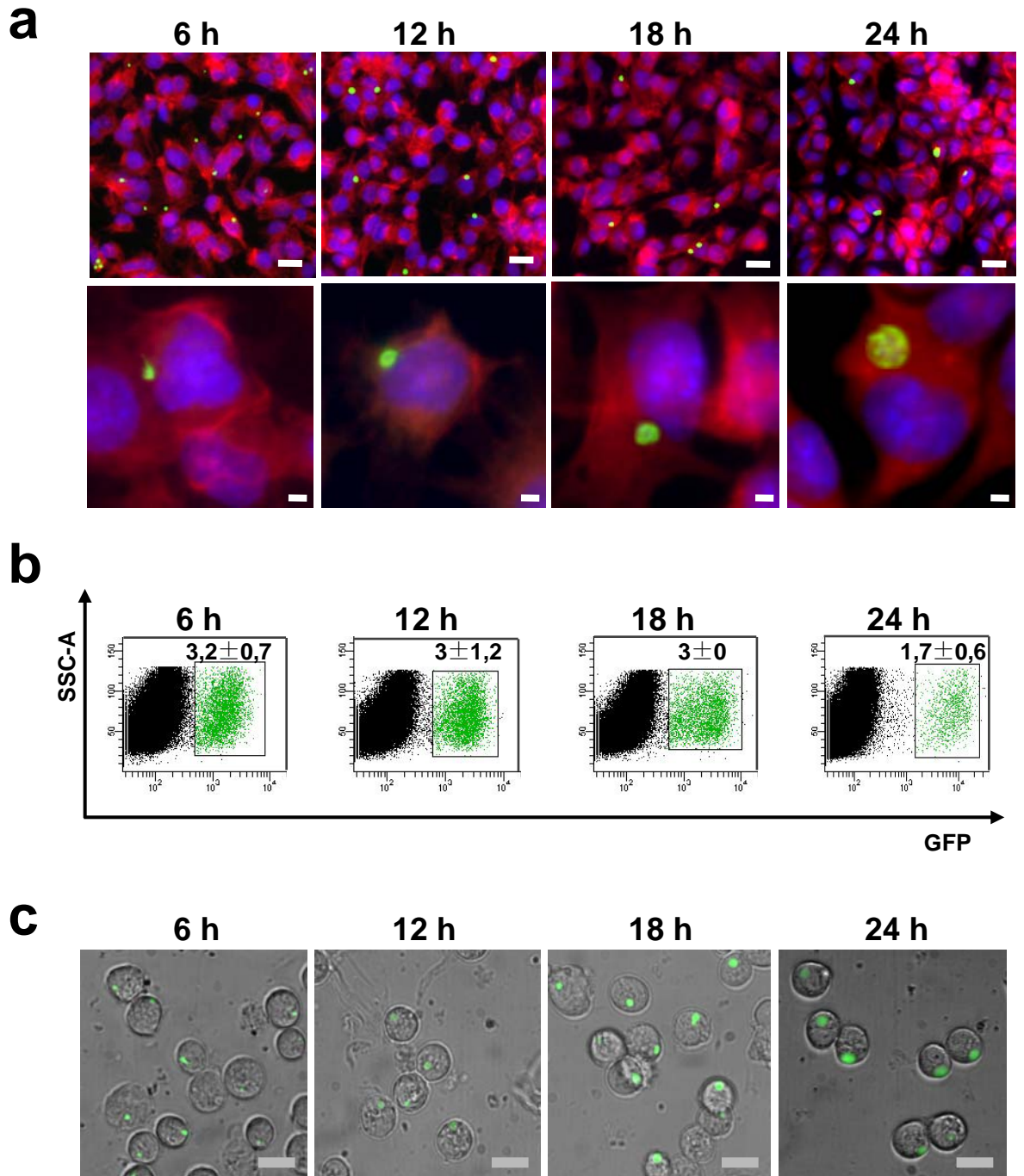
Figure 1 | Isolation of GFP-expressing *P. berghei* infected cells using FACS at different time points post-infection (p.i.).
(a) Pre-sorting fluorescence images of infected cell populations (top panels, bar = 60 µm) or isolated infected cells (bottom panels, bar = 10 µm) at the 6, 12, 18 and 24 h p.i.. Nuclei labeled by DAPI (in blue), host cell actin by Phalloidin (in red) and *P. berghei* EEFs by anti-*Pb*HSP70 antibody (in green). **(b)** FACS plot of sorting experiments performed at the respective time point's p.i. with the selected infected-population and their correspondent infection level (GFP$^+$ population gated and highlighted in green). Infection level for each time point was determined as the average ± s.d. from 3 or more independent samples. **(c)** Post-sorting imaging of infected cells at the different time points p.i.. Infected cells are shown with green EEFs inside (transmitted light and fluorescence pictures merged, bar = 60 µm).
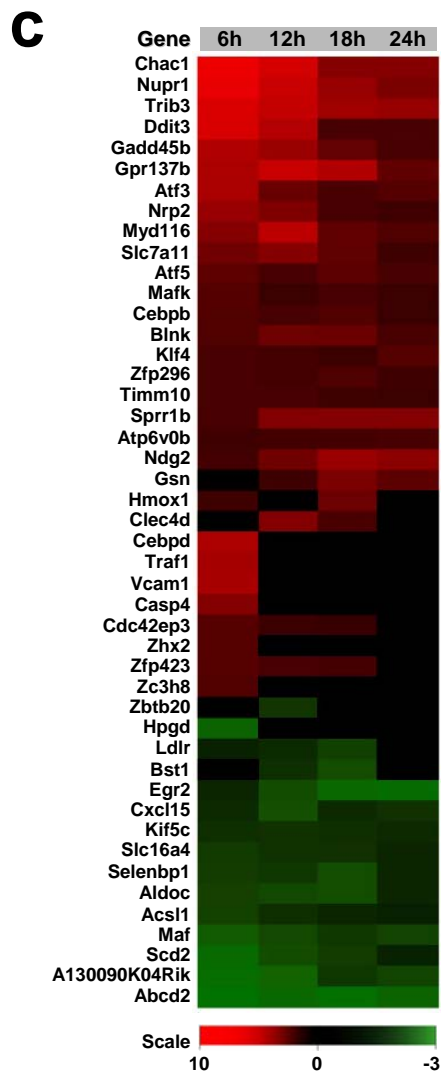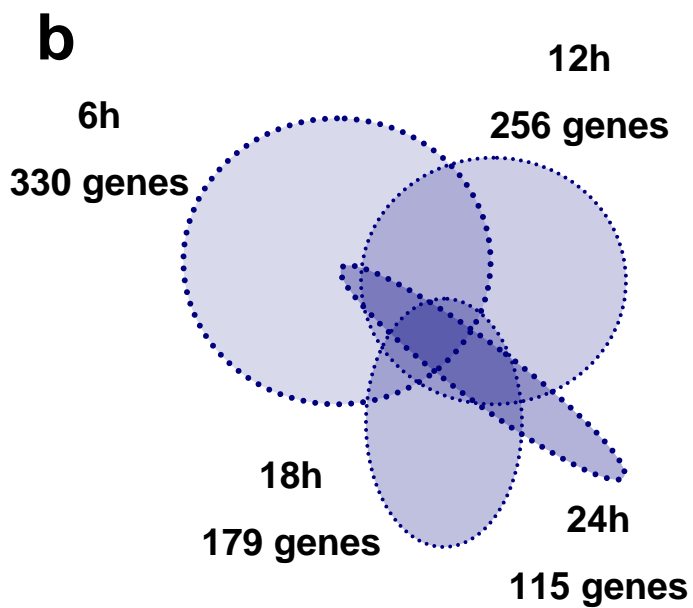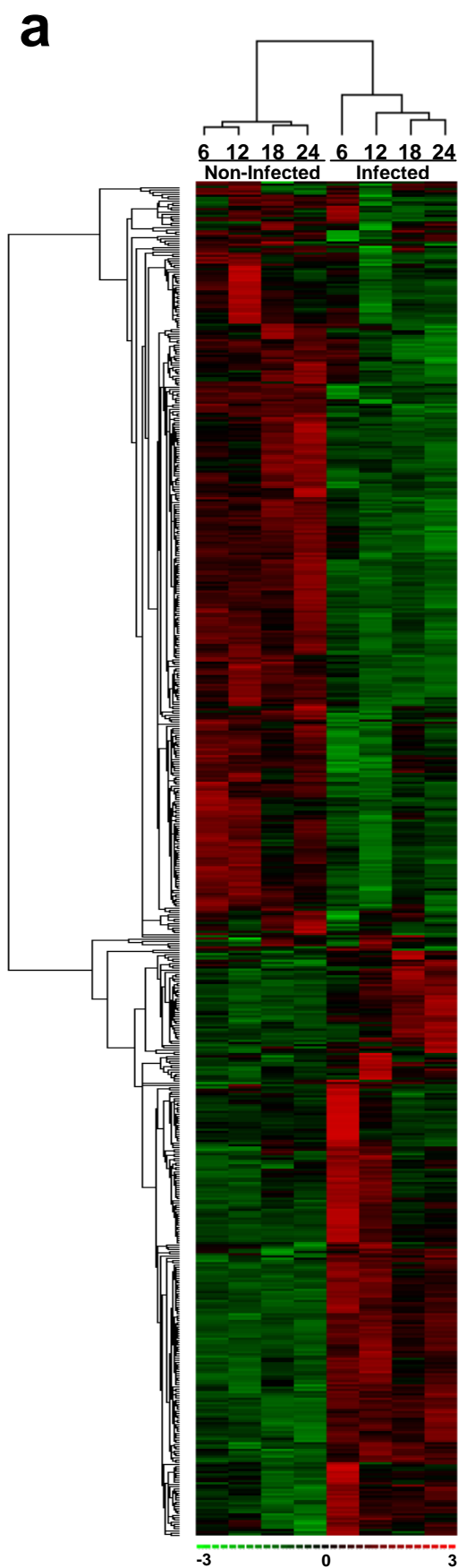
Figure 2 | Microarray analysis identifies host genes differentially expressed throughout *P. berghei* infection of Hepa1-6 cells.

(a) Heat map and cluster analysis of genes differentially expressed in *P. berghei* infected Hepa1-6 cells at different time points p.i. (6, 12, 18 and 24h p.i.) compared to non-infected samples. Gene and sample clustering branches are represented on the left and top of the map, respectively. Gene expression values vary within the [-3 to 3] scale with -3 corresponding to the brighter green (lower expression level), zero to black (median expression level) and 3 to the brighter red (higher expression level). **(b)** Venn diagram representing the distribution of host differential gene expression between and at distinct time points post-infection. Each area is proportional to the number of genes represented and the darker areas represent the common genes between the respective time points. **(c)** Expression profile of the selected 46 genes differentially expressed in *P. berghei* infected Hepa1-6 cells when compared to non-infected cells at the different p.i. time points. Gene expression values above or below a Fold Change of 1.2 are represented by the [-3 to 10] scale with -3 corresponding to the brighter green (lower expression level), zero to black (median expression level) and 10 to the brighter red (higher expression level).

a

Seed Hepa1-6 cells
in 96 well-plates

24 h

Transfection with
siRNAs

48 h

Add freshly isolated
Plasmodium spz.

24 h

Fixation & staining

**Automated Image Acquisition
& Analysis**

Hoescht | Phalloidin | GFP

Nuclei | **Confluency** | **Infection**

**1st Pass
3 siRNAs
for each genee** | **Phenotype for
1 siRNA**

**2nd Pass
Best siRNAs from 1st
+ extra siRNAs** | **Phenotype for
2 siRNA**

**3rd Pass
3 best siRNAs
+ specific-gene
qRT-PCR** | **Phenotype for
2 siRNA +
Specific-gene
modulation**

b

c

Figure 3 | RNAi screens validate the functional relevance of host genes that influence *P. berghei* sporozoite infection of Hepa1-6 cells.

(a) Schematic representation of the RNAi screen experimental workflow used to identify host factors that influence *P. berghei* sporozoite infection of Hepa1-6 cells among those selected from the microarray study. Each siRNA was used to transfect Hepa1-6 cells seeded 24 h earlier in 96-well plates. Fourty-eight h after transfection, cells were infected with $2x10^4$ *P. berghei* sporozoites and 24 h p.i. the number of *Plasmodium* EEFs, cell nuclei and confluency were determined. The candidate genes underwent three screening passes. **(b)** Plot of two independent runs of the first pass of the RNAi screen representing the effect of 150 siRNAs targeting 50 mouse genes on Hepa1-6 cell infection by *P. berghei* sporozoites and cell nuclei count. Infection rates for each experimental condition were normalized against cell confluency and calculated as a percentage of the infection rate of the negative control. The horizontal lines represent 100% ± 1.0 s.d. of the average of all data in the assay. Each circle represents one siRNA (mean of triplicate values). Negative controls appear as blue and green circles, corresponding to untreated cells and cells transfected with a non-specific control siRNA, respectively. Red circles highlight the siRNAs targeting the 11 candidate genes selected to undergo a second screening pass. **(c)** Plot of two independent runs of the second pass of the RNAi screen representing the effect of 33 siRNAs targeting a total of 11 genes on Hepa1-6 cells infection by *P. berghei* sporozoites and cell nuclei count. Experimental conditions, normalization criteria as well as colour attributions are the same as in panel **(b)**, with red circles representing the siRNAs targeting the 2 genes selected to undergo a third screening pass. The horizontal lines represent 100% ± 1.0 s.d. of the average of the average of all data in the assay.

a

Infection Rate
(% negative control)

Number of nuclei
(% plate mean)

b

Infection Rate
(% negative control)

Remaining mRNA
(% of Neg. control)
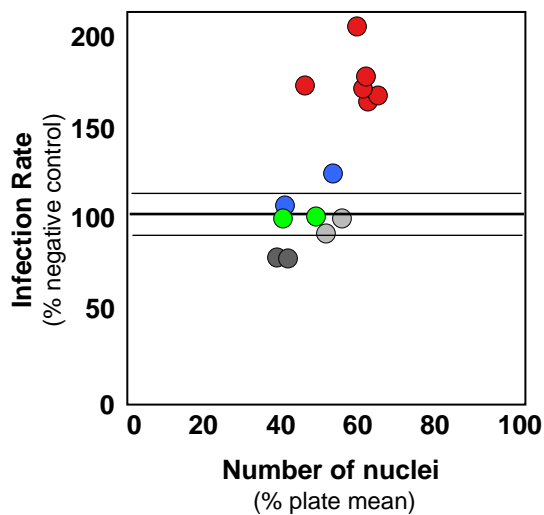
siRNA legend: ● Negative   ● Untreated   ● Atf3 hit   ● c-Myc hit   ● c-Myc

c

Atf3 mRNA level
(Atf3/HPRT, % of NI control)

BALB/c mice

NI   5h   10h   20h   40h

time point post-infection

d

Liver infection load
(*Pb* 18S/HPRT, % of control)

ATF3 -/- mice

WT   KO
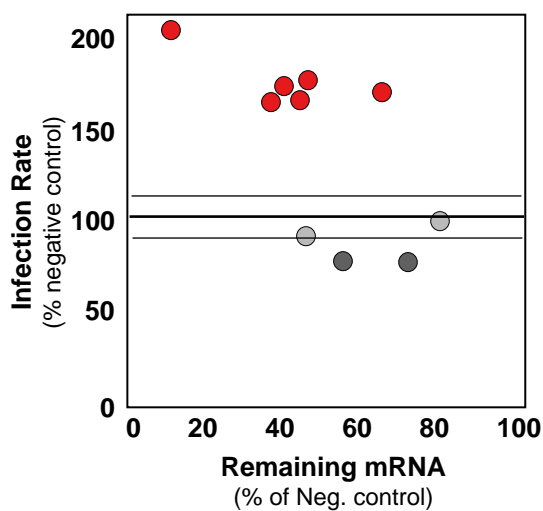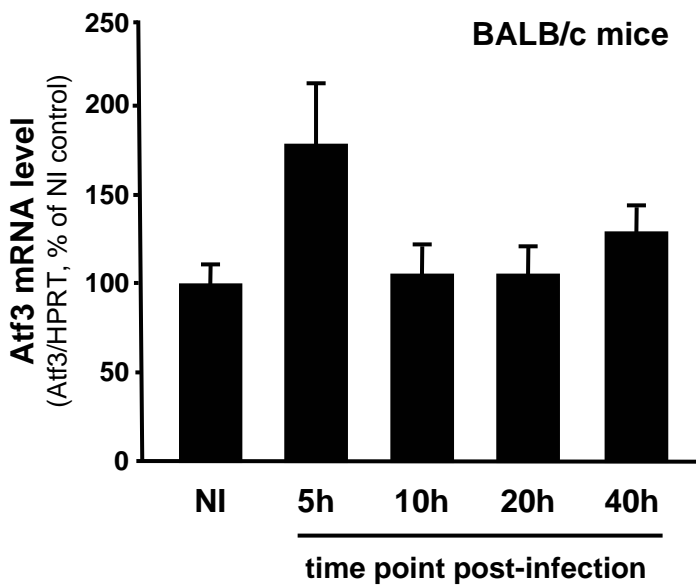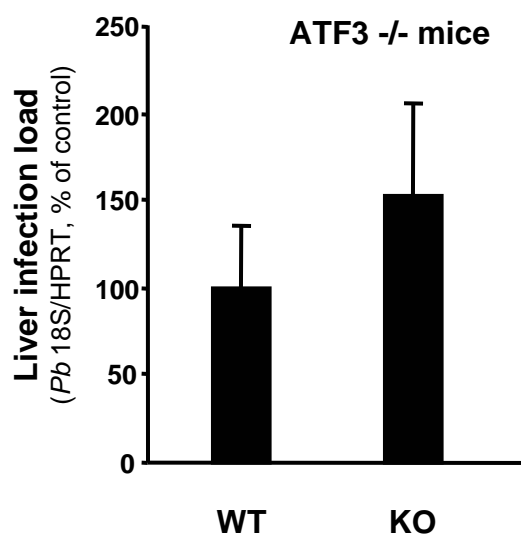
Figure 4 | Atf3 and c-Myc host genes influence *P. berghei* sporozoite infection.
(a) Plot of the third pass of the RNAi screen representing the effect of 10 siRNAs targeting 2 mouse genes on Hepa1-6 cell infection by *P. berghei* sporozoites and cell nuclei count. The horizontal lines represent 100% ± 1.0 s.d. of the average of all the negative controls in the assay. Each circle represents one siRNA (mean of triplicate values). Untreated controls appear as blue circles and negative controls as green circles. Atf3 silencing leads to an increase in infection with all the 6 distinct siRNAs tested (in red) while for c-Myc (4 siRNAs used, all in grey) a decrease in infection is only observed with 2 siRNAs (in darker grey). **(b)** Effect of each siRNA on infection rate *versus* the remaining mRNA level for the specific gene determined in the third pass RNAi screen. Colour attributions are the same as in (a). Each circle represents one siRNA (mean of triplicate values). **(c)** Atf3 mRNA level in *P. berghei in vivo* infections. BALB/c mice were infected with $2x10^4$ *P. berghei* sporozoites and the Atf3 mRNA level was determined by qRT-PCR at different time points, namely 5, 10, 20 and 40h p.i. (3 mice per experimental group). An increase on the Atf3 mRNA level is observed 5h after sporozoite injection when comparing to non-infected control mice (NI). **(d)** *P. berghei in vivo* infection in Atf3 knock-out (Atf3$^{-/-}$ or KO) and wild-type (WT) mice. Liver infection load in the two experimental groups (each with 5 mice) was determined 40 h after sporozoite i.v. injection ($2x10^4$) by qRT-PCR. Atf3 KO mice showed an increase in *P. berghei* infection when compared to that of WT mice.

a
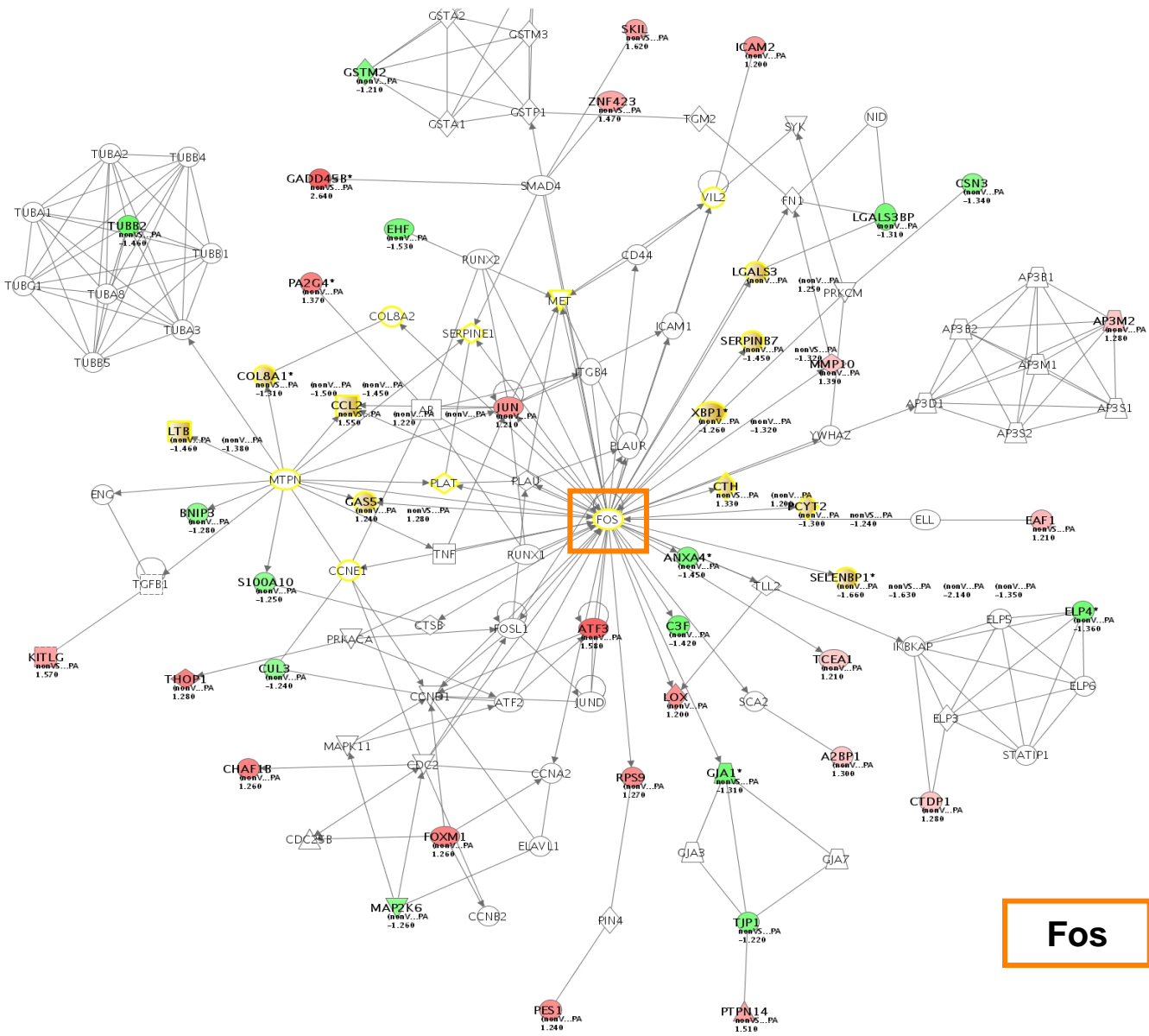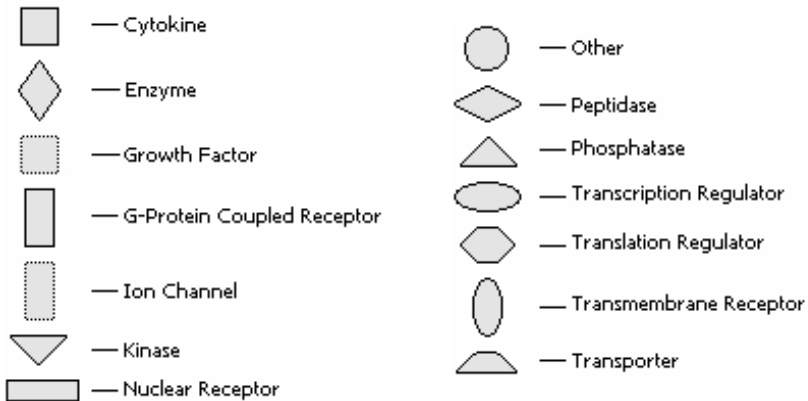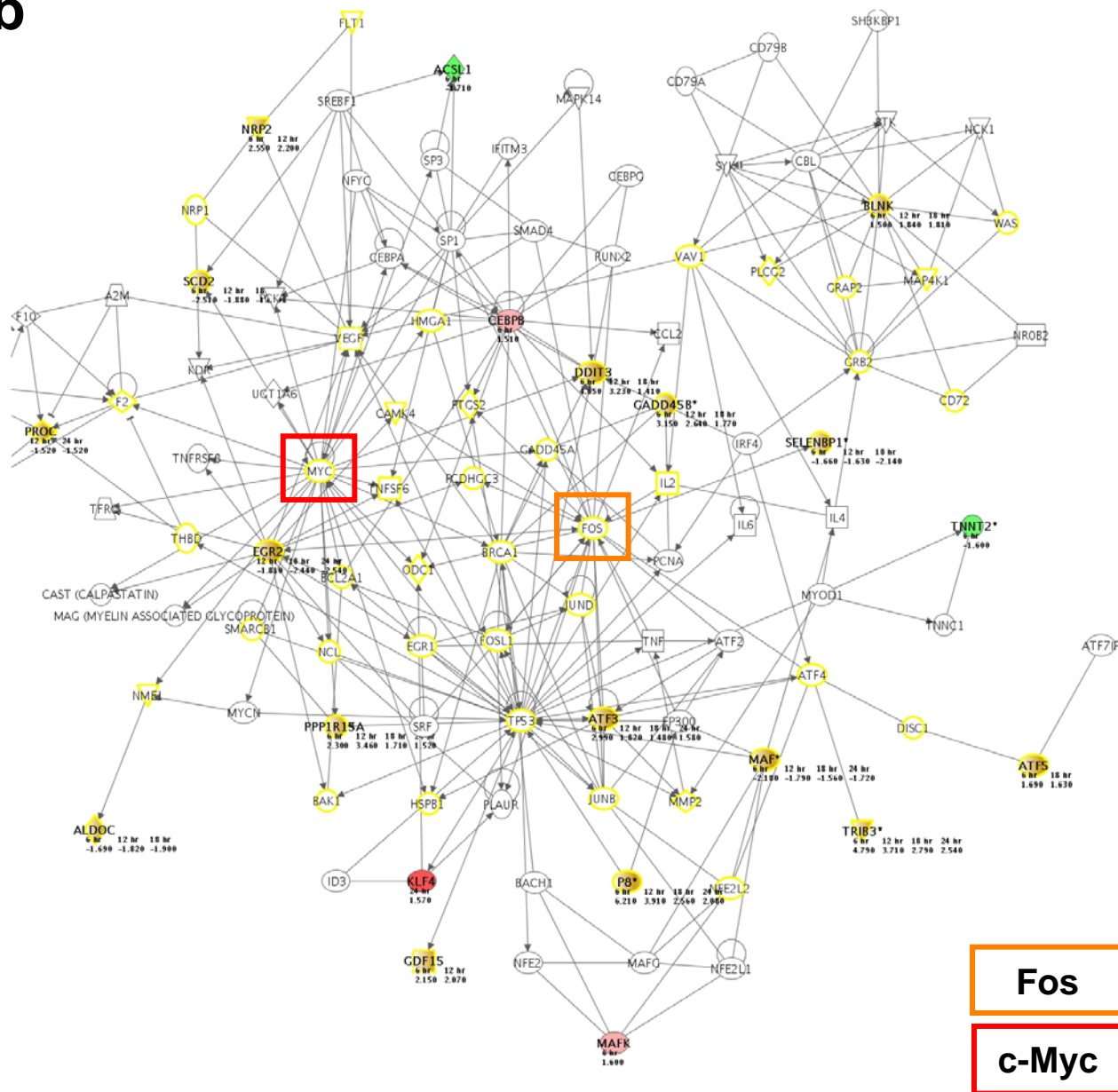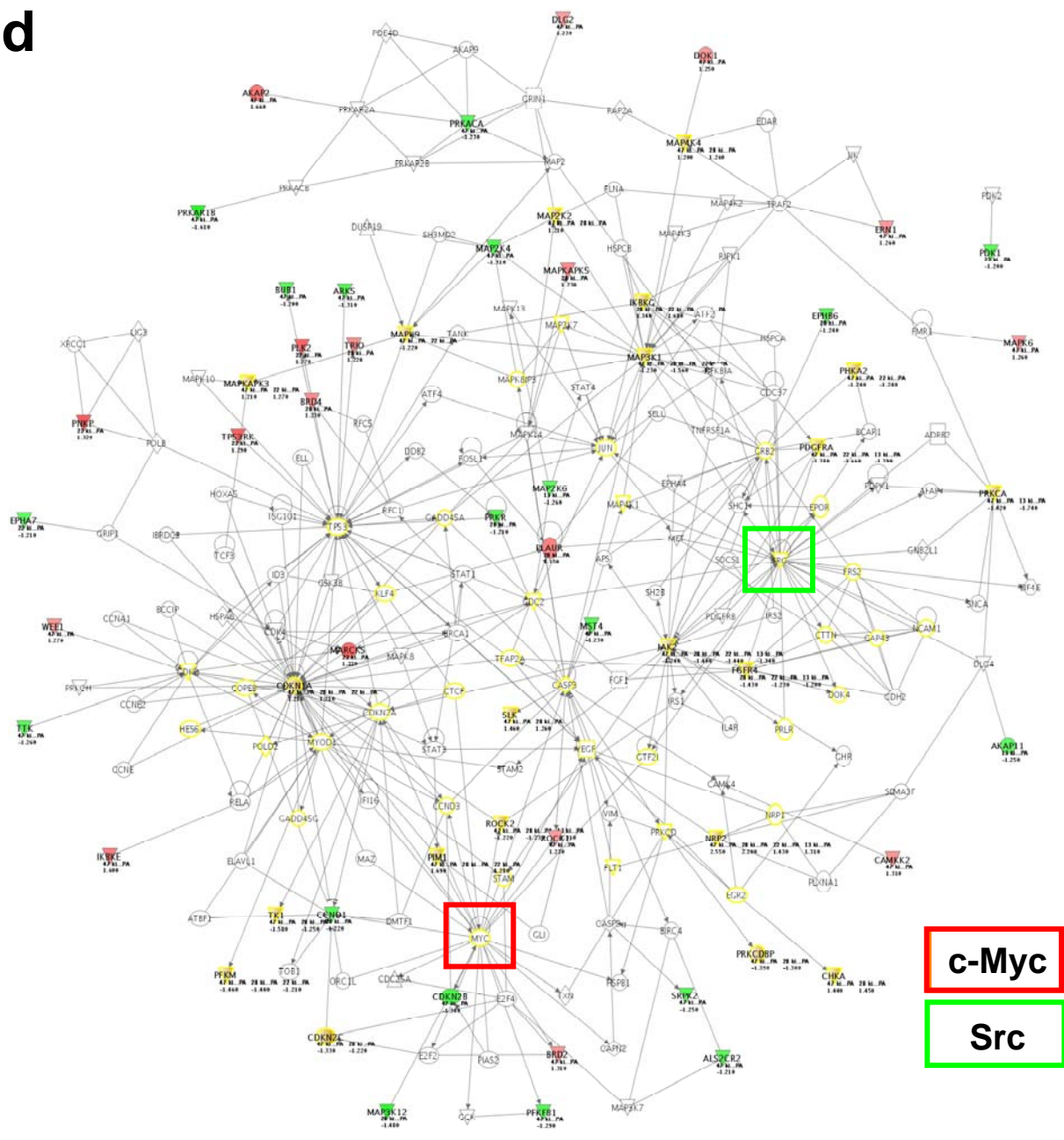
b

Supplementary Figure 1 | Microarray data analysis with Ingenuity Pathway Software revealed recurrent genes that were included in the RNAi screen.
(a-d) Microarray analysis of the genes differentially expressed throughout *Plasmodium*-hepatocyte infection (6, 12, 18 and 24 h p.i.) in terms of gene networks with the Ingenuity Pathway Software. Representative gene networks for the recurrent genes, that although not modulated during infection, were selected to be studied in the RNAi screen due to their frequent appearance in gene networks constituted by the genes differentially expressed. The latter are represented by symbols filled in red/pink if up-regulated, green in down-regulated and in yellow if modulated in more than one infection time point whereas the recurrent genes, i.e., Fos, c-Myc, Tnf and Src are respectively highlighted by orange, red, blue and green boxes.
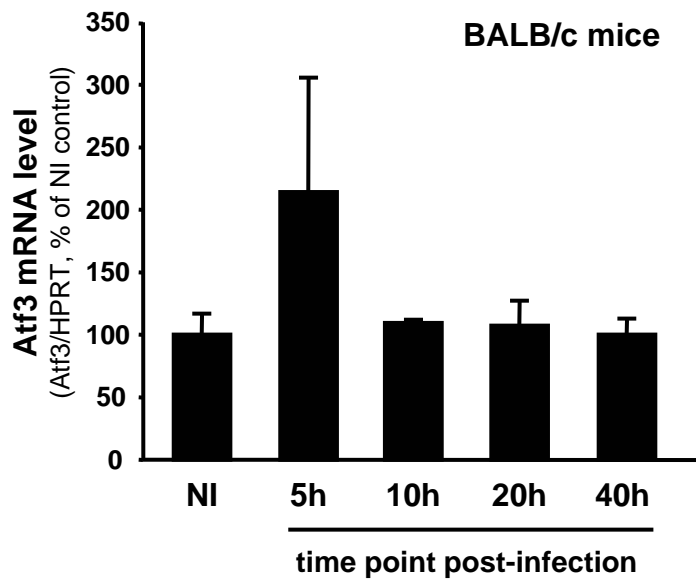
Supplementary Figure 2 | Atf3 mRNA level is up-regulated 5 h after *Plasmodium berghei* sporozoite infection *in vivo*.
BALB/c mice were infected with 10×10^4 *P. berghei* sporozoites and the Atf3 mRNA level was determined by qRT-PCR at different time points, namely 5, 10, 20 and 40h p.i. (3 mice per experimental group). An increase on the Atf3 mRNA level is observed 5h after sporozoite injection when comparing to non-infected control mice (NI).

Gene information			Microarray Fold Change ratio at different time points post-infection[1]			
Gene Official Full Name	Gene Official Symbol	NCBI Gene Accession Number	6h	12h	18h	24h
chemokine (C-X-C motif) ligand 2	Cxcl2	20310	10,35	3,2	2,06	1,08
ChaC, cation transport regulator-like 1 (E. coli)	Chac 1/ 1810008K03Rik	69065	8,88	4,44	2,32	2,27
chemokine (C-X-C motif) ligand 1	Cxcl1	14825	6,33	2,51	1,49	0,88
nuclear protein 1	Nupr1	56312	6,21	3,91	2,56	2,08
tribbles homolog 3 (Drosophila)	Trib3 / Ifld2	228775	4,79	3,71	2,79	2,54
DNA-damage inducible transcript 3	Ddit3	13198	4,65	3,23	1,41	1,48
chemokine (C-C motif) ligand 2	Ccl2	20296	4,61	1,55	1,22	1,08
chemokine (C-X-C motif) ligand 5	Cxcl5	20311	3,93	1,72	-0,79	-0,96
1200016E24Rik RIKEN cDNA 1200016E24 gene	1200016E24Rik	319202	3,26	1,01	0,77	-0,6
solute carrier family 7 (cationic amino acid transporter, y+ system), member 2	Slc7a2	11988	3,24	1,87	0,92	0,79
solute carrier family 7 (cationic amino acid transporter, y+ system), member 2	Slc7a2	11988	3,17	1,77	0,69	0,87
growth arrest and DNA-damage-inducible 45 beta	Gadd45b	17873	3,15	2,64	1,71	1,35
CCAAT/enhancer binding protein (C/EBP), delta	Cebpd	12609	3,08	1,07	0,88	0,85
activating transcription factor 3	Atf3	11910	2,99	1,82	1,48	1,58
G protein-coupled receptor 137B	Gpr137b	83924	2,99	3,76	3,19	1,73
vascular cell adhesion molecule 1	Vcam1	22329	2,93	-1,19	-0,99	-1,05
solute carrier family 7 (cationic amino acid transporter, y+ system), member 11	Slc7a11	26570	2,9	2,01	2,12	1,46
Tnf receptor-associated factor 1	Traf1	22029	2,88	0,85	0,88	0,96
interleukin 1 receptor antagonist	Il1rn	16181	2,87	3,2	1,66	0,96
chloride channel calcium activated 1	Clca1	12722	2,81	0,94	-0,67	-0,83
tumor necrosis factor, alpha-induced protein 2	Tnfaip2	21928	2,7	1,08	-0,79	-0,92
expressed sequence AI845619	AI845619	103846	2,66	1,83	1,37	1,28
carbonic anhydrase 2	Car2	12349	2,62	2,32	1,35	0,86
chloride channel calcium activated 1 /// Clca2 chloride channel calcium activated 2	Clca1 /// Clca2	12722 /// 80797	2,59	0,83	-0,42	-1,01
neuropilin 2	Nrp2	18187	2,55	2,2	1,43	1,31
ankyrin repeat and BTB (POZ) domain containing 2	Abtb2	99382	2,43	1,37	1,1	1
chemokine (C-X-C motif) ligand 16	Cxcl16	66102	2,39	1,6	1,01	1,37
myeloid differentiation primary response gene 116	Myd116	17872	2,3	3,46	1,71	1,52
caspase 4, apoptosis-related cysteine peptidase	Casp4	12363	2,24	1,15	-1,03	0,87
G protein-coupled receptor, family C, group 5, member B	Gprc5b	64297	2,24	0,6	-0,43	0,81
3110004L20Rik RIKEN cDNA 3110004L20 gene	3110004L20Rik	73102	2,21	1,33	1,2	0,98
macrophage activation 2 like [	Mpa2l	100702	2,17	-1,2	-0,88	-0,89
growth differentiation factor 15	Gdf15	23886	2,15	2,07	1,32	1,29
chemokine (C-X-C motif) ligand 10	Cxcl10	15945	2,14	-0,85	1,03	0,9
#probe design_01			2,09	1,44	1,41	1,16
a disintegrin-like and metallopeptidase (reprolysin type) with thrombospondin type 1 motif, 1	Adamts1	11504	2,08	1,55	0,86	1,09
interferon-related developmental regulator 1	Ifrd1	15982	2,05	1,46	0,93	1,02
BCL2-like 11 (apoptosis facilitator)	Bcl2l11	12125	2,04	1,41	1,14	1,12
serine (or cysteine) peptidase inhibitor, clade B, member 2	Serpinb2	18788	2,03	1,16	0,64	-0,9
Nuclear receptor subfamily 4, group A, member 2	Nr4a2	18227	2,01	1,34	1,64	0,97

Gene information			Microarray Fold Change ratio at different time points post-infection[1]			
Gene Official Full Name	Gene Official Symbol	NCBI Gene Accession Number	6h	12h	18h	24h
chemokine (C-C motif) ligand 20	Ccl20	20297	2	-0,88	-0,86	-1,09
#probe design_02			1,97	2,59	1,37	0,46
nuclear factor of kappa light chain gene enhancer in B-cells inhibitor, beta	Nfkbib	18036	1,97	1,41	1,06	1,11
solute carrier family 30 (zinc transporter), member 1	Slc30a1	22782	1,97	1,58	1,1	0,85
solute carrier family 7 (cationic amino acid transporter, y+ system), member 11	Slc7a11	26570	1,97	2,37	1,7	1,27
2310005L22Rik RIKEN cDNA 2310005L22 gene	2310005L22Rik	69471	1,95	1,7	1,27	0,93
5430416N02Rik RIKEN cDNA 5430416N02 gene	5430416N02Rik	71426	1,95	1,92	1,02	0,84
methylenetetrahydrofolate dehydrogenase (NAD+ dependent), methenyltetrahydrofolate cyclohydrolase	Mthfd2	17768	1,94	1,57	1,37	1,1
#probe design_03			1,93	1,9	1,01	1
syndecan binding protein (syntenin) 2	Sdcbp2	228765	1,93	1,95	1,48	1,17
homocysteine-inducible, endoplasmic reticulum stress-inducible, ubiquitin-like domain member 1	Herpud1	64209	1,91	1,16	-0,82	0,73
growth arrest and DNA-damage-inducible 45 gamma	Gadd45g	23882	1,9	1,9	1,46	1,02
solute carrier family 20, member 1	Slc20a1	20515	1,9	1,72	1,09	1,37
integrin beta 6	Itgb6	16420	1,86	1,18	0,91	0,88
tumor necrosis factor, alpha-induced protein 3	Tnfaip3	21929	1,86	1,09	0,95	0,91
small nucleolar RNA, C/D box 22	Snord22	83673	1,83	1,73	0,87	1,11
solute carrier family 11 (proton-coupled divalent metal ion transporters), member 2	Slc11a2	18174	1,83	-0,92	-0,85	0,71
a disintegrin-like and metallopeptidase (reprolysin type) with thrombospondin type 1 motif, 4	Adamts4	240913	1,8	1,09	-0,9	0,86
Aars alanyl-tRNA synthetase	Aars	234734	1,8	1,67	1,58	1,43
zinc finger, AN1-type domain 2A	Zfand2a	100494	1,78	1,72	1,16	1,04
mannosidase 1, alpha	Man1a	17155	1,77	1,2	-0,87	-0,87
metallothionein 2	Mt2	17750	1,77	2,95	1,31	1,15
apolipoprotein B editing complex 1	Apobec1	11810	1,74	1,28	1,04	-0,96
chloride channel calcium activated 4	Clca4	229927	1,74	1,61	-0,57	-0,54
A kinase (PRKA) anchor protein 2	Akap2	11641	1,73	1,2	1,22	1,12
activating transcription factor 4	Atf4	11911	1,73	1,78	1,23	0,92
B-cell leukemia/lymphoma 6	Bcl6	12053	1,71	1,12	1,02	0,88
SKI-like	Skil	20482	1,71	1,62	1,05	0,93
solute carrier family 7 (cationic amino acid transporter, y+ system), member 5	Slc7a5	20539	1,71	1,21	1,27	0,95
leukemia inhibitory factor	Lif	16878	1,7	1,25	1,01	0,88
aldehyde dehydrogenase 18 family, member A1	Aldh18a1	56454	1,7	1,53	1,28	1,02
activating transcription factor 5	Atf5	107503	1,69	1,39	1,63	1,45
proviral integration site 1	Pim1	18712	1,69	1,13	1,28	0,79
activating transcription factor 2	Atf2	11909	1,68	1,06	-0,94	-0,83
#probe design_04			1,68	1,16	-0,53	0,94
RIKEN cDNA 2410187C16 gene	2410187C16Rik	76773	1,68	1,1	-0,82	-0,94
transformed mouse 3T3 cell double minute 2	Mdm2	17246	1,67	1,59	1,28	0,93
solute carrier family 1 (glutamate/neutral amino acid transporter), member 4	Slc1a4	55963	1,66	1,01	1,27	0,96
RIKEN cDNA 2610034E01 gene	2610034E01Rik	69236	1,65	1,08	1,01	0,7
solute carrier family 3 (activators of dibasic and neutral amino acid transport), member 2	Slc3a2	17254	1,65	1,82	1,17	1,28
fos-like antigen 1	Fosl1	14283	1,64	1,44	1,66	0,89
#probe design_05			1,64	0,72	0,96	0,99

Gene information			Microarray Fold Change ratio at different time points post-infection[1]			
Gene Official Full Name	**Gene Official Symbol**	**NCBI Gene Accession Number**	**6h**	**12h**	**18h**	**24h**
expressed sequence AI597479	AI597479	98404	1,63	1,27	1,19	1,05
torsin family 3, member A	Tor3a	30935	1,63	1,21	-0,88	1,02
#probe design_06			1,62	-0,93	-0,94	-1,07
F-box only protein 33	Fbxo33	70611	1,61	1,5	1,15	1,17
colony stimulating factor 1 (macrophage)	Csf1	12977	1,61	1,03	1,35	0,84
6-phosphofructo-2-kinase/fructose-2,6-biphosphatase 3	Pfkfb3	170768	1,6	1,13	1,16	0,91
inhibitor of kappaB kinase epsilon	Ikbke	56489	1,6	-0,87	-0,6	0,97
syntaxin 11	Stx11	74732	1,6	-0,86	-1,06	-1,11
v-maf musculoaponeurotic fibrosarcoma oncogene family, protein K (avian)	Mafk	17135	1,6	1,25	1,39	1,28
arrestin domain containing 4	Arrdc4	66412	1,59	1,29	1,22	1,01
CDC42 effector protein (Rho GTPase binding) 3	Cdc42ep3	260409	1,59	1,25	1,21	1,01
sequestosome 1	Sqstm1	18412	1,59	1,71	1,46	1,09
*cDNA sequence_01			1,58	1,54	1,05	-0,88
keratin associated protein 6-1	Krtap6-1	16700	1,58	-0,82	-1,07	-0,97
serine (or cysteine) peptidase inhibitor, clade B, member 9g	Serpinb9g	93806	1,57	1,6	2,13	0,76
LON peptidase N-terminal domain and ring finger 1 similar to CG32369-PB, isoform B	LOC631639	631639	1,57	1,45	1,1	1,19
purine rich element binding protein B	Purb	19291	1,57	1,15	1,13	-0,82
schlafen 2	Slfn2	20556	1,57	0,95	1,09	0,94
transformation related protein 53 inducible nuclear protein 1	Trp53inp1	60599	1,57	1,35	1,69	0,93
#probe design_07			1,56	-0,86	-0,76	-1,12
Sequestosome 1	Sqstm1	18412	1,56	1,65	-0,7	1,24
RIKEN cDNA 2410018M08 gene	2410018M08Rik	71970	1,56	0,92	1,31	1,14
zinc fingers and homeoboxes protein 2	Zhx2	387609	1,56	0,89	0,91	1,1
phorbol-12-myristate-13-acetate-induced protein 1	Pmaip1	58801	1,55	1,31	1,45	0,56
zinc finger protein 423	zfp423	94187	1,55	1,47	1,39	0,83
poly (ADP-ribose) polymerase family, member 8	Parp8	52552	1,54	2,04	0,25	1,94
Rho family GTPase 1	Rnd1	223881	1,54	-1,01	0,91	0,78
melanoregulin	Mreg	381269	1,54	1,37	1,26	0,68
leucine-rich repeat-containing 5	Lrrc8d	231549	1,53	1,24	1,22	1,04
solute carrier family 7 (cationic amino acid transporter, y+ system), member 1	Slc7a1	11987	1,53	1,34	1,02	0,89
RIKEN cDNA 2700007P21 gene	2700007P21Rik	212772	1,52	1,24	1,15	0,94
TruB pseudouridine (psi) synthase homolog 2 (E. coli)	Trub2	227682	1,52	1,09	1,14	0,99
zinc finger CCCH type containing 8	Zc3h8	57432	1,52	1,16	1,2	0,89
ADP-ribosylation factor related protein 1	Arfrp1	76688	1,51	1,11	1,24	0,99
colony stimulating factor 1 (macrophage)	Csf1	12977	1,51	1,31	0,84	0,73
CCAAT/enhancer binding protein (C/EBP), beta	Cebpb	12608	1,51	1,42	1,49	1,25
immediate early response 5	Ier5	15939	1,51	1,37	1,28	1,06
repetin	Rptn	20129	1,51	-0,83	-0,69	-0,72
B-cell linker	Blnk	17060	1,5	1,84	1,81	1,45
cDNA sequence BC010981	BC010981	407830	1,5	1,17	1,09	0,68
gene model 129, (NCBI)	Gm129	229599	1,5	1,1	0,95	1
leucine-rich repeats and immunoglobulin-like domains 1	Lrig1	16206	1,5	0,91	-1	-1,02

Gene information			Microarray Fold Change ratio at different time points post-infection[1]			
Gene Official Full Name	Gene Official Symbol	NCBI Gene Accession Number	6h	12h	18h	24h
RIKEN cDNA A830080D01 gene	A830080D01Rik	382252	1,5	1,24	0,97	0,9
trinucleotide repeat containing 15	Tnrc15	227331	1,5	1,09	0,7	1
RIKEN cDNA 6720458F09 gene	6720458F09Rik	328162	1,49	1,35	1,53	0,98
HECT, UBA and WWE domain containing 1	Huwe1	59026	1,49	0,93	0,85	-0,96
aldehyde dehydrogenase 1 family, member L2	Aldh1l2	216188	1,49	1,55	1,33	1,02
RIKEN cDNA D730035F11 gene	D730035F11Rik	320010	1,49	1,22	0,92	-0,78
serine/threonine kinase 17b (apoptosis-inducing)	Stk17b	98267	1,49	1,29	1,11	1,13
*cDNA sequence_02			1,48	1,17	1,02	0,94
nuclear receptor subfamily 4, group A, member 2	Nr4a2	18227	1,48	1,22	1,11	0,76
protein tyrosine phosphatase, non-receptor type 14	Ptpn14	19250	1,48	1,51	1,25	1,13
centrosome and spindle pole associated protein 1	Cspp1	211660	1,48	0,8	1,06	-0,56
cysteine rich protein 61	Cyr61	16007	1,47	0,62	0	1,32
dipeptidylpeptidase 7	Dpp7	83768	1,47	1,53	1,39	1,83
intercellular adhesion molecule	Icam1	15894	1,47	-0,96	-1,05	-0,92
sema domain, immunoglobulin domain (Ig), and GPI membrane anchor, (semaphorin) 7A	Sema7a	20361	1,47	0,96	-1,06	-0,93
TAP binding protein-like	Tapbpl	213233	1,47	0,98	-1,04	-1,03
ornithine decarboxylase, structural 1	Odc1	18263	1,46	1,15	-0,94	0,92
STE20-like kinase (yeast)	Slk	20874	1,46	1,26	0,79	0,98
zinc finger protein 346	Zfp346	26919	1,46	1,25	1,02	0,87
BH3 interacting domain death agonist	Bid	12122	1,45	1,3	1,28	1,2
vacuolar protein sorting 37B (yeast)	Vps37b	330192	1,45	1,31	1	0,94
dual specificity phosphatase 4	Dusp4	319520	1,45	1,68	0,96	0,97
lymphotoxin B	Ltb	16994	1,45	0,86	-1,46	-1,38
protein phosphatase 1 (formerly 2C)-like	Ppm1l	242083	1,45	1,07	1,2	0,88
RIKEN cDNA 1110054O05 gene	1110054O05Rik	66209	1,45	1,31	1,46	1,04
oxidative stress induced growth inhibitor 1	Osgin1	71839	1,45	1,13	0,97	0,82
RIKEN cDNA 2610207I05 gene	2610207I05Rik	233789	1,45	1,26	0,87	0,82
choline kinase alpha	Chka	12660	1,44	1,45	-0,63	0,94
cryptochrome 1 (photolyase-like)	Cry1	12952	1,44	1,21	0,96	1,12
RAB32, member RAS oncogene family	Rab32	67844	1,44	0,94	0,9	0,89
neuron-glia-CAM-related cell adhesion molecule	Nrcam	319504	1,44	1,35	0,8	-0,9
WD repeat domain 37	Wdr37	207615	1,44	0,94	0,98	-0,86
apoptosis inhibitor 5	Api5	11800	1,43	1,1	1,21	1,04
Kruppel-like factor 4 (gut)	Klf4	16600	1,43	1,35	1,26	1,57
ESF1, nucleolar pre-rRNA processing protein, homolog (S. cerevisiae)	Esf1	66580	1,43	1,21	1,04	0,73
CD83 antigen	Cd83	12522	1,42	-1,02	-0,93	-1,03
interferon stimulated exonuclease gene 20-like 1	Isg20l1	68048	1,42	1,14	1,3	0,91
sestrin 2	Sesn2	230784	1,42	1,59	1,52	1,18
zinc finger protein 296	Zfp296	63872	1,42	1,35	1,49	1,3
zinc finger protein 566	Zfp566	72556	1,42	1,41	1,15	0,92
cDNA sequence BC022687	BC022687	217887	1,41	1,22	1,27	1,18
Growth factor receptor bound protein 2-associated protein 2	Gab2	14389	1,41	1,5	1,18	0,66

Gene information			Microarray Fold Change ratio at different time points post-infection[1]			
Gene Official Full Name	**Gene Official Symbol**	**NCBI Gene Accession Number**	**6h**	**12h**	**18h**	**24h**
#probe design_08			1,41	1,4	1,18	1,05
expressed sequence AW112010	AW112010	107350	1,41	1,06	-1,01	-0,93
gephyrin	Gphn	268566	1,41	-0,91	0,96	0,81
meningioma expressed antigen 5 (hyaluronidase)	Mgea5	76055	1,41	1,06	0,96	0,84
prostaglandin-endoperoxide synthase 1	Ptgs1	19224	1,41	0,69	1	0,58
SFT2 domain containing 2	Sft2d2	108735	1,41	1,35	1,03	1,13
trans-golgi network protein	Tgoln1	22134	1,41	1,24	0,86	1,2
translocase of inner mitochondrial membrane 10 homolog (yeast)	Timm10	30059	1,41	1,41	1,32	1,24
Nfkbiz nuclear factor of kappa light polypeptide gene enhancer in B-cells inhibitor, zeta	Nfkbiz	80859	1,4	0,94	-0,79	0,85
#probe design_09			1,4	0,77	0,75	-1,02
RIKEN cDNA 5031425E22 gene	5031425E22Rik	75977	1,4	1,24	1,07	1,07
cytochrome b5 reductase 1	Cyb5r1	72017	1,39	1,78	1,36	1,36
cache domain containing 1	Cachd1	320508	1,39	1,74	1,32	1,2
small proline-rich protein 1B	Sprr1b	20754	1,39	2,21	2,27	2,31
spermidine/spermine N1-acetyl transferase 1	Sat1	20229	1,39	1,4	1,12	1,07
fibronectin leucine rich transmembrane protein 3	Flrt3	71436	1,37	1,44	1,25	1,37
ATPase, Na+/K+ transporting, beta 1 polypeptide	Atp1b1	11931	1,35	1,49	1	0,83
#probe design_10			1,34	1,53	1,77	1,82
RIKEN cDNA 3110023B02 gene	3110023B02Rik	67291	1,33	1,41	1,25	0,9
expressed sequence AI117581	AI117581	103629	1,32	1,4	0,79	0,93
RIKEN cDNA 2610200G18 gene	2610200G18Rik	67149	1,32	1,42	1,1	1,02
TATA box binding protein (Tbp)-associated factor, RNA polymerase I, A	Taf1a	21339	1,32	1,45	1,09	0,84
heme oxygenase (decycling) 1	Hmox1	15368	1,31	0,54	1,84	1,16
acyl-CoA thioesterase 2	Acot2	171210	1,31	1,66	1,47	0,98
solute carrier family 25, member 33	Slc25a33	70556	1,31	1,5	1,15	1,16
ataxin 2 binding protein 1	A2bp1	268859	1,3	-1,12	-0,99	-1,42
phosphoserine phosphatase	Psph	100678	1,3	1,8	1,36	1,1
pyrroline-5-carboxylate reductase 1	Pycr1	209027	1,3	1,61	1,37	0,98
ribonuclease P 40 subunit (human)	Rpp40	208366	1,29	1,28	1,47	1,14
ATPase, H+ transporting, lysosomal V0 subunit B	Atp6v0b	114143	1,28	1,36	1,34	1,45
thioredoxin reductase 1	Txnrd1	50493	1,28	0,33	1,5	1,19
#probe design_11			1,27	1,41	0,96	0,99
Serine hydroxymethyltransferase 2 (mitochondrial)	Shmt2	108037	1,25	1,48	1,16	1,35
ectonucleotide pyrophosphatase/phosphodiesterase 2	Enpp2	18606	1,24	1,07	-1,42	-1,44
DEP domain containing 7	Depdc7	211896	1,24	1,22	1,49	1,24
metallothionein 1	Mt1	17748	1,24	1,92	0,88	0,85
ceroid lipofuscinosis, neuronal 3, juvenile (Batten, Spielmeyer-Vogt disease)	Cln3	12752	1,23	1,21	1,33	1,4
DPH2 homolog (S. cerevisiae)	Dph2	67728	1,23	1,26	1,44	1,32
Nur77 downstream gene 2	Ndg2	103172	1,23	1,97	2,67	2,39
4-hydroxyphenylpyruvate dioxygenase-like	Hpdl	242642	1,22	1,16	1,67	1,31
receptor accessory protein 6	Reep6	70335	1,22	1,55	1,79	1,49
Esterase D/formylglutathione hydrolase	Esd	13885	1,2	1,75	0,86	0,89

Gene information			Microarray Fold Change ratio at different time points post-infection[1]			
Gene Official Full Name	Gene Official Symbol	NCBI Gene Accession Number	6h	12h	18h	24h
phosphomannomutase 1	Pmm1	29858	1,19	1,66	1,63	1,3
serine (or cysteine) proteinase inhibitor, clade E, member 2	Serpine2	20720	1,19	1,62	1,09	0,6
zinc finger protein 142	Zfp142	77264	1,17	1,42	1,02	0,86
C-type lectin domain family 4, member d	Clec4d	17474	1,16	2,26	1,42	0,91
nucleolar and coiled-body phosphoprotein 1	Nolc1	70769	1,15	0,71	0,97	1,42
ribosomal protein S15a	Rps15a	267019	1,15	1,46	0,58	0,9
transmembrane and tetratricopeptide repeat containing 2	Tmtc2	278279	1,15	-0,86	-1,54	-1,42
Capping protein (actin filament), gelsolin-like	Capg	12332	1,14	1,49	1,02	0,75
psoriasis susceptibility 1 candidate 2 (human)	Psors1c2	57390	1,14	-1	-1,37	-1,78
calcium/calmodulin-dependent protein kinase kinase 2, beta	Camkk2	207565	1,13	0,95	1,44	0,84
#probe design_12			1,12	1,71	0,8	1,13
laminin, gamma 2	Lamc2	16782	1,12	1,51	1,69	1,32
RIKEN cDNA A830021K08 gene	A830021K08Rik	320427	1,1	1,5	1,17	1,12
target of myb1 homolog (chicken)	Tom1	21968	1,1	1,44	1,21	1,19
*cDNA sequence_03			1,08	1,13	1,43	1,04
serine (or cysteine) proteinase inhibitor, clade B, member 9b	Serpinb9b	20706	1,08	1,41	1,21	1,23
glycoprotein (transmembrane) nmb	Gpnmb	93695	1,07	1,27	1,52	1,35
heat shock protein 1A	Hspa1a	193740	1,06	1,77	-0,8	0,66
RIKEN cDNA 4932425I24 gene	4932425I24Rik	320214	1,06	0,93	1,42	1,09
arginase type II	Arg2	11847	1,05	0,82	-1,44	-0,81
#probe design_13			1,05	-1,46	-1,28	-1,22
RIKEN cDNA 2700078E11 gene	2700078E11Rik	78832	1,05	1,01	1,42	1,12
RIKEN cDNA 2310047B19 gene	2310047B19Rik	66962	1,04	1	0,98	1,48
claudin 4	Cldn4	12740	1,03	1,23	1,21	1,45
glucosamine-6-phosphate deaminase 1	Gnpda1	26384	1,03	1,01	1,6	1,21
DNA segment, Chr 5, ERATO Doi 593, expressed	D5Ertd593e	52331	1,01	1,4	0,94	1,01
spermatogenesis associated 17	Spata17	74717	1,01	1,69	-0,71	-0,74
#probe design_14			1,01	1,07	0,72	1,85
RIKEN cDNA C230093N12 gene	C230093N12Rik	98952	1,01	1,1	1,4	0,98
cDNA sequence AY036118	AY036118	170798	1	0,88	0,97	1,52
#probe design_15			1	1,58	0,85	1,29
#probe design_16			1	0,8	1,45	1,16
protocadherin 9	Pcdh9	211712	1	1,43	-0,9	-1,12
carboxypeptidase M	Cpm	70574	1	-1,23	-1,07	-1,48
glycoprotein (transmembrane) nmb	Gpnmb	93695	0,99	1,61	1,37	1,34
monoamine oxidase A	Maoa	17161	0,99	1,33	1,44	1,09
Apolipoprotein H	Apoh	11818		1,47	-0,77	0,67
heat shock protein 1B	Hspa1b	15511	0,97	2,63	1,09	0,93
epiplakin 1	Eppk1	223650	0,95	0,98	1,62	0,99
nuclear factor of kappa light polypeptide gene enhancer in B-cells inhibitor, epsilon	Nfkbie	18037	0,95	-1,42	-0,96	-1
gelsolin	Gsn	227753	0,94	1,29	2,12	1,69
kit ligand	Kitl	17311	0,94	1,57	1,61	1

Gene information			Microarray Fold Change ratio at different time points post-infection[1]			
Gene Official Full Name	Gene Official Symbol	NCBI Gene Accession Number	6h	12h	18h	24h
stannin	Snn	20621	0,94	1,23	1,44	0,98
basic helix-loop-helix domain containing, class B5	Bhlhb5	59058	0,93	-1,26	-1,34	-1,56
heat shock protein 1A /// heat shock protein 1B	Hspa1a /// Hspa1b	193740 /// 15511	0,93	2,68	1,21	0,54
RIKEN cDNA 2610528E23 gene	2610528E23Rik	66497	0,93	1,22	1,53	1,19
abhydrolase domain containing 5	Abhd5	67469	0,92	1,04	1,39	1,41
cytoplasmic polyadenylation element binding protein 2	Cpeb2	231207	0,91	-0,53	1,75	0,59
Cathepsin A	Ctsa	19025	0,91	1,13	0,85	1,46
nucleotide binding protein 2	Nubp2	26426	0,91	0,99	1,44	1,26
transmembrane protein 69	Tmem69	230657	0,91	-0,93	1,47	1,09
ets homologous factor	Ehf	13661	0,9	-1,18	-0,99	-1,53
pappalysin 2	Pappa2	23850	0,9	1,51	1,26	1,45
vomeronasal 1 receptor, C6	V1rc6	113863	0,9	1,53	-0,78	-0,64
*cDNA sequence_04			0,89	-1,01	-1,3	-1,4
insulin induced gene 1	Insig1	231070	0,89	-1,5	-0,95	-1,06
peroxisome proliferative activated receptor, gamma, coactivator 1 alpha	Ppargc1a	19017	0,88	0,99	1,34	1,47
adenosine deaminase	Ada	11486	0,87	1,08	1,46	0,9
protein tyrosine phosphatase, receptor type, E	Ptpre	19267	0,87	-1,06	-1,35	-1,43
gene model 440, (NCBI)	Gm440	242819	0,85	-1,13	-1,29	-1,43
methionine adenosyltransferase II, alpha	Mat2a	232087	0,85	-1,48	0,92	0,76
chromodomain helicase DNA binding protein 9	Chd9	109151	0,84	-0,96	-1,4	-0,99
coagulation factor II (thrombin) receptor	F2r	14062	0,84	1,47	0,85	0,8
tubulin, beta 2c	Tubb2c	227613	0,84	-1,46	-0,69	0,69
#probe design_17			0,83	1,41	-0,89	0,83
RIKEN cDNA 1700034I23 gene	1700034I23Rik	73297	0,82	0,96	0,48	2,06
inhibitor of kappaB kinase gamma	Ikbkg	16151	0,8	1,19	1,56	1,22
centaurin, delta 1	Centd1	212285	0,79	-0,83	1,43	0,84
Sorbin and SH3 domain containing 1	Sorbs1	20411	0,79	-1,5	-0,72	-0,7
alcohol dehydrogenase 7 (class IV), mu or sigma polypeptide	Adh7	11529	0,78	1,77	1,5	1,24
*cDNA sequence_05			0,77	-0,99	-1,07	-1,57
Peroxisome proliferative activated receptor, gamma, coactivator 1 alpha	Ppargc1a	19017	0,73	0,96	1,52	1,05
Baculoviral IAP repeat-containing 4	Birc4	11798	0,66	-1,42	-0,81	0,55
Ataxia telangiectasia and Rad3 related	Atr	245000	0,66	-1,42	-0,82	-0,85
*cDNA sequence_06			0,65	-1,34	-1,03	-1,56
ubiquitin specific protease 15	Usp15	14479	0,57	-1,57	1,26	0,84
Membrane associated guanylate kinase, WW and PDZ domain containing 1	Magi1	14924	0,53	-1,54	-0,39	-0,8
Myeloid ecotropic viral integration site-related gene 1	Mrg1	17536	0,52	-1,56	-0,5	-1,04
Rho-associated coiled-coil containing protein kinase 1	Rock1	19877	0,51	-1,49	-0,26	0,77
glutathione S-transferase, alpha 3	Gsta3	14859	0,51	1,31	2,28	1,39
*cDNA sequence_07			0,49	-1,61	-0,58	-0,88
RIKEN cDNA 3110047M12 gene	3110047M12Rik	73184	0,49	-1,68	-0,3	-0,66
Annexin A4	Anxa4	11746	0,47	-1,55	-0,21	-0,99
Nuclear factor of activated T-cells 5	Nfat5	54446	0,45	-1,47	-0,62	-1,04

Gene information			Microarray Fold Change ratio at different time points post-infection[1]			
Gene Official Full Name	Gene Official Symbol	NCBI Gene Accession Number	6h	12h	18h	24h
RIKEN cDNA 5230400M03 gene	5230400M03Rik	329406	0,45	-1,44	-0,49	-0,96
DENN/MADD domain containing 1B	Dennd1b	329260	0,44	-1,44	-0,75	-0,88
*cDNA sequence_08			0,42	-1,41	-0,69	-1,13
*cDNA sequence_09			0,41	-1,53	-0,44	-1,09
RIKEN cDNA 5930427L02 gene	5930427L02Rik	402754	0,4	-1,52	-0,76	-0,83
ADP-ribosylation factor guanine nucleotide-exchange factor 1(brefeldin A-inhibited)	Arfgef1	211673	0,38	-1,43	-0,29	-0,88
DNA segment, Chr 3, ERATO Doi 452, expressed	D3Ertd452e	51898	0,37	-1,45	-0,95	-1,34
Nipped-B homolog (Drosophila)	Nipbl	71175	0,35	-1,4	-0,31	-0,8
*cDNA sequence_10			0,34	-1,5	-0,64	-0,71
RIKEN cDNA 9630019E01 gene	9630019E01Rik	319967	0,33	-1,33	-0,37	-1,42
*cDNA sequence_11			0,32	-1,49	-0,65	-0,91
*cDNA sequence_12			0,19	-1,57	-0,1	-0,66
Ubiquitin-conjugating enzyme E2H	Ube2h	22214	0,17	-1,42	-0,86	-0,53
*cDNA sequence_13			0	-2,08	-0,16	-0,9
solute carrier family 12, member 2	Slc12a2	20496	0	1,42	-0,54	0,41
RAS, guanyl releasing protein 2	Rasgrp2	19395	-0,32	-0,7	-1,44	-0,76
RIKEN cDNA 2610024D14 gene	2610024D14Rik	70410	-0,51	-1,42	0,97	0,59
cysteine-rich secretory protein 1	Crisp1	11571	-0,57	-0,98	-1,59	-0,93
chemokine (C-C motif) ligand 28	Ccl28	56838	-0,59	0,74	-0,8	1,58
histone cluster 1, H2bc	Hist1h2bc	68024	-0,59	0,86	1,48	-0,67
collectin sub-family member 11	Colec11	71693	-0,69	0,68	1,19	1,52
PDZ and LIM domain 5	Pdlim5	56376	-0,69	-1,42	-1,2	-1,32
#probe design_18			-0,7	-1,43	-1,31	0,62
LUC7-like 2 (S. cerevisiae)	Luc7l2	192196	-0,72	-1,23	-0,93	-1,44
UDP-glucose ceramide glucosyltransferase	Ugcg	22234	-0,73	-1,62	-0,23	0,86
Praja 2, RING-H2 motif containing	Pja2	224938	-0,74	-0,63	-1,9	-0,1
preimplantation protein 4	Prei4	74182	-0,77	-1,45	-0,73	-0,99
zinc finger and BTB domain containing 20	Zbtb20	56490	-0,79	-1,54	-0,85	-0,75
transmembrane protein 16A	Tmem16a	101772	-0,81	1,14	1,51	1,37
#probe design_19			-0,83	-1,14	-1,5	-1,36
Interferon gamma receptor 1	Ifngr1	15979	-0,84	-1	-1,56	-1,1
CTD (carboxy-terminal domain, RNA polymerase II, polypeptide A) small phosphatase like 2	Ctdspl2	329506	-0,86	-1,49	-0,91	-0,86
interleukin 13 receptor, alpha 1	Il13ra1	16164	-0,86	-1,35	-1,71	-1,22
ubiquitin specific protease 53	Usp53	99526	-0,86	-1,68	-0,69	-1,52
ATPase, aminophospholipid transporter (APLT), class I, type 8A, member 1	Atp8a1	11980	-0,87	-1,28	-1,6	-1,5
latent transforming growth factor beta binding protein 3	Ltbp3	16998	-0,87	-1,05	-1,21	-1,42
transcription factor 7-like 2, T-cell specific, HMG-box	Tcf7l2	21416	-0,87	-1,44	-0,84	-0,95
leucine rich repeat containing 28	Lrrc28	67867	-0,88	-0,83	1,49	1,07
*cDNA sequence_14			-0,89	-1,47	-0,8	-0,65
Sterol-C4-methyl oxidase-like	Sc4mol	66234	-0,89	-1,32	-1,53	-1,01
activated leukocyte cell adhesion molecule	Alcam	11658	-0,9	-1,12	-1,42	-1,13
RIKEN cDNA D230012E17 gene	D230012E17Rik	241062	-0,9	-1,01	-1,38	-1,52

Gene information			Microarray Fold Change ratio at different time points post-infection[1]			
Gene Official Full Name	**Gene Official Symbol**	**NCBI Gene Accession Number**	**6h**	**12h**	**18h**	**24h**
adaptor protein, phosphotyrosine interaction, PH domain and leucine zipper containing 2	Appl2	216190	-0,92	-0,97	-1,66	-1,24
Wilms tumor homolog	Wt1	22431	-0,92	-1,27	-1,26	-1,41
sema domain, immunoglobulin domain (Ig), short basic domain, secreted, (semaphorin) 3G	Sema3g	218877	-0,93	-0,95	-1,74	-1,51
dedicator of cytokinesis 4	Dock4	238130	-0,93	-1,17	-1,38	-1,41
glutamate-cysteine ligase , modifier subunit	Gclm	14630	-0,93	1,64	1,66	1,46
zinc finger protein 654	Zfp654	72020	-0,93	-1,43	-1,21	-1,17
serum response factor	Srf	20807	-0,93	1,44	1,09	0,92
bromodomain and WD repeat domain containing 3	Brwd3	382236	-0,94	-0,98	-1	-1,66
#probe design_20			-0,94	-1,58	-0,78	-1,34
potassium channel tetramerisation domain containing 12	Kctd12	239217	-0,94	-1,41	-1,71	-1,54
cyclin T2	Ccnt2	72949	-0,95	-1,16	-1,49	-1,3
fibrinogen, B beta polypeptide	Fgb	110135	-0,95	-1,17	-1,68	-1,18
mitogen activated protein kinase kinase kinase 12	Map3k12	26404	-0,95	-1,48	-0,86	0,87
forkhead-associated (FHA) phosphopeptide binding domain 1	Fhad1	329977	-0,95	-1,16	-1,49	-1,19
bone marrow stromal cell antigen 1	Bst1	12182	-0,96	-1,42	-1,9	-0,79
ATPase, aminophospholipid transporter (APLT), class I, type 8A, member 1	Atp8a1	11980	-0,96	-0,88	-1,62	-1,79
3-hydroxy-3-methylglutaryl-Coenzyme A synthase 1	Hmgcs1	208715	-0,97	-1,64	-2,4	-1,31
complement component factor i	Cfi	12630	-0,97	-1,07	-1,02	-1,41
fibrinogen-like protein 1	Fgl1	234199	-0,97	-1,13	-1,24	-1,41
#probe design_21			-0,97	1,51	1,25	0,96
ERO1-like (S. cerevisiae)	Ero1l	50527	-0,98	-1,01	-1,53	-1,4
apolipoprotein C-IV	Apoc4	11425	-0,99	-1,15	-1,58	-1,07
hepatic nuclear factor 4, alpha	Hnf4a	15378	-0,99	-1,43	-0,93	-0,84
coiled-coil-helix-coiled-coil-helix domain containing 6	Chchd6	66098	-0,99	1,03	1,15	1,44
SLIT and NTRK-like family, member 6	Slitrk6	239250	-0,99	-1,29	-1,49	-1,27
carbonic anhydrase 8	Car8	12319	-1	-1,02	-1,49	-1,34
RIKEN cDNA 4930431B09 gene	4930431B09Rik	74645	-1	-1,44	-1,4	-1,4
histocompatibility 2, Q region locus 1	H2-Q1	15006	-1	-2,14	-0,53	-1,7
protein kinase, cGMP-dependent, type II	Prkg2	19092	-1	-1,07	-1,43	-1,39
cingulin-like 1	Cgnl1	68178	-1	-1,26	-1,41	-1,43
asparagine-linked glycosylation 6 homolog (yeast, alpha-1,3,-glucosyltransferase)	Alg6	320438	-1,01	-1,38	-1,42	-1,01
RIKEN cDNA 0610037L13 gene	0610037L13Rik	74098	-1,01	-1,22	-1,83	-1,13
vesicle-associated membrane protein 4	Vamp4	53330	-1,01	-1,07	-1,41	-1,21
isopentenyl-diphosphate delta isomerase	Idi1	319554	-1,02	-1,42	-1,45	-0,91
solute carrier family 36 (proton/amino acid symporter), member 4	Slc36a4	234967	-1,03	-1,11	-1,27	-1,52
myeloid/lymphoid or mixed lineage-leukemia translocation to 3 homolog (Drosophila)	Mllt3	70122	-1,04	-1,47	-0,8	-0,76
phosphomevalonate kinase	Pmvk	68603	-1,04	-1,39	-1,45	-1,09
DEAD (Asp-Glu-Ala-Asp) box polypeptide 58	Ddx58	230073	-1,05	-1,32	-1,4	-1,45
glutathione S-transferase, alpha 4	Gsta4	14860	-1,05	1,33	1,61	1,37
mal, T-cell differentiation protein 2	Mal2	105853	-1,05	-1,45	-1,21	-1,19
fatty acid desaturase 2	Fads2	56473	-1,06	-1,65	-1,39	-1
hydroxyacid oxidase 1, liver	Hao1	15112	-1,06	-1,01	-1,18	-1,45

Gene information			Microarray Fold Change ratio at different time points post-infection[1]			
Gene Official Full Name	**Gene Official Symbol**	**NCBI Gene Accession Number**	**6h**	**12h**	**18h**	**24h**
RIKEN cDNA 5730469M10 gene	5730469M10Rik	70564	-1,06	-1,41	-1,32	-1,17
butyrylcholinesterase	Bche	12038	-1,07	-1,46	-1,56	-0,91
DNA segment, Chr 11, ERATO Doi 461, expressed	Ccdc69	52570	-1,07	-1,42	-0,82	0,96
solute carrier organic anion transporter family, member 2a1	Slco2a1	24059	-1,07	-1,71	-1,13	-1,19
cytochrome P450, 51	Cyp51	13121	-1,08	-1,37	-1,62	-1
nudix (nucleoside diphosphate linked moiety X)-type motif 13	Nudt13	67725	-1,08	-0,95	-1,12	-1,42
transcription elongation factor A (SII)-like 6	Tceal6	66104	-1,08	-1,6	-0,7	-0,88
WD repeat domain 26	Wdr26	226757	-1,08	0,94	-1,05	-1,6
annexin A4	Anxa4	11746	-1,09	-1,17	-1,05	-1,43
RIKEN cDNA 1810023F06 gene	1810023F06Rik	217845	-1,09	-1,22	-1,44	-1,27
cDNA sequence BC011467	Spns2	216892	-1,1	-1,32	-1,41	-1,67
Calcium/calmodulin-dependent protein kinase II, beta	Camk2b	12323	-1,1	-1,3	-1,62	-1,52
glutamine fructose-6-phosphate transaminase 2	Gfpt2	14584	-1,1	-1,3	-1,43	-1,23
#probe design_22			-1,11	-1,39	-1,43	-1,6
phosphofructokinase, liver, B-type	Pfkl	18641	-1,11	-1,42	-1,01	-0,89
procollagen, type VIII, alpha 1	Col8a1	12837	-1,11	-1,31	-1,5	-1,45
phosphodiesterase 4D interacting protein (myomegalin)	Pde4dip	83679	-1,11	-1,11	-1,38	-1,41
heparan sulfate (glucosamine) 3-O-sulfotransferase 1	Hs3st1	15476	-1,13	-1,08	-1,43	-1,24
dedicator of cytokinesis 9	Dock9	105445	-1,14	-1,12	-1,18	-1,43
protein phosphatase 1, regulatory (inhibitor) subunit 9A	Ppp1r9a	243725	-1,14	-1,21	-1,5	-1,24
24-dehydrocholesterol reductase	Dhcr24	74754	-1,15	-1,41	-0,74	-0,67
caspase 12	Casp12	12364	-1,15	-1,38	-1,45	-1,36
zinc finger, MIZ-type containing 1	Zmiz1	328365	-1,15	-1,28	-1,35	-1,45
fibroblast growth factor receptor 4	Fgfr4	14186	-1,15	-1,43	-1,23	-1,2
inter-alpha (globulin) inhibitor H5	Itih5	209378	-1,15	-1,34	-1,51	-1,16
V-set and immunoglobulin domain containing 1	Vsig1	78789	-1,15	-1,41	-1,24	-1,04
sialyltransferase 4A (beta-galactoside alpha-2,3-sialyltransferase)	St3gal1	20442	-1,15	-0,96	-1,45	-1,03
stearoyl-Coenzyme A desaturase 1	Scd1	20249	-1,16	-1,44	-1,24	-1,01
cAMP responsive element binding protein 3-like 2	Creb3l2	208647	-1,17	-1,42	-1,22	-1,42
DNA segment, Chr 7, ERATO Doi 413, expressed	D7Ertd413e	52325	-1,17	-1,6	-0,95	-0,53
muscleblind-like 3 (Drosophila)	Mbnl3	171170	-1,17	-1,4	-0,92	-0,79
myosin, light polypeptide kinase	Mylk	107589	-1,17	-1,32	-1,45	-1,48
phospholipase C, beta 1	Plcb1	18795	-1,17	-1,39	-1,28	-1,5
proline-rich coiled-coil 1	Prrc1	73137	-1,17	-1,08	-1,06	-1,4
sestrin 3	Sesn3	75747	-1,17	-1,23	-1,2	-1,47
insulin-like growth factor binding protein 3	Igfbp3	16009	-1,18	-1,3	-1,61	-1,45
guanine nucleotide binding protein (G protein), gamma 2 subunit	Gng2	14702	-1,19	-0,8	-1,47	-1,33
SH3-domain GRB2-like (endophilin) interacting protein 1	Sgip1	73094	-1,19	-1,56	-1,51	-1,41
wingless-related MMTV integration site 5A	Wnt5a	22418	-1,19	-1,54	-1,03	-0,96
protein kinase, cGMP-dependent, type II	Prkg2	19092	-1,2	-1,32	-1,49	-1,47
ATP/GTP binding protein-like 3	Agbl3	76223	-1,2	-1,47	-1,17	-1,02
serine (or cysteine) proteinase inhibitor, clade A (alpha-1 antiproteinase, antitrypsin), member 10	Serpina10	217847	-1,2	-1,54	-1,35	-1,07

Gene information			Microarray Fold Change ratio at different time points post-infection[1]			
Gene Official Full Name	Gene Official Symbol	NCBI Gene Accession Number	6h	12h	18h	24h
myeloid/lymphoid or mixed lineage-leukemia translocation to 3 homolog (Drosophila)	Mllt3	70122	-1,21	-1,42	-0,83	-0,93
RIKEN cDNA C030045D06 gene	C030045D06Rik	109294	-1,21	-1,28	-1,69	-1,39
ATP-binding cassette, sub-family A (ABC1), member 5	Abca5	217265	-1,22	-1,37	-1,45	-1,51
BCL2/adenovirus E1B 19kDa-interacting protein 3-like	Bnip3l	12177	-1,22	-1,45	-1,22	-1,13
solute carrier family 2 (facilitated glucose transporter), member 1	Slc2a1	20525	-1,22	-1,09	-1,51	-1
mitogen activated protein kinase kinase kinase 1	Map3k1	26401	-1,23	-1,56	-1,23	-0,97
3-hydroxybutyrate dehydrogenase (heart, mitochondrial)	Bdh1	71911	-1,24	-1,5	-1,32	-0,95
chemokine (C-X-C motif) ligand 15	Cxcl15	20309	-1,24	-1,62	-1,15	-1,15
Janus kinase 2	Jak2	16452	-1,24	-1,4	-1,44	-1,19
low density lipoprotein receptor	Ldlr	16835	-1,24	-1,35	-1,69	-1,12
platelet-derived growth factor, C polypeptide	Pdgfc	54635	-1,24	0,89	1,41	1,27
early growth response 2	Egr2	13654	-1,25	-1,81	-2,44	-2,54
T-cell leukemia translocation altered gene	Tcta	102791	-1,25	-1,41	-1,08	-1,1
*cDNA sequence_15			-1,26	-1,13	-1	-1,45
smoothelin-like 2	Smtnl2	276829	-1,26	-0,95	-1,4	-1,2
aquaporin 11	Aqp11	66333	-1,27	-1,22	-1,41	-1,25
*cDNA sequence_16			-1,27	-2,43	-1,84	-1,47
insulin-like growth factor binding protein 1	Igfbp1	16006	-1,27	-1,3	-1,45	-1,06
killer cell lectin-like receptor, subfamily A, member 2	Klra2	16633	-1,27	-1,29	-1,4	-1,18
phosphofructokinase, platelet	Pfkp	56421	-1,27	-1,29	-1,47	-1,05
phosphoglucomutase 2	Pgm2	72157	-1,27	-1,4	-1,15	-0,92
potassium channel, subfamily K, member 2	Kcnk2	16526	-1,27	-1,19	-1,42	-1,5
ATPase, class V, type 10A	Atp10a	11982	-1,28	-1,4	-1,34	-1,14
butyrylcholinesterase	Bche	12038	-1,28	-1,45	-1,61	-1,21
Inositol polyphosphate-4-phosphatase, type II	Inpp4b	234515	-1,3	-1,21	-0,75	-1,43
StAR-related lipid transfer (START) domain containing 4	Stard4	170459	-1,3	-1,77	-1,48	-1,21
chemokine (C-X-C motif) ligand 15	Cxcl15	20309	-1,32	-1,92	-1,33	-1,46
TBC1 domain family, member 8B	Tbc1d8b	245638	-1,32	-1,39	-1,56	-1,63
ankyrin repeat and sterile alpha motif domain containing 1B	Anks1b	77531	-1,32	-1,21	-1,43	-1,2
RIKEN cDNA D630039A03 gene	D630039A03Rik	242484	-1,32	-1,44	-1,14	-1,18
histone 2, H2bb	Hist2h2bb	319189	-1,33	-1,21	-1,34	-1,45
calcium/calmodulin-dependent protein kinase II inhibitor 1	Camk2n1	66259	-1,33	-1,38	-1,18	-1,41
farnesyl diphosphate synthetase	Fdps	110196	-1,34	-1,42	-1,24	-0,7
spastic paraplegia 3A homolog (human)	Spg3a	73991	-1,35	-1,15	-1,51	-1,16
DNA segment, Chr 7, ERATO Doi 743, expressed	Tmem41b	233724	-1,37	-1,28	-1,44	-1,06
erythrocyte protein band 4.1-like 2	Epb4.1l2	13822	-1,38	-1,57	-1,28	-1,08
platelet derived growth factor receptor, alpha polypeptide	Pdgfra	18595	-1,38	-0,94	-1,66	-1,39
protein C	Proc	19123	-1,38	-1,52	-1,35	-1,52
protein phosphatase 1K (PP2C domain containing)	Ppm1k	243382	-1,38	-1,05	-1,54	-1,42
coatomer protein complex, subunit zeta 2	Copz2	56358	-1,39	-1,46	-1,28	-1,2
general transcription factor II E, polypeptide 2 (beta subunit)	Gtf2e2	68153	-1,4	-1,09	-1,16	-1,2
interferon activated gene 203	Ifi203	15950	-1,4	-1,53	-1,04	-0,92

Gene information			Microarray Fold Change ratio at different time points post-infection[1]			
Gene Official Full Name	**Gene Official Symbol**	**NCBI Gene Accession Number**	**6h**	**12h**	**18h**	**24h**
glutathione S-transferase, mu 7	Gstm7	68312	-1,4	-1,31	-1,02	-1,25
arylsulfatase G	Arsg	74008	-1,4	-1,63	-1,49	-1,58
t-complex 11 (mouse) like 2	Tcp11l2	216198	-1,4	-0,78	-1,2	-1,26
ubiquitin specific protease 18	Usp18	24110	-1,4	-0,92	0,93	0,95
amylo-1,6-glucosidase, 4-alpha-glucanotransferase	Agl	77559	-1,41	-1,14	-1,07	-1,46
fibroblast growth factor 1	Fgf1	14164	-1,41	-1,22	-1,14	-0,79
KH domain containing, RNA binding, signal transduction associated 3	Khdrbs3	13992	-1,41	-1,35	-0,95	-1,17
peptidyl arginine deiminase, type III	Padi3	18601	-1,41	-1,13	-0,58	-0,7
PX domain containing serine/threonine kinase	Pxk	218699	-1,41	-1,09	-1,05	-1,01
2,3-bisphosphoglycerate mutase	Bpgm	12183	-1,42	0,9	0,89	0,88
calponin 2	Cnn2	12798	-1,42	-1,04	-0,92	0,94
integrin alpha FG-GAP repeat containing 1	Itfg1	71927	-1,42	-1,28	-1,06	-1,05
GH regulated TBC protein 1	Grtp1	66790	-1,42	-1,59	-1,1	-0,88
membrane bound O-acyltransferase domain containing 5	Mboat5	14792	-1,42	-1,39	-1,22	-1,11
kinesin family member 5C	Kif5c	16574	-1,42	-1,48	-1,46	-1,37
mitochondrial tumor suppressor 1	Mtus1	102103	-1,42	-1,13	-1,56	-1,35
protein kinase C, alpha	Prkca	18750	-1,42	-1,03	-1,01	-1,74
RIKEN cDNA 1200009F10 gene	1200009F10Rik	67454	-1,42	-1,15	-1,38	-1,25
MON2 homolog (yeast)	Mon2	67074	-1,42	-0,87	-1,1	-1,2
RIKEN cDNA 6720489N17 gene	6720489N17Rik	211378	-1,42	-1,16	-0,82	-1,01
sphingomyelin phosphodiesterase 1, acid lysosomal	Smpd1	20597	-1,42	-1,02	-1,08	-0,92
CD38 antigen	Cd38	12494	-1,43	-1,15	-1,17	-1,29
lanosterol synthase	Lss	16987	-1,43	-1,63	-1,54	-1,11
thyroid hormone receptor interactor 12	Trip12	14897	-1,43	-1,17	-1,26	-1,32
proline rich 16	Prr16	71373	-1,43	-1,27	-1,19	-1,13
centaurin, beta 2	Centb2	78618	-1,43	-1,21	-0,99	-1,13
HEAT repeat containing 5B	Heatr5b	320473	-1,43	-1,01	-1,04	-1,15
stromal antigen 2	Stag2	20843	-1,43	-1,15	-1,1	-1,16
abhydrolase domain containing 3	Abhd3	106861	-1,44	-0,89	-0,91	-0,81
estrogen receptor 1 (alpha)	Esr1	13982	-1,44	-1,22	-0,98	-1,03
FK506 binding protein 14	Fkbp14	231997	-1,44	-1,3	-1,75	-1,23
glycerol-3-phosphate acyltransferase, mitochondrial	Gpam	14732	-1,44	-1,42	-1,41	-1,16
interferon consensus sequence binding protein 1	Irf8	15900	-1,44	-1,6	-1,09	-0,92
RIKEN cDNA 2510009E07 gene	2510009E07Rik	72190	-1,44	-1,23	-0,92	-1,31
solute carrier family 40 (iron-regulated transporter), member 1	Slc40a1	53945	-1,44	0,76	-1,03	-0,99
tripartite motif protein 2	Trim2	80890	-1,44	-1,09	0,79	-1,21
villin 1	Vil1	22349	-1,44	-1,19	-1,22	-1,04
C-terminal binding protein 2	Ctbp2	13017	-1,45	-1,43	0,83	-0,99
exocyst complex component 7	Exoc7	53413	-1,45	-1,08	-0,87	-0,89
F-box only protein 6b	Fbxo6	50762	-1,45	-1,21	-1,01	-0,76
microtubule-associated protein, RP/EB family, member 2	Mapre2	212307	-1,45	-1,19	0,76	0,8
odd-skipped related 1 (Drosophila)	Osr1	23967	-1,45	0,92	-0,83	0,94

Gene information			Microarray Fold Change ratio at different time points post-infection[1]			
Gene Official Full Name	Gene Official Symbol	NCBI Gene Accession Number	6h	12h	18h	24h
palmdelphin	Palmd	114301	-1,45	-1,23	-1,25	-1,14
arginine/serine-rich coiled-coil 1	Rsrc1	66880	-1,45	-1	0,85	-0,81
serine (or cysteine) proteinase inhibitor, clade B, member 7	Serpinb7	116872	-1,45	-1,32	-0,88	-0,83
ATP-binding cassette, sub-family A (ABC1), member 6	Abca6	76184	-1,46	-1,36	-0,94	-0,66
B lymphoma Mo-MLV insertion region 1	Bmi1	12151	-1,46	-1,21	-0,98	-1,02
NIMA (never in mitosis gene a)-related expressed kinase 1	Nek1	18004	-1,46	-1,16	-1,01	-1,03
phosphofructokinase, muscle	Pfkm	18642	-1,46	-1,4	-1,21	-1,13
RAS p21 protein activator 3	Rasa3	19414	-1,46	-1,19	-1,07	-1,01
retinitis pigmentosa 2 homolog (human)	Rp2h	19889	-1,46	-1,11	-0,8	-0,9
acid phosphatase-like 2	Acpl2	235534	-1,46	-1,02	-1,03	-0,98
dystrophin, muscular dystrophy	Dmd	13405	-1,47	-1,37	-1,18	-1,22
sphingomyelin synthase 1	Sgms1	208449	-1,47	-1,23	-1,36	-1,34
peptidylglycine alpha-amidating monooxygenase COOH-terminal interactor	Pamci	237504	-1,47	-1,24	-1,07	-1,21
purinergic receptor P2Y, G-protein coupled, 14	P2ry14	140795	-1,47	-1,27	-1,43	-1,01
RAS, guanyl releasing protein 3	Rasgrp3	240168	-1,47	-1,6	-1	-1,09
RIKEN cDNA 4631426J05 gene	4631426J05Rik	77590	-1,47	-1,04	-1,14	-1,08
ferrochelatase	Fech	14151	-1,48	-1,07	-1,21	-1,03
Endothelial PAS domain protein 1	Epas1	13819	-1,48	-1,78	-1,58	-1,66
growth factor receptor bound protein 14	Grb14	50915	-1,48	-1,33	-1,2	-0,95
MAD homolog 6 (Drosophila)	Smad6	17130	-1,48	-1,07	-0,9	-0,59
methylcrotonoyl-Coenzyme A carboxylase 1 (alpha)	Mccc1	72039	-1,48	-1,31	-1,56	-1,21
potassium channel tetramerisation domain containing 11	Kctd11	216858	-1,48	-1,49	-1,11	-1,2
RIKEN cDNA C730027H18 gene	C730027H18Rik	319572	-1,48	-1,44	-1,19	-1,37
7-dehydrocholesterol reductase	Dhcr7	13360	-1,49	-1,37	-1,4	-0,78
potassium inwardly-rectifying channel, subfamily J, member 8	Kcnj8	16523	-1,49	-1,05	-1,04	-1,13
RIKEN cDNA 2610027C15 gene	2610027C15Rik	230752	-1,49	-1,33	-1,23	-0,97
RIKEN cDNA 5730494M16 gene	5730494M16Rik	66648	-1,49	-0,98	-0,91	-0,78
bicaudal C homolog 1 (Drosophila)	Bicc1	83675	-1,5	-1,24	-1,11	-1,01
centrosomal protein 290	Cep290	216274	-1,5	-1,54	-1,1	-0,87
grancalcin	Gca	227960	-1,5	-1,49	-1,07	-0,95
zinc finger protein 467	Zfp467	68910	-1,5	-1,15	-1,17	-0,96
UDP glucuronosyltransferase 2 family, polypeptide B34	Ugt2b34	100727	-1,51	-1,38	-1,03	-1,08
kinesin family member 16B	Kif16b	16558	-1,51	-0,96	0,96	-0,99
RIKEN cDNA 1700011H14 gene	1700011H14Rik	67082	-1,51	-1,24	-0,8	-0,79
RIKEN cDNA 2900024C23 gene	2900024C23Rik	67266	-1,51	-1,08	-1,09	-1,07
RIKEN cDNA 9230111E07 gene	9230111E07Rik	77748	-1,52	-1,11	-0,94	-0,94
hypothetical protein 4832420M10	Kif26b	269152	-1,52	-1,28	-0,86	-1,36
flavin containing monooxygenase 2	Fmo2	55990	-1,53	-1,53	-1,29	-1,15
sulfide quinone reductase-like (yeast)	Sqrdl	59010	-1,53	-1,17	-0,86	-1,03
ankyrin repeat and SOCS box-containing protein 1	Asb1	65247	-1,54	-1,16	-1,13	-1,11
cysteinyl leukotriene receptor 1	Cysltr1	58861	-1,54	-1,09	-0,81	-0,98
methionine sulfoxide reductase B	Msrb2	76467	-1,54	-1,11	-1,08	-1,25

Gene information			Microarray Fold Change ratio at different time points post-infection[1]			
Gene Official Full Name	Gene Official Symbol	NCBI Gene Accession Number	6h	12h	18h	24h
nebulin-related anchoring protein	Nrap	18175	-1,54	-1,13	-1,1	-1,08
olfactomedin-like 2B	Olfml2b	320078	-1,54	-1	-0,99	0,82
tetratricopeptide repeat domain 8	Ttc8	76260	-1,54	-1,21	-1,2	-1,1
acetyl-Coenzyme A synthetase 2 (ADP forming)	Acss2	60525	-1,55	-1,55	-1,3	-1,18
N-glycanase 1	Ngly1	59007	-1,55	-1,01	-1,2	-1,16
PDZ and LIM domain 5	Pdlim5	56376	-1,55	-0,94	0,85	-0,7
RIKEN cDNA 1810074P20 gene	1810074P20Rik	67490	-1,55	-1,17	-1,27	-1,09
protein tyrosine phosphatase-like A domain containing 2	Ptplad2	66775	-1,55	-1,17	-1,23	-1,13
tribbles homolog 2 (Drosophila)	Trib2	217410	-1,55	-1,3	-1,1	-1,18
SUMO1/sentrin specific peptidase 7	Senp7	66315	-1,56	-1,07	-1,15	-1,16
sphingomyelin synthase 1	Sgms1	208449	-1,56	-1,09	-1,16	-0,93
erythrocyte protein band 4.1-like 4b	Epb4.1l4b	54357	-1,57	-1,65	-0,93	-1,14
thymidine kinase 1	Tk1	21877	-1,58	-1,25	-0,99	0,97
arginine vasopressin receptor 1A	Avpr1a	54140	-1,59	-1,37	-1,12	-1,23
neuritin 1	Nrn1	68404	-1,59	-1,22	-1,47	-1,16
RAD50 homolog (S. cerevisiae)	Rad50	19360	-1,6	1,11	-0,72	-0,71
RIKEN cDNA 9130213B05 gene	9130213B05Rik	231440	-1,6	-1,02	-1,27	-1,23
solute carrier family 16 (monocarboxylic acid transporters), member 4	Slc16a4	229699	-1,6	-1,43	-1,46	-1,27
troponin T2, cardiac	Tnnt2	21956	-1,6	-1,44	-1,23	-1,36
protein kinase, cAMP dependent regulatory, type I beta	Prkar1b	19085	-1,61	-1,05	-1,01	-1,05
RIKEN cDNA 1190002N15 gene	1190002N15Rik	68861	-1,61	-1,25	-1,89	-1,43
RIKEN cDNA 1110020G09 gene	1110020G09Rik	68646	-1,62	-1,43	-1,43	-1,15
RIKEN cDNA 9130005N14 gene	9130005N14Rik	68303	-1,62	-1,42	-1,28	-1,18
gene model 640, (NCBI)	Gm640	270174	-1,63	-1,33	-1,21	-1,18
*cDNA sequence_17			-1,63	-1,53	-1,12	-0,79
expressed sequence AL024069	5033414K04Rik	98496	-1,64	-2,03	-1,29	-1,2
naked cuticle 1 homolog (Drosophila)	Nkd1	93960	-1,64	-1,6	-1,21	-1,3
methionine sulfoxide reductase B3	Msrb3	320183	-1,64	-1,33	-1,17	-1,18
thiamin pyrophosphokinase	Tpk1	29807	-1,64	-1,25	-0,97	-0,89
immunity-related GTPase family, M	Irgm	15944	-1,66	-1,12	-0,79	-1,12
selenium binding protein 1	Selenbp1	20341	-1,66	-1,63	-1,9	-1,29
secernin 3	Scrn3	74616	-1,68	-0,93	-0,88	-0,99
aldolase 3, C isoform	Aldoc	11676	-1,69	-1,82	-1,9	-1,28
G protein-coupled receptor 155	Gpr155	68526	-1,69	-1,46	-1,54	-1,51
solute carrier family 38, member 4	Slc38a4	69354	-1,69	-1,35	-1,3	-1,02
UDP-glucose pyrophosphorylase 2	Ugp2	216558	-1,7	-1,37	-1,22	-1,03
acyl-CoA synthetase long-chain family member 1	Acsl1	14081	-1,71	-1,41	-1,3	-1,22
UDP glucuronosyltransferase 2 family, polypeptide B35	Ugt2b35	243085	-1,72	-1,39	-1,15	-1,21
ATP-binding cassette, sub-family A (ABC1), member 8b	Abca8b	27404	-1,73	-1,5	-1,53	-1,24
Aquaporin 11	Aqp11	66333	-1,73	-1,51	-1,45	-1,1
mannan-binding lectin serine protease 1	Masp1	17174	-1,73	-1,32	-0,91	-1,15
odd Oz/ten-m homolog 4 (Drosophila)	Odz4	23966	-1,73	-1,24	-0,86	-0,76

Gene information			Microarray Fold Change ratio at different time points post-infection[1]			
Gene Official Full Name	**Gene Official Symbol**	**NCBI Gene Accession Number**	**6h**	**12h**	**18h**	**24h**
solute carrier family 39 (metal ion transporter), member 8	Slc39a8	67547	-1,74	-1,34	-1,3	-1,34
cortactin binding protein 2	Cttnbp2	30785	-1,76	-2,22	-1,68	-1,04
pleckstrin homology domain containing, family C (with FERM domain) member 1	Plekhc1	218952	-1,76	-1,1	-1,2	-0,93
RasGEF domain family, member 1B	Rasgef1b	320292	-1,76	-1,62	-1,21	-1,11
DEP domain containing 6	Depdc6	97998	-1,77	-1,87	-1,29	-1,38
dopa decarboxylase	Ddc	13195	-1,8	-1,27	0,82	-0,72
cytochrome P450, family 2, subfamily s, polypeptide 1	Cyp2s1	74134	-1,85	-1,44	-1,32	-1,17
neuronal pentraxin 1	Nptx1	18164	-1,89	-1,41	-0,86	-0,94
Lrp2 binding protein	Lrp2bp	67620	-1,9	-1,94	-1,35	-1,12
#probe design_23			-1,95	-1,83	-1,44	-1,16
purinergic receptor P2Y, G-protein coupled 12	P2ry12	70839	-1,96	-1,53	-1,11	-1,52
UDP-glucose pyrophosphorylase 2	Ugp2	216558	-1,97	-1,56	-1,16	-1,07
transmembrane protein 71	Tmem71	213068	-1,99	-1,55	-1,45	-1,36
cytochrome P450, family 1, subfamily a, polypeptide 1	Cyp1a1	13076	-2,03	-0,93	-0,86	-0,64
hydroxyprostaglandin dehydrogenase 15 (NAD)	Hpgd	15446	-2,04	-0,75	1,15	0,9
sorbin and SH3 domain containing 2	Sorbs2	234214	-2,11	-1,52	-1,11	-0,82
angiopoietin 1	Angpt1	11600	-2,13	-1,77	-1,62	-1,01
avian musculoaponeurotic fibrosarcoma (v-maf) AS42 oncogene homolog	Maf	17132	-2,16	-1,79	-1,56	-1,72
DNA segment, human D4S114	D0H4S114	27528	-2,16	-1,16	0,9	0,82
avian musculoaponeurotic fibrosarcoma (v-maf) AS42 oncogene homolog	Maf	17132	-2,18	-1,7	-1,31	-1,56
avian musculoaponeurotic fibrosarcoma (v-maf) AS42 oncogene homolog	Maf	17132	-2,23	-1,38	-1,18	-1
RIKEN cDNA 1110059G02 gene	1110059G02Rik	68786	-2,27	-1,67	-0,72	-1,13
stearoyl-Coenzyme A desaturase 2	Scd2	20250	-2,51	-1,88	-1,67	-1,22
RIKEN cDNA A130090K04 gene	A130090K04Rik	320495	-2,55	-2,33	-1,55	-1,76
ATP-binding cassette, sub-family D (ALD), member 2	Abcd2	26874	-2,73	-2,43	-2,59	-2,4

Notes:

[1]Microarray Fold Change ratio at different time points post-infection: positive and negative values represent genes up- and down-regulated, respectively.

#probe design_numbered: Affymetrix probe design information/ target description (see Supp. Table 1b); *cDNA sequence_numbered: gene transcript description (see Supp. Table 1b).

Gene information

#probe design	Affymetrix probe design information/ target description
1	gb:AW741388 /DB_XREF=gi:7653171 /DB_XREF=ur54c07.x1 /CLONE=IMAGE:3154092 /FEA=EST /CNT=6 /TID=Mm.148901.1 /TIER=ConsEnd /STK=2 /UG=Mm.148901 /UG_TITLE=ESTs
2	gb:BQ176966 /DB_XREF=gi:20352458 /DB_XREF=UI-M-DJ2-bwa-o-19-0-UI.s1 /CLONE=UI-M-DJ2-bwa-o-19-0-UI /FEA=EST /CNT=3 /TID=Mm.117588.1 /TIER=ConsEnd /STK=2 /UG=Mm.117588 /UG_TITLE=ESTs
3	gb:BB748708 /DB_XREF=gi:16152944 /DB_XREF=BB748708 /CLONE=G030001K12 /FEA=EST /CNT=3 /TID=Mm.215937.1 /TIER=ConsEnd /STK=2 /UG=Mm.215937 /UG_TITLE=ESTs
4	gb:AW552076 /DB_XREF=gi:7197499 /DB_XREF=L0208A04-3 /CLONE=L0208A04 /FEA=EST /CNT=5 /TID=Mm.182691.1 /TIER=ConsEnd /STK=4 /UG=Mm.182691 /UG_TITLE=ESTs
5	gb:BE631223 /DB_XREF=gi:9913911 /DB_XREF=uu05g03.x1 /CLONE=IMAGE:3371092 /FEA=EST /CNT=24 /TID=Mm.2322.3 /TIER=Stack /STK=12 /UG=Mm.2322 /LL=18712 /UG_GENE=Pim1 /UG_TITLE=proviral integration site 1
6	gb:AI451554 /DB_XREF=gi:4304812 /DB_XREF=mu47b11.x1 /CLONE=IMAGE:642525 /FEA=EST /CNT=2 /TID=Mm.32490.1 /TIER=ConsEnd /STK=2 /UG=Mm.32490 /UG_TITLE=ESTs
7	gb:BB560961 /DB_XREF=gi:9647327 /DB_XREF=BB560961 /CLONE=E530118N19 /FEA=EST /CNT=7 /TID=Mm.86981.1 /TIER=ConsEnd /STK=5 /UG=Mm.86981 /UG_TITLE=ESTs
8	gb:BB447409 /DB_XREF=gi:16425180 /DB_XREF=BB447409 /CLONE=D030060G22 /FEA=EST /CNT=16 /TID=Mm.6358.1 /TIER=Stack /STK=9 /UG=Mm.6358 /UG_TITLE=ESTs
9	gb:BQ032894 /DB_XREF=gi:19768173 /DB_XREF=UI-1-CF0-axl-e-01-0-UI.s1 /CLONE=UI-1-CF0-axl-e-01-0-UI /FEA=EST /CNT=2 /TID=Mm.117583.1 /TIER=ConsEnd /STK=2 /UG=Mm.117583 /UG_TITLE=ESTs
10	gb:AW489857 /DB_XREF=gi:7060127 /DB_XREF=UI-M-BH3-aso-c-06-0-UI.s1 /CLONE=UI-M-BH3-aso-c-06-0-UI /FEA=EST /CNT=5 /TID=Mm.57956.1 /TIER=ConsEnd /STK=4 /UG=Mm.57956 /UG_TITLE=ESTs
11	gb:BE627361 /DB_XREF=gi:9907781 /DB_XREF=ut87f07.x1 /CLONE=IMAGE:3369445 /FEA=EST /CNT=30 /TID=Mm.10336.1 /TIER=Stack /STK=28 /UG=Mm.10336 /UG_TITLE=ESTs
12	gb:BB710847 /DB_XREF=gi:16064016 /DB_XREF=BB710847 /CLONE=B020018M09 /FEA=EST /CNT=3 /TID=Mm.212452.1 /TIER=ConsEnd /STK=3 /UG=Mm.212452 /UG_TITLE=ESTs
13	gb:BG069809 /DB_XREF=gi:12552378 /DB_XREF=H3080D04-3 /CLONE=H3080D04 /FEA=EST /CNT=14 /TID=Mm.24295.1 /TIER=Stack /STK=9 /UG=Mm.24295 /UG_TITLE=ESTs
14	gb:BB324785 /DB_XREF=gi:16403528 /DB_XREF=BB324785 /CLONE=B430111L14 /FEA=EST /CNT=4 /TID=Mm.210179.1 /TIER=ConsEnd /STK=2 /UG=Mm.210179 /UG_TITLE=ESTs
15	gb:AI464196 /DB_XREF=gi:4318226 /DB_XREF=vc88h09.x1 /CLONE=IMAGE:790145 /FEA=EST /CNT=2 /TID=Mm.220190.1 /TIER=ConsEnd /STK=2 /UG=Mm.220190 /LL=99653 /UG_GENE=AI464196 /UG_TITLE=expressed sequence AI464196
16	gb:BB048406 /DB_XREF=gi:8455554 /DB_XREF=BB048406 /CLONE=6430584J18 /FEA=EST /CNT=2 /TID=Mm.161167.2 /TIER=ConsEnd /STK=2 /UG=Mm.161167 /UG_TITLE=ESTs
17	gb:BG074824 /DB_XREF=gi:12557393 /DB_XREF=H3139G06-3 /CLONE=H3139G06 /FEA=EST /CNT=2 /TID=Mm.182743.1 /TIER=ConsEnd /STK=2 /UG=Mm.182743 /UG_TITLE=ESTs
18	gb:AI662750 /DB_XREF=gi:4766333 /DB_XREF=vb21d10.x1 /CLONE=IMAGE:749587 /FEA=EST /CNT=2 /TID=Mm.150125.1 /TIER=ConsEnd /STK=2 /UG=Mm.150125 /UG_TITLE=ESTs
19	gb:BB471757 /DB_XREF=gi:16427963 /DB_XREF=BB471757 /CLONE=D230040H21 /FEA=EST /CNT=2 /TID=Mm.209394.1 /TIER=ConsEnd /STK=2 /UG=Mm.209394 /UG_TITLE=ESTs
20	gb:BE949437 /DB_XREF=gi:10527196 /DB_XREF=UI-M-BH3-avi-h-07-0-UI.s1 /CLONE=UI-M-BH3-avi-h-07-0-UI /FEA=EST /CNT=8 /TID=Mm.205708.1 /TIER=ConsEnd /STK=3 /UG=Mm.205708 /UG_TITLE=ESTs
21	gb:BB258019 /DB_XREF=gi:8950852 /DB_XREF=BB258019 /CLONE=A730082I06 /FEA=EST /CNT=33 /TID=Mm.45298.1 /TIER=Stack /STK=8 /UG=Mm.45298 /LL=99692 /UG_GENE=AI649393 /UG_TITLE=expressed sequence AI649393
22	gb:AV164956 /DB_XREF=gi:15404628 /DB_XREF=AV164956 /CLONE=3110030K23 /FEA=EST /CNT=17 /TID=Mm.82292.1 /TIER=Stack /STK=15 /UG=Mm.82292 /UG_TITLE=ESTs
23	gb:BB535327 /DB_XREF=gi:16446530 /DB_XREF=BB535327 /CLONE=E030042O04 /FEA=EST /CNT=6 /TID=Mm.187844.1 /TIER=ConsEnd /STK=5 /UG=Mm.187844 /UG_TITLE=ESTs

*cDNA sequence	Gene transcript description
1	Adult male corpus striatum cDNA, RIKEN full-length enriched library, clone:C030047F10 product:unknown EST, full insert sequence
2	7 days neonate cerebellum cDNA, RIKEN full-length enriched library, clone:A730046J11 product:unclassifiable, full insert sequence
3	Adult male testis cDNA, RIKEN full-length enriched library, clone:4930525M22 product:unclassifiable, full insert sequence
4	0 day neonate skin cDNA, RIKEN full-length enriched library, clone:4632424N07 product:unknown EST, full insert sequence
5	Adult male epididymis cDNA, RIKEN full-length enriched library, clone:9230106H08 product:unclassifiable, full insert sequence
6	Adult male aorta and vein cDNA, RIKEN full-length enriched library, clone:A530047H08 product:unknown EST, full insert sequence
7	Adult female vagina cDNA, RIKEN full-length enriched library, clone:9930108O06 product:hypothetical protein, full insert sequence
8	3 days neonate thymus cDNA, RIKEN full-length enriched library, clone:A630054P20 product:unknown EST, full insert sequence
9	9.5 days embryo parthenogenote cDNA, RIKEN full-length enriched library, clone:B130031H03 product:unclassifiable, full insert sequence
10	12 days embryo male wolffian duct includes surrounding region cDNA, RIKEN full-length enriched library, clone:6720461E04 product:unknown EST, full insert sequence
11	3 days neonate thymus cDNA, RIKEN full-length enriched library, clone:A630020J17 product:unknown EST, full insert sequence
12	Adult male aorta and vein cDNA, RIKEN full-length enriched library, clone:A530021B03 product:unknown EST, full insert sequence
13	10 days neonate cerebellum cDNA, RIKEN full-length enriched library, clone:B930004G13 product:unknown EST, full insert sequence
14	0 day neonate eyeball cDNA, RIKEN full-length enriched library, clone:E130202F10 product:hypothetical protein, full insert sequence
15	10 days neonate cerebellum cDNA, RIKEN full-length enriched library, clone:B930049N01 product:unclassifiable, full insert sequence
16	Adult male olfactory brain cDNA, RIKEN full-length enriched library, clone:6430531K17 product:unclassifiable, full insert sequence
17	Transcribed locus, moderately similar to XP_001066067.1 hypothetical protein [Rattus norvegicus]

Supplementary Table 1 | Microarray data analysis reveals a total of 611 genes differentially expressed throughout *P. berghei* infection of Hepa1-6 cells.

List of the 611 genes differentially expressed during infection of Hepa1-6 cells by GFP-expressing *P. berghei* sporozoites. For each gene is indicated the microarray fold change ratio at the different infection time points (6, 12, 18 and 24 h p.i.). The fold change positive and negative values represent genes up- and down-regulated, respectively. In addition, detailed gene information is provided, i.e. the gene official full name, the official symbol and the National Center for Biotechnology Information (NCBI) gene accession number (http://www.ncbi.nlm.nih.gov/sites/entrez for Entrez Gene Database). For some cases the gene specific sequence is not assigned and therefore the information is provided either through the labeling of "probe design" or "cDNA sequence", which correspond to the Affymetrix probe design information/target description or Affymetrix gene transcript description, respectively. The different "probe design" or "cDNA sequence" were sequentially numbered in Supplementary Table 1a and their corresponding key is provided in Supplementary Table 1b.

Gene information			Microarray Fold Change ratio at different time points p.i. (FC threshold 1.2)			
Gene Official Full Name	Gene Official Symbol	NCBI Gene Accession Number	6h	12h	18h	24h
ChaC, cation transport regulator-like 1 (E. coli)	Chac 1	69065	8,88	4,44	2,32	2,27
nuclear protein 1	Nupr1	56312	6,21	3,91	2,56	2,08
tribbles homolog 3 (Drosophila)	Trib3	228775	4,79	3,71	2,79	2,54
DNA-damage inducible transcript 3	Ddit3	13198	4,65	3,23	1,41	1,48
growth arrest and DNA-damage-inducible 45 beta	Gadd45b	17873	3,15	2,64	1,71	1,35
G protein-coupled receptor 137B	Gpr137b	83924	2,99	3,76	3,19	1,73
activating transcription factor 3	Atf3	11910	2,99	1,82	1,48	1,58
neuropilin 2	Nrp2	18187	2,55	2,2	1,43	1,31
myeloid differentiation primary response gene 116	Myd116	17872	2,3	3,46	1,71	1,52
solute carrier family 7 (cationic amino acid transporter, y+ system), member 11	Slc7a11	26570	1,97	2,37	1,7	1,27
activating transcription factor 5	Atf5	107503	1,69	1,39	1,63	1,45
v-maf musculoaponeurotic fibrosarcoma oncogene family, protein K (avian)	Mafk	17135	1,6	1,25	1,39	1,28
CCAAT/enhancer binding protein (C/EBP), beta	Cebpb	12608	1,51	1,42	1,49	1,25
B-cell linker	Blnk	17060	1,5	1,84	1,81	1,45
Kruppel-like factor 4 (gut)	Klf4	16600	1,43	1,35	1,26	1,57
zinc finger protein 296	Zfp296	63872	1,42	1,35	1,49	1,3
translocase of inner mitochondrial membrane 10 homolog (yeast)	Timm10	30059	1,41	1,41	1,32	1,24
small proline-rich protein 1B	Sprr1b	20754	1,39	2,21	2,27	2,31
ATPase, H+ transporting, lysosomal V0 subunit B	Atp6v0b	114143	1,28	1,36	1,34	1,45
Nur77 downstream gene 2	Ndg2	103172	1,23	1,97	2,67	2,39
gelsolin	Gsn	227753	0	1,29	2,12	1,69
heme oxygenase (decycling) 1	Hmox1	15368	1,31	0	1,84	0
C-type lectin domain family 4, member d	Clec4d	17474	0	2,26	1,42	0
CCAAT/enhancer binding protein (C/EBP), delta	Cebpd	12609	3,08	0	0	0
Tnf receptor-associated factor 1	Traf1	22029	2,88	0	0	0

Gene information			Microarray Fold Change ratio at different time points p.i. (FC threshold 1.2)			
Gene Official Full Name	Gene Official Symbol	NCBI Gene Accession Number	6h	12h	18h	24h
vascular cell adhesion molecule 1	Vcam1	22329	2,93	0	0	0
caspase 4, apoptosis-related cysteine peptidase	Casp4	12363	2,24	0	0	0
CDC42 effector protein (Rho GTPase binding) 3	Cdc42ep3	260409	1,59	1,25	1,21	0
zinc fingers and homeoboxes protein 2	Zhx2	387609	1,56	0	0	0
zinc finger protein 423	zfp423	94187	1,55	1,47	1,39	0
zinc finger CCCH type containing 8	Zc3h8	57432	1,52	0	0	0
zinc finger and BTB domain containing 20	Zbtb20	56490	0	-1,54	0	0
hydroxyprostaglandin dehydrogenase 15 (NAD)	Hpgd	15446	-2,04	0	0	0
low density lipoprotein receptor	Ldlr	16835	-1,24	-1,35	-1,69	0
bone marrow stromal cell antigen 1	Bst1	12182	0	-1,42	-1,9	0
early growth response 2	Egr2	13654	-1,25	-1,81	-2,44	-2,54
chemokine (C-X-C motif) ligand 15	Cxcl15	20309	-1,32	-1,92	-1,33	-1,46
kinesin family member 5C	Kif5c	16574	-1,42	-1,48	-1,46	-1,37
solute carrier family 16 (monocarboxylic acid transporters), member 4	Slc16a4	229699	-1,6	-1,43	-1,46	-1,27
selenium binding protein 1	Selenbp1	20341	-1,66	-1,63	-1,9	-1,29
aldolase 3, C isoform	Aldoc	11676	-1,69	-1,82	-1,9	-1,28
acyl-CoA synthetase long-chain family member 1	Acsl1	14081	-1,71	-1,41	-1,3	-1,22
avian musculoaponeurotic fibrosarcoma (v-maf) AS42 oncogene homolog	Maf	17132	-2,16	-1,79	-1,56	-1,72
stearoyl-Coenzyme A desaturase 2	Scd2	20250	-2,51	-1,88	-1,67	-1,22
RIKEN cDNA A130090K04 gene	A130090K04Rik	320495	-2,55	-2,33	-1,55	-1,76
ATP-binding cassette, sub-family D (ALD), member 2	Abcd2	26874	-2,73	-2,43	-2,59	-2,4

Supplementary Table 2 | Genes selected from the microarray data and included in the RNAi screen to access their functional role in *Plasmodium* infection.

List of the 46 genes differentially expressed throughout *Plasmodium* infection and for which their functional relevance in infection was addressed by RNAi. For each gene is provided the relevant gene information together with the microarray fold change ratio at the different infection time points (6, 12, 18 and 24 h p.i.). The different values reflect the expression levels, with positive and negative values corresponding to up- and down-regulated genes, respectively. A fold change threshold of at least 1.2 (FC_1.2) was applied for this selection. Zero represents that the gene did not assemble the FC_1.2 criteria and therefore was considered as not differentially expressed.

Gene information			Gene emergence (in %) in IPA networks*	
Gene Official Full Name	Gene Official Symbol	NCBI Gene Acc. Nb.	Infected samples	Non-infected samples
FBJ osteosarcoma oncogene	Fos	14281	6,7	2,4
myelocytomatosis oncogene	c-Myc	17869	8,9	3,5
tumor necrosis factor	Tnf	21926	13,3	2,4
Rous sarcoma oncogene	Src	20779	4,4	0
transformation related protein 53[#]	Tp53	22059	8,9	8,2

Notes:
*Central genes emergence in Ingenuity Pathway (IPA) networks analysed in the dataset of infected samples and non-infected samples datasets. The non-infected sample dataset is considered as the control condition. All values are expressed in percentage (%). [#]Tp53 gene was considered as a positive control since it emerged equally in the infected as well as in the non-infected dataset.

Supplementary Table 3 | Central genes percentage of recurrence in gene networks composed by the genes modulated throughout *Plasmodium* infection and also other associated genes.
List of the central genes included in the RNAi screen and selected based on gene network analyses with the Ingenuity Pathway Software (IPA). The central genes emergence in IPA networks was analyzed in the dataset of infected and non-infected samples and their frequency is expressed as a percentage (%). The non-infected dataset is considered as the control condition and the Tp53 gene as a positive control, meaning that is not considerably associated with *Plasmodium* infection, since it emerged equally in the infected as well as in the non-infected dataset.

Gene Official Symbol	NCBI Gene Accession Nb	NCBI Accession ID for Targeted Transcripts	siRNA ID from Supplier	Infection Rate	Cell Proliferation
Atf3	11910	NM_007498	60299	134,47	94,83
Atf3	11910	NM_007498	60299	140,74	122,51
Bst1	12182	NM_009763	214981	152,88	101,17
Bst1	12182	NM_009763	214981	158,14	99,77
Cebpb	12608	NM_009883	214962	145,75	120,13
Cebpb	12608	NM_009883	214962	134,44	119,09
Fos	14281	NM_010234	158593	129,65	83,16
Fos	14281	NM_010234	158595	129,35	105,72
Kif5c	16574	NM_008449	215005	144,14	106,55
Kif5c	16574	NM_008449	215005	152,25	106,87
Slc7a11	26570	NM_011990	188174	143,09	99,53
Zbtb20	56490	NM_019778	214992	133,53	100,87
A130090K04Rik	320495	NM_001033391	215038	66,54	111,00
A130090K04Rik	320495	NM_001033391	215038	79,56	115,37
Ldlr	16835	NM_010700	67892	34,12	85,97
Ldlr	16835	NM_010700	67892	67,39	111,89
c-Myc	17869	NM_010849	68392	50,84	79,89
c-Myc	17869	NM_010849	68392	66,09	86,42
c-Myc	17869	NM_010849	156407	79,93	75,55
c-Myc	17869	NM_010849	156407	71,66	82,23
Src	20779	NM_009271	150978	80,27	99,24

Supplementary Table 4 | Genes identified from the first RNAi screening pass as candidates to influence *P. berghei* sporozoite infection of Hepa1-6 cells.
List of 11 genes selected from the first RNAi pass to undergo into the second confirmation round. For each gene is provided the relevant information, namely the gene official symbol, the NCBI gene accession number (Nb), the NCBI accession ID for targeted transcripts, the siRNA ID from the supplier (Ambion, Applied Biosystems) for which a phenotype was observed and the observed infection rate (corresponding to the number of EEFs normalized to confluency, shown as the percentage of plate-specific negative controls) and cell proliferation (number of cell nuclei expressed as % of plate mean).

Gene Official Symbol	NCBI Gene Accession Nb	NCBI Accession ID for Targeted Transcripts	siRNA ID from Supplier	Infection Rate	Cell Proliferation
Atf3	11910	NM_007498	60299	142,98	94,48
Atf3	11910	NM_007498	240520	158,85	145,68
Atf3	11910	NM_007498	240520	136,05	120,47
c-Myc	17869	NM_010849	68392	69,17	76,59
c-Myc	17869	NM_010849	156407	62,16	65,52

Supplementary Table 5 | Genes confirmed in the second RNAi screening pass as candidates to influence *P. berghei* sporozoite infection of Hepa1-6 cells.
The 2 genes selected from the second RNAi pass to undergo to the third confirmation round. Gene information is the same as in Supplementary Table 4.

Gene Official Symbol	NCBI Gene Acc. Nb	NCBI Accession ID for Targeted Transcripts	siRNA ID	Infection Rate	Cell Proliferation	Remaining mRNA
Atf3	11910	NM_007498	48555	172,65	88,94	39,43
Atf3	11910	NM_007498	48642	204,52	115,86	9,88
Atf3	11910	NM_007498	60393	165,17	122,19	35,97
Atf3	11910	NM_007498	159756	178,00	120,19	45,00
Atf3	11910	NM_007498	240519	170,96	118,93	64,28
Atf3	11910	NM_007498	240520	166,50	125,67	43,27
c-Myc	17869	NM_010849	47943	91,41	99,23	44,48
c-Myc	17869	NM_010849	68392	77,20	80,45	70,60
c-Myc	17869	NM_010849	156407	78,02	74,35	54,17
c-Myc	17869	NM_010849	240550	99,20	107,49	79,22

Supplementary Table 6 | Atf3 and c-Myc silencing data obtained in the third RNAi confirmation round.

Atf3 and c-Myc silencing was performed through the treatment with 6 and 4 distinct siRNAs, respectively. The infection phenotype outcome was once again accessed and in addition was also determined the specific-gene mRNA level (shown as % relative to the negative control). For both genes the relevant information is provided for all the siRNAs used, following the same criteria as explained previously in Supplementary Table 4 and 5.

Gene information		siRNA ID from Supplier (Ambion, Applied Biosystem)											
		Pass 1			Pass 2			Pass 3					
Gene Official Symbol	NCBI Gene Acc. Nb.	siRNA1	siRNA2	siRNA3	siRNA1	siRNA2	siRNA3	siRNA1	siRNA2	siRNA3	siRNA4	siRNA5	siRNA6
A130090K04Rik	320495	215037	215038	215039	215038	215039	240571						
Abcd2	26874	214995	214996	214997									
Acsl1	14081	215016	215017	215018									
Aldoc	11676	215034	215035	215036									
Atf3	11910	60299	60393	159756	60299	240519	240520	49555	48642	60393	159756	240519	240520
Atf5	107503	84801	172161	172163									
Atp6v0b	114143	214986	214987	214988	214963	214964	214986						
Blnk	17060	62728	62899	155208									
Bst1	12182	214980	214981	214982	65854	214981	240537						
Casp4	12363	60483	60674	160000									
Cdc42ep3	260409	214989	214990	214991	80897	214989	240564						
Cebpb	12608	214960	214961	214962	66041	214962	288793						
Cebpd	12609	215013	215014	215015									
Chac1	69065	81375	81464	180675									
Clec4d	17474	68179	68275	68370									
Cxcl15	20309	69078	69263	151595									
Ddit3	13198	61044	61140	61228	288790	288791	288792						
Egr2	13654	66675	158361	158362									
Fos	14281	67034	158593	158595	66846	158593	158595						
Gadd45b	17873	214977	214978	214979									
Gpr137b	83924	215007	215008	215009									
Gsn	227753	90697	90887	170256									
Hmox1	15368	67540	158978	158979									
Hpgd	15446	214983	214984	214985									
Kif5c	16574	215004	215005	215006	155043	155044	215005						

Gene Official Symbol	NCBI Gene Acc. Nb.	siRNA ID from Supplier (Ambion, Applied Biosystem)											
		Pass 1			Pass 2			Pass 3					
		siRNA1	siRNA2	siRNA3	siRNA1	siRNA2	siRNA3	siRNA1	siRNA2	siRNA3	siRNA4	siRNA5	siRNA6
Klf4	16600	215025	215026	215027	67853	215027	240545						
Ldlr	16835	67892	156096	156097	67988	67892	156096						
Maf	17132	215031	215032	215033									
Mafk	17135	68032	68126	156226	67937	156224	156226						
Myc	17869	68203	68392	156407	47943	68392	156407	47943	68392	156407	240550		
Myd116	17872	63095	63187	155481	63003	63187	155481						
Ndg2	103172	214974	214975	214976									
Nrp2	18187	215010	215011	215012	166858	215010	215012						
Nupr1	56312	74306	185512	185513	74124	74306	185513						
Scd2	20250	215019	215021										
Selenbp1	20341	214957	214958	214959									
Slc16a4	229699	90710	170275	170277	90806	90900	170275						
Slc7a11	26570	70494	70588	188174	70588	188172	188174						
Sprr1b	20754	101439	101530	101606									
Src	20779	64804	150978	150979	150978	240568	240567						
Timm10	30059	71849	71944	184165									
Tnf	21926	71316	188363	188364									
Traf1	22029	215022	215023	215024									
Trib3	228775	215001	215002	215003									
Vcam1	22329	214998	214999	215000									
Zbtb20	56490	214992	214993	214994									
Zc3h8	57432	75183	165931	165932									
Zfp296	63872	76296	76487	182288									
Zfp423	94187	85277	85372	166171									
Zhx2	387609	215028	215029	215030									

Supplementary Table 7 | siRNAs used to access the functional role of the corresponding target gene in *Plasmodium* infection throughout the three confirmation phases of the RNAi approach.

The list of the RNAi screened genes together with the number and siRNAs ID used in the different confirmation phases is supplied. The siRNAs for which an increase or decrease in infection was observed are highlighted in red and green, respectively.

Chapter 3 | Results

Kinome-wide RNAi screen identifies host PKCζ as a critical kinase for *Plasmodium* sporozoite infection

Miguel Prudêncio[1,2*], Cristina D. Rodrigues[1,2*], Michael Hannus[3], Cécilie Martin[3], Lígia A. Gonçalves[2], Silvia Portugal[1], Akin Akinc[4], Philipp Hadwiger[5], Adrian J.F. Luty[6], Robert Sauerwein[6], Dominique Mazier[7], Victor Koteliansky[4], Hans-Peter Vornlocher[5], Christophe J. Echeverri[3], Maria M. Mota[1,2†]

[1]Unidade de Malária, Instituto de Medicina Molecular, Universidade de Lisboa, 1649-028 Lisboa, Portugal. [2]Instituto Gulbenkian de Ciência, 2780-156 Oeiras, Portugal. [3]Cenix BioScience GmbH, Tatzberg 47, Dresden 01307, Germany. [4]Alnylam Pharmaceuticals, 300 Third Street, Cambridge, MA02142, USA. [5]Alnylam Europe AG, Fritz-Hornschuch-Strasse 9, 95326 Kulmbach, Germany. [6]Department of Medical Microbiology, University Medical Centre, P.O. Box 9101, 6500 HB Nijmegen, The Netherlands. [7]Inserm U511, Université Pierre et Marie Curie-Paris, Centre Hospitalier Universitaire Pitié-Salpêtrière, Paris, France.

[*]These authors contributed equally to this work.

[#]Correspondence should be addressed to M.M.M. (mmota@fm.ul.pt).

When sporozoites of *Plasmodium*, the causative agent of malaria, are injected into their vertebrate host through the bite of an infected *Anopheles* mosquito, they travel to the liver where they invade hepatocytes and develop into merozoites that are then released into the blood and give rise to the clinical phase of infection. Since the combined activities of kinases and phosphatases can tightly control numerous cellular processes, we sought to examine the role of host kinases in *P. berghei* sporozoites infection of hepatocytes using RNA interference. Quantification of infection of Huh7 cells following transfection with 2306 siRNAs identified at least 6 host kinases playing crucial roles during *P. berghei* sporozoite infection. This screen represents the first comprehensive identification of novel host factors involved in *Plasmodium* sporozoite infection. Moreover, in order to provide a final validation of the screen, we have studied one of these kinases for which available tools, such as a pseudo-subtrate inhibitor, exist and showed that the host aPKCς plays a role in *P. berghei* and *P. falciparum* sporozoite infection of hepatocytes. Moreover, down-modulation of aPKCς *in vivo* in the liver leads to a reduction of liver infection up to 90%.

Intracellular phosphorylation and dephosphorylation events are enzymatically catalysed by kinases and phosphatases, respectively, and constitute the most important signalling mechanisms known in eukaryotic cells (Hunter, 2000). The phosphorylation state of a protein can determine its activity and, thereby, regulate the pathway(s) in which it is involved.

Malaria, caused by the protozoan parasite of the genus *Plasmodium*, is transmitted through the bite of an infected female *Anopheles* mosquito. *Plasmodium* sporozoites enter the mammalian host and travel to the liver. Once there, they cross several hepatocytes before invading a final one, with formation of a parasitophorous vacuole (Mota *et al.*, 2001). Each invading parasite then replicates asexually into several thousand merozoites that constitute a so-called exoerythrocytic form (EEF) of *Plasmodium*. This asymptomatic stage of infection is followed by the release of merozoites into the blood stream, where they invade erythrocytes, initiating the blood-stage of infection, which is responsible for the malaria-associated symptoms. *Plasmodium* sporozoites display a marked tropism for hepatocytes, the only cells where they are able to undergo the huge replication process that results in the formation of thousands of merozoites from each invading parasite [reviewed in (Prudencio *et al.*, 2006)]. In fact, in hepatocytes, *Plasmodium* achieves one of the fastest growth rates among eukaryotic cells. In addition, there is increasing evidence that the asymptomatic hepatic stage of infection, triggers an immune response in the vertebrate host (Waters *et al.*, 2005; Renia *et al.*, 2006). In conjunction, these facts constitute a clear indication that the host liver cells do not play a passive role during *Plasmodium* infection and that host factors that strongly influence its fate must exist. Since the combined activities of kinases and phosphatases can tightly control numerous cellular processes, it seems logical to assume that they can modulate the cell's behaviour during the infection process by an intracellular pathogen. For this reason, we decided to use RNA interference (RNAi) to selectively silence the expression of 727 genes in the human genome, encoding all the known proteins with putative kinase activity, as well as several kinase-interacting proteins (Supplementary Table 1). The effect of gene knock-down on *Plasmodium* infection of Huh7 cells, a human hepatoma cell line, was monitored by high-throughput, high-content immuno-fluorescence microscopy.

Short interfering RNA oligonucleotides (siRNAs) with sequences complementary to those of the genes of interest were designed and used to transfect Huh7 cells seeded 24 h earlier in 96-well plates. Forty-eight h after transfection cells were infected with *P. berghei* sporozoites freshly extracted from the salivary glands of infected *Anopheles stephensi* mosquitoes. Cells were fixed and immuno-stained for parasite, host cell

nuclei and actin 24 h after infection. Following image acquisition, the number of EEFs, nuclei and cell confluency were automatically determined. Candidate genes underwent three screening passes with increasing stringency criteria (Figure 1a). Infection was quantified by normalizing the number of EEFs against the cell confluency in each well. In order to compare results across different plates, a second level of normalization was introduced by calculating the infection level in each experimental well as a percentage of the average infection of the whole plate. In order to account for proliferation or cell toxicity effects, infection data obtained in this way were plotted against the number of nuclei in the same experimental well, expressed as a percentage of the average number of nuclei within the plate.

To validate the experimental procedure outlined above Huh7 cells were transfected with 2 siRNAs targeting the *Met* gene, whose knock-down is known to lead to a decrease in infection of HepG2 cells by *Plasmodium* (Carrolo *et al.*, 2003). *Met* knock-down was confirmed by quantitative Real-Time PCR (qRT-PCT) and a significant decrease in infection was observed relative to controls (data not shown). Two types of negative controls, untransfected cells and cells transfected with a negative control siRNA not targeting any annotated genes in the human genome, were included in every experimental plate and all experimental conditions were assayed in triplicate wells.

The 727 selected genes were initially screened by targeting each of them with three independent siRNA oligonucleotides (Supplementary Table 1). This corresponds to a total of 2181 siRNAs in twenty-four 96-well plates that were used to transfect a total of 72 experimental cell plates. Approximately 10% of these genes were selected to undergo a second screening pass. In order to minimize the number of false negative results, genes were selected for which the knock-down in expression with at least one siRNA led to a statistically significant effect on infection levels with a negligible effect on cell proliferation (Figure 1b).

Seventy-four genes were selected to undergo a confirmation round of the screen. For most of these, an additional two siRNAs were designed and included in the assay (Supplementary Table 1). Infection increase or decrease was considered significant when it was greater or smaller than 2.0 standard deviations of the average of all the negative controls in the assay, respectively. To minimize the chances of false positive results at this stage, selection of candidate genes required that at least two independent siRNAs targeting the same gene met the selection criteria, leading to either a significant increase or decrease in infection (Figure 1c). All the siRNAs were assayed in triplicate and in two independent experiments yielding very consistent results, demonstrating the robustness of the experimental approach employed (Figure

1d). Only those siRNAs for which the selection criteria were met in both experiments were considered as candidates for the next confirmation round.

The 19 genes selected for further verification were targeted with the siRNAs yielding the strongest infection increase or decrease phenotypes in the previous round of the screen. In order to increase the stringency of the selection, genes were selected for the final confirmation step only if at least two siRNAs targeting each of them led to an infection increase or decrease greater or smaller than 3.0 standard deviations of the average of all the negative controls in the assay, respectively (Figure 2a).

The knock-down level attained for the eight genes that met these criteria was then assessed by qRT-PCR. A good correlation between the infection phenotypes observed when targeting these genes by RNAi and their corresponding mRNA levels at the time of sporozoite addition was observed for 6 of these genes (Figure 2b, Table 1). It can thus be concluded that MET, PKCι, PKCζ, PRKWNK1, SGK2 and STK35 are likely to play important roles during infection of host hepatocytes by *Plasmodium*. It should be noted that the present data does not fully rule out the possible involvement of other genes among those tested here, as negative results in RNAi screens are generally inconclusive (Echeverri *et al.*, 2006).

The protein kinase (PK) complement of the human genome was thoroughly analyzed in a seminal paper by Manning *et al.* (Manning *et al.*, 2002) that divided the human kinome in ten major groups, based on sequence comparison of their catalytic domains, sequence similarities, domain structures and biological functions. In addition to these PKs, the present screen also included a number of additional genes that can be included in three additional classes: lipid kinases, other non-protein kinases (*i.e.*, proteins that phosphorylate substrates other than proteins and lipids) and proteins without kinase activity but known or proposed to interact with kinases (such as kinase anchors or inhibitors). The relative representations of these groups throughout the screen were analysed (Figure 2c). The eight genes in Table 1 belong to 4 different classes, with the "AGC" and "other" groups having the larger representations. An analysis of the selected genes in terms of their ontology (Figure 2d) can be indicative of the cellular processes that are likely to be preferentially exploited or subverted by the parasite during infection. Agaisse *et al.* (Agaisse *et al.*, 2005) have used RNAi to identify host factors that influence infection of *Drosophila* cells by intracellular bacterial pathogens. They conclude that these factors span a wide range of cellular functions with particular emphasis for gene products involved in cell cycle, vesicular trafficking and cytoskeleton. The genes identified by the present screen have also been implicated in various cellular processes, suggesting a complex

response of the host to the invading parasite. The list includes genes involved in cell cycle control, cytoskeleton regulation and stress/immune response.

MET encodes the hepatocyte growth factor (HGF) receptor and has previously been shown to influence *Plasmodium* infection of hepatocytes (Carrolo *et al.*, 2003; Leiriao *et al.*, 2005). It has been demonstrated that HGF/MET signaling facilitates infection, an effect that has been proposed to occur through inhibition of apoptosis (Leiriao *et al.*, 2005). MET was used to establish the validity of the screening method and, reassuringly, underwent all the steps in the screen emerging as one of the genes whose knock-down consistently led to a decrease in infection.

Both SGK2 and PRKWNK1 are serine/threonine kinases that have been implicated in osmotic control through the regulation of Na^+ and K^+ transport channels (Gamper *et al.*, 2002; Friedrich *et al.*, 2003; Moriguchi *et al.*, 2005; Anselmo *et al.*, 2006). Down-modulation of both of these osmotic and oxidative stress-responsive proteins led to a reduced infection in the present screen. Although their exact role in *Plasmodium* infection is not obvious, it is tempting to speculate that their function is exploited by the parasite in order to create an osmotic balance that favors infection.

STK35 is a poorly characterized gene product, known to interact with CLP-36, a PDZ-LIM protein, and re-localize from the nucleus to actin stress fibres. This suggested that STK35 may act as a regulator of the actinmyosin cytoskeleton in non-muscle cells (Vallenius and Makela, 2002). In the present screen, knock-down of STK35 led to a decrease in infection by *Plasmodium*. It has been suggested that host cell actin cytoskeleton reorganization processes may be important for *Plasmodium* infection (Carrolo *et al.*, 2003). Thus, it is possible that recruitment of STK35 may be enhanced by the parasite in a way that favors cell infection.

Protein kinase C (PKC) is a family of proteins that has been implicated in numerous cellular processes. PKC isotypes constitute a family of 10–15 members, divided in 4 groups (Mellor and Parker, 1998). One of these groups, known as the atypical PKCs (aPKCs) (Moscat and Diaz-Meco, 2000), comprises the PKCζ (PKCzeta) (Ono *et al.*, 1989) and PKCλ/ι (PKCiota/lambda) (Akimoto *et al.*, 1994) isoforms, both of which were targets in the present screen. The aPKCs have been implicated in numerous processes, including cell growth and survival, regulation of NF-κB activation and polarity (reviewed in (Moscat and Diaz-Meco, 2000; Moscat *et al.*, 2006; Suzuki and Ohno, 2006)). In the present screen, the down-modulation of PKCλ/ι caused an increase in infection whereas the knock-down in the expression of PKCζ led to an infection decrease. This is particularly interesting since these two proteins that have a 72% overall amino acid identity (Akimoto *et al.*, 1994) were, for a long time, considered redundant. In fact, only recently has a distribution of functions between

the two aPKC isoforms begun to emerge (Suzuki *et al.*, 2003; Soloff *et al.*, 2004; Muscella *et al.*, 2005), the exact details of which remain largely to be understood. The results presented here clearly suggest that these two proteins do indeed serve different purposes in the cell, in what may be viewed as a manifestation of the intricate relations that exist between molecular structure and function.

In order to provide a final validation for the results of the RNAi screen, the aPKCζ was selected for further investigation, to ascertain whether it indeed plays a role in *Plasmodium* infection of hepatocytes. The screen results show that knock-down of PKCζ leads to a decrease in Huh7 cell infection by *P. berghei* sporozoites. This RNAi-based identification of PKCζ was further validated by testing the effects on infection of a known PKCζ pseudo-substrate inhibitor (PKCζInh). Addition of the PKCζInh to cells 1 h prior to sporozoite addition led to a marked, dose-dependent decrease in infection rate as compared to control samples, measured by flow citometry 24 h after *P. berghei* sporozoite addition, in two different hepatoma cell lines (Figure 3a and Supplementary Figure 1). Importantly, infection rates were not affected by pre-incubation of *Plasmodium* sporozoites with PKCζInh for 1 h prior to addition to cells, showing that PKCζInh has no effect on sporozoite viability (Figure 3b). The efect of PKCζInh on infection was further confirmed using a qRT-PCR-based assay that quantifies infection rates by measuring levels of *Plasmodium* 18S RNA found within Huh7 cell extracts harvested 24 h after *P. berghei* sporozoite addition (Prudêncio *et al.*, 2007) (Figure 3c). Our results show that a 20 μM concentration of PKCζInh leads to ~50% reduction in *Plasmodium* infection rates. Interestingly, this is in agreement with the IC_{50} of 10-20 μM reported for this compound (Standaert *et al.*, 1997). As the above experiments were all performed using hepatoma cell lines infected with the rodent malaria parasite *P. berghei*, we sought to validate the role of PKCζ in *Plasmodium* infection under more physiologically relevant conditions. To this end, we first confirmed that inhibition of PKCζ also leads to a reduction in *P. berghei* infection of primary mouse hepatocytes (Figure 3d). In addition, the role of PKCζ was also tested for *P. falciparum* infection, the most pathogenic *Plasmodium* spp. for humans, in primary human hepatocytes 72h after sporozoite addition, using a similar qRT-PCR-based assay. Once again, PKCζInh treatment of human primary hepatocytes caused a significant and specific decrease of *P. falciparum* infection in these cells (Figure 3e, $P < 0.05$).

Finally, we also confirmed the relevance of these findings *in vivo*, using systemically-delivered, liposome-formulated siRNAs to silence PKCζ expression in adult mice and subjecting these to infection by *P. berghei* sporozoites. Here, the qRT-PCR-based assay was used to quantify infection rates by measuring levels of *Plasmodium* 18S RNA

found within extracts of liver samples harvested 40 h after intravenous (i.v.) sporozoite injection. *In vivo* RNAi treatments have previously yielded potent gene-specific knock-downs in rodent livers using cholesterol-conjugated siRNAs or in non-human primates after systemic administration of siRNAs encapsulated in stable lipid-nanoparticles. In our experiments, PKCζ expression was also reduced successfully in adult mouse livers using 3 distinct PKCζ-specific siRNAs, each of which yielded ~56-73% remaining PKCζ mRNA, as measured by qRT-PCR of tissue extracts taken 76 h after a single i.v. injection and normalization to PKCζ mRNA levels in the livers of adult mice treated with control siRNA (Fig 3f). When compared to control siRNA treatment, this administration of PKCζ-specific siRNAs resulted in a significant reduction of liver infection by *P. berghei* sporozoites, yielding ~9-40% of control infection loads, as measured by qRT-PCR of *P. berghei* 18S rRNA in samples taken 40h after sporozoite injection (Fig 3f, $P < 0.01$, black bars). In a parallel experiment, mice treated with one of the PKCζ siRNAs also showed a reduction in the number of parasites reaching the bloodstream, when compared to their controls (Figure 3g, $P < 0.001$). While by day 4 after sporozoite injection, all mice in the control group were positive for blood stages, none of the 6 mice in the group pre-treated with PKCζ-specific siRNA were positive. In fact, by day 5 only 2 mice became positive in this last group.

Although the dissection of the role of the aPKCs in the establishment of a malaria infection clearly merits further attention, these results clearly demonstrate that this approach constitutes a valid and important strategy for the identification of genes that clearly influence the infection of hepatocytes by *Plasmodium* under physiological conditions.

The RNAi technology has been successfully employed to systematically address the role of specific groups of genes in various cellular processes using both *Drosophila* cell lines (Ramet *et al.*, 2002; Lum *et al.*, 2003; Boutros *et al.*, 2004; Agaisse *et al.*, 2005) and more recently mammalian cells (Berns *et al.*, 2004; Fraser, 2004; Paddison *et al.*, 2004; Pelkmans *et al.*, 2005). However, the approach described here constitutes, to our knowledge, the first report of a kinome-wide RNAi screen of factors that influence the outcome of a parasitic infection in human cells. This RNAi approach enabled the unequivocal establishment of an important role for several genes in facilitating or hampering *Plasmodium* infection of a human hepatoma cell line, shedding light on the fundamental biology of this process and opening avenues for further investigation. Attention should be drawn to the fact that the list of potentially important genes should not be restricted to those outlined in Table 1. In fact, RNAi is an evolving field, with algorithms of increasing efficiency in designing siRNA oligonucleotides able of

effectively silencing the expression of their target genes constantly being developed. Moreover, depending on the specific turnover of the proteins encoded by each targeted gene and on the efficiency of the knock-down process itself, the down-modulation of certain genes may be more prone to having a detectable effect with the phenotypic assessment method used. Due to the very stringent criteria employed throughout the screen, it is not unlikely that certain genes may not have reached the final screening stage despite their relevance for infection. Thus, all phenotype details for all siRNAs used are described (Supplementary Table 1). Altogether, these results contribute towards an understanding of host-pathogen interactions, which may help fostering the rational design of prophylactic and/or therapeutic strategies against infectious diseases in general and malaria in particular.

Methods

Cells, mice and parasites

Huh7 cells were maintained in RPMI medium (Gibco/Invitrogen) supplemented with 10% fetal calf serum (FCS, Gibco/Invitrogen), 1% glutamine (Gibco/Invitrogen), 1% non-essential aminoacids (Gibco/Invitrogen) and 1% HEPES, pH 7.0 (Gibco/Invitrogen) in the presence of penicillin/streptomycin (pen/strep, Gibco/Invitrogen) and grown at 37 °C and 5% CO_2.

C57BL/6 mouse primary hepatocytes were isolated by perfusion of mouse liver lobules with liver perfusion medium and liver digest medium (Gibco/Invitrogen) and purified using a 1.12 g/ml; 1.08 g/ml and 1.06 g/ml Percoll gradient. Cells were cultured in William´s E medium containing 4% FCS, 1% pen/strep, 50 mg/ml epidermal growth factor (EGF), 10 µg/ml transferrin, 1 µg/ml insulin and 3.5 µM hydrocortisone in 24 well plates coated with 0,2% Gelatine in PBS. Cells were maintained in culture at 37°C and 5% CO_2.

Human primary hepatocytes were isolated from the healthy parts of liver biopsies from patients undergoing a partial hepatectomy with informed consent provided, as previously described (Mazier *et al.*, 1985). Freshly isolated human primary hepatocytes were cultured in Williams Medium E supplemented with 10% FCS, 1% glutamine, 1% insuline/transferrine/selenium (Invitrogen), 10^{-7} M dexamethasone (Sigma), 1% sodium piruvate, 2% pen/strep in 48 well plates coated with rat tail collagen, type I. Cells were maintained in culture at 37°C and 5% CO_2. Medium was supplemented with 2% DMSO after complete cell adhesion (12-24h) and until 1 h before infection.

C57BL/6 mice were bred and housed in the pathogen-free facilities of the Instituto Gulbenkian de Ciência and Instituto de Medicina Molecular, respectively. All protocols were approved by the Animal Care Committee of both Institutes.

Green fluorescent protein (GFP)-expressing *P. berghei* (parasite line 259cl2) sporozoites (Franke-Fayard *et al.*, 2004) or *P. falciparum* sporozoites (NF 54 strain) were obtained from dissection of infected female *Anopheles stephensi* mosquito salivary glands.

siRNA design, siRNA library and screening controls

Custom siRNA library sets were designed (Cenix Bioscience GmbH) and synthesized (Ambion/Applied Biosystems, Austin USA) with three siRNA duplexes for each gene target (Supplementary Table 1). For selected genes, two additional siRNAs were designed and synthesized. Negative control samples included untransfected cells and

cells transfected with a negative control siRNA not targeting any annotated genes in the human genome. A pre-validated siRNA targeting the *met* gene (see text), leading to a decrease in infection, was included as positive control in all plates. The siRNA duplexes were arrayed in a 96-well format.

High-throughput siRNA screening of *Plasmodium* infection

Huh7 cells (4500 per well) were seeded in 100 µl complete RPMI medium in optical 96-well plates (Costar) and incubated at 37°C in 5% CO_2. Twenty-four h after seeding, cells were transfected with individual siRNAs in a final concentration of 100 nM per lipofection. Each siRNA was transfected in triplicate. Briefly, for each well, cell supernatant was replaced by 80 µl of serum-free culture medium without antibiotics. One µl of 10 µM siRNA diluted in 16 µl of Opti-MEM (Invitrogen.) was complexed with 0.4 µl Oligofectamine (Invitrogen) diluted with 2.6 µl Opti-MEM and added onto the cells following the manufacturer's protocol. Four h after addition of the complex, 50 µl of fresh RPMI medium, supplemented with 30% FCS, 3% pen/strep, 3% non-essential amino acid, 3% glutamine and 3% HEPES were added to the cells. Two days after siRNA transfection, cells were infected with 10^4 *P. berghei* sporozoites/well. Twenty-four h after infection, cells were fixed with 4% paraformaldehyde (PFA) in PBS and permeabilized with 0.2% saponin in PBS. Cell nuclei were stained with Hoechst-33342 (Molecular Probes/Invitrogen), filamentous actin was stained with Phalloidin AlexaFluor488 (Molecular Probes/Invitrogen), EEFs were detected using the mouse monoclonal antibody 2E6 (Tsuji *et al.*, 1994) and an AlexaFluor555-labeled goat anti-mouse secondary antibody (Molecular Probes/Invitrogen).

Automated image acquisition and analysis

Plates were acquired with a Discovery1 automated fluorescence microscope (Molecular Devices Corporation, CA, USA) using a 10x lens. In each well, cell nuclei, actin and EEFs were imaged in 9 fields covering a total area of 2.7 x 2.0 mm. Image data was analyzed using a custom MetaMorph (Molecular Devices Corporation, CA, USA) based algorithm extracting the following values for each imaged field: cell proliferation as measured by the number of nuclei per imaged field (Hoechst staining), cell confluency as measured by the percentage of the imaged field covered by actin staining and number of EEFs as number of compact, high contrast objects in a size range from 16 to 150 pixels. Within each field, the number of EEFs was normalized to the cell confluency. Normalized EEF numbers and number of nuclei were averaged between the 9 imaged fields within each well. Mean and standard

deviations were calculated for each experimental triplicate. Final readouts included number of EEFs and number of nuclei, shown as a percentage of the plate mean.

Gene-specific expression and infection quantification by qRT-PCR

For gene-specific expression *in vitro*, total RNA was isolated from Huh7 cells 48 h post-transfection (Invitek Invisorb 96-well plate kit) and converted into cDNA (ABI's HighCapacity cDNA reagents) with random hexamers, following the manufacturer recommendations. qRT-PCR used the SybrGreen method with Quantace qPCR mastermix at 11 µl total reaction volume, containing 500 nM of the target-specific primers, and primers that were designed to specifically amplify a fragment of the selected genes. Real-time PCR reactions were performed on an ABI Prism 7900HT system. Relative amounts of remaining mRNA levels of RNAi targets were calculated against the level of *RPL13A* or *18S* rRNA, as housekeeping genes. Remaining mRNA levels of RNAi-treated samples were compared with those of samples transfected with Negative unspecific siRNA. *RPL13A*-specific primer sequences were: 5′-CCT GGA GGA GAA GAG GAA AGA GA-3′ and 5′-TTG AGG ACC TCT GTG TAT TTG TCA A-3′. *18S* rRNA-specific primer sequences were: 5′-CGG CTT AAT TTG ACT CAA CAC G-3′ and 5′-TTA GCA TGC CAG AGT CTC GTT C-3′.

For infection determination *in vivo, in vitro* or *ex vivo*, total RNA was isolated from livers, Huh7 cells or primary hepatocytes using Qiagen's RNeasy Mini or Micro kits, respectively for livers and cells, following the manufacturer's instructions. The determination of liver parasite load *in vivo*, was performed according to the method developed for *P. yoelii* infections (Bruna-Romero *et al.*, 2001). Livers were collected and homogenized in denaturing solution (4 M guanidine thiocyanate; 25 mM sodium citrate pH 7, 0.5 % sarcosyl and 0.7 % β-Mercaptoethanol in DEPC-treated water), 40 h after sporozoite injection. Total RNA was extracted using Qiagen's RNeasy Mini kit, following the manufacturer's instructions. RNA for infection measurements was converted into cDNA using Roche's Transcriptor First Strand cDNA Synthesis kit, according to the manufacturer's protocol. The qRT-PCR reactions used Applied Biosystems' Power SYBR Green PCR Master Mix and were performed according to the manufacturer's instructions on an ABI Prism 7000 system (Applied Biosystems). Amplification reactions were carried out in a total reaction volume of 25 µl, containing 0,8 pmoles/µl or 0,16 pmoles/µl of the *Plasmodium-* or housekeeping gene-specific primers, respectively. Relative amounts of *Plasmodium* mRNA were calculated against the Hypoxanthine Guanine Phosphoribosyltransferase (*HPRT*) housekeeping gene. *18S* Pb*A*- and mouse *HPRT*-specific primer sequences were 5′- AAG CAT TAA ATA AAG CGA ATA CAT CCT TAC – 3′ and 5′ - GGA GAT TGG TTT TGA CGT TTA

TGT G – 3'and 5' – GTA ATG ATC GTC GTC AAC GGG GGA – 3´ and 5' – CCA GCA AGC TTG CAA CCT TAA CCA – 3', respectively. *18S* Pf- and human *HPRT*-specific primer sequences were 5'- CTG GTT TGG GAA AAC CAA AT – 3' and 5' – CTC AAT CAT GAC TAC CCG TCT G – 3'and 5' – TGC TCG AGA TGT GAT GAA GG – 3´ and 5' – TCC CCT GTT GAC TGG TCA TT – 3'. For PKCζ mRNA level determination by qRT-PCT, mouse or human *PKCζ*-specific primers (from SuperArray, USA; catalog number PPM05103A and PPH02321B, respectively) were used according to the manufacturer's protocol.

PKCζ inhibition in Huh7 cells

Freshly-prepared serial dilutions of PKCζ pseudo-substrate inhibitor, Myristoylated (PKCζInh, from Calbiochem/Merck KGaA, Germany) were added to Huh7 cells 1h before sporozoite addition. Infection level was determined 24 after sporozoite addition (1-3 × 10^4 per well, depending on the experiment) by FACS or qRT-PCR, depending on the experiment. As control, a dilution of PBS, matching that present in the most concentrated inhibitor preparation was used.

Infection level determination by FACS was performed through the quantification of the percentage of parasite-containing cells (cell population GFP+). Cell samples for FACS analysis were washed with 1 ml PBS, incubated with 150 μl trypsin for 5 min at 37 °C and collected in 400 μl 10% FCS in PBS at the selected time-points post-sporozoite addition. Cells were then centrifuged at 0.1 *g* for 3 min at 4 °C and ressuspended in 150 μl 2% FCS in PBS. Cells were analysed on a Becton Dickinson FACScalibur with the appropriate settings for the fluorophores used. Data acquisition and analysis were carried out using the CELLQuest (version 3.2.1fl1, Becton Dickinson) and FlowJo (version 6.3.4, FlowJo) software packages, respectively.

For infection measurement by qRT-PCR, as described above, cell samples were collected for RNA extraction in 150 μl of RLT buffer (Qiagen) containing 0.1% β-mercaptoethanol.

PKCζ inhibition in mouse and human primary hepatocytes

C57BL/6 mouse primary hepatocytes (10 × 10^4 per well) were incubated with 20 μM PKCζInh one h prior to infection with 5 × 10^4 freshly extracted *P. berghei* sporozoites. Forty-eight h after infection, cells were collected in 150 μl of RLT buffer (Qiagen) containing 0.1% β-mercaptoethanol for RNA extraction and infection measurement by qRT-PCR.

Human primary hepatocytes (10×10^4 cells per well) were incubated with 20 μM PKCζInh one h prior to infection with 10×10^4 freshly extracted *P. falciparum* sporozoites. Three days after infection, cells were collected in 150 μl of RLT buffer (Qiagen) containing 0.1% β-mercaptoethanol for RNA extraction and infection measurement by qRT-PCR.

In vivo RNAi

C57BL/6 mice (male, 6-8 weeks) were treated with a single intravenous (i.v.) administration of 5 mg/kg of siRNA formulated in liposomal nanoparticles (Alnylam, Germany). Three different modified siRNAs targeting PKCζ, were used. A modified siRNA targeting luciferase was used as control. Thirty-six h after siRNA administration mice were infected by i.v. injection of 2×10^4 *P. berghei* sporozoites. Remaining PKCζ mRNA levels and parasite load in the livers of infected mice were determined by qRT-PCR 40 h after sporozoite injection, 76 h after siRNA administration. Infection of mice treated with one PKCζ siRNA was allowed to proceed onto the blood stage and parasitemia (% of infected red blood cells) was measured daily.

Statistical analysis

Statistical analysis was performed using unpaired Student *t* or ANOVA parametric tests. $P < 0.05$ and $P < 0.051$ were considered statistically significant.

Ackowledgements

References

Agaisse, H., Burrack, L.S., Philips, J.A., Rubin, E.J., Perrimon, N., and Higgins, D.E. (2005). Genome-wide RNAi screen for host factors required for intracellular bacterial infection. Science *309*, 1248-1251.

Akimoto, K., Mizuno, K., Osada, S., Hirai, S., Tanuma, S., Suzuki, K., and Ohno, S. (1994). A new member of the third class in the protein kinase C family, PKC lambda, expressed dominantly in an undifferentiated mouse embryonal carcinoma cell line and also in many tissues and cells. J Biol Chem *269*, 12677-12683.

Anselmo, A.N., Earnest, S., Chen, W., Juang, Y.C., Kim, S.C., Zhao, Y., and Cobb, M.H. (2006). WNK1 and OSR1 regulate the Na+, K+, 2Cl- cotransporter in HeLa cells. Proc Natl Acad Sci U S A *103*, 10883-10888.

Berns, K., Hijmans, E.M., Mullenders, J., Brummelkamp, T.R., Velds, A., Heimerikx, M., Kerkhoven, R.M., Madiredjo, M., Nijkamp, W., Weigelt, B., Agami, R., Ge, W., Cavet, G., Linsley, P.S., Beijersbergen, R.L., and Bernards, R. (2004). A large-scale RNAi screen in human cells identifies new components of the p53 pathway. Nature *428*, 431-437.

Boutros, M., Kiger, A.A., Armknecht, S., Kerr, K., Hild, M., Koch, B., Haas, S.A., Paro, R., and Perrimon, N. (2004). Genome-wide RNAi analysis of growth and viability in Drosophila cells. Science *303*, 832-835.

Bruna-Romero, O., Hafalla, J.C., Gonzalez-Aseguinolaza, G., Sano, G., Tsuji, M., and Zavala, F. (2001). Detection of malaria liver-stages in mice infected through the bite of a single Anopheles mosquito using a highly sensitive real-time PCR. Int J Parasitol *31*, 1499-1502.

Carrolo, M., Giordano, S., Cabrita-Santos, L., Corso, S., Vigario, A.M., Silva, S., Leiriao, P., Carapau, D., Armas-Portela, R., Comoglio, P.M., Rodriguez, A., and Mota, M.M. (2003). Hepatocyte growth factor and its receptor are required for malaria infection. Nat Med *9*, 1363-1369.

Echeverri, C.J., Beachy, P.A., Baum, B., Boutros, M., Buchholz, F., Chanda, S.K., Downward, J., Ellenberg, J., Fraser, A.G., Hacohen, N., Hahn, W.C., Jackson, A.L., Kiger, A., Linsley, P.S., Lum, L., Ma, Y., Mathey-Prevot, B., Root, D.E., Sabatini, D.M., Taipale, J., Perrimon, N., and Bernards, R. (2006). Minimizing the risk of reporting false positives in large-scale RNAi screens. Nat Methods *3*, 777-779.

Franke-Fayard, B., Trueman, H., Ramesar, J., Mendoza, J., van der Keur, M., van der Linden, R., Sinden, R.E., Waters, A.P., and Janse, C.J. (2004). A Plasmodium berghei reference line that constitutively expresses GFP at a high level throughout the complete life cycle. Mol Biochem Parasitol *137*, 23-33.

Fraser, A. (2004). RNA interference: human genes hit the big screen. Nature *428*, 375-378.

Friedrich, B., Feng, Y., Cohen, P., Risler, T., Vandewalle, A., Broer, S., Wang, J., Pearce, D., and Lang, F. (2003). The serine/threonine kinases SGK2 and SGK3 are potent stimulators of the epithelial Na+ channel alpha,beta,gamma-ENaC. Pflugers Arch *445*, 693-696.

Gamper, N., Fillon, S., Feng, Y., Friedrich, B., Lang, P.A., Henke, G., Huber, S.M., Kobayashi, T., Cohen, P., and Lang, F. (2002). K+ channel activation by all three isoforms of serum- and glucocorticoid-dependent protein kinase SGK. Pflugers Arch *445*, 60-66.

Hunter, T. (2000). Signaling--2000 and beyond. Cell *100*, 113-127.

Leiriao, P., Albuquerque, S.S., Corso, S., van Gemert, G.J., Sauerwein, R.W., Rodriguez, A., Giordano, S., and Mota, M.M. (2005). HGF/MET signalling protects Plasmodium-infected host cells from apoptosis. Cell Microbiol 7, 603-609.

Lum, L., Yao, S., Mozer, B., Rovescalli, A., Von Kessler, D., Nirenberg, M., and Beachy, P.A. (2003). Identification of Hedgehog pathway components by RNAi in Drosophila cultured cells. Science *299*, 2039-2045.

Manning, G., Whyte, D.B., Martinez, R., Hunter, T., and Sudarsanam, S. (2002). The protein kinase complement of the human genome. Science *298*, 1912-1934.

Mazier, D., Beaudoin, R.L., Mellouk, S., Druilhe, P., Texier, B., Trosper, J., Miltgen, F., Landau, I., Paul, C., Brandicourt, O., and et al. (1985). Complete development of hepatic stages of Plasmodium falciparum in vitro. Science *227*, 440-442.

Mellor, H., and Parker, P.J. (1998). The extended protein kinase C superfamily. Biochem J *332 (Pt 2)*, 281-292.

Moriguchi, T., Urushiyama, S., Hisamoto, N., Iemura, S., Uchida, S., Natsume, T., Matsumoto, K., and Shibuya, H. (2005). WNK1 regulates phosphorylation of cation-chloride-coupled cotransporters via the STE20-related kinases, SPAK and OSR1. J Biol Chem *280*, 42685-42693.

Moscat, J., and Diaz-Meco, M.T. (2000). The atypical protein kinase Cs. Functional specificity mediated by specific protein adapters. EMBO Rep *1*, 399-403.

Moscat, J., Rennert, P., and Diaz-Meco, M.T. (2006). PKCzeta at the crossroad of NF-kappaB and Jak1/Stat6 signaling pathways. Cell Death Differ *13*, 702-711.

Mota, M.M., Pradel, G., Vanderberg, J.P., Hafalla, J.C., Frevert, U., Nussenzweig, R.S., Nussenzweig, V., and Rodriguez, A. (2001). Migration of Plasmodium sporozoites through cells before infection. Science *291*, 141-144.

Muscella, A., Storelli, C., and Marsigliante, S. (2005). Atypical PKC-zeta and PKC-iota mediate opposing effects on MCF-7 Na+/K+ATPase activity. J Cell Physiol *205*, 278-285.

Ono, Y., Fujii, T., Ogita, K., Kikkawa, U., Igarashi, K., and Nishizuka, Y. (1989). Protein kinase C zeta subspecies from rat brain: its structure, expression, and properties. Proc Natl Acad Sci U S A *86*, 3099-3103.

Paddison, P.J., Silva, J.M., Conklin, D.S., Schlabach, M., Li, M., Aruleba, S., Balija, V., O'Shaughnessy, A., Gnoj, L., Scobie, K., Chang, K., Westbrook, T., Cleary, M., Sachidanandam, R., McCombie, W.R., Elledge, S.J., and Hannon, G.J. (2004). A resource for large-scale RNA-interference-based screens in mammals. Nature *428*, 427-431.

Pelkmans, L., Fava, E., Grabner, H., Hannus, M., Habermann, B., Krausz, E., and Zerial, M. (2005). Genome-wide analysis of human kinases in clathrin- and caveolae/raft-mediated endocytosis. Nature *436*, 78-86.

Prudêncio, M., Rodrigues, C.D., Ataíde, R., and Mota, M.M. (2007). Dissecting in vitro host cell infection by Plasmodium sporozoites using flow cytometry. Cell Microbiol *In Press*.

Prudencio, M., Rodriguez, A., and Mota, M.M. (2006). The silent path to thousands of merozoites: the Plasmodium liver stage. Nat Rev Microbiol *4*, 849-856.

Ramet, M., Manfruelli, P., Pearson, A., Mathey-Prevot, B., and Ezekowitz, R.A. (2002). Functional genomic analysis of phagocytosis and identification of a Drosophila receptor for E. coli. Nature *416*, 644-648.

Renia, L., Gruner, A.C., Mauduit, M., and Snounou, G. (2006). Vaccination against malaria with live parasites. Expert Rev Vaccines *5*, 473-481.

Soloff, R.S., Katayama, C., Lin, M.Y., Feramisco, J.R., and Hedrick, S.M. (2004). Targeted deletion of protein kinase C lambda reveals a distribution of functions between the two atypical protein kinase C isoforms. J Immunol *173*, 3250-3260.

Standaert, M.L., Galloway, L., Karnam, P., Bandyopadhyay, G., Moscat, J., and Farese, R.V. (1997). Protein kinase C-zeta as a downstream effector of phosphatidylinositol 3-kinase during insulin stimulation in rat adipocytes. Potential role in glucose transport. J Biol Chem *272*, 30075-30082.

Suzuki, A., Akimoto, K., and Ohno, S. (2003). Protein kinase C lambda/iota (PKClambda/iota): a PKC isotype essential for the development of multicellular organisms. J Biochem (Tokyo) *133*, 9-16.

Suzuki, A., and Ohno, S. (2006). The PAR-aPKC system: lessons in polarity. J Cell Sci *119*, 979-987.

Vallenius, T., and Makela, T.P. (2002). Clik1: a novel kinase targeted to actin stress fibers by the CLP-36 PDZ-LIM protein. J Cell Sci *115*, 2067-2073.

Waters, A.P., Mota, M.M., van Dijk, M.R., and Janse, C.J. (2005). Parasitology. Malaria vaccines: back to the future? Science *307*, 528-530.
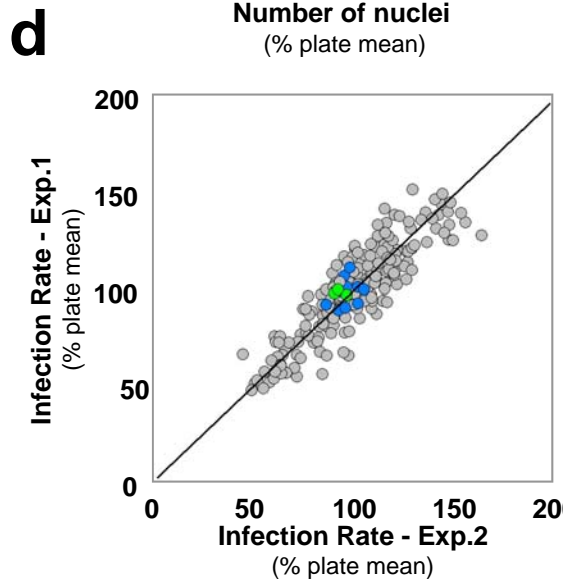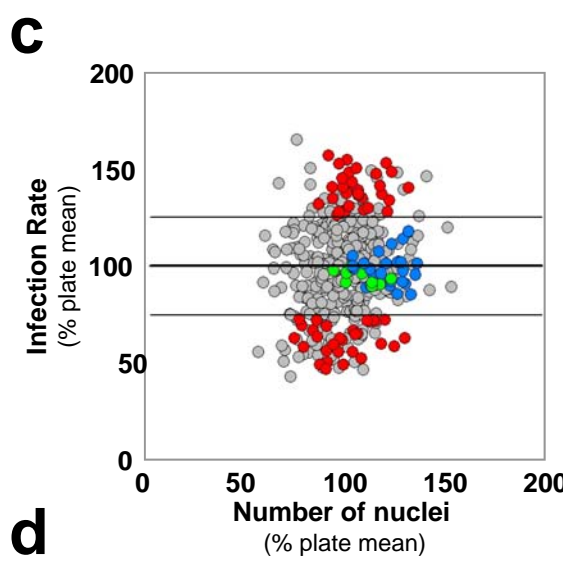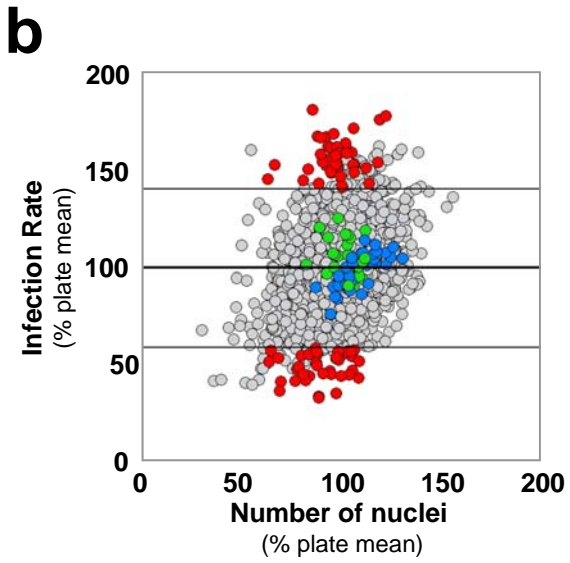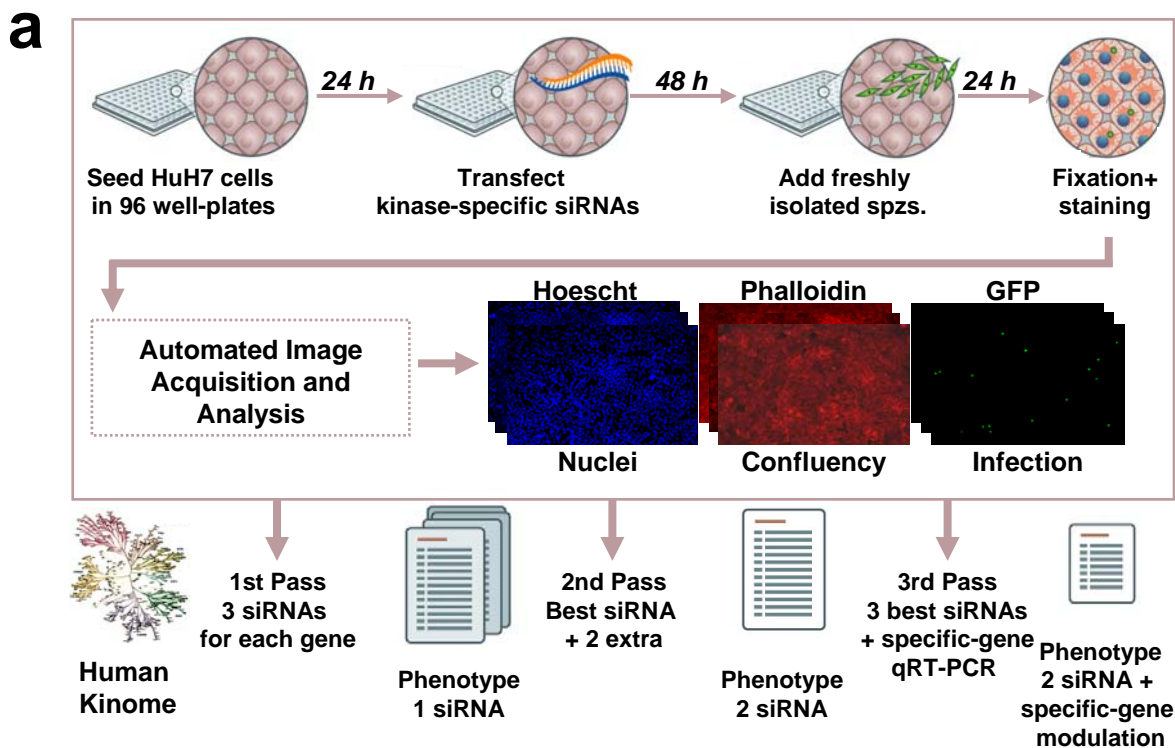
Figure 1 | A kinome-wide RNAi screen identifies candidate host genes that influence *P. berghei* sporozoite infection of Huh7 cells.

(a) Schematic illustration of the experimental workflow for the cell-based RNAi screening approach used to explore the influence of known proteins with putative kinase activity, as well as several kinase-interacting proteins in the outcome of *P. berghei* sporozoite infection of Huh7 cells. The candidate genes underwent three screening passes with increasing stringency criteria. **(b)** Plot of pass 1 of the RNAi screen representing the effect of 2181 siRNAs targeting 727 human genes on Huh7 cell infection by *P. berghei* sporozoites and cell nuclei count. Infection rates for each experimental condition were normalized against cell confluency. The horizontal lines represent 100% ± 2.0 s.d. of the average of all data in the assay. Each circle represents one siRNA (mean of triplicate values). Negative controls appear as blue and green circles, corresponding to untreated cells and cells transfected with a non-specific control siRNA, respectively. Red circles highlight the siRNAs targeting the 74 candidate genes selected to undergo a second screening pass. **(c)** Plot of 2 independent runs of pass 2 of the RNAi screen representing the effect of 229 siRNAs targeting 74 human genes on Huh7 cell infection by *P. berghei* sporozoites and cell nuclei count. Experimental conditions, normalization criteria as well as colour attributions are the same as in panel (b), with red circles representing the siRNAs targeting the 19 genes selected to undergo a third screening pass. The horizontal lines represent 100% ± 2.0 s.d. of the average of all the negative controls in the assay. **(d)** Plot comparison of the 2 runs of pass 2 of the RNAi screen. Colour attributions are the same as in panel (b). The comparison reveals a high correlation (R = 0.88) between the duplicate pass 2 of the screen.
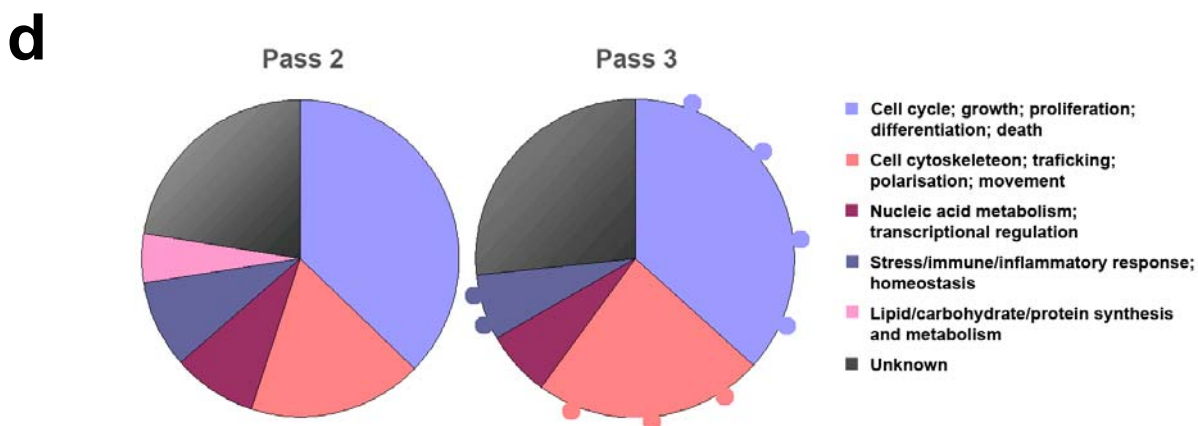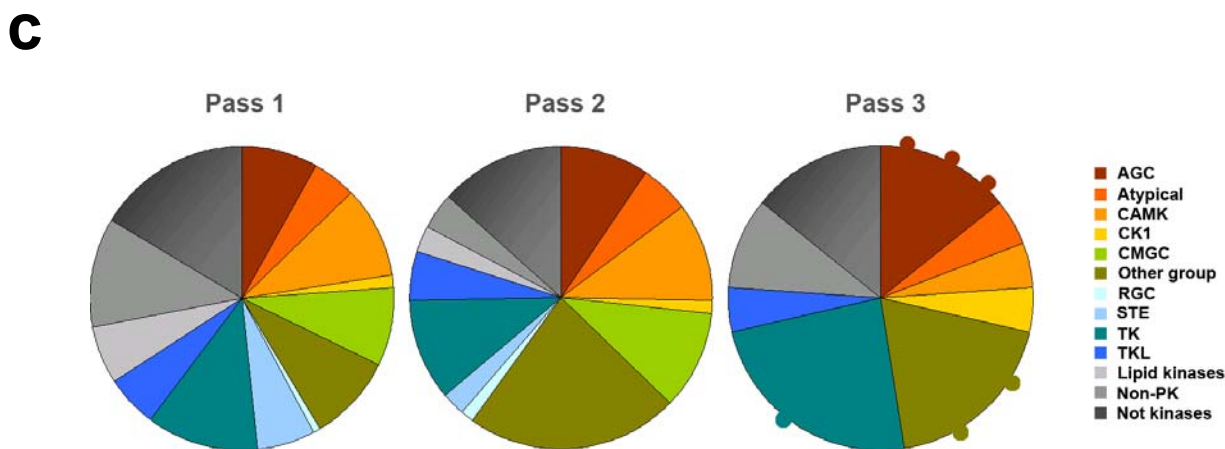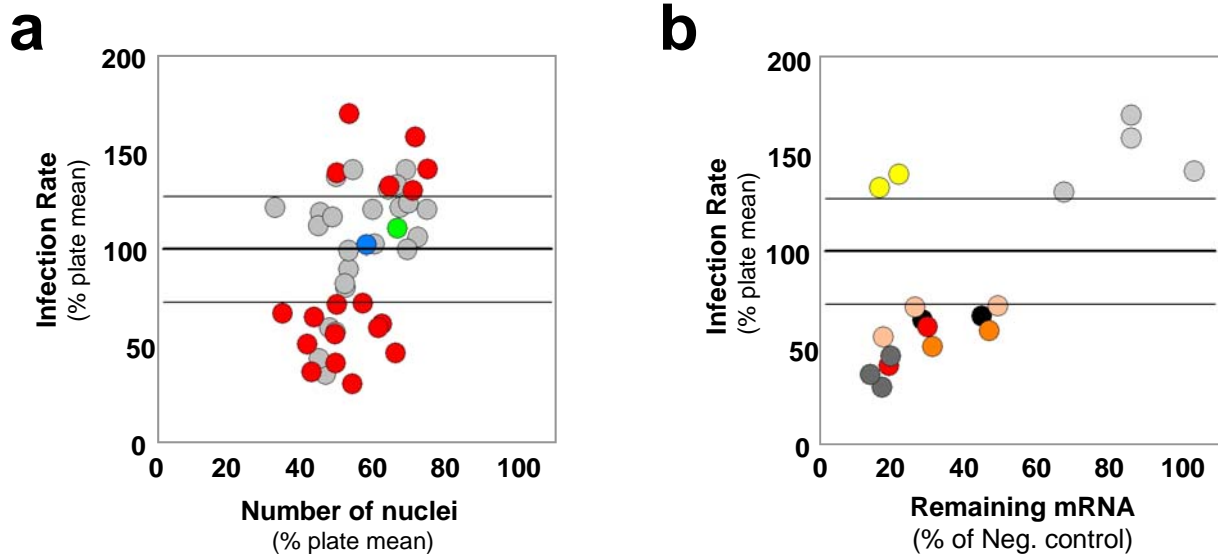
Figure 2 | Identification and analysis of host kinases and related genes affecting infection by *P. berghei* sporozoites.

(a) Plot of pass 3 of the RNAi screen representing the effect of 43 siRNAs targeting 19 human genes on Huh7 cell infection by *P. berghei* sporozoites and cell nuclei count. Colour attributions are the same as in Figure 1. Red circles highlight genes selected for final confirmation. The horizontal lines represent $100\% \pm 3.0$ s.d. of the average of all the negative controls in the assay. **(b)** Effect of siRNA on infection rates *versus* remaining mRNA levels for genes selected on pass 3 of the screen. Each circle represents one siRNA (mean of triplicate values) with the siRNAs targeting PKCι in yellow, STK35 in light orange, WNK1 in orange, PKCζ in red, SGK2 in dark grey and MET in black. For all genes except GUK1 and ULK1, represented in light grey, a positive correlation between infection rate and remaining gene-specific mRNA levels is observed. **(c)** Data analysis for the RNAi screen in terms of gene distribution through kinase and kinase-related families and **(d)** based on gene ontology and molecular function.
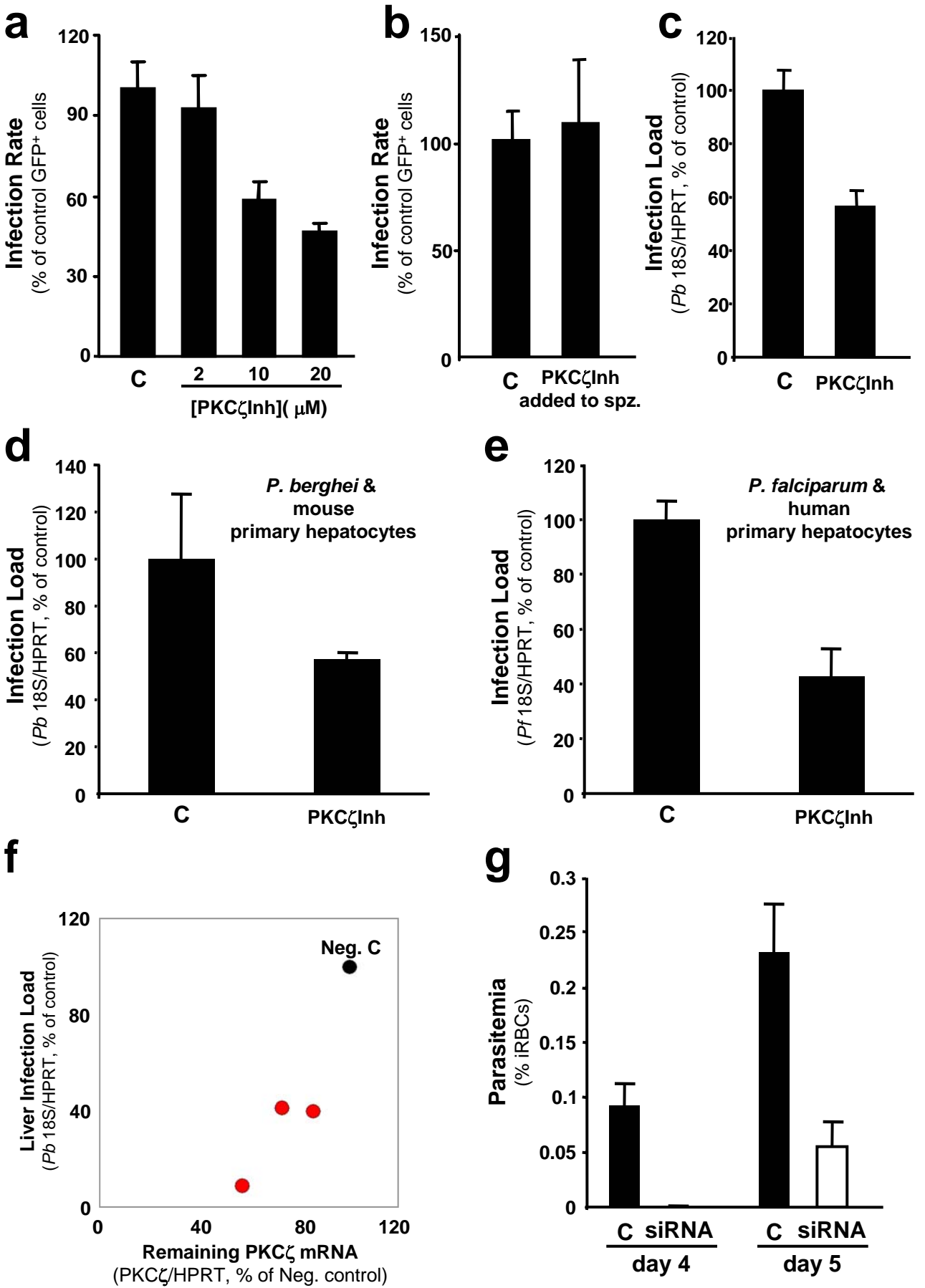
Figure 3 | PKCζ inhibition effect on infection confirms the physiological relevance of the RNAi screen results.

(a) PKCζ inhibition by a pseudo-substrate inhibitor (PKCζInh) decreases *P. berghei* sporozoite infection of Huh7 cells in a dose-dependent manner. PKCζInh was added to Huh7 cells 1 h before GFP-expressing *P. berghei* sporozoite addition and infection rate was measured 24 h later, by flow cytometry. **(b)** Infection load was not affected by pre-incubating *P. berghei* sporozoites with PKCζInh for 1 h prior to addition to cells. Results are expressed as the mean ± s.d. of GFP⁺ cells (%) in 3 independent infections. **(c-e)** PKCζInh (20 μM) reduces *P. berghei* load in Huh7 cells **(c)** or mouse primary hepatocytes **(d)** and *P. falciparum* load in human primary hepatocytes **(e).** Parasite loads were measured by qRT-PCR 24 h, 48 h or 5 days after sporozoite addition, respectively. Results are expressed as the mean ± s.d. of triplicate samples. "C" indicates solvent-treated cells used as control and results were normalized to C levels (100%). **(f)** Effect of siRNA-mediated *in vivo* silencing of PKCζ on mouse liver infection by *P. berghei*, measured by qRT-PCR analysis of liver extracts taken 40 h after sporozoite i.v. injection. Results are plotted as the percentage of the mean of negative control samples "C". The remaining mRNA levels for PKCζ were measured by qRT-PCR in the same liver samples. Each circle represents one siRNA (mean of 5 mice per group). Black circle represents the negative control (luciferase-targeting siRNA). Red circles highlight the 3 independent siRNAs targeting the PKCζ gene. **(g)** Knock-down of PKCζ expression by RNAi delays the onset of blood stage infection, as measured by parasitemia quantification (percentage of infected red blood cells, iRBC) using flow cytometry. Results are expressed as the mean ± s.d. of 6 mice per group**.**
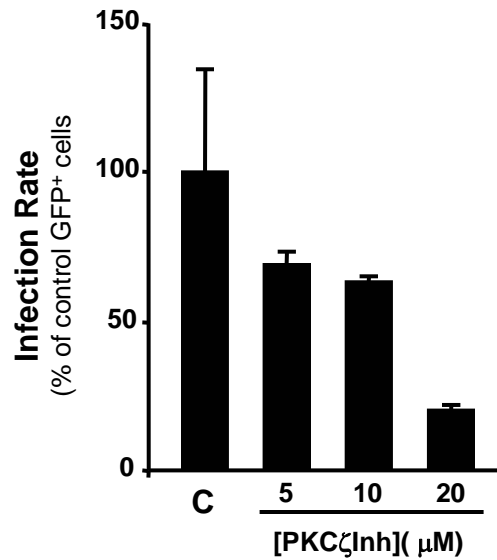
Supplementary Figure 1 | PKCζ inhibition effect on *P. berghei* infection of Hepa1-6 cells.

(a) PKCζ inhibition by a pseudo-substrate inhibitor (PKCζInh) decreases *P. berghei* sporozoite infection of Hepa1-6 cells in a dose-dependent manner. PKCζInh was added to Hepa1-6 cells 1 h before GFP-expressing *P. berghei* sporozoite addition and infection rate was measured 24 h later, by flow cytometry.

Gene name	Kinome Group	Main described functions	NCBI Gene Accession Number
MET	TK	Cell growth and proliferation	4233
PRKCI	AGC	Cell growth and survival; cytoskeleton organisation	5584
PRKCZ	AGC	Cell growth and survival; cytoskeleton organisation	5590
SGK2	AGC	Regulation of transport; apoptosis	10110
PRKWNK1	Other Group	Regulation of salt transport; cell growth	65125
STK35	Other Group	Regulation of actin stress fibers	140901

Gene name	NCBI Accession ID for Targeted Transcripts	siRNA ID from Supplier[1]	Infection Rate[2]	Cell Proliferation[3]	Remaining mRNA[4]
MET	NM_000245	242542; 242543	76,2	78,4	35,7
PRKCI	NM_002740	311; 242360	130,2	98,1	18,0
PRKCZ	NM_002744	103575; 242362	75,6	86,3	23,4
SGK2	NM_170693;NM_016276	1485; 1579; 1669	66,2	100,0	38,2
PRKWNK1	NM_018979	1269; 242540	74,2	103,7	15,7
STK35	NM_080836	1135; 103377; 103461	71,7	97,4	30,1

[1]Ambion, Applied Biosystems; [2]number of EEFs normalised to confluency, shown as % of plate mean; [3]number of cell nuclei, shown as % of plate mean; [4]% relative to negative control.

Table 1 | Host kinases and related genes identified as important for Huh7 infection by *P. berghei* sporozoites.
The NCBI gene accession number and accession ID for targeted transcripts, as well as the kinome group and main described function are provided for the genes identified in the RNAi screen. In addition the infection rate (corresponding to the number of EEFs normalized to confluency, shown as % of plate mean), cell proliferation (number of cell nuclei, shown as % of plate mean) and remaining mRNA (% relative to negative control) data from Pass 3 are also shown. The values correspond to the average of the data of the siRNAs yielding a phenotype change for each gene.

Gene Information		Pass 1				Pass 2				Pass 3		
Gene Name	LocusLink ID	siRNA-1	siRNA-2	siRNA-3	siRNA1	siRNA2	siRNA3	siRNA4	siRNA5	siRNA1	siRNA2	siRNA3
ABL1	25	1241	1336	1431								
ABL2	27	1478	1662	**103346**	103346	242409	242410					
ACVR1	90	**76**	77	78	76	242344	242345					
ACVR1B	91	1331	103589	111240								
ACVR2	92	143	144	103568								
ACVR2B	93	79	80	81								
ACVRL1	94	11	12	13								
ADK	132	1474	1568	1658								
ADRBK1	156	147	103304	103391								
ADRBK2	157	628	629	630								
AK1	203	65	66	110741								
AK2	204	41652	41815	147152								
AK3	205	915	**916**	917	916	242490	242491					
AKT1	207	632	42811	118270								
AKT2	208	149	150	103305								
ALK	238	499	500	501								
AMHR2	269	1044	1045	1046								
ARAF1	369	151	152	153								
ATM	472	111194	118231	118232								
ATR	545	82	83	103302								
AXL	558	1218	1313	1408								
BCR	613	1237	1332	110844								
BLK	640	154	155	156								
BMPR1A	657	502	503	504								
BMPR1B	658	85	87	103565								
BMPR2	659	1438	1623	110763								
BMX	660	157	158	159								
BRAF	673	506	507	110846								
BRDT	676	160	161	162								
BTK	695	14	15	16								
BUB1	699	508	509	510								
BUB1B	699	88	89	90								
DDR1	780	1221	1316	1411								
CALM1	801	146695	146696	146697								
CALM2	805	145935	145936	145937								
CALM3	808	634	636	111245								
CAMK4	814	163	164	165								

Gene Information		Pass 1			Pass 2					Pass 3		
Gene Name	LocusLink ID	siRNA-1	siRNA-2	siRNA-3	siRNA1	siRNA2	siRNA3	siRNA4	siRNA5	siRNA1	siRNA2	siRNA3
CAMK2A	815	1484	1578	1668								
CAMK2B	816	9477	9571	9662								
CAMK2D	817	91	93	118256								
CAMK2G	818	40536	40631	40719								
CDC2	983	1625	42819	103821								
CDC2L1	984	41656	214537	214538	41656	214537	214538			41656	214537	214538
CDK2	1017	1314	1409	42820								
CDK3	1018	94	95	96								
CDK4	1019	44756	44852	213350								
CDK5	1020	1466	1560	1650								
CDK6	1021	98	99	42822								
CDK7	1022	166	167	168								
CDK8	1024	100	101	102								
CDK9	1025	103	104	103567								
CDKN1A	1026	1436	1531	1621	1436	242474	242475					
CDKN1B	1027	118712	118713	118714	118712	242378	242379			118712	242378	
CDKN1C	1028	2789	118537	119424	119424	242331	242332					
CDKN2A	1029	118858	119508	119509								
CDKN2B	1030	118739	118740	118741								
CDKN2C	1031	118622	118623	119531								
CDKN2D	1032	118644	118645	118646								
CDKN3	1033	637	45016	45105								
CHEK1	1111	106	107	108								
CHKA	1119	109	110	111	109	242492	242493					
CHKB	1120	202425	202426	202427								
CHUK	1147	112	113	114								
CKB	1152	170	118235	118236								
CKM	1158	172	173	110772								
CKMT1	1159	1178	1273	1368								
CKMT2	1160	175	176	177								
CLK1	1195	479	480	110837								
CLK2	1196	43833	43929	44017								
CLK3	1198	1233	1328	1423								
PLK3	1263	103318	103806	103809	103809	242380	242381					
MAP3K8	1326	118272	118273	118274								
MAPK14	1432	1217	1312	111198								
CSF1R	1436	641	642	643								
CSK	1445	511	512	513								
CSNK1A1	1452	178	179	180								

Gene Information		Pass 1			Pass 2					Pass 3		
Gene Name	LocusLink ID	siRNA-1	siRNA-2	siRNA-3	siRNA1	siRNA2	siRNA3	siRNA4	siRNA5	siRNA1	siRNA2	siRNA3
CSNK1D	1453	1220	1315	1410								
CSNK1E	1454	1441	1536	1626								
CSNK1G2	1455	115	117	118258								
CSNK1G3	1456	103320	103404	103486								
CSNK2A1	1457	1146	1242	1337								
CSNK2A2	1459	181	183	103306								
CSNK2B	1460	9710	9806	9896								
DGKA	1606	118	119	120								
DGKB	1607	1235	1330	1425								
DGKG	1608	121	122	123								
DGKQ	1609	124	125	126								
DAPK1	1612	598	599	600								
DAPK3	1613	129	103790	103795								
DCK	1633	68	69	103564								
DGUOK	1716	1514	1606	1695								
DLG1	1739	146326	146327	146328								
DLG3	1741	146766	146767	146768								
DLG4	1742	145816	145817	145818								
DMPK	1760	517	518	519								
DOK1	1796	145825	145826	145827								
DTYMK	1841	1152	45179	45274								
DYRK1A	1859	1439	1534	1624								
EGFR	1956	644	42833	110895								
EPHA2	1969	**520**	521	110852	**520**	**242384**	242385			**520**	242384	
MARK2	2011	1582	**103359**	**103443**	**103359**	**103443**	242440	242441		**103359**	**103443**	
EPHA1	2041	647	648	649								
EPHA3	2042	652	**103330**	**103414**	**103330**	**103414**				**103330**	103414	
EPHA4	2043	523	524	525								
EPHA5	2044	1460	1555	1645								
EPHA7	2045	527	528	103321								
EPHA8	2046	1041	1042	118289								
EPHB1	2047	1149	1245	1340								
EPHB2	2048	1487	1581	1671								
EPHB3	2049	529	530	531								
EPHB4	2050	533	103322	103406								
EPHB6	2051	535	536	537								
ERBB2	2064	42836	103546	103552								
ERBB3	2065	184	185	186								

Gene Information		Pass 1			Pass 2					Pass 3		
Gene Name	LocusLink ID	siRNA-1	siRNA-2	siRNA-3	siRNA1	siRNA2	siRNA3	siRNA4	siRNA5	siRNA1	siRNA2	siRNA3
ERBB4	2066	103331	103415	103497								
ERF	2077	3387	3483	115797								
ERN1	2081	130	131	132								
PTK2B	2185	484	103319	103403								
FER	2241	657	658	103594								
FES	2242	187	188	189								
FGFR1	2260	1216	1311	118296								
FGFR3	2261	103815	110725	110728								
FGFR2	2263	1215	118291	118292								
FGFR4	2264	103307	103394	103816								
FGR	2268	1468	1562	1652								
FLT1	2321	190	191	192								
FLT3	2322	487	488	489								
FLT3LG	2323	44790	44886	144682								
FLT4	2324	193	194	195								
FRK	2444	1147	1243	1338								
FRAP1	2475	601	602	**603**	603	242386	242387					
FYN	2534	1442	1537	1627								
GAK	2580	661	103332	103416								
GALK1	2584	20	21	22								
GALK2	2585	198	103570	103624								
GCK	2645	1507	1600	1690								
GCKR	2646	144707	144708	144709								
GK	2710	24	25	103562								
GK2	2712	1200	1295	1390								
GRK4	2868	662	663	664								
GRK5	2869	666	667	110898								
GRK6	2870	199	200	201								
MKNK2	2872	1157	1252	1347								
GSK3A	2931	1492	1586	1676								
GSK3B	2932	202	203	204								
GUCY2C	2984	604	605	606								
GUCY2F	2986	133	134	135								
GUK1	2987	**71**	**72**	103786	**71**	**72**	242335	242336		**71**	**72**	
GUCY2D	3000	26	27	28								
HCK	3055	**205**	**206**	**207**	**205**	206	**207**			**205**	**207**	
HK1	3098	1506	1599	1689								
HK2	3099	1433	1528	1618								
HK3	3101	208	209	210								

Gene Information		Pass 1			Pass 2					Pass 3		
Gene Name	LocusLink ID	siRNA-1	siRNA-2	siRNA-3	siRNA1	siRNA2	siRNA3	siRNA4	siRNA5	siRNA1	siRNA2	siRNA3
IGF1R	3480	74	103301	110754								
IKBKB	3551	147120	147121	147122								
ILK	3611	1461	1556	1646								
INSR	3643	103297	103384	103467								
INSRR	3645	103722	103730	103738								
IRAK1	3654	136	137	138								
IRAK2	3656	139	140	141								
ITK	3702	701	702	703								
ITPK1	3705	921	922	923								
ITPKA	3706	211	212	213								
ITPKB	3707	214	215	216								
JAK1	3716	217	218	219								
JAK2	3717	607	608	609								
JAK3	3718	32	33	34								
KDR	3791	220	221	222								
KHK	3795	103298	103385	103468								
KIT	3815	35	36	37								
LCK	3932	668	669	670								
LIMK1	3984	1223	1318	1413								
LIMK2	3984	1469	1563	1653								
LTK	4058	223	224	111201								
LYN	4067	226	227	103571								
MARCKS	4082	11454	143479	143480								
MAK	4117	734	735	736								
MARK1	4139	1173	1268	1363								
MARK3	4140	229	230	231								
MATK	4145	1443	1538	1628								
MAP3K1	4214	202512	202513	202514								
MAP3K3	4215	234	103572	103626								
MAP3K4	4216	1470	1564	1654								
MAP3K5	4217	737	738	739								
MET	4233	42825	**242542**	**242543**	**242542**	**242543**	242544			242542	242543	
SCGB2A1	4246	44821	143538	**143539**	**143539**	**242352**	**242353**			143539	**242352**	242353
MAP3K9	4293	202330	202394	202395								
MAP3K10	4294	1444	1539	1629								
MAP3K11	4296	235	236	103787								
MOS	4342	671	**672**	673	672	242388	242389					
MST1R	4486	237	103308	103395								

Gene Information		Pass 1			Pass 2					Pass 3		
Gene Name	LocusLink ID	siRNA-1	siRNA-2	siRNA-3	siRNA1	siRNA2	siRNA3	siRNA4	siRNA5	siRNA1	siRNA2	siRNA3
MUSK	4593	704	705	706								
MVK	4598	56	57	58								
MYLK	4638	1603	1692	103376								
NEK1	4750	147471	147472	147473								
NEK2	4751	**240**	241	242	240	242354	242355					
NEK3	4752	1445	**1540**	**1630**	1540	1630	242356	242357				
NME1	4830	41	42	43								
NME2	4831	244	245	111203								
NME3	4832	42872	42968	118241								
NME4	4833	610	612	110871								
NPR1	4881	1437	1532	1622								
NPR2	4882	1234	1424	**110833**	110833	242337	242338					
NRGN	4900	17411	17506	144200								
NTRK1	4914	42873	42969	43056								
NTRK2	4915	752	753	754								
NTRK3	4916	246	247	248								
ROR1	4919	613	614	615								
ROR2	4920	541	542	543								
DDR2	4921	757	118276	118277								
PAK1	5058	249	250	251								
PAK2	5062	252	110776	110779								
PAK3	5063	**255**	256	257	255	242358	242359					
PCM1	5108	144220	144221	144222								
PCTK1	5127	1472	1566	1656								
PCTK2	5128	258	259	260								
PCTK3	5129	202294	202295	202296								
PDGFRA	5156	758	759	760								
PDGFRB	5159	1446	1541	1631								
PDK1	5163	261	103573	103627								
PDK2	5164	264	265	266								
PDK3	5165	674	675	676								
PDK4	5166	267	268	269								
PDPK1	5170	270	271	272								
PFKFB1	5207	273	274	275								
PFKFB2	5208	761	762	763								
PFKFB3	5209	103323	103407	103489								
PFKFB4	5210	547	548	549								
PFKL	5211	276	277	278								
PFKM	5213	44	46	103563								

Gene Information		Pass 1			Pass 2					Pass 3		
Gene Name	LocusLink ID	siRNA-1	siRNA-2	siRNA-3	siRNA1	siRNA2	siRNA3	siRNA4	siRNA5	siRNA1	siRNA2	siRNA3
PFKP	5214	279	280	281								
PFTK1	5218	118282	118283	118284								
PGK1	5230	48	103299	110731								
PGK2	5232	1204	1299	1394								
PHKA1	5255	143791	143792	143793								
PHKA2	5256	143277	143278	143279								
PHKB	5257	143280	143281	143282								
PHKG1	5260	764	**765**	766	**765**	242394	242395					
PHKG2	5261	110737	118254	118293								
PIK3C2A	5286	143796	143797	143798								
PIK3C2B	5287	143799	143800	143801								
PIK3C2G	5288	143925	143926	143927								
PIK3C3	5289	143802	143803	143804								
PIK3CA	5290	144250	144251	144252								
PIK3CB	5291	144253	144254	144255								
PIM1	5292	1447	1542	1632								
PIK3CD	5293	143975	143976	143977								
PIK3CG	5294	143807	143808	143809								
PIK3R1	5295	118085	118086	118087								
PIK3R2	5296	143978	143979	143980								
PIK4CA	5297	1511	1604	1693								
PIK4CB	5298	282	283	284								
PIP5K2A	5305	616	617	618								
PKLR	5313	53	54	55								
PKM2	5315	285	286	287								
PLK1	5347	1341	42856	103548								
PRKAA1	5562	**767**	768	769	767	242396	242397					
PRKAA2	5563	772	103599	103652								
PRKAB1	5564	142927	142928	142929								
PRKAB2	5565	142837	142838	142839								
PRKACA	5566	292	293	103574								
PRKACB	5567	294	295	118253								
PRKACG	5568	297	298	299								
PKIA	5569	143005	143006	143007								
PKIB	5570	34178	34263	143137								
PRKAG1	5571	11916	12010	12098								
PRKAR1A	5573	42857	44836	44930								
PRKAR1B	5575	142277	142278	142279								
PRKAR2A	5576	490	491	492								

Gene Information		Pass 1			Pass 2					Pass 3		
Gene Name	LocusLink ID	siRNA-1	siRNA-2	siRNA-3	siRNA1	siRNA2	siRNA3	siRNA4	siRNA5	siRNA1	siRNA2	siRNA3
PRKAR2B	5577	142280	142281	142282								
PRKCA	5578	300	301	302								
PRKCB1	5579	304	103309	103396								
PRKCD	5580	774	775	103600								
PRKCE	5581	677	678	679								
PRKCG	5582	306	307	308								
PRKCH	5583	777	778	103822								
PRKCI	5584	**309**	**311**	110781	309	**311**	**242360**	242361		**311**	**242360**	
PKN1	5585	312	314	111207								
PKN2	5586	779	780	781								
PRKCM	5587	103310	103397	103479								
PRKCQ	5588	782	783	784								
PRKCSH	5589	11918	12012	12100								
PRKCZ	5590	**103575**	103629	103679	**103575**	**242362**	242363			**103575**	**242362**	
PRKDC	5591	842	844	103604								
PRKG1	5592	785	786	787								
PRKG2	5593	790	103337	103421								
MAPK1	5594	1449	1544	1634								
MAPK3	5595	142304	142305	202320								
MAPK4	5596	318	319	320								
MAPK6	5597	1450	**1545**	1635	**1545**	242364	242365					
MAPK7	5598	1414	110787	110792								
MAPK8	5599	1225	1320	1415								
MAPK11	5600	103311	103807	103810								
MAPK9	5601	1452	1547	1637								
MAPK10	5602	1517	1608	103378								
MAPK13	5603	321	322	323								
MAP2K1	5604	324	325	326								
MAP2K2	5605	1080	1081	1082								
MAP2K3	5606	1518	1609	1698								
MAP2K5	5607	1519	1699	118252								
MAP2K6	5608	1226	1321	103576								
MAP2K7	5609	103744	103745	103746								
PRKR	5610	328	329	42855								
PRKRIR	5612	142801	142802	142803								
PRKX	5613	1151	1247	1342								
PRKY	5616	332	103312	103805								
PRPS1	5631	335	111211	118242								
PRPS2	5634	336	337	338								

Gene Information		Pass 1			Pass 2					Pass 3		
Gene Name	LocusLink ID	siRNA-1	siRNA-2	siRNA-3	siRNA1	siRNA2	siRNA3	siRNA4	siRNA5	siRNA1	siRNA2	siRNA3
PSKH1	5681	1476	1570	1660								
PTK2	5747	708	103596	103649								
PTK6	5753	**740**	**741**	**742**	740	741	742					
PTK7	5754	339	340	341								
PTK9	5756	342	343	344								
ALDH18A1	5832	345	346	347								
MAP4K2	5871	550	103590	103643								
RAGE	5891	**924**	925	926	924	242421	242422					
RAF1	5894	1548	1638	42858								
RET	5979	1435	1530	1620								
GRK1	6011	**349**	111213	**111215**	349	111215	242366	242367				
RNASEL	6041	1179	1274	1369								
BRD2	6046	118266	118267	118268								
ROCK1	6093	680	681	682								
ROS1	6098	353	110795	110797								
RPS6KA1	6195	354	355	356								
RPS6KA2	6196	1053	1054	1055								
RPS6KA3	6197	553	554	555								
RPS6KB1	6198	1454	1639	110802								
RPS6KB2	6199	469	470	471								
RYK	6259	357	358	103579								
MAPK12	6300	360	44843	44935								
MAP2K4	6416	363	103580	103634								
SGK	6446	711	103597	103650								
SKIV2L	6499	143038	143039	143040								
SKP2	6502	142899	142900	142901								
SRC	6714	683	684	103333								
SRMS	6725	1131	1132	1133								
SRPK1	6732	365	366	367								
SRPK2	6733	103743	103749	103752								
NEK4	6787	371	373	103581								
STK3	6788	791	792	103601								
STK4	6789	**794**	**795**	103602	794	795	242398	242399				
STK6	6790	425	426	427								
CDKL5	6792	374	375	376								
STK10	6793	743	744	745								
STK11	6794	59	60	61								
AURKC	6795	378	379	111219								

Gene Information		Pass 1			Pass 2					Pass 3		
Gene Name	LocusLink ID	siRNA-1	siRNA-2	siRNA-3	siRNA1	siRNA2	siRNA3	siRNA4	siRNA5	siRNA1	siRNA2	siRNA3
SYK	6850	380	381	382								
TAF1	6872	103547	103553	103559								
MAP3K7	6885	1522	1613	1702								
TEC	7006	383	384	385								
TEK	7010	64	103300	103387								
TESK1	7016	797	798	**799**	799	242400	242401					
TGFBR1	7046	556	557	103324								
TGFBR2	7048	386	387	388								
TIE	7075	686	687	688								
TK1	7083	389	390	391								
TK2	7084	559	560	561								
TRIO	7204	849	103343	103427								
TTK	7272	392	393	394								
TTN	7273	1515	1607	**1696**	1696	242370	242371					
TXK	7294	395	396	397								
TYK2	7297	398	399	400								
TYRO3	7301	800	801	802								
UGP2	7360	830	831	832								
UCK2	7371	893	894	895								
VRK1	7443	401	402	403								
VRK2	7444	803	804	**805**	805	242402	242403					
WEE1	7465	405	103582	103636								
YES1	7525	690	103334	103418								
ZAP70	7535	103736	110756	110759								
MAP3K12	7786	103338	103422	103503								
MAPKAPK3	7867	562	563	564								
BRD3	8019	869	**111249**	111251	**111249**	242411	**242412**			111249	242412	
MLL2	8085	107160	107161	115436								
AKAP1	8165	139096	139097	139098								
TRRAP	8295	408	**103314**	103399	103314	242374	242375					
CDC7	8317	410	411	412								
NME5	8382	13281	13442	139132								
PIP5K1A	8394	415	103583	118245								
PIP5K1B	8395	139134	139135	139136								
PIP5K2B	8396	1227	1322	110806								
ULK1	8408	118259	118260	**118261**	118261	242376	242377					
STK24	8428	419	420	421								
DYRK3	8444	424	103315	103400								
DYRK2	8445	103339	103423	103504								

Gene Information		Pass 1			Pass 2					Pass 3		
Gene Name	LocusLink ID	siRNA-1	siRNA-2	siRNA-3	siRNA1	siRNA2	siRNA3	siRNA4	siRNA5	siRNA1	siRNA2	siRNA3
CDC42BPA	8476	**430**	**22066**	**103791**	430	22066	103791	242428	242429			
MAP4K3	8491	1455	1550	1640								
PIK3R3	8503	139246	139247	139248								
IKBKG	8517	139260	139261	139262								
IKBKAP	8518	139263	139264	139265								
DGKZ	8525	432	433	111093								
DGKE	8526	434	435	436								
DGKD	8527	1228	1323	1418								
CAMK1	8536	437	438	439								
MAPKAPK5	8550	1229	1419	103379								
CDK10	8558	1420	111225	111229								
PDXK	8566	440	441	442								
MADD	8567	139308	139309	139310								
MKNK1	8569	445	111234	111236								
CASK	8573	446	447	448								
PRKRA	8575	449	450	451								
STK16	8576	**1457**	1552	103584	1457	242342	242343					
CDC2L5	8621	1231	1326	1421								
SCAP1	8631	139355	139356	139357								
MAP2K1IP1	8649	**138573**	138574	138575	138573	242456	242457					
TNK1	8711	477	110823	110827								
RIPK1	8737	452	453	454								
RIPK2	8767	455	456	103585								
RIOK3	8780	1232	1327	1422								
DYRK4	8798	43832	43928	44016								
TIF1	8805	103317	103402	103484								
CDKL1	8814	1459	1554	1644								
CDK5R1	8851	459	46067	110814								
AKAP4	8852	137315	137316	137317								
STK19	8859	1504	1597	1687								
SPHK1	8877	1181	1276	1371								
PRPF4B	8899	460	461	462								
RPS6KA4	8986	463	464	103586								
CDKL2	8999	466	467	468								
MAP3K14	9020	474	118262	118263								
STK29	9024	13849	13942	14032								
PAPSS2	9060	1463	1557	1647								
PAPSS1	9061	693	694	103595								

Gene Name	LocusLink ID	Pass 1 siRNA-1	siRNA-2	siRNA-3	Pass 2 siRNA1	siRNA2	siRNA3	siRNA4	siRNA5	Pass 3 siRNA1	siRNA2	siRNA3
MAP3K6	9064	1558	103325	103491								
PKMYT1	9088	41898	41988	118297								
LATS1	9113	565	566	567								
HGS	9146	137616	137617	137618								
DYRK1B	9149	1239	1334	1429								
DGKI	9162	571	572	573								
MAP3K13	9175	103327	103411	103493								
DCAMKL1	9201	576	103591	110854								
AURKB	9212	494	495	103587								
RPS6KA5	9252	580	581	103592								
MFHAS1	9258	14331	14426	14519								
MAPKAPK2	9261	1598	1688	103613								
STK17B	9262	498	103588	118265								
STK17A	9263	585	110861	110863								
TAO1	9344	118285	118286	118287								
MAP4K4	9448	1240	1335	1430								
EIF2AK3	9451	592	594	103593								
PRKCABP	9463	138239	138240	138241								
AKAP7	9465	138632	138633	138634								
AKAP6	9472	137533	137534	137535								
ROCK2	9475	595	596	110867								
MAPK8IP1	9479	16356	16447	137929								
AKAP5	9495	15339	137774	137775								
CDC42BPB	9578	746	747	103598								
AKAP12	9590	137856	137857	137858								
IKBKE	9641	**918**	919	920	918	242417	242418					
ULK2	9706	954	955	**956**	956	242427						
SLK	9748	957	958	959								
IHPK1	9807	1213	1308	1403								
MELK	9833	960	961	103349								
KIAA0626	9848	1180	1275	1370								
TLK1	9874	**884**	885	886	**884**	242415	242416					
ARK5	9891	964	103350	103843								
MRC2	9902	749	750	751								
XYLB	9942	103329	103413	103495								
OSR1	9943	625	626	627								
AKT3	10000	695	697	110901								
GNE	10020	698	699	700								
SGK2	10110	**1485**	**1579**	**1669**	**1485**	**1579**	**1669**	242482	242483	**1485**	**1579**	1669

Gene Information		Pass 1			Pass 2					Pass 3		
Gene Name	**LocusLink ID**	**siRNA-1**	**siRNA-2**	**siRNA-3**	**siRNA1**	**siRNA2**	**siRNA3**	**siRNA4**	**siRNA5**	**siRNA1**	**siRNA2**	**siRNA3**
HIPK3	10114	713	714	715								
AKAP9	10142	138647	138648	138649								
TRIM28	10155	716	717	718								
ACK1	10188	721	103335	103419								
NME6	10201	722	723	724								
TRIB1	10221	103365	103449	103529								
CNKSR1	10256	122592	122593	122594								
AKAP8	10270	135514	135515	135516								
APEG1	10290	42121	42210	42274								
BCKDK	10295	729	730	110905								
PAK4	10298	731	732	733								
TESK2	10420	852	**853** 🟥	110925	853	242408 🟩						
MAP3K7IP1	10454	17476	17569	135631								
MERTK	10461	809	810	811								
STK25	10494	812	813	814								
CIB2	10518	135730	135731	135732								
AKAP3	10566	135788	135789	135790								
ERN2	10595	1201	1296	1391								
LIM	10611	126673	**126674** 🟩	126675	126674 🟩	242404 🟥	242405					
CAMKK2	10645	815	816	110919								
PMVK	10654	818	819	820								
PLK4	10733	103348	**103432** 🟥	103512	103432 🟥	242423	242424					
MAP3K2	10746	824	825	103340								
PLK2	10769	827	828	829								
NEK6	10783	939	940	941								
FASTK	10922	44224	44317	44407								
ASK	10926	126686	126687	126688								
TLK2	11011	103342	103426	103507								
RIPK3	11035	836	837	110923								
PIM2	11040	839	840	**841** 🟥	841	242406	242407					
CIT	11113	103721	103729	103737								
TRAD	11139	845	846	847								
PKIG	11142	19143	19235	136230								
MAP4K5	11183	822	103603	103656								
MAP4K1	11184	854	855	856								
CHEK2	11200	1477	118278	118298								
IRAK3	11213	857	858	859								
AKAP11	11215	136937	136938	136939								
AKAP10	11216	136307	136308	136309								

Gene Information			Pass 1			Pass 2					Pass 3		
Gene Name	LocusLink ID	siRNA-1	siRNA-2	siRNA-3	siRNA1	siRNA2	siRNA3	siRNA4	siRNA5	siRNA1	siRNA2	siRNA3
AKAP2	11217	202406	202407	202408								
PACSIN2	11252	136338	136339	136340								
PNKP	11284	860	861	103345								
STK38	11329	863	864	865								
PTK9L	11344	868	118279	118281								
Ksr	16706	71029	71124	71216								
AAK1	22848	103351	103435	103515								
LMTK2	22853	969	970	971								
ICK	22858	972	974	103352								
SEPHS2	22928	881	882	883								
SEPHS1	22929	878	879	880								
STK38L	23012	1481	1575	1665								
MAST3	23031	202506	202507	202508								
KIAA0551	23043	202509	202510	202511								
SMG1	23049	44241	44334	44424								
CDK11	23097	**103723**	**103731**	**103739**	103723	103731	103739	214337				
MAP3K7IP2	23118	136739	136740	136741								
MAST2	23139	975	977	103353								
MAPK8IP3	23162	136770	136771	136772								
PASK	23178	978	103354	110953								
SIK2	23235	122759	122760	122761								
KIAA0999	23387	1591	1681	103611								
PIP5K1C	23396	136520	136521	136522								
BRD4	23476	1512	1605	1694								
P101-PI3K	23533	140138	140139	140140								
MAPK8IP2	23542	19889	19983	20076								
OSRF	23548	126713	126714	126715								
CCRK	23552	875	876	111072								
DAPK2	23604	930	932	110948								
PRKCBP1	23613	135457	135458	135459								
STK22B	23617	46442	103793	103798								
SGKL	23678	1479	1573	1663								
PRKCN	23683	727	103336	103420								
CARKL	23729	902	903	904								
PRKD2	25865	1011	1013	111257								
DKFZP586B1621	26007	981	982	983								
FBXW3	26226	213333	213334	213335								
AK5	26289	872	873	874								
HSPB8	26353	933	934	935								

Gene Information		Pass 1			Pass 2					Pass 3		
Gene Name	LocusLink ID	siRNA-1	siRNA-2	siRNA-3	siRNA1	siRNA2	siRNA3	siRNA4	siRNA5	siRNA1	siRNA2	siRNA3
LATS2	26524	948	949	950								
STK23	26576	936	937	**938**	938	242425	242426					
RPS6KC1	26750	890	891	892								
AKAP8L	26993	21328	21422	147522								
TPK1	27010	1184	1279	1374								
HRI	27102	942	943	944								
STK36	27148	1482	1576	1666								
RPS6KA6	27330	945	946	947								
STK39	27347	896	897	898								
TRIB2	28951	1061	103364	103448								
HIPK2	28996	1375	116346	116347								
TBK1	29110	899	900	901								
PACSIN3	29763	24054	24241	134898								
EEF2K	29904	905	906	907								
NME7	29922	908	45196	45290								
PKN3	29941	909	910	911								
NRBP	29959	913	914	103605								
PACSIN1	29993	1496	1589	1679								
SH3KBP1	30011	135342	135343	135344								
HUNK	30811	951	952	953								
PIK3R4	30849	1480	1574	103606								
MINK	50488	985	986	103382								
AK3L1	50808	1002	1004	103356								
TNNI3K	51086	987	**988**	989	**988**	**242432**	242433			**988**	242432	
IRAK4	51135	993	994	995								
VRK3	51231	1008	1009	1010								
CRIM1	51232	135025	135026	135027								
CDKL3	51265	**1154**	1249	1344	1154	242438	242439					
JIK	51347	999	1000	1001								
PRKAG2	51422	134877	**134878**	134879	**134878**	242434	242435					
IHPK2	51447	134946	134947	134948								
NIPA	51530	126921	126922	126923								
TRIM33	51592	103355	103439	103519								
NLK	51701	996	997	998								
UMP-CMPK	51727	1005	1006	1007								
CRK7	51755	1153	**1248**	1343	**1248**	242436	242437					
MST4	51765	1155	1250	1345								
ZAK	51776	1016	103358	110959								
PANK1	53354	1614	1704	103380								

Gene Information		Pass 1			Pass 2					Pass 3		
Gene Name	LocusLink ID	siRNA-1	siRNA-2	siRNA-3	siRNA1	siRNA2	siRNA3	siRNA4	siRNA5	siRNA1	siRNA2	siRNA3
PRKAG3	53632	24967	25060	131929								
MYO3A	53904	1486	1580	1670								
CSNK1G1	53944	1062	1064	110992								
RIPK4	54101	1177	1272	113613								
TRPM7	54822	1490	103360	103444								
SNRK	54861	1159	1349	103607								
PXK	54899	1585	1675	110964								
UCKL1	54963	1161	1256	1351								
FLJ20574	54986	1257	**103361**	**103445**	103361	103445						
AKIP	54998	25730	45342	123005								
P15RS	55197	1164	1259	1354								
ETNK2	55224	1165	1260	1355								
PANK4	55229	132362	132363	132364								
PI4K2B	55300	1167	1262	1357								
RFK	55312	1168	1358	110971								
STK32B	55351	1023	1024	1025								
STYK1	55359	1169	1264	**1359**	1359	242448	242449					
PI4KII	55361	1170	1265	1360								
ALS2CR2	55437	1171	1266	1361								
CaMKIINalpha	55450	123137	202303	202322								
ETNK1	55500	1172	1267	103362								
NAGK	55577	1156	1251	1346								
BMP2K	55589	1489	1583	**111088**	111088	242488	242489					
FLJ10074	55681	110966	110968	110969								
FLJ10842	55750	**1166**	1261	1356	1166	242444	242445					
RIOK2	55781	1022	110975	110977								
TOPK	55872	1026	1027	1028								
TEX14	56155	1086	1087	1088								
STK31	56164	1594	1684	103369								
SPHK2	56848	1587	1677	103792								
PAK6	56924	1029	1030	1031								
CDC42SE2	56990	42453	42532	127235								
CABC1	56997	1032	1033	110979								
CAMK1D	57118	1035	1036	1037								
ADCK1	57143	1176	1271	103609								
PAK7	57144	42902	42997	43083								
PACE-1	57147	103780	103782	111074								
CAMK1G	57172	103363	103447	103527								

Gene Information		Pass 1			Pass 2					Pass 3		
Gene Name	LocusLink ID	siRNA-1	siRNA-2	siRNA-3	siRNA1	siRNA2	siRNA3	siRNA4	siRNA5	siRNA1	siRNA2	siRNA3
CLK4	57396	**1048**	**1049**	**110988**	1048	1049	110988	212808				
SCYL1	57410	1050	1051	1052								
MIDORI	57538	1495	1588	1678								
KIAA1446	57596	140672	140673	140674								
TRIB3	57761	1056	1057	1058								
MARK4	57787	1089	1090	111028								
LY6G5B	58496	42389	42474	42549								
TSKS	60385	125326	125327	125328								
RBKS	64080	1182	1277	1372								
FN3K	64122	1183	1278	1373								
NJMU-R1	64149	140704	140705	**140706**	**140706**	**242458**	242459			140706	242458	
C9orf12	64768	**1186**	**1281**	1376	**1186**	**1281**	**242460**	242461		1186	1281	242460
CERK	64781	110997	111000	111002								
FLJ12476	64799	1188	1283	1378								
PINK1	65018	1199	1294	103372								
ALS2CR7	65061	1140	1141	1142								
PRKWNK1	65125	1174	**1269**	1364	**1269**	**242450**	242451			1269	242450	
FLJ13052	65220	1189	1284	1379								
PRKWNK4	65266	1104	1105	1106								
PRKWNK3	65267	103724	103732	103740								
PRKWNK2	65268	130209	130210	130211								
STK33	65975	1683	103367	103451								
MGC8407	79012	1065	1066	1067								
MAPKAP1	79109	130548	130549	130550								
PANK3	79646	130622	130623	130624								
FN3KRP	79672	1190	1285	1380								
LRRK1	79705	1497	1590	1680								
PIP5K2C	79837	1191	1286	1381								
NEK11	79858	1192	1287	1382								
ADCK4	79934	1068	1069	1070								
PANK2	80025	131832	131833	131834								
FLJ23074	80122	1071	1072	1073								
LAK	80216	1075	1076	103610								
ITPKC	80271	1193	1288	1383								
GKAP1	80318	1384	127538	127539								
T3JAM	80342	123566	123567	123568								
COASY	80347	1195	1290	111026								
CDADC1	81602	1196	1291	103612								
STK22C	81629	1122	1123	1124								

Gene Information		Pass 1			Pass 2					Pass 3		
Gene Name	LocusLink ID	siRNA-1	siRNA-2	siRNA-3	siRNA1	siRNA2	siRNA3	siRNA4	siRNA5	siRNA1	siRNA2	siRNA3
SNARK	81788	1083	**1084**	103368	1084	242464	242465					
UCK1	83549	103370	103454	103534								
RPS6KL1	83694	1198	1293	1388								
RIOK1	83732	44297	44389	44477								
GSG2	83903	1093	1094	**103371**	103371	242466	242467					
MGC4796	83931	103725	103733	103741								
STK22D	83942	1097	111259	118249								
SSTK	83983	42598	42691	42768								
FLJ23356	84197	1098	1099	1100								
CAMKK1	84254	103383	103466	103544								
KIAA1811	84446	1502	1595	1685								
KIAA1804	84451	1503	103373	103457								
MASTL	84930	1108	1109	111039								
MYLK2	85366	103375	**103459**	103539	103459	242468	242469					
KIAA1765	85443	202523	202524	202525								
PSKH2	85481	1119	1120	1121								
NYD-SP25	89882	1508	1601	1691								
ADCK2	90956	1125	103614	103666								
NEK9	91754	1113	1114	1115								
LOC91807	91807	**103772**	103775	**103778**	103772	103778						
LYK5	92335	42950	43040	43116								
MGC16169	93627	1110	1111	103374								
PRKCDBP	112464	45706	129307	129308								
TP53RK	112858	1202	1297	1392								
STK11IP	114790	128863	128864	128865								
HAK	115701	1128	**1130**	111041	**1130**	242470	242471					
IHPK3	117283	1203	1298	1393								
CIB3	117286	147982	147983	147984								
PIK3AP1	118788	129419	129420	129421								
CSNK1A1L	122011	1520	1611	1700								
AK7	122481	129427	129428	129429								
FLJ25006	124923	1207	1397	103615								
KIS	127933	1208	1303	**1398**	1398	242484	242485					
ACVR1C	130399	1521	1612	1701								
GRK7	131890	**1206**	**1301**	**1396**	1206	1301	1396					
ASB10	136371	**1513**	45582	45672	**1513**	242476	242477					
PIP5KL1	138429	40615	40705	46550								
TAF1L	138474	40303	40394	40482								

Gene Information		Pass 1			Pass 2					Pass 3		
Gene Name	LocusLink ID	siRNA-1	siRNA-2	siRNA-3	siRNA1	siRNA2	siRNA3	siRNA4	siRNA5	siRNA1	siRNA2	siRNA3
PNCK	139728	124469	202319	202347								
MYO3B	140469	1137	1138	1139								
NEK7	140609	45587	45677	103794								
TRPM6	140803	1158	1253	1348								
STK35	140901	**1135**	**103377**	**103461**	**1135**	**103377**	**103461**			1135	103377	103461
TTBK2	146057	40791	40887	40980								
HIPK4	147746	1143	1144	1145								
LOC149420	149420	1526	1616	**1706**	1706	242480	242481					
SNF1LK	150094	40587	40679	40762								
FLJ32685	152110	103550	103556	111053								
MAGI1	154043	129762	129763	129764								
C9orf98	158067	1525	1615	111057								
AKAP28	158798	**128414**	202311	202312	128414	242340	242341					
DGKH	160851	129947	129948	129949								
MGC45428	166614	39203	39298	39391								
MGC42105	167359	42951	43041	43117								
FUK	197258	111047	111049	111051								
FLJ34389	197259	42942	43032	43109								
ADCK5	203054	43144	103781	103783								
HIPK1	204851	39638	111081	111083								
MGC26597	206426	103381	103808	103811								
C6orf199	221264	1209	1304	1399								
ERK8	225689	1205	1300	1395								
IPMK	253430	38438	38524	148096								
ANKK1	255239	103771	103774	103777								
MAGI-3	260425	123257	123258	123259								
STK32C	282974	40863	45762	45854								
KSR2	283455	41069	41165	111068								
C14orf20	283629	41401	41491	41571								
LOC283846	283846	202497	202498	202499								
NEK8	284086	103726	103734	103742								
LOC375133	375133	202463	202630	202631								
LOC375449	375449	202348	202364	202379								

Supplementary Table 1 | siRNAs used throughout the RNAi screen to access the functional role of the corresponding target gene in *Plasmodium* infection.

List with all the siRNAs screened for each gene in the different phases of the RNAi screen. Highlighted in red and green are the siRNAs for which an increase or decrease in *Plasmodium* infection was observed, respectively.

Chapter 4 | Results

SR-BI is a crucially required host factor with a dual role in the establishment of malaria liver infection

Cristina D. Rodrigues[1,2*], Michael Hannus[3*], Miguel Prudêncio[1,2*], Cécilie Martin[3], Lígia A. Gonçalves[2], Silvia Portugal[1], Akin Akinc[4], Philipp Hadwiger[5], Kerstin Jahn-Hofmann[5], Ingo Röhl[5], Geert-Jan van Gemert[6], Jean-François Franetich[7], Adrian J.F. Luty[6], Robert Sauerwein[6], Dominique Mazier[7], Victor Koteliansky[4], Hans-Peter Vornlocher[5], Christophe J. Echeverri[3], Maria M. Mota[1,2]

[1]Unidade de Malária, Instituto de Medicina Molecular, Universidade de Lisboa, 1649-028 Lisboa, Portugal. [2]Instituto Gulbenkian de Ciência, 2780-156 Oeiras, Portugal. [3]Cenix BioScience GmbH, Tatzberg 47, Dresden 01307, Germany. [4]Alnylam Pharmaceuticals, 300 Third Street, Cambridge, MA02142, USA. [5]Alnylam Europe AG, Fritz-Hornschuch-Strasse 9, 95326 Kulmbach, Germany. [6]Department of Medical Microbiology, University Medical Centre, P.O. Box 9101, 6500 HB Nijmegen, The Netherlands. [7]Inserm U511, Université Pierre et Marie Curie-Paris, Centre Hospitalier Universitaire Pitié-Salpêtrière, Paris, France.

[*]These authors contributed equally to this work.

[#]Correspondence should be addressed to M.M.M. (mmota@fm.ul.pt).

An obligatory first step of malaria is the asymptomatic invasion of host hepatocytes by *Plasmodium* sporozoites, which develop therein to form thousands of erythrocyte-infective merozoites. While host factors required for liver infection offer powerful prophylactic potential, they remain poorly understood. Having found that modified forms of LDL can competitively inhibit the infection of human hepatoma cells by *P. berghei* sporozoites, we have used RNAi to screen host lipoprotein pathway genes, identifying the class B, type I scavenger receptor (SR-BI) as crucially required for infection. Compound- or antibody-inhibition of SR-BI function in cultured Huh7 cells similarly reduced *P. berghei* infection. Importantly, *in vivo* RNAi silencing of liver SR-BI expression in adult mice, and inhibition of SR-BI activity in human primary hepatocytes also reduced infection by *P. berghei* and *P. falciparum*, respectively, thus supporting the patho-physiological relevance of our findings. With detailed analyses further revealing the SR-BI requirement in both sporozoite invasion and development, our study offers important mechanistic insights into the processes underlying *Plasmodium* liver infection, while also opening a powerful new interventional strategy for the development of novel anti-malarial prophylactics.

Malaria, caused by the protozoan parasite *Plasmodium*, is a major health problem, mainly in Sub-Saharan Africa and in some parts of Asia and South America. Each year there are about 600 million new clinical cases and at least one million individuals, mostly children, die from malaria (Greenwood and Mutabingwa, 2002). Moreover, malaria presents a serious risk to the economic potential of many countries in the world. Various attempts at eradicating this disease have so far been unsuccessful and in fact within the last 10 to 15 years the burden of malaria has been increasing (Greenwood and Mutabingwa, 2002) mainly because of the emergence of *P. falciparum* variants that are resistant to the drugs in use (Marsh, 1998; White, 2004). These realities have compounded the urgency of finding novel treatment strategies that will be less vulnerable to the development of parasite resistance, a goal that necessarily requires a better understanding of the underlying parasite-host interactions.

After the bite of an infected mosquito delivers *Plasmodium* sporozoites into a human host, the parasite first accumulates in the liver where it migrates through the cytoplasm of several hepatocytes before invading the one in which it will develop into an exoerythrocytic form (EEF) (Mota *et al.*, 2001). During this asymptomatic liver infection the parasite proliferates and changes from a motile sporozoite into its next form, the merozoite, which will allow the symptomatic infection of red blood cells. In doing so, its exploitation of host liver resources represents an important and as-yet under-investigated vulnerability to prophylactic intervention. In our ongoing study of such host factors needed for the liver infection stage, we have herein followed-up on observations from earlier reports which suggested a link between host lipoprotein clearance pathways and *Plasmodium* sporozoite infection of the liver (Shakibaei and Frevert, 1996; Sinnis *et al.*, 1996).

Modified forms of LDL but not HDL inhibit *Plasmodium* infection of Huh7 cells

As an initial step, we examined whether different types of lipoprotein particles display differential effects on *Plasmodium* sporozoite infection of host liver cells. To test this, cultured human Huh7 hepatoma cells grown in medium containing lipoprotein-deficient serum (LPDS) were infected with isolated *Plasmodium berghei* sporozoites in the presence of defined amounts of human high density lipoprotein (HDL), low density lipoprotein (LDL), acetylated LDL (acLDL) or oxidized LDL (oxLDL). Throughout these and all subsequent infection experiments in the present study, *Plasmodium* sporozoites were used fresh on the same day after isolation from the salivary glands of infected female *Anopheles stephensi* mosquitoes. Infected cell

cultures were fixed 24 h after sporozoite addition, stained for nuclear DNA and immunolabeled for a *Plasmodium* EEF-specific antigen, as well as host cell actin. Infection rates were then quantified by fluorescence microscopy, using automated image analysis to count the number of stained EEFs that had developed inside the Huh7 cells, and normalizing these values to cell confluency, as determined by actin staining, to compensate for potential differences in total cell surface available for infection in each well. Both modified forms of LDL (modLDL) reproducibly reduced the infection levels ($P < 0.01$ and $P < 0.001$ for concentrations equal or higher than 100 µg/ml of oxLDL and acLDL, respectively), whereas LDL or HDL did not (Figure 1a). In fact, HDL at low concentrations showed a mildly positive effect on EEF number counted after 24h (Figure 1a; $P < 0.05$). As such, these initial results are indeed consistent with the earlier proposed link between *Plasmodium* infection and lipoprotein pathways in the liver (Shakibaei and Frevert, 1996; Sinnis *et al.*, 1996).

We therefore continued by analyzing the specific impact of this lipoprotein-mediated inhibition on two major steps of liver infection: invasion and development. Under the conditions of our 24 h *in vitro* infection assay, >95% of invasion events take place over the first 2 h following addition of sporozoites to the cells, consistent with the transient traversing of neighbouring cells prior to productive invasion events, which we reported previously (Mota *et al.*, 2001). The expected inhibition of infection was only observed when the added acLDL or oxLDL were present during the first 2 h after sporozoite addition to the cells, i.e. the invasion phase (Figure 1b, $P < 0.001$). When lipoproteins were only added after this phase, i.e. more than 2h after sporozoite addition, once >95% of invasion events have already occurred, no significant reduction in infection level was detected (Figure 1b). These results strongly suggest that elevated levels of modLDL reduce *Plasmodium* infection of hepatoma cells primarily by inhibiting the sporozoite invasion step.

Host scavenger receptor BI (SR-BI) is required for *P. berghei* infection of Huh7 cells

A possible explanation for the observed lipoprotein-mediated inhibition of invasion would be the competitive binding of lipoproteins and sporozoites to the same cell surface protein(s). We therefore sought to further analyze the role of lipoprotein pathway genes in the liver stage of *Plasmodium* infection by applying our *in vitro* assay in the context of a systematic RNAi-induced loss-of-function screen. To this end, we assembled a library of 206 siRNAs targeting 53 genes expressed in the liver and annotated as having validated or putative roles in lipoprotein assembly, binding or uptake (Supplementary Table 1). Each gene was targeted with at least 3 distinct

siRNA sequences, applying the experimental workflow outlined in Figure 2a. Briefly, each siRNA was transfected individually into Huh7 cells 24 h after seeding, and 48 h later, cells were either infected with *P. berghei* sporozoites, or lysed for quantitative RT-PCR (qRT-PCR) analysis of target mRNA knock-down levels at the onset of infection. Infected samples were subjected to the same microscopy-based assay procedure described above, including fixation 24 h post infection and subsequent staining for EEFs, host actin and nuclear DNA to yield the quantification of infection rates, also as described above.

This library of siRNAs was screened in two independent runs, generating phenotypic loss-of-function data for all tested siRNAs and conclusive qRT-PCR analysis of remaining target mRNA levels for 155 siRNAs targeting 40 genes (see detailed data in Supplementary Table 1). The vast majority of siRNAs did not significantly affect viability of the Huh7 host cells, as determined by number of cell nuclei (Figure 2b, Supplementary Table 1). Although several genes exhibited a single siRNA showing a notable up- or down-regulation of the infection rate, the lack of confirmation from other siRNAs targeting those genes rendered their significance unclear without further analysis. This is readily illustrated by plotting the mean results from all siRNAs for each targeted gene (Figure 2c). Only one gene, scavenger receptor BI (SR-BI), stood out from the rest by showing significant reductions in infection rates with 3 distinct siRNA sequences (Figure 2b, d, $P < 0.001$). This effect on infection occurred without any detectable side effects on cell proliferation, as measured by nuclear counts (Figure 2b, Supplementary Table 1). Importantly, the multiplicity of siRNA sequences underlying this result argues strongly that the observed phenotype is indeed a specific consequence of down-regulating SR-BI expression, and is not arising through off-target effects [see (Echeverri *et al.*, 2006)]. As further confirmation of specificity, the phenotypic severity (i.e. degree of inhibition of infection) was found to correlate closely with SR-BI knock-down, as quantified at the mRNA level by qRT-PCR (Figure 2d), using 4 distinct SR-BI-targeting siRNA sequences in multiple independent experiments. The SR-BI knock-down was also confirmed at the protein level by quantitative Western blotting (Figure 2e). Together, these results strongly implicate host SR-BI expression as a key requirement for *Plasmodium* infection of liver cells. It should be noted that the present data does not rule out the possible involvement of other genes among those tested here, as negative results in RNAi screens are generally inconclusive [see (Echeverri *et al.*, 2006)]. Indeed, the present analysis already suggests that two other genes, ApoA1BP and MSR1, which displayed more moderate effects, may also warrant further examination in the future (Figure 2d).

The above RNAi-based identification of SR-BI was further validated by testing the effects on infection of known SR-BI inhibitors, including a SR-BI blocking antibody (Silver, 2002) and several small synthetic molecules previously reported to inhibit the SR-BI-mediated selective uptake of lipids from HDL [termed "blockers of lipid transport", or BLTs (Nieland *et al.*, 2002)]. Addition of the SR-BI blocking antibody to cells 1 h prior to sporozoite addition led to a marked, dose-dependent decrease in infection rate as compared to control samples, measured by the *in vitro* microscopy-based Huh7 infection assay described above (Figure 3a). Similar dose dependent decreases in *P. berghei* sporozoite infection rates were observed when cells were similarly incubated with either BLT-1, BLT-2 or BLT-4 throughout the 24 h infection period, showing IC_{50} values of 0.9, 5.2 and 19.9 µM respectively (Figure 3b-d). Interestingly, the relative efficiencies with which the different BLT compounds inhibited sporozoite infection closely mirrored their previously reported effects on the selective uptake of lipids, with BLT-1 being 5 and 20 times more efficient than BLT-2 and BLT-4, respectively (Nieland *et al.*, 2002), thus suggesting a close structural link between the two activities. Infection rates were not affected by pre-incubation of *Plasmodium* sporozoites with BLT-1 for 1 hour prior to addition to cells, showing that BLT-1 has no effect on sporozoite viability (data not shown). Altogether, these results using RNAi, blocking antibodies and synthetic inhibitors clearly demonstrate a critical role for SR-BI during *P. berghei* sporozoite infection of Huh7 cells.

Patho-physiological relevance of host SR-BI is confirmed with *in vivo* mouse infection model and *P. falciparum* infection of primary human hepatocytes

As the above experiments were all performed *in vitro* using the human hepatoma cell line Huh7, we sought to validate the requirement for SR-BI in *Plasmodium* infection under more physiologically relevant conditions. To this end, we first confirmed that silencing or inhibition of SR-BI also leads to a reduction in *P. berghei* infection of primary mouse hepatocytes (Supplementary Figure 1).

Next, we also confirmed the relevance of these findings *in vivo*, using systemically-delivered, liposome-formulated siRNAs to silence SR-BI expression in adult mice and subjecting these to infection by *P. berghei* sporozoites. Here, a qRT-PCR-based assay was used to quantify infection rates by measuring levels of *Plasmodium* 18S RNA found within extracts of liver samples harvested 40 h after intravenous (i.v.) sporozoite injection. *In vivo* RNAi treatments have previously yielded potent gene-specific knock-downs in rodent livers using cholesterol-conjugated siRNAs (Soutschek *et al.*, 2004) or in non-human primates after systemic administration of siRNAs encapsulated in stable lipid-nanoparticles (Zimmermann *et al.*, 2006). In our

experiments, SR-BI expression was also reduced successfully in adult mouse livers using 3 distinct SR-BI-specific siRNAs, each of which yielded ~25-45% remaining SR-BI mRNA, as measured by qRT-PCR of tissue extracts taken 76 h after a single i.v. injection and normalization to SR-BI mRNA levels in the livers of adult mice treated with control siRNA (Figure 4a, $P < 0.001$, grey bars). When compared to control siRNA treatment, this administration of SR-BI specific siRNAs resulted in a significant reduction of liver infection by *P. berghei* sporozoites that correlated proportionally with the SR-BI mRNA silencing levels, yielding 30-50% of control infection loads, as measured by qRT-PCR of *P. berghei* 18S rRNA in samples taken 40h after sporozoite injection (Figure 4a, $P < 0.001$, black bars). In a parallel experiment, mice treated with one of the SR-BI siRNAs also showed a reduction in the number of parasites reaching the blood stream, when compared to their controls (Figure 4b, $P < 0.05$). While by day 4 after sporozoite injection, all mice in the control group were positive for blood stages, only 2 of 6 mice were positive in the group pre-treated with SR-BI siRNA.

Finally, we note that all of the above experiments were carried out using *P. berghei*, whose natural preference for rodent hosts entails the possibility that its infection strategy may differ in certain respects from that of *Plasmodium* species such as *P. falciparum*, known to be pathogenic to humans. The role of SR-BI was therefore also tested for *P. falciparum* infection in primary human hepatocytes 72 h after sporozoite addition, using the same qRT-PCR-based assay of *Plasmodium* 18S RNA used above. Once again, BLT-1 treatment of human primary hepatocytes caused a significant and specific decrease of *P. falciparum* infection in these cells (Figure 4c, $P < 0.001$).

Altogether, these data unequivocally confirm the requisite role of host SR-BI expression in the liver stage of *Plasmodium* infection not only *in vitro* but also *in vivo*, and not only for the rodent malaria parasite, *P. berghei*, but also for *P. falciparum*, the deadliest of human malarial pathogens.

Host cell SR-BI is required for both invasion and development of *Plasmodium* inside the parasitophorous vacuole

The responses observed with the different BLT compounds, in yielding such similar profiles for both their anti-malarial and anti-lipid uptake activities (Figure 3b-d) (Nieland *et al.*, 2002), suggest that the role of SR-BI in *Plasmodium* infection is closely related to its normal function in selective uptake of lipids from HDL particles. In fact, SR-BI has been described not only as a key component of HDL metabolism, but also as an efficient receptor for LDL, oxLDL and acLDL (Gillotte-Taylor *et al.*, 2001), all of which are apparently processed via separable extracellular subdomains (Gu *et al.*, 2000). This is of particular interest in view of our present observations that excess

amounts of oxLDL and acLDL, but not HDL or LDL, inhibit *Plasmodium* infection in Huh7 cells (Figure 1a and b). One direct interpretation of that data would be that during invasion, *Plasmodium* sporozoites are competing directly or indirectly with certain lipid particles for access to a common rate-limiting interaction site and/or biochemical activity, implying, therefore, that these could be on or from SR-BI. In order to probe this hypothesis, we conducted a more detailed phenotypic dissection of the effects of SR-BI inhibition on sporozoite infection in Huh7 cells, to determine whether this might be linked mechanistically to the observed lipoprotein-mediated inhibition.

To this end, we first determined whether SR-BI silencing or inhibition affects a crucial step of sporozoite infection, i.e. invasion (Figure 5a), as was observed for the lipoproteins tested (Figure 1b). In order to quantify invaded cells prior to EEF development most accurately, we used a FACS-based assay. Briefly, Huh7 cells were infected with GFP-expressing *P. berghei* sporozoites in the presence of rhodamine dextran. Two hours after sporozoite addition, cells were harvested and analyzed by FACS. Cells which had previously been transiently traversed by sporozoites were identified as rhodamine-dextran positive but GFP negative, while cells successfully invaded by sporozoites were identified by the presence of GFP and the absence of rhodamine-dextran (Mota *et al.*, 2001) (Supplementary Figure 2). Pre-treatments with three distinct SR-BI-targeting siRNAs, as characterized above, again yielded significant reductions in the proportion of Huh7 cells invaded by *P. berghei* sporozoites, as compared to controls (black bars in Figure 5a, $P < 0.001$). Similarly, treatment with BLT-1 also led to a dose-dependent decrease in invaded cells measured 2 h after sporozoite addition (grey bars in Figure 5a). These results reveal a critical role for SR-BI during the initial invasion step of sporozoite infection, mirroring that which we had observed with excess amounts of acLDL and oxLDL.

We next examined whether SR-BI also has a role in the following step of sporozoite infection, i.e. development of the EEF within the parasitophorous vacuole. Pre-treatments with SR-BI-specific siRNAs, or exposure to blocking antibody or small molecule inhibitors (BLTs) throughout the full 24h infection period of our *in vitro* microscopy assay all yielded marked decreases in EEF size, as measured using automated image analysis algorithms (Figure 5b, Supplementary Figure 3). The absence of larger EEF classes noted using this analysis in treated cells suggested a possible blockage of EEF development. Detailed FACS analysis of Huh7 cells infected with GFP-expressing *P. berghei* also suggested an effect of BLT-1 treatment on EEF development (Figure 5c). This analysis showed that, in addition to the marked decrease in number of infected cells already noted 2 h after sporozoite addition

(Figure 5a, grey bars), a significant decrease in GFP intensity becomes apparent within the infected cells at the 24 h time point (Figure 5c). These results are consistent with a defect in *P. berghei* development, resulting in decreased size and/or numbers of EEFs.

However, since invasion was also affected under the above assay conditions, we conducted more precise tests to address the development stage more unambiguously. We investigated whether BLT-1 retains its inhibitory effect on infection when added only after completion of sporozoite invasion, *i.e.*, 2 h after sporozoite addition to cells under our assay conditions. The resulting infected cells, when compared with negative controls 24 h after sporozoite addition using the same microscopy assay and analysis algorithms described above, still showed a clear and comparable downward shift in the size profile of EEFs (Figure 5d). This result was also confirmed by FACS analysis of equivalently-treated samples, which revealed a significant drop in GFP intensity among infected cells (data not shown), as had been seen with the full 24-h exposure to BLT-1 (Figure 5c). Together, these data indicate that host liver cell SR-BI function is required not only for sporozoite invasion but also for the subsequent development of EEFs within the parasitophorous vacuole.

Finally, in view of the above findings, we examined whether SR-BI's role in *Plasmodium* infection correlates with its being brought into close subcellular proximity with the parasite itself, as it develops within the parasitophorous vacuole. Using a polyclonal antibody directed against the extracellular domain of SR-BI, control uninfected Huh7 cells exhibited highly reproducible staining patterns defining a high density of discrete, fine granular or punctate structures suggestive of sub-micron-sized vesicles, distributed very homogenously throughout the cytoplasm (Figure 5e). In *Plasmodium*-infected cells, SR-BI staining revealed a marked accumulation of the same vesicle-like structures around the immediate periphery of 79.5 ± 6.3 % of intracellular EEFs (Figure 5e). This suggests that SR-BI may be residing within the parasitophorous vacuole membrane itself or accumulating in membranous compartments around EEFs, presumably catalyzing the lipid transfer between these compartments and the parasitophorous membrane. While more detailed, higher resolution analyses will be required to further elucidate this question, the present evidence of a clear subcellular accumulation of SR-BI around EEFs is consistent with all of our present findings that, besides its role in invasion, SR-BI also fulfills a requisite function in *Plasmodium* development inside liver cells.

Discussion

Together with our past studies, which revealed how *Plasmodium* sporozoites transiently traverse several hepatocytes before initiating a productive invasion event (Mota *et al.*, 2001), the present study adds significant new insights into the host molecules and cellular processes underlying this parasite's infection of the liver. In particular, our results confirm and extend earlier suggested links between liver infection and lipoprotein pathways (Shakibaei and Frevert, 1996; Sinnis *et al.*, 1996). By using several types of inhibitors including RNAi both *in vitro* in cultured human cells and *in vivo* in a mouse model of infection, we have identified a major lipoprotein receptor, SR-BI, as being crucial for both sporozoite invasion and EEF development.

Our data strongly suggest that the inhibition of parasite invasion that we observe with modified forms of LDL occurs via competition between the excess lipoproteins and the parasite for a common SR-BI binding site or activity. This observation supports the hypothesis that SR-BI may be fulfilling some or all functions of a liver receptor for *Plasmodium* sporozoites. Such a hypothesis would imply at least one of two activities: first a binding or docking activity, and second, an internalization activity. SR-BI has been characterized as an efficient receptor for HDL, as well as native and modified forms of LDL, including acLDL and oxLDL. Our results showing that only modified forms of LDL, but not HDL or LDL, inhibit sporozoite invasion, may yield at least two models of the molecular interactions underlying *Plasmodium* binding to hepatocytes: the "HDL-piggyback" model and the "modLDL-mimic" model. In the former, *Plasmodium* sporozoites interact directly with HDL particles and benefit from their high affinity binding to SR-BI. Interestingly, in this case, the sporozoite would not need to come into direct contact with any host cell components at all, as this direct interaction would be assured by the HDL particle on which it is "piggybacking", thereby explaining HDL's slight positive effect on invasion. Further posits of this model would be that the parasite cannot similarly "piggyback" on modified forms of LDL and that the latter's interaction mode with SR-BI must overlap sufficiently with that of the HDL-sporozoite complex so as to result in the observed competition effect between the two. In the "modLDL-mimic" model, the parasite does interact directly with SR-BI, using a mode of binding that overlaps with that of modLDL forms, but not with that normally used by HDL, therefore explaining the observed competition effects. The fact that SR-BI shows distinct and separable binding activities for different lipoprotein ligands (Gu *et al.*, 2000) is consistent with this notion.

Beyond these models for initial "docking", the next key step of *Plasmodium* invasion must necessarily be internalization of the bound parasite, leading to establishment of

the parasitophorous vacuole. Here, the best-characterized activity of SR-BI with respect to bound lipoproteins proves less supportive of a conventional receptor role. SR-BI is known to primarily mediate selective uptake of cholesteryl esters from bound HDL or LDL without triggering an endocytic or phagocytic event (Nieland *et al.*, 2005). While this main activity does not immediately suggest an obvious mechanism for facilitating internalization, some have nonetheless noted that HDL can enter HepG2 cells by endocytosis, followed by rapid recycling to the surface without reaching late endosomes or lysosomes (Wustner *et al.*, 2004). It is also interesting to note that the SR-BII isoform, which arises through alternative splicing from the *SR-BI* gene, undergoes endocytosis by a clathrin-dependent, caveolae-independent mechanism (Eckhardt *et al.*, 2006). Our finding that siRNA-mediated silencing of SR-BII expression by >70% has no detectable effect on *P. berghei* infection *in vitro* (Supplementary Table 1), argues against its involvement here, though not conclusively. As a further alternative, it has been suggested that *Plasmodium* sporozoites might enter the host cell in an active process from the parasite side without the need of the host endocytic or phagocytic machinery (Sibley, 2004), as previously demonstrated for the *Plasmodium* related parasite *Toxoplasma gondii* (Dobrowolski and Sibley, 1996). In this case, the so-called receptor activity needed by the parasite would only be restricted to the docking role, as the parasite itself would take care of the subsequent internalization. Further work is now under way to test these models.

In addition to the role of SR-BI in *Plasmodium* sporozoite invasion, our results also show that SR-BI is critical for EEF development. Inside hepatocytes, *Plasmodium* sporozoites undergo a major transformation, with each giving rise to thousands of merozoites. However, the sporozoite's requirements and the strategies it has developed to survive and to be successful remain poorly understood [reviewed in (Prudencio *et al.*, 2006)]. Regardless, the parasite's extensive proliferation during this stage necessarily requires the availability of sufficient lipids for the synthesis of large amounts of additional membranes. It is therefore tempting to speculate that our observations reflect a direct involvement of the host cell SR-BI's selective lipid uptake activity in "feeding" cholesteryl esters and other lipids to the parasite across the parasitophorous vacuole membrane. While all of our present data are consistent with this hypothesis, more detailed analyses will be required to further test its validity. It will be of particular interest in this context to further examine the functional contributions of other known SR-BI pathway components to *Plasmodium* infection in liver.

Finally, the present study establishes an important proof of principle for the use of non-essential host factors as novel prophylactic or therapeutic drug targets to combat malaria and other infectious diseases. So far, most anti-malarial drug development has focused on targeting the *Plasmodium* parasite itself. However, targeting host components offers major advantages including the inherently lower vulnerability of such drugs to the development of resistance by the parasite (Cunha-Rodrigues *et al.*, 2006), arguably the biggest problem faced in all infectious disease fields today. Indeed, one or two mutations within a parasite gene can render useless virtually any drug targeting its encoded protein. By contrast, the need for the parasite to significantly re-direct its entire infection strategy to compensate for a missing host factor is a much more difficult obstacle to overcome through natural selective variation. As a second key advantage, the host factor approach also offers significantly higher potential for accelerated drug discovery and development through synergies with ongoing output from other disease pipelines, including so-called "mainstream" ones. Host factors needed for parasitic infections are more likely to have been the focus of previous or even ongoing therapeutic development work in other fields, thus opening the possibility of finding anti-infective activities as second medical uses for existing drugs. This potential emerges particularly well in the present case of SR-BI, which has recently been proposed to function as a receptor for several pathogens, including hepatitis C virus (HCV) (Scarselli *et al.*, 2002; Cocquerel *et al.*, 2006), mycobacteria (Philips *et al.*, 2005) and bacteria (Vishnyakova *et al.*, 2006). Interestingly, it has been proposed that HCV requires functional cooperation between the host's SR-BI and tetraspanin CD81, the latter having also been implicated in *Plasmodium* sporozoite invasion (Silvie *et al.*, 2003; Silvie *et al.*, 2006; Silvie *et al.*, 2007). Thus, our present evidence, implicating for the first time host SR-BI in malaria infection, may in fact help to advance our understanding of several other important infectious diseases. By further exploring the parallels between these infection pathways, one can now hope for increasing synergies between all of these fields for years to come.

Methods

Cells and Parasites

Huh7 cells, a human hepatoma cell line, were cultured in RPMI (Gibco/Invitrogen) medium supplemented with 10% fetal calf serum (FCS, Gibco/Invitrogen), 1% non-essential amino acid (Gibco/Invitrogen), 1% penicillin/streptomycin (pen/strep, Gibco/Invitrogen), 1% glutamine (Gibco/Invitrogen) and 1% HEPES, pH 7 (Gibco/Invitrogen) and maintained at 37°C with 5% CO_2.

Mouse primary hepatocytes were isolated by perfusion of mouse liver lobules with liver perfusion medium (Gibco/Invitrogen) and purified using a 1.12 g/ml; 1.08 g/ml and 1.06 g/ml Percoll gradient. Cells were cultured in William´s E medium containing 4% FCS, 1% pen/strep, 50 mg/ml epidermal growth factor (EGF), 10 µg/ml transferrin, 1 µg/ml insulin and 3.5 µM hydrocortisone in 24 well plates coated with 0,2% Gelatine in PBS. Cells were maintained in culture at 37°C and 5% CO_2.

Human primary hepatocytes were isolated from the healthy parts of liver biopsies from patients undergoing a partial hepatectomy with informed consent provided, as previously described (Mazier *et al.*, 1985). Freshly isolated human primary hepatocytes were cultured in Williams Medium E supplemented with 10% FCS, 1% glutamine, 1% insuline/transferrine/selenium (Invitrogen), 10^{-7} M dexamethasone (Sigma), 1% sodium piruvate, 2% pen/strep in 48 well plates coated with rat tail collagen, type I. Cells were maintained in culture at 37ºC and 5% CO_2. Medium was supplemented with 2% DMSO after complete cell adherence (12-24h) and until 1 hour before infection.

Green fluorescent protein (GFP)-expressing *P. berghei* (parasite line 259cl2) sporozoites (Franke-Fayard *et al.*, 2004) or *P. falciparum* sporozoites (NF 54 strain) were obtained from dissection of infected female *Anopheles stephensi* mosquito salivary glands.

Cell treatment with lipoproteins

Human low density lipoprotein (LDL), oxidised LDL (oxLDL), acetylated LDL (acLDL) and high density lipoprotein (HDL) (Biomedical Technologies Inc., USA) solutions were prepared in medium containing 1% lipoprotein deficient serum (Sigma Aldrich, Germany). Huh7 cells were incubated with different concentrations of lipoproteins during the periods described in the text, measured relative to sporozoite addition (10^4 per well).

siRNA design, siRNA library and screening controls

All siRNAs were purchased from Ambion's *Silencer* genome wide library (Ambion/Applied Biosystems, Austin USA). The siRNA library screened included validated or putative lipoprotein receptors and genes involved in lipoprotein assembly. Each gene was targeted by at least 3 distinct siRNAs used individually in all cases. Negative control samples included untransfected cells, and cells transfected with a negative control siRNA not targeting any annotated genes in the human genome. A full list of gene names, siRNA ID numbers and sequences, and associated screening data are shown in Supplementary Table 1.

High-throughput siRNA screening of *Plasmodium* infection

Huh7 cells (4500 per well) were seeded in 100 µl complete RPMI medium in optical 96-well plates (Costar) and incubated at 37ºC in 5% CO_2. Twenty-four hours after seeding, cells were transfected with individual siRNAs in a final concentration of 100 nM per lipofection. Each siRNA was transfected in triplicate. Briefly, for each well, cell supernatant was replaced by 80 µl of serum-free culture medium without antibiotics. One µl of 10 µM siRNA diluted in 16 µl of Opti-MEM (Invitrogen.) was complexed with 0.4 µl Oligofectamine (Invitrogen) diluted with 2.6 µl Opti-MEM and added onto the cells following the manufacturer's protocol. Four hours after addition of the complex, 50 µl of fresh RPMI medium, supplemented with 30% FCS, 3% pen/strep, 3% non-essential amino acid, 3% glutamine and 3% HEPES were added to the cells. Two days after siRNA transfection, cells were infected with 10^4 *P. berghei* sporozoites/well. Twenty-four hours after infection, cells were fixed with 4% paraformaldehyde (PFA) in PBS and permeabilized with 0.2% saponin in PBS. Cell nuclei were stained with Hoechst-33342 (Molecular Probes/Invitrogen), filamentous actin was stained with Phalloidin AlexaFluor488 (Molecular Probes/Invitrogen), EEFs were detected using the mouse monoclonal antibody 2E6 (Tsuji *et al.*, 1994) and an AlexaFluor555 labeled goat anti-mouse secondary antibody (Molecular Probes/Invitrogen).

Automated image acquisition and analysis

Plates were acquired with a Discovery1 automated fluorescence microscope (Molecular Devices Corporation, CA, USA) using a 10x lens. In each well, cell nuclei, actin and EEFs were imaged in 9 fields covering a total area of 2.7 x 2.0 mm. Image data was analyzed using a custom MetaMorph (Molecular Devices Corporation, CA, USA) based algorithm extracting the following values for each imaged field: Cell

proliferation as measured by the number of nuclei per imaged field (Hoechst staining), cell confluency as measured by the percentage of the imaged field covered by actin staining and number of EEFs as number of compact, high contrast objects in a size range from 16 to 150 pixels. Within each field, the number of EEFs was normalized to the cell confluency. Normalized EEF numbers and number of nuclei were averaged between the 9 imaged fields within each well. Mean and standard deviations were calculated for each experimental triplicate. Final readouts included number of EEFs and number of nuclei, shown as a percentage of the plate mean. For size analysis of EEFs (Figure 5c and 5e, Supplementary Figure 3), EEF classes were classified as follows: class 1 (3 to 15 pixels), class 2 (16 to 28 pixels), class 3 (29 to 75 pixels) and class 4 (76 to 150 pixels).

Gene-specific expression and infection quantification by qRT-PCR

For gene-specific expression *in vitro*, total RNA was isolated from Huh7 cells 48 h post-transfection (Invitek Invisorb 96-well plate kit) and converted into cDNA (ABI's HighCapacity cDNA reagents) with random hexamers, following the manufacturer recommendations. qRT-PCR used the SybrGreen method with Quantace qPCR mastermix at 11 µl total reaction volume, containing 500 nM of the target-specific primers, and primers that were designed to specifically amplify a fragment of the selected genes. Real-time PCR reactions were performed on an ABI Prism 7900HT system. Relative amounts of remaining mRNA levels of RNAi targets were calculated against the level of RPL13A or 18S rRNA, as housekeeping genes. Remaining mRNA levels of RNAi-treated samples were compared with those of samples transfected with Negative unspecific siRNA. *RPL13A*-specific primer sequences were: 5'-CCT GGA GGA GAA GAG GAA AGA GA-3' and 5'-TTG AGG ACC TCT GTG TAT TTG TCA A-3'. *18S* rRNA-specific primer sequences were: 5'-CGG CTT AAT TTG ACT CAA CAC G-3' and 5'-TTA GCA TGC CAG AGT CTC GTT C-3'.

For infection determination *in vivo* or *ex vivo*, total RNA was isolated from livers or primary hepatocytes using Qiagen's RNeasy Mini or Micro kits, respectively, following the manufacturer's instructions. The determination of liver parasite load *in vivo*, was performed according to the method developed for *P. yoelii* infections (Bruna-Romero *et al.*, 2001). Livers were collected and homogenized in denaturing solution (4 M guanidine thiocyanate; 25 mM sodium citrate pH 7, 0.5 % sarcosyl and 0.7 % β-Mercaptoethanol in DEPC-treated water), 40 h after sporozoite injection. Total RNA was extracted using Qiagen's RNeasy Mini kit, following the manufacturer's instructions. RNA for infection measurements was converted into cDNA using

Roche's Transcriptor First Strand cDNA Synthesis kit, according to the manufacturer's protocol. The qRT-PCR reactions used Applied Biosystems' Power SYBR Green PCR Master Mix and were performed according to the maunufacturer's instructions on an ABI Prism 7000 system (Applied Biosystems). Amplification reactions were carried out in a total reaction volume of 25 µl, containing 0,8 pmoles/µl or 0,16 pmoles/µl of the *Plasmodium-* or housekeeping gene-specific primers, respectively. Relative amounts of *Plasmodium* mRNA were calculated against the Hypoxanthine Guanine Phosphoribosyltransferase (*HPRT*) housekeeping gene. *18S* Pb*A-* and mouse *HPRT*-specific primer sequences were 5'- AAG CAT TAA ATA AAG CGA ATA CAT CCT TAC – 3' and 5' - GGA GAT TGG TTT TGA CGT TTA TGT G – 3'and 5' – GTA ATG ATC GTC GTC AAC GGG GGA – 3´ and 5' – CCA GCA AGC TTG CAA CCT TAA CCA – 3', respectively. *18S* Pf- and human *HPRT*-specific primer sequences were 5'- CTG GTT TGG GAA AAC CAA AT – 3' and 5' – CTC AAT CAT GAC TAC CCG TCT G – 3'and 5' – TGC TCG AGA TGT GAT GAA GG – 3´ and 5' – TCC CCT GTT GAC TGG TCA TT – 3'. For SR-BI mRNA level determination by qRT-PCT, *SR-BI*-specific primers were used, namely for mouse *SR-BI,* 5' – AAG CTG TTC TTG GTC TGA ACC C – 3' and 5' –ACT ACT GGC TCG ATC TTC CCT G – 3' and human *SR-BI,* 5´- AGA ATA AGC CCA TGA CCC TGA A - 3' and 5´- TGA GCT CAG CAA ATA ATC CGA A – 3´, respectively.

Quantification of host SR-BI protein expression using Western blot

Huh7 cells were seeded and transfected in optical 96-well plates as described above. After an additional 48 h of incubation at 37°C in 5% CO_2, cells were harvested in RIPA buffer (150 mM NaCl; 20 mM Tris, pH 8.0; 2% Triton X100, 0.5% deoxycholic acid and 0.1% SDS) containing 50 U/ml Benzonase (Merck, Germany) and complete EDTA-free protease inhibitor cocktail (Roche, Germany). The cell lysate was incubated for 20 min on ice. After centrifugation, reducing buffer (NuPAGE LDS Sample Buffer and NuPAGE Sample Reducing Agent, Invitrogen) was added to the supernatant. Proteins were resolved on a NuPAGE 4-12% Bis-Tris gel (Invitrogen) and transferred on a semi-dry transfer cell (Bio-Rad, Germany) to a nitrocellulose blotting membrane (Invitrogen) at 100 mA per blot for 2 hours. The membrane was blocked for one hour at room temperature (RT) in PBS containing 0.05% Tween 20 and 3 % nonfat dried milk and incubated subsequently over night at 4°C with the primary antibody (rabbit anti-SR-BI or mouse anti-GAPDH, Acris Antibodies GmbH, Germany). Then, the membrane was incubated for 1 h at RT with horseradish peroxidase-conjugated secondary antibodies (Goat anti-rabbit or Donkey anti-mouse, Dianova, Germany and

Jackson ImmunoResearch, UK, respectively). The secondary antibody was detected by chemiluminescence with the ECL Western Blotting Analysis System, according to the manufacturer's instructions (Amersham Bioscience, Germany) using the LAS-3000 Luminescent Image Analyzer (Fujifilm). Protein quantification was performed with the program AIDA Image Analyzer (Raytest, USA).

SR-BI blockage with anti-SR-BI antibody

Freshly-prepared serial dilutions of anti-SR-BI antibody (NB 400-134 from Novus Biologicals, USA) were added to Huh7 cells 1 h before sporozoite addition. Infection level and EEF size were determined 24 after sporozoite addition (10^4 per well). As control, a dilution of 0.02% Na azide, matching that present in the most concentrated antibody preparation was used. Huh7 cells were incubated with anti-SR-BI antibody during the periods described in the text, measured relative to sporozoite addition.

Effect of BLTs on infection of Huh7 cells

Stock solutions at 50 mM of BLT-1, BLT-2 and BLT-4 (ChemBridge Corporation, San Diego, USA) were prepared in DMSO. One hour prior to sporozoite addition ($1-3 \times 10^4$ per well, depending on the experiment). Huh7 cells were incubated with serial dilutions of each compound in complete medium, all of which contained DMSO in a final concentration of 0.1%. Negative controls were treated with 0.1% DMSO in complete medium. Infection level and EEF size were determined 24 h after sporozoite addition. Huh7 cells were incubated with BLT-1 during the periods described in the text, measured relative to sporozoite addition.

SR-BI silencing in mouse primary hepatocytes

Mouse primary hepatocytes (10×10^4 per well) were seeded in 700 µl complete Williams E medium in 24-well plates and incubated at 37°C in 5% CO_2. Forty-eight hours after seeding, cells were transfected with individual SR-BI siRNAs. As control a negative siRNA was used. Each siRNA was transfected in triplicate. Briefly, the culture medium was replaced by 200 µl of serum-free culture medium without antibiotics. Four µl of 10 µM siRNA diluted in 37,5 µl Opti-MEM (Invitrogen.) were complexed with 1 µl Oligofectamine (Invitrogen) diluted with 6,5 µl Opti-MEM and added to the cells following the manufacturer's recommended protocol. Four hours after addition of the complex, 125 µl of fresh Williams E medium, supplemented with 12 % FCS and 3% pen/strep, were added to the cells. Two days later, cells were infected with 5×10^4 *P. berghei* sporozoites per well. Forty-eight hours after infection,

cells were collected in 150 µl of RLT buffer (Qiagen) containing 0.1% β-mercaptoethanol for RNA extraction and infection measurement by qRT-PCR.

Effect of BLT-1 on infection of mouse and human primary hepatocytes

Mouse primary hepatocytes (10×10^4 per well) were incubated with 10 µM BLT-1 one hour prior to infection with 5×10^4 freshly extracted *P. berghei* sporozoites. Forty-eight hours after infection, cells were collected in 150 µl of RLT buffer (Qiagen) containing 0.1% β-mercaptoethanol for RNA extraction and infection measurement by qRT-PCR. Human primary hepatocytes (10×10^4 cells per well) were incubated with 10 µM BLT-1 one hour prior to infection with 10×10^4 freshly extracted *P. falciparum* sporozoites. Three days after infection, cells were collected in 150 µl of RLT buffer (Qiagen) containing 0.1% β-mercaptoethanol for RNA extraction and infection measurement by qRT-PCR.

Fluorescence Activated Cell Sorting (FACS) analysis

FACS analysis at 2 and 24 h after sporozoite addition was performed to determine the percentage of parasite-containing cells. For infection level measurement at 2 h, 2 mg/ml Dextran tetramethylrhodamine 10000 MW, lysine fixable (fluoro-ruby) (Molecular Probes/ Invitrogen) were added to the cells immediately prior to sporozoite addition. Cell samples for FACS analysis were washed with 1 ml PBS, incubated with 150 µl trypsin for 5 min at 37ºC and collected in 400 µl 10% FCS in PBS at the selected time-points post-sporozoite addition. Cells were then centrifuged at 0.1 *g* for 3 min at 4 ºC and ressuspended in 150 µl 2% FCS in PBS. Cells were analysed on a Becton Dickinson FACScalibur with the appropriate settings for the fluorophores used. Data acquisition and analysis were carried out using the CELLQuest (version 3.2.1fl1, Becton Dickinson) and FlowJo (version 6.3.4, FlowJo) software packages, respectively.

Host SR-BI staining

Huh-7 cells were seeded on coverslips in a 24-well plate (4×10^4 cells per well) and incubated at 37ºC in 5% CO_2 for 48 h. The medium was then replaced by fresh complete medium and incubated at 37ºC in 5% CO_2 for 24h. Three days after seeding, cells were infected with 5×10^4 *P. berghei* sporozoites/well. Twenty-four hours after infection, cells were fixed with 4% PFA in PBS and permeabilized with 0.01% saponin in PBS. Cell nuclei were stained with Hoechst-33342 (Molecular Probes/Invitrogen), EEFs were detected using the mouse monoclonal antibody 2E6 (Tsuji *et al.*, 1994) and

an AlexaFluor 488-labeled goat anti-mouse secondary antibody (Molecular Probes/Invitrogen). Host SR-BI was stained using the rabbit polyclonal antibody anti-SR-BI (GTX30467 from GeneTex) and an AlexaFluor 555-labeled donkey anti-rabbit secondary antibody (Molecular Probes/Invitrogen). Stained cells were imaged with an Olympus fluorescence microscope (BX61) using an oil immersion 100× lens. A total of 252 EEFs were randomly imaged from three independent coverslips using identical acquisition settings and classified by the presence and intensity of SR-BI staining in their vicinity.

In vivo RNAi

C57Bl/6 mice (male, 6-8 weeks) were treated with a single intravenous (i.v.) administration of 5 mg/kg of siRNA formulated in liposomal nanoparticles (Alnylam, Germany). Three different modified siRNAs targeting SR-BI were used. A modified siRNA targeting luciferase was used as control. Thirty-six h after siRNA administration mice were infected by i.v. injection of 2×10^4 *P. berghei* sporozoites. Remaining SR-BI mRNA levels and parasite load in the livers of infected mice were determined by qRT-PCR 40 h after sporozoite injection, 76 h after siRNA administration. Infection of mice treated with one SR-BI siRNA was allowed to proceed onto the blood stage and parasitemia (% of infected red blood cells) was measured daily.

Statistical analysis

For samples in which n > 5, statistical analysis were performed using unpaired Student *t* or ANOVA parametric tests. Normal distributions were confirmed using the Kolmogorov-Smirnov test. For samples in which n < 5, statistical analysis were performed using Kruskall-Wallis or Wilcoxon non-parametric tests. $P < 0.05$ was considered significant, $P < 0.001$ was considered highly significant.

Acknowledgments

References

Bruna-Romero, O., Hafalla, J.C., Gonzalez-Aseguinolaza, G., Sano, G., Tsuji, M., and Zavala, F. (2001). Detection of malaria liver-stages in mice infected through the bite of a single Anopheles mosquito using a highly sensitive real-time PCR. Int J Parasitol *31*, 1499-1502.

Cocquerel, L., Voisset, C., and Dubuisson, J. (2006). Hepatitis C virus entry: potential receptors and their biological functions. J Gen Virol *87*, 1075-1084.

Cunha-Rodrigues, M., Prudencio, M., Mota, M.M., and Haas, W. (2006). Antimalarial drugs - host targets (re)visited. Biotechnol J *1*, 321-332.

Dobrowolski, J.M., and Sibley, L.D. (1996). Toxoplasma invasion of mammalian cells is powered by the actin cytoskeleton of the parasite. Cell *84*, 933-939.

Echeverri, C.J., Beachy, P.A., Baum, B., Boutros, M., Buchholz, F., Chanda, S.K., Downward, J., Ellenberg, J., Fraser, A.G., Hacohen, N., Hahn, W.C., Jackson, A.L., Kiger, A., Linsley, P.S., Lum, L., Ma, Y., Mathey-Prevot, B., Root, D.E., Sabatini, D.M., Taipale, J., Perrimon, N., and Bernards, R. (2006). Minimizing the risk of reporting false positives in large-scale RNAi screens. Nat Methods *3*, 777-779.

Eckhardt, E.R., Cai, L., Shetty, S., Zhao, Z., Szanto, A., Webb, N.R., and Van der Westhuyzen, D.R. (2006). High density lipoprotein endocytosis by scavenger receptor SR-BII is clathrin-dependent and requires a carboxyl-terminal dileucine motif. J Biol Chem *281*, 4348-4353.

Franke-Fayard, B., Trueman, H., Ramesar, J., Mendoza, J., van der Keur, M., van der Linden, R., Sinden, R.E., Waters, A.P., and Janse, C.J. (2004). A Plasmodium berghei reference line that constitutively expresses GFP at a high level throughout the complete life cycle. Mol Biochem Parasitol *137*, 23-33.

Gillotte-Taylor, K., Boullier, A., Witztum, J.L., Steinberg, D., and Quehenberger, O. (2001). Scavenger receptor class B type I as a receptor for oxidized low density lipoprotein. J Lipid Res *42*, 1474-1482.

Greenwood, B., and Mutabingwa, T. (2002). Malaria in 2002. Nature *415*, 670-672.

Gu, X., Lawrence, R., and Krieger, M. (2000). Dissociation of the high density lipoprotein and low density lipoprotein binding activities of murine scavenger receptor class B type I (mSR-BI) using retrovirus library-based activity dissection. J Biol Chem *275*, 9120-9130.

Marsh, K. (1998). Malaria disaster in Africa. Lancet *352*, 924.

Mazier, D., Beaudoin, R.L., Mellouk, S., Druilhe, P., Texier, B., Trosper, J., Miltgen, F., Landau, I., Paul, C., Brandicourt, O., and et al. (1985). Complete development of hepatic stages of Plasmodium falciparum in vitro. Science *227*, 440-442.

Mota, M.M., Pradel, G., Vanderberg, J.P., Hafalla, J.C., Frevert, U., Nussenzweig, R.S., Nussenzweig, V., and Rodriguez, A. (2001). Migration of Plasmodium sporozoites through cells before infection. Science *291*, 141-144.

Nieland, T.J., Ehrlich, M., Krieger, M., and Kirchhausen, T. (2005). Endocytosis is not required for the selective lipid uptake mediated by murine SR-BI. Biochim Biophys Acta *1734*, 44-51.

Nieland, T.J., Penman, M., Dori, L., Krieger, M., and Kirchhausen, T. (2002). Discovery of chemical inhibitors of the selective transfer of lipids mediated by the HDL receptor SR-BI. Proc Natl Acad Sci U S A *99*, 15422-15427.

Philips, J.A., Rubin, E.J., and Perrimon, N. (2005). Drosophila RNAi screen reveals CD36 family member required for mycobacterial infection. Science *309*, 1251-1253.

Prudencio, M., Rodriguez, A., and Mota, M.M. (2006). The silent path to thousands of merozoites: the Plasmodium liver stage. Nat Rev Microbiol *4*, 849-856.

Scarselli, E., Ansuini, H., Cerino, R., Roccasecca, R.M., Acali, S., Filocamo, G., Traboni, C., Nicosia, A., Cortese, R., and Vitelli, A. (2002). The human scavenger receptor class B type I is a novel candidate receptor for the hepatitis C virus. Embo J *21*, 5017-5025.

Shakibaei, M., and Frevert, U. (1996). Dual interaction of the malaria circumsporozoite protein with the low density lipoprotein receptor-related protein (LRP) and heparan sulfate proteoglycans. J Exp Med *184*, 1699-1711.

Sibley, L.D. (2004). Intracellular parasite invasion strategies. Science *304*, 248-253.

Silver, D.L. (2002). A carboxyl-terminal PDZ-interacting domain of scavenger receptor B, type I is essential for cell surface expression in liver. J Biol Chem *277*, 34042-34047.

Silvie, O., Franetich, J.F., Boucheix, C., Rubinstein, E., and Mazier, D. (2007). Alternative invasion pathways for Plasmodium berghei sporozoites. Int J Parasitol *37*, 173-182.

Silvie, O., Greco, C., Franetich, J.F., Dubart-Kupperschmitt, A., Hannoun, L., van Gemert, G.J., Sauerwein, R.W., Levy, S., Boucheix, C., Rubinstein, E., and Mazier, D. (2006). Expression of human CD81 differently affects host cell susceptibility to malaria sporozoites depending on the Plasmodium species. Cell Microbiol *8*, 1134-1146.

Silvie, O., Rubinstein, E., Franetich, J.F., Prenant, M., Belnoue, E., Renia, L., Hannoun, L., Eling, W., Levy, S., Boucheix, C., and Mazier, D. (2003). Hepatocyte CD81 is required for Plasmodium falciparum and Plasmodium yoelii sporozoite infectivity. Nat Med *9*, 93-96.

Sinnis, P., Willnow, T.E., Briones, M.R., Herz, J., and Nussenzweig, V. (1996). Remnant lipoproteins inhibit malaria sporozoite invasion of hepatocytes. J Exp Med *184*, 945-954.

Soutschek, J., Akinc, A., Bramlage, B., Charisse, K., Constien, R., Donoghue, M., Elbashir, S., Geick, A., Hadwiger, P., Harborth, J., John, M., Kesavan, V., Lavine, G., Pandey, R.K., Racie, T., Rajeev, K.G., Rohl, I., Toudjarska, I., Wang, G., Wuschko, S., Bumcrot, D., Koteliansky, V., Limmer, S., Manoharan, M., and Vornlocher, H.P. (2004). Therapeutic silencing of an endogenous gene by systemic administration of modified siRNAs. Nature *432*, 173-178.

Tsuji, M., Mattei, D., Nussenzweig, R.S., Eichinger, D., and Zavala, F. (1994). Demonstration of heat-shock protein 70 in the sporozoite stage of malaria parasites. Parasitol Res *80*, 16-21.

Vishnyakova, T.G., Kurlander, R., Bocharov, A.V., Baranova, I.N., Chen, Z., Abu-Asab, M.S., Tsokos, M., Malide, D., Basso, F., Remaley, A., Csako, G., Eggerman, T.L., and Patterson, A.P. (2006). CLA-1 and its splicing variant CLA-2 mediate bacterial adhesion and cytosolic bacterial invasion in mammalian cells. Proc Natl Acad Sci U S A *103*, 16888-16893.

White, N.J. (2004). Antimalarial drug resistance. J Clin Invest *113*, 1084-1092.

Wustner, D., Mondal, M., Huang, A., and Maxfield, F.R. (2004). Different transport routes for high density lipoprotein and its associated free sterol in polarized hepatic cells. J Lipid Res *45*, 427-437.

Zimmermann, T.S., Lee, A.C., Akinc, A., Bramlage, B., Bumcrot, D., Fedoruk, M.N., Harborth, J., Heyes, J.A., Jeffs, L.B., John, M., Judge, A.D., Lam, K., McClintock, K., Nechev, L.V., Palmer, L.R., Racie, T., Rohl, I., Seiffert, S., Shanmugam, S., Sood, V., Soutschek, J.,

Toudjarska, I., Wheat, A.J., Yaworski, E., Zedalis, W., Koteliansky, V., Manoharan, M., Vornlocher, H.P., and MacLachlan, I. (2006). RNAi-mediated gene silencing in non-human primates. Nature *441*, 111-114.
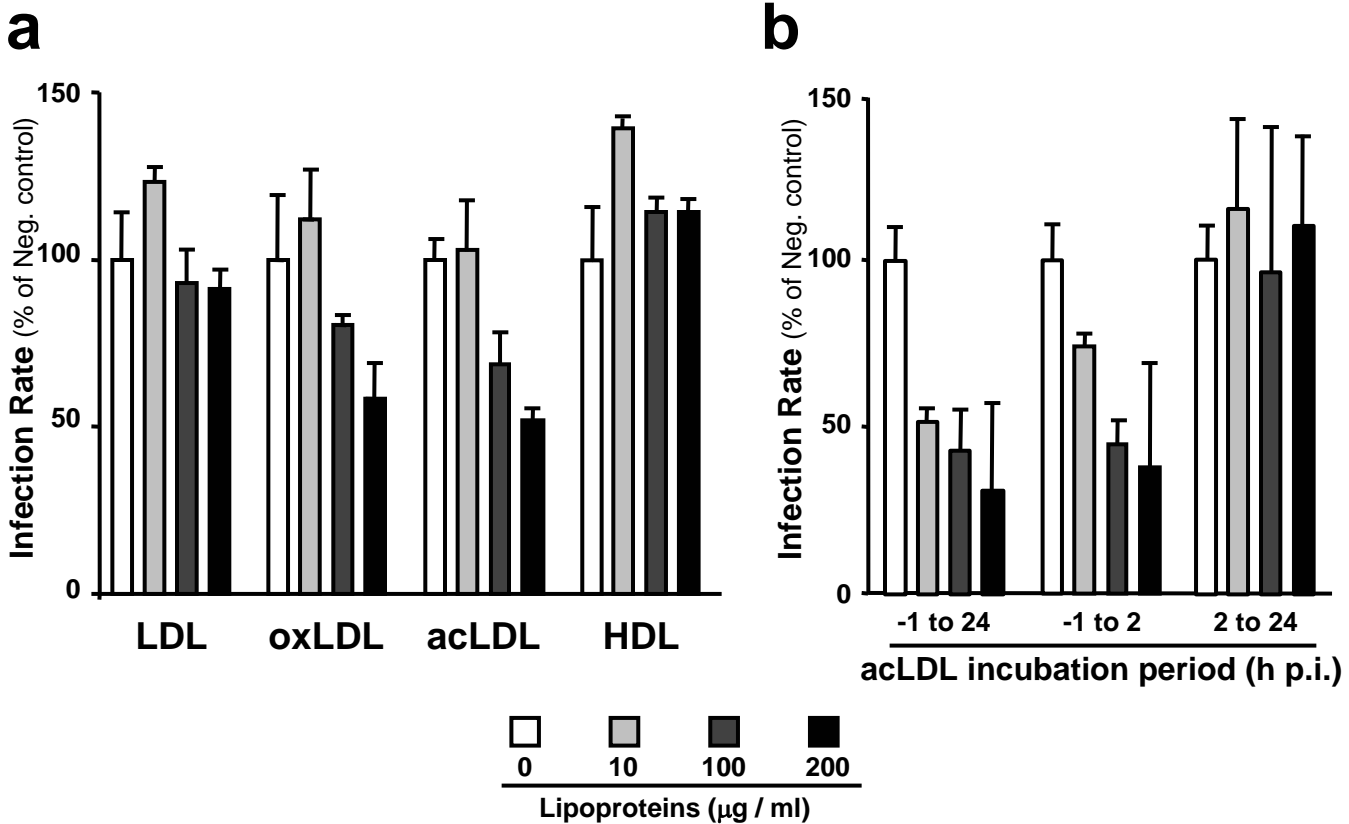
Figure 1 | Modified forms of LDL reduce *P. berghei* sporozoite infection of Huh7 cells.
(a) Effect of different concentrations of LDL, oxLDL, acLDL and HDL on Huh7 cell infection by *P. berghei* sporozoites. **(b)** Quantification of infection of Huh7 cells incubated with acLDL for various time periods relative to addition of *P. berghei* sporozoites. All infections were measured 24 h after sporozoite addition. Results are expressed as the mean ± s.d. of 3 independent infections.

221
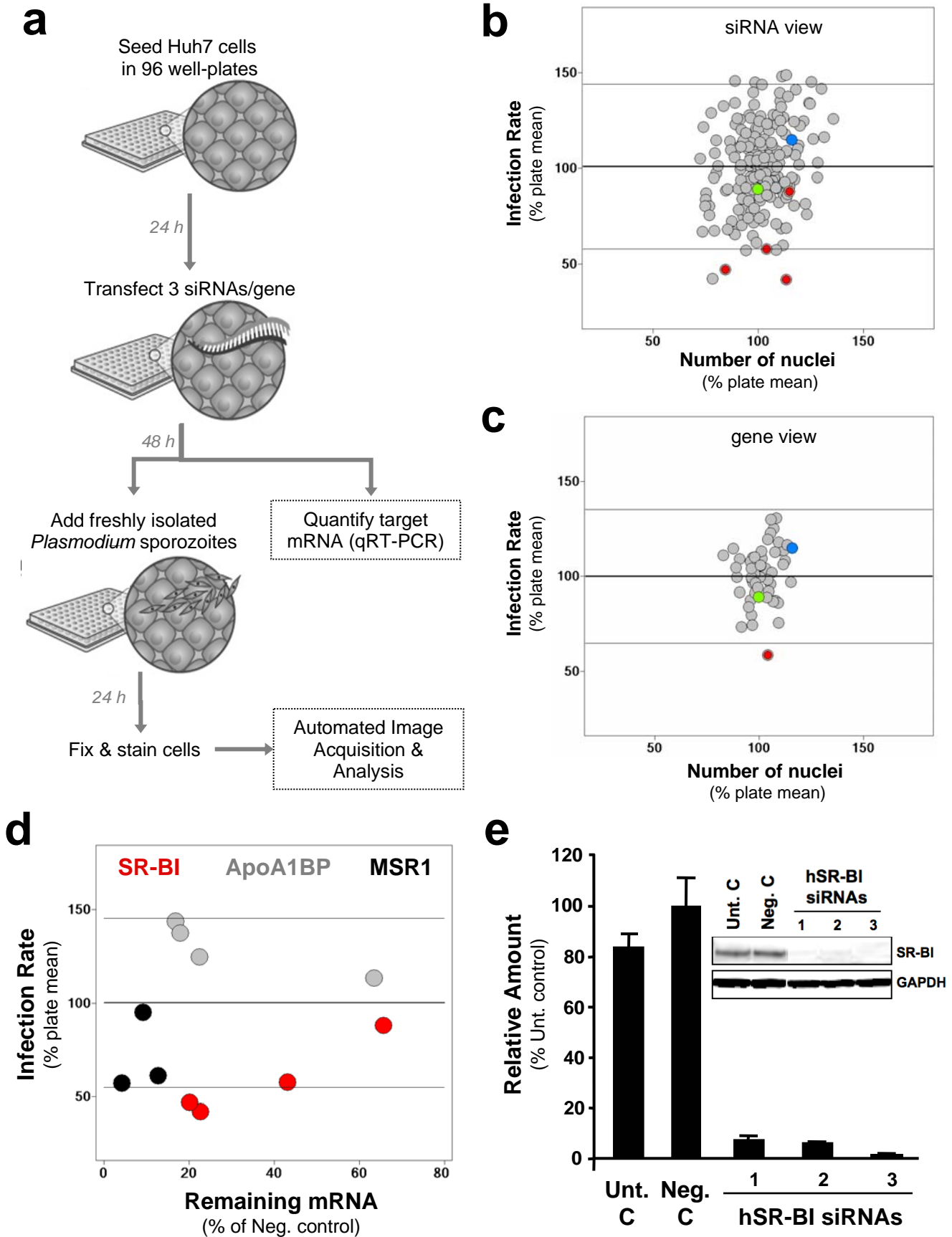
Figure 2 | RNAi screen of lipoprotein pathway genes identifies host SR-BI as critical requirement for infection of Huh7 cells by *P. berghei* sporozoites.

(a) Schematic representation of experimental workflow for cell-based RNAi screening assay to probe role of lipoprotein pathway genes in *P. berghei* sporozoite infection of Huh7 cells. **(b)** Effects of 206 siRNA treatments targeting 53 lipoprotein pathway genes on Huh7 cell proliferation (X axis) and infection by *P. berghei* sporozoites (Y axis), both measured 24 h after sporozoite addition and 72 h after siRNA transfection. Cell proliferation was estimated as the percentage of Huh7 nuclei relative to the mean from all experimental wells on each plate. Infection rates were calculated for each sample well as number of EEFs/cell confluency (as described in main text), also plotted here as a percentage relative to the mean from all experimental wells on each plate. For convenience, horizontal lines marking ± 2 s.d. of the whole dataset are also shown. Each circle represents one siRNA (mean of triplicate values, see also Supplementary Table 1 for exact values). Negative controls appear as blue and green circles, corresponding to untreated cells and cells transfected with a non-specific control siRNA, respectively. Red circles correspond to siRNAs targeting SR-BI. **(c)** Same dataset as shown in panel b, with each circle representing one of the 53 tested genes, and corresponding to the mean value from all siRNAs targeting each gene. Color attributions are the same as in panel b. **(d)** Comparison of effects of siRNA treatments on infection rate *versus* remaining mRNA levels for genes showing at least one positive siRNA (beyond 2 s.d. above or below mean infection rate for entire dataset), and for which the relationship between infection rate and remaining mRNA supports a proportional dosage effect. The horizontal grey lines represent 2 s.d. from the mean infection rate for entire dataset. Each circle represents one siRNA (mean of triplicate values), with red, grey and black circles corresponding to siRNAs targeting SR-BI, ApoA1BP and MSR1, respectively. **(e)** Effect of siRNA treatments on SR-BI protein levels in Huh7 cells, measured by semi-quantitative Western blotting of extracts taken at the time of infection, i.e. 48 h after siRNA transfection, from untransfected cells (Unt. C), cells transfected with a negative control non-specific siRNA (Neg. C), or cells transfected with human SR-BI-specific siRNAs (hSR-BI siRNAs). Results were normalized to Neg. C levels (100%).
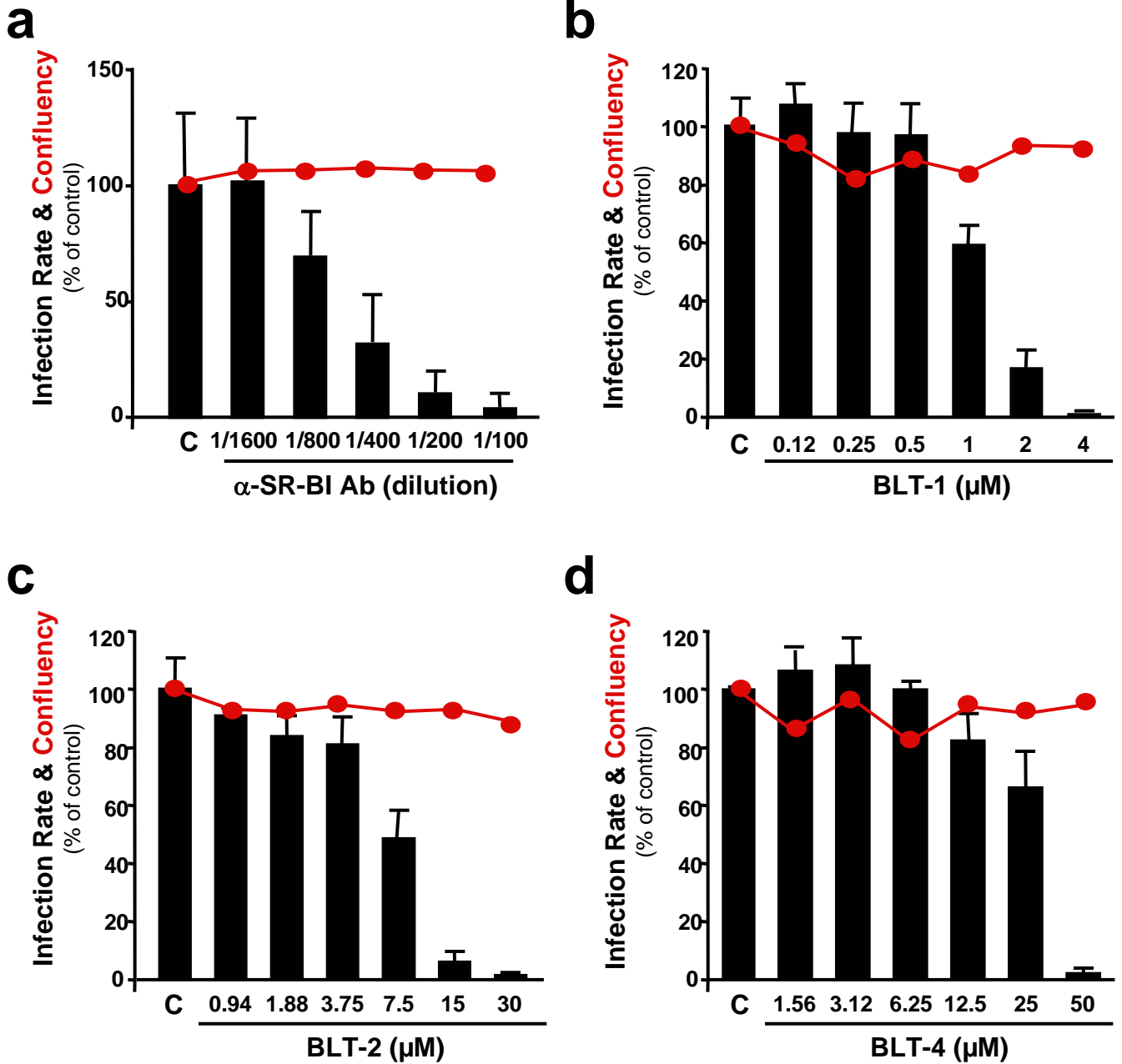
Figure 3 | Inhibition of host SR-BI protein function reduces *P. berghei* sporozoite infection of Huh7 cells.

(a) Effect of a serial dilution of a SR-BI blocking antibody on *P. berghei* infection rate of Huh7 cells. "C" indicates solvent-treated cells used as control. (b-d) Effect of known chemical inhibitors of SR-BI (BLT-1, 2 and 4, respectively) used at different concentrations, as shown, on *P. berghei* infection rate in Huh7 cells, as measured by quantification of the number of EEFs. "C" indicates solvent-treated cells used as negative control. (a-d) Antibody and all compounds were added to Huh7 cells 1 h before sporozoite addition, and infection rates were measured 24 h after sporozoite addition, by quantification of the number of EEFs, as described in main text. Results are expressed as the mean ± s.d. of EEFs (%) in 3 independent infections. Red symbols and lines represent the mean levels of cell confluence based on automated analysis of actin staining, as measured for each set of triplicate samples.
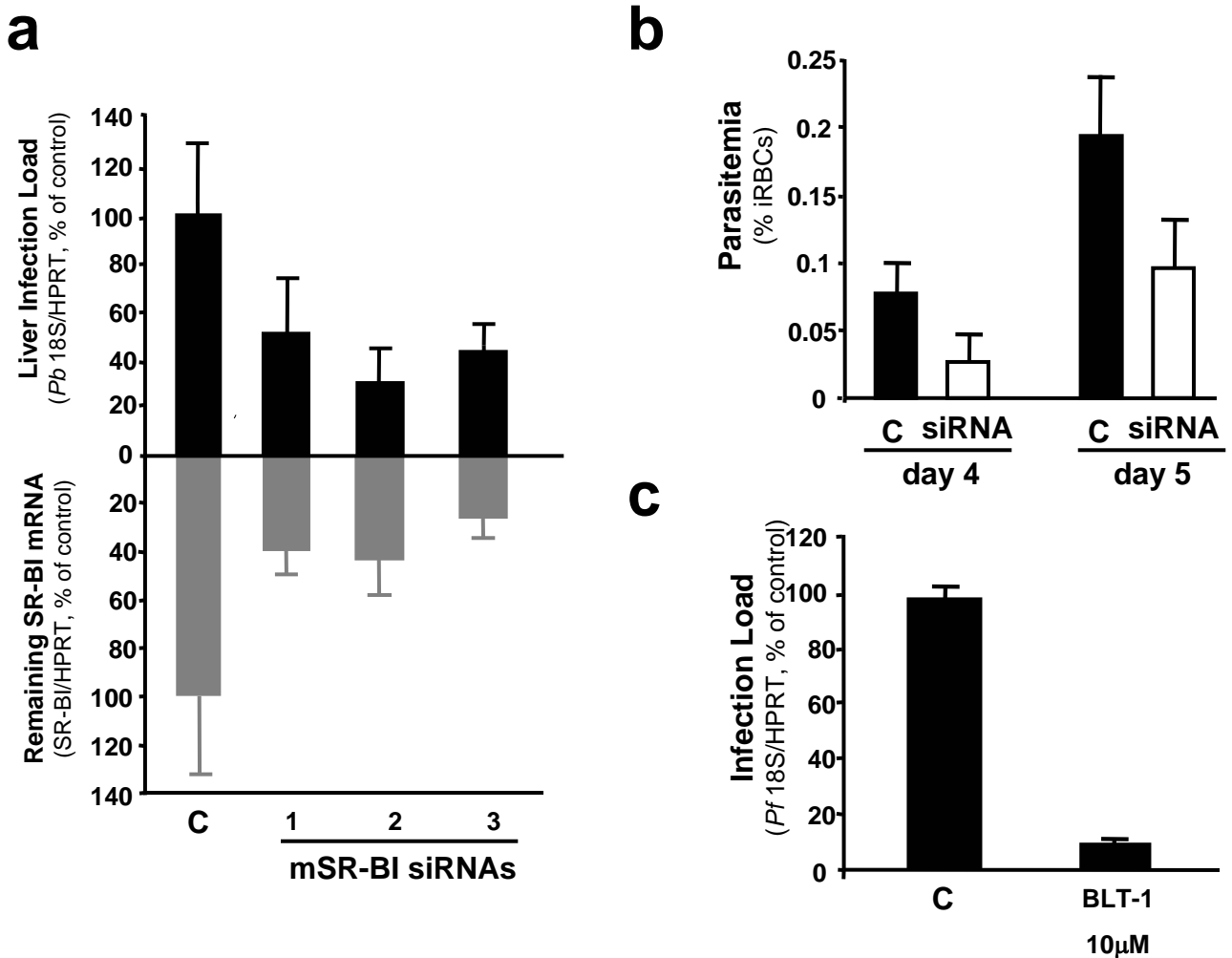
Figure 4 | Host SR-BI is crucial for *P. berghei* infection in adult mice *in vivo* and *P. falciparum* infection in primary human hepatocytes.

(a-b) Effect of siRNA-mediated *in vivo* knock-down of SR-BI on mouse liver stage **(a)** and blood stage **(b)** infection by *P. berghei.* Liver infection load (a, black bars) was measured by qRT-PCR analysis of *P. berghei* 18S rRNA normalized to HPRT in liver extracts taken 40 h after sporozoite i.v. injection, and plotted as percentage of the mean of negative control samples (C). Grey bars in (a) represent the remaining mRNA levels for the targeted mSR-BI gene in the same liver samples. Results are expressed as the mean ± s.d. of 5 mice per group. Effect on blood stage of treatment of one SR-BI siRNA (b) was measured by parasitemia quantification (percentage of infected red blood cells, iRBC) using FACS. Mice treated with a siRNA targeting luciferase were used as control. **(c)** Effect of BLT-1 on *P. falciparum* infection in human primary hepatocytes, measured by qRT-PCR as described for (b) above. BLT-1 was added to cells 1 h before sporozoite addition, and infection load was measured in cell extracts taken 72 h after sporozoite addition, as described in main text. Results are expressed as the mean ± s.d. of triplicate samples..

231
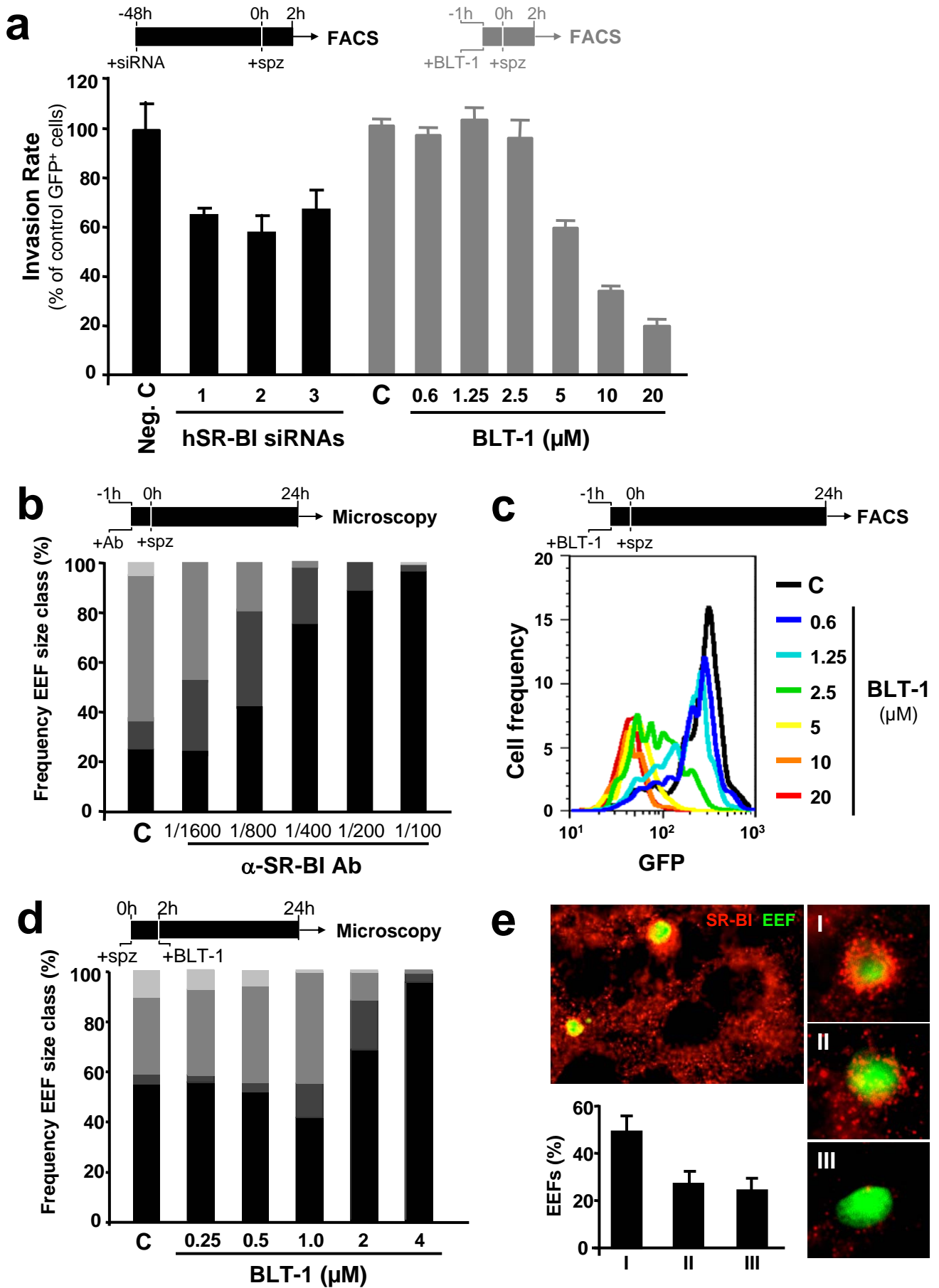
Figure 5 | Host SR-BI plays a role in both invasion and development of *P. berghei* in Huh7 cells.

(a) FACS analysis of effects of siRNA-mediated knock-down of SR-BI (black bars) or different concentrations of BLT-1 treatment (grey bars) on invasion phase of infection in Huh7 cells, using GFP-expressing *P. berghei* sporozoites. As indicated in diagrams above bar chart, cells were harvested for flow cytometry 2 h after sporozoite addition, and invasion rate was measured as percentage of GFP$^+$ cells compared to control values. For siRNA-treated samples, control samples (Neg. C) were treated with a non-specific siRNA. For BLT-1-treated samples, control (DMSO) was treated with drug dilution buffer containing same level of DMSO found in most concentrated drug treatment. Results are expressed as the mean ± s.d. of triplicate samples. **(b)** Effect of serial dilutions of a SR-BI blocking antibody on *P. berghei* development within host Huh7 cells, as determined by EEF size classification using automated analysis of microscopy images from cells fixed 24 h after sporozoite addition. Data shown are from same samples used for infection rate analysis in Figure 3a. Four classes of EEF sizes are represented as different grey levels used in bar fills, ranging from black for EEFs with smallest diameter, up to lightest grey tone for largest EEFs. Negative control (C) represents cells exposed to antibody dilution buffer containing same azide concentration present in most concentrated antibody treatment. As indicated in diagram above bar chart, antibody was added 1 h before sporozoite addition. Results are expressed as the mean of triplicate samples. **(c)** Effect of BLT-1 treatment at different concentrations on *P. berghei* development within host Huh7 cells, as measured by FACS in cells harvested 24 h after addition of GFP-expressing sporozoites. Negative control (C) represents cells treated with drug dilution buffer containing same level of DMSO found in most concentrated drug treatment. As indicated in diagram above chart, drug was added 1 h before sporozoite addition. The graph represents a representative dataset of triplicate experimental samples. **(d)** Effect of BLT-1 treatment at different concentrations added 2 h after sporozoite addition on *P. berghei* EEF size, determined as described in (b) above, from cells fixed 24 h after sporozoite addition. Negative control (C) is as described in (c) above. Results are expressed as the mean of triplicate samples. **(e)** Immunofluorescence analysis of SR-BI localization in infected Huh7 cells fixed 24 h after addition of *P. berghei* sporozoites. The plot represents the quantification of the percentage of EEFs (green in images) with different levels of SR-BI (red in images) in immediate proximity, according to classification shown in small images (I, II, III). Results are expressed as the mean ± s.d. of EEFs (%) in 3 independent infections.
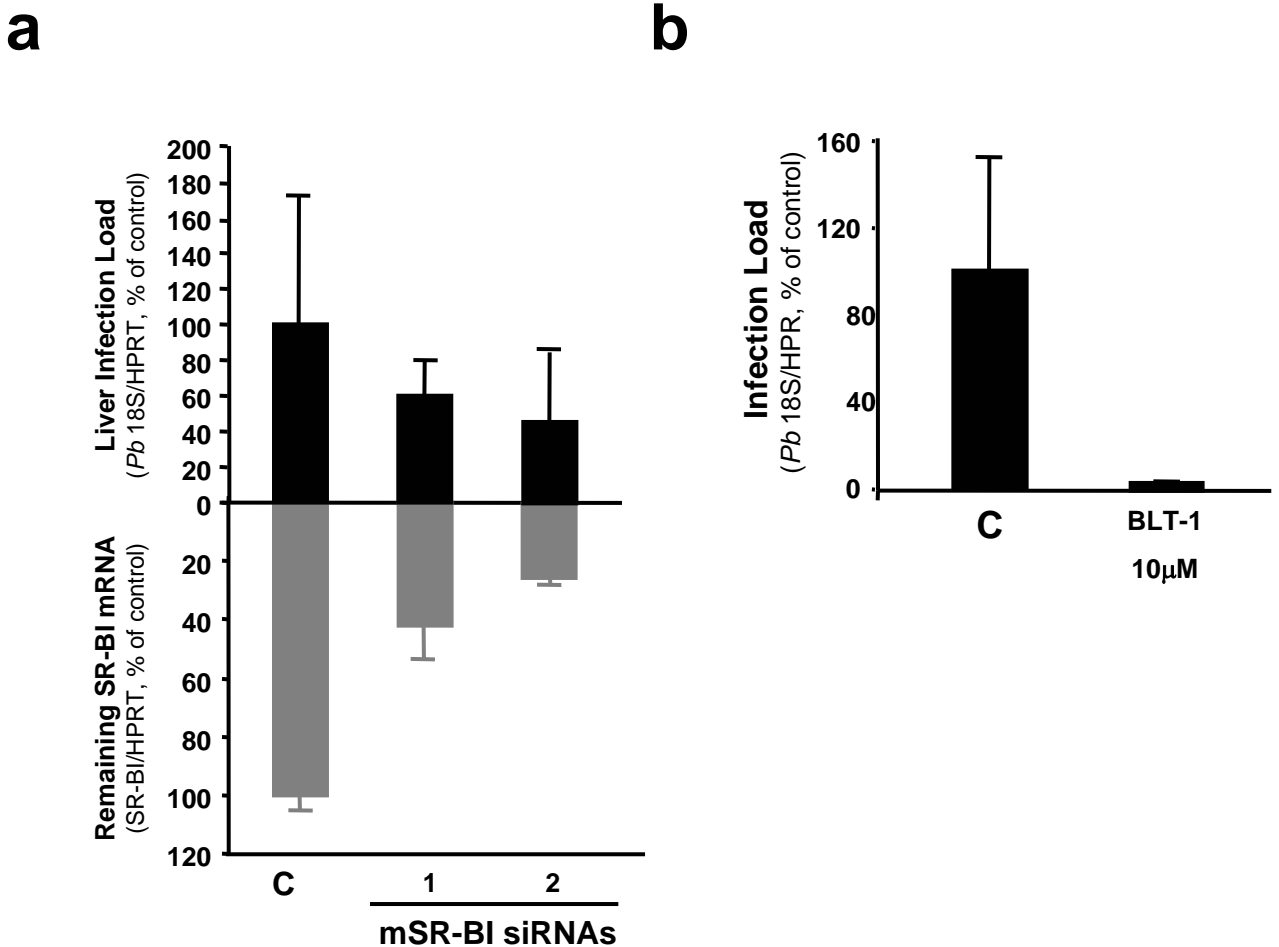
Supplementary Figure 1 | SR-BI is crucial for mouse primary hepatocyte infection by *P. berghei* sporozoites.
(a) Effect of SR-BI siRNAs in mRNA-specific levels (grey bars) and *P. berghei* infection (black bars), both measured 48 h after sporozoite addition by qRT-PCR. (b) Effect of BLT-1 on infection of mouse primary hepatocytes by *P. berghei*, as measured 48 h after sporozoite addition by qRT-PCR.
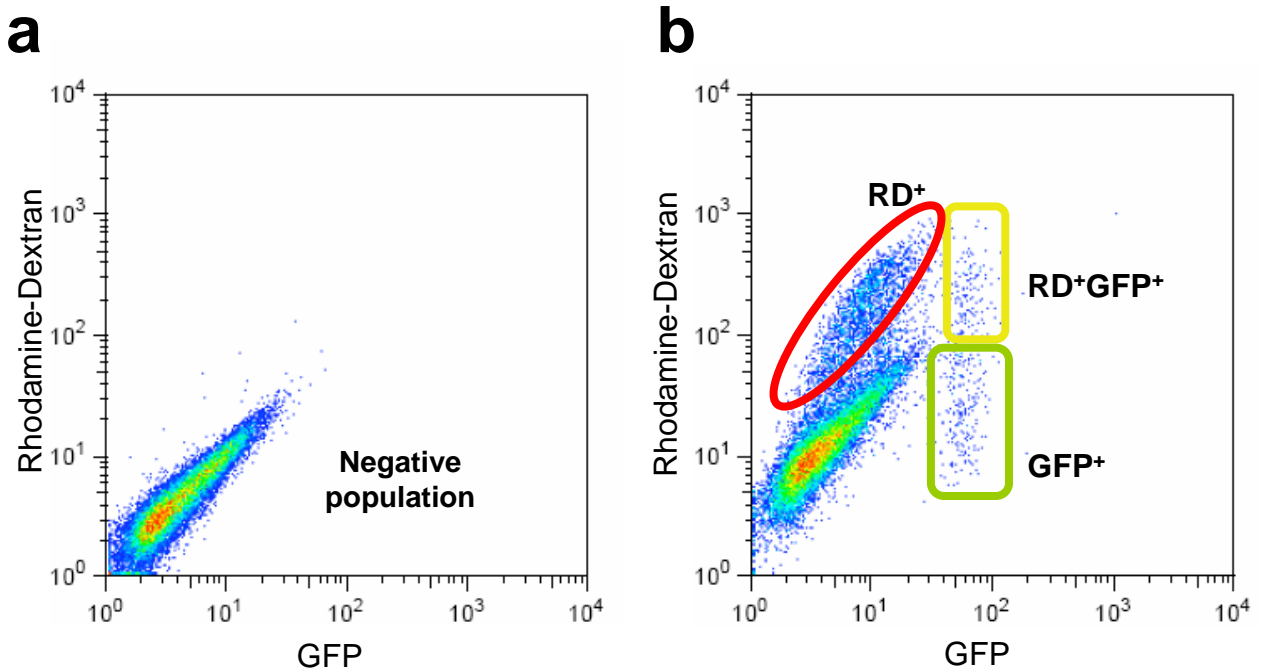
Supplementary Figure 2 | FACS assessment of sporozoite migration through cells and invasion during infection.
(a) Cells not incubated with sporozoites (negative population). (b) Traversal *vs* invasion were assessed in cells incubated with PbGFP sporozoites (1.5×10^4) for 2 hours. The gates contain RD-positive (RD⁺, red gate), GFP-positive (GFP⁺, green gate) or double-positive cells (RD⁺GFP⁺, yellow gate).
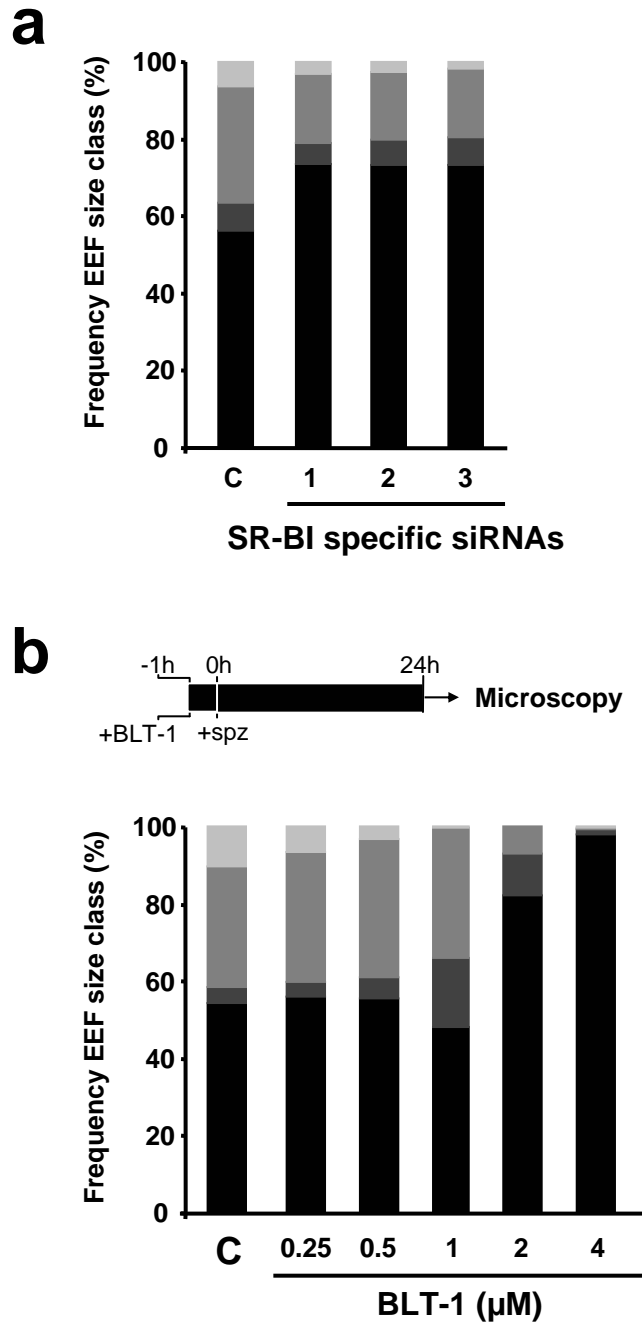
Figure 3 | SR-BI plays a role in *P. berghei* EEF development inside Huh7 cells.
(a) Effect of siRNA-mediated knockdown of SR-BI on EEF size, determined 24 h after sporozoite addition. **(b)** Effect of BLT-1 on EEF size, determined 24 h after sporozoite addition. Results are expressed as the mean $\pm$ s.d. of triplicates.

Gene Name	NCBI Gene Accession Number	NCBI Accession ID for Targeted Transcripts	siRNA ID from Supplier[1]	Infection Rate[2]	Cell Proliferation[3]	Remaining mRNA[4]
ABCA1	19	NM_005502	107729	95,9	97,2	38,4
ABCA1	19	NM_005502	107730	91,3	91,8	38,0
ABCA1	19	NM_005502	117341	95,6	96,3	27,8
ABCA1	19	NM_005502	117342	101,3	95,6	30,4
ABCA1	19	NM_005502	118165	102,5	98,0	27,6
ABCA1	19	NM_005502	212921	109,7	105,5	25,3
APOA1	335	NM_000039, XM_496536	122559	89,7	99,2	18,7
APOA1	335	NM_000039, XM_496536	2250	78,9	96,0	15,2
APOA1	335	NM_000039, XM_496536	2346	110,6	88,9	26,5
APOA1	335	NM_000039, XM_496536	2436	126,4	111,9	20,9
APOA1BP	128240	NM_144772	129257	137,4	114,2	17,9
APOA1BP	128240	NM_144772	129258	113,3	106,1	63,4
APOA1BP	128240	NM_144772	37558	143,7	101,7	16,8
APOA1BP	128240	NM_144772	37652	124,6	100,5	22,5
APOA2	336	NM_001643	10053	116,8	95,6	25,6
APOA2	336	NM_001643	10143	128,8	77,7	15,9
APOA2	336	NM_001643	10229	87,0	75,2	19,3
APOA5	116519	NM_052968	128930	77,8	96,8	37,7
APOA5	116519	NM_052968	35650 *	75,7	76,6	37,3
APOA5	116519	NM_052968	35746 *	89,9	94,1	71,5
APOA5	116519	NM_052968	35835 *	92,7	112,7	17,3
APOB	338	NM_000384	120962	86,0	99,3	58,2
APOB	338	NM_000384	120963	120,8	98,8	34,7
APOB	338	NM_000384	120964	92,8	115,2	50,8
APOB	338	NM_000384	2257	116,1	99,1	20,1
APOC1	341	NM_001645	10231	65,0	97,4	19,0
APOC1	341	NM_001645	10327	95,4	109,3	15,8
APOC1	341	NM_001645	10421	94,2	117,1	26,8
APOC1	341	NM_001645	147168	94,8	107,6	135,6
APOC2	344	NM_000483	8600	107,8	79,4	27,3
APOC2	344	NM_000483	8696	133,1	98,1	22,5
APOC2	344	NM_000483	8789	86,6	94,2	16,3

Gene Name	NCBI Gene Accession Number	NCBI Accession ID for Targeted Transcripts	siRNA ID from Supplier[1]	Infection Rate[2]	Cell Proliferation[3]	Remaining mRNA[4]
APOC3	345	NM_000040, XM_496537	146890	120,7	100,1	11,7
APOC3	345	NM_000040, XM_496537	45917	117,6	112,8	10,4
APOC3	345	NM_000040, XM_496537	7767	104,4	107,0	7,0
APOC3	345	NM_000040, XM_496537	7862	112,0	119,1	3,6
APOC4	346	NM_001646	10232	127,7	95,7	inconc
APOC4	346	NM_001646	10328	115,7	97,3	inconc
APOC4	346	NM_001646	147169	102,9	97,7	inconc
APOC4	346	NM_001646	45988	90,7	114,7	inconc
APOE	348	NM_000041	146891 *	87,4	97,3	68,1
APOE	348	NM_000041	41598	110,1	118,6	47,1
APOE	348	NM_000041	41694	114,5	79,9	62,0
APOE	348	NM_000041	41775	95,2	128,1	13,9
APOF	319	NM_001638	147163	82,2	109,8	inconc
APOF	319	NM_001638	2322	110,8	105,0	inconc
APOF	319	NM_001638	2414	125,9	135,6	inconc
APOF	319	NM_001638	2500	68,6	110,8	inconc
APOH	350	NM_000042	146892	59,9	111,7	20,9
APOH	350	NM_000042	146893	115,4	126,1	32,0
APOH	350	NM_000042	146894	67,4	79,2	11,4
APOH	350	NM_000042	7768	101,9	119,4	8,1
APOL1	8542	NM_003661, NM_145343, NM_145344	6709	145,5	88,8	inconc
APOL1	8542	NM_003661, NM_145343, NM_145344	6800	88,5	103,2	inconc
APOL1	8542	NM_003661, NM_145343, NM_145344	6886	134,2	124,1	inconc
APOL2	23780	NM_030882, NM_145637	135325	133,6	124,5	42,3

Gene Name	NCBI Gene Accession Number	NCBI Accession ID for Targeted Transcripts	siRNA ID from Supplier[1]	Infection Rate[2]	Cell Proliferation[3]	Remaining mRNA[4]
APOL2	23780	NM_030882, NM_145637	135326	141,6	130,1	19,7
APOL2	23780	NM_030882, NM_145637	135327	102,1	102,3	14,6
APOL2	23780	NM_030882, NM_145637	6179	89,0	97,4	34,0
APOL3	80833	NM_014349, NM_030644, NM_145639, NM_145640, NM_145641, NM_145642	38103	104,0	99,4	inconc
APOL3	80833	NM_014349, NM_030644, NM_145639, NM_145640, NM_145641, NM_145642	38196	57,5	108,6	inconc
APOL3	80833	NM_014349, NM_030644, NM_145639, NM_145640, NM_145641, NM_145642	38278	105,4	102,8	inconc
APOM	55937	NM_019101	27747 *	91,6	113,5	19,4
APOM	55937	NM_019101	27840 *	81,7	122,4	33,1
APOM	55937	NM_019101	27926 *	145,0	98,5	87,1
ARH	26119	NM_015627	108752	90,0	108,2	43,7
ARH	26119	NM_015627	23202	101,7	91,8	59,1
ARH	26119	NM_015627	23298	86,7	113,9	101,7
ARH	26119	NM_015627	23391	69,0	113,3	58,1
CAV1	857	NM_001753	10297	90,5	110,6	48,1
CAV1	857	NM_001753	10392	93,5	104,8	20,1
CAV1	857	NM_001753	10479	116,2	131,3	69,4
CAV1	857	NM_001753	145951 *	83,7	74,9	29,9

Gene Name	NCBI Gene Accession Number	NCBI Accession ID for Targeted Transcripts	siRNA ID from Supplier[1]	Infection Rate[2]	Cell Proliferation[3]	Remaining mRNA[4]
CAV2	858	NM_001233, NM_198212	145680 *	107,5	105,6	2,0
CAV2	858	NM_001233, NM_198212	145681 *	119,9	104,9	17,1
CAV2	858	NM_001233, NM_198212	9481 *	114,1	97,1	3,0
CAV2	858	NM_001233, NM_198212	9575 *	97,4	80,1	14,2
CD36	948	NM_000072, NM_001001547, NM_001001548	105939	132,5	83,5	68,3
CD36	948	NM_000072, NM_001001547, NM_001001548	110587 *	109,8	89,3	24,3
CD36	948	NM_000072, NM_001001547, NM_001001548	7788	95,0	79,0	33,4
CD36	948	NM_000072, NM_001001547, NM_001001548	7883	125,6	91,4	35,9
CD36	948	NM_000072, NM_001001547, NM_001001548	7974	110,0	95,3	51,8
CD5L	922	NM_005894	107864	108,8	109,2	inconc
CD5L	922	NM_005894	107865	72,5	102,2	inconc
CD5L	922	NM_005894	2589	98,9	101,3	inconc

Gene Name	NCBI Gene Accession Number	NCBI Accession ID for Targeted Transcripts	siRNA ID from Supplier[1]	Infection Rate[2]	Cell Proliferation[3]	Remaining mRNA[4]
CD5L	922	NM_005894	2679	112,2	103,6	inconc
CETP	1071	NM_000078	120947	98,8	107,2	inconc
CETP	1071	NM_000078	120948	84,4	99,2	inconc
CETP	1071	NM_000078	120949	91,9	105,3	inconc
CETP	1071	NM_000078	2251	93,4	106,7	inconc
CXCL16	58191	NM_022059	121892 *	106,1	99,9	29,3
CXCL16	58191	NM_022059	121893 *	74,3	100,5	21,8
CXCL16	58191	NM_022059	29610 *	120,0	91,9	13,4
CXCL16	58191	NM_022059	29705 *	85,2	100,7	26,0
DKFZP434F0318	81575	NM_030817	123591 *	96,3	100,9	1,3
DKFZP434F0318	81575	NM_030817	32719 *	118,5	94,2	63,2
DKFZP434F0318	81575	NM_030817	32811 *	111,3	95,5	100,6
DKFZP434F0318	81575	NM_030817	32898 *	113,6	100,9	60,6
HDLBP	3069	NM_005336, NM_203346	145235 *	99,5	91,5	12,2
HDLBP	3069	NM_005336, NM_203346	145236 *	90,0	98,6	18,7
HDLBP	3069	NM_005336, NM_203346	2329 *	91,1	103,2	25,5
HDLBP	3069	NM_005336, NM_203346	2419 *	113,2	92,4	26,5
LCAT	3931	NM_000229	110616	124,5	121,4	inconc
LCAT	3931	NM_000229	110617	88,6	84,5	inconc
LCAT	3931	NM_000229	110618	105,6	102,7	inconc
LCAT	3931	NM_000229	8062	79,1	93,2	inconc
LDLR	3949	NM_000527	106132	134,0	88,9	inconc
LDLR	3949	NM_000527	106134 *	127,2	101,0	32,7
LDLR	3949	NM_000527	110672 *	110,2	97,9	29,8
LDLR	3949	NM_000527	110674 *	80,6	116,9	19,9
LIPC	3990	NM_000236	143213 *	86,9	112,0	7,0
LIPC	3990	NM_000236	8068 *	106,9	117,6	1,4
LIPC	3990	NM_000236	8161 *	93,1	95,1	45,6
LIPC	3990	NM_000236	8252 *	145,1	125,3	12,7
LIPG	9388	NM_006033	138162 *	99,2	107,6	42,0
LIPG	9388	NM_006033	17152 *	78,5	92,9	18,5
LIPG	9388	NM_006033	17246 *	148,7	113,3	36,1

Gene Name	NCBI Gene Accession Number	NCBI Accession ID for Targeted Transcripts	siRNA ID from Supplier[1]	Infection Rate[2]	Cell Proliferation[3]	Remaining mRNA[4]
LIPG	9388	NM_006033	17336 *	124,3	117,0	28,0
LISCH7	51599	NM_015925, NM_205834, NM_205835	23479 *	85,2	105,6	83,9
LISCH7	51599	NM_015925, NM_205834, NM_205835	23575 *	105,1	72,3	14,9
LISCH7	51599	NM_015925, NM_205834, NM_205835	23670 *	123,0	89,1	26,5
LOC338328	338328	NM_015925, NM_205834, NM_205835	116788	89,2	85,3	inconc
LOC338328	338328	NM_178172	128376	123,1	104,0	inconc
LOC338328	338328	NM_178172	128377	111,3	91,7	inconc
LOC338328	338328	NM_178172	217244	93,1	104,4	inconc
LOC388633	388633	NM_001010978	254859	125,9	90,1	inconc
LOC388633	388633	NM_001010978	285064	100,6	108,9	inconc
LOC388633	388633	NM_001010978	285065	90,4	103,2	inconc
LOC401944	401944	NM_001013693	255653	139,7	97,5	inconc
LOC401944	401944	NM_001013693	255654	131,9	110,9	inconc
LOC401944	401944	NM_001013693	255655	86,2	104,1	inconc
LRP1	4035	NM_002332	106763	102,9	109,9	32,5
LRP1	4035	NM_002332	111141	91,1	103,2	44,9
LRP1	4035	NM_002332	111142	114,0	86,6	42,6
LRP1	4035	NM_002332	11437	113,5	102,9	27,6
LRP10	26020	NM_014045	108464	82,9	95,4	29,7
LRP10	26020	NM_014045	134173	105,7	88,7	36,1
LRP10	26020	NM_014045	134174	80,4	74,8	52,7
LRP10	26020	NM_014045	20779	97,4	103,5	52,2

Gene Name	NCBI Gene Accession Number	NCBI Accession ID for Targeted Transcripts	siRNA ID from Supplier[1]	Infection Rate[2]	Cell Proliferation[3]	Remaining mRNA[4]
LRP11	84918	NM_032832	109824	126,2	96,3	29,1
LRP11	84918	NM_032832	34821	42,5	78,4	29,9
LRP11	84918	NM_032832	34917	95,3	115,8	35,9
LRP11	84918	NM_032832	35005	112,1	106,6	11,7
LRP4	4038	NM_002334	202503	87,2	96,3	29,8
LRP4	4038	NM_002334	213206	67,0	73,4	35,5
LRP4	4038	NM_002334	213207	123,6	105,9	36,1
LRP4	4038	NM_002334	213208	108,2	113,0	88,9
LRP5	4041	NM_002335	106765	66,7	88,2	88,7
LRP5	4041	NM_002335	111147	100,8	101,3	54,8
LRP5	4041	NM_002335	111149	76,0	102,7	49,2
LRP5	4041	NM_002335	11438	75,2	92,8	35,4
LRP6	4040	NM_002336	106766	109,1	113,5	30,6
LRP6	4040	NM_002336	106767	122,2	119,7	117,1
LRP6	4040	NM_002336	11345	122,8	108,8	31,8
LRP6	4040	NM_002336	11439	99,9	105,2	29,0
LRP8	7804	NM_001018054, NM_004631, NM_017522, NM_033300	107482	84,7	113,3	60,0
LRP8	7804	NM_001018054, NM_004631, NM_017522, NM_033300	111478	71,0	108,4	62,9
LRP8	7804	NM_001018054, NM_004631, NM_017522, NM_033300	111480	70,5	92,2	105,9
LRP8	7804	NM_001018054, NM_004631, NM_017522, NM_033300	6039	76,2	123,0	72,1

Gene Name	NCBI Gene Accession Number	NCBI Accession ID for Targeted Transcripts	siRNA ID from Supplier[1]	Infection Rate[2]	Cell Proliferation[3]	Remaining mRNA[4]
LRPAP1	4043	NM_002337	11346	71,9	97,9	24,9
LRPAP1	4043	NM_002337	11440	101,1	80,9	19,6
LRPAP1	4043	NM_002337	11528	89,8	108,6	18,3
MGC45780	286133	NM_173833	128312	74,1	95,3	inconc
MGC45780	286133	NM_173833	43900	72,6	87,3	inconc
MGC45780	286133	NM_173833	43994	68,3	85,3	inconc
MGC45780	286133	NM_173833	44079	79,1	98,0	inconc
MSR1	4481	NM_002445, NM_138715, NM_138716	110010	84,2	92,3	inconc
MSR1	4481	NM_002445, NM_138715, NM_138716	110011 *	61,3	99,2	12,7
MSR1	4481	NM_002445, NM_138715, NM_138716	36772 *	57,3	94,1	4,2
MSR1	4481	NM_002445, NM_138715, NM_138716	36859 *	95,2	101,3	9,1
MTP	4547	NM_000253	143239	147,9	111,4	59,4
MTP	4547	NM_000253	8075	105,4	96,4	38,1
MTP	4547	NM_000253	8168	128,0	107,1	21,2
MTP	4547	NM_000253	8259	141,0	117,9	72,6
NPC1	4864	NM_000271	106017 *	135,2	110,4	56,6
NPC1	4864	NM_000271	114040 *	112,4	98,2	54,9
NPC1	4864	NM_000271	114041 *	124,9	110,3	76,3
NPC1	4864	NM_000271	8092 *	127,7	109,2	31,5
PLTP	5360	NM_006227, NM_182676	121016	116,5	98,3	32,7
PLTP	5360	NM_006227, NM_182676	121017	102,9	128,3	114,7
PLTP	5360	NM_006227, NM_182676	17445	65,6	89,0	43,2
PLTP	5360	NM_006227, NM_182676	17538	80,5	76,6	47,9
SR-BI	949	NM_005505	107731	57,9	104,0	43,1

Gene Name	NCBI Gene Accession Number	NCBI Accession ID for Targeted Transcripts	siRNA ID from Supplier[1]	Infection Rate[2]	Cell Proliferation[3]	Remaining mRNA[4]
SR-BI	949	NM_005505	107732	88,1	114,8	65,6
SR-BI	949	NM_005505	111573	47,1	84,4	20,1
SR-BI	949	NM_005505	16481	42,0	113,2	22,7
SR-BII	950	NM_005506	107735	89,4	90,5	30,9
SR-BII	950	NM_005506	16297	102,2	99,0	11,1
SR-BII	950	NM_005506	16392	121,5	74,0	23,6
SR-BII	950	NM_005506	16482	85,1	94,0	17,8
SCARF1	8578	NM_003693, NM_145349, NM_145350, NM_145351, NM_145352	111342	111,9	101,8	inconc
SCARF1	8578	NM_003693, NM_145349, NM_145350, NM_145351, NM_145352	111343	113,4	96,3	inconc
SCARF1	8578	NM_003693, NM_145349, NM_145350, NM_145351, NM_145352	13507	95,3	98,1	inconc
SCARF1	8578	NM_003693, NM_145349, NM_145350, NM_145351, NM_145352	13603	109,6	86,9	inconc
STAB1	23166	NM_015136	136773	78,6	90,6	inconc
STAB1	23166	NM_015136	136774	114,3	92,9	inconc
STAB1	23166	NM_015136	22421	100,5	105,8	inconc
STAB1	23166	NM_015136	22517	104,0	95,9	inconc
TLR6	10333	NM_006068	107933 *	107,0	109,9	68,6
TLR6	10333	NM_006068	17169 *	139,4	110,2	40,0
TLR6	10333	NM_006068	17263 *	119,6	111,1	67,5
TLR6	10333	NM_006068	17353	105,1	106,4	inconc

Gene Name	NCBI Gene Accession Number	NCBI Accession ID for Targeted Transcripts	siRNA ID from Supplier[1]	Infection Rate[2]	Cell Proliferation[3]	Remaining mRNA[4]
VLDLR	7436	NM_001018056, NM_003383	107087 *	83,4	100,8	86,0
VLDLR	7436	NM_001018056, NM_003383	107088 *	112,6	96,0	17,5
VLDLR	7436	NM_001018056, NM_003383	4545 *	93,9	91,8	40,6
VLDLR	7436	NM_001018056, NM_003383	4641 *	114,9	102,9	51,0
neg1			103860	89,3	99,8	na
untreated			na	114,8	115,8	na

Notes:

[1] (Ambion, Applied Biosystem)

[2] (nb EEFs normalized to confluency, shown as % of plate mean)

[3] (nb of cell nuclei, shown as % of plate mean)

[4] (% relative to negative control)

* siRNAs with one single experimental triplicate

"inconc": qRT-PCR yielded inconclusive or uninterpretable results despite testing multiple primer pairs (most likely due to low expression of gene or undocumented splice variants)

Supplementary Table 1 | The relevance of lipoprotein pathway genes for the liver stage of *Plasmodium* infection was addressed by RNAi.

A library of 206 siRNAs targeting 53 genes expressed in the liver and annotated as having validated or putative roles in lipoprotein assembly, binding or uptake was assembled and screened by RNAi. For each gene is provided relevant information, namely the gene name, the NCBI (National Center for Biotechnology Information, Entrez Gene Database; http://www.ncbi.nlm.nih.gov/sites/entrez) gene accession number and NCBI accession ID for targeted transcript together with the data obtained. The siRNAs used [distinguished by the siRNA ID from the supplier (Ambion, Applied Biosystems)] and their respective infection rate (corresponding to the number of EEFs normalized to confluency, shown as the % of plate-specific negative controls), cell proliferation (number of cell nuclei expressed as % of plate mean) and remaining mRNA (% relative to negative control) are provided.

Chapter 5 | General Discussion

Malaria is one of the most prevalent infectious diseases worldwide with forty percent of the world's population at risk of infection. As is the case for any parasitic disease, malaria infection depends upon the occurrence of interactions between the parasite and its host [see (Leiriao *et al.*, 2004; Bano *et al.*, 2007)]. Every stage of *Plasmodium* infection relies, to different extents, on the presence of host molecules that enable or facilitate its invasion, survival and multiplication [reviewed in (Prudêncio *et al.*, 2006a)]. As the development of *Plasmodium* sporozoites inside hepatocytes is an obligatory step before the onset of disease, understanding the parasite's requirements during this stage not only offers a new perspective into mammalian cell biology but also contributes to the design of rational prophylactic approaches against malaria infection. Despite this fact, to date, not much is known about the host molecules that play a role in malaria liver infection, particularly in what concerns *Plasmodium* invasion and development within hepatocytes. The work developed in the present PhD thesis used RNAi and microarray approaches to identify novel host factors playing a role in the establishment of a malaria infection.

Microarray technology has revolutionized the analysis of gene expression since it allows monitoring the RNA products of thousands of genes at the same time. This is possible through the use of arrays, which consist of an orderly arrangement of DNA samples that act as a probe for the specific gene. Thus, in a single experiment, it is possible to address the expression level of hundreds or thousands of genes within a cell by measuring the amount of mRNA (previously converted into cDNA) bound to each probe on the array. This amount of mRNA can be precisely measured and used to generate a profile of gene expression in the cell(s) (Alberts *et al.*, 2002). Together with the use of model systems of infection, microarrays are particularly useful to analyze a pathogen's response to its host environment as well as to examine how a pathogen alters its gene expression profile in response to its host [reviewed in (Jenner and Young, 2005)].

In chapter 2, entitled "Identification of host molecules involved in the liver stage of malaria infection using transcriptional profiling followed by RNAi analysis", a microarray approach was used to obtain a comprehensive view of the changes in the host cell transcription throughout *Plasmodium* infection. An *in vitro* model of *Plasmodium* hepatocyte infection, the infection of the mouse hepatoma cell line Hepa1-6 with the murine *P. berghei* parasite, was employed to identify the host genes that are differentially expressed during infection. However, the information obtained cannot distinguish between the host genes that constitute just a host cell response to the parasite infection from the ones that play an important role for the infection outcome. To this end, an RNAi approach was applied to a group of genes, which

presented an interesting gene expression signature during *Plasmodium* infection of hepatocytes, as revealed by the microarray analysis.

RNAi technology is based on a biological mechanism that consists on a sequence-specific post-transcriptional gene silencing as a response to dsRNA. The discovery of RNAi as a biological response to dsRNA was first made in the nematode *Caenorhabditis elegans*, in which, through the injection of dsRNAs, it was possible to silence the genes with complementary sequences to the introduced dsRNAs (Fire *et al.*, 1998). RNAi was characterized as an evolutionarily conserved mechanism as it was observed in different species, such as fungi (Cogoni and Macino, 1999), *Drosophila* (Kennerdell and Carthew, 1998; Hammond *et al.*, 2000), plants (Waterhouse *et al.*, 1998; Hamilton and Baulcombe, 1999) and mammals (Caplen *et al.*, 2001; Elbashir *et al.*, 2001). The mechanisms behind this remarkable pathway have been extensively studied and are reviewed in (Hammond, 2005; Sontheimer, 2005; Tomari and Zamore, 2005; Sen and Blau, 2006; Rana, 2007). Briefly, the dsRNA is processed into siRNAs by the RNase III enzyme Dicer. These siRNAs are incorporated into an effector complex called the RNA-induced silencing complex (RISC) that identifies and silences the complementary mRNA.

RNAi was soon employed from small-scale experimentation to genome-wide scale screening in *Caenorhabditis elegans* using dsRNAs (Fraser *et al.*, 2000; Gonczy *et al.*, 2000). Hopes were raised that this method might also be applicable in mammalian cells, providing a direct causal link between gene sequence and functional data in the form of targeted loss-of-function phenotypes. However, although this method quickly proved successful in cultured *Drosophila melanogaster* cells (Clemens *et al.*, 2000), the use of long dsRNAs to trigger RNAi in mammalian cells was initially hampered by the observation that they elicit an innate antiviral immune response by inducing interferon-linked pathways. Long sequences of dsRNA induce the activation of a cellular dsRNA-dependent protein kinase (PKR) that causes nonspecific destruction of RNA and the inhibition of protein synthesis [see (Williams, 1999)]. Fundamental insights into mammalian RNAi came with the knowledge that target mRNA degradation was guided by the siRNAs resultant from the dsRNAs (Zamore *et al.*, 2000). This indicated that siRNAs induce RNAi in mammalian cells without eliciting a PKR response or inducing antiviral pathways. In fact it was later reported that siRNAs could be transfected into mammalian cells to efficiently induce sequence-specific gene silencing (Caplen *et al.*, 2001; Elbashir *et al.*, 2001). Shortly after, RNAi became a standard laboratory procedure to study gene functions in mammalian systems since it enables the experimental knockdown of a specific gene and through the observation of the subsequent phenotype allows the inference of the function of

the targeted gene. RNAi has been widely used in high-throughput screens in both basic and applied biology [reviewed in (Carpenter and Sabatini, 2004; Friedman and Perrimon, 2004; Willingham *et al.*, 2004; Moffat and Sabatini, 2006; Fuchs and Borkhardt, 2007)] and has also become an excellent method for development of therapeutic agents, from target discovery and validation to the analysis of the mechanisms of action of small molecules [see (Kramer and Cohen, 2004; Ricke *et al.*, 2006)].

The work presented in this PhD thesis took advantage of RNAi and constitutes an additional example of how this technique can be used to address basic biology questions. Furthermore it represents, to our knowledge, the first time that this technology was used as a screening tool to identify factors that influence the outcome of a parasitic infection.

The basic question behind this work was to identify hepatocyte host factors that modulate *Plasmodium* infection. To this end an RNAi approach was applied to *in vitro* *Plasmodium* infection models and the infection phenotype, as a consequence of gene loss-of-function, was evaluated. As mentioned above, chapter 2 describes the use of RNAi to address the functional relevance of a selection of genes found to be differentially expressed throughout *Plasmodium* infection, as revealed by a previous microarray analysis. In chapter 3, entitled "Kinome-wide RNAi screen identifies host PKCζ as a critical kinase for *Plasmodium* sporozoite infection", RNAi was used to address the role of all the known proteins with putative kinase activity, as well as several kinase-interacting proteins, in *P. berghei* sporozoite infection of hepatocytes. In chapter 4, "SR-BI is a crucially required host factor with a dual role in the establishment of malaria liver infection", RNAi was decisive to identify the requirement of the host SR-BI for *Plasmodium* infection.

The extensive use of RNAi to identify host factors important for hepatocyte infection by *Plasmodium* was only successful by following certain guidelines. As with any experiment, the use of appropriate negative controls is, in the case of RNAi, extremely important. The negative controls used in the RNAi screens performed consisted of a negative siRNA, not targeting any annotated genes in the human genome, and of untransfected cells, in which no siRNA was used to transfect the cells. The negative siRNA control is quite valuable because, as it is processed intracellularly, it reflects the effects of using the cell's RNAi processing machinery in the read-out phenotype [see (Huppi *et al.*, 2005)]. Both controls have allowed evaluating the success of each experiment and were essential during data analysis.

Systematic RNAi screens typically comprise multiple passes to achieve an optimal balance between comprehensive coverage, minimization of false negatives and

elimination of false positives, all at acceptable costs and within reasonable timelines [reviewed in (Echeverri and Perrimon, 2006)]. In the first pass, all genes were targeted using at least 3 independent siRNAs and the positive hits, i.e., siRNAs that led to a detectable phenotype, were chosen to undergo a follow-up step. It is commonly accepted that the initial hits will probably include a significant number of false positives due to reagent-specific off-target effects [see (Echeverri *et al.*, 2006; Echeverri and Perrimon, 2006)] and, therefore, the second screening pass is important to refine the relevance of the selected hits with respect to the biological process of interest. In the second pass of the screens all the candidate hit genes were re-tested using the hit siRNA(s) and new siRNA(s) in order to test again a total of 3 siRNAs per gene. At this stage only the genes for which a positive loss-of-function phenotype was confirmed with more than one siRNA were considered as hits. As the specific pattern of transcripts silenced with a given siRNA derives directly from its own nucleotide sequence, the likelyhood that several siRNAs with completely distinct sequences share the same sequence-dependent off-target effect(s) is very low. Therefore, confirmation of an observed phenotype with redundant siRNAs (at least 2), offers the most straightforward and compelling way of demonstrating RNAi target specificity in large-scale screens [see (Echeverri *et al.*, 2006)]. Finally, genes confirmed as "true positives" in the second pass were subjected to a final pass. In the latter the functional phenotypic read-out was repeated in parallel with an assay to measure target gene silencing, namely qRT-PCR, therefore, allowing the confirmation of a direct link between the two.

The success of RNAi screens depends on the overall quality of the final data set, which is associated with the degree to which all sources of variability affect the experimental reproducibility. These comprise factors such as the experimental design, technical implementation, data processing and intrinsic biological variability. The latter was undoubtedly the most important and difficult to control, ranging from cell confluency at the time of transfection and infection to the number of sporozoites obtained from infected mosquitoes and quality of the infections (i.e., the parasite's development within each experiment). In order to evaluate and minimize the data variability from these factors, when possible, the different screening passes were performed twice.

Besides all the different aspects mentioned above there are still other intrinsic aspects of the technique that should be considered. The most basic limitation of all RNAi-based screens is that negative results, that is, the absence of a detectably altered phenotype, cannot be conclusively interpreted. This is due to the fact that RNAi is inherently a knock-down rather than a knock-out technology. Therefore, although

algorithms are developed to design highly efficient siRNAs, the silencing level achieved is rarely of 100% and it is inevitable that these lead to varying loss-of-function degrees. Consequently, some level of the target protein will remain and, depending on the type and turnover of the protein, this may help explain the observation of wild-type phenotypes. Indeed, the threshold (i.e., the degree of silencing) required for achieving a detectable loss-of-function phenotype differs markedly between proteins and depends also on the detection sensitivity of the assay [see (Sachse *et al.*, 2005)]. Taking this into consideration it should be noted that it is possible that, among genes with negative results in the screens performed, there might be host genes that play a role in hepatocyte infection by *Plasmodium* and which we were not able to identify.

On the other hand, while evaluating the positive results, one should keep in mind that it is possible that a stringent direct correlation between the infection phenotype and remaining mRNA is not observed. This might be due to the fact that the activity of some proteins is concentration-dependent and, thus, small differences in the degree of down regulation by different siRNAs against the same target may be sufficient to originate different phenotype levels [see (Huppi *et al.*, 2005)]. Moreover, it is possible that these small differences in the degree of down regulation are not completely distinguished with qRT-PCR, due to biological and/or experimental variability.

The topics presented here were considered while performing the analysis of the data from the different RNAi screens that led to the identification of host factors that seem to modulate hepatocyte infection by *Plasmodium* sporozoites. The work presented in chapter 2 has revealed the host genes Atf3 and c-Myc through the combined use of microarray and RNAi technologies applied to the *in vitro* infection model constituted by the mouse hepatoma cell line Hepa1-6 and *P. berghei* sporozoites. In chapter 3, an RNAi screen comprising a total of 727 human genes, encoding all the known proteins with putative kinase activity as well as several kinase-interacting proteins, was performed using the *in vitro* infection model of human hepatoma Huh7 cells infected with *P. berghei* sporozoites. In this screen six host kinases, specifically MET, PKCι, PKCζ, PRKWNK1, SGK2 and STK35, were identified as playing important roles during *P. berghei* sporozoite infection. Another host factor, SR-BI, was revealed by RNAi as crucially required for *P. berghei* sporozoite infection of Huh7 cells, as described in chapter 4.

Therefore, in conclusion, the use of RNAi has enabled the identification of several host factors as being essential for hepatocyte infection by *Plasmodium* sporozoites. The study of their relevance and specific role during *Plasmodium* infection merits further attention. For instance to assess their relevance in the several steps that constitute a

successful hepatocyte infection by *Plasmodium*, namely cell traversal, hepatocyte invasion and intrahepatocyte parasite development would be extremely important. In fact, some of these questions can be rapidly and efficiently addressed *in vitro* through flow cytometry in conjunction with GFP-expressing *Plasmodium* sporozoites [(Prudêncio *et al.*, 2007), for more details consult this publication, which is provided in Appendix].

A previous study has shown that hepatocyte wounding by sporozoite migration induces the secretion of HGF, which renders hepatocytes susceptible to infection through the activation of MET, HGF's receptor (Carrolo *et al.*, 2003). The malaria parasite exploits MET not as a primary binding site, but as a mediator of signals. HGF/MET signaling induces rearrangements of the host cell actin cytoskeleton that are required for parasite early development within hepatocytes (Carrolo *et al.*, 2003). Moreover, HGF/MET signaling is also essential for protection of *Plasmodium*-infected hepatocytes from apoptosis (Leiriao *et al.*, 2005). This is in agreement with our observation that MET knock-down led to a decrease in infection.

For all the other host factors identified by the RNAi screens, follow-up experiments have to be performed in order to validate and understand their involvement in *Plasmodium* infection. To date we have focused, to different extents, on Atf3, PKCζ and SR-BI and the results obtained support a role for these host factors in *Plasmodium* sporozoite infection of hepatocytes.

Atf3's relevance for *in vivo* infections was successfully proved and evidence suggests that hepatocytes may respond to *P. berghei* infection by increasing expression of Atf3, which, in turn, plays a role in countering infection. Atf3 is a transcription factor linked to several cellular functions, such as stress response, regulation of the cell cycle and apoptosis (Hartman *et al.*, 2004; Yan *et al.*, 2005; Lu *et al.*, 2006; Lu *et al.*, 2007). The exact role that Atf3 plays in *Plasmodium* infection has to be determined. Still, it is quite interesting that Atf3 has been demonstrated by several microarray studies as one of the host genes regulated by diverse microbe infections [reviewed in (Jenner and Young, 2005)].

PKCζ's involvement in *Plasmodium* sporozoite infection has been confirmed with two different approaches. The first consisted of treating cells with a PKCζ pseudo-substrate inhibitor (PKCζInh), which led to a decrease in *P. berghei* infection, both in Hepa1-6 and Huh7 cells as well as mouse primary hepatocytes. Moreover, PKCζInh treatment of human primary hepatocytes also led to a decrease of *P. falciparum* infection in these cells. In addition, PKCζ's relevance was also proved for *in vivo* *Plasmodium* infection, since PKCζ silencing in adult mice by RNAi significantly reduced liver infection by *P. berghei* sporozoites. PKCζ has been implicated in several

signal transduction pathways regulating differentiation, proliferation and apoptosis of mammalian cells [see (Hirai and Chida, 2003; Moscat *et al.*, 2006)]. The specific function of PKCζ in the establishment of a malaria liver infection as well as the mechanism involved clearly merit further attention.

Finally, SR-BI is another host factor identified by our work and for which follow-up experiments have already been performed in order to validate its role in *Plasmodium* infection. SR-BI's requirement for *P. berghei* sporozoite infection of Huh7 cells was recognized originally by siRNAi-gene silencing and further validated through compound- and antibody-inhibition of its function. SR-BI *in vitro* silencing or inhibition had as outcome a decrease in *Plasmodium* infection. Moreover, SR-BI relevance for infection was proved by *ex vivo* and *in vivo* experiments. It was shown that SR-BI silencing or inhibition in mouse primary hepatocytes as well as SR-BI *in vivo* silencing leads to a decrease in *P. berghei* sporozoite infection. Furthermore, inhibition of SR-BI activity in human primary hepatocytes also reduced infection by the human parasite, *P. falciparum.* SR-BI involvement in infection was analyzed in detail and it was observed a role in both sporozoite invasion and subsequent EEF development within the parasitophorous vacuole inside hepatocytes.

SR-BI is an 82-kDa membrane glycoprotein containing a large extracellular domain and two transmembrane domains with short cytoplasmic amino- and carboxy-terminal domains [reviewed in (Krieger, 1999; Zannis *et al.*, 2006)]. SR-BI functions as a multiligand receptor, able to bind with high affinity to a wide variety of apparently unrelated ligands. These include native (VLDL, LDL and HDL) and chemically modified lipoproteins (oxLDL and acLDL), maleylated bovine serum albumin, advanced glycation end-product modified proteins, liposomes containing anionic phospholipids and apoptotic cells [see (Trigatti *et al.*, 2000; Trigatti *et al.*, 2003)].

SR-BI was initially identified as a binding receptor for acLDL, oxLDL and native LDL (Acton *et al.*, 1994). Later, SR-BI was reported as the first molecularly well-defined and functionally active cell-surface HDL receptor capable of mediating selective lipid uptake (Acton *et al.*, 1996). Interestingly, it has been shown that SR-BI interaction with HDL differs from that with LDL (Gu *et al.*, 2000b). While HDL competes effectively for the binding of LDL to SR-BI, LDL can only partially compete for HDL binding to SR-BI. This phenomenon suggests that SR-BI possesses multiple binding sites with differing ligand binding properties [see (Krieger, 2001)].

The cellular uptake of cholesterol from the hydrophobic cores of lipoproteins by SR-BI occurs initially through the binding of the lipoprotein to the cell outer surface, as is the case for the classic LDLR. However, SR-BI's mechanism of lipid uptake after lipoprotein binding differs markedly from that of LDLR. Whereas LDLR mediates

endocytosis of the intact lipoprotein particle via coated pits and vesicles and its subsequent hydrolysis in lysosomes [reviewed in (Hussain *et al.*, 1999)], SR-BI mediates the selective uptake of HDL's cholesteryl esters. During this selective uptake the lipid is efficiently transferred from the lipoprotein's hydrophobic core to cells while the lipid-depleted apolipoprotein-containing shell is released to the extracellular space [see (Krieger, 2001)]. In addition to its role in the selective uptake of HDL cholesteryl esters, SR-BI stimulates the bi-directional flux of free cholesterol between cells and HDL and in fact the rate of cholesterol efflux from various cell types correlates with the expression of SR-BI (de la Llera-Moya *et al.*, 1999; Gu *et al.*, 2000a; Yancey *et al.*, 2000).

SR-BI is highly conserved and, although expressed in various cells, its highest expression occurs in organs with critical roles in cholesterol metabolism (i.e. liver) and steroidogenesis (i.e. adrenal, ovary, testis) (Acton *et al.*, 1994; Acton *et al.*, 1996; Calvo *et al.*, 1997). Studies using Chinese hamster ovary cells (CHO) have shown that SR-BI localizes to caveolae (Babitt *et al.*, 1997; Graf *et al.*, 1999), which are cholesterol- and sphingomyelin-rich microdomains in the plasma membrane [see (Parton and Simons, 2007)]. Surprisingly, in mouse hepatocyte couplets, SR-BI has been localized on both canalicular (apical) and sinusoidal (basolateral) membranes but, also in juxtanuclear compartments, which were identified as the endosomal recycling compartment (ERC) [(Silver *et al.*, 2001) and reviewed in (Rhainds and Brissette, 2004)]. Moreover, evidence of SR-BI internalization has been provided, which suggests that SR-BI can undergo rapid endocytosis from the cell surface (Silver *et al.*, 2001).

SR-BI has been involved in several pathogen infections. Recently, a *Drosophila* RNAi screen aiming the identification of host factors required for uptake and growth of mycobacteria has shown that SR-BI mediates the uptake of *Mycobacterium fortuitum*, *Escherichia coli* and *Staphylococcus aureus* (Philips *et al.*, 2005). In addition, a different study has provided evidence that SR-BI mediates *E. coli* K1 and K12, *S. aureus*, *Salmonella typhimurium* and *Listeria monocytogenes* bacterial adhesion and cytosolic invasion in mammalian cells (Vishnyakova *et al.*, 2006).

SR-BI was also identified as a novel receptor for the Hepatitis C Virus (HCV) (Scarselli *et al.*, 2002). Several studies have tried to define the role of SR-BI in HCV cell entry [reviewed in (Tellinghuisen *et al.*, 2007)]. It has been shown that antibodies against SR-BI, BLT-2 and BLT-4, and siRNAs targeting SR-BI inhibit HCV infection (Bartosch *et al.*, 2003b; Lavillette *et al.*, 2005; Voisset *et al.*, 2005) while SR-BI expression level in Huh7.5 cells modulates the level of HCV infection (Grove *et al.*, 2007). Moreover, HDL and oxLDL, two natural ligands of SR-BI, were shown to modulate HCV infectivity in different ways. While HDL facilitates HCV entry into host cells in an SR-BI-dependent

manner (Bartosch *et al.*, 2005; Voisset *et al.*, 2005), oxLDL is a potent HCV entry inhibitor (von Hahn *et al.*, 2006). In addition it has been observed that LDL and VLDL have no effect on HCV infection of host cells (Bartosch *et al.*, 2005; Voisset *et al.*, 2005). SR-BI has been shown to interact with HCV envelope glycoprotein E2 (Scarselli *et al.*, 2002), suggesting that it might be involved at some step of HCV's entry into its host. However, the exact role of SR-BI in invasion by HCV is far from understood. Ectopic expression of this molecule in non-liver cell lines does not lead to HCV entry, which suggests that additional molecule(s) is/are required for HCV entry (Bartosch *et al.*, 2003b). Alternatively, it has been suggested that SR-BI may have the capacity to traffic HCV virions to low pH compartments where the fusion of HCV may occur or that SR-BI might modulate the lipid composition of the plasma membrane to render the membrane permissive to HCV entry [reviewed in (Cocquerel *et al.*, 2006)].

Although its role is not fully understood, SR-BI's importance for HCV infection has already been extensively addressed. Our work describes for the first time SR-BI's involvement in *Plasmodium* infection. Our results show that, like for HCV, SR-BI silencing by RNAi or its blockage with specific antibodies or chemical inhibitors have an inhibitory effect on *Plasmodium* infection. Similarly, we have observed that HDL has a mild positive effect on infection while oxLDL or acLDL inhibit infection and LDL has no effect. Furthermore, we have shown that SR-BI plays a role not only in invasion but also on parasite development inside the hepatocyte. Its exact function(s) in these two steps still remain(s) to be elucidated.

SR-BI's role in both HCV and *Plasmodium* infection, two liver infectious agents, suggests that these pathogens have developed common strategies that allow them to infect their host cells. This notion is further supported by the fact that both *Plasmodium* sporozoites (Pancake *et al.*, 1992; Frevert *et al.*, 1993) and HCV (Barth *et al.*, 2003; Koutsoudakis *et al.*, 2006) interact with heparan sulfate proteoglycans and also by the observation that another host molecule, the tetraspanin CD81, is involved in both HCV and *Plasmodium* infection.

CD81 was identified as a candidate HCV receptor based on its ability to bind the virus envelope protein E2 (Pileri *et al.*, 1998). Several studies have confirmed CD81's involvement in HCV entry [see (Favre and Muellhaupt, 2005; Cocquerel *et al.*, 2006)]. Indeed, it was observed that HCV presents a restricted tropism for human hepatic cell lines expressing CD81 (Bartosch *et al.*, 2003a; Bartosch *et al.*, 2003b; Hsu *et al.*, 2003; Cormier *et al.*, 2004; Zhang *et al.*, 2004). Moreover, anti-CD81 mAbs inhibit the entry of HCV into hepatoma cell lines (Hsu *et al.*, 2003; Cormier *et al.*, 2004; Zhang *et al.*, 2004; Lindenbach *et al.*, 2005) and CD81 siRNA-silencing abolishes infection of Huh7 cells by HCV (Zhang *et al.*, 2004). In addition, it has also been shown that the human

hepatoma cell line HepG2, which does not express CD81 and, therefore, is not infected by HCV, becomes susceptible to infection upon CD81 ectopic expression (Bartosch *et al.*, 2003b; Cormier *et al.*, 2004; Zhang *et al.*, 2004; Lavillette *et al.*, 2005; Lindenbach *et al.*, 2005).

The exact role of CD81 in HCV entry is also not well understood. Nevertheless, although its role in virus entry has been confirmed, CD81 ectopic expression in non-hepatic cell lines does not lead to HCV entry, which again suggests that additional molecule(s) is/are needed for HCV entry (Bartosch *et al.*, 2003b; Cormier *et al.*, 2004). It has been proposed that CD81 may function as a post-attachment entry co-receptor, i.e., that CD81 might play a role after binding of the particle to a first receptor (Cormier *et al.*, 2004). This hypothesis is supported by the fact that tetraspanins are able to form lateral associations with multiple partner proteins and with each other in a dynamic assembly, described as the "tetraspanin web" [see (Boucheix and Rubinstein, 2001)]. Additional experimental evidence is still needed to confirm such a role.

CD81 was also identified as an important molecule required for hepatocyte invasion by the rodent *P. yoelii* and the human malaria *P. falciparum* parasites (Silvie *et al.*, 2003). It was shown that *P. yoelii* sporozoites fail to infect CD81-deficient mouse hepatocytes and antibodies against human and mouse CD81 inhibit the hepatic development of *P. falciparum* and *P. yoelii*, respectively (Silvie *et al.*, 2003). On the other hand, the rodent parasite *P. berghei* can use both CD81-dependent and -independent pathways to enter the hepatocyte (Silvie *et al.*, 2003; Silvie *et al.*, 2007). It has been shown that *P. berghei* sporozoites use a CD81-independent pathway to infect CD81-negative cells, such as HepG2 and CD81 KO mouse hepatocytes, as well as CD81-positive cells, such as Huh7 or HeLa, in which it was observed that CD81 silencing or antibody-blockage does not alter *P. berghei* infection (Silvie *et al.*, 2003; Silvie *et al.*, 2007). Conversely, similarly to *P. yoelii*, *P. berghei* sporozoites use a CD81-dependent pathway to infect Hepa1-6 cells, since in these cells infection is blocked/reduced by anti-CD81 antibody, CD81 siRNA and cholesterol depletion (Silvie *et al.*, 2007).

To date, the precise role of CD81 in *P. yoelii* and *P. falciparum* infection remains elusive. Tetraspanin-enriched microdomains, which depend on membrane cholesterol, have been shown to contribute to CD81-dependent infection by *P. yoelii* and *P. falciparum* sporozoites (Silvie *et al.*, 2006a). In addition, attempts to identify a sporozoite ligand for CD81 have not yet revealed a binding partner for this protein (Silvie *et al.*, 2003). Taking this into consideration, it has been proposed that within tetraspanin-enriched microdomains, CD81 may regulate the activity of a partner host

membrane molecule which plays an essential role during sporozoite invasion (Silvie *et al.*, 2006a). Additionally, it has also been proposed that CD81 may play a role during the early stages of PV formation, since it was observed that the few *P. yoelii* sporozoites that do invade CD81-negative cells are found without a vacuole, developing in the nucleus (Silvie *et al.*, 2006b).

Thus, since SR-BI, HSPGs and CD81 have been revealed as important for HCV and *Plasmodium* infection, it is tempting to speculate that altogether these host factors might account for pathogen tissue tropism towards the liver and pathogenicity. A synergy between SR-BI and CD81 functions has already been described in HCV infection (Kapadia *et al.*, 2007). It would be extremely important to address this issue in *Plasmodium* infection. In order to do so, CD81-dependent infection models would have to be used namely the *P. yoelii* and/or *P. falciparum* parasites. It would also be possible to use *P. berghei* but only in combination with Hepa1-6, since it has been shown that this infection model is CD81-dependent, contrary to Huh7 infection by *P. berghei*, which is CD81-independent. For example, this question could initially be addressed by cell treatment with specific antibodies against CD81 and SR-BI or by siRNA-gene silencing for both genes.

It should also be considered that CD81 and SR-BI are probably not the only host cell factors important for HCV and *Plasmodium* infection. Actually, for *Plasmodium* infection, other host factors, namely HGF, L-FABP and ApoA1, have already been disclosed as playing important roles in this process. To reconcile their functions is quite challenging.

Regarding SR-BI, the work that has already been developed and is presented in Chapter 4 provides strong evidence of its crucial role for *Plasmodium* infection. Still to complement the RNAi *in vivo* experiments, in which SR-BI was silenced and *Plasmodium* liver infection was determined, it would be extremely important to test if SR-BI-deficient mice are susceptible to *Plasmodium* liver infection. In fact, we have already observed a reduction in *P. berghei* liver infection in SR-BI heterozygous in comparison to wild-type mice (data not show). However, to test homozygous KO mice would be an appropriate strategy, but until now, this has not been possible due to difficulties in obtaining these mice. These difficulties are related to the fact that homozygous female SR-BI KO mice are infertile, therefore, homozygous *vs.* homozygous breedings are nonproductive (Miettinen *et al.*, 2001). Moreover, intercrosses of SR-BI heterozygous mice on a mixed C57BL6/129 background result in a non-Mendelian transmission of the SR-BI KO allele and subsequently a low frequency of homozygous mice is obtained (Rigotti *et al.*, 1997). An alternative option would be to test *Plasmodium* infection *in vivo* in PDZK1-deficient mice. PDZK1 is a

multi-PDZ domain containing adaptor protein, known to interact with SR-BI [see (Yesilaltay *et al.*, 2005)]. It has been shown that PDZK1 controls in a tissue-specific and post-transcriptional fashion SR-BI *in vivo* expression. PDZK1-deficient mice have greatly diminished surface expression of SR-BI in the liver, i.e., a 85-95% reduction of SR-BI protein expression has been observed (Kocher *et al.*, 2003). Recently, these mice have become commercially available through The Jackson Laboratory (http://www.jax.org/) and they will be tested earlier in the future.

A different strategy to prove that SR-BI is essential for host cell infection by *Plasmodium*, already ongoing in our laboratory, consists on testing the effect of SR-BI overexpression in different cell lines. It can be expected that SR-BI overexpression in hepatic cells known to support *Plasmodium* sporozoite infection will lead to an infection increase, while SR-BI overexpression in non-hepatic cells that do not support sporozoite infection would turn them susceptible to infection. However, it is also possible that the latter assumption cannot be observed, which would suggest that, although SR-BI is important, additional host molecule(s) is/are needed for *Plasmodium* infection.

As previously mentioned, SR-BI plays a dual role in *Plasmodium* infection, it is important for sporozoite invasion and also for parasite intracellular development. Therefore, understanding SR-BI's exact function in these two steps of *Plasmodium* infection constitutes one of our next objectives.

In terms of invasion one can speculate on a direct or on an indirect interaction between sporozoites and SR-BI. A direct interaction between sporozoites and SR-BI is supported by the observation that modLDL, in particular oxLDL and acLDL, inhibit sporozoite invasion. It is tempting to picture a "modLDL-mimic" model, in which the sporozoite would be interacting directly with SR-BI through a mode of binding similar with that of modLDL forms, but not with that normally used by HDL. This hypothesis can be ascertained by the observation of a direct binding between sporozoites and SR-BI and, furthermore, by the identification of the sporozoite molecule that interacts with SR-BI. An indirect interaction would imply that the sporozoites would interact directly with HDL particles and benefit from their high affinity binding to SR-BI. This "HDL-piggyback" model would be based on the sporozoite's ability to associate with HDL and would explain HDL's slightly positive effect on invasion.

Besides how SR-BI and sporozoites interact, another important question is if and how does SR-BI contribute to sporozoite internalization? It is possible that SR-BI might not play an active role during sporozoite invasion and instead this host factor would only serve as a "docking" site. In this scenario the sporozoite would enter the host cell by

engaging an active process, as previously shown for *Toxoplasma gondii* (Dobrowolski and Sibley, 1996). If, on the other hand, SR-BI plays an active role during *Plasmodium* invasion, this must somehow be related with its mode of action. SR-BI has been mainly characterized to mediate the selective uptake of cholesteryl esters from bound HDL or LDL without triggering an endocytic or phagocytic event [see (Krieger, 2001)]. Taking into consideration only this SR-BI mode of action it is not obvious how sporozoites would be able to enter the hepatocyte. However, it has also been shown that HDL is able to enter HepG2 cells by endocytosis (Wustner *et al.*, 2004), therefore, it is possible and more logical that sporozoites could invade hepatocytes by endocytosis.

Moreover, it is also possible that our observations are due to a side effect of interfering with SR-BI's pathway, such as an alteration of the membrane composition (i.e. re-arrangement or destruction of lipid rafts) and, in fact, downstream signalling events and/or another receptor would be involved in *Plasmodium* invasion.

Concerning SR-BI's role in *Plasmodium* development within hepatocytes, it is tempting to speculate that SR-BI may participate in a mechanism that would provide cholesteryl esters and other lipids to the parasite across the PV membrane, since during this phase the parasite undergoes an amazing proliferation process. The knowledge that other cholesterol-related proteins, ApoA1 and L-FABP, are also important for *Plasmodium* infection supports this hypoyhesis.

ApoA1 is the major structural apolipoprotein of HDL, and it has been observed to interact with the UIS4 sporozoite protein and co-localize in the PV 24 hours after sporozoite infection [Mueller and Matuschewski, unpublished data referenced in (Prudêncio *et al.*, 2006b)]. Our observation of a subcellular accumulation of SR-BI around EEFs together with this knowledge of ApoA1 co-localization on PV supports the hypothesis that SR-BI would be "feeding" the parasite with cholesteryl esters and other lipids.

L-FABP, is the main cytoplasmic carrier of fatty acids in hepatocytes. Down-regulation of its expression in hepatocytes severely impairs parasite growth while its overexpression promotes growth. L-FABP has been shown to interact with the UIS3 sporozoite protein through a two-hybrid system and, although no direct interaction has been shown in infected hepatocytes, it has been suggested that the UIS3 parasite association with L-FABP would allow the parasite to acquire fatty acids (Mikolajczak *et al.*, 2007). Thus, this can represent a totally different alternative mechanism that the parasite has to access cholesterol or, instead it might be linked to SR-BI "feeding" mechanism. It is known that free cholesterol obtained from the SR-BI pathway normally reaches the endoplasmic reticulum, a cholesterol regulatory compartment,

through cholesterol diffusion into membranes. However, it is possible that intracellular transport proteins may help to deliver cholesterol to cell surface-remote compartments and, in hepatocytes, L-FABP would be a good candidate for this transport, since it binds fatty acids and cholesterol, both of which are products of cholesteryl ester hydrolysis [see (Rhainds and Brissette, 2004)]. This hypothesis is further supported by the observation that SR-BI overexpression in HepG2 cells increases L-FABP expression (Rhainds *et al.*, 2004).

In addition, it has recently been shown that *Plasmodium* preferentially develops in the host juxtanuclear region and its PV forms an association with the host endoplasmic reticulum (Bano *et al.*, 2007). Moreover, it was reported that during intrahepatic development *Plasmodium* actively modifies the permeability of its vacuole to allow the transfer of a large variety of molecules from the host cytosol to the vacuolar space through open channels (Bano *et al.*, 2007).

Altogether the data presented and referenced strongly indicate that the parasite needs cholesterol and that it is able to acquire it through the manipulation of one or more pathways. In order to access if any of the hypothesis formulated are true it is important to explore the combined function of these cholesterol-related host factors during *Plasmodium* development. Although quite challenging, this approach will certainly reveal new insights into *Plasmodium* liver stage infection.

In conclusion, we have identified a number of host factors that are important for hepatocyte infection by *Plasmodium*. This study provides a crucial basis for the more extensive studies that are required to understand the role of the now-revealed host molecules as well as to identify additional ones. The study of *Plasmodium* liver stage infection is extremely important to develop prophylactic strategies. In fact, if infection is blocked at this stage, there will be no pathology and consequently no disease. The major concerns regarding the prophylaxis strategies are drug resistance and toxicity if the drug target is parasite or host-derived, respectively. With increasing knowledge of the molecular mechanisms underlying parasite invasion and development in the liver, it might become possible to design drugs that do not interfere with normal liver functions but do prevent infection.

References

Acton, S., Rigotti, A., Landschulz, K.T., Xu, S., Hobbs, H.H., and Krieger, M. (1996). Identification of scavenger receptor SR-BI as a high density lipoprotein receptor. Science *271*, 518-520.

Acton, S.L., Scherer, P.E., Lodish, H.F., and Krieger, M. (1994). Expression cloning of SR-BI, a CD36-related class B scavenger receptor. J Biol Chem *269*, 21003-21009.

Alberts, B., Johnson, A., Lewis, J., Raff, M., Roberts, K., and Walter, P. (2002). Methods: Manipulating Proteins, DNA, and RNA. Studying Gene Expression and Function. In: Molecular biology of the cell, 4th Edition. Garland Science, Taylor & Francis Group, New York,.

Babitt, J., Trigatti, B., Rigotti, A., Smart, E.J., Anderson, R.G., Xu, S., and Krieger, M. (1997). Murine SR-BI, a high density lipoprotein receptor that mediates selective lipid uptake, is N-glycosylated and fatty acylated and colocalizes with plasma membrane caveolae. J Biol Chem *272*, 13242-13249.

Bano, N., Romano, J.D., Jayabalasingham, B., and Coppens, I. (2007). Cellular interactions of Plasmodium liver stage with its host mammalian cell. Int J Parasitol.

Barth, H., Schafer, C., Adah, M.I., Zhang, F., Linhardt, R.J., Toyoda, H., Kinoshita-Toyoda, A., Toida, T., Van Kuppevelt, T.H., Depla, E., Von Weizsacker, F., Blum, H.E., and Baumert, T.F. (2003). Cellular binding of hepatitis C virus envelope glycoprotein E2 requires cell surface heparan sulfate. J Biol Chem *278*, 41003-41012.

Bartosch, B., Dubuisson, J., and Cosset, F.L. (2003a). Infectious hepatitis C virus pseudo-particles containing functional E1-E2 envelope protein complexes. J Exp Med *197*, 633-642.

Bartosch, B., Verney, G., Dreux, M., Donot, P., Morice, Y., Penin, F., Pawlotsky, J.M., Lavillette, D., and Cosset, F.L. (2005). An interplay between hypervariable region 1 of the hepatitis C virus E2 glycoprotein, the scavenger receptor BI, and high-density lipoprotein promotes both enhancement of infection and protection against neutralizing antibodies. J Virol *79*, 8217-8229.

Bartosch, B., Vitelli, A., Granier, C., Goujon, C., Dubuisson, J., Pascale, S., Scarselli, E., Cortese, R., Nicosia, A., and Cosset, F.L. (2003b). Cell entry of hepatitis C virus requires a set of co-receptors that include the CD81 tetraspanin and the SR-B1 scavenger receptor. J Biol Chem *278*, 41624-41630.

Boucheix, C., and Rubinstein, E. (2001). Tetraspanins. Cell Mol Life Sci *58*, 1189-1205.

Calvo, D., Gomez-Coronado, D., Lasuncion, M.A., and Vega, M.A. (1997). CLA-1 is an 85-kD plasma membrane glycoprotein that acts as a high-affinity receptor for both native (HDL, LDL, and VLDL) and modified (OxLDL and AcLDL) lipoproteins. Arterioscler Thromb Vasc Biol *17*, 2341-2349.

Caplen, N.J., Parrish, S., Imani, F., Fire, A., and Morgan, R.A. (2001). Specific inhibition of gene expression by small double-stranded RNAs in invertebrate and vertebrate systems. Proc Natl Acad Sci U S A *98*, 9742-9747.

Carpenter, A.E., and Sabatini, D.M. (2004). Systematic genome-wide screens of gene function. Nat Rev Genet *5*, 11-22.

Carrolo, M., Giordano, S., Cabrita-Santos, L., Corso, S., Vigario, A.M., Silva, S., Leiriao, P., Carapau, D., Armas-Portela, R., Comoglio, P.M., Rodriguez, A., and Mota, M.M. (2003).

Hepatocyte growth factor and its receptor are required for malaria infection. Nat Med *9*, 1363-1369.

Clemens, J.C., Worby, C.A., Simonson-Leff, N., Muda, M., Maehama, T., Hemmings, B.A., and Dixon, J.E. (2000). Use of double-stranded RNA interference in Drosophila cell lines to dissect signal transduction pathways. Proc Natl Acad Sci U S A *97*, 6499-6503.

Cocquerel, L., Voisset, C., and Dubuisson, J. (2006). Hepatitis C virus entry: potential receptors and their biological functions. J Gen Virol *87*, 1075-1084.

Cogoni, C., and Macino, G. (1999). Gene silencing in Neurospora crassa requires a protein homologous to RNA-dependent RNA polymerase. Nature *399*, 166-169.

Cormier, E.G., Tsamis, F., Kajumo, F., Durso, R.J., Gardner, J.P., and Dragic, T. (2004). CD81 is an entry coreceptor for hepatitis C virus. Proc Natl Acad Sci U S A *101*, 7270-7274.

de la Llera-Moya, M., Rothblat, G.H., Connelly, M.A., Kellner-Weibel, G., Sakr, S.W., Phillips, M.C., and Williams, D.L. (1999). Scavenger receptor BI (SR-BI) mediates free cholesterol flux independently of HDL tethering to the cell surface. J Lipid Res *40*, 575-580.

Dobrowolski, J.M., and Sibley, L.D. (1996). Toxoplasma invasion of mammalian cells is powered by the actin cytoskeleton of the parasite. Cell *84*, 933-939.

Echeverri, C.J., Beachy, P.A., Baum, B., Boutros, M., Buchholz, F., Chanda, S.K., Downward, J., Ellenberg, J., Fraser, A.G., Hacohen, N., Hahn, W.C., Jackson, A.L., Kiger, A., Linsley, P.S., Lum, L., Ma, Y., Mathey-Prevot, B., Root, D.E., Sabatini, D.M., Taipale, J., Perrimon, N., and Bernards, R. (2006). Minimizing the risk of reporting false positives in large-scale RNAi screens. Nat Methods *3*, 777-779.

Echeverri, C.J., and Perrimon, N. (2006). High-throughput RNAi screening in cultured cells: a user's guide. Nat Rev Genet *7*, 373-384.

Elbashir, S.M., Harborth, J., Lendeckel, W., Yalcin, A., Weber, K., and Tuschl, T. (2001). Duplexes of 21-nucleotide RNAs mediate RNA interference in cultured mammalian cells. Nature *411*, 494-498.

Favre, D., and Muellhaupt, B. (2005). Potential cellular receptors involved in hepatitis C virus entry into cells. Lipids Health Dis *4*, 9.

Fire, A., Xu, S., Montgomery, M.K., Kostas, S.A., Driver, S.E., and Mello, C.C. (1998). Potent and specific genetic interference by double-stranded RNA in Caenorhabditis elegans. Nature *391*, 806-811.

Fraser, A.G., Kamath, R.S., Zipperlen, P., Martinez-Campos, M., Sohrmann, M., and Ahringer, J. (2000). Functional genomic analysis of C. elegans chromosome I by systematic RNA interference. Nature *408*, 325-330.

Frevert, U., Sinnis, P., Cerami, C., Shreffler, W., Takacs, B., and Nussenzweig, V. (1993). Malaria circumsporozoite protein binds to heparan sulfate proteoglycans associated with the surface membrane of hepatocytes. J Exp Med *177*, 1287-1298.

Friedman, A., and Perrimon, N. (2004). Genome-wide high-throughput screens in functional genomics. Curr Opin Genet Dev *14*, 470-476.

Fuchs, U., and Borkhardt, A. (2007). The application of siRNA technology to cancer biology discovery. Adv Cancer Res *96*, 75-102.

Gonczy, P., Echeverri, C., Oegema, K., Coulson, A., Jones, S.J., Copley, R.R., Duperon, J., Oegema, J., Brehm, M., Cassin, E., Hannak, E., Kirkham, M., Pichler, S., Flohrs, K., Goessen, A., Leidel, S., Alleaume, A.M., Martin, C., Ozlu, N., Bork, P., and Hyman, A.A.

(2000). Functional genomic analysis of cell division in C. elegans using RNAi of genes on chromosome III. Nature *408*, 331-336.

Graf, G.A., Connell, P.M., van der Westhuyzen, D.R., and Smart, E.J. (1999). The class B, type I scavenger receptor promotes the selective uptake of high density lipoprotein cholesterol ethers into caveolae. J Biol Chem *274*, 12043-12048.

Grove, J., Huby, T., Stamataki, Z., Vanwolleghem, T., Meuleman, P., Farquhar, M., Schwarz, A., Moreau, M., Owen, J.S., Leroux-Roels, G., Balfe, P., and McKeating, J.A. (2007). Scavenger receptor BI and BII expression levels modulate hepatitis C virus infectivity. J Virol *81*, 3162-3169.

Gu, X., Kozarsky, K., and Krieger, M. (2000a). Scavenger receptor class B, type I-mediated [3H]cholesterol efflux to high and low density lipoproteins is dependent on lipoprotein binding to the receptor. J Biol Chem *275*, 29993-30001.

Gu, X., Lawrence, R., and Krieger, M. (2000b). Dissociation of the high density lipoprotein and low density lipoprotein binding activities of murine scavenger receptor class B type I (mSR-BI) using retrovirus library-based activity dissection. J Biol Chem *275*, 9120-9130.

Hamilton, A.J., and Baulcombe, D.C. (1999). A species of small antisense RNA in posttranscriptional gene silencing in plants. Science *286*, 950-952.

Hammond, S.M. (2005). Dicing and slicing: the core machinery of the RNA interference pathway. FEBS Lett *579*, 5822-5829.

Hammond, S.M., Bernstein, E., Beach, D., and Hannon, G.J. (2000). An RNA-directed nuclease mediates post-transcriptional gene silencing in Drosophila cells. Nature *404*, 293-296.

Hartman, M.G., Lu, D., Kim, M.L., Kociba, G.J., Shukri, T., Buteau, J., Wang, X., Frankel, W.L., Guttridge, D., Prentki, M., Grey, S.T., Ron, D., and Hai, T. (2004). Role for activating transcription factor 3 in stress-induced beta-cell apoptosis. Mol Cell Biol *24*, 5721-5732.

Hirai, T., and Chida, K. (2003). Protein kinase Czeta (PKCzeta): activation mechanisms and cellular functions. J Biochem (Tokyo) *133*, 1-7.

Hsu, M., Zhang, J., Flint, M., Logvinoff, C., Cheng-Mayer, C., Rice, C.M., and McKeating, J.A. (2003). Hepatitis C virus glycoproteins mediate pH-dependent cell entry of pseudotyped retroviral particles. Proc Natl Acad Sci U S A *100*, 7271-7276.

Huppi, K., Martin, S.E., and Caplen, N.J. (2005). Defining and assaying RNAi in mammalian cells. Mol Cell *17*, 1-10.

Hussain, M.M., Strickland, D.K., and Bakillah, A. (1999). The mammalian low-density lipoprotein receptor family. Annu Rev Nutr *19*, 141-172.

Jenner, R.G., and Young, R.A. (2005). Insights into host responses against pathogens from transcriptional profiling. Nat Rev Microbiol *3*, 281-294.

Kapadia, S.B., Barth, H., Baumert, T., McKeating, J.A., and Chisari, F.V. (2007). Initiation of hepatitis C virus infection is dependent on cholesterol and cooperativity between CD81 and scavenger receptor B type I. J Virol *81*, 374-383.

Kennerdell, J.R., and Carthew, R.W. (1998). Use of dsRNA-mediated genetic interference to demonstrate that frizzled and frizzled 2 act in the wingless pathway. Cell *95*, 1017-1026.

Kocher, O., Yesilaltay, A., Cirovic, C., Pal, R., Rigotti, A., and Krieger, M. (2003). Targeted disruption of the PDZK1 gene in mice causes tissue-specific depletion of the high density

lipoprotein receptor scavenger receptor class B type I and altered lipoprotein metabolism. J Biol Chem *278*, 52820-52825.

Koutsoudakis, G., Kaul, A., Steinmann, E., Kallis, S., Lohmann, V., Pietschmann, T., and Bartenschlager, R. (2006). Characterization of the early steps of hepatitis C virus infection by using luciferase reporter viruses. J Virol *80*, 5308-5320.

Kramer, R., and Cohen, D. (2004). Functional genomics to new drug targets. Nat Rev Drug Discov *3*, 965-972.

Krieger, M. (1999). Charting the fate of the "good cholesterol": identification and characterization of the high-density lipoprotein receptor SR-BI. Annu Rev Biochem *68*, 523-558.

Krieger, M. (2001). Scavenger receptor class B type I is a multiligand HDL receptor that influences diverse physiologic systems. J Clin Invest *108*, 793-797.

Lavillette, D., Tarr, A.W., Voisset, C., Donot, P., Bartosch, B., Bain, C., Patel, A.H., Dubuisson, J., Ball, J.K., and Cosset, F.L. (2005). Characterization of host-range and cell entry properties of the major genotypes and subtypes of hepatitis C virus. Hepatology *41*, 265-274.

Leiriao, P., Albuquerque, S.S., Corso, S., van Gemert, G.J., Sauerwein, R.W., Rodriguez, A., Giordano, S., and Mota, M.M. (2005). HGF/MET signalling protects Plasmodium-infected host cells from apoptosis. Cell Microbiol *7*, 603-609.

Leiriao, P., Rodrigues, C.D., Albuquerque, S.S., and Mota, M.M. (2004). Survival of protozoan intracellular parasites in host cells. EMBO Rep *5*, 1142-1147.

Lindenbach, B.D., Evans, M.J., Syder, A.J., Wolk, B., Tellinghuisen, T.L., Liu, C.C., Maruyama, T., Hynes, R.O., Burton, D.R., McKeating, J.A., and Rice, C.M. (2005). Complete replication of hepatitis C virus in cell culture. Science *309*, 623-626.

Lu, D., Chen, J., and Hai, T. (2007). The regulation of ATF3 gene expression by mitogen-activated protein kinases. Biochem J *401*, 559-567.

Lu, D., Wolfgang, C.D., and Hai, T. (2006). Activating transcription factor 3, a stress-inducible gene, suppresses Ras-stimulated tumorigenesis. J Biol Chem *281*, 10473-10481.

Miettinen, H.E., Rayburn, H., and Krieger, M. (2001). Abnormal lipoprotein metabolism and reversible female infertility in HDL receptor (SR-BI)-deficient mice. J Clin Invest *108*, 1717-1722.

Mikolajczak, S.A., Jacobs-Lorena, V., MacKellar, D.C., Camargo, N., and Kappe, S.H. (2007). L-FABP is a critical host factor for successful malaria liver stage development. Int J Parasitol *37*, 483-489.

Moffat, J., and Sabatini, D.M. (2006). Building mammalian signalling pathways with RNAi screens. Nat Rev Mol Cell Biol *7*, 177-187.

Moscat, J., Rennert, P., and Diaz-Meco, M.T. (2006). PKCzeta at the crossroad of NF-kappaB and Jak1/Stat6 signaling pathways. Cell Death Differ *13*, 702-711.

Pancake, S.J., Holt, G.D., Mellouk, S., and Hoffman, S.L. (1992). Malaria sporozoites and circumsporozoite proteins bind specifically to sulfated glycoconjugates. J Cell Biol *117*, 1351-1357.

Parton, R.G., and Simons, K. (2007). The multiple faces of caveolae. Nat Rev Mol Cell Biol *8*, 185-194.

Philips, J.A., Rubin, E.J., and Perrimon, N. (2005). Drosophila RNAi screen reveals CD36 family member required for mycobacterial infection. Science *309*, 1251-1253.

Pileri, P., Uematsu, Y., Campagnoli, S., Galli, G., Falugi, F., Petracca, R., Weiner, A.J., Houghton, M., Rosa, D., Grandi, G., and Abrignani, S. (1998). Binding of hepatitis C virus to CD81. Science *282*, 938-941.

Prudêncio, M., Rodrigues, C.D., Ataide, R., and Mota, M.M. (2007). Dissecting in vitro host cell infection by Plasmodium sporozoites using flow cytometry. Cell Microbiol.

Prudêncio, M., Rodrigues, C.D., and Mota, M.M. (2006a). The relevance of host genes in malaria. SEB Exp Biol Ser *58*, 47-91.

Prudêncio, M., Rodriguez, A., and Mota, M.M. (2006b). The silent path to thousands of merozoites: the Plasmodium liver stage. Nat Rev Microbiol *4*, 849-856.

Rana, T.M. (2007). Illuminating the silence: understanding the structure and function of small RNAs. Nat Rev Mol Cell Biol *8*, 23-36.

Rhainds, D., Bourgeois, P., Bourret, G., Huard, K., Falstrault, L., and Brissette, L. (2004). Localization and regulation of SR-BI in membrane rafts of HepG2 cells. J Cell Sci *117*, 3095-3105.

Rhainds, D., and Brissette, L. (2004). The role of scavenger receptor class B type I (SR-BI) in lipid trafficking. defining the rules for lipid traders. Int J Biochem Cell Biol *36*, 39-77.

Ricke, D.O., Wang, S., Cai, R., and Cohen, D. (2006). Genomic approaches to drug discovery. Curr Opin Chem Biol *10*, 303-308.

Rigotti, A., Trigatti, B.L., Penman, M., Rayburn, H., Herz, J., and Krieger, M. (1997). A targeted mutation in the murine gene encoding the high density lipoprotein (HDL) receptor scavenger receptor class B type I reveals its key role in HDL metabolism. Proc Natl Acad Sci U S A *94*, 12610-12615.

Sachse, C., Krausz, E., Kronke, A., Hannus, M., Walsh, A., Grabner, A., Ovcharenko, D., Dorris, D., Trudel, C., Sonnichsen, B., and Echeverri, C.J. (2005). High-throughput RNA interference strategies for target discovery and validation by using synthetic short interfering RNAs: functional genomics investigations of biological pathways. Methods Enzymol *392*, 242-277.

Scarselli, E., Ansuini, H., Cerino, R., Roccasecca, R.M., Acali, S., Filocamo, G., Traboni, C., Nicosia, A., Cortese, R., and Vitelli, A. (2002). The human scavenger receptor class B type I is a novel candidate receptor for the hepatitis C virus. Embo J *21*, 5017-5025.

Sen, G.L., and Blau, H.M. (2006). A brief history of RNAi: the silence of the genes. Faseb J *20*, 1293-1299.

Silver, D.L., Wang, N., Xiao, X., and Tall, A.R. (2001). High density lipoprotein (HDL) particle uptake mediated by scavenger receptor class B type 1 results in selective sorting of HDL cholesterol from protein and polarized cholesterol secretion. J Biol Chem *276*, 25287-25293.

Silvie, O., Charrin, S., Billard, M., Franetich, J.F., Clark, K.L., van Gemert, G.J., Sauerwein, R.W., Dautry, F., Boucheix, C., Mazier, D., and Rubinstein, E. (2006a). Cholesterol contributes to the organization of tetraspanin-enriched microdomains and to CD81-dependent infection by malaria sporozoites. J Cell Sci *119*, 1992-2002.

Silvie, O., Franetich, J.F., Boucheix, C., Rubinstein, E., and Mazier, D. (2007). Alternative invasion pathways for Plasmodium berghei sporozoites. Int J Parasitol *37*, 173-182.

Silvie, O., Greco, C., Franetich, J.F., Dubart-Kupperschmitt, A., Hannoun, L., van Gemert, G.J., Sauerwein, R.W., Levy, S., Boucheix, C., Rubinstein, E., and Mazier, D. (2006b). Expression of human CD81 differently affects host cell susceptibility to malaria sporozoites depending on the Plasmodium species. Cell Microbiol *8*, 1134-1146.

Silvie, O., Rubinstein, E., Franetich, J.F., Prenant, M., Belnoue, E., Renia, L., Hannoun, L., Eling, W., Levy, S., Boucheix, C., and Mazier, D. (2003). Hepatocyte CD81 is required for Plasmodium falciparum and Plasmodium yoelii sporozoite infectivity. Nat Med *9*, 93-96.

Sontheimer, E.J. (2005). Assembly and function of RNA silencing complexes. Nat Rev Mol Cell Biol *6*, 127-138.

Tellinghuisen, T.L., Evans, M.J., von Hahn, T., You, S., and Rice, C.M. (2007). Studying hepatitis C virus: making the best of a bad virus. J Virol *81*, 8853-8867.

Tomari, Y., and Zamore, P.D. (2005). Perspective: machines for RNAi. Genes Dev *19*, 517-529.

Trigatti, B.L., Krieger, M., and Rigotti, A. (2003). Influence of the HDL receptor SR-BI on lipoprotein metabolism and atherosclerosis. Arterioscler Thromb Vasc Biol *23*, 1732-1738.

Trigatti, B.L., Rigotti, A., and Braun, A. (2000). Cellular and physiological roles of SR-BI, a lipoprotein receptor which mediates selective lipid uptake. Biochim Biophys Acta *1529*, 276-286.

Vishnyakova, T.G., Kurlander, R., Bocharov, A.V., Baranova, I.N., Chen, Z., Abu-Asab, M.S., Tsokos, M., Malide, D., Basso, F., Remaley, A., Csako, G., Eggerman, T.L., and Patterson, A.P. (2006). CLA-1 and its splicing variant CLA-2 mediate bacterial adhesion and cytosolic bacterial invasion in mammalian cells. Proc Natl Acad Sci U S A *103*, 16888-16893.

Voisset, C., Callens, N., Blanchard, E., Op De Beeck, A., Dubuisson, J., and Vu-Dac, N. (2005). High density lipoproteins facilitate hepatitis C virus entry through the scavenger receptor class B type I. J Biol Chem *280*, 7793-7799.

von Hahn, T., Lindenbach, B.D., Boullier, A., Quehenberger, O., Paulson, M., Rice, C.M., and McKeating, J.A. (2006). Oxidized low-density lipoprotein inhibits hepatitis C virus cell entry in human hepatoma cells. Hepatology *43*, 932-942.

Waterhouse, P.M., Graham, M.W., and Wang, M.B. (1998). Virus resistance and gene silencing in plants can be induced by simultaneous expression of sense and antisense RNA. Proc Natl Acad Sci U S A *95*, 13959-13964.

Williams, B.R. (1999). PKR; a sentinel kinase for cellular stress. Oncogene *18*, 6112-6120.

Willingham, A.T., Deveraux, Q.L., Hampton, G.M., and Aza-Blanc, P. (2004). RNAi and HTS: exploring cancer by systematic loss-of-function. Oncogene *23*, 8392-8400.

Wustner, D., Mondal, M., Huang, A., and Maxfield, F.R. (2004). Different transport routes for high density lipoprotein and its associated free sterol in polarized hepatic cells. J Lipid Res *45*, 427-437.

Yan, C., Lu, D., Hai, T., and Boyd, D.D. (2005). Activating transcription factor 3, a stress sensor, activates p53 by blocking its ubiquitination. Embo J *24*, 2425-2435.

Yancey, P.G., de la Llera-Moya, M., Swarnakar, S., Monzo, P., Klein, S.M., Connelly, M.A., Johnson, W.J., Williams, D.L., and Rothblat, G.H. (2000). High density lipoprotein phospholipid composition is a major determinant of the bi-directional flux and net movement of cellular free cholesterol mediated by scavenger receptor BI. J Biol Chem *275*, 36596-36604.

Yesilaltay, A., Kocher, O., Rigotti, A., and Krieger, M. (2005). Regulation of SR-BI-mediated high-density lipoprotein metabolism by the tissue-specific adaptor protein PDZK1. Curr Opin Lipidol *16*, 147-152.

Zamore, P.D., Tuschl, T., Sharp, P.A., and Bartel, D.P. (2000). RNAi: double-stranded RNA directs the ATP-dependent cleavage of mRNA at 21 to 23 nucleotide intervals. Cell *101*, 25-33.

Zannis, V.I., Chroni, A., and Krieger, M. (2006). Role of apoA-I, ABCA1, LCAT, and SR-BI in the biogenesis of HDL. J Mol Med *84*, 276-294.

Zhang, J., Randall, G., Higginbottom, A., Monk, P., Rice, C.M., and McKeating, J.A. (2004). CD81 is required for hepatitis C virus glycoprotein-mediated viral infection. J Virol *78*, 1448-1455.

Appendix

Curriculum Vitae & Publications

Curriculum Vitae

Personal Data

Name	Cristina Dias Rodrigues
Birth place and date	Lisboa, Portugal 06th of May 1980
Nacionality	Portuguese
Home address	Rua do Tejo, lote 7, 1ºA, Quinta da Piedade 2ª fase 2625-204 Póvoa de Santa Iria, Portugal
Work address	Unidade de Malária, Instituto de Medicina Molecular, Av. Prof. Egas Moniz, Ed. Egas Moniz Piso 3B-41 1649-028 Lisboa, Portugal
Contacts	Mobile (+351) 965601973 E-mail: crodrig@igc.gulbenkian.pt, cdrodrigues@fm.ul.pt

Education

July 2003	Degree in Genetics and Microbial Biology by the Faculdade de Ciências da Universidade de Lisboa, Portugal, with 16 out of 20 as final classification
2003 – 2005	Frequency of several theoretical courses as part of the Doctoral Programme of Instituto Gulbenkian da Ciência – PDIGC

Scientific experience

Nov 2002 to July 2003	Undergraduate student at Instituto Gulbenkian de Ciência, Oeiras, Portugal, under the supervision of Prof. Maria Mota, with the project "Interactions between Liver- and Blood-stages of Malaria"
Nov 2003 to Oct 2007	PhD student (FCT fellow) in the Malaria group, at Instituto de Medicina Molecular, Lisboa, Portugal and Instituto Gulbenkian da Ciência, Oeiras, Portugal. Supervision by Dr. Maria M. Mota, with the project "Revealing Host Factors Important for Hepatocyte infection by Plasmodium"

Publications

2004	Leirião P., **Rodrigues C.D.**, Albuquerque S.S., Mota M.M. (2004) Survival of protozoan intracellular parasites in host cells, EMBO Reports, 5(12): 1142-7. Review.

2006 — Prudêncio M., **Rodrigues C.D**., Mota M.M. (2006) "The relevance of host genes in Malaria", In: Parrington, J. and Coward, K. (Eds) Comparative Genomics and Proteomics in the Identification of New Drug Targets, Taylor & Francis, Oxford, UK. Review.

2007 — Pamplona A., Ferreira A., Balla J., Jeney V., Balla G., Epiphanio S., Chora A., **Rodrigues C.D.** Cunha-Rodrigues M., Gregoire I.P., Portugal S., Soares M.P. and Mota M.M. (2007) Heme oxygenase-1 and carbon monoxide suppress the pathogenesis of experimental cerebral malaria, Nature Medicine, 13(6):703-10.

2007 — Prudêncio M, **Rodrigues C.D.,** Ataíde R., Mota M.M., (2007) Dissecting *in vitro* host cell infection by *Plasmodium* sporozoites using flow cytometry, Cellular Microbiology, *in press.*

2007 — <u>Albuquerque S.S.</u>*****, **<u>Rodrigues C.D.**</u>***,** <u>Prudêncio M.</u>*****, Hannus M., Martin C., Epiphanio S., van Gemert G-J, Luty A.J.F., Sauerwein R., Echeverri C.J. and Mota M.M. (2007) Identification of host molecules involved in the liver stage of malaria infection using transcriptional profiling followed by RNAi analysis, *in preparation*

2007 — <u>Prudêncio M.</u>*****, **<u>Rodrigues C.D.</u>***, Hannus M., Martin C., Gonçalves L.A., Portugal S., Akinc A., Hadwiger P., Luty A.J.F., Sauerwein R., Mazier D., Koteliansky V., Vornlocher H.P., Echeverri C.J. and Mota M.M. (2007) Kinome-wide RNAi screen identifies host PKCζ as a critical kinase for *Plasmodium* sporozoite infection, *in preparation.*

2007 — **<u>Rodrigues C.D.</u>***, <u>Hannus M.</u>*****, <u>Prudêncio M.</u>*****, Martin C., Gonçalves L.A., Portugal S., Akinc A., Hadwiger P., Jahn-Hofmann K., Röhl I., van Gemert G.-J., Franetich J.-F., Luty A.J.F., Sauerwein R., Mazier D., Koteliansky V., Vornlocher H.P., Echeverri C.J. and Mota M.M. (2007) SR-BI is a crucially required host factor with a dual role in the establishment of malaria liver infection, *submitted to Nature.*

* These authors contributed equally to this work.

Oral Communications in International Scientific Meetings

2006 | **Rodrigues C.D.**, Albuquerque S.S., Prudêncio M., Martin C., van Gemert G.-J., Sauerwein R.W., Carmo N., Henriques R., Hannus M., Mota M.M., "Identification of host factors required for liver stage infection by *Plasmodium* using RNA interference", Keystone Symposium, Malaria: Functional Genomics to Biology to Medicine, 28 February - 5 March 2006, Taos, NM, USA.

Posters in International Scientific Meetings

2004 | Epiphanio S., Garcia C.R., Rodrigues-Cunha M., **Rodrigues C.D.**, Leirião P., van Gemert G.-J., Sauerwein R., Mota M.M. "Influence of melatonin in malaria hepatic stage", Apicomplexa Biology in the post-genomic era Meeting, COST Action 857, May 2004, Lisbon, Portugal.

Pamplona A., **Rodrigues C.D.**, Soares M.P. and Mota M.M. "Heme oxygenase-1 Activation Protects Mice from Cerebral Malaria", 15th Annual Molecular Parasitology Meeting, 19-23 September 2004, Woods Hole, MA, USA.

2006 | Prudêncio M., **Rodrigues C.D.**, Martin C., van Gemert G.-J., Sauerwein R.W., Carmo N., Hannus M., Mota M.M. "An RNA interference screen of the kinome to identify host factors important during the liver stage of a malaria infection", Keystone Symposium, Malaria: Functional Genomics to Biology to Medicine, 28 February - 5 March 2006, Taos, NM, USA.

Rodrigues C.D., Albuquerque S.S., Prudêncio M., Martin C., van Gemert G.-J., Sauerwein R.W., Carmo N., Henriques R., Hannus M., Mota M.M. "Identification of host factors required for liver stage infection by *Plasmodium* using RNA interference", Keystone Symposium, Malaria: Functional Genomics to Biology to Medicine, 28 February- 5 March 2006, Taos, NM, USA.

Albuquerque S.S., **Rodrigues C.D.**, Prudêncio M., Mota M.M. "Hepatocyte genes functionally required for *P. berghei* sporozoites development", 12th International Congress on Infectious Diseases, 15-18 June 2006, Lisbon, Portugal.

2006	Albuquerque S.S., **Rodrigues C.D.**, Prudêncio M., Mota M.M. "Hepatocyte genes functionally required for *P. berghei* sporozoites development", 11th International Congress of Parasitology (ICOPA XI), 6-11 August 2006, SECC, Glasgow, Scotland.
2007	Hannus M., **Rodrigues C.D.**, Prudêncio M., Martin C., van Gemert G.-J., Sauerwein RW, Echeverri C.J., and Mota M.M. "RNAi-based Discovery and Validation of Novel Anti-Malarial Targets & Lead Compounds" Keystone Symposium, Drugs Against Protozoan Parasites, 28 January – 1 February 2007, Tahoe City, California, USA.

Pamplona A., Ferreira A., Balla J., Jeney V., Balla G., Epiphanio S., Chora A., **Rodrigues C.D.** Cunha-Rodrigues M., Gregoire I.P., Portugal S., Soares M.P. and Mota M.M. "Heme oxygenase-1 and carbon monoxide suppress the pathogenesis of experimental cerebral malaria", Third Annual BioMalPar Conference on Biology and Pathology of the Malaria Parasite, 10-12 April 2007, Heidelberg, Germany.

Rodrigues C.D., Prudêncio M., Hannus M., Martin C., Gonçalves L.A., van Gemert G.-J., Sauerwein R.W., Echeverri C.J. and Mota M.M. "Identification of host factors required for *Plasmodium* liver stage infection - a role for SR-BI", Third Annual BioMalPar Conference on Biology and Pathology of the Malaria Parasite, 10-12 April 2007, Heidelberg, Germany. **Awarded the 1st Poster Prize**.

Dissecting *in vitro* host cell infection by *Plasmodium* sporozoites using flow cytometry

Miguel Prudêncio,[1,2]* **Cristina D. Rodrigues,**[1,2]
Ricardo Ataíde[1] **and Maria M. Mota**[1,2]**
[1]*Unidade de Malária, Instituto de Medicina Molecular, Universidade de Lisboa, 1649-028 Lisboa, Portugal.*
[2]*Instituto Gulbenkian de Ciência, 2780-156 Oeiras, Portugal.*

Summary

The study of the liver stage of malaria has been hampered by limitations in the experimental approaches required to effectively dissect and quantify hepatocyte infection by *Plasmodium*. Here, we report on the use of flow cytometry, in conjunction with GFP-expressing *Plasmodium* sporozoites, to assess the various steps that constitute a successful malaria liver infection: cell traversal, hepatocyte invasion and intrahepatocyte parasite development. We show that this rapid, efficient and inexpensive method can be used to overcome current limitations in the independent quantification of those steps, facilitating routine or large-scale studies of host–pathogen molecular interactions.

Introduction

The liver stage of the life cycle of *Plasmodium* is the first, obligatory step in any natural malaria infection. During this asymptomatic phase, the sporozoites injected into the mammalian host through the bite of an infected mosquito reach the liver, where they traverse several hepatocytes before invading a final one with formation of a parasitophorous vacuole (PV) (Mota *et al.*, 2001; Frevert *et al.*, 2005). Inside hepatocytes, the parasites develop and multiply, forming a so-called exoerythrocytic form (EEF). During this process, which takes 5–7 days for the human parasite *Plasmodium falciparum* and *c.* 42 h for the rodent *Plasmodium berghei* parasite, the EEF grows in size and eventually releases 20 000–30 000 merozoites into the blood, where they will invade erythrocytes and cause the symptoms of the disease (reviewed in Prudencio *et al.*, 2006).

Although the liver stage of malaria constitutes an ideal target for prophylactic intervention, only recently have the processes that take place during this stage begun to be understood. This is largely due to practical issues hampering the study of what goes on when sporozoites invade and develop inside hepatic cells. In fact, unlike blood stages that can be easily obtained from frozen-infected blood, sporozoites need to be freshly extracted from the salivary glands of infected mosquitoes, which poses constraints to their availability. Moreover, studies in human volunteers or in endemic populations are not feasible due to ethic constraints and to the fact that this stage of disease is asymptomatic. This leaves researchers with a few important tools to study liver stage malaria, namely, *in vivo* animal models, *ex vivo* primary hepatocytes and *in vitro* hepatoma cell lines. The latter constitute a valuable resource to study the fundamental aspects of EEF formation and development and to evaluate drug candidates that may interfere with these processes.

Recently, genetic manipulation of *Plasmodium* has allowed the generation of parasites that express green fluorescent protein (GFP) (Kadekoppala *et al.*, 2001; Natarajan *et al.*, 2001; Franke-Fayard *et al.*, 2004; Tarun *et al.*, 2006; Ono *et al.*, 2007), which enables cells infected with these parasites to be analysed by fluorescence-activated cell sorting (FACS). This technique has been successfully used to separate infected hepatocytes or hepatoma cells (Natarajan *et al.*, 2001; Tarun *et al.*, 2006) as well as to monitor infection of red blood cells in mice (Janse *et al.*, 2006; Ono *et al.*, 2007).

In this report we describe how flow cytometry can be employed to obtain crucial quantitative information regarding the hepatic stage of malaria. Our results show that this technique can be used to determine the efficiency of infection of a hepatoma cell line by the GFP-expressing rodent malaria parasite *P. berghei* (PbGFP). In particular, it enables the quantitative assessment of the cell traversal process that precedes invasion, as well as of both the invasion and development processes essential for the establishment of a successful infection.

Results and discussion

Quantification of cell traversal by migrating sporozoites

When sporozoites traverse hepatocytes before the final invasion, they disrupt the membrane of the host cell,
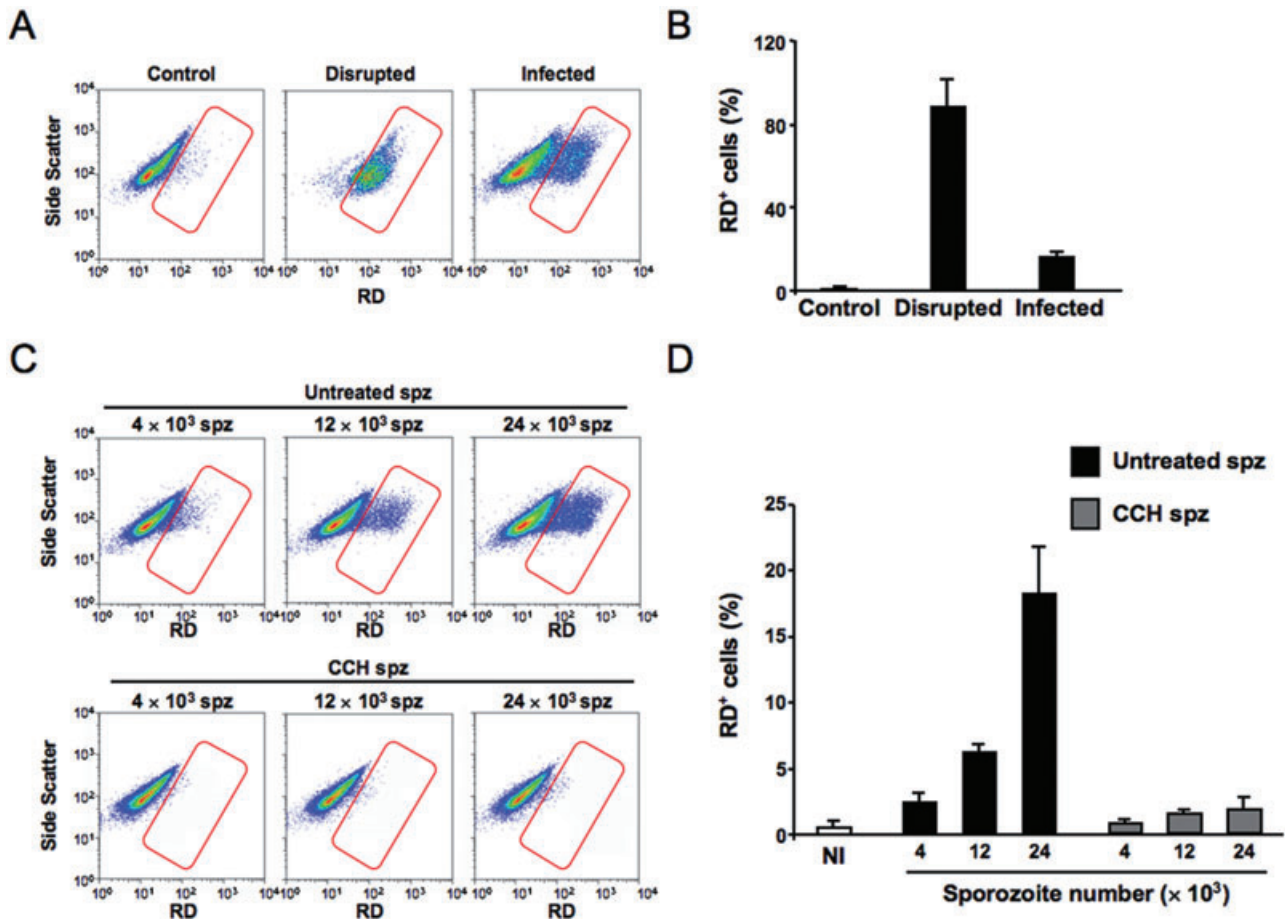
Fig. 1. FACS assessment of cell wounding during sporozoite traversal.
A. Cell wounding was assessed in a RD-based assay by fluorescence intensity. Dot plots represent undisrupted-uninfected cells (control), mechanically disrupted cells and cells incubated with sporozoites (15×10^3) for 2 h. The gate contains RD+ cells.
B. Bar plot represents the percentage of RD+ cells in the conditions in (A) ($n = 3$). Error bars represent SD.
C. Cell wounding by sporozoites was assessed in a RD-based assay by fluorescence intensity. Dot plots represent cells incubated for 2 h with different numbers of sporozoites (spz), previously treated with cytochalasin (CCH) or not (Untreated). The gate contains RD+ cells. Non-infected cells were used as control.
D. Bar plot represents the percentage of RD+ cells in the conditions in (C) ($n = 3$). NI corresponds to non-infected cells used as control. Error bars represent SD.

which then quickly reseals (Mota *et al.*, 2001). Cell traversal can be monitored and quantified by fluorescence microscopy by a cell wounding assay employing rhodamine dextran (RD), which, if present in the medium upon sporozoite addition, is trapped within the cell before resealing occurs (Mota *et al.*, 2001). Generally, such quantification is laborious and time-consuming, as it involves the visual inspection of RD-positive (RD+) cells and their quantification. A very recent report uses FACS to compare cell wounding by mutant and wild-type sporozoites but does not provide any controls to show that this technique can be used to quantify cell traversal (Labaied *et al.*, 2007). We have sought to establish whether FACS can be used to quantitatively assess cell traversal by sporozoites. RD was added to the cells immediately prior to sporozoite addition and cells were collected and analy-

sed by FACS 2 h later. Non-infected cells incubated with RD during the same period as the infected ones and cells that were mechanically disrupted in the presence of RD were used as controls (Fig. 1A and B). The percentage of RD+ cells in untreated cultures is minimal, when compared with those in which cells were either incubated with sporozoites or mechanically disrupted, showing that membrane wounding by traversing sporozoites can be detected by this approach (Fig. 1B). In order to determine whether the technique can give quantitative information about cell traversal, cells were incubated with different amounts of sporozoites for 2 h (Fig. 1C and D). Cells incubated with sporozoites treated with cytochalasin (CCH), whose motility is impaired (Stewart *et al.*, 1986), and uninfected cells, were used as controls (Fig. 1C and D). The results obtained show that the percentage of RD+

cells correlates with the number of sporozoites added to cells (Fig. 1D). When cells are incubated with a fixed number of sporozoites for periods of time between 15 min and 2 h, the percentage of RD+ cells correlates with the time of incubation (data not shown). These results show that flow cytometry can indeed be used to successfully quantify hepatocyte traversal by sporozoites.

Quantification of invasion

Invasion of hepatoma cells by sporozoites is usually assumed to be complete within the first 2 h following parasite addition to the cells (Mota *et al.*, 2001). Thus, by determining the extent of infection 2 h after sporozoite addition, one can, conceivably, assess the efficiency of the invasion process. Quantification of invasion by any of the techniques traditionally employed to study hepatocyte infection is difficult. Until now, it has relied on a parasite surface molecule double immunostaining, performed before and after cell permeabilization (Sinnis, 1998). This method distinguishes between parasites attached to the cells and invading ones, but it is a time-consuming procedure requiring pre-labelled, parasite-specific antibodies. Another approach that can be employed to determine infection levels *in vitro* is quantitative real-time reverse transcription polymerase chain reaction (qRT-PCR), using primers specific for the parasite in parallel with primers for a housekeeping gene to allow normalization of the results, as described for the quantification of *in vivo* liver infections (Bruna-Romero *et al.*, 2001). However, quantification by qRT-PCR is not only a time-consuming approach but also an expensive one, rendering it unsuitable for large-scale or routine studies. Now, we demonstrate that these limitations can be overcome by using FACS to analyse cells 2 h after sporozoite addition.

We infected Huh7 cells with fixed numbers of PbGFP sporozoites and analysed them by FACS 2 h later. Non-infected cells were used as control (Fig. 2A and B). Our results show that the infected cell population can be successfully quantified using this technique and that, as expected, the percentage of PbGFP-containing cells depends on the number of sporozoites added (Fig. 2B). CCH treatment of sporozoites does not impair their ability to attach to cells but renders them unable to invade (Stewart *et al.*, 1986). Cells incubated with CCH-treated sporozoites for 2 h and then analysed by FACS show only negligible amounts of GFP fluorescence, when compared with that of cells incubated with untreated sporozoites and similar to those displayed by non-infected cells (Fig. 2A and B). This shows that tripsinization of cells prior to FACS analysis ensures that all GFP-positive (GFP+) events observed correspond to parasite-containing cells and not to cells with sporozoites attached to their surface. In a parallel experiment, we incubated cells with the

supernatant of infected cells, collected 2 h after parasite addition. Two hours later, cells to which this supernatant was added were collected and analysed by FACS, revealing only residual amounts of infected cells (data not shown). This result is in agreement with the notion that successful infection is accomplished within the first 2 h that follows sporozoite addition.

The traversal and invasion processes can be simultaneously assessed in RD-treated cell samples infected with PbGFP sporozoites (Fig. 2C and D). By carefully gating the various cell populations, FACS can be used to determine the percentage of cells whose membrane has been disrupted (RD+) and of those containing a parasite at the time of measurement (GFP+). Furthermore, a double-positive population (RD+GFP+) consisting of cells either that contain parasites 'in transit' or that were traversed and subsequently invaded can be identified (Fig. 2D). Approximately 50% of the GFP+ cell population is RD-negative and therefore these cells have been unequivocally invaded. On the other hand, invasion with PV formation may or may not have occurred in the remaining 50% of the GFP+ cell population, which corresponds to RD+GFP+ cells. Hence, data from double-fluorescence FACS measurements should be taken into account when the estimation of the percentage of invaded, non-traversed cells is of relevance.

Quantification of EEF development

By itself, flow cytometry information collected 2 h after sporozoite addition is useful to evaluate the ability of parasites to invade cells in culture, but provides little insight into the extent of their intracellular development. The latter can be assessed by quantifying infection at later time points after sporozoite addition. Traditionally, this was done by immunofluorescence staining of the parasite and EEF quantification by microscopy. This is a time-consuming approach, made easier by developments in automatic image acquisition and treatment techniques, but is still impractical for the assessment of the early developmental stages of infection. As an alternative to microscopy, qRT-PCR can be used to quantify the number of parasite copies at specific times following sporozoite addition. However, in addition to the disadvantages mentioned earlier, qRT-PCR has limitations regarding an effective differentiation between the invasion and development processes, if samples are analysed at a single time point of EEF development. This can be circumvented by analysing samples at different times after sporozoite addition, but this further increases both the price and time of data acquisition. In order to overcome these drawbacks, we sought to determine whether FACS can be used to reliably estimate the extent of intrahepatocyte parasite development.
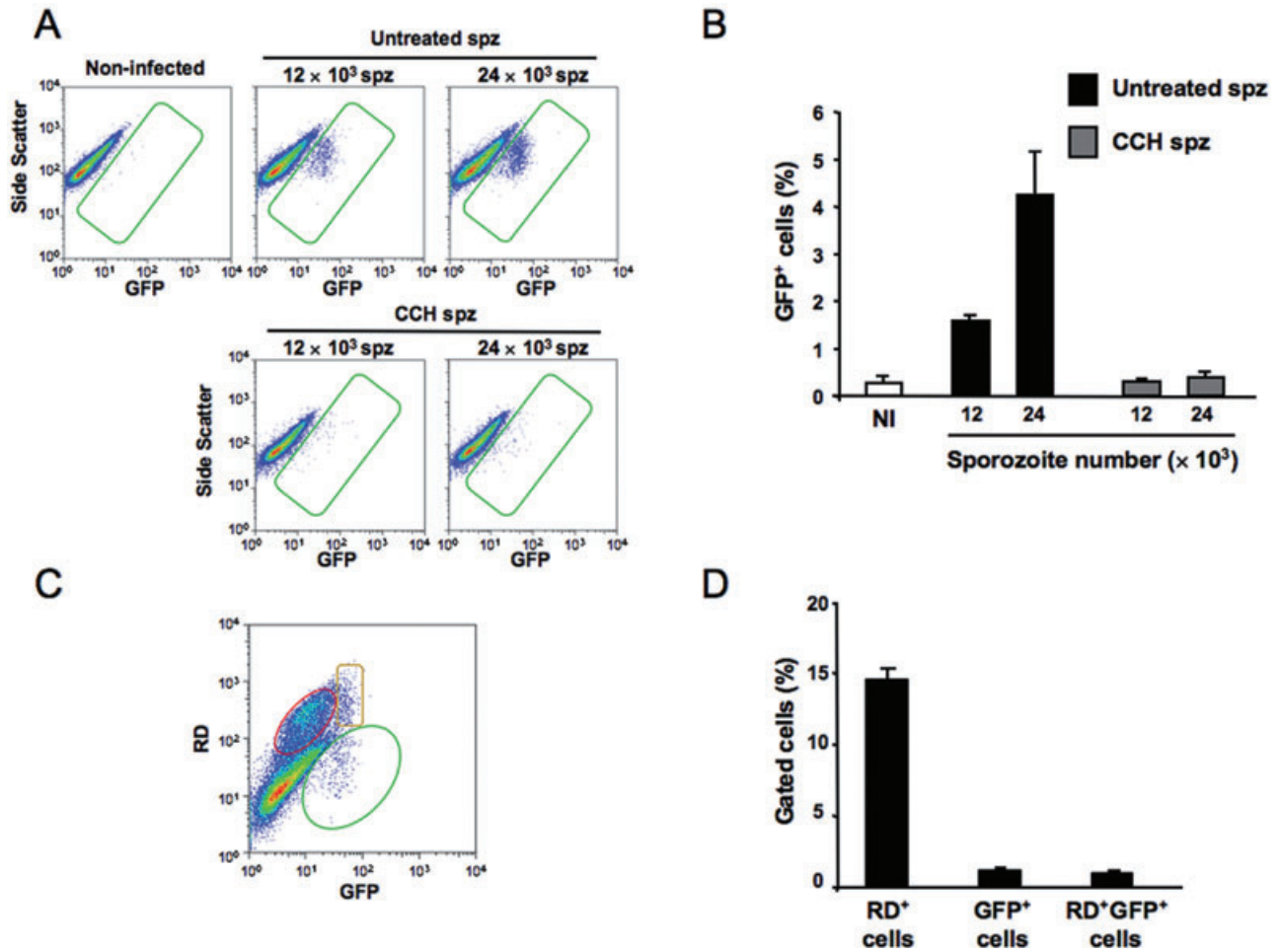
Fig. 2. FACS assessment of cell invasion.
A. Cell invasion was quantified by determining the proportion of GFP+ cells in Huh7 cells incubated with PbGFP sporozoites. Dot plots represent non-infected cells and cells incubated for 2 h with different numbers of PbGFP sporozoites (spz), previously treated with cytochalasin (CCH) or not (Untreated). The gate contains GFP+ cells.
B. Bar plot represents the percentage of GFP+ cells in the conditions in (A) ($n = 3$). NI corresponds to non-infected cells used as control. Error bars represent SD.
C. Traversal versus invasion were assessed in cells incubated with PbGFP sporozoites (15×10^3) for 2 h. The gates contain RD+ (red) GFP+ (green) or RD+GFP+ (yellow) cells.
D. Bar plot represents the percentages of RD+, GFP+ or RD+GFP+ cells ($n = 3$). Error bars represent SD.

We infected Huh7 cells with a fixed number of PbGFP sporozoites and analysed them by FACS at various time points post infection (Fig. 3A and B). As control, we used radiation-attenuated PbGFP sporozoites (RASPbGFP), which are known to retain their ability to invade cells but fail to develop and multiply (Suhrbier *et al.*, 1990). As expected, the percentage of PbGFP-infected cells decreases for later time points of infection, as a result of the multiplication of cells in culture (Fig. 3A). When the FACS data are plotted as a histogram, it becomes apparent that the maximum fluorescence of the PbGFP-infected cells increases as the infection is allowed to proceed for longer (Fig. 3B). These data show that although the relative proportion of PbGFP-infected cells is decreasing as the time post infection increases, the fluorescence emitted by these

cells is increasing during the same period, as a result of EEF development. When cells are infected with RASPb-GFP sporozoites, the percentage of infected cells also decreases with time (Fig. 3A). However, the maximum fluorescence of RASPbGFP-infected cells does not change significantly in the same period (Fig. 3B), in agreement with the knowledge that development of irradiated parasites is impaired (Suhrbier *et al.*, 1990).

In order to determine whether there is a correlation between the position of the GFP+ curve and the number of copies of parasite at a given time post infection, we analysed cells infected under similar conditions as those described above by qRT-PCR (Fig. 3C). We observed that, as expected, the number of parasite copies in PbGFP-infected cells increases up until 36 h post infection and is
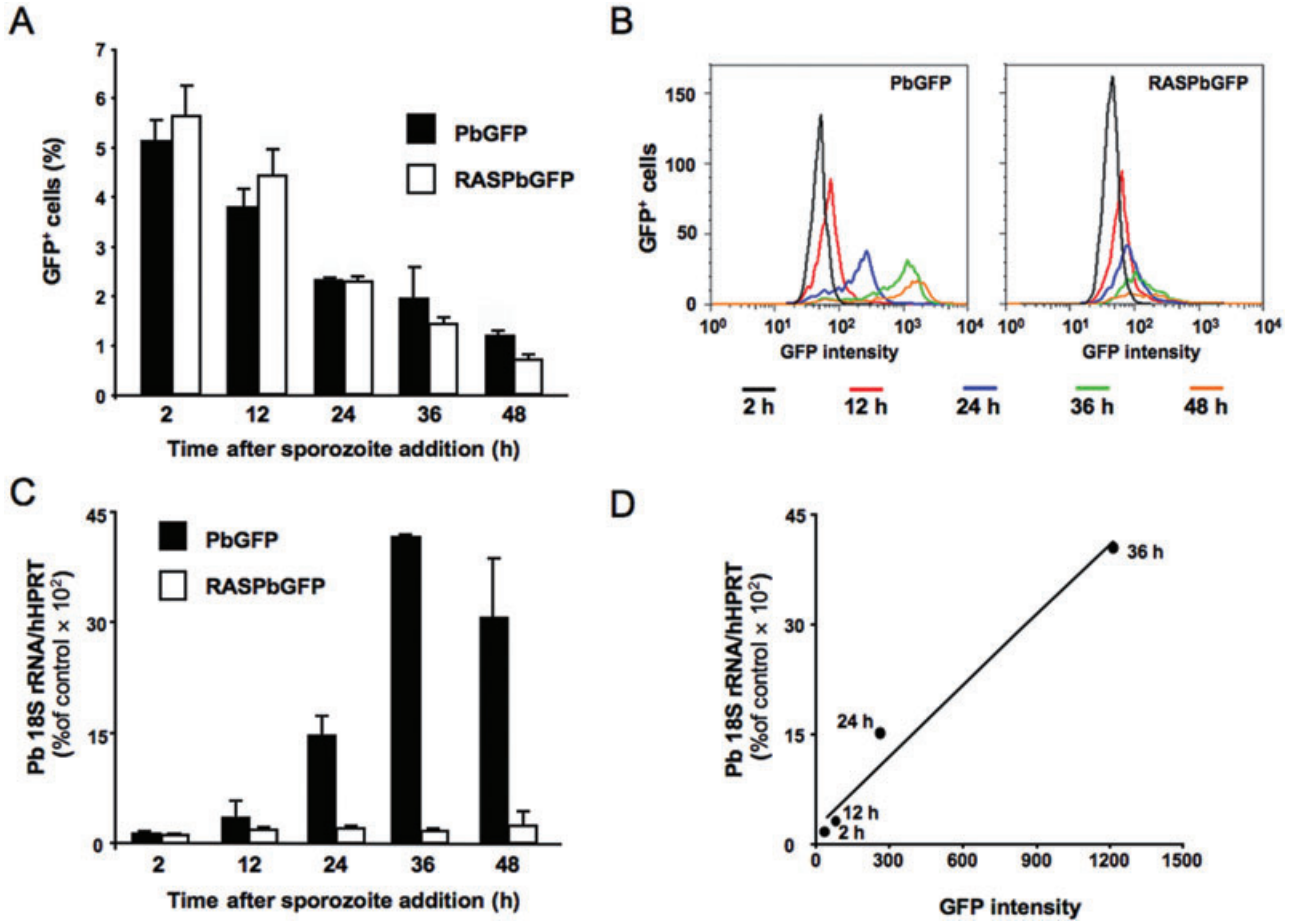
Fig. 3. Assessment of infection at various times after sporozoite (30×10^3) addition to cells.
A. Proportion of infected cells was quantified during infection with PbGFP (black bars) or RASPbGFP (white bars) ($n = 3$).
B. EEF development was assessed by fluorescence intensity of GFP^{+} cells. The graphs show one representative data set of triplicate samples.
C. Infection was quantified by parasite-specific qRT-PCR 2, 12, 24, 36 and 44 h post infection with PbGFP or RASPbGFP ($n = 3$). Infection is expressed as percentage of control (2 h time point of cells infected with RASPbGFP). Error bars represent SD.
D. Positive correlation ($R^2 = 0.98$) between the parasite load measured by qRT-PCR and the maximum intensity of the GFP[+] band in the FACS histograms.

reduced at 48 h post infection. The number of parasite copies in RASPbGFP-infected cells increases slightly between 2 and 12 h post infection and then remains roughly constant up until 48 h after sporozoite addition, a result that is in agreement with previous observations (Suhrbier *et al.*, 1990). Our results also indicate that the number of PbGFP copies decreases between 36 and 48 h after infection, possibly due to detachment of infected cells or release of merozoites (Sturm *et al.*, 2006). This is not observed for RASPbGFP-infected cells, suggesting that *Plasmodium* release by the host cells is dependent on the development of the parasites within them.

The correlation between the number of parasite copies and the intensity of the GFP[+] band in PbGFP-infected cells was further established by plotting the former against the latter (Fig. 3D). This shows that intracellular parasite development takes place exponentially until parasite

release starts to occur. Moreover, it shows that the fluorescence corresponding to the maximum of the GFP peak in a FACS histogram correlates linearly with the number of copies of parasite in the cells and can thus be used as a quick and effective way of estimating the intracellular development of the parasite.

Finally, we assessed parasite development in cells that are either RD[-]GFP[+] or RD[+]GFP[+], by independently plotting the histograms of each of these cell populations at time points between 2 and 48 h following sporozoite addition. Our results reveal that RD[-]GFP^{+} cells contain EEFs that develop normally during this period, showing that the parasites in these cells have undergone productive invasion with formation of a PV. On the contrary, parasites in RD[+]GFP^{+} cells develop poorly if at all and their GFP intensity decreases at the later time points assessed (data not shown).

The method presented in this report has various important applications as it constitutes an efficient way of assessing *Plasmodium* infection of hepatocytes under different experimental conditions. Compared with other available methods to address this, it presents advantages both in terms of speed of data acquisition and in terms of cost-effectiveness. Furthermore, it distinguishes between invasion and developmental stages of *Plasmodium* within a hepatocyte, overcoming limitations presented by other available techniques in this respect. The method can, for instance, be used to address the effectiveness of a given drug in impairing the invasion and/or the development of the parasite in the liver. It can also serve to study the role of specific host genes in *Plasmodium* invasion and/or development, either by employing genetically modified cell lines or by using RNA interference to down-modulate the expression of the gene(s) of interest. Finally, the method provides a quick way to address the potential invasion and/or developmental consequences of introducing specific gene mutations or deletions in the parasite. The methodology described here greatly extends the potential of combining GFP-expressing pathogens with flow cytometry to address host–pathogen interactions.

Experimental procedures

Cell, parasites and infection

Huh7 cells, a human hepatoma cell line, were cultured in RPMI (Gibco/Invitrogen) medium supplemented with 10% fetal calf serum (FCS) (Gibco/Invitrogen), 1% non-essential amino acids (Gibco/Invitrogen), 1% penicillin/streptomycin (Gibco/Invitrogen), 1% glutamine (Gibco/Invitrogen) and 10 mM Hepes, pH 7 (Gibco/Invitrogen) and maintained at 37°C with 5% CO_2. GFP-expressing *P. berghei* (parasite line 259 cL2) sporozoites were obtained by disruption of the salivary glands of freshly dissected infected female *Anopheles stephensi* mosquitoes, bred at the Insectary of the Instituto de Medicina Molecular. Radiation-attenuated sporozoites were obtained by irradiation of sporozoites with 160 Gy on a Compagnie Oris Industrie IBL 437C irradiator, at room temperature, for approximately 80 min. Non-irradiated sporozoites used in development experiments were left at room temperature during the same period. Sporozoite motility was impaired by incubation with 10 µM cytochalasin (Calbiochem) for 10 min at room temperature prior to addition to cells. Non-treated sporozoites used in these experiments were left at room temperature during the same period. Cells (17.5×10^4 per well) were seeded on 24-well plates the day before infection. Cells were infected by addition of specific numbers of sporozoites, followed by centrifugation at 1700 *g* for 7 min at 37°C. For membrane disruption assessment, 2 mg ml^{-1} Dextran tetramethylrhodamine 10 000 MW, lysine fixable (fluoro-ruby) (Molecular Probes/Invitrogen) were added to the cells immediately prior to sporozoite addition. Cells used as positive controls for the membrane disruption assay were mechanically disrupted by passage through a 27 G syringe five times, in the presence of 2 mg ml^{-1} Dextran.

Fluorescence-activated cell sorting (FACS)

Cell samples for FACS analysis were washed with 1 ml of PBS, incubated with 150 µl of trypsin for 5 min at 37°C and collected in 400 µl of 10% FCS in PBS at the selected time points post sporozoite addition. Cells were then centrifuged at 0.1 *g* for 3 min at 4°C and re-suspended in 150 µl of 2% FCS in PBS. Cells were analysed on a Becton Dickinson FACScalibur with the appropriate settings for the fluorophores used. Data acquisition and analysis were carried out using the CELLQuest (version 3.2.1fl1, Becton Dickinson) and FlowJo (version 6.3.4, FlowJo) software packages respectively.

Quantification of parasite copy numbers by qRT-PCR

Cells were washed with 1 ml of PBS and collected at the selected time points in 150 µl of RLT buffer (Qiagen) containing 1% β-mercaptoethanol and immediately stored at −80°C until further processing. Total RNA was isolated from Huh7 cells with Qiagen's Micro RNeasy kit, following the manufacturer's instructions, and converted into cDNA using Roche's Transcriptor First Strand cDNA Synthesis kit, according to the manufacturer's protocol. The qRT-PCR reactions used Applied Biosystems' Power SYBR Green PCR Master Mix and were performed according to the manufacturer's instructions on an ABI Prism 7000 system (Applied Biosystems). Amplification reactions were carried out in a total reaction volume of 25 µl, containing 0.8 pmoles µl^{-1} or 0.16 pmoles µl^{-1} of the PbA- or housekeeping gene-specific primers respectively. Relative amounts of PbA mRNA were calculated against the Hypoxanthine Guanine Phosphoribosyltransferase (HPRT) housekeeping gene. PbA- and HPRT-specific primer sequences were 5′-AAG CAT TAA ATA AAG CGA ATA CAT CCT TAC-3′ and 5′-GGA GAT TGG TTT TGA CGT TTA TGT G-3′, and 5′-TGC TCG AGA TGT GAT GAA GG-3′ and 5′-TCC CCT GTT GAC TGG TCA TT-3′ respectively.

References

Bruna-Romero, O., Hafalla, J.C., Gonzalez-Aseguinolaza, G., Sano, G., Tsuji, M., and Zavala, F. (2001) Detection of malaria liver-stages in mice infected through the bite of a single Anopheles mosquito using a highly sensitive real-time PCR. *Int J Parasitol* **31:** 1499–1502.

Franke-Fayard, B., Trueman, H., Ramesar, J., Mendoza, J., van der Keur, M., van der Linden, R., *et al.* (2004) A *Plasmodium berghei* reference line that constitutively expresses GFP at a high level throughout the complete life cycle. *Mol Biochem Parasitol* **137:** 23–33.

Frevert, U., Engelmann, S., Zougbede, S., Stange, J., Ng, B.,

Matuschewski, K., *et al.* (2005) Intravital observation of *Plasmodium berghei* sporozoite infection of the liver. *PLoS Biol* **3:** e192.

Janse, C.J., Franke-Fayard, B., and Waters, A.P. (2006) Selection by flow-sorting of genetically transformed, GFP-expressing blood stages of the rodent malaria parasite, *Plasmodium berghei*. *Nat Protoc* **1:** 614–623.

Kadekoppala, M., Cheresh, P., Catron, D., Ji, D.D., Deitsch, K., Wellems, T.E., *et al.* (2001) Rapid recombination among transfected plasmids, chimeric episome formation and trans gene expression in *Plasmodium falciparum*. *Mol Biochem Parasitol* **112:** 211–218.

Labaied, M., Harupa, A., Dumpit, R.F., Coppens, I., Mikolajczak, S.A., and Kappe, S.H. (2007) *Plasmodium yoelii* sporozoites with simultaneous deletion of P52 and P36 are completely attenuated and confer sterile immunity against infection. *Infect Immun* **75:** 3758–3768.

Mota, M.M., Pradel, G., Vanderberg, J.P., Hafalla, J.C., Frevert, U., Nussenzweig, R.S., *et al.* (2001) Migration of *Plasmodium* sporozoites through cells before infection. *Science* **291:** 141–144.

Natarajan, R., Thathy, V., Mota, M.M., Hafalla, J.C., Menard, R., and Vernick, K.D. (2001) Fluorescent *Plasmodium berghei* sporozoites and pre-erythrocytic stages: a new tool to study mosquito and mammalian host interactions with malaria parasites. *Cell Microbiol* **3:** 371–379.

Ono, T., Tadakuma, T., and Rodriguez, A. (2007) *Plasmodium yoelii yoelii* 17XNL constitutively expressing GFP throughout the life cycle. *Exp Parasitol* **115:** 310–313.

Prudencio, M., Rodriguez, A., and Mota, M.M. (2006) The silent path to thousands of merozoites: the *Plasmodium* liver stage. *Nat Rev Microbiol* **4:** 849–856.

Sinnis, P. (1998) An immunoradiometric assay for the quantification of *Plasmodium* sporozoite invasion of HepG2 cells. *J Immunol Methods* **221:** 17–23.

Stewart, M.J., Nawrot, R.J., Schulman, S., and Vanderberg, J.P. (1986) *Plasmodium berghei* sporozoite invasion is blocked *in vitro* by sporozoite-immobilizing antibodies. *Infect Immun* **51:** 859–864.

Sturm, A., Amino, R., van de Sand, C., Regen, T., Retzlaff, S., Rennenberg, A., *et al.* (2006) Manipulation of host hepatocytes by the malaria parasite for delivery into liver sinusoids. *Science* **313:** 1287–1290.

Suhrbier, A., Winger, L.A., Castellano, E., and Sinden, R.E. (1990) Survival and antigenic profile of irradiated malarial sporozoites in infected liver cells. *Infect Immun* **58:** 2834–2839.

Tarun, A.S., Baer, K., Dumpit, R.F., Gray, S., Lejarcegui, N., Frevert, U., and Kappe, S.H. (2006) Quantitative isolation and *in vivo* imaging of malaria parasite liver stages. *Int J Parasitol* **36:** 1283–1293.

Heme oxygenase-1 and carbon monoxide suppress the pathogenesis of experimental cerebral malaria

Ana Pamplona[1,2], Ana Ferreira[1], József Balla[3], Viktória Jeney[3], György Balla[3], Sabrina Epiphanio[1,2], Ângelo Chora[1], Cristina D Rodrigues[1,2], Isabel Pombo Gregoire[1], Margarida Cunha-Rodrigues[1,2], Silvia Portugal[1,2], Miguel P Soares[1,4] & Maria M Mota[1,2,4]

Cerebral malaria claims more than 1 million lives per year. We report that heme oxygenase-1 (HO-1, encoded by *Hmox1*) prevents the development of experimental cerebral malaria (ECM). BALB/c mice infected with *Plasmodium berghei* ANKA upregulated HO-1 expression and activity and did not develop ECM. Deletion of *Hmox1* and inhibition of HO activity increased ECM incidence to 83% and 78%, respectively. HO-1 upregulation was lower in infected C57BL/6 compared to BALB/c mice, and all infected C57BL/6 mice developed ECM (100% incidence). Pharmacological induction of HO-1 and exposure to the end-product of HO-1 activity, carbon monoxide (CO), reduced ECM incidence in C57BL/6 mice to 10% and 0%, respectively. Whereas neither HO-1 nor CO affected parasitemia, both prevented blood-brain barrier (BBB) disruption, brain microvasculature congestion and neuro-inflammation, including CD8^{+} T-cell brain sequestration. These effects were mediated by the binding of CO to hemoglobin, preventing hemoglobin oxidation and the generation of free heme, a molecule that triggers ECM pathogenesis.

Plasmodium, the causative agent of malaria, causes extensive hemolysis. About 40% of the hemoglobin contained within each infected red blood cell can be released and readily oxidized[1]. This leads to the generation of free heme (reviewed in ref. 2), a molecule cytotoxic to the parasite when generated within red blood cells[3] and to the host when released into the circulation[4]. *Plasmodium* has developed strategies to cope with free heme generated within red blood cells, polymerizing it into hemozoin[1]. When exposed to free heme, host cells (human or rodent) upregulate the expression of heme oxygenase-1 (HO-1), a stress-responsive enzyme that catabolizes heme into iron (Fe), biliverdin and carbon monoxide (CO)[5]. As previously shown, CO can limit the deleterious effects of inflammation (ref. 6, and reviewed in ref. 7). We hypothesized that CO might counter the pathogenesis of cerebral malaria, an inflammatory syndrome that can develop in the course of malaria infection and lead to neurological disturbances revealed clinically by abnormal behavior, impairment of consciousness, seizures and irreversible coma, ultimately leading to death[8].

C57BL/6 mice infected with *P. berghei* ANKA die within 6–12 d, due to the development of a complex neurological syndrome consisting of hemi- or paraplegia, head deviation, a tendency to roll over on stimulation, ataxia and convulsions (reviewed in ref. 9). Given its similarities to human cerebral malaria, this neurological syndrome is referred to as experimental cerebral malaria (ECM). Certain mouse strains, for example, BALB/c, are less likely to develop ECM when infected with *P. berghei* ANKA; these strains, if not treated to control parasitemia, die within 3 to 4 weeks of infection due to severe anemia

and hyperparasitemia but do not exhibit neurological symptoms (reviewed in refs. 9,10).

RESULTS

HO-1 prevents the development of ECM in BALB/c mice

Infection of BALB/c mice with *P. berghei* ANKA led to the upregulation of HO-1 in the brain, as assessed at the mRNA level by quantitative RT-PCR (qRT-PCR) ($P < 0.01$ comparing day 6 versus day 0; **Fig. 1a**), at the protein level by western blot ($P < 0.05$, days 9–12 versus day 0; **Fig. 1b** and **Supplementary Fig. 1** online) and at a functional level by assessment of HO enzymatic activity ($P < 0.05$, day 6–12 versus day 0; **Fig. 1c**). Expression of *Hmox1* mRNA reached maximal levels 6 d after infection, decreasing thereafter until day 12, the last day analyzed (**Fig. 1a**). HO-1 protein expression (**Fig. 1b**) and HO activity (**Fig. 1c**) reached maximal levels 9 d after infection, and the protein remained highly expressed and functional at day 12, the last day analyzed. Expression of HO-2, the constitutive form of HO, remained unchanged in the brains of infected mice, as assessed by western blot (**Fig. 1b** and **Supplementary Fig. 1**). *Hmox1* mRNA expression in the liver and lungs increased steadily until day 12 after infection (**Supplementary Fig. 2** online).

Upregulation of HO-1 explains the low incidence of ECM in BALB/c mice infected with *P. berghei* ANKA (ref. 11), as incidence of death with ECM-like symptoms increased from 0% in wild-type ($Hmox1^{+/+}$) mice to 83.3% in HO-1 deficient ($Hmox1^{-/-}$) BALB/c mice ($P < 0.001$; **Fig. 1d**). Heterozygous ($Hmox1^{+/-}$) and $Hmox1^{+/+}$ BALB/c
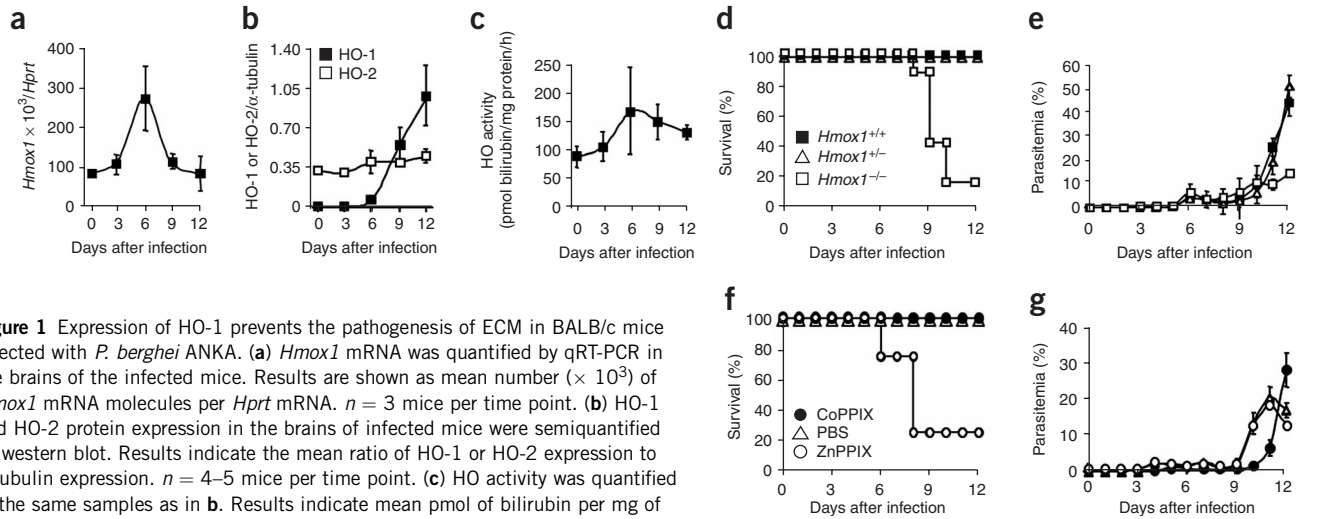
Figure 1 Expression of HO-1 prevents the pathogenesis of ECM in BALB/c mice infected with *P. berghei* ANKA. (**a**) *Hmox1* mRNA was quantified by qRT-PCR in the brains of the infected mice. Results are shown as mean number ($\times 10^3$) of *Hmox1* mRNA molecules per *Hprt* mRNA. $n = 3$ mice per time point. (**b**) HO-1 and HO-2 protein expression in the brains of infected mice were semiquantified by western blot. Results indicate the mean ratio of HO-1 or HO-2 expression to α-tubulin expression. $n = 4–5$ mice per time point. (**c**) HO activity was quantified in the same samples as in **b**. Results indicate mean pmol of bilirubin per mg of brain protein per hour. $n = 4–5$ mice per time point. (**d,e**) Survival and mean parasitemia of infected *Hmox1*^+/+^ mice ($n = 20$), *Hmox1*^+/−^ mice ($n = 14$) and *Hmox1*^−/−^ mice ($n = 12$). (**f,g**) Effects of HO inhibition by ZnPPIX ($n = 10$) and HO-1 induction by CoPPIX ($n = 10$) on survival and mean parasitemia of infected mice. PBS-treated mice were used as a control. $n = 5$ mice per group. Error bars represent s.d.

mice behaved similarly in that neither group developed ECM. Despite having increased ECM incidence, *Hmox1*^−/−^ mice did not have increased parasitemia, as compared to *Hmox1*^+/+^ and *Hmox1*^+/−^ mice (**Fig. 1e**). This suggests that the protective effect of HO-1 does not rely on the modulation of parasitemia. We observed an apparent decrease in parasitemia in two of six *Hmox1*^−/−^ mice that did not die of ECM (**Fig. 1e**); however, this decrease was not statistically significant ($P > 0.05$) and therefore its importance is difficult to ascertain.

Pharmacologic inhibition of HO enzymatic activity by zinc protoporphyrin (ZnPPIX) resulted in the death of 77.5% of infected *Hmox1*^+/+^ BALB/c mice, with symptoms consistent with the development of ECM (**Fig. 1f**). ZnPPIX did not influence parasitemia (**Fig. 1g**), suggesting again that the protective effect of HO-1 does not rely on the inhibition of parasitemia. Infected mice treated with cobalt protoporphyrin (CoPPIX), a protoporphyrin that induces HO-1 expression and activity, did not develop ECM (0% incidence; **Fig. 1f**). CoPPIX delayed parasitemia between days 9 and 11 after infection ($P < 0.05$ versus PBS controls), an effect lost shortly after its administration was discontinued (that is, on day 9 after infection; **Fig. 1g**). As is the case with other non-iron porphyrins[12], CoPPIX might interfere with the ability of the parasite to polymerize heme into hemozoin, thereby decreasing parasitemia.

HO-1 induction or exposure to CO prevent ECM onset

In contrast to BALB/c mice, C57BL/6 mice develop ECM when infected with *P. berghei* ANKA, dying within 6 to 9 d after infection[11]. ECM incidence was associated with lower levels of *Hmox1* mRNA expression in the brains of C57BL/6 mice, as compared to BALB/c mice ($P < 0.05$; **Fig. 2a**). We hypothesized that lower HO-1 expression contributes in a critical manner to the incidence of ECM in C57BL/6 mice infected with *P. berghei* ANKA. Pharmacologic induction of HO-1 using CoPPIX reduced the incidence of ECM and death to 10%, from 100% in PBS- and ZnPPIX-treated controls (**Fig. 2b**). Here too, CoPPIX led to a significant delay in parasitemia ($P < 0.05$ versus PBS-treated controls; **Fig. 2c**), which, as argued above, may result from interference with parasite heme clearance[12]. As parasitemia was not treated, infected mice that did not die due to ECM died later due to the development of hyperparasitemia ($>60\%$ infected red blood cells; **Fig. 2b,c**).

CO (250 p.p.m.) given for 24 h (**Fig. 2d**) or 72 h (**Supplementary Fig. 3a** online), starting at day 3 after infection, prevented death and all ECM symptoms in C57BL/6 mice infected with *P. berghei* ANKA. None of the C57BL/6 mice exposed to CO developed ECM (**Fig. 2d**). This finding is in keeping with previous observations that inhaled CO can mimic the protective effects of HO-1 in several experimental
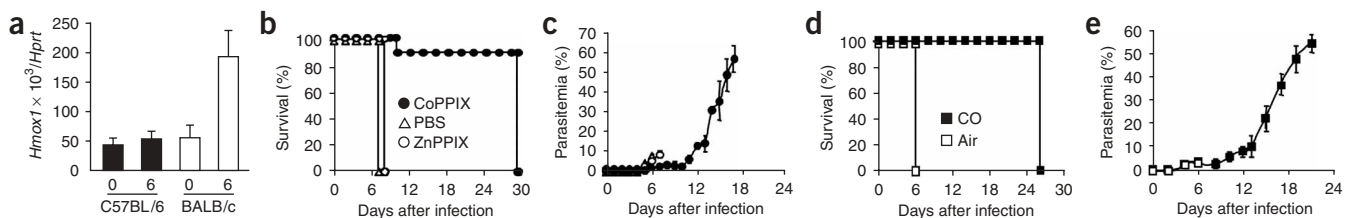
Figure 2 Induction of HO-1 or exposure to CO suppresses ECM onset in C57BL/6 mice infected with *P. berghei* ANKA. (**a**) *Hmox1* mRNA was quantified by qRT-PCR in uninfected mice ('0') or infected mice on day 6 after infection ('6'). $n = 6$ mice per group. (**b,c**) Effect of HO-1 induction by CoPPIX (5 mg/kg/d, i.p., starting 2 d before infection and ending 9 d thereafter) on survival and parasitemia of infected mice. ZnPPIX and PBS were used as controls. $n = 10$ mice per group. (**d,e**) Effects of inhalation of air or CO (for 24 h, starting at day 3 after infection) on survival and mean parasitemia. $n = 10$ mice per group. Error bars represent s.d.
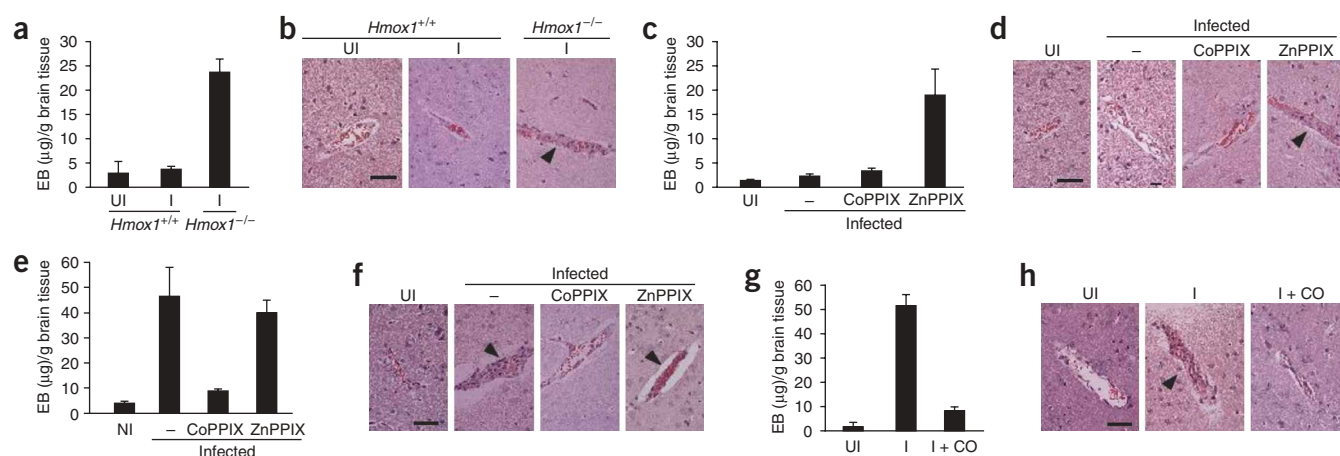
Figure 3 HO-1 and CO prevent BBB disruption and brain microvascular congestion. BBB disruption was assessed by Evans blue (EB) quantification and microvascular congestion was assessed by H&E staining of brain sections in C57BL/6 mice (at 6 d after infection) and BALB/c mice (at 9–12 d after infection). Evans blue quantification is shown as mean μg of Evans blue (EB) per g of brain tissue. $n = 5$ mice per group. H&E staining of brain sections (5 μm thick) was analyzed in parallel experiments. (**a,b**) *Hmox1+/+* and *Hmox1−/−* BALB/c mice, uninfected (UI) or infected with *P. berghei* ANKA (I). (**c,d**) BALB/c mice, uninfected or infected with *P. berghei* ANKA. Infected mice were untreated (−), or treated with CoPPX or ZnPPIX. (**e,f**) As in **c** and **d**, but for C57BL/6 mice. (**g,h**) As in **e** and **f**, but with exposure to air (I) or CO (I + CO), instead of treatment with CoPPX or ZnPPIX. Images in **b,d,f** and **h** are representative of 15 mice in 3 independent experiments. Arrowheads indicate microvascular congestion. Scale bars, 100 μm. Error bars represent s.d.

conditions (ref. 6, and reviewed in ref. 7). This protective effect was still observed (80% reduction in ECM incidence) when CO was administered at day 4 after infection, for 24 h (**Supplementary Fig. 3**). CO administration starting at day 5 after infection was not effective, even when given before the onset of ECM clinical symptoms (data not shown). We observed no significant changes in parasitemia upon CO exposure (**Fig. 2e** and **Supplementary Fig. 3**; $P > 0.05$), suggesting that, as with HO-1 induction, the protective effect of CO does not rely on the inhibition of parasitemia. These data suggest that at a dosage as low as 250 p.p.m., CO can be used therapeutically—that is, treatment with CO following infection can prevent ECM even when applied as late as 2 d before the expected time of death from ECM.

We assessed whether biliverdin, another end product of HO-1 activity, could mimic the protective effects of HO-1. In C57BL/6 mice infected with *P. berghei* ANKA, exogenous biliverdin did not suppress the development of ECM when administered on day 2 after infection and every 8 h thereafter until day 4 (a schedule that mimics the protective effect of HO-1 in other inflammatory conditions, ref. 13; **Supplementary Fig. 3**).

HO-1 and CO prevent BBB disruption and neuroinflammation

We confirmed ECM incidence under the different experimental conditions described above by quantifying blood-brain barrier (BBB) disruption, a hallmark of ECM as well as of cerebral malaria in humans. We also performed histological examination of brain tissue 6 to 12 d after infection.

In BALB/c mice, infection with *P. berghei* ANKA did not lead to BBB disruption (**Fig. 3a**). In contrast, *Hmox1* deletion led to BBB disruption, as revealed by a 10- to 20-fold increase in Evans blue accumulation in brain parenchyma of infected BALB/c mice, as compared to infected wild-type controls ($P < 0.0001$; **Fig. 3a**). Other major pathological features associated with ECM include brain microvascular congestion with activated leukocytes and red blood cells, and brain parenchymal hemorrhages. These features were clearly detectable in *Hmox1−/−* BALB/c mice infected with *P. berghei* ANKA, but not in uninfected or infected wild-type BALB/c controls (**Fig. 3b** and **Supplementary Fig. 4** online).

In a similar manner to *Hmox1* deletion, pharmacological inhibition of HO activity by ZnPPIX also resulted in disruption of BBB (**Fig. 3c**), brain microvascular congestion (**Fig. 3d**) and hemorrhage (**Supplementary Fig. 4**) in infected BALB/c mice, but not in untreated or CoPPIX-treated infected controls (**Fig. 3c,d** and **Supplementary Fig. 4**).

In C57BL/6 mice, *P. berghei* ANKA infection resulted in BBB disruption: there was a 20- to 50-fold increase in Evans blue accumulation in the brain parenchyma, as compared to that in uninfected controls (**Fig. 3e**). HO-1 induction by CoPPIX reduced BBB disruption by $75.6 \pm 4.2\%$ (mean $\pm$ s.d.; $P < 0.0001$; **Fig. 3e**), and abolished brain microvascular congestion (**Fig. 3f**) and hemorrhage (**Supplementary Fig. 4**) associated with the onset of ECM; these effects were not seen in untreated or ZnPPIX-treated controls (**Fig. 3e,f** and **Supplementary Fig. 4**).

Likewise, exposure to CO reduced BBB disruption by $80.2 \pm 8.1\%$ in infected C57BL/6 mice, as compared to air-treated controls ($P < 0.0001$; **Fig. 3g** and **Supplementary Fig. 4**), and abolished brain microvascular congestion (**Fig. 3h**) and hemorrhage (**Supplementary Fig. 4**). On the basis of previous results[14,15], the inhibition of BBB disruption, brain microvascular congestion and hemorrhage is likely to have a major effect in suppressing the pathogenesis of ECM.

We carried out a more detailed histological analysis of the protective effect of CO with regard to suppressing brain microvascular congestion. Development of ECM in C57BL/6 mice was associated with moderate to severe microvasculature occlusion in $58.4 \pm 13.6\%$ of brain arterioles, capillaries or postcapillary venules. Up to $79.2 \pm 10.3\%$ of congested microvessels presented intraluminal accumulation of both infected and uninfected red blood cells and leukocytes (91 vessels analyzed in 4 mice). Exposure to CO reduced the percentage of occluded microvessels to $24 \pm 8.3\%$ ($P < 0.001$ versus air control). Only $42.6 \pm 10.8\%$ of these microvessels contained infected red blood cells and leukocytes (250 vessels analyzed in 10 mice). In uninfected mice, $10.8 \pm 12.5\%$ of brain microvessels had low levels of red blood cell intravascular congestion, and only $5.5 \pm 6.8\%$ of these vessels contained leukocytes (56 vessels analyzed in 4 mice). Taken together, these data suggest that both HO-1 induction and CO exposure
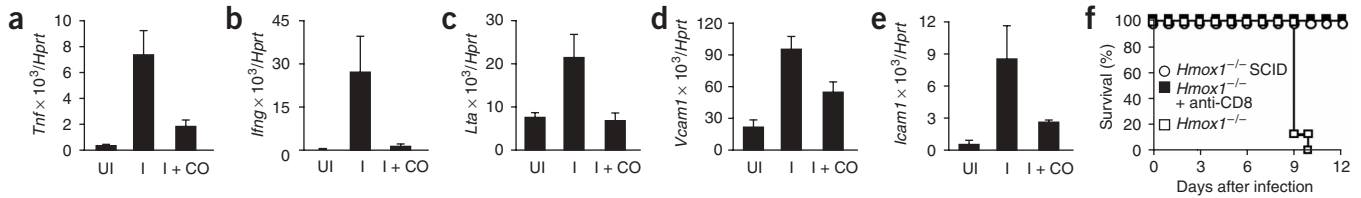
Figure 4 CO inhibits neuroinflammation and CD8+ T-cell brain sequestration. Uninfected and *P. berghei* ANKA–infected mice (at day 6 after infection) were analyzed. CO was supplied by inhalation. (**a**–**e**) mRNA expression in the brain was quantified by qRT-PCR and is shown as the mean number of mRNA molecules of the indicated gene per *Hprt* mRNA ($\times 10^3$). $n = 5$ mice per group. UI, uninfected. Infected C57BL/6 mice were exposed to air (I) or to CO (I + CO). (**f**) Survival of $Hmox1^{-/-}$ and $Hmox1^{-/-}$ SCID BALB/c mice infected with *P. berghei* ANKA. A separate group of $Hmox1^{-/-}$ BALB/c infected mice was treated with a CD8-specific depleting antibody. $n = 5$ mice per group. (**g**) Quantification of total CD8+, activated CD69+CD8+ and IFN-γ+CD8+ T cells in the brains of C57BL/6 mice. Error bars represent s.d.

prevent microvascular congestion and hemorrhage in the brain, two key pathologic features of ECM and cerebral malaria (ref. 11; and reviewed in ref. 16).

We asked whether CO could modulate the expression of tumor necrosis factor (TNF)[17], lymphotoxin-α (LT-α)[18] and interferon-γ (IFN-γ)[19], pro-inflammatory cytokines known to be upregulated during the pathogenesis of ECM and to contribute to its onset (reviewed in ref. 16). Expression of *Tnf* (**Fig. 4a**), *Ifng* (**Fig. 4b**) and *Lta* (**Fig. 4c**) mRNAs were significantly upregulated in the brains of C57BL/6 mice infected with *P. berghei* ANKA, as compared to uninfected controls (*Tnf*, $P < 0.001$; *Ifng*, $P < 0.005$; and *Lta*, $P < 0.05$; day 6 after infection). Exposure to CO reduced *Tnf*, *Ifng* and *Lta* mRNA expression by $76 \pm 13\%$ ($P < 0.002$), $98 \pm 1\%$ ($P < 0.005$) and $68 \pm 20\%$ ($P < 0.005$), respectively, as compared to that in infected controls (**Fig. 4a–c**). Taking into consideration the critical role of pro-inflammatory cytokines in the pathogenesis of ECM (reviewed in ref. 16), it is likely that the protective effect of CO is mediated at least in part through their inhibition.

Expression of intracellular adhesion molecule-1 (ICAM-1/CD54)[14] and presumably that of vascular cell adhesion molecule-1 (VCAM-1/CD106) promote the pathogenesis of ECM. *Icam1* and *Vcam1* mRNA expression was increased in the brains of C57BL/6 mice showing ECM symptoms ($P < 0.001$ and $P < 0.005$, respectively: infected versus uninfected mice; **Fig. 4d,e**). Exposure to CO led to a $71 \pm 9\%$ and a $41 \pm 4\%$ decrease in ICAM-1 and VCAM-1 expression ($P < 0.001$ and $P < 0.05$, respectively, infected versus infected exposed to CO), as assessed on day 6 after infection (**Fig. 4d,e**).

In addition, we assessed whether pharmacological induction of HO-1 or exposure to CO inhibited the recruitment of CD8+ T cells into the brain, another critical event in the pathogenesis of ECM (refs. 20,21). When backcrossed into the severe combined immunodeficiency (SCID) background, $Hmox1^{-/-}$ BALB/c mice infected with *P. berghei* ANKA did not develop ECM symptoms, and all mice survived (**Fig. 4f**). This demonstrates that HO-1 counters the deleterious effects of B or T cells that lead to ECM. Further, depletion of CD8+ T cells using a CD8-specific monoclonal antibody was sufficient to prevent the onset of ECM in infected $Hmox1^{-/-}$ BALB/c mice (**Fig. 4f**). This result suggests that HO-1 prevents CD8+ T cells from triggering ECM (refs. 20,21). Moreover, we assessed whether exposure to CO (**Fig. 4g**) or the induction of HO-1 by CoPPIX (data not shown) could suppress CD8+ T-cell sequestration in the brain. In infected C57BL/6 mice, CO decreased the total number of CD8+ T cells in the brain (including activated CD8+CD69+ and

IFN-γ–secreting CD8+ T cells) by 65–75%, as compared to air-treated controls ($P < 0.05$; **Fig. 4g**). CO also inhibited monocyte/macrophage (CD45RB^{high}CD11b+) and polymorphonuclear (PMN; CD45RB^{high}GR1+) recruitment into the brain (data not shown). Induction of HO-1 by CoPPIX yielded similar results to CO inhalation, whereas ZnPPIX had no effect (data not shown). These results suggest that CO suppresses the sequestration of CD8+ T cells in brains of mice infected with *P. berghei* ANKA, an effect that should contribute to the suppression of ECM onset[20,21].

CO inhibits heme release from oxidized hemoglobin

Malaria is associated with a severe hemolysis that generates extracellular ferrous (Fe^{2+}) hemoglobin, which in the presence of reactive oxygen species (ROS) is readily oxidized into methemoglobin (MetHb) (Fe^{3+}). We asked whether CO could arrest this process. Generation of carboxyHb (COHb; 100%) by exposure of purified ferrous (Fe^{2+}) hemoglobin to CO *in vitro* suppressed MetHb formation driven by either H_2O_2 or activated polymorphonuclear (PMN) cells ($>85\%$ inhibition versus that in air-treated controls, $P < 0.0001$; **Supplementary Fig. 5** online). These effects were dose dependent, as increasing the percentage of COHb led to increased inhibition of MetHb formation (**Supplementary Fig. 5**), and were not observed when PMN were exposed to CO instead of Fe^{2+} hemoglobin (data not shown). These results suggested that CO prevents hemoglobin oxidation through a mechanism that relies on its binding to Fe^{2+} hemoglobin. To ascertain whether similar effects occur *in vivo*, we measured MetHb concentration in whole blood from infected C57BL/6 mice that had or had not been exposed to CO. MetHb concentration increased significantly in infected versus uninfected mice ($P < 0.05$; **Fig. 5a**). Exposure of the infected mice to CO (250 p.p.m.; $23 \pm 6\%$ COHb; **Supplementary Fig. 6** online) decreased MetHb concentration to basal levels (that is, to levels observed in uninfected mice; **Fig. 5a**).

MetHb is highly unstable, releasing free heme[22]. The ability of H_2O_2 or activated PMN cells to release heme from Fe^{2+} hemoglobin was suppressed when hemoglobin was exposed to CO before oxidation ($>95\%$ inhibition versus air-treated controls, $P < 0.0001$; **Fig. 5b**). These data indicate that once bound to Fe^{2+} hemoglobin, CO suppresses not only its oxidation but also the subsequent generation of free heme. To assess whether a similar mechanism occurs *in vivo*, we measured the concentration of extracellular (non-protein-bound) heme in the circulation of infected C57BL/6 mice (**Fig. 5c**). Free heme concentration increased significantly upon infection ($P < 0.001$;

Figure 5 HO-1 and CO prevent BBB disruption and the development of ECM by inhibiting free heme release from oxidized hemoglobin. Uninfected (UI) and *P. berghei* ANKA–infected (I) mice were analyzed. (**a**) Mean percentage of methemoglobin (MetHb) in whole blood of C57BL/6 mice. Measurements were performed on day 6 after infection. $n = 5$ mice per group. (**b**) Hemoglobin (Hb, 200 μM) was exposed to air or to CO (100% bubbled at a flow rate of 10 ml/min for 10 s) to generate carboxyhemoglobin (COHb) and then subjected to oxidation by H_2O_2 (2 mM, 1 h, 37 °C) or by activated polymorphonuclear (PMN) cells (4×10^7 per ml, 1 h). (−), no addition. Free heme captured by low density lipoprotein (LDL) is shown as mean number of heme molecules per LDL particle. $n = 3$ independent experiments. (**c**) Mean free heme concentration in protein-free plasma of uninfected and infected C57BL/6 mice. Infected mice were exposed to air (−) or CO, or treated with CoPPIX or ZnPPIX. Measurements were performed on day 6 after infection. $n = 4$–7 mice per group. (**d**) Survival of infected C57BL/6 mice exposed to CO and receiving heme or vehicle (PBS). (**e**) BBB disruption in uninfected versus *P.* infected C57BL/6 mice exposed to air (−), CO or CO + heme. Evans blue (EB) quantification is shown as mean μg of Evans blue per g of brain tissue. $n = 4$–5 mice per group. (**f**) Permeability of confluent bMVEC-B cells to 10 kDa fluorescent dextran was quantified in a transwell chamber, after exposure to heme, H_2O_2 or heme + H_2O_2. Results are shown as mean percentage of fluorescent tracer in the lower chamber. $n = 3$. Error bars represent s.d.
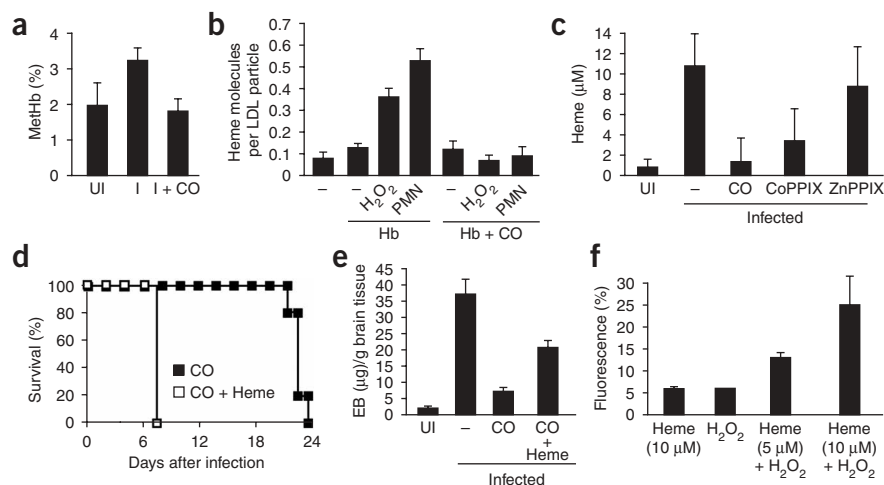
Fig. 5c). Both exposure to CO and the induction of HO-1 using CoPPIX reduced plasma free heme concentration—by 88 ± 22% and 69 ± 31%, respectively—as compared to that in untreated infected controls ($P < 0.01$; **Fig. 5c**). With ZnPPIX treatment, plasma free heme concentration was not different than that in untreated infected controls (**Fig. 5c**).

CO did not modulate red blood cell counts (data not shown), heme red blood cell content, lactate dehydrogenase (LDH) levels or bilirubin concentration in the circulation of infected C57BL/6 mice (**Supplementary Fig. 6**). These results suggest that CO inhibits the accumulation of free heme in the circulation of these mice by a process that does not involve the inhibition of red blood cell lysis.

Free heme triggers ECM

We asked whether the accumulation of free heme in the circulation of infected C57BL/6 mice was involved in the pathogenesis of ECM. Heme administration 3 d after infection was sufficient to reverse the protective effect of CO, causing death in 100% of infected mice, with symptoms consistent with ECM, compared to 0% of vehicle-treated mice (**Fig. 5d**). Heme had no deleterious effects when administered to uninfected C57BL/6 mice at the same dose and on the same schedule (data not shown). Heme administration reverted the protective effect of CO and triggered BBB disruption, a key pathological feature of ECM and cerebral malaria (**Fig. 5e**). These data reveal not only that accumulation of free heme in the circulation of infected mice is a central component in the pathogenesis of ECM, but also that CO suppresses ECM by inhibiting this process, presumably by blocking hemoglobin oxidation.

We tested whether the ability of different *Plasmodium* strains to trigger ECM was functionally linked to the amount of free heme that accumulates in the host circulation. Plasma free heme concentration was reduced by 44 ± 19% ($P < 0.001$) in C57BL/6 mice infected with *P. berghei* NK65 versus *P. berghei* ANKA. The former group did not succumb, whereas the latter succumbed 6–7 d after infection, with symptoms consistent with ECM (**Supplementary Fig. 7** online). After this time period, free heme concentrations remained constant in mice infected with *P. berghei* ANKA NK65: at days 10 and 15 after infection, concentrations were 33 ± 11% and 34 ± 19%, respectively, of those in

mice infected with *P. berghei* ANKA ($P < 0.001$; **Supplementary Fig. 7**). Heme administration to C57BL/6 mice infected with *P. berghei* ANKA NK65 (60 mg per kg body weight; at 6 d after infection) led to death in 100% of mice, with symptoms consistent with ECM (**Supplementary Fig. 7**). Heme administration to uninfected C57BL/6 mice at the same dose and on the same schedule was not lethal (data not shown).

We then asked whether the absence of ECM in *P. berghei* ANKA–infected BALB/c mice compared to its occurrence in *P. berghei* ANKA–infected C57BL/6 mice was also functionally linked to the accumulation of circulating free heme. Plasma free heme concentration was reduced by 36 ± 9% ($P < 0.001$) in BALB/c versus C57BL/6 mice (**Supplementary Fig. 7**). At the time of development of ECM symptoms, plasma free heme concentration in BALB/c mice was reduced by 36 ± 9% and 28 ± 32% at days 10 and 15 after infection, respectively, from the levels in infected C57BL/6 mice ($P < 0.001$; **Supplementary Fig. 7**). Heme administration to BALB/c mice infected with *P. berghei* ANKA (60 mg/kg; i.p.; 6 d after infection) led to death in 100% of the mice, with symptoms consistent with ECM (**Supplementary Fig. 7**). Heme administration to uninfected BALB/c mice was not lethal (data not shown). Taken together, these data support the notion that accumulation of free heme in the circulation of a malaria-infected host plays a critical role in dictating the host's susceptibility to ECM.

We hypothesized that free heme might affect BBB tight-junction function in a manner that would promote BBB disruption. We tested this hypothesis using a well-established *in vitro* BBB model, in which confluent bovine brain microvascular endothelial cells (bMVEC-B cells) form functional tight junctions, revealed by the exclusion of a fluorescent 10-kDa dextran tracer in a transwell assay (**Fig. 5f**). Tight-junction functional integrity was not disrupted when bMVEC-B cells were exposed to either H_2O_2 or heme alone. However, when bMVEC-B cells were pre-exposed to heme, further addition of H_2O_2 caused loss of functional tight-junction integrity, as revealed by a 2–5 fold increase in fluorescent dextran tracer permeability. The effect of heme was dose dependent, with higher concentrations leading to increased permeability. We obtained similar results using Madin-Darby canine kidney (MDCK) cells (data not shown), which also form tight junctions
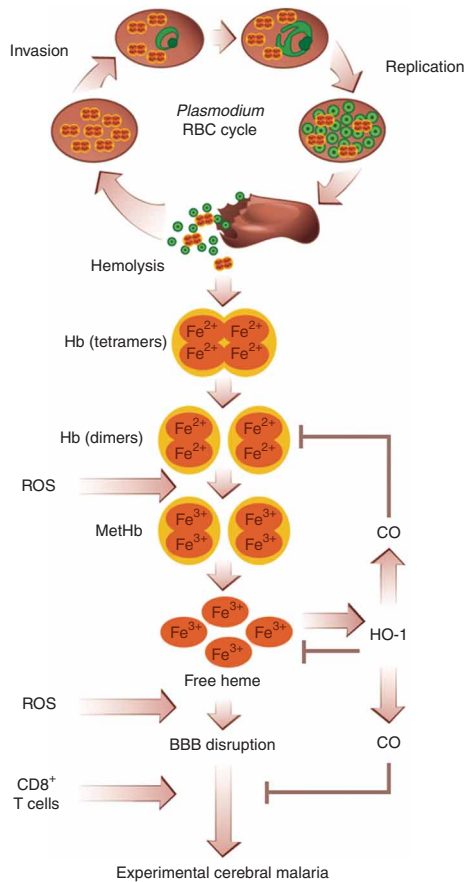
Figure 6 Mechanism underlying the protective actions of HO-1 and CO. Hemolysis is inherently associated with cycles of *Plasmodium* invasion, replication and egress (hemolysis) in red blood cells (RBC). This process leads to the release of hemoglobin into the circulation. Cell-free hemoglobin dimerizes spontaneously and in the presence of ROS is readily oxidized into MetHb. This process of hemoglobin oxidation readily leads to the release of heme. In the presence of ROS, cell-free heme promotes BBB disruption; activated $CD8^+$ T cells can then promote the onset of ECM. Both heme and ROS upregulate the expression of HO-1, a stress-responsive enzyme that generates CO by degrading heme. CO binds cell-free hemoglobin dimers, blocking their oxidation and thus the generation of circulating free heme. In addition, CO prevents the recruitment of $CD8^+$ T cells in the brain microvasculature. These effects may together afford potent protection against the development of ECM.

in vitro. These data suggest that in the presence of a ROS (that is, H_2O_2), heme can disrupt BBB tight-junction function, which could explain the BBB disruption associated with the pathogenesis of ECM. By blocking the generation of free heme, CO may act to prevent BBB disruption.

DISCUSSION

Understanding the pathogenesis of malaria infection is crucial for the development of more efficient clinical interventions. Sequestration of infected red blood cells and leukocytes (that is, $CD8^+$ T cells in the brain[20,21,23]), and the inflammatory response triggered by malaria infection are thought to be the two key events in the pathogenesis of cerebral malaria[8]. Our present data show that HO-1 expression and enzymatic activity in the host counter the pathogenesis of ECM. Moreover, we have demonstrated that the administration of exogenous CO via inhalation can be used therapeutically to suppress the pathogenesis of ECM. The protective effects of CO administration were associated with inhibition of BBB disruption, brain microvascular congestion and hemorrhage, as well as with suppression of neuroinflammation, including inhibition of adhesion molecule expression in the brain microvasculature and the suppression of activated $CD8^+$ T cell sequestration in the brain.

The ability of CO to suppress the accumulation of free heme in the circulation of the infected host seems critical for its protective effects. Malaria infection is associated with severe hemolysis and therefore with the oxidation of cell-free hemoglobin[2], leading to the release of free heme and its accumulation in plasma. We have shown that circulating free heme is a central effector in the pathogenesis of

ECM, promoting BBB disruption by means of a mechanism targeting the tight junctions that maintain BBB functional integrity. Binding of CO to Fe^{2+} in the heme groups of ferrous hemoglobin prevents hemoglobin oxidation, heme release from oxidized hemoglobin, accumulation of free heme in the circulation, BBB disruption and, consequently, the development of ECM.

Other researchers have shown that, as in other hemolytic diseases (for example, sickle cell anemia[24]), scavenging of nitric oxide (NO) by cell-free hemoglobin generated during malaria infection promotes the onset of ECM (ref. 25). It is possible therefore that CO and NO might interact functionally to suppress the pathogenesis of ECM. Once bound to cell-free hemoglobin, CO may limit NO scavenging, an effect that would increase NO bioavailability and thus suppress the pathogenesis of ECM (ref. 25). According to this notion, the protective effect of CO might be 'NO dependent'. On the other hand, the protective effect of NO might itself be 'CO dependent', as NO is a potent inducer of HO expression[26]. NO might act in a protective manner through the induction of HO-1 and the subsequent generation of CO, shown here to prevent the onset of ECM. These hypotheses remain to be tested experimentally.

The proposed mechanism for the protective action of CO (**Fig. 6**) may have important implications for understanding the pathogenesis of cerebral malaria. Expression of HO-1 occurs during malaria infection in humans[27,28], suggesting that a similar protective mechanism may operate to suppress the development of cerebral malaria. Although ECM may not fully reflect human cerebral malaria, it allows for the identification of genes that control both of these pathologic processes, as shown for the involvement of *TNF* (refs. 29–32) and *ICAM1* (also known as CD54)[33,34] in ECM and cerebral malaria (reviewed in ref. 35). Thus, although our data do not allow to conclude unequivocally that *HMOX1* is a gene that determines susceptibility to cerebral malaria, it is likely that variations in HO-1 expression, known to occur in human populations as a result of a (GT)n microsatellite polymorphism in the promoter region of the human *HMOX1* gene (reviewed in ref. 36), can dictate susceptibility to cerebral malaria.

Preliminary evidence suggests that the incidence of the homozygous short GT(< 28) polymorphism, which presumably affords a high level of HO-1 induction during malaria infection, is markedly increased in malaria patients who succumb to cerebral malaria[37], a finding that is in apparent discrepancy with the notion that HO-1 prevents the onset of ECM. This might be explained by the observation that HO-1 is highly induced in the liver during the initial liver stage of malaria infection in mice, which occurs before the blood stage. Moreover, we found that the liver stage of infection was reduced by 70–80% in $Hmox1^{-/-}$ mice (S.E. *et al.*, unpublished data). These findings suggest that a successful host-*Plasmodium* interaction leading to long-lasting

infection in a viable host is quite complex and is dependent on the regulated expression of HO-1 in different tissues at different stages of the *Plasmodium* life cycle.

This study reveals that the pathogenesis of cerebral malaria might be controlled through the expression of a so-called 'protective gene' in the host[38]. We have shown this for HO-1 in the context of ECM, but we do not exclude the possibility that other 'protective genes'[39] might act in a similar manner to prevent the onset of cerebral malaria or other forms of severe acute malaria in humans. These findings provide new insights into the pathogenesis of ECM and may lead to new therapeutic approaches to suppress the pathogenesis of human cerebral malaria based on the modulation of HO-1 expression or the administration of CO.

METHODS

Mice. C57BL/6 and BALB/c mice were bred and housed in the pathogen-free facilities of the Instituto de Gulbenkian de Ciência. All protocols were approved by the Animal Care Committee of the Instituto Gulbenkian de Ciência. We generated $Hmox1^{-/-}$ mice by mating $Hmox1^{+/-}$ mice (backcrossed for ten generations into the BALB/c background), as previously described[40]. We backcrossed BALB/c $Hmox1^{+/-}$ mice into the severe combined immuno-deficient (SCID) background (Jackson Laboratory). We isolated genomic DNA from the tail and determined the *Hmox* genotype by PCR using the following primers: 5′-TCTTGACGAGTTCTTCTGAG-3′ and 5′-ACGAAGT GACGCCATCTGT-3′; 5′-GGTGACAGAAGAGGCTAAG-3′ and 5′-CTGTAA CTCCACCTCCAAC-3′. We repeated each PCR reaction at least three times before experiments on the mice were performed and once more afterward. As controls, we used littermate $Hmox1^{+/-}$ and $Hmox1^{+/+}$ mice.

Parasites, infection and disease assessment. In all experiments, we used red blood cells infected with green fluorescent protein (GFP)-transgenic *P. berghei* ANKA (ref. 41) or *P. berghei* NK65 to infect C57BL/6 or BALB/c mice. Mice were infected by intraperitoneal (i.p.) inoculation of 10^5 infected red blood cells, except in experiments using *Hmox1*-deficient mice, in which 10^4 infected red blood cells were used. Infected mice were monitored twice daily for clinical symptoms of ECM including hemi- or paraplegia, head deviation, tendency to roll over on stimulation, ataxia and convulsions. We determined parasitemia by flow cytometry for mice infected with GFP-transgenic *P. berghei* ANKA and by Giemsa staining followed by microscopic counting for mice infected with *P. berghei* NK65. These results are expressed as percentage of infected red blood cells, as previously described[41].

Protoporphyrins. Iron protoporphyrin-IX (FePPIX, hemin), zinc protopor-phyrin-IX (ZnPPIX), cobalt protoporphyrin-IX (CoPPIX) and biliverdin hydrochloride (BV) (Frontier Scientific Inc.), were dissolved in 0.2 M NaOH, neutralized (to pH 7.2) with 1 M HCl, and adjusted to concentrations of 1 mg/ml (ZnPPIX, CoPPIX) or 3.8 mg/ml (BV) with distilled water. Aliquots were stored at –80 °C and protected from light until used. For BBB studies, we treated mice with FePPIX (40 mg/kg body weight) every 12 h, starting on day 3 after infection. For survival studies, we administered FePPIX (60 mg/kg body weight) every 12 h, starting on day 5 after infection. CoPPIX (5 mg/kg body weight per d) and ZnPPIX (5 mg/kg/d) were administered i.p. and were started 2 d before infection and continued for 9 d thereafter. We administered biliverdin every 8 h (35 mg/kg i.p.) between days 2 and 4 after infection.

CO exposure. Mice were placed in a gastight 60-liter capacity chamber and exposed to CO for the times indicated in the figure legends, as described elsewhere[6,42]. Briefly, 1% CO (Aga Linde) was mixed with air in a stainless steel cylinder to obtain a final concentration of 250 p.p.m. CO was provided continuously at a flow rate of ∼12 liter/min, starting on day 3 after infection and continuing for 72 h, unless otherwise stated. We monitored CO concen-tration using a CO analyzer (Interscan Corporation). Controls were maintained in a similar chamber without CO. We measured levels of COHb using a portable CO-oximeter (AVOXImeter 4000, Avox Systems).

BBB permeability. We injected mice intravenously (i.v.) with 0.2 ml of 1–2% Evans blue (Sigma) when clinical symptoms of ECM were observed (that is, head deviation, convulsions, ataxia and paraplegia). Mice were killed 1 h thereafter, and brains were weighed and placed in formamide (2 ml, 37 °C, 48 h; Merck) to extract Evans blue dye from the tissue, essentially as previously described[43]. Absorbance was measured at $\lambda = 620$ nm (Bio Rad SmartSpec 3000). We calculated Evans blue concentration using a standard curve. Data are expressed as μg of Evans blue per g of brain tissue.

CD8-specific antibody depletion. $Hmox1^{-/-}$ BALB/c mice infected with *P. berghei* ANKA received 0.8 mg of CD8-specific monoclonal antibody (clone 2.43, ATCC) on days 5 and 8 after infection, a protocol leading to CD8$^+$ T-cell depletion and suppression of ECM (ref. 20).

Heme quantification in vivo. Blood was drawn into heparinized tubes by heart puncture and centrifuged (5 min, 4 °C, 1,100g). We collected red blood cells, centrifuged the plasma (5 min, 4 °C, 1,100g) to remove contaminating red blood cells and passed it through a Microcon YM-3 column (Millipore)(60 min at 14 °C, 21,000g) to remove proteins (MW > 3 kDa). We quantified heme (that is, free heme) in protein-depleted plasma using a chromogenic assay according to the manufacturer's instructions (QuantiChrom heme assay kit, Bioassay Systems). We washed red blood cells in a choline washing solution (160 mM choline chloride, 10 mM glucose, 10 mM Tris.MOPS, pH 7.4); the cells were incubated in washing solution for 5 min at 4 °C, then centrifuged at 1,100g, and this was repeated 4 times. We lysed the cells in H_2O (1/100 vol) and measured heme concentration using the same chromogenic assay as above.

Statistical analysis. For samples in which $n > 5$, statistical analyses were performed using the unpaired Student's t-test or analysis of variance (ANOVA) parametric tests. Normal distributions were confirmed using the Kolmogorov-Smirnov test. For samples in which $n < 5$, statistical analyses were performed using Kruskall-Wallis or Wilcoxon nonparametric tests. The log-rank test was used for all experiments in which survival was assessed as an end point. $P < 0.05$ was considered significant; $P < 0.001$ was considered highly significant.

Note: Supplementary information is available on the Nature Medicine website.

AUTHOR CONTRIBUTIONS
A.P. performed the majority of the experimental work. A.F. contributed critically to defining the role of free heme in the onset of ECM. Both A.P. and A.F. contributed to the study design and helped in drafting the manuscript. J.B., V.J. and G.B. performed the *in vitro* studies that defined the ability of CO to inhibit hemoglobin oxidation. S.E. performed all histological procedures and analysis. A.C., C.D.R., I.P.G., M.C.-R. and S.P. contributed to the experimental work. M.M.M. formulated the initial hypothesis that HO-1 and CO might counter the onset of ECM, and M.P.S. formulated the hypothesis that CO might act on hemoglobin to arrest ECM triggered by free heme. Both M.P.S. and M.M.M. conceived and designed the experimental procedures and wrote the manuscript. All authors read and approved the manuscript.

COMPETING INTERESTS STATEMENT
The authors declare no competing financial interests.

ARTICLES

1. Francis, S.E., Sullivan, D.J., Jr. & Goldberg, D.E. Hemoglobin metabolism in the malaria parasite Plasmodium falciparum. *Annu. Rev. Microbiol.* **51**, 97–123 (1997).
2. Balla, J. *et al.* Heme, heme oxygenase and ferritin in vascular endothelial cell injury. *Mol. Nutr. Food Res.* **49**, 1030–1043 (2005).
3. Orjih, A.U., Banyal, H.S., Chevli, R. & Fitch, C.D. Hemin lyses malaria parasites. *Science* **214**, 667–669 (1981).
4. Balla, G. *et al.* Ferritin: a cytoprotective antioxidant strategem of endothelium. *J. Biol. Chem.* **267**, 18148–18153 (1992).
5. Tenhunen, R., Marver, H.S. & Schmid, R. The enzymatic conversion of heme to bilirubin by microsomal heme oxygenase. *Proc. Natl. Acad. Sci. USA* **61**, 748–755 (1968).
6. Sato, K. *et al.* Carbon monoxide generated by heme oxygenase-1 suppresses the rejection of mouse to rat cardiac transplants. *J. Immunol.* **166**, 4185–4194 (2001).
7. Otterbein, L.E., Soares, M.P., Yamashita, K. & Bach, F.H. Heme oxygenase-1: unleashing the protective properties of heme. *Trends Immunol.* **24**, 449–455 (2003).
8. Clark, I.A., Cowden, W.B. & Rockett, K.A. The pathogenesis of human cerebral malaria. *Parasitol. Today* **10**, 417–418 (1994).
9. Schofield, L. & Grau, G.E. Immunological processes in malaria pathogenesis. *Nat. Rev. Immunol.* **5**, 722–735 (2005).
10. Lou, J., Lucas, R. & Grau, G.E. Pathogenesis of cerebral malaria: recent experimental data and possible applications for humans. *Clin. Microbiol. Rev.* **14**, 810–820 (2001).
11. Hansen, D.S., Siomos, M.A., Buckingham, L., Scalzo, A.A. & Schofield, L. Regulation of murine cerebral malaria pathogenesis by CD1d-restricted NKT cells and the natural killer complex. *Immunity* **18**, 391–402 (2003).
12. Basilico, N., Monti, D., Olliaro, P. & Taramelli, D. Non-iron porphyrins inhibit beta-haematin (malaria pigment) polymerisation. *FEBS Lett.* **409**, 297–299 (1997).
13. Yamashita, K. *et al.* Biliverdin, a natural product of heme catabolism, induces tolerance to cardiac allografts. *FASEB J.* **18**, 765–767 (2004).
14. Favre, N. *et al.* Role of ICAM-1 (CD54) in the development of murine cerebral malaria. *Microbes Infect.* **1**, 961–968 (1999).
15. Thumwood, C.M., Hunt, N.H., Clark, I.A. & Cowden, W.B. Breakdown of the blood-brain barrier in murine cerebral malaria. *Parasitology* **96**, 579–589 (1988).
16. Good, M.F., Xu, H., Wykes, M. & Engwerda, C.R. Development and regulation of cell-mediated immune responses to the blood stages of malaria: implications for vaccine research. *Annu. Rev. Immunol.* **23**, 69–99 (2005).
17. Grau, G.E. *et al.* Tumor necrosis factor (cachectin) as an essential mediator in murine cerebral malaria. *Science* **237**, 1210–1212 (1987).
18. Engwerda, C.R. *et al.* Locally up-regulated lymphotoxin alpha, not systemic tumor necrosis factor alpha, is the principle mediator of murine cerebral malaria. *J. Exp. Med.* **195**, 1371–1377 (2002).
19. Grau, G.E. *et al.* Monoclonal antibody against interferon gamma can prevent experimental cerebral malaria and its associated overproduction of tumor necrosis factor. *Proc. Natl. Acad. Sci. USA* **86**, 5572–5574 (1989).
20. Belnoue, E. *et al.* On the pathogenic role of brain-sequestered alphabeta CD8+ T cells in experimental cerebral malaria. *J. Immunol.* **169**, 6369–6375 (2002).
21. Yanez, D.M., Manning, D.D., Cooley, A.J., Weidanz, W.P. & van der Heyde, H.C. Participation of lymphocyte subpopulations in the pathogenesis of experimental murine cerebral malaria. *J. Immunol.* **157**, 1620–1624 (1996).
22. Balla, J. *et al.* Endothelial-cell heme uptake from heme proteins: induction of sensitization and desensitization to oxidant damage. *Proc. Natl. Acad. Sci. USA* **90**, 9285–9289 (1993).
23. Berendt, A.R., Tumer, G.D. & Newbold, C.I. Cerebral malaria: the sequestration hypothesis. *Parasitol. Today* **10**, 412–414 (1994).
24. Reiter, C.D. *et al.* Cell-free hemoglobin limits nitric oxide bioavailability in sickle-cell disease. *Nat. Med.* **8**, 1383–1389 (2002).
25. Gramaglia, I. *et al.* Low nitric oxide bioavailability contributes to the genesis of experimental cerebral malaria. *Nat. Med.* **12**, 1417–1422 (2006).
26. Bouton, C. & Demple, B. Nitric oxide-inducible expression of heme oxygenase-1 in human cells. Translation-independent stabilization of the mRNA and evidence for direct action of nitric oxide. *J. Biol. Chem.* **275**, 32688–32693 (2000).
27. Clark, A.R., Dean, J.L. & Saklatvala, J. Post-transcriptional regulation of gene expression by mitogen-activated protein kinase p38. *FEBS Lett.* **546**, 37–44 (2003).
28. Schluesener, H.J., Kremsner, P.G. & Meyermann, R. Heme oxygenase-1 in lesions of human cerebral malaria. *Acta Neuropathol. (Berl.)* **101**, 65–68 (2001).
29. Grau, G.E. *et al.* Tumor-necrosis-factor (cachectin) as an essential mediator in murine cerebral malaria. *Science* **237**, 1210–1212 (1987).
30. McGuire, W., Hill, A.V.S., Allsopp, C.E.M., Greenwood, B.M. & Kwiatkowski, D. Variation in the Tnf-alpha promoter region associated with susceptibility to cerebral malaria. *Nature* **371**, 508–511 (1994).
31. Grau, G.E. *et al.* Tumor necrosis factor and disease severity in children with falciparum-malaria. *N. Engl. J. Med.* **320**, 1586–1591 (1989).
32. Wilson, A.G., Symons, J.A., McDowell, T.L., McDevitt, H.O. & Duff, G.W. Effects of a polymorphism in the human tumor necrosis factor alpha promoter on transcriptional activation. *Proc. Natl. Acad. Sci. USA* **94**, 3195–3199 (1997).
33. Grau, G.E. *et al.* Late administration of monoclonal-antibody to leukocyte function-antigen 1 abrogates incipient murine cerebral malaria. *Eur. J. Immunol.* **21**, 2265–2267 (1991).
34. Ockenhouse, C.F. *et al.* Human vascular endothelial-cell adhesion receptors for plasmodium-falciparum infected erythrocytes: roles for endothelial leukocyte adhesion molecule-1 and vascular cell-adhesion molecule-1. *J. Exp. Med.* **176**, 1183–1189 (1992).
35. Hunt, N.H. & Grau, G.E. Cytokines: accelerators and brakes in the pathogenesis of cerebral malaria. *Trends Immunol.* **24**, 491–499 (2003).
36. Exner, M., Minar, E., Wagner, O. & Schillinger, M. The role of heme oxygenase-1 promoter polymorphisms in human disease. *Free Radic. Biol. Med.* **37**, 1097–1104 (2004).
37. Takeda, M. *et al.* Microsatellite polymorphism in the heme oxygenase-1 gene promoter is associated with susceptibility to cerebral malaria in Myanmar. *Jpn. J. Infect. Dis.* **58**, 268–271 (2005).
38. Bach, F.H., Hancock, W.W. & Ferran, C. Protective genes expressed in endothelial cells: a regulatory response to injury. *Immunol. Today* **18**, 483–486 (1997).
39. Nathan, C. Points of control in inflammation. *Nature* **420**, 846–852 (2002).
40. Yet, S.F. *et al.* Hypoxia induces severe right ventricular dilatation and infarction in heme oxygenase-1 null mice. *J. Clin. Invest.* **103**, R23–R29 (1999).
41. Franke-Fayard, B. *et al.* A Plasmodium berghei reference line that constitutively expresses GFP at a high level throughout the complete life cycle. *Mol. Biochem. Parasitol.* **137**, 23–33 (2004).
42. Otterbein, L.E. *et al.* Carbon monoxide has anti-inflammatory effects involving the mitogen-activated protein kinase pathway. *Nat. Med.* **6**, 422–428 (2000).
43. van der Heyde, H.C. *et al.* Assessing vascular permeability during experimental cerebral malaria by a radiolabeled monoclonal antibody technique. *Infect. Immun.* **69**, 3460–3465 (2001).

Comparative Genomics and Proteomics in Drug Discovery

EXPERIMENTAL BIOLOGY REVIEWS

Comparative Genomics and Proteomics in Drug Discovery

Edited by

JOHN PARRINGTON
Department of Pharmacology, University of Oxford, Oxford, UK

KEVIN COWARD
Department of Pharmacology, University of Oxford, Oxford, UK

Taylor & Francis
Taylor & Francis Group

Contents

Contributors

Sergio Callejas and Sara Melville, University of Cambridge, UK

CS Peacock, Wellcome Trust Sanger Institute, UK

Maria M. Mota, Miguel Prudêncio and Cristina Rodrigues, Universidade de Lisboa, Portugal

David B. Sattelle, Andrew K. Jones, Laurence A. Brown, Steven D. Buckingham, Christopher J. Mee and Luanda Pym, University of Oxford, UK

Jeff Clare, GlaxoSmithKline, UK

John Bilello, GlaxoSmithKline, USA

David Wishart, University of Alberta, Canada

Preface

This book arose from a one-day symposium arranged as part of the Annual Meeting of the Society for Experimental Biology (UK) in Barcelona in 2005 and takes up the important question of how emerging genomic and proteomic technologies are making significant contributions to global drug discovery programmes, and in particular the key role that comparative genomic and proteomic strategies play.

Rapid progress in our understanding of cellular and molecular biology has led to the field of biomedical science undergoing a major revolution over the last 30 years or so. Of particular note is the dramatic development of genomic and proteomic technologies and their associated application in biology and medicine.

Genomics is the study of an organism's genome and involves isolation, identification and mapping of genes along with associated functional dynamics and interaction. The Human Genome Project has revealed that the human genome is composed of 20,000 to 25,000 genes. However, since each gene can be translated into a variety of different proteins via a variety of cellular and molecular mechanisms, it is estimated that the human proteome consists of approximately 1,000,000 differently modified proteins. This in turn means that there are significantly more potential biomarkers or drug targets to be discovered using proteomic approaches rather than genomic approaches. Expression of these proteins is known to vary in response to environmental change and is related to genetic history. Unlike variation in gene expression, any change in protein expression usually results in alteration of function. Genomics and proteomics are thus considered as being highly complementary approaches to the molecular study of disease.

Written by widely respected authorities from both academic and pharmaceutical backgrounds, this book is composed of seven concise chapters. In Chapter 1, Sara Melville (Cambridge University, UK), introduces the use of comparative genomics in drug discovery in one of the three main human pathogens associated with kinetoplastids, the trypanosomatids, parasitic protozoa responsible for a wide range of diseases including African sleeping sickness, Chagas disease and leishmaniasis. In Chapter 2, Chris Peacock (Wellcome Trust Sanger Institute, UK) describes how comparative genomics is being used to assist in developing treatments against the kinetoplastids, a remarkable group of organisms that include major pathogens responsible for thousands of deaths each year and serious illness to millions. Maria Mota (Universidade de lisboa, Portugal) then considers the relevance of host genes in malaria (Chapter 3), a devastating disease that affects extensive areas of Africa, Asia and South/Central America causing up to 2.7 million deaths per year. In Chapter 4, David Sattelle (University of Oxford, UK) describes how comparative genomics has contributed to the study of nicotinic acetylcholine receptors as drug/chemical targets for a number of conditions including genetic and autoimmune disorders. Chapter 5 (Jeff Clare, GlaxoSmithKline, UK) discusses how genomic and proteomic strategies are being used in gene family-based drug discovery projects aimed at isolating novel sodium channel inhibitors. A sub-population of voltage-gated sodium channels are expressed primarily in nerves involved in pain signalling; these are hence of major interest to the pharmaceutical industry as potential targets for improved analgesics. In Chapter 6,

John Bilello (GlaxoSmithKline, USA) discusses how information resulting from genomic and proteomic studies can be translated into disease understanding and effective management of therapy. Finally, in Chapter 7, David Wishart (University of Alberta, Canada) discusses how advances in genomic and information technology have led to the possibility of *in silico* drug target discovery.

The purpose of this book is to provide an introduction to the concepts behind the dynamic and powerful fields of comparative genomics and proteomics and their specific application in drug discovery. To some extent, the book assumes knowledge of basic molecular biology and is targeted at students, researchers and academics in related areas of biomedicine and pharmaceutics and to a more general readership interested in specific applications of genomic and proteomic technologies.

We would like to thank all of the contributing authors and the Society for Experimental Biology (SEB, UK) for helping us to put this book together. We would also like to extend our thanks to Elizabeth Owen and Kirsty Lyons at Taylor & Francis for their extensive assistance in the final compilation of this book.

Oxford, April 2006.   John Parrington & Kevin Coward

The relevance of host genes in malaria

Miguel Prudêncio, Cristina D. Rodrigues and Maria M. Mota

1 Introduction

Malaria is a devastating disease that affects extensive areas of Africa, Asia and South and Central America, causing up to 2.7 million deaths per year, mainly children under the age of five (Webster and Hill, 2003). The disease is caused by a protozoan parasite from the genus *Plasmodium* and transmitted through the bite of the female *Anopheles* mosquito. When a mosquito infected with *Plasmodium* bites a mammalian host, it probes for a blood source under the skin and, during this process, deposits saliva containing sporozoites. These sporozoites reach the circulatory system and are transported to the liver. Once there, they migrate through several hepatocytes by breaching their plasma membranes before infecting a final cell with the formation of a parasitophorous vacuole. After several days of development inside a hepatocyte, thousands of merozoites are released into the bloodstream where they invade red blood cells (RBCs), initiating the symptomatic erythrocytic stage of the disease (*Figure 1*).

Malaria infection depends upon the occurrence of interactions between the *Plasmodium* parasite and the host. Every stage of an infection by *Plasmodium* relies, to different extents, on the presence of host molecules that enable or facilitate its invasion, survival and multiplication. Therefore, host genes play a crucial role in determining the resistance or susceptibility to malaria and may constitute potential targets for preventive or therapeutic intervention. Analysis of the genetic basis of susceptibility to major infectious diseases is, arguably, the most complex area in the genetics of complex disease (Hill, 2001). In this chapter, we will examine the progress made towards identifying mammalian host molecules that play a role in the modulation of malaria infections.

2 The pre-erythrocytic stage: hepatocyte, liver and beyond

The hepatic stage of a *Plasmodium* infection constitutes an appealing target for the development of an intervention strategy since this would act before the onset of pathology, which only occurs during the blood stage of the parasite's life cycle. In fact, until now, the only demonstrably effective vaccine shown to confer a sterile and lasting protection both in mice (Nussenzweig *et al.*, 1967) and in humans (Clyde *et al.*, 1973;
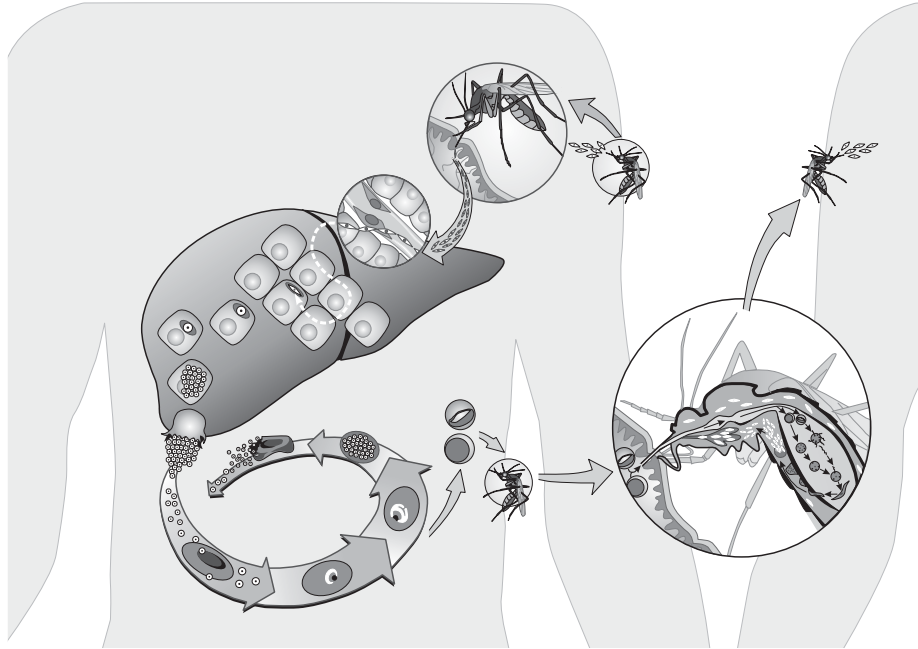
Figure 1. *The life cycle of* Plasmodium *in the mammalian and mosquito hosts.*

Rieckmann *et al*., 1974; Herrington *et al*., 1991) was the inoculation of γ-irradiation-attenuated sporozoites, that are able to invade but not fully mature inside the hepatocyte (see Carvalho *et al*., 2002; Gruner *et al*., 2003; Bodescot *et al*., 2004; Todryk and Walther, 2005; Waters *et al*., 2005).

Despite being symptomatically silent, the liver stage of a malaria infection is immunologically very complex. Unlike RBCs, liver cells are able to promote cell-mediated immune response mechanisms through expression of class I Major Histocompatibility Complex (MHC) proteins. Class I MHC proteins present antigens to cytotoxic T lymphocytes (CTLs) (Lowell, 1997), which are known to play an important role in the generation of a protective immune response in many microbial infections (Esser *et al*., 2003). The activation of T cells by antigen-presenting cells (APCs) is required to initiate specific immune responses. Different APCs have been shown to be important in this process, including dendritic cells (DC) (Bruna-Romero and Rodriguez, 2001; Jung *et al*., 2002; Leiriao *et al*., 2005) and Kupffer cells (Steers *et al*., 2005).

Human leucocyte antigens (HLAs) are encoded by genes of the MHC, which are known to be among the most polymorphic of all human genes (reviewed in Williams, 2001). Although most of the human MHC *loci* are relatively stable, the *HLA-B locus* has been shown to undergo rapid changes, especially in isolated populations (McAdam *et al*., 1994). *HLA-B* encodes an MHC class I heavy chain that is part of the *HLA-B* antigen-presentation complex (Kwiatkowski, 2005). On the other hand, the *HLA-DR* antigen-presenting complex includes an HLA class II β chain, which is encoded by *HLA-DRB1*. HLA-DR is found in B lymphocytes, DC and macrophages where it plays an essential role in the production of antibodies (Kwiatkowski, 2005). Both the *HLA-B53* allele and the *DRB1*1302-DQB1*0501* haplotype were shown to be

associated with protection against severe malaria (SM) in The Gambia (Hill *et al.*, 1991) and the latter was also found to be associated with protection from malaria anaemia and malarial reinfections in Gabonese children (May *et al.*, 2001).

The analysis of the peptides from a vast range of malaria antigens that bind to HLA-B53-restricted CTLs in malaria-immune Africans led to the identification of a single conserved peptide from liver-stage-specific antigen-1 (LSA-1) (Hill *et al.*, 1992), making LSA-1 an interesting malaria vaccine candidate (Migot-Nabias *et al.*, 2001). Of the four most prevalent allelic variants of the protein recognized by HLA-B53, only two are indeed epitopes, binding this protein *in vitro* (Gilbert *et al.*, 1998). Moreover, these results suggest that cohabiting parasite strains, each of which being an individually effective target for CTLs, may have the ability to use altered peptide ligand (APL) antagonism mechanisms to suppress the CTL response to the other strain, thereby increasing each other's chances of survival. This observation has obvious implications in terms of vaccine development, since it suggests that including all allelic peptide variants in a prospective vaccine might be counterproductive because one given variant may antagonize immunity to other variants.

During *Plasmodium* sporozoite development inside hepatocytes there is an amazing multiplication, with each parasite giving rise to 10,000–30,000 merozoites in 2–7 days (depending on *Plasmodium* spp.). Moreover, there is a high level of specificity of *Plasmodium* sporozoite development, which only occurs in certain types of cells. This strongly suggests an important role for the host cell in supporting the full development of the parasite. However, not much is known about *Plasmodium* requirements, strategies developed to survive and be successful, or how much the host cell contributes to this. An intriguing characteristic of *Plasmodium* sporozoites is their ability to migrate through hepatocytes prior to invading a final one with the formation of a vacuole for further development. Sporozoites breach the plasma membrane of the cell, traverse through its cytosol and leave by wounding the membrane (Mota *et al.*, 2001). This unusual process is frequently observed *in vitro*, where sporozoites traverse mammalian cells at a speed of approximately one cell per minute. Migration through host hepatocytes is also observed *in vivo* in the liver of mice infected with *Plasmodium* sporozoites (Mota *et al.*, 2001; Frevert *et al.*, 2005). Wounding of host hepatocytes induces an alteration in traversed cells which includes the secretion of host cell factor(s), which render(s) neighbouring hepatocytes susceptible to infection. One such factor is hepatocyte growth factor (HGF), which, by activating its receptor MET, seems to be required for the early development of parasites within host cells (Carrolo *et al.*, 2003). These results, however, appear to be contradicted by evidence provided by *spect*-deficient sporozoites, which do not migrate through cells *in vitro* (Ishino *et al.*, 2004). It would be expected that *spect*-deficient sporozoites would not induce host cells to produce HGF and, therefore, infection would be inhibited. However, these sporozoites efficiently infect host cells *in vitro* (Ishino *et al.*, 2004). This apparent discrepancy may be due to particular characteristics of the *in vitro* cell system used for infection (Mota and Rodriguez, 2004), or to alternative ways used by the parasite to fully develop inside host cells.

3 The erythrocytic stage and disease

The erythrocytic stage of *Plasmodium's* life cycle corresponds to the symptomatic phase of a malaria infection. During this phase, *Plasmodium* merozoites invade RBCs and degrade haemoglobin (Hb), releasing heme that is converted into haemozoin

(malarial pigment). The invading merozoites multiply in the RBCs and, upon ruptur-ing the erythrocytic membrane, are eventually released into the blood where they target new RBCs. The interaction between *Plasmodium* and the RBCs occurs in two stages: first, the identification and binding of RBC surface molecules that will enable invasion; subsequently, the intracellular interaction with Hb and the multiplication of the parasite.

3.1 *Erythrocyte invasion –* P. vivax *versus* P. falciparum

The human malaria parasite, *P. vivax*, and the related monkey malaria, *P. knowlesi*, use the Duffy blood group antigen as a receptor to invade human RBCs (Miller *et al.*, 1976). The Duffy antigen, encoded by the *FY* gene, is a chemokine receptor on the surface of the RBCs. It belongs to the superfamily of G-protein coupled receptors (GCRs) (Neote *et al.*, 1994) and is also termed DARC (for Duffy antigen receptor for chemokines). The Duffy blood group locus is polymorphic and has three main alleles designated *FY*A*, *FY*B* and *FY*O*. The *FY*A* allele is very frequent in Asia and the Pacific, whereas in Europe and the Americas the *FY*A* and *FY*B* alleles are at inter-mediate frequencies. The *FY*O* allele is at or near fixation in most sub-Saharan African populations, but is very rare outside Africa (Hamblin and Di Rienzo, 2000). *FY*O* arises from a mutation at position -46 in the promoter of the *FY*B* allele, leading to a Fy(a-b-) phenotype in which RBCs lack both Fy^a and Fy^b antigens (Tournamille *et al.*, 1995). Fy(a-b-) RBCs resist invasion *in vitro* by *P. knowlesi* parasites and indi-viduals homozygous for the *FY*O* allele are completely resistant to *P. vivax* malaria (Miller *et al.*, 1976). The correlation between the Duffy-negative serological pheno-type and resistance to *P. vivax* malaria is now clear. *P. vivax* relies on a single path-way to invade RBCs. The lack of redundancy in *P. vivax* invasion pathways may explain the near absence of this parasite from West Africa, where almost 95% of the population have the Duffy-negative phenotype and are resistant to *P. vivax* malaria (Chitnis and Miller, 1994). The extreme degree of between-population differentiation of allele frequency of the Duffy blood group gene shows evidence of human directional selection by *P. vivax* (Hamblin *et al.*, 2002). Furthermore, it has important implica-tions in drug or vaccine design (Yazdani *et al.*, 2004).

Unfortunately, things are a lot more complicated when it comes to the much more deadly *P. falciparum* malaria parasite.

Contrary to *P. vivax*, *P. falciparum* displays the ability to invade RBCs following multiple, alternative pathways, with significant redundancy. Research into the identifi-cation of RBC receptors involved in merozoite invasion has made use of RBCs that lack specific surface molecules or enzymes that modify protein and carbohydrate domains on those molecules. The main enzymes used have been neuraminidase (which cleaves sialic acid groups from surface glycoproteins and glycolipids) and trypsin (which cleaves the peptide backbone of a number of surface proteins) (Baum *et al.*, 2003). These studies have revealed several surface receptors that are involved in invasion of the RBC by *P. falciparum* merozoites. Three neuraminidase-sensitive molecules that have received particular attention are glycophorin A (GYPA) (Pasvol *et al.*, 1982), glycophorin B (GYPB) (Dolan *et al.*, 1994), and glycophorins C and D (GYPC/D) (Mayer *et al.*, 2001; Maier *et al.*, 2003). GYPC and GYPD are encoded by the same gene, but use alternative start codons. Deletion of exon 3 in the *GYPC/D* gene

changes the serologic phenotype of the Gerbich (Ge) blood group system, resulting in Ge-negativity. Ge-negative RBCs exhibit a shortened GYPC and lack GYPD (Mayer *et al.*, 2001). This is of particular relevance if we consider that the Ge-negative phenotype is found at high allele frequencies in some regions of Papua New Guinea, which coincide with regions of malaria hyperendemicity. This strongly suggests that selection of Ge-negativity in these populations confers at least partial protection against *P. falciparum* malaria. It should be noted that this is in contrast to a study in which no correlation between the prevalence of *P. falciparum* infection and Ge-negativity in the Wosera region of Papua New Guinea was found (Patel *et al.*, 2001). More recently, the existence of yet another sialic acid-dependent receptor, termed 'Receptor Y', has been demonstrated (Rayner *et al.*, 2001). It would seem apparent that *P. falciparum* shows a near-exclusive preference for sialic acid-dependent (i.e. neuraminidase-sensitive) glycophorins for RBC invasion. This, however, is now known not to be the case. Several reports have shown that alternative, sialic acid-independent, invasion pathways are commonly used by *P. falciparum* (Mitchell *et al.*, 1986; Hadley *et al.*, 1987; Dolan *et al.*, 1994). Moreover, *P. falciparum* seems capable not only of sialic acid-independent RBC invasion, but also of switching between sialic acid-dependent and sialic acid-independent pathways (Dolan *et al.*, 1990; Reed *et al.*, 2000; Duraisingh *et al.*, 2003). Very recently, the molecular mechanism for this switching process was elucidated (Stubbs *et al.*, 2005).

As we have seen, the surface of the RBC presents various types of sialic acid-dependent and sialic acid-independent receptors that can mediate *P. falciparum* invasion with at least a certain degree of redundancy. Furthermore, it is clear that the relative importance of each receptor is strain-dependent (Rayner *et al.*, 2001). These observations have important implications for vaccine development. While the existence of a single RBC invasion pathway for *P. vivax* yields good reasons to hope for a successful vaccine, this is clearly not the case for *P. falciparum*.

3.2 *Intraerythrocytic stage – globin and non-globin genes*

Following invasion of RBCs, *Plasmodium* parasites develop and multiply, leading to the appearance of the symptoms of malaria infection. Almost 90% of the intraerythrocytic space is taken up by Hb. Therefore, it is to be expected that *Plasmodium* will interact closely with this molecule and be influenced by its overwhelming presence. Thus, it is perfectly conceivable that Hb alterations will affect the development of the parasite, as well as the parasitized RBC itself.

Normal Hbs are tetrameric proteins composed of two pairs of unlike globin chains. After birth, the vast majority of Hb is composed of two α-globin and two β-globin chains (reviewed in Weatherall and Clegg, 2001; Richer and Chudley, 2005). The molecular pathology of most of the haemoglobinopathies is well defined (Weatherall and Clegg, 2001). The Hb disorders resulting from mutations in the α- or β-globin gene clusters are the most common single-gene disorders in humans (Weatherall, 2001). Inherited haemoglobinopathies can be divided into two main groups: structural Hb variants, mostly resulting from single amino acid substitutions in the α- or β-chains, and thalassaemias, arising due to the ineffective synthesis of the α- and/or β-chains (reviewed in Weatherall and Clegg, 2001). These two classes of Hb disorders constitute one of the most striking illustrations of why malaria is considered

the strongest known selective pressure in the recent history of the human genome (Kwiatkowski, 2005).

Structural Hb variants. Of the more than 700 structural Hb variants identified, only those coding for 'haemoglobin S' (or 'sickle haemoglobin', HbS), 'haemoglobin C' (HbC) and 'haemoglobin E' (HbE) have reached polymorphic frequencies. Each of the alleles *HbS*, *HbC* and *HbE* results from a single point mutation in the *HBB* gene. Although often lethal in the homozygous state, the unusually high prevalence of these alleles in areas of malaria endemicity has long been attributed to a selective pressure exerted by *Plasmodium* on the human host genome (Min-Oo and Gros, 2005).

In HbS, the glutamate at position 6 of the β-globin chain is replaced by a valine residue. The resulting protein contains 'sickle' β-globin ($β^S$-globin) chains and tends to polymerize at low oxygen concentrations, causing the RBC to acquire a sickle-like shape (Brittenham *et al.*, 1985). This results in a condition known as 'sickle cell' anaemia, an autosomal recessive genetic disorder characterized by chronic anaemia and periodic vaso-occlusive crises (Shiu *et al.*, 2000). Although the homozygous state (HbSS) is often lethal, the heterozygous state (HbAS) is referred to as sickle cell trait and is usually clinically silent. The HbAS state has been shown to confer significant protection to malaria (reviewed in Kwiatkowski, 2005; see also Aidoo *et al.*, 2002; Williams *et al.*, 2005a). The exact mechanisms through which HbAS protects against malaria are unclear. A few possible explanations have, however, been put forward, including the enhanced sickling of the infected RBCs (iRBCs) (Luzzatto *et al.*, 1970), the suppression of parasite growth in individuals with the sickling disorders (Pasvol *et al.*, 1978) and increased spleen clearance (Shear *et al.*, 1993), enhanced phagocytosis (Ayi *et al.*, 2004) and enhanced acquisition of natural immunity to malaria, possibly due to the accelerated acquisition of antibodies against altered host antigens expressed on the surface of the infected RBCs (iRBCs) and/or against parasite-derived proteins (Williams *et al.*, 2005b).

In HbC, the glutamate at position 6 of the β-globin chain is replaced by a lysine residue. The resulting condition is considerably less serious than sickle cell anaemia. Even in the homozygous state (HbCC), only occasional pathologic developments are observed whereas heterozygotes (HbAC) are asymptomatic (Agarwal *et al.*, 2000; Kwiatkowski, 2005). This Hb variant has been implicated in protection against malaria in both the HbAC and the HbCC states (reviewed in Kwiatkowski, 2005; Min-Oo and Gros, 2005), although contrasting results have been reported concerning the heterozygous state (discussed in Modiano *et al.*, 2001). Three recent reports propose complementary explanations for the protective effect of HbC against malaria, all implying modifications that occur at the host cell surface (Tokumasu *et al.*, 2005; Arie *et al.*, 2005; Fairhurst *et al.*, 2005).

HbE results from a glutamate → lysine mutation at position 27 of the β-globin chain. It is the most common structural variant of Hb and is innocuous both in its heterozygous (HbEA) and homozygous (HbEE) states (Weatherall and Clegg, 2001). There is no unequivocal proof that HbE protects against malaria but it has been suggested that an alteration in the RBC membrane in HbEA cells renders the majority of the RBCs population relatively resistant to invasion by *P. falciparum* (Chotivanich *et al.*, 2002).

Thalassaemias. The β- and α-thalassaemias are disorders of globin chain synthesis that appear as a consequence of deletions or point mutations in the non-coding portion of

the β- and α- globin genes, respectively (reviewed in Weatherall, 2001; Richer and Chudley, 2005). Because the synthesis of the β-globin chain is determined by two alleles of the *HBB* gene, whereas that of α-globin is encoded by the four alleles on the equivalent *HBA1* and *HBA2* genes, there is a wide range of possible thalassaemic genetic variants, with different clinical manifestations. In general, homozygous thalassaemia is severe or even fatal, whereas the heterozygous state is clinically benign. However, when either the *HBA1* or the *HBA2* gene, but not both, is defective, a condition termed α-thalassaemia occurs, for which homozygous individuals show only mild anaemia (Kwiatkowski, 2005). Evidence for protection against malaria by thalassaemia has been shown in different reports (reviewed in Min-Oo and Gros, 2005; Williams *et al.*, 2005a). The nature of protection against malaria by thalassaemias is unclear. Again, several suggestions have been mentioned including impaired parasite growth and increased susceptibility to phagocytosis (Yuthavong *et al.*, 1988, 1990), altered expression of parasite-induced surface neoantigens in β- and α-thalassaemia allowing greater binding of specific antibody to iRBCs and their subsequent clearance (Luzzi *et al.*, 1991a, 1991b) and enhanced phagocytosis of ring-stage iRBCs of β- (but not α-) thalassaemia individuals (Ayi *et al.*, 2004).

In addition to Hb, other RBC molecules also seem to play an important role in the parasite's development and in the host's susceptibility to malaria.

G6PD deficiency. The haeme liberated in the process of intra-erythrocytic Hb degradation by *Plasmodium* is polymerized to haemozoin or broken down non-enzymatically. Non-enzymatic cleavage of haeme liberates iron and generates hydrogen peroxide, a potential source of oxidative stress (Schwarzer *et al.*, 2003). Glucose-6-phosphate dehydrogenase (G6PD) catalyses the oxidation of glucose-6-phosphate to 6-phosphogluconate, while concomitantly reducing nicotinamide adenine dinucleotide phosphate ($NADP^+$ to NADPH). G6PD is the only erythrocytic enzyme that produces NADPH, a compound that is crucial for the defence of the RBCs against oxidative stress (Beutler, 1996). G6PD deficiency is the most common human enzymopathy known, affecting over 400 million people (Beutler, 1990). There are numerous variants of the *G6PD* gene and only those that significantly hamper enzyme activity lead to haemolytic anaemia, a phenotype that is exacerbated under oxidative stress conditions (Kwiatkowski, 2005). Evidence for the geographical correlation between G6PD deficiency and protection against malaria comes from various population-based studies and suggests evolutionary selection by the latter (reviewed in Kwiatkowski, 2005; Min-Oo and Gros, 2005). Although reduced parasite replication in G6PD-deficient RBCs was initially proposed as the mechanism of protection (Luzzatto *et al.*, 1969), the invasion and maturation of the parasite seems not to be significantly different between normal and G6PD-deficient RBCs (Cappadoro *et al.*, 1998). Instead, ring-stage iRBCs present on their surface a higher density of phagocytic removal markers than normal iRBCs and are, therefore, phagocytozed more efficiently. This suggestion has been extended to explain the protective nature of other erythrocytic defects against malaria (Ayi *et al.*, 2004), as previously mentioned.

Band 3 protein. Band 3 protein, encoded by *AE1*, is a ~100 kDa membrane protein that acts as an anion permeation channel, exchanging intracellular bicarbonate for chloride through the RBC lipid bilayer (Rothstein *et al.*, 1976; Alper *et al.*, 2002).

A 27-base-pair deletion in the *AE1* gene (known as Band3Δ27), has been shown to cause a condition known as South-East Asian ovalocytosis (SAO), characterized by slightly oval or elliptical shaped RBCs, defective anion transport activity, increased acidosis and haemolytic anaemia (Schofield *et al.*, 1992). Whereas the homozygous state is lethal, population-based studies have shown that the heterozygous state confers protection against cerebral malaria (CM), a condition characterized by progressing coma, unconsciousness, multiple convulsions and, often, death (Rasti *et al.*, 2004; Genton *et al.*, 1995; Allen *et al.*, 1999). Again, the mechanism of protection is unknown but several hypothesis have arisen, such as membrane alterations in SAO RBCs affecting parasite invasion (Kidson *et al.*, 1981) and involvement of Band 3 protein in iRBC cytoadherence, a process described below (Winograd and Sherman, 1989; Winograd *et al.*, 2005; Shimizu *et al.*, 2005).

PK deficiency. RBCs do not have mitochondria and are, therefore, dependent on glycolysis for energy. Pyruvate kinase (PK) is a key enzyme in glucose metabolism, catalysing the conversion of phosphoenolpyruvate into pyruvate, with simultaneous production of ATP. Thus, PK-deficient RBCs have impaired glycolysis and difficulty in maintaining normal levels of ATP and NAD. The degree of severity of PK-deficiency depends on the mutation(s) in one or both genes coding for PK in the human genome (Min-Oo and Gros, 2005). No formal evidence exists of a protective effect of PK deficiency against malaria in humans (Min-Oo and Gros, 2005). However, such a correlation is likely to exist, as suggested by recent studies carried out in mouse models (Min-Oo *et al.*, 2003, 2004).

3.3 *Cytoadherence and sequestration – selective pressures and therapeutic value*

P. falciparum is the most virulent of all four *Plasmodium* parasites that infect humans. Two features are strongly suggested to contribute decisively to the outstanding pathogenicity of *P. falciparum*: its remarkable potential to multiply to high parasite burdens and its unique ability to cause iRBCs to adhere to the linings of small blood vessels. The latter process is termed cytoadherence and the ensuing sequestration of iRBCs is frequently suggested to be a key feature in the pathogenesis of SM (see Ho and White, 1999; Kyes *et al.*, 2001; Miller *et al.*, 2002 for reviews).

The most widely suggested justification for sequestration in *P. falciparum* malaria is that adhesion of iRBCs to the endothelium allows the parasite to escape peripheral circulation and be cleared by the spleen. Another *Plasmodium* survival advantage is that sequestration in the deep tissue microvasculature provides the parasites with a microaerophilic venous environment that promotes maturation and faster asexual replication (Cranston *et al.*, 1984). Alternative, but not necessarily exclusive, explanations include sheltering of the iRBCs against destruction by the immune system of the host, enhanced survival of the gametocyte and immunomodulation by inhibition of the maturation and activation of DC (reviewed in Sherman *et al.*, 2003).

It has been suggested that parasite accumulation in specific organs is an important factor in malaria pathogenesis. Indeed, post-mortem examinations of people who have died from *P. falciparum* malaria show sequestered iRBCs within the small vessels of several tissues. The best-documented situation regards the sequestration of iRBCs in the endothelium of small vessels of the brain, which can lead to CM

(Kyes *et al.*, 2001; Rasti *et al.*, 2004). The proportion of iRBCs was higher in *P. falciparum* malaria patients dying with CM than in those that showed no CM symptoms (MacPherson *et al.*, 1985; Silamut *et al.*, 1999; Taylor *et al.*, 2004). The most prevalent hypothesis to explain the clinical manifestations of CM seems to be that sequestration obstructs blood flow, and, consequently, decreases the levels of oxygen and nutrients, whilst increasing the accumulation of waste products in the brain (Miller *et al.*, 1994). A complementary hypothesis is that an inflammatory response to the infection activates leukocytes and promotes their adhesion to receptors in the endothelium (Sun *et al.*, 2003). Another organ where sequestration seems to play a particularly important pathogenic role is the placenta. Maternal or placental malaria (PM) in *P. falciparum*-infected pregnant women is associated with disease and death of both mother and child. The characteristic feature of infection during pregnancy is the selective accumulation of iRBCs in the intervillous blood spaces of the placenta, leading to hypoxia, inflammatory reactions and intervillositis (reviewed in Beeson *et al.*, 2001; Andrews and Lanzer, 2002; Duffy and Fried, 2003).

Besides the cytoadherence of iRBCs to endothelial cells (sequestration), other distinctive patterns of iRBCs adherence can be distinguished at the cellular level. These involve different types of interactions between iRBCs and other host cells, such as RBCs (rosetting) (Udomsangpetch *et al.*, 1989; 1992), platelets ('platelet-mediated clumping', formerly known as autoagglutination) (Roberts *et al.*, 1992; Pain *et al.*, 2001a) or DC (Urban *et al.*, 1999, 2001). All these different types of interactions have been suggested to have implications in the course of infection as well as in disease severity (Udomsangpetch *et al.*, 1989; Urban *et al.*, 1999; Pain *et al.*, 2001a).

Over the last few years, significant progress has been made towards the identification of both parasite and host molecules that participate in these interactions. An array of host molecules have been identified that mediate cytoadherence of the iRBCs to various host cells. Among the most important ones identified so far are CD36 (Barnwell *et al.*, 1985), thrombospondin (TSP) (Roberts *et al.*, 1985), intercellular adhesion molecule-1 (ICAM-1) (Berendt *et al.*, 1989), vascular cell adhesion molecule-1 (VCAM-1) (Ockenhouse *et al.*, 1992), E-selectin (endothelial leukocyte adhesion molecule 1, ELAM-1) (Ockenhouse *et al.*, 1992), chondroitin sulphate A (CSA) (Rogerson *et al.*, 1995), platelet/endothelial cell adhesion molecule-1 (PECAM-1/CD31) (Treutiger *et al.*, 1997), complement receptor 1 (CR1) (Rowe *et al.*, 1997), hialuronic acid (HA) (Beeson *et al.*, 2002) and heparan sulphate (HS) (Vogt *et al.*, 2003). Nevertheless, the exact role of each of these molecules in pathogenesis remains largely unclear. Whilst some host ligands appear to be nearly ubiquitous, others seem to be organ- or cell-specific. This specificity has implications in terms of disease severity and adhesion mechanisms. Moreover, sequestration in an organ is likely to involve multiple receptors, and different combinations of specific receptors for adhesion may determine the site at which parasites adhere and accumulate (Beeson and Brown, 2002). Furthermore, receptors can act synergistically in mediating the adhesion of iRBCs (McCormick *et al.*, 1997; Yipp *et al.*, 2000; Heddini *et al.*, 2001b) and *in vivo* sequestration has been shown to involve a multi-step adhesive cascade of events where iRBCs initially roll along the endothelial surface and are subsequently arrested (Ho *et al.*, 2000).

CD36. CD36 (encoded by *CD36*), also known as GP88 or platelet glycoprotein IV, is an 88 kDa cell surface class B scavenger receptor and is expressed in endothelial cells,

monocytes, platelets and erythroblasts (Barnwell *et al.*, 1989; Ho and White, 1999). CD36 has been implicated in the interaction with a variety of natural ligands (reviewed in Ho and White, 1999; Serghides *et al.*, 2003) and it was identified *in vitro* as a receptor for iRBCs (Barnwell *et al.*, 1985, 1989). Since then, evidence for the involvement of CD36 in malarial cytoadherence became abundant and unequivocal, although its implications in disease severity are not always clear-cut. Whilst some reports describe a contribution of CD36 to malaria severity (Udomsangpetch *et al.*, 1992; Pain *et al.*, 2001a; Urban *et al.*, 2001; Prudhomme *et al.*, 1996), others suggest that it might be advantageous for host survival (Rogerson and Beeson, 1999; Serghides *et al.*, 2003; McGilvray *et al.*, 2000; Traore *et al.*, 2000). Several *CD36* polymorphisms have been identified. In Africa, the most common of these substitutions is a T1264G stop mutation in exon 10 (Aitman *et al.*, 2000). Studies of the effects of this polymorphism in disease severity have again yielded contradictory results and do not provide definitive answers regarding a possible selective pressure by malaria in endemic areas (Aitman *et al.*, 2000; Pain *et al.*, 2001b; Omi *et al.*, 2003).

The role of CD36 in the pathogenicity of malaria is still ambiguous. This has important implications in terms of the development of therapies or vaccines that target the interaction between PfEMP-1 and the CD36 receptor. The *in vitro*-based assumption that adherence to CD36 contributes to disease severity, and results in negative clinical outcomes, triggered research aimed towards interfering with this interaction that did not always yield agreeing results (Barnwell *et al.*, 1985; Baruch *et al.*, 1997; Cooke *et al.*, 1998; Yipp *et al.*, 2003). One way to try and circumvent this problem is by making use of appropriate animal, ideally rodent, models. The sequences of human and rat CD36 differ in a single amino acid (His242 in humans is Tyr242 in rat) and both are able to bind *P. falciparum*-infected RBCs (Serghides *et al.*, 1998). It has been shown that RBCs infected with the murine parasite *P. chabaudi chabaudi* AS adhere *in vitro* to purified CD36 and are sequestered from circulation in an organ-specific way *in vivo* (Mota *et al.*, 2000). Recently, a novel system that enables real-time *in vivo* imaging luciferase-expressing rodent malaria parasite *P. berghei* was used to monitor sequestration (Franke-Fayard *et al.*, 2005). Using CD36$^{-/-}$ mice, it was shown that nearly all detectable iRBC sequestration depends on CD36 and that murine CM pathology still develops in the absence of this receptor, implying that CD36-mediated sequestration in nonerythroid organs does not constitute the molecular basis of rodent CM. Despite the obvious advantages of using animal models to study sequestration, caution should be employed when extrapolating results to the *P. falciparum*/human situation.

ICAM-1. Intercellular adhesion molecule-1 (ICAM-1), encoded by *ICAM-1*, is a surface glycoprotein member of the immunoglobulin superfamily. ICAM-1, also known as CD54, plays a central role in immune response generation by functioning as an endothelial and immune-cell ligand for integrin-expressing leukocytes (reviewed in Ho and White, 1999; Kwiatkowski, 2005). ICAM-1 is widely distributed in endothelial cells including, unlike CD36, those of the brain microvascular system (Adams *et al.*, 2000). Also unlike CD36, the expression of *ICAM-1* can be up-regulated by a number of factors, most notably pro-inflammatory cytokines such as tumour necrosis factor-α (TNF-α), interleukin-1 (IL-1) and interferon-γ (IFN-γ) (reviewed in Dietrich, 2002), which seem to correlate with disease severity.

P. falciparum iRBCs have been shown to bind with different affinities to ICAM-1 *in vitro* (Berendt *et al.*, 1989). Unequivocal *in vivo* evidence of the involvement of ICAM-1 in sequestration, mainly in the brain, has been reported in both humans (Turner *et al.*, 1994) and mice models (Willimann *et al.*, 1995; Kaul *et al.*, 1998). The evidence gathered in these studies has led to the notion that ICAM-1 may play an important role in CM by either sequestering iRBCs or adhering to activated leukocytes. Furthermore, this receptor has also been shown to contribute to the cytoadherence of iRBCs within the intervillous spaces of the *P. falciparum*-infected placenta, supporting a possible role of ICAM-1 in PM (Sugiyama *et al.*, 2001), as previously suggested (Sartelet *et al.*, 2000). Moreover, ICAM-1 can synergize with CD36 to promote iRBC adhesion under flow conditions (McCormick *et al.*, 1997, Ho *et al.*, 2000; Yipp *et al.*, 2000). For these reasons, it is generally accepted that ICAM-1 plays a role in iRBC sequestration and in the severity of disease.

A high-frequency coding polymorphism in the *ICAM-1* gene of individuals from Kilifi (Kenya), an area of high malaria endemicity, has been identified (Fernandez-Reyes *et al.*, 1997). The mutant protein, termed ICAM-1[Kilifi], contains a lysine → methionine replacement at position 29 (Fernandez-Reyes *et al.*, 1997). Intuitively, one would be led to think that the prevalence of this polymorphism in malaria-endemic regions would be associated with protection against severe forms of disease. However, studies attempting to correlate this polymorphism with malaria severity, yielded surprising and contradictory results (Fernandez-Reyes *et al.*, 1997; Kun *et al.*, 1999; Bellamy *et al.*, 1998; Ohashi *et al.*, 2001; Amodu *et al.*, 2005). The obvious difficulties that arise when attempting to reconcile those results constitute an illustration of the extreme complexity of malaria pathogenesis and suggest that different biological selective forces might simultaneously be at play in the studied populations (Craig *et al.*, 2000). In a very recent report, an ICAM-1 exon 6 polymorphism (lysine → glutamate replacement at position 469 in the protein) was seen to positively correlate with an increased risk of SM (Amodu *et al.*, 2005).

PECAM-1/CD31. Platelet/endothelial cell adhesion molecule-1 (PECAM-1, also known as CD31), encoded by *PECAM-1*, is a highly glycosylated transmembrane glycoprotein of the immunoglobulin superfamily (Newman *et al.*, 1990). It is expressed on endothelial cells and platelets, as well as on granulocytes, monocytes, neutrophils and naïve T lymphocytes (Newman *et al.*, 1990; Mannel and Grau, 1997).

The role of PECAM-1 as an endothelial receptor for adherence of *P. falciparum*-infected RBCs was demonstrated *in vitro* by Treutiger *et al.* (1997). These authors further demonstrated that binding could be blocked by monoclonal antibodies (mAbs) specific for the N-terminus of PECAM-1 whereas it could be increased by IFN-γ, a proinflammatory cytokine associated with the development of CM. In addition to serving as an endothelial receptor, the fact that PECAM-1 is expressed on platelets raises the possibility that it may also be involved in platelet adhesion of iRBCs, although no direct evidence exists for this. Platelets have been proposed as important effectors of neurovascular injury in CM, both in mice and in humans (reviewed in Mannel and Grau, 1997). Furthermore, the PECAM-1 receptor is quite commonly recognized by wild *P. falciparum* isolates (Heddini *et al.*, 2001a). In this particular study, over 50% of the fresh patient-isolates tested recognized PECAM-1, a number that is not matched by any other endothelial receptor, with the exception of CD36.

A functional mutation in codon 125 of the *PECAM-1* gene (leucine → valine replacement in the protein) was analysed in terms of its possible influence on malaria resistance (Casals-Pascual *et al.*, 2001). This study, carried out in Madang (Papua New Guinea) and Kilifi (Kenya) revealed no association between codon 125 polymorphism and disease severity in either of the populations. In another study, carried out in Thailand, a *PECAM-1* haplotype that is significantly associated with CM was reported (Kikuchi *et al.*, 2001).

It seems clear that our knowledge of the role of PECAM-1 in the pathogenicity of malaria is, at present, quite limited. This may be partly explained by the fact that, despite being an apparently high affinity receptor for iRBCs, PECAM-1 has been identified as such more recently than, for example, CD36 and ICAM-1. The use of appropriate animal models and larger-scale assessment of human *PECAM-1* polymorphisms would be a welcome source of potentially valuable information concerning this molecule.

CR1. Complement receptor 1 (CR1; C3b/C4b receptor; CD35), encoded by *CR1*, is a glycoprotein expressed on the surface of human RBCs and leukocytes (see Moulds *et al.*, 1991). CR1 was first implicated in malaria when its involvement in rosette formation, a phenotype associated with disease severity, was shown (Rowe *et al.*, 1997). CR1-dependent rosette formation is common in *P. falciparum* field isolates and the region of CR1 involved in rosetting was mapped (Rowe *et al.*, 2000).

The common blood group antigens, Kn(a)/Kn(b) (Knops); McC(a)/McC(b) (McCoy); Sl(a)/Vil (Swain-Langley/Villien) (now known as Sl:1/Sl:2); and Yk(a) (York) have been shown to be expressed on CR1 and, thus, correspond to alleles that encode polymorphisms in this receptor (Moulds *et al.*, 1991, 2000, 2001). The null phenotypes for the CR1-related blood group (also known as the Knops blood group) antigens are associated with the expression of a low number of CR1 molecules on the erythrocytic surface (Moulds *et al.*, 1991). The Sl(a⁻) and the McC(b⁺) phenotypes had a significantly higher prevalence in a Malian population when compared to other African and European-American populations (Moulds *et al.*, 2000). However, no correlation was found between either the Sl(a⁻) or the McC(b⁺) phenotypes (or, in fact, the *Sl:2/McC(b⁺)* allele) and protection against malaria in The Gambia (Zimmerman *et al.*, 2003).

CR1 is also polymorphic with respect to molecular weight (Wilson and Pearson, 1986; Wong *et al.*, 1989). A *HindIII*-RFLP (restriction fragment length polymorphism), was identified and shown to correlate with differential quantitative expression of CR1 on RBCs in Caucasian populations (Wong *et al.*, 1989). Homozygotes for a 7.4 kilobase (kb) *HindIII* genomic fragment (the H allele) have high RBC CR1 density, whereas homozygotes for a 6.9 kb *HindIII* genomic fragment (the L allele) have low CR1 expression, with HL heterozygotes having intermediate CR1 levels (Wong *et al.*, 1989). Surprisingly, in a Thai population, malaria severity was most prevalent in individuals homozygous for the L allele, compared with heterozygous individuals and individuals homozygous for the H allele (Nagayasu *et al.*, 2001). However, a recent study has found no correlation between the level of erythrocytic CR1 and the H and L alleles in an African population (Rowe *et al.*, 2002), raising doubts about the *HindIII*-RFLP importance in determining CR1 density on RBCs. To add to the confusion, a recent report in Papua New Guinea showed that HH individuals were at most risk of

developing SM whereas HL individuals were significantly protected and LL individuals showed statistically insignificant, albeit reduced, odds (Cockburn *et al.*, 2004).

It is clear that further studies are needed in order to fully understand the actual role of CR1-mediated rosetting in determining malaria severity and in establishing a clear correlation between CR1 polymorphisms and protection against severe disease. Studies involving murine models are unlikely to provide any further insights into this issue. In fact, although mouse leukocytes have been shown to contain CR1, it has been shown that mouse RBCs are CR1-negative, in contrast to human RBCs (Rabellino *et al.*, 1978; Kinoshita *et al.*, 1988). Moreover, recent work carried out with the rodent malaria laboratory model *P. chabaudi* showed that rosetting does occur in mice but suggested that the molecules involved may differ from those in human-infecting parasite species (Mackinnon *et al.*, 2002).

The results obtained when studying adhesion molecule polymorphisms in relation to malaria severity were, in all cases described, ambiguous, if not contradictory. This raises intriguing questions regarding *Plasmodium*-driven selection as well as important issues of therapeutic relevance.

3.4 *Host's immune response*

Any infectious disease is characterized, at the host level, by a complex reaction from the host immune system. The counteraction of host invasion by replicating pathogens demands a rapid response, generally provided by components of the innate immune system, which develops promptly and precedes the time-consuming clonal expansion of antigen-specific lymphocytes (Ismail *et al.*, 2002). Recent research has collected evidence of the importance of innate immunity in shaping the subsequent adaptive immune response to malaria blood-stage infection. It is now known that during blood-stage infection there is a 'cross-talk' between the parasite and cells of the innate immune system, such as DC, monocytes/macrophages, natural killer (NK) cells, NKT cells, and γ6 T cells. The activity of NK cells was found to be high in uncomplicated cases of malaria while in patients suffering CM there was a profound depression of NK activity (Stach *et al.*, 1986). Murine malaria studies also presented evidence that NK cells play a role in providing protection against the early stages of *P. berghei* or *P. chabaudi* infections (Solomon *et al.*, 1985; Mohan *et al.*, 1997). Recently, using the murine model *P. berghei* ANKA, it was shown that the natural killer complex (NKC) regulates CM, pulmonary edema and severe anaemia, and influences acquired immune responses to infection (Hansen *et al.*, 2005).

Although several recent studies have partially elucidated the role of NK cells during malaria infection (Orago and Facer, 1991; Artavanis-Tsakonas *et al.*, 2003; Artavanis-Tsakonas and Riley, 2002; Baratin *et al.*, 2005), the ligands and receptors responsible for NK-cell activation are still unknown. However, there are some data suggesting an association between NK cell reactivity to *P. falciparum*-infected RBCs and killer Ig-like receptors (KIR) genotype (Artavanis-Tsakonas *et al.*, 2003). This observation raises the fascinating possibility that genetic variation at the *KIR* locus might explain heterogeneity of human NK cell responses to parasitized iRBCs and that the parasite might express ligands to inhibit or activate KIR (Stevenson and Riley, 2004). Nonetheless, these findings highlight the need for large-scale population-based

studies in order to address associations between KIR genotype, NK responses and susceptibility to malaria.

The host's immune response to a malaria infection involves not only molecules from the rapid innate immune response but also molecules from a more specific immune response.

IL4. Interleukin-4 (IL4) is a cytokine that regulates the differentiation of precursor T helper cells into the T_H2 subset, which enhance the antigen-presenting capacity of B cells and specific antibody production (Romagnani, 1995). IL4 serves as an important regulator in isotype switching from IgM/IgG to IgE. Several studies have pointed towards IL-4 as an important factor in malaria resistance. A causal relationship between the activation of IL4-producing T-cell subsets and production of the anti-Pf155/RESA-specific antibodies in individuals with immunity induced by a natural malaria infection has been established (Troye-Blomberg *et al.*, 1990). More recently, it was shown that in the Fulani (Burkina Faso), known for having a lower susceptibility to *P. falciparum* infection than their neighbours, the IL4-524T allele (SNP C → T transition at position −524T from the transcription initiation site) was associated with high IgG levels against malaria antigens (Luoni *et al.*, 2001). However, others did not find this association (Verra *et al.*, 2004).

The possible association between three polymorphisms in the IL4 gene with SM in Ghanaian children has been addressed (Gyan *et al.*, 2004). One of these polymorphisms is located in the repeat region (intron3) of the *IL4* gene while the other two are in the promoter region (IL4+33T, SNP at position +33 relative to the transcription initiation site and the previously mentioned IL4-589T). A significantly higher frequency for +33 and −589 loci (IL4+33T/-589T allele) was observed in patients with CM and this was associated with elevated levels of total IgE.

Studies using the murine *P. chabaudi* and *P. berghei* models and IL4-deficient mice failed to show any role for this molecule in parasitaemia control or resistance to infection (von der Weid *et al.*, 1994; Saeftel *et al.*, 2004).

CD40L. CD40 ligand (CD40L) is a glycoprotein expressed in activated T cells. When it binds to CD40 in B cells it regulates their proliferation, antigen-presenting activity and IgG class switching (Durie *et al.*, 1994). CD40L is encoded by the gene *TNFSF5*. The study of CD40L-726 (C/T mutation in the promoter region) and CD40L+220 (C/T mutation in exon 1) polymorphisms association with resistance to SM in *P. falciparum* infections led to the observation that Gambian males with the CD40L-726C allele were protected from CM and severe anaemia (Sabeti *et al.*, 2002). This observation provides evidence to implicate CD40L as a factor in immunity or pathogenesis of malaria infections. The role of CD40L in the course of malaria infections was also explored in *P. berghei* infection, a mouse model of SM (Piguet *et al.*, 2001). CD40L-deficient mice are protected from CM, which seems to occur because the CD40/CD40L system is involved in the breakdown of the blood–brain barrier, macrophage sequestration and platelet consumption.

Fc receptors. The Fc receptors (FcRs) are a family of cell-surface molecules that bind the Fc portion of immunoglobulins. FcRs are widely distributed on cells of the immune system and establish a crucial connection between the humoral and the cellular immune

responses (Ravetch and Kinet, 1991). There are three families of FcγR (FcγRI, FcγRII and FcγRIII) that contain multiple distinct genes and alternative splicing forms. Few studies have focused on polymorphisms in different FcγRs. The FcγRIIA presents a polymorphism at position 131 that consists of a single histidine → arginine amino acid substitution (FcγRIIA-131H/R). It was shown that infants with the FcγRIIA-R/R genotype were significantly less likely to be at risk from high-density *P. falciparum* infection, compared with infants with the FcγRIIA-H/R. A later study focused on this same polymorphism and on another receptor polymorphism, FcγRIIIB-NA1/NA2, known to influence the phagocytic capacity of neutrophils (Omi *et al.*, 2002). This work, performed in northwest Thailand, has shown that malaria severity in this area is not associated with the FcγRIIA-131H/R or the FcγRIIIB-NA1/NA2 polymorphisms individually. However, the FcγRIIIB-NA2 allele together with the genotype FcγRIIA-131H/H was shown to be associated with susceptibility to CM. It has been also shown that in West Africa the polymorphism FcγRIIA-131H/R is related to disease severity since the FcγRIIA-131H/H genotype is significantly associated with increased susceptibility to SM (Cooke *et al.*, 2003).

The importance of Fc receptors in a malaria infection was addressed using transgenic mice in two different studies using *P. yoelii yoelii* and *P. berghei* XAT rodent models that showed that host resistance is mediated by antibodies (Rotman *et al.*, 1998; Yoneto *et al.*, 2001). Overall, the different studies indicate that Fc receptors have an important role in malaria infections.

TNF-α. Tumour necrosis factor-α (TNF-α) is a pro-inflammatory cytokine, produced by macrophages, NK cells and T cells, involved in local inflammation and endothelial activation (Janeway, 2001). This cytokine plays a pivotal role in the modulation of immune functions to infection and it was shown to limit the spread of pathogens (reviewed in Beutler and Grau, 1993). In a malaria infection TNF-α production by monocytes/macrophages mainly occurs during the blood stage when RBCs rupture and the schizonts, together with parasite-soluble antigens, are released into the bloodstream (Bate *et al.*, 1988; Kwiatkowski *et al.*, 1989; Taverne *et al.*, 1990a, 1990b; Pichyangkul *et al.*, 1994; Kwiatkowski, 1995).

TNF-α's role in malaria has been extensively studied and both a protective and a pathogenic role for this cytokine have been observed during infection. TNF-α's dual actions are related to its ability to activate endothelial cells, leading to the release of pro-inflammatory cytokines (Pober and Cotran, 1990), to the impairment of the blood–brain barrier (Sharief *et al.*, 1992; Sharief and Thompson, 1992) and to the up-regulation of adhesion molecules (reviewed in Meager, 1999). Of all up-regulated adhesion molecules, TNF-α's interplay with ICAM-1 seems to be extremely important to malaria pathogenesis (Dietrich, 2002; reviewed in Gimenez *et al.*, 2003). TNF-α also induces nitric oxide (NO) release by endothelial cells (Lamas *et al.*, 1991; Rockett *et al.*, 1992) which seems to play an important role during malaria infections (see NO section below). TNF-α was shown to play a beneficial role by inhibiting *P. falciparum* growth *in vitro* (Haidaris *et al.*, 1983; Rockett *et al.*, 1988). However, this effect was not observed using recombinant TNF (Taverne *et al.*, 1987). TNF was also reported to inhibit infection in murine malaria *in vivo* (Clark *et al.*, 1987; Taverne *et al.*, 1987). These and other later studies suggest that TNF is important in the control of malarial parasites (Ferrante *et al.*, 1990; Kumaratilake *et al.*, 1997). Nevertheless,

TNF-α has also an important role in SM pathogenesis (reviewed in Richards, 1997; Mazier *et al.*, 2000; Odeh, 2001; Gimenez *et al.*, 2003; Clark *et al.*, 2004). High TNF-α levels and malaria severity have been associated in several clinical studies (Grau *et al.*, 1989b; Kwiatkowski *et al.*, 1990; el-Nashar *et al.*, 2002; Esamai *et al.*, 2003) and the ratio of the antagonistic cytokines TNF-α and Interleukin-10 (IL-10) has been shown to be important to the outcome of malaria infection (May *et al.*, 2000) (see IL-10 section). It was shown that the balance between the protective and pathological actions of TNF-α depends on several factors, namely the amount, timing, and duration of TNF-α production, as well as the organ-specific site of synthesis (Beutler and Cerami, 1988; Jacobs *et al.*, 1996b).

TNF-α's unquestionable role in malaria pathogenesis has led to research focused on *TNF* polymorphisms and their association with malaria severity. Several polymorphisms in the *TNF* gene, with special emphasis for 2 promoter polymorphism, the TNF-308 and TNF-238, located -308 and -238 nucleotides relative to the gene transcriptional start, have been shown to be important for infection severity (McGuire *et al.*, 1994; Wattavidanage *et al.*, 1999; Aidoo *et al.*, 2001; Wilson *et al.*, 1997; Abraham and Kroeger, 1999; McGuire *et al.*, 1999; Knight *et al.*, 1999; Meyer *et al.*, 2002; Mombo *et al.*, 2003; Flori *et al.*, 2003). While many studies suggest a positive association between the mentioned TNF-α polymorphisms and malaria severity, other studies have failed to find these associations (Ubalee *et al.*, 2001; Stirnadel *et al.*, 1999; Bayley *et al.*, 2004). However, most evidence supports the idea that TNF polymorphisms may be part of the genetic determinants for human malaria resistance/susceptibility. More studies and functional analysis need to be carried out in order to understand the mechanisms involved. Nevertheless the TNF polymorphisms studies performed to date have provided more biological evidence for the role of TNF-α in human malaria.

A different set of studies, following a more therapeutic approach, has assessed the clinical outcome of SM using antibodies to neutralize TNF-α levels (Kwiatkowski *et al.*, 1993; van Hensbroek *et al.*, 1996; Looareesuwan *et al.*, 1999; Jacobs *et al.*, 1996b; Hermsen *et al.*, 1997; Grau *et al.*, 1987) and pentoxifylline to inhibit TNF-α (Sullivan *et al.*, 1988; Strieter *et al.*, 1988; Kremsner *et al.*, 1991; Stoltenburg-Didinger *et al.*, 1993; Di Perri *et al.*, 1995; Hemmer *et al.*, 1997; Looareesuwan *et al.*, 1998; Das *et al.*, 2003) both in human infections and rodent models of infection. A recent report explores a new way to treat CM by inhibiting TNF-α through the use of LMP-420, an anti-inflammatory drug (Wassmer *et al.*, 2005). Data from this report suggest that LMP-420, through the inhibition of endothelial activation, should be considered as a potential way to treat CM. However, the experimental results were based only on *in vitro* assays and further *in vivo* experiments are required to assess LMP-420 as a new therapeutic treatment.

While some observations suggest that TNF-α inhibition therapies would be of great value for malaria pathology control, others show that they may not hold any benefit. This lack of consensus may reflect the dual action that TNF-α seems to have during malaria infection.

IFN-γ. Interferon-γ (IFN-γ), mainly produced by NK cells and helper T cells is a pro-inflammatory cytokine involved in macrophage activation, Ig class switching, increased expression of MHC molecules and antigen processing components (Mohan *et al.*, 1997; Janeway *et al.*, 2001; Seixas *et al.*, 2002). IFN-γ plays a central role in the

immune response to several infectious diseases (Pfefferkorn and Guyre, 1984; Suzuki *et al.*, 1988; Rossi-Bergmann *et al.*, 1993; van den Broek *et al.*, 1995).

IFN-γ has been shown to be produced during malaria infections (Brake *et al.*, 1988; Meding *et al.*, 1990; Waki *et al.*, 1992; Mohan *et al.*, 1997; Artavanis-Tsakonas *et al.*, 2003; Artavanis-Tsakonas and Riley, 2002; Hailu *et al.*, 2004), and both a protective and a pathological function have been reported. Concerning its protective effect, it was demonstrated that an early IFN-γ-driven Th1-type response is required for an effective control of parasite multiplication in a primary blood-stage infection (Clark, 1987; Shear *et al.*, 1989; Stevenson *et al.*, 1990b; Taylor-Robinson, 1995; Favre *et al.*, 1997; Choudhury *et al.*, 2000; Kobayashi *et al.*, 2000). During infection, IFN-γ activates monocytes/macrophages (Bate *et al.*, 1988) and neutrophils (Kumaratilake *et al.*, 1991), which were shown to be involved in the recognition and removal of either merozoites or iRBCs (Khusmith *et al.*, 1982; Kharazmi *et al.*, 1984; Kharazmi and Jepsen, 1984; Ockenhouse *et al.*, 1984; Bouharoun-Tayoun *et al.*, 1995). This protective effect is strongly supported by several studies with rodent models using exogenous IFN-γ (Clark, 1987; Shear *et al.*, 1989) or an anti-IFN-γ mouse antibody (Kobayashi *et al.*, 2000). Furthermore, others have shown a correlation between IFN-γ production and a more positive outcome of malaria infections in both *P. chabaudi* and *P. yoelii* (Shear *et al.*, 1989; Stevenson *et al.*, 1990a). Endogenous IFN-γ has also been shown to play a role in the development of protective immunity using IFN-γ and IFN-γ receptor-deficient mice (van der Heyde *et al.*, 1997; Favre *et al.*, 1997). Altogether, these studies with different mouse strains combined with different *Plasmodium* spp. support a beneficial role for IFN-γ. Several human studies also point toward a protective role for IFN-γ in a malaria infection (Luty *et al.*, 1999; Torre *et al.*, 2001, 2002).

Despite this, several studies have clearly linked IFN-γ to the onset of pathology in mice as well as in humans. The detrimental effects of IFN-γ are thought to be due to its ability to activate macrophages, which, in turn, produce TNF-α, IL-1 and IL-6, leading to activation of an inflammatory cascade (Kern *et al.*, 1989; Day *et al.*, 1999). Grau *et al.* (1989a) showed that treatment of *P. berghei* ANKA CBA infected mice with a neutralizing anti-IFN-γ mouse antibody prevented development of CM and was associated with a significant decrease of TNF-α serum levels. This study supports the idea that there may be a fine balance between the levels of IFN-γ and TNF-α and protective immunity or pathological consequences. Furthermore, a synergy between IFN-γ and TNF-α, particularly with respect to the effects on endothelial cells, has also been observed (Pober *et al.*, 1986). Additional data correlating IFN-γ production with the susceptibility to CM are provided by the observation that CM-susceptible mice exhibit a preferential expansion of Th1-like clones characterized by a marked production of IFN-γ (de Kossodo and Grau, 1993). In addition, IFN-γ receptor deficient mice are completely protected from CM (Rudin *et al.*, 1997; Amani *et al.*, 2000). IFN-γ association with malaria pathology in humans is based on the fact that patients with acute *P. falciparum* malaria present high IFN-γ serum levels (Ringwald *et al.*, 1991; Ho *et al.*, 1995; Wenisch *et al.*, 1995; Nagamine *et al.*, 2003) and individuals at risk for SM produce more IFN-γ in an antigen-specific manner (Chizzolini *et al.*, 1990; Riley *et al.*, 1991).

IFN-γ and its receptor are encoded by the *IFNG* and *IFNGR1* genes, respectively. It was shown that in the Mandika, the predominant Gambian ethnic group, those that are heterozygous for IFNGR1-56 polymorphism (SNP at position -56 (T→C) in the promoter region), presented a two-fold protection against CM and a four-fold

protection against death resulting from CM (Koch *et al.*, 2002). Later, it was shown that this polymorphic allele reduces *IFNGR1* gene expression (Juliger *et al.*, 2003).

Only recently has research focused on *IFNG* polymorphisms. SNPs in the region of *IFNG* and the neighbouring *IL22* and *IL26* genes were analysed but no evidence of a strong association between SM and *IFNG* markers was found (Koch *et al.*, 2005). Recently it was shown that in children from Mali the −183T allele is associated with a lower risk of CM (Cabantous *et al.*, 2005). This allele is the polymorphic form of the IFNG-183G/T (G replaced by a T) polymorphism located in the gene promoter region and has been shown to create an AP1-binding site for a nuclear transcription factor, leading to the increase of gene transcription (Bream *et al.*, 2002; Chevillard *et al.*, 2002). IFN-γ clearly plays an important role during malaria infection, which can lead towards protection or pathology. The knowledge of IFN-γ exact involvement in malaria is important for the understanding of infection progression and, consequently, for the assessment of possible therapies against malaria.

NO. Nitric oxide (NO), a labile and highly reactive gas, results from the oxidative deamination of L-arginine to produce L-citruline through a reaction catalysed by the enzyme inducible nitric oxide synthase (iNOS) (Leone *et al.*, 1991). NO has been shown to inhibit the growth and function of diverse infectious agents, such as bacteria, fungi and protozoan parasites, by inactivating some of their critical metabolic pathways (reviewed in James, 1995). Increased NO production has been reported in murine (Taylor-Robinson *et al.*, 1993; Jacobs *et al.*, 1995) and human infections (Kremsner *et al.*, 1996). NO is produced by macrophages (Ahvazi *et al.*, 1995; Tachado *et al.*, 1996) but also by hepatocytes (Mellouk *et al.*, 1991; Nussler *et al.*, 1991) and endothelial cells (Oswald *et al.*, 1994; Tachado *et al.*, 1996). Cytokines such as IFN-γ and TNF-α are critical for the regulation of NO production (Jacobs *et al.*, 1996a). Tachado *et al.* (1996) demonstrated that glycosylphosphatidylinositols (GPI) induce NO release in a time- and dose-dependent manner in macrophages and vascular endothelial cells, and regulate iNOS expression in macrophages. In addition, it was shown that another parasite metabolite, haemozoin, is able to increase IFN-γ-dependent NO production by macrophages (Jaramillo *et al.*, 2003).

Both beneficial and pathological roles have been assigned to NO during malaria infection (Sobolewski *et al.*, 2005a). It is generally accepted that NO kills intraerythrocytic malarial parasites (Brunet, 2001; Clark and Cowden, 2003; Stevenson and Riley, 2004). However, it has been recently proposed that the blood stages are virtually immune to the cytotoxic effects of NO and other reactive oxygen species as a consequence of Hb NO scavenging and reactive oxygen species (ROS) suppression within RBCs (Sobolewski *et al.*, 2005b). Excess of NO can also contribute to malarial immunosuppression (Rockett *et al.*, 1994; Ahvazi *et al.*, 1995) as well as to CM development in *P. falciparum* infections (Clark *et al.*, 1991; Al Yaman *et al.*, 1996). It was proposed that overproduction of NO in the brain might affect local neuronal function by mimicking and exaggerating the physiological effects of endogenous NO (Clark and Cowden, 2003; Clark *et al.*, 1992). However, this hypothesis is not consensual as there is evidence suggesting that NO production may be limited in malaria due to the presence of hypoargininaemia in patients (Lopansri *et al.*, 2003). Furthermore, both plasma and urine NO*x* levels, as well as the iNOS protein and mRNA levels, correlate inversely with disease severity (Anstey *et al.*, 1996; Boutlis *et al.*, 2003; Perkins *et al.*, 1999; Chiwakata *et al.*, 2000).

A genomic approach, based on the association of *iNOS* gene polymorphisms with malaria infection has been applied to address NO role in malaria. Two SNPs, −954G → C and −1173 C → T, and a pentanucleotide (CCTTT) polymorphism have been studied in terms of malaria clinical outcome. However, reports show controversial data regarding the association of these *iNOS* gene promoter polymorphisms with severe *P. falciparum* malaria. Several reports show that NOS2A-954C allele is associated with protection from SM and resistance to reinfection both in Gabon and Uganda (Kun *et al.*, 1998, 2001; Parikh *et al.*, 2004). However, data from The Gambia, Tanzania and Ghana did not detect this association (Levesque *et al.*, 1999; Burgner *et al.*, 2003; Cramer *et al.*, 2004). A protective role for the *iNOS* -1173 C → T polymorphism has been shown in Tanzania (Hobbs *et al.*, 2002) but not in The Gambia and Ghana (Burgner *et al.*, 2003; Cramer *et al.*, 2004). Both these SNPs were shown to increase NO synthesis (Kun *et al.*, 2001; Hobbs *et al.*, 2002).

A pentanucleotide (CCTTT) microsatellite -2,5 kb of the transcription start site has also been studied. Short microsatellites (<11) have been shown to occur more frequently in fatal CM in The Gambia (Burgner *et al.*, 1998) while longer microsatellite alleles (≥13) were shown to be associated with SM in Thailand and Ghana (Ohashi *et al.*, 2002; Cramer *et al.*, 2004).

These contradictory results may be explained by the fact that the studies reported were carried out in different regions and again by the dual effect that host some molecules seem to have during malaria infection.

IL-10. Interleukin-10 (IL-10) is an anti-inflammatory cytokine produced by T cells and macrophages (Janeway *et al.*, 2001). Expression of IL-10 was shown to increase in response to high TNF-α levels and to down-regulate the production of the latter *in vivo* (Gerard *et al.*, 1993; Howard *et al.*, 1993), possibly representing an attempt of the host to counteract excessive activity of pro-inflammatory cytokines (van der Poll *et al.*, 1994).

Evidence for a beneficial role of IL-10 in malaria stems from an array of different population-based and animal model-based studies. IL-10-deficient mice infected with the rodent model parasite *P. chabaudi chabaudi* have been shown to have higher disease severity and mortality than their wild-type counterparts (Li *et al.*, 1999, 2003; Sanni *et al.*, 2004). The levels of both IL-10 and TNF-α are increased in patients with SM (Day et al., 1999). Several studies have attempted to correlate the IL-10:TNF-α ratio with disease severity (Kurtzhals *et al.*, 1998; Day *et al.*, 1999; Kurtzhals *et al.*, 1999; May *et al.*, 2000; Nussenblatt *et al.*, 2001). The general consensus seems to be that ratios <1 constitute a risk factor for severe anaemia, suggesting that an imbalance between the anti- and the pro-inflammatory responses may constitute a determinant of mortality. Furthermore, a study involving the simian model parasites *P. cynomolgi* and *P. knowlesi*, a role for IL-10 in controlling anaemia during primary infection has been suggested (Praba-Egge *et al.*, 2002).

The available evidence of a protective role for IL-10 against malaria would suggest that strategies to increase the production of this cytokine might hold therapeutic value. However, this may be less simple than it appears. Studies with rodent models have shown that an early pro-inflammatory response may be required to enhance the mechanisms that are essential for elimination of the parasites (Shear *et al.*, 1989; Stevenson *et al.*, 1995; De Souza *et al.*, 1997). In fact, a positive correlation between the IL-10 levels and parasitaemia in *P. falciparum*-infected individuals before the start

of anti-malarial treatment has been found (Luty *et al.*, 2000). These results were extended in a recent study that showed a clear association between IL-10 levels and reduced parasite clearance ability in a Tanzanian population undergoing four different treatment regimens with distinct parasite clearance rates (Hugosson *et al.*, 2004). In another study using the rodent parasite model *P. yoelii yoelii*, it was found that mice injected with anti-IL-10 antibody had significantly prolonged survival, suggesting that IL-10 is associated with disease exacerbation rather than protection. Taken together, these observations indicate that enhancing the level of IL-10 might actually be beneficial for the parasite since it could interfere with production of pro-inflammatory cytokines and enable *Plasmodium* to escape effective killing (Hugosson *et al.*, 2004).

Genetic factors substantially influence production of cytokines and may account for as much as 75% of inter-individual differences in IL-10 production (Westendorp *et al.*, 1997). Furthermore, a clear association exists between a variety of IL-10 polymorphisms and susceptibility to several inflammatory diseases, such as rheumatoid arthritis (Eskdale *et al.*, 1998) and systemic lupus erythematosus (Gibson *et al.*, 2001). Thus, the possible correlation between five IL-10 polymorphisms (defining six haplotypes) and malaria severity in a population in The Gambia was investigated (Wilson *et al.*, 2005). One of these haplotypes, termed HAP3, defined by three SNPs at positions +4949, −1117 and −3585, showed a significant association with protection against CM and severe anaemia. However, this case-control association between malaria and HAP3 was not confirmed by a transmission disequilibrium test analysis of the same population. No evidence was found of a correlation between disease severity and any of the individual polymorphisms under study, suggesting that resistance either depends on other SNPs not addressed in this study or on specific combinations of *IL10* polymorphisms (Wilson *et al.*, 2005).

It seems clear that a certain level of IL-10 is required to balance the effect of pro-inflammatory cytokines. Still, an early pro-inflammatory response may be required to enhance the mechanisms that are essential for elimination of the parasites The balance between pro- and anti-inflammatory cytokines during a malaria infection is clearly difficult to ascertain and has important consequences in terms of disease progression. If it is true that fine tuning the inflammatory responses during disease appears as an attractive way to improve its outcome, it is nonetheless obvious that our current knowledge of the complex immunological response that takes place during infection needs to be improved before this can be done in a manner that ensures a promising outcome.

4 Final remarks: exploring the host potential in the 'post-omics era'

The contact between *Plasmodium* and its mammalian host involves a number of interactions that result in a series of different scenarios that range from complete or partial protection to infection and/or disease to SM leading to death. Both sides of this relationship are quite variable and many different possibilities of interaction may occur in the same population. Still, the survival of the *Plasmodium* parasite depends not only on its interaction with host molecules but also on efficiently coping with the host's immune responses. Thus, not only host-driven genetic selection acts on malaria parasite populations, but also *Plasmodium* is likely to exert evolutionary pressure on

human gene frequencies. In malaria endemic regions, we might guess that infection contributes positively to the allele frequency of variants associated with protection. The gene conferring the Duffy blood group is one of the most striking examples of this selection pressure; people of this blood type are completely resistant to *P. vivax* blood-stage infection, as they lack a RBC receptor required for *P. vivax* invasion (Hamblin and Di Rienzo, 2000; Chitnis and Miller, 1994). Another striking example is the sickle cell anaemia allele. While severely deleterious in the homozygous state, this allele is associated with malaria protection in the heterozygous state, although the protection mechanisms involved are not fully understood (Aidoo *et al.*, 2002). Importantly, as one might expect, host components involved in the symptomatic phase of infection (blood stage) do not seem to be the only ones implicated in determining the severity of malaria infection. In fact, some alleles on the MHC Class I B53 loci are associated with protective clinical responses in African populations, due to interactions occurring during the silent liver stage of infection (Hill *et al.*, 1991). Presumably this association has contributed to the high frequency of MHC-B53 observed in populations living in areas of high malaria endemicity. Moreover, one should keep in mind that the blood and liver stages of infection can coexist in populations living in endemic areas. Therefore, the final result observed in human populations should not be extrapolated without taking into account possible interactions or common pathways that may occur between the two infection stages.

The sequence of both mice (rodent models of malaria infection) and human genomes can prove to be very useful. Moreover, the use of high-throughput technologies to determine the host molecules altered during the course of an infection, already used for some systems with interesting results (Delahaye *et al.*, 2006), together with systems that allow functional genomics studies, such as RNA interference, will be powerful tools to determine the role of these host molecules during the course of malaria infections.

References

Abraham, L.J. & Kroeger, K.M. (1999) Impact of the -308 TNF promoter polymorphism on the transcriptional regulation of the TNF gene: relevance to disease. *J Leukoc Bio*, **66:** 562–566.

Adams, S., Turner, G.D., Nash, G.B., Micklem, K., Newbold, C.I. & Craig, A.G. (2000) Differential binding of clonal variants of *Plasmodium falciparum* to allelic forms of intracellular adhesion molecule 1 determined by flow adhesion assay. *Infect Immun* **68:** 264–269.

Agarwal, A., Guindo, A., Cissoko, Y., Taylor, J.G., Coulibaly, D., Kone, A., Kayentao, K., Djimde, A., Plowe, C.V., Doumbo, O., Wellems, T.E. & Diallo, D. (2000) Hemoglobin C associated with protection from severe malaria in the Dogon of Mali, a West African population with a low prevalence of hemoglobin S. *Blood* **96:** 2358–2363.

Ahvazi, B.C., Jacobs, P. & Stevenson, M.M. (1995) Role of macrophage-derived nitric oxide in suppression of lymphocyte proliferation during blood-stage malaria. *J Leukoc Biol* **58:** 23–31.

Aidoo, M., McElroy, P.D., Kolczak, M.S., Terlouw, D.J., Ter kuile, F.O., Nahlen, B., Lal, A.A. & Udhayakumar, V. (2001) Tumor necrosis factor-alpha promoter

variant 2 (TNF2) is associated with pre-term delivery, infant mortality, and malaria morbidity in western Kenya: Asembo Bay Cohort Project IX. *Genet Epidemiol* **21**: 201–211.

Aidoo, M., Terlouw, D.J., Kolczak, M.S., McElroy, P.D., Ter kuile, F.O., Kariuki, S., Nahlen, B.L., Lal, A.A. & Udhayakumar, V. (2002) Protective effects of the sickle cell gene against malaria morbidity and mortality. *Lancet* **359**: 1311–1312.

Aitman, T.J., Cooper, L.D., Norsworthy, P.J., Wahid, F.N., Gray, J.K., Curtis, B.R., Mckeigue, P.M., Kwiatkowski, D., Greenwood, B.M., Snow, R.W., Hill, A.V. & Scott, J. (2000) Malaria susceptibility and CD36 mutation. *Nature* **405**: 1015–1016.

Al yaman, F.M., Mokela, D., Genton, B., Rockett, K.A., Alpers, M.P. & Clark, I.A. (1996) Association between serum levels of reactive nitrogen intermediates and coma in children with cerebral malaria in Papua New Guinea. *Trans R Soc Trop Med Hyg* **90**: 270–273.

Allen, S.J., O'Donnell, A., Alexander, N.D., Mgone, C.S., Peto, T.E., Clegg, J.B., Alpers, M.P. & Weatherall, D.J. (1999) Prevention of cerebral malaria in children in Papua New Guinea by southeast Asian ovalocytosis band 3. *Am J Trop Med Hyg* **60**: 1056–1060.

Alper, S.L., Darman, R.B., Chernova, M.N. & Dahl, N.K. (2002) The AE gene family of Cl/HCO3- exchangers. *J Nephrol* **15**: suppl 5, s41–s53.

Amani, V., Vigario, A.M., Belnoue, E., Marussig, M., Fonseca, L., Mazier, D. & Renia, L. (2000) Involvement of IFN-gamma receptor-medicated signaling in pathology and anti-malarial immunity induced by *Plasmodium berghei* infection. *Eur J Immunol* **30**: 1646–1655.

Amodu, O.K., Gbadegesin, R.A., Ralph, S.A., Adeyemo, A.A., Brenchley, P.E., Ayoola, O.O., Orimadegun, A.E., Akinsola, A.K., Olumese, P.E. & Omotade, O.O. (2005) *Plasmodium falciparum* malaria in south-west Nigerian children: is the polymorphism of ICAM-1 and E-selectin genes contributing to the clinical severity of malaria? *Acta Trop* **95**: 248–255.

Andrews, K.T. & Lanzer, M. (2002) Maternal malaria: *Plasmodium falciparum* sequestration in the placenta. *Parasitol Res* **88**: 715–723.

Anstey, N.M., Weinberg, J.B., Hassanali, M.Y., Mwaikambo, E.D., Manyenga, D., Misukonis, M.A., Arnelle, D.R., Hollis, D., Mcdonald, M.I. & Granger, D.L. (1996) Nitric oxide in Tanzanian children with malaria: inverse relationship between malaria severity and nitric oxide production/nitric oxide synthase type 2 expression. *J Exp Med* **184**: 557–567.

Arie, T., Fairhurst, R.M., Brittain, N.J., Wellems, T.E. & Dvorak, J.A. (2005) Hemoglobin C modulates the surface topography of *Plasmodium falciparum*-infected erythrocytes. *J Struct Biol* **150**: 163–169.

Artavanis-Tsakonas, K. & Riley, E.M. (2002) Innate immune response to malaria: rapid induction of IFN-gamma from human NK cells by live *Plasmodium falciparum*-infected erythrocytes. *J Immunol* **169**: 2956–2963.

Artavanis-Tsakonas, K., Eleme, K., McQueen, K.L., Cheng, N.W., Parham, P., Davis, D.M. & Riley, E.M. (2003) Activation of a subset of human NK cells upon contact with *Plasmodium falciparum*-infected erythrocytes. *J Immunol* **171**: 5396–5405.

Ayi, K., Turrini, F., Piga, A. & Arese, P. (2004) Enhanced phagocytosis of ring-parasitized mutant erythrocytes: a common mechanism that may explain protection against *falciparum* malaria in sickle trait and beta-thalassemia trait. *Blood* **104:** 3364–3371.

Baratin, M., Roetynck, S., Lepolard, C., Falk, C., Sawadogo, S., Uematsu, S., Akira, S., Ryffel, B., Tiraby, J.G., Alexopoulou, L., Kirschning, C.J., Gysin, J., Vivier, E. & Ugolini, S. (2005) Natural killer cell and macrophage cooperation in MyD88-dependent innate responses to *Plasmodium falciparum*. *Proc Natl Acad Sci USA* **102:** 14747–14752.

Barnwell, J.W., Ockenhouse, C.F. & Knowles, D.M., 2nd (1985) Monoclonal antibody OKM5 inhibits the *in vitro* binding of *Plasmodium falciparum*-infected erythrocytes to monocytes, endothelial, and C32 melanoma cells. *J Immunol* **135:** 3494–3497.

Barnwell, J.W., Asch, A.S., Nachman, R.L., Yamaya, M., Aikawa, M. & Ingravallo, P. (1989) A human 88-kD membrane glycoprotein (CD36) functions *in vitro* as a receptor for a cytoadherence ligand on *Plasmodium falciparum*-infected erythrocytes. *J Clin Invest* **84:** 765–772.

Baruch, D.I., Ma, X.C., Singh, H.B., Bi, X, Pasloske, B.L. & Howard, R.J. (1997) Identification of a region of PfEMP1 that mediates adherence of *Plasmodium falciparum* infected erythrocytes to CD36: conserved function with variant sequence. *Blood* **90:** 3766–3775.

Bate, C.A., Taverne, J. & Playfair, J.H. (1988) Malarial parasites induce TNF production by macrophages. *Immunology* **64:** 227–231.

Baum, J., Pinder, M. & Conway, D.J. (2003) Erythrocyte invasion phenotypes of *Plasmodium falciparum* in The Gambia. *Infect Immun* **71:** 1856–1863.

Bayley, J.P., Ottenhoff, T.H. & Verweij, C.L. (2004) Is there a future for TNF promoter polymorphisms? *Genes Immun* **5:** 315–329.

Beeson, J.G. & Brown, G.V. (2002) Pathogenesis of *Plasmodium falciparum* malaria: the roles of parasite adhesion and antigenic variation. *Cell Mol Life Sci* **59:** 258–271.

Beeson, J.G., Reeder, J.C., Rogerson, S.J. & Brown, G.V. (2001) Parasite adhesion and immune evasion in placental malaria. *Trends Parasitol* **17:** 331–337.

Beeson, J.G., Rogerson, S.J. & Brown, G.V. (2002) Evaluating specific adhesion of *Plasmodium falciparum*-infected erythrocytes to immobilized hyaluronic acid with comparison to binding of mammalian cells. *Int J Parasitol* **32:** 1245–1252.

Bellamy, R., Kwiatkowski, D. & Hill, A.V. (1998) Absence of an association between intercellular adhesion molecule 1, complement receptor 1 and interleukin 1 receptor antagonist gene polymorphisms and severe malaria in a West African population. *Trans R Soc Trop Med Hyg* **92:** 312–316.

Berendt, A.R., Simmons, D.L., Tansey, J., Newbold, C.I. & Marsh, K. (1989) Intercellular adhesion molecule-1 is an endothelial cell adhesion receptor for *Plasmodium falciparum*. *Nature* **341:** 57–59.

Beutler, B. & Cerami, A. (1988) Tumor necrosis, cachexia, shock, and inflammation: a common mediator. *Annu Rev Biochem* **57:** 505–518.

Beutler, B. & Grau, G.E. (1993) Tumor necrosis factor in the pathogenesis of infectious diseases. *Crit Care Med* **21:** S423–S435.

Beutler, E. (1990) The genetics of glucose-6-phosphate dehydrogenase deficiency. *Semin Hematol* **27:** 137–164.

Beutler, E. (1996) G6PD: population genetics and clinical manifestations. *Blood Rev* **10:** 45–52.

Bodescot, M., Silvie, O., Siau, A., Refour, P., Pino, P., Franetich, J.F., Hannoun, L., Sauerwein, R. & Mazier, D. (2004) Transcription status of vaccine candidate genes of *Plasmodium falciparum* during the hepatic phase of its life cycle. *Parasitol Res* **92:** 449–452.

Bouharoun-Tayoun, H., Oeuvray, C., Lunel, F. & Druilhe, P. (1995) Mechanisms underlying the monocyte-mediated antibody-dependent killing of *Plasmodium falciparum* asexual blood stages. *J Exp Med* **182:** 409–418.

Boutlis, C.S., Tjitra, E., Maniboey, H., Misukonis, M.A., Saunders, J.R., Suprianto, S., Weinberg, J.B. & Anstey, N.M. (2003) Nitric oxide production and mononuclear cell nitric oxide synthase activity in malaria-tolerant Papuan adults. *Infect Immun* **71:** 3682–3689.

Brake, D.A., Long, C.A. & Weidanz, W.P. (1988) Adoptive protection against *Plasmodium chabaudi adami* malaria in athymic nude mice by a cloned T cell line. *J Immunol* **140:** 1989–1993.

Bream, J.H., Ping, A., Zhang, X., Winkler, C. & Young, H.A. (2002) A single nucleotide polymorphism in the proximal IFN-gamma promoter alters control of gene transcription. *Genes Immun* **3:** 165–169.

Brittenham, G.M., Schechter, A.N. & Noguchi, C.T. (1985) Hemoglobin S polymerization: primary determinant of the hemolytic and clinical severity of the sickling syndromes. *Blood* **65:** 183–189.

Bruna-Romero, O. & Rodriguez, A. (2001) Dendritic cells can initiate protective immune responses against malaria. *Infect Immun* **69:** 5173–5176.

Brunet, L.R. (2001) Nitric oxide in parasitic infections. *Int Immunopharmacol* **1:** 1457–1467.

Burgner, D., Xu, W., Rockett, K., Gravenor, M., Charles, I.G., Hill, A.V. & Kwiatkowski, D. (1998) Inducible nitric oxide synthase polymorphism and fatal cerebral malaria. *Lancet* **352:** 1193–1194.

Burgner, D., Usen, S., Rockett, K., Jallow, M., Ackerman, H., Cervino, A., Pinder, M. & Kwiatkowski, D.P. (2003) Nucleotide and haplotypic diversity of the NOS2A promoter region and its relationship to cerebral malaria. *Hum Genet* **112:** 379–386.

Cabantous, S., Poudiougou, B., Traore, A., Keita, M., Cisse, M.B., Doumbo, O., Dessein, A.J. & Marquet, S. (2005) Evidence that interferon-gamma plays a protective role during cerebral malaria. *J Infect Dis* **192:** 854–860.

Cappadoro, M., Giribaldi, G., O'Brien, E., Turrini, F., Mannu, F., Ulliers, D., Simula, G., Luzzatto, L. & Arese, P. (1998) Early phagocytosis of glucose-6-phosphate dehydrogenase (G6PD)-deficient erythrocytes parasitized by *Plasmodium falciparum* may explain malaria protection in G6PD deficiency. *Blood* **92:** 2527–2534.

Carrolo, M., Giordano, S., Cabrita-Santos, L., Corso, S., Vigario, A.M., Silva, S., Leiriao, P., Carapau, D., Armas-Portela, R., Comoglio, P.M., Rodriguez, A. & Mota, M.M. (2003) Hepatocyte growth factor and its receptor are required for malaria infection. *Nat Med* **9:** 1363–1369.

Carvalho, L.J., Daniel-Ribeiro, C.T. & Goto, H. (2002) Malaria vaccine: candidate antigens, mechanisms, constraints and prospects. *Scand J Immunol* **56:** 327–343.

Casals-Pascual, C., Allen, S., Allen, A., Kai, O., Lowe, B., Pain, A. & Roberts, D.J. (2001) Short report: codon 125 polymorphism of CD31 and susceptibility to malaria. *Am J Trop Med Hyg* **65:** 736–737.

Chevillard, C., Henri, S., Stefani, F., Parzy, D. & Dessein, A. (2002) Two new polymorphisms in the human interferon gamma (IFN-gamma) promoter. *Eur J Immunogenet* **29**: 53–56.

Chitnis, C.E. & Miller, L.H. (1994) Identification of the erythrocyte binding domains of *Plasmodium vivax* and *Plasmodium knowlesi* proteins involved in erythrocyte invasion. *J Exp Med* **180**: 497–506.

Chiwakata, C.B., Hemmer, C.J. & Dietrich, M. (2000) High levels of inducible nitric oxide synthase mRNA are associated with increased monocyte counts in blood and have a beneficial role in *Plasmodium falciparum* malaria. *Infect Immun* **68**: 394–399.

Chizzolini, C., Grau, G.E., Geinoz, A. & Schrijvers, D. (1990) T lymphocyte interferon-gamma production induced by *Plasmodium falciparum* antigen is high in recently infected non-immune and low in immune subjects. *Clin Exp Immunol* **79**: 95–99.

Chotivanich, K., Udomsangpetch, R., Pattanapanyasat, K., Chierakul, W., Simpson, J., Looareesuwan, S. & White, N. (2002) Hemoglobin E: a balanced polymorphism protective against high parasitemias and thus severe *P. falciparum* malaria. *Blood* **100**: 1172–1176.

Choudhury, H.R., Sheikh, N.A., Bancroft, G.J., Katz, D.R. & de Souza, J.B. (2000) Early nonspecific immune responses and immunity to blood-stage nonlethal *Plasmodium yoelii* malaria. *Infect Immun* **68**: 6127–6132.

Clark, I.A. (1987) Cell-mediated immunity in protection and pathology of malaria. *Parasitol Today* **3**: 300–305.

Clark, I.A. & Cowden, W.B. (2003) The pathophysiology of *falciparum* malaria. *Pharmacol Ther* **99**: 221–260.

Clark, I.A., Hunt, N.H., Butcher, G.A. & Cowden, W.B. (1987) Inhibition of murine malaria (*Plasmodium chabaudi*) *in vivo* by recombinant interferon-gamma or tumor necrosis factor, and its enhancement by butylated hydroxyanisole. *J Immunol* **139**: 3493–3496.

Clark, I.A., Rockett, K.A. & Cowden, W.B. (1991) Proposed link between cytokines, nitric oxide and human cerebral malaria. *Parasitol Today* **7**: 205–207.

Clark, I.A., Rockett, K.A. & Cowden, W.B. (1992) Possible central role of nitric oxide in conditions clinically similar to cerebral malaria. *Lancet* **340**: 894–896.

Clark, I.A., Alleva, L.M., Mills, A.C. & Cowden, W.B. (2004) Pathogenesis of malaria and clinically similar conditions. *Clin Microbiol Rev* **17**: 509–539, table of contents.

Clyde, D.F., Most, H., McCarthy, V.C. & Vanderberg, J.P. (1973) Immunization of man against sporozite-induced *falciparum* malaria. *Am J Med Sci* **266**: 169–177.

Cockburn, I.A., MacKinnon, M.J., O'Donnell, A., Allen, S.J., Moulds, J.M., Baisor, M., Bockarie, M., Reeder, J.C. & Rowe, J.A. (2004) A human complement receptor 1 polymorphism that reduces *Plasmodium falciparum* rosetting confers protection against severe malaria. *Proc Natl Acad Sci USA* **101**: 272–277.

Cooke, B.M., Nicoll, C.L., Baruch, D.I. & Coppel, R.L. (1998) A recombinant peptide based on PfEMP-1 blocks and reverses adhesion of malaria-infected red blood cells to CD36 under flow. *Mol Microbiol* **30**: 83–90.

Cooke, G.S., Aucan, C., Walley, A.J., Segal, S., Greenwood, B.M., Kwiatkowski, D.P. & Hill, W.V. (2003) Association of Fcgamma receptor IIa (CD32) polymorphism with severe malaria in West Africa. *Am J Trop Med Hyg* **69**: 565–568.

Craig, A., Fernandez-Reyes, D., Mesri, M., McDowall, A., Altieri, D.C., Hogg, N. & Newbold, C. (2000) A functional analysis of a natural variant of intercellular adhesion molecule-1 (ICAM-1Kilifi). *Hum Mol Genet* **9**: 525–530.

Cramer, J.P., Mockenhaupt, F.P., Ehrhardt, S., Burkhardt, J., Otchwemah, R.N., Dietz, E., Gellert, S. & Bienzle, U. (2004) iNOS promoter variants and severe malaria in Ghanaian children. *Trop Med Int Health* **9**: 1074–1080.

Cranston, H.A., Boylan, C.W., Carroll, G.L., Sutera, S.P., Williamson, J.R., Gluzman, I.Y. & Krogstad, D.J. (1984) *Plasmodium falciparum* maturation abolishes physiologic red cell deformability. *Science* **223**: 400–403.

Das, B.K., Mishra, S., Padhi, P.K., Manish, R., Tripathy, R., Sahoo, P.K. & Ravindran, B. (2003) Pentoxifylline adjunct improves prognosis of human cerebral malaria in adults. *Trop Med Int Health* **8**: 680–684.

Day, N.P., Hien, T.T., Schollaardt, T., Loc, P.P., Chuong, L.V., Chau, T.T., Mai, N.T., Phu, N.H., Sinh, D.X., White, N.J. & Ho, M. (1999) The prognostic and pathophysiologic role of pro- and antiinflammatory cytokines in severe malaria. *J Infect Dis* **180**: 1288–1297.

De Kossodo, S. & Grau, G.E. (1993) Profiles of cytokine production in relation with susceptibility to cerebral malaria. *J Immunol* **151**: 4811–4820.

De Souza, J.B., Williamson, K.H., Otani, T. & Playfair, J.H. (1997) Early gamma interferon responses in lethal and nonlethal murine blood-stage malaria. *Infect Immun* **65**: 1593–1598.

Delahaye, N.F., Coltel, N., Puthier, D., Flori, L., Houlgatte, R., Iraqi, F.A., Nguyen, C., Grau, G.E. & Rihet, P. (2006) Gene-expression profiling discriminates between cerebral malaria (CM)-susceptible mice and CM-resistant mice. *J Infect Dis* **193**: 312–321.

Di perri, G., Di perri, I.G., Monteiro, G.B., Bonora, S., Hennig, C., Cassatella, M., Micciolo, R., Vento, S., Dusi, S., Bassetti, D. *et al.* (1995) Pentoxifylline as a supportive agent in the treatment of cerebral malaria in children. *J Infect Dis* **171**: 1317–1322.

Dietrich, I.B. (2002) The adhesion molecule ICAM-1 and its regulation in relation with the blood–brain barrier. *J Neuroimmunol* **128**: 58–68.

Dolan, S.A., Miller, L.H. & Wellems, T.E. (1990) Evidence for a switching mechanism in the invasion of erythrocytes by *Plasmodium falciparum*. *J Clin Invest* **86**: 618–624.

Dolan, S.A., Proctor, J.L., Alling, D.W., Okubo, Y., Wellems, T.E. & Miller, L.H. (1994) Glycophorin B as an EBA-175 independent *Plasmodium falciparum* receptor of human erythrocytes. *Mol Biochem Parasitol* **64**: 55–63.

Duffy, P.E. & Fried, M. (2003) *Plasmodium falciparum* adhesion in the placenta. *Curr Opin Microbiol* **6**: 371–376.

Duraisingh, M.T., Maier, A.G., Triglia, T. & Cowman, A.F. (2003) Erythrocyte-binding antigen 175 mediates invasion in *Plasmodium falciparum* utilizing sialic acid-dependent and -independent pathways. *Proc Natl Acad Sci USA* **100**: 4796–4801.

Durie, F.H., Foy, T.M., Masters, S.R., Laman, J.D. & Noelle, R.J. (1994) The role of CD40 in the regulation of humoral and cell-mediated immunity. *Immunol Today* **15**: 406–411.

El-nashar, T.M., El-kholy, H.M., El-shiety, A.G. & Al-zahaby, A.A. (2002) Correlation of plasma levels of tumor necrosis factor, interleukin-6 and nitric oxide with the severity of human malaria. *J Egypt Soc Parasitol* **32**: 525–535.

Esamai, F., Ernerudh, J., Janols, H., Welin, S., Ekerfelt, C., Mining, S. & Forsberg, P. (2003) Cerebral malaria in children: serum and cerebrospinal fluid TNF-alpha and TGF-beta levels and their relationship to clinical outcome. *J Trop Pediatr* **49:** 216–223.

Eskdale, J., McNicholl, J., Wordsworth, P., Jonas, B., Huizinga, T., Field, M. & Gallagher, G. (1998) Interleukin-10 microsatellite polymorphisms and IL-10 locus alleles in rheumatoid arthritis susceptibility. *Lancet* **352:** 1282–1283.

Esser, M.T., Marchese, R.D., Kierstead, L.S., Tussey, L.G., Wang, F., Chirmule, N. & Washabaugh, M.W. (2003) Memory T cells and vaccines. *Vaccine* **21:** 419–430.

Fairhurst, R.M., Baruch, D.I., Brittain, N.J., Ostera, G.R., Wallach, J.S., Hoang, H.L., Hayton, K., Guindo, A., Makobongo, M.O., Schwartz, O.M., Tounkara, A., Doumbo, O.K., Diallo, D.A., Fujioka, H., Ho, M. & Wellems, T.E. (2005) Abnormal display of PfEMP-1 on erythrocytes carrying haemoglobin C may protect against malaria. *Nature* **435:** 1117–1121.

Favre, N., Ryffel, B., Bordmann, G. & Rudin, W. (1997) The course of *Plasmodium chabaudi chabaudi* infections in interferon-gamma receptor deficient mice. *Parasite Immunol* **19:** 375–383.

Fernandez-Reyes, D., Craig, A.G., Kyes, S.A., Peshu, N., Snow, R.W., Berendt, A.R., Marsh, K. & Newbold, C.I. (1997) A high frequency African coding polymorphism in the N-terminal domain of ICAM-1 predisposing to cerebral malaria in Kenya. *Hum Mol Genet* **6:** 1357–1360.

Ferrante, A., Kumaratilake, L., Rzepczyk, C.M. & Dayer, J.M. (1990) Killing of *Plasmodium falciparum* by cytokine activated effector cells (neutrophils and macrophages). *Immunol Lett* **25:** 179–187.

Flori, L., Sawadogo, S., Esnault, C., Delahaye, N.F., Fumoux, F. & Rihet, P. (2003) Linkage of mild malaria to the major histocompatibility complex in families living in Burkina Faso. *Hum Mol Genet* **12:** 375–378.

Franke-Fayard, B., Janse, C.J., Cunha-Rodrigues, M., Ramesar, J., Buscher, P., Que, I., Lowik, C., Voshol, P.J., den Boer, M.A., van Duinen, S.G., Febbraio, M., Mota, M.M. & Waters, A.P. (2005) Murine malaria parasite sequestration: CD36 is the major receptor, but cerebral pathology is unlinked to sequestration. *Proc Natl Acad Sci USA* **102:** 11468–11473.

Frevert, U., Engelmann, S., Zougbede, S., Stange, J., Ng, B., Matuschewski, K., Liebes, L. & Yee, H. (2005) Intravital observation of *Plasmodium berghei* sporozoite infection of the liver. *Plos Biol* **3:** e192.

Genton, B., Al-yaman, F., Mgone, C.S., Alexander, N., Paniu, M.M., Alpers, M.P. & Mokela, D. (1995) Ovalocytosis and cerebral malaria. *Nature* **378:** 564–565.

Gerard, C., Bruyns, C., Marchant, A., Abramowicz, D., Vandenabeele, P., Delvaux, A., Fiers, W., Goldman, M. & Velu, T. (1993) Interleukin 10 reduces the release of tumor necrosis factor and prevents lethality in experimental endotoxemia. *J Exp Med* **177:** 547–550.

Gibson, A.W., Edberg, J.C., Wu, J., Westendorp, R.G., Huizinga, T.W. & Kimberly, R.P. (2001) Novel single nucleotide polymorphisms in the distal IL-10 promoter affect IL-10 production and enhance the risk of systemic lupus erythematosus. *J Immunol* **166:** 3915–3922.

Gilbert, S.C., Plebanski, M., Gupta, S., Morris, J., Cox, M., Aidoo, M., Kwiatkowski, D., Greenwood, B.M., Whittle, H.C. & Hill, A.V. (1998)

Association of malaria parasite population structure, HLA, and immunological antagonism. *Science* **279**: 1173–1177.

Gimenez, F., Barraud de Lagerie, S., Fernandez, C., Pino, P. & Mazier, D. (2003) Tumor necrosis factor alpha in the pathogenesis of cerebral malaria. *Cell Mol Life Sci* **60**: 1623–1635.

Grau, G.E., Fajardo, L.F., Piguet, P.F., Allet, B., Lambert, P.H. & Vassalli, P. (1987) Tumor necrosis factor (cachectin) as an essential mediator in murine cerebral malaria. *Science* **237**: 1210–1212.

Grau, G.E., Heremans, H., Piguet, P.F., Pointaire, P., Lambert, P.H., Billiau, A. & Vassalli, P. (1989a) Monoclonal antibody against interferon gamma can prevent experimental cerebral malaria and its associated overproduction of tumor necrosis factor. *Proc Natl Acad Sci USA* **86**: 5572–5574.

Grau, G.E., Taylor, T.E., Molyneux, M.E., Wirima, J.J., Vassalli, P., Hommel, M. & Lambert, P.H. (1989b) Tumor necrosis factor and disease severity in children with *falciparum* malaria. *N Engl J Med* **320**: 1586–1591.

Gruner, A.C., Snounou, G., Brahimi, K., Letourneur, F., Renia, L. & Druilhe, P. (2003) Pre-erythrocytic antigens of *Plasmodium falciparum*: from rags to riches? *Trends Parasitol* **19**: 74–78.

Gyan, B.A., Goka, B., Cvetkovic, J.T., Kurtzhals, J.L., Adabayeri, V., Perlmann, H., Lefvert, A.K., Akanmori, B.D. & Troye-Blomberg, M. (2004) Allelic polymorphisms in the repeat and promoter regions of the interleukin-4 gene and malaria severity in Ghanaian children. *Clin Exp Immunol* **138**: 145–150.

Hadley, T.J., Klotz, F.W., Pasvol, G., Haynes, J.D., McGinniss, M.H., Okubo, Y. & Miller, L.H. (1987) *Falciparum* malaria parasites invade erythrocytes that lack glycophorin A and B (MkMk). Strain differences indicate receptor heterogeneity and two pathways for invasion. *J Clin Invest* **80**: 1190–1193.

Haidaris, C.G., Haynes, J.D., Meltzer, M.S. & Allison, A.C. (1983) Serum containing tumor necrosis factor is cytotoxic for the human malaria parasite *Plasmodium falciparum*. *Infect Immun* **42**: 385–393.

Hailu, A., van der Poll, T., Berhe, N. & Kager, P.A. (2004) Elevated plasma levels of interferon (IFN)-gamma, IFN-gamma inducing cytokines, and IFN-gamma inducible CXC chemokines in visceral leishmaniasis. *Am J Trop Med Hyg* **71**: 561–567.

Hamblin, M.T. & Di Rienzo, A. (2000) Detection of the signature of natural selection in humans: evidence from the Duffy blood group locus. *Am J Hum Genet* **66**: 1669–1679.

Hamblin, M.T., Thompson, E.E. & Di Rienzo, A. (2002) Complex signatures of natural selection at the Duffy blood group locus. *Am J Hum Genet* **70**: 369–383.

Hansen, D.S., Evans, K.J., D'Ombrain, M.C., Bernard, N.J., Sexton, A.C., Buckingham, L., Scalzo, A.A. & Schofield, L. (2005) The natural killer complex regulates severe malarial pathogenesis and influences acquired immune responses to *Plasmodium berghei* ANKA. *Infect Immun* **73**:2288–2297.

Heddini, A., Chen, Q., Obiero, J., Kai, O., Fernandez, V., Marsh, K., Muller, W.A. & Wahlgren, M. (2001a) Binding of *Plasmodium falciparum*-infected erythrocytes to soluble platelet endothelial cell adhesion molecule-1 (PECAM-1/CD31): frequent recognition by clinical isolates. *Am J Trop Med Hyg* **65**: 47–51.

Heddini, A., Pettersson, F., Kai, O., Shafi, J., Obiero, J., Chen, Q., Barragan, A., Wahlgren, M. & Marsh, K. (2001b) Fresh isolates from children with severe *Plasmodium falciparum* malaria bind to multiple receptors. *Infect Immun* **69:** 5849–5856.

Hemmer, C.J., Hort, G., Chiwakata, C.B., Seitz, R., Egbring, R., Gaus, W., Hogel, J., Hassemer, M., Nawroth, P.P., Kern, P. & Dietrich, M. (1997) Supportive pentoxifylline in *falciparum* malaria: no effect on tumor necrosis factor alpha levels or clinical outcome: a prospective, randomized, placebo-controlled study. *Am J Trop Med Hyg* **56:** 397–403.

Hermsen, C.C., Crommert, J.V., Fredix, H., Sauerwein, R.W. & Eling, W.M. (1997) Circulating tumour necrosis factor alpha is not involved in the development of cerebral malaria in *Plasmodium berghei*-infected c57bl mice. *Parasite Immunol* **19:** 571–577.

Herrington, D., Davis, J., Nardin, E., Beier, M., Cortese, J., Eddy, H., Losonsky, G., Hollingdale, M., Sztein, M., Levine, M., *et al.* (1991) Successful immunization of humans with irradiated malaria sporozoites: humoral and cellular responses of the protected individuals. *Am J Trop Med Hyg* **45:** 539–547.

Hill, A.V. (2001) The genomics and genetics of human infectious disease susceptibility. *Annu Rev Genomics Hum Genet* **2:** 373–400.

Hill, A.V., Allsopp, C.E., Kwiatkowski, D., Anstey, N.M., Twumasi, P., Rowe, P.A., Bennett, S., Brewster, D., McMichael, A.J. & Greenwood, B.M. (1991) Common West African HLA antigens are associated with protection from severe malaria. *Nature* **352:** 595–600.

Hill, A.V., Elvin, J., Willis, A.C., Aidoo, M., Allsopp, C.E., Gotch, F.M., Gao, X.M., Takiguchi, M., Greenwood, B.M., Townsend, A.R. *et al.* (1992) Molecular analysis of the association of HLA-B53 and resistance to severe malaria. *Nature* **360:** 434–439.

Ho, M. & White, N.J. (1999) Molecular mechanisms of cytoadherence in malaria. *Am J Physiol* **276:** c1231–c1242.

Ho, M., Sexton, M.M., Tongtawe, P., Looareesuwan, S., Suntharasamai, P. & Webster, H.K. (1995) Interleukin-10 inhibits tumor necrosis factor production but not antigen-specific lymphoproliferation in acute *Plasmodium falciparum* malaria. *J Infect Dis* **172:** 838–844.

Ho, M., Hickey, M.J., Murray, A.G., Andonegui, G. & Kubes, P. (2000) Visualization of *Plasmodium falciparum*-endothelium interactions in human microvasculature: mimicry of leukocyte recruitment. *J Exp Med* **192:** 1205–1211.

Hobbs, M.R., Udhayakumar, V., Levesque, M.C., Booth, J., Roberts, J.M., Tkachuk, A.N., Pole, A., Coon, H., Kariuki, S., Nahlen, B.L., Mwaikambo, E.D., Lal, A.L., Granger, D.L., Anstey, N.M. & Weinberg, J.B. (2002) A new NOS2 promoter polymorphism associated with increased nitric oxide production and protection from severe malaria in Tanzanian and Kenyan children. *Lancet* **360:** 1468–1475.

Howard, M., Muchamuel, T., Andrade, S. & Menon, S. (1993) Interleukin 10 protects mice from lethal endotoxemia. *J Exp Med* **177:** 1205–1208.

Hugosson, E., Montgomery, S.M., Premji, Z., Troye-Blomberg, M. & Bjorkman, A. (2004) Higher IL-10 levels are associated with less effective clearance of *Plasmodium falciparum* parasites. *Parasite Immunol* **26:** 111–117.

Ishino, T., Yano, K., Chinzei, Y. & Yuda, M. (2004) Cell-passage activity is required for the malarial parasite to cross the liver sinusoidal cell layer. *Plos Biol* **2:** e4.

Ismail, N., Olano, J.P., Feng, H.M. & Walker, D.H. (2002) Current status of immune mechanisms of killing of intracellular microorganisms. *Fems Microbiol Lett* **207:** 111–120.

Jacobs, P., Radzioch, D. & Stevenson, M.M. (1995) Nitric oxide expression in the spleen, but not in the liver, correlates with resistance to blood-stage malaria in mice. *J Immunol* **155:** 5306–5313.

Jacobs, P., Radzioch, D. & Stevenson, M.M. (1996a) *In vivo* regulation of nitric oxide production by tumor necrosis factor alpha and gamma interferon, but not by interleukin-4, during blood stage malaria in mice. *Infect Immun* **64:** 44–49.

Jacobs, P., Radzioch, D. & Stevenson, M.M. (1996b) A Th1-associated increase in tumor necrosis factor alpha expression in the spleen correlates with resistance to blood-stage malaria in mice. *Infect Immun* **64:** 535–541.

James, S.L. (1995) Role of nitric oxide in parasitic infections. *Microbiol Rev* **59:** 533–547.

Janeway C.A, T.P., Walport M, Shlomchik M (2001) Cytokines and their receptors. *Immunobiology: The Immune System in Health and Disease*, 5 edn. Garland Science Textbooks, Taylor and Francis, New York and London.

Jaramillo, M., Gowda, D.C., Radzioch, D. & Olivier, M. (2003) Hemozoin increases IFN-gamma-inducible macrophage nitric oxide generation through extracellular signal-regulated kinase- and NF-kappa B-dependent pathways. *J Immunol* **171:** 4243–4253.

Juliger, S., Bongartz, M., Luty, A.J., Kremsner, P.G. & Kun, J.F. (2003) Functional analysis of a promoter variant of the gene encoding the interferon-gamma receptor chain I. *Immunogenetics* **54:** 675–680.

Jung, S., Unutmaz, D., Wong, P., Sano, G., De Los Santos, K., Sparwasser, T., Wu, S., Vuthoori, S., Ko, K., Zavala, F., Pamer, E.G., Littman, D.R. & Lang, R.A. (2002) *In vivo* depletion of CD11c(+) dendritic cells abrogates priming of CD8(+) t cells by exogenous cell-associated antigens. *Immunity* **17:** 211–220.

Kaul, D.K., Liu, X.D., Nagel, R.L. & Shear, H.L. (1998) Microvascular hemodynamics and *in vivo* evidence for the role of intercellular adhesion molecule-1 in the sequestration of infected red blood cells in a mouse model of lethal malaria. *Am J Trop Med Hyg* **58:** 240–247.

Kern, P., Hemmer, C.J., van Damme, J., Gruss, H.J. & Dietrich, M. (1989) Elevated tumor necrosis factor alpha and interleukin-6 serum levels as markers for complicated *Plasmodium falciparum* malaria. *Am J Med* **87:** 139–143.

Kharazmi, A. & Jepsen, S. (1984) Enhanced inhibition of *in vitro* multiplication of *Plasmodium falciparum* by stimulated human polymorphonuclear leucocytes. *Clin Exp Immunol* **57:** 287–292.

Kharazmi, A., Jepsen, S. & Valerius, N.H. (1984) Polymorphonuclear leucocytes defective in oxidative metabolism inhibit *in vitro* growth of *Plasmodium falciparum*. Evidence against an oxygen-dependent mechanism. *Scand J Immunol* **20:** 93–96.

Khusmith, S., Druilhe, P. & Gentilini, M. (1982) Enhanced *Plasmodium falciparum* merozoite phagocytosis by monocytes from immune individuals. *Infect Immun* **35:** 874–879.

Kidson, C., Lamont, G., Saul, A. & Nurse, G.T. (1981) Ovalocytic erythrocytes from Melanesians are resistant to invasion by malaria parasites in culture. *Proc Natl Acad Sci USA* **78:** 5829–5832.

Kikuchi, M., Looareesuwan, S., Ubalee, R., Tasanor, O., Suzuki, F., Wattanagoon, Y., Na-Bangchang, K., Kimura, A., Aikawa, M. & Hirayama, K. (2001) Association of adhesion molecule PECAM-1/CD31 polymorphism with susceptibility to cerebral malaria in Thais. *Parasitol Int* **50:** 235–239.

Kinoshita, T., Takeda, J., Hong, K., Kozono, H., Sakai, H. & Inoue, K. (1988) Monoclonal antibodies to mouse complement receptor type 1 (CR1). Their use in a distribution study showing that mouse erythrocytes and platelets are CR1-negative. *J Immunol* **140:** 3066–3072.

Knight, J.C., Udalova, I., Hill, A.V., Greenwood, B.M., Peshu, N., Marsh, K. & Kwiatkowski, D. (1999) A polymorphism that affects OCT-1 binding to the TNF promoter region is associated with severe malaria. *Nat Genet* **22:** 145–150.

Kobayashi, F., Ishida, H., Matsui, T. & Tsuji, M. (2000) Effects of *in vivo* administration of anti-IL:-10 or anti-IFN-gamma monoclonal antibody on the host defense mechanism against *Plasmodium yoelii yoelii* infection. *J Vet Med Sci* **62:** 583–587.

Koch, O., Awomoyi, A., Usen, S., Jallow, M., Richardson, A., Hull, J., Pinder, M., Newport, M. & Kwiatkowski, D. (2002) IFNGR1 gene promoter polymorphisms and susceptibility to cerebral malaria. *J Infect Dis* **185:** 1684–1687.

Koch, O., Rockett, K., Jallow, M., Pinder, M., Sisay-Joof, F. & Kwiatkowski, D. (2005) Investigation of malaria susceptibility determinants in the IFNG/IL26/IL22 genomic region. *Genes Immun* **6:** 312–318.

Kremsner, P.G., Grundmann, H., Neifer, S., Sliwa, K., Sahlmuller, G., Hegenscheid, B. & Bienzle, U. (1991) Pentoxifylline prevents murine cerebral malaria. *J Infect Dis* **164:** 605–608.

Kremsner, P.G., Winkler, S., Wildling, E., Prada, J., Bienzle, U., Graninger, W. & Nussler, A.K. (1996) High plasma levels of nitrogen oxides are associated with severe disease and correlate with rapid parasitological and clinical cure in *Plasmodium falciparum* malaria. *Trans R Soc Trop Med Hyg* **90:** 44–47.

Kumaratilake, L.M., Ferrante, A., Jaeger, T. & Morris-Jones, S.D. (1997) The role of complement, antibody, and tumor necrosis factor alpha in the killing of *Plasmodium falciparum* by the monocytic cell line THP-1. *Infect Immun* **65:** 5342–5345.

Kumaratilake, L.M., Ferrante, A. & Rzepczyk, C. (1991) The role of T lymphocytes in immunity to *Plasmodium falciparum*. Enhancement of neutrophil-mediated parasite killing by lymphotoxin and IFN-gamma: comparisons with tumor necrosis factor effects. *J Immunol* **146:** 762–767.

Kun, J.F., Mordmuller, B., Lell, B., Lehman, L.G., Luckner, D. & Kremsner, P.G. (1998) Polymorphism in promoter region of inducible nitric oxide synthase gene and protection against malaria. *Lancet* **351:** 265–266.

Kun, J.F., Klabunde, J., Lell, B., Luckner, D., Alpers, M., May, J., Meyer, C. & Kremsner, P.G. (1999) Association of the ICAM-1Kilifi mutation with protection against severe malaria in Lambarene, Gabon. *Am J Trop Med Hyg* **61:** 776–779.

Kun, J.F., Mordmuller, B., Perkins, D.J., May, J., Mercereau-Puijalon, O., Alpers, M., Weinberg, J.B. & Kremsner, P.G. (2001) Nitric oxide synthase 2(Lambarene)

(G-954C), increased nitric oxide production, and protection against malaria. *J Infect Dis* **184:** 330–336.

Kurtzhals, J.A., Adabayeri, V., Goka, B.Q., Akanmori, B.D., Oliver-Commey, J.O., Nkrumah, F.K., Behr, C. & Hviid, L. (1998) Low plasma concentrations of interleukin 10 in severe malarial anaemia compared with cerebral and uncomplicated malaria. *Lancet* **351:** 1768–1772.

Kurtzhals, J.A., Akanmori, B.D., Goka, B.Q., Adabayeri, V., Nkrumah, F.K., Behr, C. & Hviid, L. (1999) The cytokine balance in severe malarial anemia. *J Infect Dis* **180:** 1753–1755.

Kwiatkowski, D. (1995) Malarial toxins and the regulation of parasite density. *Parasitol Today* **11:** 206–212.

Kwiatkowski, D., Cannon, J.G., Manogue, K.R., Cerami, A., Dinarello, C.A. & Greenwood, B.M. (1989) Tumour necrosis factor production in *falciparum* malaria and its association with schizont rupture. *Clin Exp Immunol* **77:** 361–366.

Kwiatkowski, D., Hill, A.V., Sambou, I., Twumasi, P., Castracane, J., Manogue, K.R., Cerami, A., Brewster, D.R. & Greenwood, B.M. (1990) TNF concentration in fatal cerebral, non-fatal cerebral, and uncomplicated *Plasmodium falciparum* malaria. *Lancet* **336:** 1201–1204.

Kwiatkowski, D., Molyneux, M.E., Stephens, S., Curtis, N., Klein, N., Pointaire, P., Smit, M., Allan, R., Brewster, D.R., Grau, G.E., *et al.* (1993) Anti-TNF therapy inhibits fever in cerebral malaria. *Q J Med* **86:** 91–98.

Kwiatkowski, D.P. (2005) How malaria has affected the human genome and what human genetics can teach us about malaria. *Am J Hum Genet* **77:** 171–192.

Kyes, S., Horrocks, P. & Newbold, C. (2001) Antigenic variation at the infected red cell surface in malaria. *Annu Rev Microbiol* **55:** 673–707.

Lamas, S., Michel, T., Brenner, B.M. & Marsden, P.A. (1991) Nitric oxide synthesis in endothelial cells: evidence for a pathway inducible by TNF-alpha. *Am J Physiol* **261:** c634–c641.

Leiriao, P., Mota, M.M. & Rodriguez, A. (2005) Apoptotic Plasmodium-infected hepatocytes provide antigens to liver dendritic cells. *J Infect Dis* **191:** 1576–1581.

Leone, A.M., Palmer, R.M., Knowles, R.G., Francis, P.L., Ashton, D.S. & Moncada, S. (1991) Constitutive and inducible nitric oxide synthases incorporate molecular oxygen into both nitric oxide and citrulline. *J Biol Chem* **266:** 23790–23795.

Levesque, M.C., Hobbs, M.R., Anstey, N.M., Vaughn, T.N., Chancellor, J.A., Pole, A., Perkins, D.J., Misukonis, M.A., Chanock, S.J., Granger, D.L. & Weinberg, J.B. (1999) Nitric oxide synthase type 2 promoter polymorphisms, nitric oxide production, and disease severity in Tanzanian children with malaria. *J Infect Dis* **180:** 1994–2002.

Li, C., Corraliza, I. & Langhorne, J. (1999) A defect in interleukin-10 leads to enhanced malarial disease in *Plasmodium chabaudi chabaudi* infection in mice. *Infect Immun* **67:** 4435–4442.

Li, C., Sanni, L.A., Omer, F., Riley, E. & Langhorne, J. (2003) Pathology of *Plasmodium chabaudi chabaudi* infection and mortality in interleukin-10-deficient mice are ameliorated by anti-tumor necrosis factor alpha and exacerbated by anti-transforming growth factor beta antibodies. *Infect Immun* **71:** 4850–4856.

Looareesuwan, S., Wilairatana, P., Vannaphan, S., Wanaratana, V., Wenisch, C., Aikawa, M., Brittenham, G., Graninger, W. & Wernsdorfer, W.H. (1998) Pentoxifylline as an ancillary treatment for severe *falciparum* malaria in Thailand. *Am J Trop Med Hyg* **58**: 348–353.

Looareesuwan, S., Sjostrom, L., Krudsood, S., Wilairatana, P., Porter, R.S., Hills, F. & Warrell, D.A. (1999) Polyclonal anti-tumor necrosis factor-alpha Fab used as an ancillary treatment for severe malaria. *Am J Trop Med Hyg* **61**: 26–33.

Lopansri, B.K., Anstey, N.M., Weinberg, J.B., Stoddard, G.J., Hobbs, M.R., Levesque, M.C., Mwaikambo, E.D. & Granger, D.L. (2003) Low plasma arginine concentrations in children with cerebral malaria and decreased nitric oxide production. *Lancet* **361**: 676–678.

Lowell, C. (1997) Fundamentals of cell biology. In: Daniel P. Stites, A. I. T., Tristram G. Parslow (eds) *Medical Immunology,* 9 edn. Prentice-Hall International Inc, New Jersey.

Luoni, G., Verra, F., Arca, B., Sirima, B.S., Troye-Blomberg, M., Coluzzi, M., Kwiatkowski, D. & Modiano, D. (2001) Antimalarial antibody levels and IL4 polymorphism in the Fulani of West Africa. *Genes Immun* **2**: 411–414.

Luty, A.J., Lell, B., Schmidt-Ott, R., Lehman, L.G., Luckner, D., Greve, B., Matousek, P., Herbich, K., Schmid, D., Migot-Nabias, F., Deloron, P., Nussenzweig, R.S. & Kremsner, P.G. (1999) Interferon-gamma responses are associated with resistance to reinfection with *Plasmodium falciparum* in young African children. *J Infect Dis* **179**: 980–988.

Luty, A.J., Perkins, D.J., Lell, B., Schmidt-Ott, R., Lehman, L.G., Luckner, D., Greve, B., Matousek, P., Herbich, K., Schmid, D., Weinberg, J.B. & Kremsner, P.G. (2000) Low interleukin-12 activity in severe *Plasmodium falciparum* malaria. *Infect Immun* **68**: 3909–3915.

Luzzatto, L., Usanga, F.A. & Reddy, S. (1969) Glucose-6-phosphate dehydrogenase deficient red cells: resistance to infection by malarial parasites. *Science* **164**: 839–842.

Luzzatto, L., Nwachuku-Jarrett, E.S. & Reddy, S. (1970) Increased sickling of parasitized erythrocytes as mechanism of resistance against malaria in the sickle-cell trait. *Lancet* **1**: 319–321.

Luzzi, G.A., Merry, A.H., Newbold, C.I., Marsh, K. & Pasvol, G. (1991a) Protection by alpha-thalassaemia against *Plasmodium falciparum* malaria: modified surface antigen expression rather than impaired growth or cytoadherence. *Immunol Lett* **30**: 233–2340.

Luzzi, G.A., Merry, A.H., Newbold, C.I., Marsh, K., Pasvol, G. & Weatherall, D.J. (1991b) Surface antigen expression on *Plasmodium falciparum*-infected erythrocytes is modified in alpha- and beta-thalassemia. *J Exp Med* **173**: 785–791.

MacKinnon, M.J., Walker, P.R. & Rowe, J.A. (2002) *Plasmodium chabaudi*: rosetting in a rodent malaria model. *Exp Parasitol* **101**: 121–128.

Macpherson, G.G., Warrell, M.J., White, N.J., Looareesuwan, S. & Warrell, D.A. (1985) Human cerebral malaria. A quantitative ultrastructural analysis of parasitized erythrocyte sequestration. *Am J Pathol* **119**: 385–401.

Maier, A.G., Duraisingh, M.T., Reeder, J.C., Patel, S.S., Kazura, J.W., Zimmerman, P.A. & Cowman, A.F. (2003) *Plasmodium falciparum* erythrocyte invasion through glycophorin C and selection for Gerbich negativity in human populations. *Nat Med* **9**: 87–92.

Survival of protozoan intracellular parasites in host cells

Patrícia Leirião, Cristina D. Rodrigues, Sónia S. Albuquerque & Maria M. Mota[+]

Instituto Gulbenkian de Ciência, Oeiras, Portugal

The most common human diseases are caused by pathogens. Several of these microorganisms have developed efficient ways in which to exploit host molecules, along with molecular pathways to ensure their survival, differentiation and replication in host cells. Although the contribution of the host cell to the development of many intracellular pathogens (particularly viruses and bacteria) has been unequivocally established, the study of host-cell requirements during the life cycle of protozoan parasites is still in its infancy. In this review, we aim to provide some insight into the manipulation of the host cell by parasites through discussing the hurdles that are faced by the latter during infection.

Introduction

After entering the host, intracellular pathogens need to recognize and exploit host-cell resources for their own benefit. Although this might seem obvious, the importance of a detailed understanding of the host-cell environment has only recently been generally acknowledged in the parasitology research field. The extent of the manipulation of host function by protozoan parasites can be seen, for example, in the uncontrolled proliferation of cells that are infected by *Theileria* (Dobbelaere & Kuenzi, 2004) and in the microarray analysis of a *Toxoplasma*-infected cell versus a non-infected cell, which highlighted important differences in several regulatory and biosynthetic activities (Blader *et al*, 2001). Therefore, the host-cell composition should no longer be considered as a 'black box'; rather, it should be seen as an ideal 'milieu' of molecular interactions in which the parasite strives towards success.

Reaching and entering the host cell

To infect a host, parasites must reach and recognize their specific target cell, as most infect only one or a few cell types in their host. In the phylum Apicomplexa, for example, *Plasmodium* invades hepatocytes and erythrocytes, whereas *Theileria* and *Babesia* spp. infect leukocytes. *Toxoplasma* spp. are an exception as they can survive in all types of nucleated cell, which implies that they recognize target molecules that are present on all cells and/or have developed many redundant mechanisms of infection.

On the transmission of *Plasmodium* by anopheline mosquitoes, sporozoites (the stage injected by a mosquito bite) rapidly reach the liver. Once there, they traverse several cells by breaching their plasma membranes before they finally invade their target cell through the formation of a vacuole (Mota *et al*, 2001). The migration of *Plasmodium* sporozoites through different cells before infection might be an example of a parasite seeking its required target cell. Migration has also been observed during the sporozoite and ookinete (the stage that traverses the mosquito gut after fertilization) stages of other apicomplexan parasites, such as *Toxoplasma* and *Eimeria*, although no migration has been seen during the merozoite and tachyzoite stages (the second and third invasive stages in the vertebrate host; Mota & Rodriguez, 2001). Therefore, the sporozoite and ookinete stages are the invasive forms that encounter, and must overcome, host cellular barriers to reach their replication sites. Recently, mutant *Plasmodium* parasites have been generated by disruption of the gene that encodes sporozoite microneme protein essential for cell traversal (*spect*). Although *spect* mutants are unable to migrate through cells and are not infectious *in vivo,* they are still able to infect hepatocytes *in vitro* (Ishino *et al*, 2004). The reason for this behaviour is under investigation.

Once their target has been reached, different parasites have developed distinct strategies for entering the host cell. Professional phagocytic cells, such as neutrophils and macrophages, use phagocytosis to internalize and destroy not only foreign objects and apoptotic cells but also microbial pathogens. However, several intracellular pathogens are able to subvert this defence mechanism to gain access to the cells. The invasion of macrophages by *Leishmania* parasites, for example, is mediated by classical phagocytic receptors that are coupled to the vigorous actin-driven uptake machinery of these cells (Peters *et al*, 1995; Mosser & Brittingham, 1997).This process is mediated by serum opsonins that coat the parasite and requires the activation of Rho, Cdc42 and Rac1 in the macrophage. *Leishmania* parasites can also enter host cells by a non-opsonic pathway through a phagocyte-like actin-mediated process that does not involve Rac1 activation (Morehead *et al*, 2002). Conversely, the invasion of *Trypanosoma cruzi* is distinct from phagocytosis and is actually enhanced by inhibitors of actin polymerization (Kipnis *et al*, 1979; Schenkman

Instituto Gulbenkian de Ciência, Rua da Quinta Grande 6, 2780-156 Oeiras, Portugal
[+]Corresponding author. Tel: +351 21 446 4517; Fax: +351 21 440 7970;
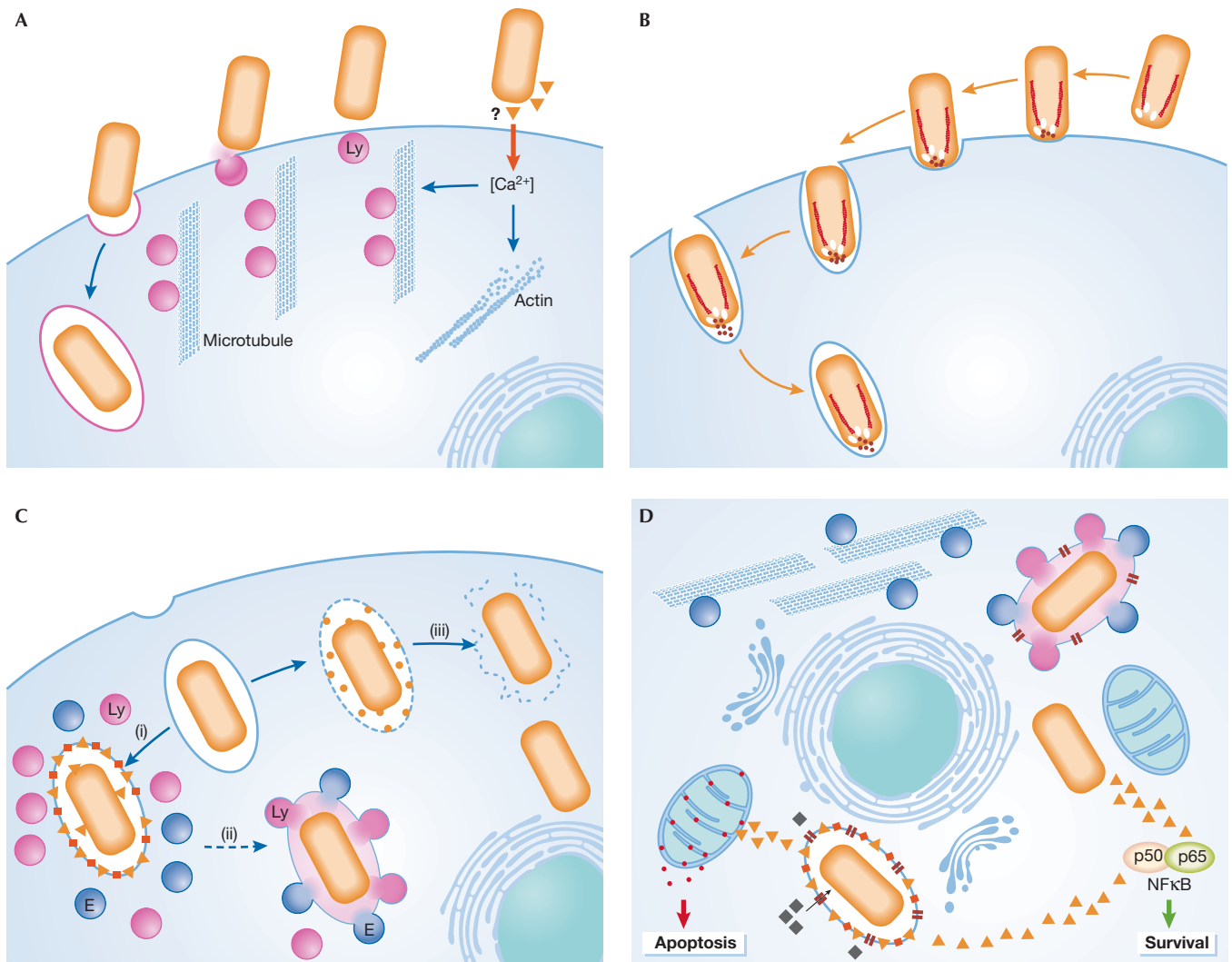E-mail: mmota@igc.gulbenkian.pt

Fig 1 | Recognition, entrance and survival: a schematic representation of some of the strategies adopted by pathogens. (**A**) Induced recruitment of lysosomes to fuse with the host-cell plasma membrane to form the required vacuole for *Trypanosoma cruzi*. (**B**) A parasite, such as *Toxoplasma,* uses its own form of motility to propel itself into the host cell. (**C**) Once inside, intracellular pathogens follow different routes: they either reside inside the vacuole (i), which sometimes fuses with the exocytic/endocytic pathways (ii), or they reside in the host cytosol (iii). The same pathogen might use different strategies at different stages of development. (**D**) Independent of the route taken, all pathogens face similar problems, which include how to ensure that the cell is alive or dead at the appropriate times, how to acquire nutrients, how to avoid host-recognition systems and how to increase in size. Parasites and their proteins are shown in orange. E, endosomes; Ly, lysosomes.

et al, 1991; Tardieux *et al*, 1992; Rodriguez *et al*, 1999). This parasite uses a unique calcium-regulated microtubule-mediated pathway that directs the recruitment and fusion of lysosomes to the plasma membrane of host cells. The binding of *T. cruzi* to cells causes a transient increase in intracellular calcium, which induces actin disruption and the mobilization of lysosomes along microtubules towards the site of parasite attachment by associated kinesin motors. *T. cruzi* exploits this lysosomal-derived membrane to form a parasitophorous vacuole inside the host cell (Fig 1A; Schenkman *et al*, 1988; Rodriguez *et al*, 1996). Not surprisingly, other parasites have also developed strategies for cell invasion that are not dependent on particular components of the host cell. Some apicomplexans, for example, use an actin–myosin motor that is present in their own cytoskeleton to generate the motile force that

is necessary to actively propel themselves into cells. This movement is known as gliding motility and is required for the active process of invasion that is mediated by the parasite. In the best-studied example—*Toxoplasma* invasion—the host cell has little or no active role in uptake (Fig 1B). No change is detected in host membrane ruffling, in the actin cytoskeleton or in the phosphorylation of host-cell proteins (Morisaki *et al*, 1995; Dobrowolski & Sibley, 1996). Host-cell actin polymerization is necessary, however, for the invasion of some apicomplexan parasites, such as *Cryptosporidium parvum* (Fayer & Hammond, 1967; Elliott & Clark, 2000; Elliott *et al*, 2001). Recent work indicates that *C. parvum* invades target epithelia by activating a Cdc42 GTPase signalling pathway that induces host-cell actin remodelling at the attachment site (Chen *et al*, 2004).

Plasmodium sporozoites invade hepatocytes, whereas the merozoites invade erythrocytes. The effects of actin-depolymerizing agents on *Plasmodium* invasion are difficult to interpret as they affect not only the cytoskeleton of the host but also *Plasmodium* motility, which is required for invasion. The invasion of red blood cells by the merozoite begins with the initial attachment of the parasite and its subsequent reorientation such that its apical end is directed towards the erythrocyte. A moving junction is formed and the parasite pulls itself into the cell, where it stays inside a vacuole that is formed by the host plasma membrane (Chitnis & Blackman, 2000). In all of the apicomplexan parasite examples discussed here, parasite ligands for host-cell receptors are required for invasion. However, many of these adhesins are not displayed statically on the surface of the parasite; instead, they are stored in apically located secretory organelles that are known as micronemes. Constitutive secretion from these organelles is probably sufficient for gliding motility. Nevertheless, enhanced microneme secretion is probably required for invasion. This occurs when parasites contact host cells or migrate through cells, for example, in the cases of *Toxoplasma* tachyzoites and *Plasmodium* sporozoites, respectively (Carruthers & Sibley, 1997; Gantt *et al*, 2000; Mota *et al*, 2002). However, another exception in the Apicomplexa is the invasion of *Theileria*, the invasive stages of which are non-motile with no micronemes, and which require neither apical attachment to the host cell nor apical organelle secretion for invasion. In addition, invasion is neither dependent on the parasite actin cytoskeleton, nor does it involve substantial remodelling of the host cell surface. It has therefore been proposed that entry is accomplished by a physical process of zippering, which seems to be sufficient to cause internalization by a passive process (Webster *et al*, 1985; Shaw, 1999, 2003).

Vacuole or cytoplasm?

Parasites can survive and replicate in a vacuole or a phagolysosome inside the cell, or, less commonly, free in the host-cell cytosol (Fig 1C).

Inside a vacuole. The vacuolar compartment that is formed during parasite entry has an acidic environment, which is poor in nutrients, and undergoes progressive fusions with early endosomes, late endosomes and lysosomes. Parasites must therefore avoid, or modify, these compartments to escape destruction.

A general strategy that is used by pathogens to avoid the hostile lysosomal environment is to arrest the process of vacuole maturation at different stages. The maturation of vacuoles might be arrested not only by the persistence but also by the exclusion of host proteins that are known to regulate the endocytic/phagocytic pathway. For example, in infections by *Toxoplasma gondii*, which resist typical phagosome–lysosome fusion (Jones & Hirsch, 1972; Sibley *et al*, 1985), host-cell integral membrane proteins are largely excluded from the parasitophorous vacuole, whereas those of the parasite are incorporated (Sibley & Krahenbuhl, 1988; Beckers *et al*, 1994). This results in the formation of a membrane that is unique in its biochemical and biophysical properties, and leads to the creation of a non-fusogenic vacuole.

Conversely, some parasites survive in, and might even depend on, the harsh acidic environment of the phagolysosome. Although these pathogens must be resistant to acid hydrolases, the molecular mechanisms of this protection have yet to be clarified. *Leishmania donovani* is an interesting example, as it applies a dual strategy at distinct stages of its life cycle. *L. donovani* promastigotes, which are sensitive to acid, seem to inhibit phagosome–endosome fusion through unique lipophosphoglycan molecules on their cell surface (Miao *et al*, 1995; Descoteaux & Turco, 1999). After the amastigote transformation occurs, this inhibition is lifted and *L. donovani* multiplies in the now acidic intracellular compartment. Indeed, the amastigotes are metabolically most active when their environment is acidic (Joshi *et al*, 1993).

Free in the host-cell cytoplasm. Intracellular parasites can avoid the harsh environment that results from the fusion of their vacuole with degradative endocytic compartments by escaping rapidly from the nascent vacuole into the cytoplasm. Surprisingly, this strategy is used by only a few parasites, including *T. cruzi* and *Theileria*. Little is known about the molecular events that precede vacuole lysis. The exit of *T. cruzi* from the vacuole involves a parasite-secreted molecule, Tc-TOX, which has membrane pore-forming activity at acidic pHs (Andrews & Whitlow, 1989; Andrews *et al*, 1990; Ley *et al*, 1990). In the case of *Theileria*, escape into the cytoplasm coincides with the discharge of the parasite apical organelles, but their contents remain unknown (Shaw, 2003). *Theileria* also secretes proteins that contain AT-rich DNA-binding domains (AT-hook motifs) and that localize to the host-cell nucleus during infection (Swan *et al*, 1999, 2001, 2003). Recently, it has been shown that transfection of an uninfected, transformed bovine macrophage cell line with a plasmid that encodes the AT-hook parasite protein modulates cellular morphology and alters the expression pattern of a cytoskeletal polypeptide in a manner similar to that observed during the infection of leukocytes by the parasite (Shiels *et al*, 2004). Putative polypeptides that bear AT-hook motifs are present in the genomes of other parasites, such as *T. gondii* (http://ToxoDB.org; accession number TgTwinScan_4661) and several *Plasmodium* spp. (http://PlasmoDB.org; accession numbers PFC0325c, PB001090, Q7R873 and Q7RDC7). However, whether they are involved in host-cell modulation remains to be determined.

Problems of an intracellular lifestyle

Once inside the host cell, intracellular pathogens are faced with several obstacles and, in particular, must circumvent host defences, acquire nutrients and either kill or maintain the host cell according to their needs.

Host-cell defences. Parasites rarely reside in the cytosol, so it might be expected to contain many protective proteins or other antimicrobial agents. However, surprisingly, no cytosolic agents with direct antimicrobial activity have yet been identified. Most antimicrobial agents are either delivered into 'infected' vacuoles or are secreted into the extracellular space. The only known example of a cytosolic antimicrobial peptide is ubiquicidin, which is produced by the post-translational processing of the Fau protein, and part of which is very similar to ubiquitin. The peptide has strong antimicrobial activity against several bacteria, including *Listeria monocytogenes* (Hiemstra *et al*, 1999). However, it is not known whether this peptide is active against protozoan parasites.

Replication and growth. One of the problems faced by an intracellular pathogen is how to create sufficient space for replication. For this process to occur inside the vacuole, a considerable

expansion of the compartment is required. Therefore, vacuoles must acquire large amounts of additional membrane lipids. As the cytoskeleton is involved in membrane transport events, modulation of its structure and/or function is an obvious strategy through which pathogens might alter vacuole formation and behaviour. A mesh of microtubules has been described around *Toxoplasma* vacuoles (Melo *et al*, 2001), but whether this provides a means for vacuole expansion is not yet known. No other strategy has been described for the enlargement of a parasitophorous vacuole by a protozoan parasite.

Nutrient acquisition. Acquisition of nutrients is crucial for pathogen survival. Although it provides protection from host defences, the membrane of non-fusogenic vacuoles restricts the access of the intravacuolar pathogens to the nutrient-rich cytoplasm. Therefore, pathogens must modify the vacuole membrane to allow them to scavenge the necessary nutrients and metabolites from the cytosol. During the blood stages of its life cycle, *Plasmodium* is inside a cell in which haemoglobin is extremely abundant, and this serves as the main source of amino acids for the parasite. As the parasite matures, it develops a special organelle, called the cytostome, for the uptake of host cytoplasm (Goldberg, 1993). In addition, *Plasmodium* (in the erythrocytic stages) and other apicomplexan parasites, such as *Toxoplasma* and *Eimeria,* have been shown to render the parasitophorous vacuole membrane freely permeable to small cytosolic molecules through the introduction of high-capacity channels or pores (Desai *et al*, 1993; Schwab *et al*, 1994; Desai & Rosenberg, 1997; Werner-Meier & Entzeroth, 1997). Conversely, results obtained for *Leishmania* imply that such pores or channels are not present in their vacuoles (Antoine *et al*, 1990). In the case of *Leishmania* amastigotes, the vacuole fuses with lysosomes and endosomes, which provides a relatively constant supply of nutrients. However, in promastigotes, the vacuole membrane does not fuse with vesicles of the endocytic or lysosomal compartments (Heinzen *et al*, 1996). It has been proposed that the association of vacuolar membranes with host-cell organelles, such as mitochondria and the endoplasmic reticulum, might have a role in nutrient acquisition in *Toxoplasma* (Jones & Hirsch, 1972; Sinai *et al*, 1997; Fig 1D).

Host-cell death and survival. Pathogens often kill cells and sometimes even the whole host organism, but at the same time they are heavily dependent on living cells and many of their functions. It is therefore not surprising that they have developed mechanisms for both the promotion of, and protection against, cell death. Although the apoptotic pathways that are regulated by virus- and bacteria-derived molecules have been extensively characterized at the molecular level, the details of these pathways in protozoan parasites are only just beginning to be revealed (reviewed in Heussler *et al*, 2001; Luder *et al*, 2001). The intracellular parasites *T. parva*, *Toxoplasma* and *Leishmania* can all inhibit apoptosis of the infected host cell (Moore & Matlashewski, 1994; Nash *et al*, 1998; Heussler *et al*, 1999). For both *T. parva* and *Toxoplasma,* activation of the transcription factor nuclear factor-κB (NF-κB) seems to be crucial in protecting infected cells against apoptosis (Heussler *et al*, 2002; Molestina *et al*, 2003; Payne *et al*, 2003). In *Theileria*, NF-κB activation in infected transformed cells is known to be mediated by the recruitment of the multisubunit IκB kinase (IKK) into large activated foci on the surface of a specific parasite stage (Heussler *et al*, 2002). This indicates that the parasite seems to bypass the conventional pathways that link surface-receptor stimulation to IKK activation (Heussler *et al*, 2002). However, the precise mechanism by which the parasite recruits IKK signalosomes remains unknown. How *Toxoplasma* infection mediates NF-κB activation is also poorly understood and, in fact, is an area of some controversy (reviewed in Sinai *et al*, 2004). *T. cruzi* shows dual activity: it inhibits apoptotic pathways in the infected cell while simultaneously inducing apoptosis in T cells (Lopes *et al*, 1995; Clark & Kuhn, 1999; Nakajima-Shimada *et al*, 2000). It has been reported that *Cryptosporidium* infections induce apoptosis in *in vitro*-infected cell lines that were derived from primary hosts (Chen *et al*, 1999; McCole *et al*, 2000). More recently, and using a different *in vitro* cell system, it has been shown that *Cryptosporidium* induces non-apoptotic death in host cells as it leaves them (Elliott & Clark, 2003). The relevance of each of these observations to the outcome of the infection remains to be clarified. The erythrocytic stages of a malaria infection are unusual, as *Plasmodium* parasitizes one of the few types of cell that is thought to have limited ability to undergo apoptosis. However, apoptosis in erythrocytes has been characterized (Bratosin *et al*, 2001), and erythrocytes that are infected with mature stages of *Plasmodium* seem to contain phosphatidylserine on their surface (Eda & Sherman, 2002). This membrane phospholipid is present on the external surface of cells that are undergoing apoptosis or oxidative stress. It is not yet known whether, in this case, it is related to apoptosis. Conversely, in the hepatic stages of infection, hepatocytes infected with *Plasmodium berghei* and *Plasmodium yoelii* are protected against apoptosis, and this resistance seems to be triggered by both host and parasite molecules (P.L., S.S.A. and M.M.M., unpublished data).

Escape from the host cell

A final important step in the intracellular life of pathogens is their ability to exit the host cell after intracellular replication. The free pathogens can then infect new cells in the same host, or can be transmitted into a new host, depending on the life cycle of the pathogen. Parasites that have replicated inside a vacuole need to exit from both the vacuole and the cell, whereas those in the cytoplasm only need to escape from the cell itself. In *Plasmodium* merozoites, distinct proteases are involved in leaving the vacuole and the cell (Salmon *et al*, 2001; Wickham *et al*, 2003). Although the signals that trigger pathogens to leave cells are not yet known, in *Toxoplasma*, an increase in intraparasitic Ca^{2+} signalling occurs before exit of the parasite (Moudy *et al*, 2001; Arrizabalaga & Boothroyd, 2004).

Conclusions

Although the study of infectious diseases has spanned more than 100 years, we have only recently begun to appreciate the intricate interactions and the delicate balance that occur between pathogens and their host cells. Signalling pathways abound in cells and represent potential mechanisms by which a pathogen can cause profound effects in a host cell. Understanding these intricate interactions not only offers a new perspective on mammalian cell biology, but also allows the design of rational approaches to combat infectious diseases.

REFERENCES

Andrews NW, Whitlow MB (1989) Secretion by *Trypanosoma cruzi* of a hemolysin active at low pH. *Mol Biochem Parasitol* **33:** 249–256

Andrews NW, Abrams CK, Slatin SL, Griffiths G (1990) A *T. cruzi*-secreted protein immunologically related to the complement component C9: evidence for membrane pore-forming activity at low pH. *Cell* **61:** 1277–1287

Antoine JC, Prina E, Jouanne C, Bongrand P (1990) Parasitophorous vacuoles of *Leishmania amazonensis*-infected macrophages maintain an acidic pH. *Infect Immun* **58:** 779–787

Arrizabalaga G, Boothroyd JC (2004) Role of calcium during *Toxoplasma gondii* invasion and egress. *Int J Parasitol* **34:** 361–368

Beckers CJ, Dubremetz JF, Mercereau-Puijalon O, Joiner KA (1994) The *Toxoplasma gondii* rhoptry protein ROP2 is inserted into the parasitophorous vacuole membrane, surrounding the intracellular parasite, and is exposed to the host cell cytoplasm. *J Cell Biol* **127:** 947–961

Blader IJ, Manger ID, Boothroyd JC (2001) Microarray analysis reveals previously unknown changes in *Toxoplasma gondii*-infected human cells. *J Biol Chem* **276:** 24223–24231

Bratosin D *et al* (2001) Programmed cell death in mature erythrocytes: a model for investigating death effector pathways operating in the absence of mitochondria. *Cell Death Differ* **8:** 1143–1156

Carruthers VB, Sibley LD (1997) Sequential protein secretion from three distinct organelles of *Toxoplasma gondii* accompanies invasion of human fibroblasts. *Eur J Cell Biol* **73:** 114–123

Chen XM, Gores GJ, Paya CV, LaRusso NF (1999) *Cryptosporidium parvum* induces apoptosis in biliary epithelia by a Fas/Fas ligand-dependent mechanism. *Am J Physiol* **277:** G599–G608

Chen XM, Huang BQ, Splinter PL, Orth JD, Billadeau DD, McNiven MA, LaRusso NF (2004) Cdc42 and the actin-related protein/neural Wiskott–Aldrich syndrome protein network mediate cellular invasion by *Cryptosporidium parvum*. *Infect Immun* **72:** 3011–3021

Chitnis CE, Blackman MJ (2000) Host cell invasion by malaria parasites. *Parasitol Today* **16:** 411–415

Clark RK, Kuhn RE (1999) *Trypanosoma cruzi* does not induce apoptosis in murine fibroblasts. *Parasitology* **118:** 167–175

Desai SA, Rosenberg RL (1997) Pore size of the malaria parasite's nutrient channel. *Proc Natl Acad Sci USA* **94:** 2045–2049

Desai SA, Krogstad DJ, McCleskey EW (1993) A nutrient-permeable channel on the intraerythrocytic malaria parasite. *Nature* **362:** 643–646

Descoteaux A, Turco SJ (1999) Glycoconjugates in *Leishmania* infectivity. *Biochim Biophys Acta* **1455:** 341–352

Dobbelaere DA, Kuenzi P (2004) The strategies of the *Theileria* parasite: a new twist in host–pathogen interactions. *Curr Opin Immunol* **16:** 524–530

Dobrowolski JM, Sibley LD (1996) *Toxoplasma* invasion of mammalian cells is powered by the actin cytoskeleton of the parasite. *Cell* **84:** 933–939

Eda S, Sherman IW (2002) Cytoadherence of malaria-infected red blood cells involves exposure of phosphatidylserine. *Cell Physiol Biochem* **12:** 373–384

Elliott DA, Clark DP (2000) *Cryptosporidium parvum* induces host cell actin accumulation at the host–parasite interface. *Infect Immun* **68:** 2315–2322

Elliott DA, Clark DP (2003) Host cell fate on *Cryptosporidium parvum* egress from MDCK cells. *Infect Immun* **71:** 5422–5426

Elliott DA, Coleman DJ, Lane MA, May RC, Machesky LM, Clark DP (2001) *Cryptosporidium parvum* infection requires host cell actin polymerization. *Infect Immun* **69:** 5940–5942

Fayer R, Hammond DM (1967) Development of first-generation schizonts of *Eimeria bovis* in cultured bovine cells. *J Protozool* **14:** 764–772

Gantt S, Persson C, Rose K, Birkett AJ, Abagyan R, Nussenzweig V (2000) Antibodies against thrombospondin-related anonymous protein do not inhibit *Plasmodium* sporozoite infectivity *in vivo*. *Infect Immun* **68:** 3667–3673

Goldberg DE (1993) Hemoglobin degradation in *Plasmodium*-infected red blood cells. *Semin Cell Biol* **4:** 355–361

Heinzen RA, Scidmore MA, Rockey DD, Hackstadt T (1996) Differential interaction with endocytic and exocytic pathways distinguish parasitophorous vacuoles of *Coxiella burnetii* and *Chlamydia trachomatis*. *Infect Immun* **64:** 796–809

Heussler VT, Machado J Jr, Fernandez PC, Botteron C, Chen CG, Pearse MJ, Dobbelaere DA (1999) The intracellular parasite *Theileria parva* protects infected T cells from apoptosis. *Proc Natl Acad Sci USA* **96:** 7312–7317

Heussler VT, Kuenzi P, Rottenberg S (2001) Inhibition of apoptosis by intracellular protozoan parasites. *Int J Parasitol* **31:** 1166–1176

Heussler VT *et al* (2002) Hijacking of host cell IKK signalosomes by the transforming parasite *Theileria*. *Science* **298:** 1033–1036

Hiemstra PS, van den Barselaar MT, Roest M, Nibbering PH, van Furth R (1999) Ubiquicidin, a novel murine microbicidal protein present in the cytosolic fraction of macrophages. *J Leukoc Biol* **66:** 423–428

Ishino T, Yano K, Chinzei Y, Yuda M (2004) Cell-passage activity is required for the malarial parasite to cross the liver sinusoidal cell layer. *PLoS Biol* **2:** E4

Jones TC, Hirsch JG (1972) The interaction between *Toxoplasma gondii* and mammalian cells. II. The absence of lysosomal fusion with phagocytic vacuoles containing living parasites. *J Exp Med* **136:** 1173–1194

Joshi M, Dwyer DM, Nakhasi HL (1993) Cloning and characterization of differentially expressed genes from *in vitro*-grown 'amastigotes' of *Leishmania donovani*. *Mol Biochem Parasitol* **58:** 345–354

Kipnis TL, Calich VL, da Silva WD (1979) Active entry of bloodstream forms of *Trypanosoma cruzi* into macrophages. *Parasitology* **78:** 89–98

Ley V, Robbins ES, Nussenzweig V, Andrews NW (1990) The exit of *Trypanosoma cruzi* from the phagosome is inhibited by raising the pH of acidic compartments. *J Exp Med* **171:** 401–413

Lopes MF, da Veiga VF, Santos AR, Fonseca ME, DosReis GA (1995) Activation-induced CD4+ T cell death by apoptosis in experimental Chagas' disease. *J Immunol* **154:** 744–752

Luder CG, Gross U, Lopes MF (2001) Intracellular protozoan parasites and apoptosis: diverse strategies to modulate parasite–host interactions. *Trends Parasitol* **17:** 480–486

McCole DF, Eckmann L, Laurent F, Kagnoff MF (2000) Intestinal epithelial cell apoptosis following *Cryptosporidium parvum* infection. *Infect Immun* **68:** 1710–1713

Melo EJ, Carvalho TM, De Souza W (2001) Behaviour of microtubules in cells infected with *Toxoplasma gondii*. *Biocell* **25:** 53–59

Miao L, Stafford A, Nir S, Turco SJ, Flanagan TD, Epand RM (1995) Potent inhibition of viral fusion by the lipophosphoglycan of *Leishmania donovani*. *Biochemistry* **34:** 4676–4683

Molestina RE, Payne TM, Coppens I, Sinai AP (2003) Activation of NF-κB by *Toxoplasma gondii* correlates with increased expression of antiapoptotic genes and localization of phosphorylated IκB to the parasitophorous vacuole membrane. *J Cell Sci* **116:** 4359–4371

Moore KJ, Matlashewski G (1994) Intracellular infection by *Leishmania donovani* inhibits macrophage apoptosis. *J Immunol* **152:** 2930–2937

Morehead J, Coppens I, Andrews NW (2002) Opsonization modulates Rac-1 activation during cell entry by *Leishmania amazonensis*. *Infect Immun* **70:** 4571–4580

Morisaki JH, Heuser JE, Sibley LD (1995) Invasion of *Toxoplasma gondii* occurs by active penetration of the host cell. *J Cell Sci* **108:** 2457–2464

Mosser DM, Brittingham A (1997) *Leishmania*, macrophages and complement: a tale of subversion and exploitation. *Parasitology* **115** (Suppl.)**:** S9–S23

Mota MM, Rodriguez A (2001) Migration through host cells by apicomplexan parasites. *Microbes Infect* **3:** 1123–1128

Mota MM, Pradel G, Vanderberg JP, Hafalla JC, Frevert U, Nussenzweig RS, Nussenzweig V, Rodriguez A (2001) Migration of *Plasmodium* sporozoites through cells before infection. *Science* **291:** 141–144

Mota MM, Hafalla JC, Rodriguez A (2002) Migration through host cells activates *Plasmodium sporozoites* for infection. *Nat Med* **8:** 1318–1322

Moudy R, Manning TJ, Beckers CJ (2001) The loss of cytoplasmic potassium upon host cell breakdown triggers egress of *Toxoplasma gondii*. *J Biol Chem* **276:** 41492–41501

Nakajima-Shimada J, Zou C, Takagi M, Umeda M, Nara T, Aoki T (2000) Inhibition of Fas-mediated apoptosis by *Trypanosoma cruzi* infection. *Biochim Biophys Acta* **1475:** 175–183

Nash PB, Purner MB, Leon RP, Clarke P, Duke RC, Curiel TJ (1998) *Toxoplasma gondii*-infected cells are resistant to multiple inducers of apoptosis. *J Immunol* **160:** 1824–1830

Payne TM, Molestina RE, Sinai AP (2003) Inhibition of caspase activation and a requirement for NF-κB function in the *Toxoplasma gondii*-mediated blockade of host apoptosis. *J Cell Sci* **116:** 4345–4358

Peters C, Aebischer T, Stierhof YD, Fuchs M, Overath P (1995) The role of macrophage receptors in adhesion and uptake of *Leishmania mexicana* amastigotes. *J Cell Sci* **108:** 3715–3724

Rodriguez A, Samoff E, Rioult MG, Chung A, Andrews NW (1996) Host cell invasion by trypanosomes requires lysosomes and microtubule/kinesin-mediated transport. *J Cell Biol* **134:** 349–362

Rodriguez A, Martinez I, Chung A, Berlot CH, Andrews NW (1999) cAMP regulates Ca²⁺-dependent exocytosis of lysosomes and lysosome-mediated cell invasion by trypanosomes. *J Biol Chem* **274:** 16754–16759

Salmon BL, Oksman A, Goldberg DE (2001) Malaria parasite exit from the host erythrocyte: a two-step process requiring extraerythrocytic proteolysis. *Proc Natl Acad Sci USA* **98:** 271–276

Schenkman S, Andrews NW, Nussenzweig V, Robbins ES (1988) *Trypanosoma cruzi* invade a mammalian epithelial cell in a polarized manner. *Cell* **55:** 157–165

Schenkman S, Diaz C, Nussenzweig V (1991) Attachment of *Trypanosoma cruzi* trypomastigotes to receptors at restricted cell surface domains. *Exp Parasitol* **72:** 76–86

Schwab JC, Beckers CJ, Joiner KA (1994) The parasitophorous vacuole membrane surrounding intracellular *Toxoplasma gondii* functions as a molecular sieve. *Proc Natl Acad Sci USA* **91:** 509–513

Shaw MK (1999) *Theileria parva*: sporozoite entry into bovine lymphocytes is not dependent on the parasite cytoskeleton. *Exp Parasitol* **92:** 24–31

Shaw MK (2003) Cell invasion by *Theileria sporozoites*. *Trends Parasitol* **19:** 2–6

Shiels BR, McKellar S, Katzer F, Lyons K, Kinnaird J, Ward C, Wastling JM, Swan D (2004) A *Theileria annulata* DNA binding protein localized to the host cell nucleus alters the phenotype of a bovine macrophage cell line. *Eukaryot Cell* **3:** 495–505

Sibley LD, Krahenbuhl JL (1988) Modification of host cell phagosomes by *Toxoplasma gondii* involves redistribution of surface proteins and secretion of a 32 kDa protein. *Eur J Cell Biol* **47:** 81–87

Sibley LD, Weidner E, Krahenbuhl JL (1985) Phagosome acidification blocked by intracellular *Toxoplasma gondii*. *Nature* **315:** 416–419

Sinai AP, Webster P, Joiner KA (1997) Association of host cell endoplasmic reticulum and mitochondria with the *Toxoplasma gondii* parasitophorous vacuole membrane: a high affinity interaction. *J Cell Sci* **110:** 2117–2128

Sinai AP, Payne TM, Carmen JC, Hardi L, Watson SJ, Molestina RE (2004) Mechanisms underlying the manipulation of host apoptotic pathways by *Toxoplasma gondii*. *Int J Parasitol* **34:** 381–391

Swan DG, Phillips K, Tait A, Shiels BR (1999) Evidence for localisation of a *Theileria* parasite AT hook DNA-binding protein to the nucleus of immortalised bovine host cells. *Mol Biochem Parasitol* **101:** 117–129

Swan DG, Stern R, McKellar S, Phillips K, Oura CA, Karagenc TI, Stadler L, Shiels BR (2001) Characterisation of a cluster of genes encoding *Theileria annulata* AT hook DNA-binding proteins and evidence for localisation to the host cell nucleus. *J Cell Sci* **114:** 2747–2754

Swan DG, Stadler L, Okan E, Hoffs M, Katzer F, Kinnaird J, McKellar S, Shiels BR (2003) TashHN, a *Theileria annulata* encoded protein transported to the host nucleus displays an association with attenuation of parasite differentiation. *Cell Microbiol* **5:** 947–956

Tardieux I, Webster P, Ravesloot J, Boron W, Lunn JA, Heuser JE, Andrews NW (1992) Lysosome recruitment and fusion are early events required for trypanosome invasion of mammalian cells. *Cell* **71:** 1117–1130

Webster P, Dobbelaere DA, Fawcett DW (1985) The entry of sporozoites of *Theileria parva* into bovine lymphocytes *in vitro*. Immunoelectron microscopic observations. *Eur J Cell Biol* **36:** 157–162

Werner-Meier R, Entzeroth R (1997) Diffusion of microinjected markers across the parasitophorous vacuole membrane in cells infected with *Eimeria nieschulzi* (Coccidia, Apicomplexa). *Parasitol Res* **83:** 611–613

Wickham ME, Culvenor JG, Cowman AF (2003) Selective inhibition of a two-step egress of malaria parasites from the host erythrocyte. *J Biol Chem* **278:** 37658–37663

Clockwise from top left: Sónia S. Albuquerque, Maria M. Mota, Patricia Leirião & Cristina D. Rodrigues

Now this is not the end.
It is not even the beginning of the end.
But it is, perhaps, the end of the beginning.

Sir Winston Churchill